IMPROVING OUR UNDERSTANDING OF EVOLUTIONARY PALEOECOLOGY

A CELEBRATION OF THE WORK AND CAREER OF TOMASZ K. BAUMILLER

Image Credit: M. Veitch

A SPECIAL VOLUME IN THE CONTRIBUTIONS FROM THE MUSEUM OF PALEONTOLOGY JOURNAL SERIES

IMPROVING OUR UNDERSTANDING OF EVOLUTIONARY PALEOECOLOGY

A CELEBRATION OF THE WORK AND CAREER OF TOMASZ K. BAUMILLER

A special thank you to the many authors and contributors who made this special volume possible.
And thank you to Jennifer E. Bauer and William I. Ausich, who worked as special editors for this volume.

Museum of Paleontology, The University of Michigan
1105 North University Avenue, Ann Arbor, Michigan 48109-1085
Matt Friedman, Director

Contributions from the Museum of Paleontology, University of Michigan is a medium for publication of reports based chiefly on museum collections and field research sponsored by the museum. Jennifer Bauer and William Ausich, Guest Editors;
Jeffrey Wilson Mantilla, Editor.

Publications of the Museum of Paleontology are accessible online at: http://deepblue.lib.umich.edu/handle/2027.42/41251

Print (ISSN 0097-3556), Online (ISSN 2771-2192)
Published June 27, 2022

TABLE OF CONTENTS

Photo taken of Tom in a submarine off the coast of Roatán where he was studying extant stalked crinoids. Photo courtesy of Andreas Kroh.

DR. TOMASZ K. BAUMILLER – A CAREER IN EVOLUTIONARY PALEOECOLOGY

by
J.E. Bauer, W.I. Ausich, R.E. Plotnick, W.J. Sanders, and M.E. Veitch

Dr. Tomasz K. Baumiller is an extraordinary scientist with an innate flair for finding elegant solutions for complex problems. Tom's research is concentrated primarily on both extant and fossil crinoids, where he has provided critical insights in functional morphology, predation and regeneration ecology, parasitism, functional morphology in dinosaurs and the Ediacaran fauna, and taphonomy in echinoderms and mollusks. He has also published important manuscripts on gastropod drilling into brachiopods, bivalves, echinoids, and blastoids. As such, his work has been and continues to be collaborative with biologists and paleontologists from around the world.

Tom began his academic journey at the Department of Geophysical Sciences, University of Chicago (A.B., 1979), where he was a terror on the soccer field and distinguished himself as the only student of his cohort who could understand the lectures of Leigh Van Valen. He earned an M.S. degree from the Department of Geological Sciences, University of Illinois at Chicago (1985, "The function of the wing plates of *Pterotocrinus* and the anal tube of *Abatocrinus*"), where he worked under the direction of Roy Plotnick. He returned to the University of Chicago to complete his Ph.D. with a dissertation entitled, "Crinoid Functional Morphology and the

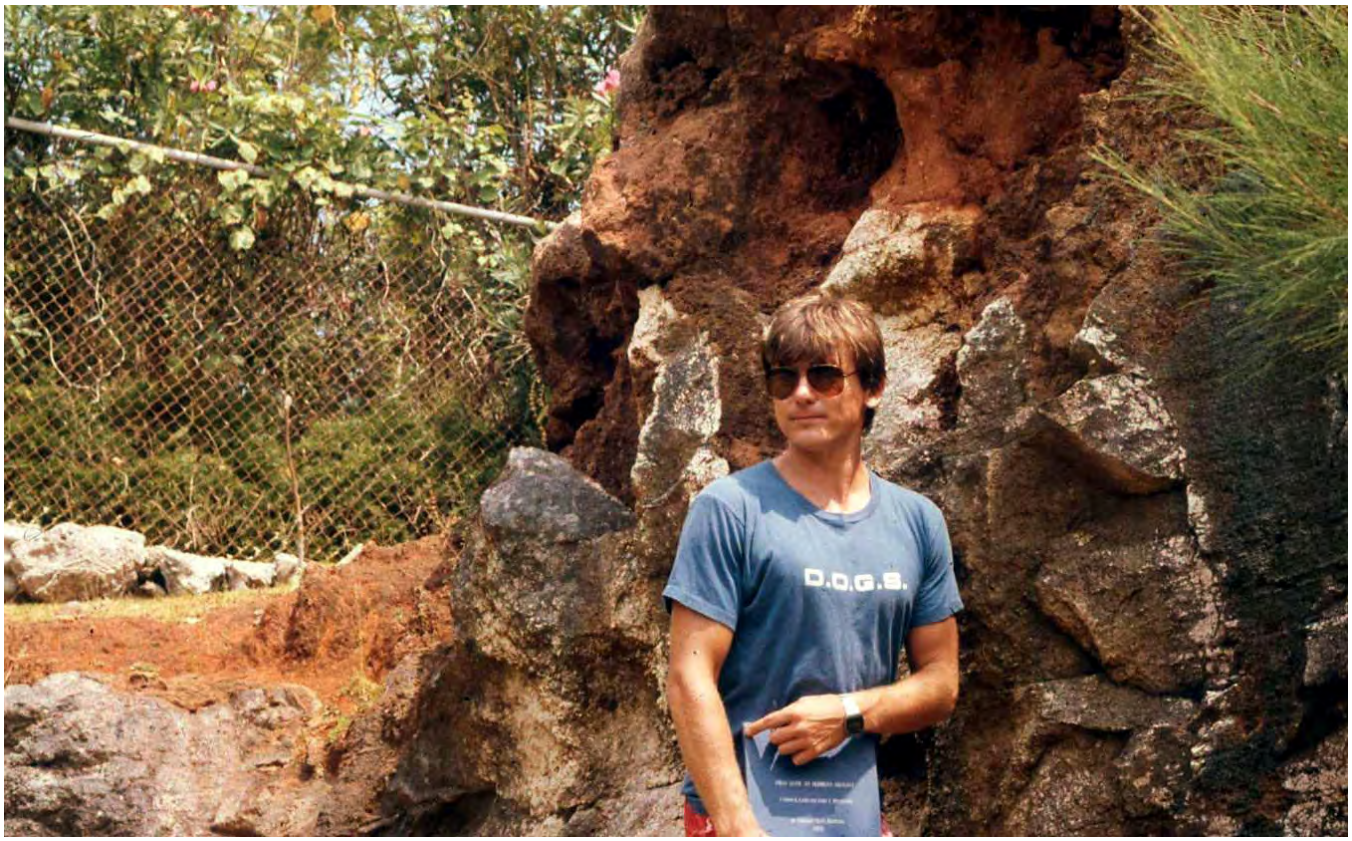

Photo taken of Tom in the field in Bermuda 1985. Photo courtesy of Roy Plotnick.

Energetics of Passive Suspension Feeding: Implications to the Evolutionary History of Paleozoic Crinoidea" (Ph.D. 1990, advisor: Michael LaBarbera).

Tom spent one academic year as a post-doctoral scholar working with William I. Ausich at the Ohio State University. Work initiated at Ohio State includes Phanerozoic crinoid column taphonomy (broken stick), biology, and functional morphology based of connective tissues; muscles versus ligaments in the arms of Paleozoic crinoids; Paleozoic crinoid evolutionary faunas, differential species longevity in Mississippian crinoids. His first academic position was at Harvard University (1991–1996) as an Assistant/Associate Curator at the Museum of Comparative Zoology and Assistant/Associate Professor in the Department of Earth and Planetary Sciences, after which he joined the faculty at the University of Michigan with a joint position as Curator for the Museum of Paleontology and Professor in the Department of Earth and Environmental Sciences, from which he retired in Spring 2020.

A primary thrust of Tom's research was bringing fossil crinoids "back to life." This was accomplished with a joint research focus on the biology of living crinoids and on applying these data to fossil crinoids using engineering principles and rigorous numerical methods. These studies included work on fluid flow, soft tissues, predation, taphonomy, regeneration, isotope geochemistry, paleoecology, and functional morphology. Using a flow tank, that he helped construct in the lab of Roy Plotnick, he showed that that the wingplates in a camerate crinoid acted to maintain stability of their feeding posture and that the weird anal tube of batocrinids functioned as a chimney to flush their wastes downstream. He introduced many terms into the crinoid lexicon, including broken stick, cantilever beam, shaving-brush trauma posture, and starburst trauma posture to name a few. One of Tom's more interesting papers, working with Forest Gahn, was on the association between platyceratid gastropods and crinoids. Long described as a durophage on crinoids, Tom and Forest were able to convincingly demonstrate that they were clearly parasites.

Tom also spent the latter half of his career studying extant crinoids, including feather stars in the Indo-Pacific, and stalked

crinoids present in deep water of the Caribbean Sea. His work on these crinoids included ecology, predation, regeneration, taxonomy, and functional morphology. One remarkable video, produced along with his long-time collaborator Charles Messing, showed a living isocrinid crinoid detached from its holdfast and crawling along the sea-floor off Grand Bahama Island. His work off Roatán, Honduras includes several study sites of stalked crinoids across three different orders, various bottom environments, and a range of depths. The data gathered from these crinoids is seminal in deep water stalked crinoid studies for being among the first that observed a known population across several years, allowing new insights to crinoid ecology and functional morphology, including age estimates, regeneration rates, and population ecology. His temporal consideration of regeneration rates in crinoids changed how predation studies should be viewed for these echinoderms. Crinoid arm injuries are ephemeral and eventually leave no detectable trace, and the rate at which an injury disappears via regeneration is critical to estimate predation intensity. Simply counting the number of injuries in a population leads to an incorrect estimate. The many trips down in the submersible off Roatán, also displayed Tom's admiration and fascination of stalked crinoids. Few people would get into a submersible built by a guy in his backyard once, let alone again after events such as leaks, power shorts, and being squashed next to a terribly sea-sick grad student for six hours.

Tom has always been a generous and engaging mentor who has positively impacted the careers of students and colleagues alike. As many as a dozen graduate students have completed their degrees with Tom, and many more students have benefitted from his critical thinking and quest for well-constrained, rigorous solutions for understanding the paleobiologic history of ancient life. Tom excelled in allowing his students to push themselves outside of research as well, supporting internships, teaching retreats, professional development, and more, leading to success for his students both in and outside of academia. He never limited his influence to just his students in the lab, being an undergraduate advisor for many years, pushing for new courses and department initiatives, and constantly working to improve his teaching lectures. Collectively, we thank Tom for his wisdom, counseling, insights, and statistical coaching; and we hope that he continues his scientific quest during retirement.

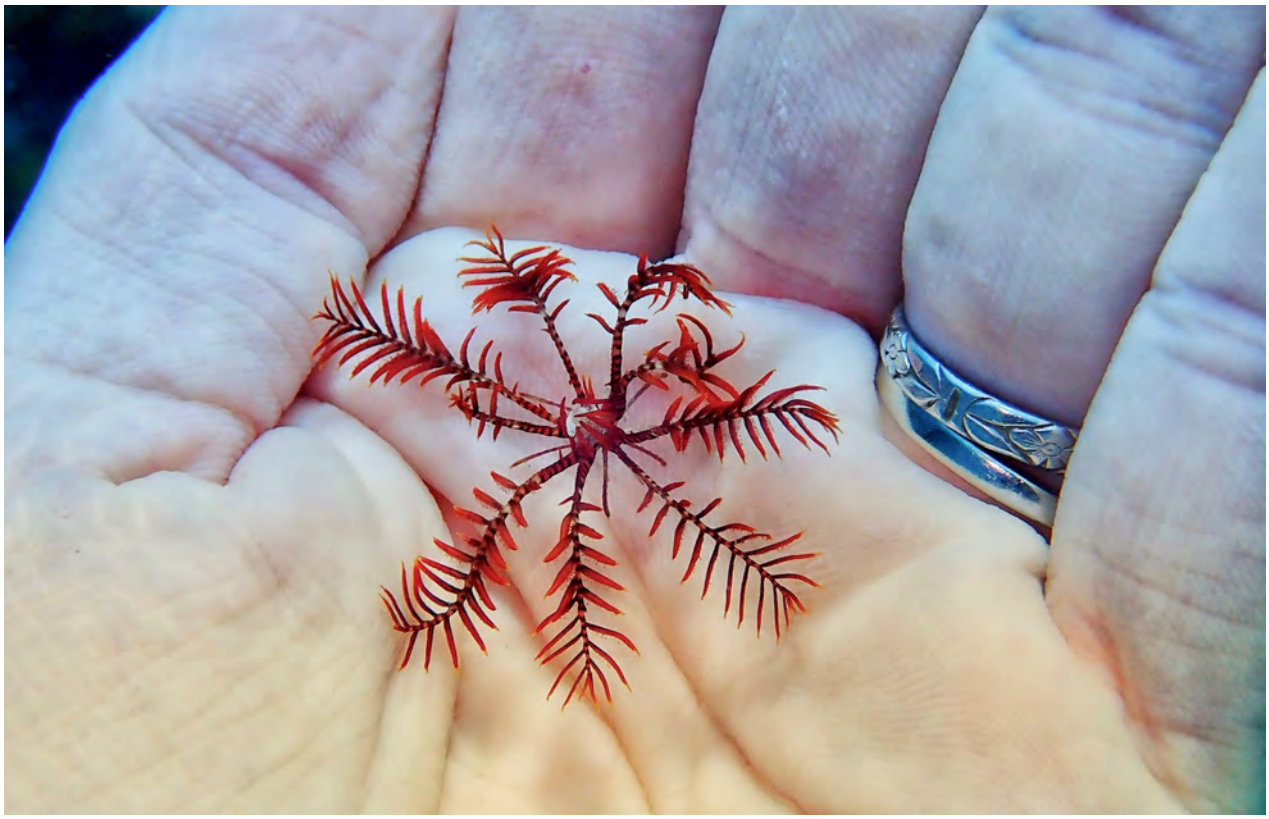

Tom holding a juvenile Stephanometra. *Photo courtesy of Angela Stevenson.*

Graduation picture taken with former student and volume contributor Devapriya Chattopadhyay in 2009. Photo courtesy of Chattopadhyay

Contributions

from the Museum of Paleontology, University of Michigan
VOL. 34, NO. 1, PP. 1–4 JANUARY 18, 2022

SYRINGOPORA GOLDFUSS (TABULATA) ON AN ENIGMATIC SUBSTRATE, MISSISSIPPIAN, THE NETHERLANDS

BY

S. KENNETH DONOVAN[1]

Abstract — This paper reports only the second example of a *Syringopora* – substrate association in the common Mississippian building stones of the Netherlands. The present specimen is in a bridge coping stone in Hoofddorp, province of Noord Holland. The first example had a readily identifiable molluscan substrate; in contrast, that discussed herein remains enigmatic. The substrate is preserved as an irregular, lobate mass of recrystallized, white calcite. This is unlikely to be an inorganic clast, but, if organic in origin, its affinities are puzzling. Most likely it was a sponge or colonial invertebrate which was subsequently recrystallized. This distinctive and peculiar organism-substrate association is recorded, but its precise interpretation remains elusive.

INTRODUCTION

I lived in the Netherlands for more than 19 years. It was only in the last few years of my residence that I took an active interest in its Upper Paleozoic geology. This is not apparent except in very rare *in situ* exposures (various papers in Wong et al., 2007); there are no exposures of fossiliferous carbonate rocks of pre-Mesozoic age buried under a thick succession of Cenozoic sands and muds. However, imported carbonate rocks are common as building stones, particularly Mississippian limestones, such as described by Dubelaar et al. (2011, 2014) and Donovan (2019: figs 1b, 5b, 6a, c), and coeval erratic clasts in the bedload of the rivers Maas and Rhine (see Van der Lijn, 1974; Bosch, 1992; Blankers and Nelissen, 2013; Donovan et al., 2016, 2020, 2021, and references therein).

Studying the paleontology of Mississippian building stones has its problems. Except for rare, lucky specimens, situated at corners of rock slabs, fossils are apparent only in two-dimensions. Specimens can only be collected by camera; there are no hammers and no excavation or slabbing of rocks in the laboratory. Most specimens, with the notable exception of corals (Van Ruiten and Donovan, 2018), can be determined only to a high taxonomic level, such as productid brachiopods or fenestrate bryozoans (Donovan and Harper, 2018; Donovan and Wyse Jackson, 2018). However, there are rare and notable examples of organism – organism interactions apparent in two-dimensions, such as corals encrusting shelly substrates (Donovan, 2016).

[1]Apartment 5 Worsley Point, 251 Worsley Road, Swinton, Manchester M27 0YE, UK (SKennethDono@gmail.com)

FIGURE 1 — A view of the locality, a canal bridge on Hoofdweg – Westzijde, Hoofddorp, the Netherlands. It is photographed from near the corner of Graan voor Visch and Hoofdweg – Oostzijde. The windmill – Korenmolen De Eersteling – is a notable local landmark. This site is about 1.3 km northwest of Hoofddorp railway station, on the Amsterdam Schiphol to Leiden line. The asterisk (*) marks the position of the fossiliferous coping stone of interest.

In consequence, it is significant to record a feature that I have seen many times without being able to interpret it adequately. Publishing details of this association may spark the interest in someone more knowledgeable in recrystallized fossils and/or sedimentary structures; I hope so. The feature was of particular interest in that it is exposed in a bridge cladding within a few hundred meters of my former home in Hoofddorp, the Netherlands. In a country with no natural outcrops of Mississippian limestones, this man-made edifice exposes an enigmatic association between a tabulate coral and a recrystallized structure of unknown organic(?) origin.

LOCALITY

Hoofddorp in the province of Noord-Holland is the first railroad station southwest from Amsterdam Schiphol International Airport, on the line to Leiden, Den Haag, and Belgium. Approximately 1.3 km northwest of the station, following the road Graan voor Visch, is a crossroads with the Hoofdweg separated into two sides — Westzijde and Oostzijde — by a major canal. The site of interest is a canal bridge on the Hoofdweg – Westzijde (Fig. 1), northeast of the crossroads, but close to it, and near to a major local landmark, the Korenmolen De Eersteling, a large windmill that still produces flour.

The specimen of interest (Figs. 2, 3) is in a coping stone at the northeast end of the bridge on the southeastern side (Fig. 1). The coping stones of this bridge are Mississippian limestones. These rocks contain a marine fauna typical of such limestones, particularly crinoid debris, brachiopods, and colonial corals (rugose *Michelinia* sp. and tabulate *Syringopora* sp.).

DESCRIPTION

The specimen of interest consists of two distinct structures, but, in truth, there is little to describe. Most prominent is an irregularly rounded, lobate mass of crystalline, white calcite (Figs. 2, 3). This was drilled by man near its upper edge, as illustrated; this presumably once supported a fence post but is now infilled by cement.

To the upper and upper right of the calcite mass there is a colony of the tabulate coral *Syringopora* sp. This colony curves around the calcite crystals in this region (best seen in Fig. 3). Individual corallites are conspicuously raised above the surface of the coping stone, having been etched out by weak acid rain, and more than one example of branching is apparent.

DISCUSSION

It is assumed that the coping stone was cut parallel to bedding, so the Figures 2 and 3 show a transverse section of the limestone bed. This specimen poses two simple questions:

FIGURE 2 — Detail of the coping stone, a highly fossiliferous Mississippian limestone. The lobate mass of white calcite crystals, left of center, was presumably organic in origin, but is now unidentifiable. After slabbing, it was bored, but this hole is now infilled with cement. *Syringopora* sp. is prominent towards the top. Scale bar represents 50 mm.

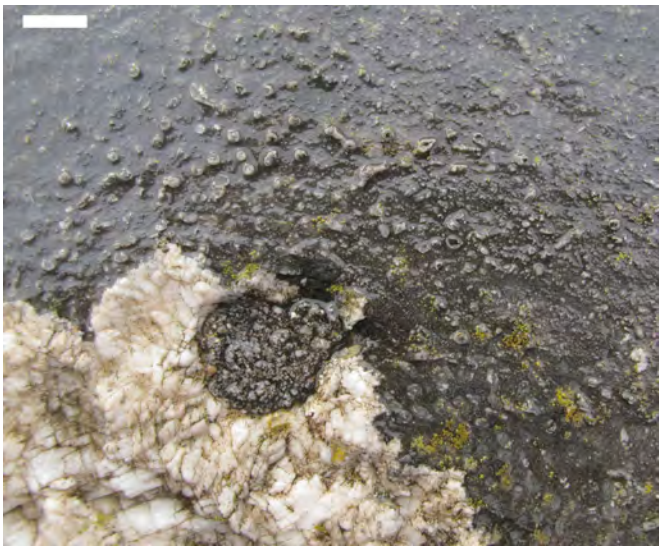

FIGURE 3 — Detail of Figure 2, showing corallites of *Syringopora* sp. etched out of the surface. Scale bar represents 10 mm.

was the coral colony growing attached to what is now a recrystallized mass of calcite; and, if so, what was the nature of the substrate at that time? The former question is the easier and answerable in the affirmative. Although rare, at least one other *Syringopora* — substrate association has been reported from Dutch building stone, the coral growing on a coiled mollusk (gastropod or cephalopod(?)) shell (Donovan, 2016; Van Ruiten and Donovan, 2018). An analogous association is determinable in the present specimen. Evidence includes some corallites of the colony occurring within a few millimeters of the calcite mass and the colony itself curving around the presumed substrate (Figs 2, 3). An intimate relationship during the life of the colony was thus highly likely, perhaps near-certain.

A more difficult problem of interpretation is presented by the crystalline calcite mass. Was it crystalline calcite when encrusted by the coral or, as seems probable, does this represent a later diagenetic alteration? If the former, was it an inorganic clast? Alternately, could it be a reworked bioclast of unusual outline that was already recrystallized? Neither seems likely, particularly an inorganic clast; there is nothing else in this shelly limestone that suggests a conglomeratic origin. Further, the lobate shape with an internal crystalline structure would not have survived energetic transport.

Could the calcite mass be some form of stromatactis, with an early diagenetic infill subsequently exposed by seafloor erosion (see, for example, Bathurst, 1982, 1998; Bourque and Boulvain, 1993; Bourque, 2003)? It seems unlikely: the shelly limestone is not a marine carbonate mudrock; and there is no evidence of a biohermal association or a series of labyrinthine cavities. The two-dimensional shape is superficially stromatactis-like, but not stromatactis.

Alternately, is the calcite mass a recrystallized bioclast, with recrystallization only occurring after final burial? This is the preferred interpretation, yet it is pulled up short by the outline which does not confidently propose any particular biotic affinity. The irregular outline suggests some massive organism, such as a coral, or a sponge or stromatoporoid, but, if so, why is it recrystallized? *Michelinia* sp. occurs in coping stones in this bridge without any indication of major diagenetic alteration. Perhaps most probably, but uncertainly, it was a non-calcareous sponge preserved by diagenetic alteration after encrustation and final burial. Only further specimens available for laboratory study can test the accuracy of this speculation.

ACKNOWLEDGMENTS

I thank my external reviewers, Carl W. Stock, University of Alabama, and John W.M. Jagt, Natuurhistorisch Museum Maastricht, for their constructive comments on an earlier incarnation of this paper.

LITERATURE CITED

BATHURST, R. G. C. 1982. Genesis of stromatactis cavities between submarine crusts in Palaeozoic carbonate mud buildups. Journal of the Geological Society, London, 139: 165–181.

BATHURST, R. G. C. 1998. The world's most spectacular carbonate mud mounds (Middle Devonian, Algerian

Sahara) – Discussion. Journal of Sedimentary Research, 68: 1051.

BLANKERS, P., and L. NELISSEN. 2013. Het Limburgse Heuvelland. Landschap en gesteenten in Zuid-Limburg. Dagblad 'De Limburger'/IVN Spau-Beek, Maastricht en Beek/Spaubeek, 88 pp.

BOSCH, P. W. 1992. De herkomstgebieden van de Maasgesteenten. Grondboor & Hamer, 46: 57–64.

BOURQUE, P. A. 2003. Stromatactis. In G. V. Middleton, M. J. Church, M. Coniglio, L. A. Hardie, and F. J. Longstaffe (eds.), Encyclopedia of Sediments and Sedimentary Rocks. Springer Nature, Switzerland. DOI: https://doi.org/10.1007/978-1-4020-3609-5_223.

BOURQUE, P.-A., and F. BOULVAIN. 1993. A model for the origin and petrogenesis of the red stromatactis limestone of Paleozoic carbonate mounds. Journal of Sedimentary Petrology, 63: 607–619.

DONOVAN, S. K. 2016. A mollusc-coral interaction in a paving slab, Leiden, the Netherlands. Bulletin of the Mizunami Fossil Museum, 42: 45–46.

DONOVAN, S. K. 2019. Urban geology: Mississippian in the Mainstreet. Geology Today, 35: 135–139.

DONOVAN, S. K., M. J. M. DECKERS, J. W. M. JAGT, and A. J. DE WINTER. 2021. Palaeozoic micropelmatozoan thecae from the bedload of the River Maas (province of Limburg, the Netherlands). Proceedings of the Geologists' Association, 132: 66-69.

DONOVAN, S. K., and D. A. T. HARPER. 2018. Urban geology: productid brachiopods in Amsterdam and Utrecht. Deposits, 56: 10–12.

DONOVAN, S. K., J. W. M. JAGT, and M. J. M. DECKERS. 2016. Reworked crinoidal cherts and screwstones (Mississippian, Tournaisian/Visean) in the bedload of the River Maas, south-east Netherlands. Swiss Journal of Palaeontology, 135: 343–348.

DONOVAN, S. K., J. W. M. JAGT, and B. W. LANGEVELD. 2020. A Palaeozoic crinoid from Marker Wadden, a man-made island in north-central Netherlands. Bulletin of the Mizunami Fossil Museum, 46: 11–15.

DONOVAN, S. K., and P. N. WYSE JACKSON. 2018. Well-preserved fenestrate bryozoans in Mississippian building stones, Utrecht, The Netherlands. Swiss Journal of Palaeontology, 137: 99–102.

DUBELAAR, C. W., P. J. M. KISTERS, and J. W. STROUCKEN. 2011. A natural-stone city walk through Maastricht, the Netherlands. In J. W. M. Jagt, E. A. Jagt-Yazykova, and W. J. H. Schins (eds.), A tribute to the late Felder brothers – pioneers in Limburg geology and prehistoric archaeology. Netherlands Journal of Geosciences, 90: 65–71.

VAN DER LIJN, P. 1974. Het Keienboek. Mineralen, gesteenten en fossielen in Nederland (Zesde druk, herzien en bewerkt door Dr. G.J. Boekschoten). W.J. Thieme & Cie, Zutphen, 361 pp.

VAN RUITEN, D. M. and S. K. DONOVAN. 2018. Provenance, systematics and palaeoecology of Mississippian (Lower Carboniferous) corals (subclasses Rugosa, Tabulata) preserved in an urban environment, Leiden, the Netherlands. Bulletin of the Mizunami Fossil Museum, 44: 39–50.

WONG, T. E., D. A. J. BATJES, and J. DE JAGER (eds.). 2007. Geology of the Netherlands. Edita-KNAW (Royal Netherlands Academy of Arts and Sciences), Amsterdam, 354 pp.

Museum of Paleontology, The University of Michigan
1105 North University Avenue, Ann Arbor, Michigan 48109-1085
Matt Friedman, Director

Contributions from the Museum of Paleontology, University of Michigan is a medium for publication of reports based chiefly on museum collections and field research sponsored by the museum. Jennifer Bauer and William Ausich, Guest Editors;
Jeffrey Wilson Mantilla, Editor.

Publications of the Museum of Paleontology are accessible online at: http://deepblue.lib.umich.edu/handle/2027.42/41251

Print (ISSN 0097-3556), Online (ISSN 2771-2192)

Contributions

from the Museum of Paleontology, University of Michigan
VOL. 34, NO. 2, PP. 5–16 JANUARY 18, 2022

DEVONIAN EURYPTERIDS FROM INDIANA AND PENNSYLVANIA

BY

ROY E. PLOTNICK[1]

Abstract — The collection of the University of Michigan Museum of Paleontology contains specimens from two previously undescribed Devonian eurypterid localities. Specimens assigned to *Pterygotus* sp. come from the now flooded Northern Indiana Stone Quarry from Rensselaer, Jasper County, Indiana. The material is preserved as carbonaceous films in dolomites, probably from the Middle Devonian Muscatatuck Group. These are the youngest known specimens of pterygotid eurypterids. A single large body plate is described from the Famennian Oswayo Sandstone of Port Allegany, McKean Co., Pennsylvania and tentatively assigned to the huge stylonurid eurypterid *Hallipterus*. There are a number of fragmentary eurypterids described from the Upper Devonian of Pennsylvania, but no new material has been described since the 1930s.

INTRODUCTION

Although never common in the fossil record, eurypterid diversity, in terms of both species and genera, peaked during the late Silurian and declined throughout the Devonian (Lamsdell and Selden, 2017). One of major groups lost during the Devonian are pterygotids, which include the largest arthropods of all time (Plotnick and Baumiller, 1988; Braddy et al., 2007; Lamsdell and Braddy, 2010). Although most of the Silurian and Devonian eurypterid occurrences are in a variety of marine settings, especially shallow and marginal marine, non-marine occurrences become proportionally more common from the Early Devonian onwards (Plotnick, 1999). Many Late Devonian forms, such as *Hallipterus* Kjellesvig-Waering, 1963 are also quite large (Tetlie, 2008).

The collections of the University of Michigan contain specimens that document two previously undescribed Devonian eurypterid occurrences. The first of these are specimens of the genus *Pterygotus* Agassiz, 1844 from marginal marine deposits in the Middle Devonian of Indiana. This may represent the youngest occurrence of this once diverse family. The second is a large isolated tergite from non-

[1]Department of Earth and Environmental Sciences, University of Illinois at Chicago, 845 West Taylor Street, Chicago, Illinois 60607, U.S.A. (plotnick@uic.edu)

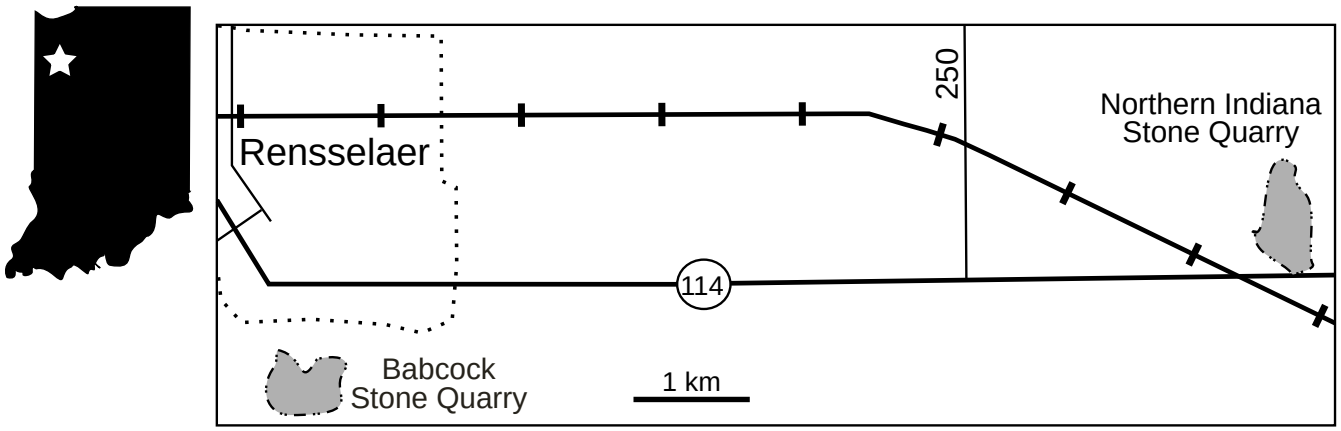

FIGURE 1 — Silhouette map of Indiana showing location of Rensselaer, Jasper Co. (star). Map at right shows locations of now flooded Northern Indiana Stone Quarry at Pleasant Ridge, east of Rensselaer, and the Babcock Stone Quarry, south of Rensselaer.

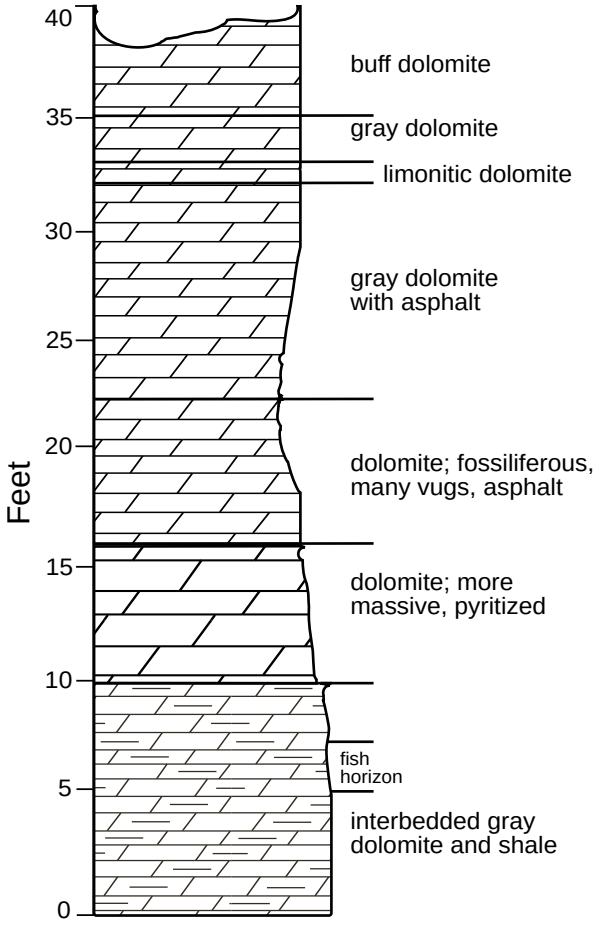

FIGURE 2 — Geologic section of the Northern Indiana Stone Quarry, based on the field notes and sketch of W. G. Melton Jr. on June 18, 1962.

marine sediments in the uppermost Devonian of Pennsylvania, possibly belonging to the genus *Hallipterus*.

As is common for eurypterids, the specimens are incomplete fragments. Nevertheless, they add important documentation to the history of this interesting clade. In addition, I summarize the eurypterid fossil record of the Upper Devonian of Pennsylvania.

A Middle Devonian Pterygotid from Indiana

William G. Melton Jr. collected the eurypterids on June 18, 1962. They came from the now flooded Northern Indiana Stone Quarry (*aka* Rensselaer Stone Company Quarry or A Metz. Inc.), 6.9 km E east of Rensselaer, Jasper County, Indiana, and just west of Pleasant Ridge on Indiana 114 (N 40.93349 W 87.07043; Fig. 1).

Figure 2 shows a redrawn section of the quarry produced by Melton during his visit. According to his field notes, he was accompanied by James Malick and Phillip Bjork; they found "bone through the dolomite as well as in the shale partings, especially in the upper 5 feet." It can be assumed that this is the "fish horizon" in the measured section. He also mentions the presence of 11' of Silurian below, "near the contractor's shack." Based on a note with the specimens, a dipnoan tooth identified by D. Dunkle (Sept. 6. 1963) supported a Devonian age. All the specimen labels indicate Devonian.

The quarry was visited by geologists from the Indiana Geological Survey (IGS) several times between 1963 and 1993, when it was flooded and abandoned (unpublished IGS reports). A 1963 visit by L.F. Rooney and R. R. French recorded a similar section to that drawn by Melton, with an upper 6.8' unit of buff dolomite, then 27' of dark gray dolomite very bituminous and vuggy, with pyrite and molds of corals, underlain by 5' of argillaceous light gray dolomite and shale. This lower unit appears to correspond to the "Fish horizon" identified by Melton, and they suggested it was Silurian. In a 1983 visit, C.A. Ault identified the entire sequence as Devonian, with the upper 33.8' being Traverse Formation

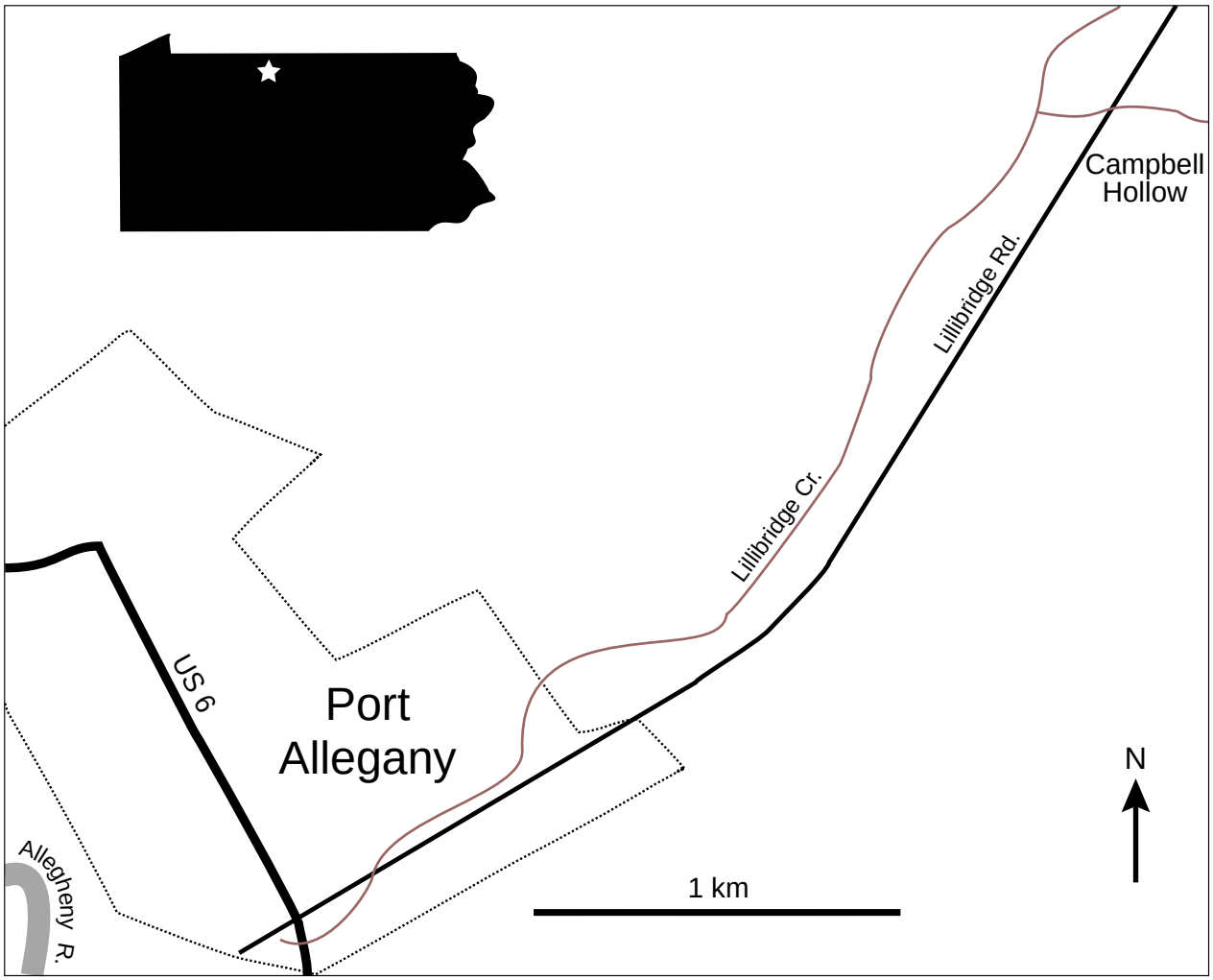

FIGURE 3 — Silhouette map of Pennsylvania showing location of Port Allegany (star). Larger map shows location of Campbell Hollow locality relative to Port Allegany, McKean County.

and the lower unit being Traverse or Detroit River Formation with a total thickness of 14.7'. The Devonian is underlain unconformably by the reefal Silurian Wabash Formation (Salina Group), with some 15' of relief on the unconformity in the quarry. A similar unconformity is described in the nearby Babcock Stone Quarry, where the Devonian is again described as vuggy and oily, with a lower shale marker bed.

The Traverse and Detroit River Formations are part of the Middle Devonian Muscatatuck Group (Doheny et al., 1975), with Detroit River Formation being latest Emsian–Eifelian and the Traverse Formation being Givetian (Shaver et al., 1986; Klapper and Oliver, 1995). Orr and Rebuck (1972) examined conodonts from Traverse Formation outcrops in the Rensselaer area, in the dark grey vuggy dolomite, and placed then in the Givetian *Polygnathus varcus* zone. The Traverse Formation is predominantly limestone with shale beds, and more fossiliferous whereas laminated dolostones are more characteristic of the Detroit River Formation, considered to have been deposited in penesaline to hypersaline environments. Unfortunately, there is insufficient evidence to confidentially determine which of the formations the eurypterids come from, so the age cannot be specified beyond probably Middle Devonian. The presence of shale beds supports a correlation with the Traverse Formation.

The quarry was well known for its sulfide group mineral specimens (Brock, 1986), including marcasite and pyrite. These are present in the vugs in the upper horizons in the quarry, greyish brown sparry dolostones, along with calcite and dolomite crystals. Most cavities are also oil-filled, making collection "indescribably filthy" (Brock, 1986).

The dolomites are also fossiliferous. The Yale Peabody Museum collections contain an unidentified stromatoporoid listed as coming from the middle part of the quarry. The collections of the Indiana State Museum (ISM) include

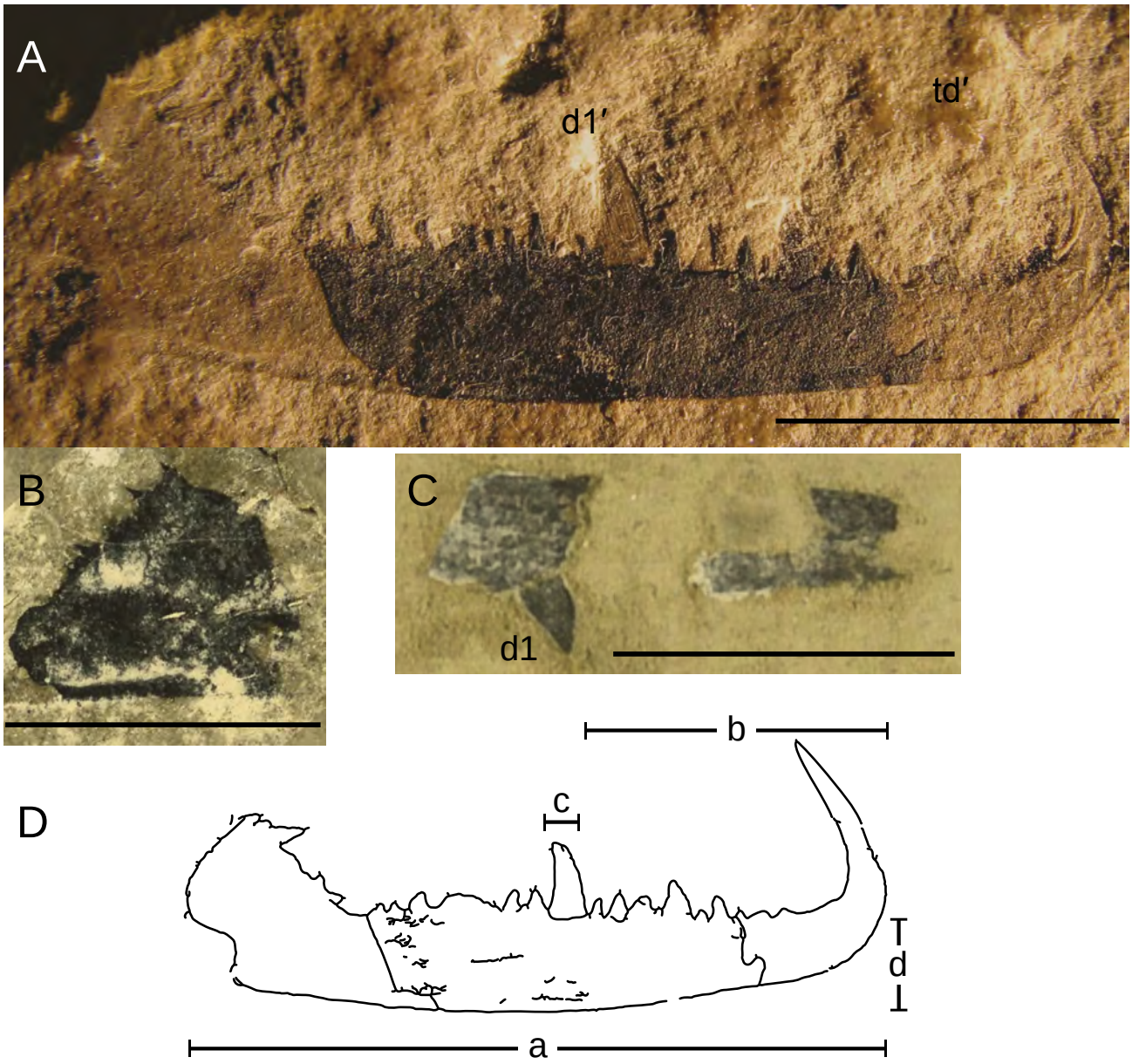

FIGURE 4 — Chelicerae of *Pterygotus* sp. **A**, free finger of UMMP 64135. **B**, base of free finger of UMMP 64137, which may be the counterpart of 64135. **C**, fragments of fixed finger of UMMP 64134. **D**, schematic showing measurements made on UMMP 64135 (Table 1). Dactyl designations and measurements from Miller (2007). All scales equal 1 cm. Abbreviations: *d1*, principal dactyl of fixed finger; *d1′*, principal dactyl of free finger; *td′*, terminal dactyl of free finger.

specimens of brachiopods (*Atrypa reticularis; Pseudoatrypa devoniana; Schizophoria* sp.) and corals, preserved as mineralized casts and molds. According to Peggy Fisherkeller (ISM), hundreds of fossil and mineral specimens from the quarry have had to be deaccessioned due to pyrite disease.

In addition to the eurypterids, specimen UMMP 64141 labelled as being collected by G.M. Ehlers, R.V. Kesling, and A. Boucot on the same date, appears to be a fragment of a placoderm. Based on a photo, L. Sallan and M. Brazeau identified this as likely an arthrodire placoderm, either *Coccosteus* or a close relative, based on size and the rounded ornament (pers. comm., 08/2020), although M. Friedman is not convinced the material is vertebrate. The ornamentation, however, is not consistent with that of eurypterids (agreed with by J. Lamsdell, pers. comm. to J. Bauer, 12/2020). The specimen clearly requires further study.

A Upper Devonian Stylonurid from Pennsylvania

A single specimen (UMMP 26196) was collected by J. C. Galloway, of Port Allegany, McKean Co., Pennsylvania and given to Chester A. Arnold in 1931. It came from a small quarry, known as the DeLong Quarry, 2 miles northeast of Port Allegany at Campbell Hollow (N 41.829, W 78.241) about 30 m above the local valley floor (Fig. 3).

Arnold (1933, 1939) described the lithology and paleobotany of the locality. The described section consists of 3 – 4 meters of massive sandstone, overlain by an approximately 0.5 meter bed of yellow mud and sand with associated pyrite. Plant remains include fronds of *Archaeopteris latifolia* Arnold, 1939 and pyritized wood (*Callixylon*) of *Archaeopteris*, a possible lycopod strobilus (tentatively assigned by Arnold to *Sigillaria*), and the lycopods *Prolepidodendron breviinternodium* Arnold, 1939 and *Lepidostrobus gallowayi* Arnold, 1935.

Stratigraphically, Arnold (1933, 1939) placed this locality in the Oswayo Sandstone. The Pennsylvania geological survey maps this area as "Shenango through Oswayo undivided" (Berg and Dodge, 1981). This puts the unit in the uppermost Famennian (Richardson and Ahmed, 1988).

Richardson and Ahmed (1988) assigned the Oswayo to the "Cattaraugus facies" of Rickard (1975). These are variable nearshore and alluvial sediments, including non-marine sandstones with abundant plants. This is compatible with Arnold (1939), who believed this deposit represented a deltaic environment.

INSTITUTIONAL ABBREVIATIONS

NYSM — New York State Museum
SMP — State Museum of Pennsylvania
UMMP — University of Michigan Museum of Paleontology
YPM — Yale Peabody Museum

SYSTEMATIC PALEONTOLOGY

EURYPTERIDA Burmeister, 1843
EURYPTERINA Burmeister, 1843
PTERYGOTOIDEA Clarke and Ruedemann, 1912
PTERYGOTIDAE Clarke and Ruedemann, 1912
PTERYGOTUS Agassiz, 1844
PTERYGOTUS sp.

Referred Specimens.— UMMP 64135 (moveable finger of chelicera), UMMP 64137 (probable counterpart of 64135); Paratype UMMP 64138 (telson, part and counterpart), UMMP 64134 (fragments of fixed finger of chelicera), UMMP 64136 (podomeres of swimming leg?); UMMP 64139 (fourteen pieces, unidentifiable fragments), UMMP 64140 (sixteen pieces, unidentifiable fragments).

Locality and Horizon.— Northern Indiana Stone Quarry 6.9 km E east of Rensselaer, Jasper County, Indiana. Probably Muscatatuck Group, Middle Devonian.

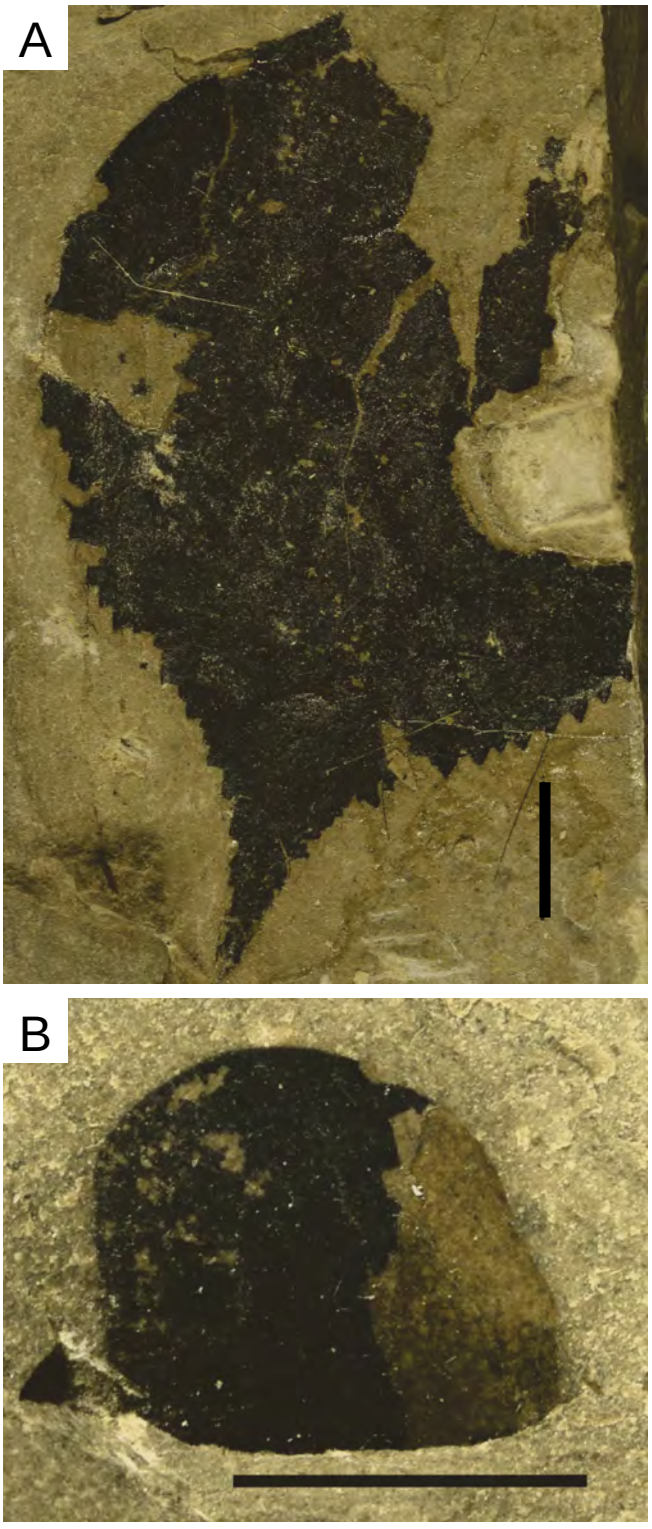

FIGURE 5 — **A**, telson of *Pterygotus* sp. (UMMP 64138). **B**, unidentified fragment; possibly podomeres 7 and 7a of swimming leg (UMMP 64136). Scales equal 1 cm.

FIGURE 6 — **A**, isolated tergite from the Upper Devonian of Pennsylvania. UMMP 29196. **B**, closeup showing the ornamentation. Scales equal 1 cm.

Description.— Specimen UMMP 64135 (Fig. 4A) is an isolated moveable finger of chelicerae, 32.4 mm in length, terminal dactyl recurved proximally. There is a single major sharp denticle, clearly striated, with a height of 3.6 mm and width of 1.76 mm, designated d1′, using the notation of (Miller, 2007: text-fig. 13). A second more distal denticle, corresponding in position to d3′, is 2.0 mm in height, Additional small denticles occur along the length of finger, including on the base. The denticles on the base are clearly shown in UMMP 64137 (Fig. 4B), which is almost certainly the counterpart of UMMP 64135.

Table 1 includes measurements of the free fingers of given in Miller (2007) plus those of the specimen discussed here (Fig. 4D). Although the specimen from Indiana is smaller, the proportions given as ratios in the table are indistinguishable.

UMMP 64134 (Fig. 4C) is a fragment of a finger, with a single large denticle, 1.7 mm in height, broad at the base and inclined distally. This specimen is interpreted as a fragment of the fixed finger and the denticle as d1. Poschmann and Tetlie (2006) noted an inclined denticle is characteristic of the fixed finger of the Silurian *Acutiramus macrophthalmus* (Hall, 1859).

Specimen UMMP 64138 (part and counterpart; Fig. 5A) is a laterally expanded telson diagnostic of pterygotid eurypterids (Plotnick and Baumiller, 1988). The posterior end is pointed, and the posterolateral margins are serrated. The anterolateral margins appear smooth. There is no evidence of a median keel, although we may be looking at the ventral surface. The telson length is >69.5 mm, with a width of ~47 mm. The approximate length-to-width ratio of 1.48 compares to 1.35 for a much larger specimen described by Miller (2007). A reduced major axis analysis of nine telsons of *Acutiramus* by Plotnick and Baumiller (1988) showed a strong positive allometry of width with size, with length/width ratios in small individuals being about 1.4 and large individuals close to 1.0. Poschmann and Tetlie (2006), based on 62 specimens of telsons of *A. macrophthalmus* (Hall, 1859), also noted an allometric decrease in the length to width proportion, from nearly 2.5 in very small individuals and about 1.0 in large ones. The length/ratio of UMMP 64138 is greater than what was observed in similar sized *A. macrophthalmus* but are what would be expected in a juvenile pterygotid.

There are numerous other small fragments, but no others are diagnostic. UMMP 64136 (Fig. 5B) may be a portion of the swimming paddle of the sixth prosomal appendage, possibly podomeres 7 and 7a.

A Note on Pterygotid Chelicerae.— At least as far back as Huxley and Salter (1859), pterygotid papers have termed the two components of the pterygotid chelicerae the "fixed ramus" and the "free ramus." This persists despite the usual usage of ramus in arthropod biology, to refer to separate, multiple podomere branches of appendages, such as the endopods and exopods of crustaceans. An examination of the literature of living chelicerates reveals a wide disparity of terminology among papers on *Limulus* and arachnids (Shultz, 2001; Carrera et al., 2009; Bird et al., 2015; Bicknell et al., 2018). As a result, I am using the terminology fixed finger and moveable finger, similar to that used for the cheliped of decapods Snodgrass (1965).

Discussion.— The material from Rensselaer, Indiana represents fragments of a small, possibly juvenile, pterygotid eurypterid. Although somewhat smaller, it is not readily distinguished from *Pterygotus anglicus* Agassiz, 1844 as described by Miller (2007) from the Emsian Campbellton Formation of New Brunswick. *P. anglicus* was originally identified by Agassiz (1844) and discussed in detail by Huxley and Salter (1859) and Woodward (1866–1878). One of the first eurypterids described, it is from "Lower Old Red Sandstone" of Scotland (Arbuthnott Group, Gedinnian). If these specimens are indeed conspecific, then *P. anglicus* has a wide stratigraphic and geographic range. However, following Lamsdell and Legg (2010), the modest amount of material neither justifies creating a new species nor allows certainty in the taxonomic assignment, beyond *Pterygotus* sp.

In addition, if the Middle Devonian date is correct, these specimens represent the last occurrence of the pterygotid eurypterids (Tetlie, 2007). Russell (1954) described *P. gaspesiensis* from the Devonian Battery Point Formation of Gaspé Bay, Quebec and gave it a Middle Devonian age (Russell, 1947). However, more recent work has assigned

TABLE 1 — Comparison of the four moveable fingers of *P. anglicus* given in Miller (2007) to UMMP 64135. Measurements in millimeters are a) total length of finger; b) distance from the distal base of the primary denticle (d1′) to outside terminal denticle (td′), c) width of base of primary denticle, d) width finger from base primary denticle. See Figure 4D. NBMG = New Brunswick Museum; GSC = Geological Survey of Canada.

Specimen	a. Total Length	b.Distance Primary to Terminal Denticle	c. Basal Width Primary Denticle	d. Width Finger at Primary Denticle	Ratio b/a	Ratio c/a	Ratio d/a
NBMG 10237	71	33	4	9+	0.46	0.06	0.13
NBMG 9774	135	52	7	18	0.39	0.05	0.13
NBMG 10000	101	54	4–5	15	0.53	0.04	0.15
GSC 3239	50.5	>18	3	6.5	0.36	0.06	0.13
UMMP 64135	32.4	13.8	1.76	4.04	0.43	0.05	0.12

TABLE 2 — Upper Devonian Eurypterids of Pennsylvania (see text).

Higher taxon	Species	Formation	Locality	Age
Hardieopteridae	*Hallipterus excelsior*	Catskill	Meshoppen	Late Frasnian-Famennian
Stylonurina	*Stylonurella (?) arnoldi*	Catskill	Port Allegany	Late Famennian
	Stylonurella (?) beecheri	Chadakoin	Warren	Famennian
	Stylonurus (?) shaffneri	Lock Haven	Galeton	Late Frasnian-Famennian
Adelophthalmidae	*Adelophthalmus approximatus*	Venango	Warren	Late Famennian
	Adelophthalmus		Burtville	Famennian

these strata to the Cap-aux-Os Member of that formation, which has an Emsian age based on spores (McGregor, 1979; Griffing et al., 2000). In an informal report, Giesen and Poschmann (2012) described an isolated pterygotid metastoma from Wuppertal-Elberfeld, Germany. It is likely from the upper Eifelian Brandenberg Formation, but may be lowermost Givetian (M. Poschmann, pers. comm., 1/2021).

The only other described Middle Devonian form is *P. bolivianus* Kjellesvig-Waering, 1964, described solely on a supposed fragment of the ramus of the chelicera. The locality is described as in the "*Metacryphaeus caffer* Zone of the upper part of the Sicasica Series… near the farm of Belen (Finca de Belen)…La Paz Department, Bolivia" (Kjellesvig-Waering 1964: 348). According to Farjat (2005) and a column supplied by A. Farjat (pers. comm., 7/2020), this unit would be Eifelian. However, the figured specimen does not resemble any other pterygotid. Based on photographs supplied by J. Lamsdell and P. Mayer, Phillipe Janvier identified the specimen as the lower jaw of the chondrichthyan *Pucapampella*, with superbly preserved teeth (pers. comm. 12/2020). This genus was described from the same locality by Janvier and Suarez Riglos (1986). A specimen from the Upper Devonian of Colombia (Olive et al., 2019) was misidentified as possibly being *P. bolivianus*; it is probably arthropod but is too fragmentary to identify further (J. Lamsdell, pers. comm. 1/2021).

STYLONURINA Diener, 1924
KOKOMOPTEROIDEA Kjellesvig-Waering, 1966
HARDIEOPTERIDAE Tollerton, 1989
Hallipterus? Kjellesvig-Waering, 1963
Hallipterus excelsior? Hall 1884

Referred material.— UMMP 29196.

Locality and Horizon.— DeLong Quarry at Campbell Hollow, 2 miles northeast of Port Allegany, Pennsylvania. Oswayo Sandstone, Late Devonian (Famennian).

Description.— The specimen is a large, probably incomplete isolated sclerite (Fig. 6A). The preserved portion is about 100 mm wide and 40 mm maximum length. The presence of cracks on the left side of the specimen (as oriented in the photo), the broken edge on the right side, and the lack of bilateral symmetry in length (longer on the right side), all suggest the original width was significantly greater.

One margin of the sclerite (lower edge in the figure) is serrate, with small pits on the surface. The opposite margin appears corrugate. The shapes of the margins resemble those shown for tergites of the Carboniferous eurypterids *Dunsopterus* Waterston, 1968 (see Waterston, 1957: pl. 3, fig. 1) and *Cyrtoctenus* Waterston, Oelofsen, and Oosthuizen 1985 (see their fig. 11e). As a result, this plate is interpreted as a tergite, with the corrugate margin being anterior.

The tergite is covered with broad lunules (Fig. 6B; Selden, 1981). In the central part of the plate, they appear to be oriented laterally from the upper left to the lower right. On the left side, they are oriented more longitudinally.

Discussion.— Although extremely rare, Upper Devonian

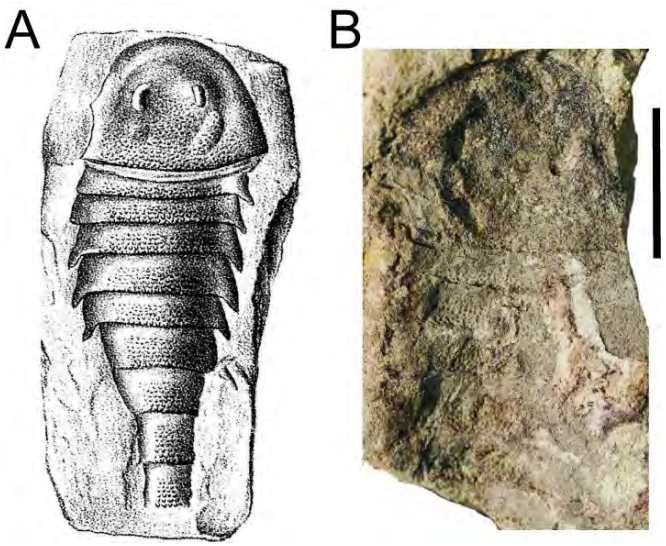

FIGURE 7 — *Adelophthalmus approximatus*. **A**, drawing of missing holotype from Hall and Clarke (1888). **B**, photograph of specimen SMP IP-12793 in State Museum of Pennsylvania, which is the probable counterpart of holotype. Scale equals 1 cm. Photo courtesy of Andrew Bush.

(Frasnian and Famennian) eurypterids have been known from Pennsylvania since the nineteenth century. Surprisingly, none have been described since 1935 (Ehlers, 1935), despite intensive paleontological work on these rocks since then (e.g., Broussard et al., 2018). Unfortunately, the original descriptions often use outdated stratigraphic nomenclature, and the locality data tends to be generalized. I have summarized these occurrences, including their currently used taxonomy (Table 2; Tetlie, 2007, 2008; Lamsdell et al., 2010) and a best estimate of their stratigraphy based primarily on publications and maps of the Pennsylvania Geological Survey (Berg and Dodge, 1981; Dodge, 1992; Berg et al., 1993; Harper, 1999).

Claypole (1883) described a large carapace from the "sandstone of the Catskill group at Meshoppen" Wyoming county. This specimen was very similar to a fossil collected at nearly the same time from New York, which led to a complex nomenclatural history, ably reviewed by Tetlie (2008). There were also competing inaccurate but spectacular reconstructions of a 1.5 m long animal. Tetlie (2008) places both specimens in the genus *Hallipteris excelsior,* a member of the stylonurid eurypterid Family Hardieopteridae (Lamsdell, et al., 2010). He also provides a new reconstruction showing an approximately 100 cm long eurypterid. The state geological map of the area shows Catskill formation as the sole Devonian unit, ranging in age this area from the Late Frasnian to the Famennian (Dodge, 1992; Harper, 1999).

Based on its geographic location, stratigraphy, environments and size, the specimen described here is tentatively assigned to *H. excelsior*. This is also supported by the similarity of the posterior margin of the tergite to that of the prosoma of *H. excelsior* (Tetlie, 2008: fig. 1A).

FIGURE 8 — Holotype of *Stylonurella* (?) *beecheri* (YPM 24347). Photograph of specimen in negative relief. Scale equals 1 cm. Photo by Susan Butts.

Other Late Devonian Eurypterids from Pennsylvania.— Hall and Clarke (1888) illustrated, as a drawing, a small eurypterid from "three miles south of Warren, Warren county, Pennsylvania" and named it *Eurypterus approximatus*. There was only a short description of the species in the caption. The species is now placed in the genus *Adelophthalmus*, a diverse and cosmopolitan taxon that survived until the Middle Permian (Tetlie, 2007; Tetlie and Poschmann, 2008). The original specimen seems to be lost, with the New York State Museum catalog listing only a "plastotype" (NYSM 4459). In 2012, however, Andrew Bush located in the collections of the State Museum of Pennsylvania a specimen collected by the 1800's by the Second Pennsylvania Geological Survey (Second Survey #9651, State Museum Pennsylvania #: SMP IP-12793). It appears to be the counterpart of the holotype (Fig. 7). This is supported by the locality data, which is given as "R2.Tanner's Hill Red Rock. Second Oil Sand? Grey SS. 3 miles S. W. of Warren, PA." The Tanners Hill Red beds are from the Venango Formation in Warren County, making this occurrence Upper Famennian (Dodge, 1993; S. Jasinski, pers. comm., 05/2021). Given the loss of the part, this specimen should be considered the holotype for *A. approximatus.*

In the same publication, Hall and Clarke (1888) illustrated *Eurypterus beecheri* from a sandstone in the "Chemung" (currently Chadakoin) beds of Warren, Warren County, originally described by (Hall, 1884). No other locality information is available. Since a photo of this specimen has not been previously published, I am including it here as Figure 8. The drawing in Hall (1884) is based on a plaster cast and is thus reversed and in positive relief. Tetlie (2008) lists this as an "enigmatic stylonurid" under the name *Stylonurella (?) beecheri*.

Willard (1933) published a new "Chemung eurypterid" from a locality "along the west side of State Highway number 144, three and one-fourth miles south of the town of Galeton in Potter County". The eurypterid, which he named *Stylonurus shaffneri*, is based solely on what is interpreted as a single appendage. Tetlie (2008) considered it doubtfully assigned to the genus *Stylonurus* and indicated it was an "enigmatic stylonurid." The specimen is apparently lost. Lithologically, the specimen is in soft greenish gray shale, associated with lingulids, small bivalves (*Leptodesma*, *Nucula*, and *Grammysia*) and fragments of a bothriolepid. The state survey maps this region as Catskill Formation, underlain by Lock Haven Formation, equal to the no longer used Chemung. Based on fossil content of the site, the eurypterid probably came from the Lock Haven (late Frasnian–Famennian; Broussard et al., 2020).

Another "enigmatic stylonurid" according to Tetlie (2007), despite being relatively complete, is *Stylonurella (?) arnoldi*, described as *Eurypterus arnoldi* by Ehlers (1935). This specimen is from a roadcut along U.S. 6 between Smethport and Port Allegany, McKean County, Pennsylvania, at a place locally known as Bush Hill, about six miles west of Port Allegany. The eurypterid was found in soft, clayey shale containing *Archaeopteris*, lingulid brachiopods, and

fragments of *Holoptychius*. Richardson and Ahmed (1988) placed this section in the upper part of the Cattaraugus Formation and assigned an age, based on miospores, of Late Famennian ("Strunian"). According to S. Jasinski (pers. comm., 05/2021) this is the Catskill Formation. It should be noted that this form has very large eyes relative to the size of the carapace, suggesting it may be juvenile, possibly of *H. excelsior* (Lamsdell et al., 2019).

An undescribed small *Adelophthalmus* in the collections of the New York State Museum (BU 320) was collected ca. 1969 by Ray Baschnagel, from an outcrop on Route 6, near Burtville, Potter County, 4.6 miles east of the junction with Route 155 at Port Allegany. The label gives the age as Famennian.

These specimens suggest that there are numerous additional eurypterid remains to be discovered in the Devonian rocks of northern Pennsylvania and adjacent areas. Future discoveries should help clarify taxonomic ambiguities, as well as improve our knowledge of biostratigraphy and paleoenvironments. These will be important for determining the impact of the Late Devonian extinctions on eurypterids (Lamsdell and Selden, 2017).

ACKNOWLEDGEMENTS

This paper is on honor of Tomasz Baumiller (my very first master's student!) on the occasion of his retirement. My thanks to J. Bauer and W. Ausich for the invitation to complete this paper and finally get these descriptions off my back burner. I also thank P. Fisherkeller, P. McLaughlin, N. Hasenmueller and W. Harrison for invaluable assistance on Indiana Devonian stratigraphy and paleontology; A. Farjat, B. Lieberman, and P. Janvier for advice on the Devonian of Bolivia; M. Poschmann, G. Edgecombe, J-B. Caron, J. Lamsdell, and J. Dunlop for their various comments on pterygotid fragments and chelicerae; J. Huntley for drawing state and county maps; A. Bush for the photo of *A. approximatus* and for bringing the specimen to my attention; S. Butts for the photo of *Stylonurella (?) beecheri*; and to L. Sallan, M. Brazeau, and M. Friedman for their thoughts on a possible placoderm. S. Jasinski corrected the Late Devonian stratigraphy of Pennsylvania. Highly useful comments on the manuscript came from reviewers J. Lamsdell and M. Poschmann.

LITERATURE CITED

AGASSIZ, J. L. 1844. Monographie des poissons fossiles du vieux grès rouge, ou système dèvonien (Old Red Sandstone) des Iles Britanniques et de Russie. Jent et Gassman, Neuchâtel, 171 p.

ARNOLD, C. A. 1933. Fossil plants from the Pocono (Oswayo) sandstone of Pennsylvania. Papers of the Michigan Academy of Science, Arts and Letters, 17: 51–56.

_____ 1935. Notes on some American species of *Lepidostrobus*. American Journal of Botany, 22:23-25.

_____ 1939. Observations on fossil plants from the Devonian of eastern North America. IV. Plant remains from the Catskill Delta deposits of northern Pennsylvania and southern New York. Contributions from the Museum of Paleontology, University of Michigan, 5(11): 271–314.

BERG, T. M., and C. M. DODGE. 1981. Atlas of preliminary geologic quadrangle maps of Pennsylvania. Pennsylvania Geological Survey, 61.

_____, M. MCINERNEY, J. WAY, and D. MACLACHLAN. 1993. Stratigraphic correlation chart of Pennsylvania (slightly revised): Pennsylvania Geological Survey, ser. 4. General Geology Report, 75(1).

BICKNELL, R. D. C., A. J. KLINKHAMER, R. J. FLAVEL, S. WROE, and J. R. PATERSON. 2018. A 3D anatomical atlas of appendage musculature in the chelicerate arthropod *Limulus polyphemus*. PLoS One, 13(2): e0191400.

BIRD, T., R. WHARTON, and L. PRENDINI. 2015. Cheliceral morphology in Solifugae (Arachnida) : primary homology, terminology, and character survey. Bulletin of the American Museum of Natural History, 394: 1–355.

BRADDY, S. J., M. POSCHMANN, AND O. E. TETLIE. 2007. Giant claw reveals the largest ever arthropod. Biology Letters, 4(1):106-109.

BROCK, K. J. 1986. Minerals of the Rensselaer Stone Co. Quarry. Rocks & Minerals, 61(3): 111–115.

BROUSSARD, D. R., J. M. TROP, J. A. BENOWITZ, E. B. DAESCHLER, J. A. CHAMBERLAIN, and R. B. CHAMBERLAIN. 2018. Depositional setting, taphonomy and geochronology of new fossil sites in the Catskill Formation (Upper Devonian) of north–central Pennsylvania, USA, including a new early tetrapod fossil. Palaeogeography, Palaeoclimatology, Palaeoecology, 511: 168–187.

_____, C. J. TREASTER, J. M. TROP, E. B. DAESCHLER, P. A. ZIPPI, M. B. VRAZO, and M. C. RYGEL. 2020. Vertebrate taphonomy, paleontology, sedimentology, and palynology of a fossiliferous Late Devonian fluvial succession, Catskill Formation, North–Central Pennsylvania, USA. PALAIOS, 35(11): 470–494.

BURMEISTER, H. 1843. Die Organisation der Trilobiten, aus ihren lebenden Verwandten entwickelt; nebst einer systematischen Uebersicht aller zeither Arten. G. Reimer, Berlin, 148 p.

CARRERA, P. C., C. I. MATTONI, and A. V. PERETTI. 2009. Chelicerae as male grasping organs in scorpions: sexual dimorphism and associated behaviour. Zoology, 112(5): 332–350.

CLARKE, J. M., and R. RUEDEMANN. 1912. The Eurypterida of New York. New York State Museum Memoir 14: 1– 439.

CLAYPOLE, E. W. 1883. Note on a Large Crustacean from the Catskill Group of Pennsylvania. Proceedings of the American Philosophical Society, 21(114): 236–239.

DIENER, C. 1924. Eurypterida, *In* C. Diener (ed.), Fossilium Catalogus I: Animalia.Volume 25. W. Junk, Berlin, pp. 1-26.

DODGE, C. 1992. Bedrock lithostratigraphy of Warren County, Pennsylvania. Guidebook for the 57th Annual Field Conference of Pennsylvania Geologists, Field Conference of Pennsylvania Geologists Inc: 1–20.

DOHENY, E. J., J. B. DROSTE, and R. H. SHAVER. 1975. Stratigraphy of the Detroit River Formation (Middle Devonian) of Northern Indiana. Indiana Department of Natural Resources, Geological Survery Bulletin, 53: 1–86.

EHLERS, G. M. 1935. A new eurypterid from the Upper Devonian of Pennsylvania. Contributions from the Museum of Paleontology. University of Michigan, 4(18): 291–295.

FARJAT, A. D. 2005. Los géneros *Praectenodonta*, *Praenucula* y *Notonucula* (Palaeotaxodonta: Bivalvia) en el Siluro–Devónico de Bolivia. Geobios, 38(2): 171–186.

GIESEN, P., and M. POSCHMANN. 2012. Riesen–Seeskorpione im Bergischen Land. Archäologie im Rheinland 2012: 53–54.

GRIFFING, D. H., J. S. BRIDGE, and C. L. HOTTON. 2000. Coastal–fluvial palaeoenvironments and plant palaeoecology of the Lower Devonian (Emsian), Gaspe Bay, Quebec, Canada. Geological Society, London, Special Publications, 180(1): 61–84.

HALL, J. 1859. Palæontology of New York.Volume 3, Containing Descriptions and Figures of the Organic Remains of the Lower Helderberg Group and the Oriskany Sandstones. Albany, New York, 532 pp.

_____. 1884. Note on Eurypteridae of the Devonian and Carboniferous formations of Pennsylvania. Pennsylvania Geological Survey, 2nd series, Report P3: 28–39.

_____, and J. M. CLARKE. 1888. Palæontology of New York.Volume 7, Descriptions of the trilobites and other crustacea of the Oriskany, Upper Helderberg, Hamilton, Portage, Chemung, and Catskill groups, Albany, New York, 236 pp.

HARPER, J. A. 1999. Chapter 7 – Devonian, In C. H. Schultz (ed.), The Geology of Pennsylvania. Pennsylvanian Geological Survey and Pittsburgh Geological Society, pp. 109–127.

HUXLEY, T., and J. SALTER. 1859. On the anatomy and affinities of the genus *Pterygotus* and description of new species of *Pterygotus*. Memoirs of the Geological Survey of the United Kingdom, 1: 1- 105.

JANVIER, P., and M. SUAREZ RIGLOS. 1986. The Silurian and Devonian vertebrates of Bolivia. Bulletin de L'Institut Francais d'Etudes Andines, 15: 73–114.

KJELLESVIG–WAERING, E. N. 1963. Revision of some Upper Devonian Stylonuridae (Eurypterida) from New York and Pennsylvania. Journal of Paleontology, 37(2): 490–495.

_____. 1964. A synopsis of the family Pterygotidae Clarke and Ruedemann, 1912 (Eurypterida). Journal of Paleontology, 38(2): 331–361.

_____. 1966. A revision of the families and genera of the Stylonuracea (Eurypterida). Fieldiana: Geology, 14: 169–197.

KLAPPER, G., and J. W. A. OLIVER. 1995. The Detroit River Group is Middle Devonian: Discussion on "Early Devonian age of the Detroit River Group, inferred from Arctic stromatoporoids". Canadian Journal of Earth Sciences, 32(7): 1070–1073.

LAMSDELL, J. C., and D. A. LEGG. 2010. An isolated pterygotid ramus (Chelicerata: Eurypterida) from the Devonian Beartooth Butte Formation, Wyoming. Journal of Paleontology, 84(6): 1206–1208.

_____, and P. A. SELDEN. 2017. From success to persistence: Identifying an evolutionary regime shift in the diverse Paleozoic aquatic arthropod group Eurypterida, driven by the Devonian biotic crisis. Evolution, 71(1): 95–110.

_____, and S. J. BRADDY. 2010. Cope's Rule and Romer's theory: patterns of diversity and gigantism in eurypterids and Palaeozoic vertebrates. Biology Letters, 6(2): 265–269.

_____, _____, and O. E. TETLIE. 2010. The systematics and phylogeny of the Stylonurina (Arthropoda: Chelicerata: Eurypterida). Journal of Systematic Palaeontology, 8(1): 49–61.

_____, L. LAGEBRO, G. D. EDGECOMBE, G. E. BUDD, AND P. GUERIAU. 2019. Stylonurine eurypterids from the Strud locality (Upper Devonian, Belgium): new insights into the ecology of freshwater sea scorpions. Geological Magazine:156:1708-1714.

MCGREGOR, D. C. 1979. Devonian miospores of North America. Palynology, 3: 31–52.

MILLER, R. F. 2007. *Pterygotus anglicus* Agassiz (Chelicerata: Eurypterida) from Atholville, Lower Devonian Campbellton Formation, New Brunswick, Canada. Palaeontology, 50(4): 981–999.

OLIVE, S., A. PRADEL, C. MARTINEZ–PÉREZ, P. JANVIER, J. C. LAMSDELL, P. GUERIAU, N. RABET, P. DURANLEAU–GAGNON, A. L. CÁRDENAS–ROZO, P. A. ZAPATA RAMÍREZ, and H. BOTELLA. 2019. New insights into Late Devonian vertebrates and associated fauna from the Cuche Formation (Floresta Massif, Colombia). Journal of Vertebrate Paleontology, 39(3): DOI: 10.1080/02724634.2019.1620247

ORR, W. R., and W. D. REBUCK. 1972. Age and correlation of Middle Devonian Strata of Jasper County, Indiana. Proceedings of the Indiana Academy of Science, 82: 187.

PLOTNICK, R. E. 1999. Habitat of Llandoverian-Lochkovian eurypterids, In A. J. Boucot and J. D. Lawson (eds.), Paleocommunities: a Case Study From the Silurian and Lower Devonian. Cambridge University Press, Cambridge, pp. 106-131.

_____, and T. K. BAUMILLER. 1988. The pterygotid telson as a biological rudder. Lethaia, 21(1): 13–27.

POSCHMANN, M., AND O. E. TETLIE. 2006. On the Emsian

(Lower Devonian) arthropods of the Rhenish Slate Mountains: 5. Rare and poorly known eurypterids from Willwerath, Germany. Palaeontologische Zeitschrift, 80(4): 325-343.

RICHARDSON, J. B., and S. AHMED. 1988. Miospores, zonation and correlation of Upper Devonian Sequences from western New York State and Pennsylvania, In N. J. McMillan, A. F. Embry, and D. J. Glass (eds.), Devonian of the World: Proceedings of the 2nd International Symposium on the Devonian System — Canadian Society Petroleum Geology Memoir 14, Volume III, pp. 541–558.

RICKARD, L. V. 1975. Correlation of the Silurian and Devonian rocks in New York State. New York State Museum & Science Service, Map and Chart Series, 24:1-16.

RUSSELL, L. S. 1947. A new locality for fossil fishes and eurypterids in the Middle Devonian of Gaspe, Quebec. Royal Ontario Museum Palaeontology Contributions, 12: 6.

_____. 1954. A new species of eurypterid from the Devonian of Gaspé. Annual Report of the National Museum for the Fiscal Year 1952–1953, Bulletin, 132: 83–91.

SELDEN, P. A. 1981. Functional morphology of the prosoma of *Baltoeurypterus tetragonophthalmus* (Fischer) (Chelicerata: Eurypterida). Transaction of the Royal Society of Edinburgh: Earth Sciences, 72: 9–48.

SHAVER, R. H., C. H. AULT, A. M. BURGER, D. D. CARR, J. B. DROSTE, D. L. EGGERT, H. H. GRAY, D. HARPER, N. R. HASENMUELLER, W. A. HASENMUELLER, A. S. HOROWITZ, H. C. HUTCHISON, B. D. KEITH, S. J. KELLER, J. B. PATTON, C. B. REXROAD, and C. E. WIER. 1986. Compendium of Paleozoic rock–unit stratigraphy in Indiana; a revision. Indiana Geological Survey Bulletin, 59: 1- 203

SHULTZ, J. W. 2001. Gross muscular anatomy of *Limulus polyphemus* (Xiphosura, Chelicerata) and its bearing on evolution in the Arachnida. The Journal of Arachnology, 29(3): 283–303.

SNODGRASS, R. E. 1965. A Textbook of Arthropod Anatomy. Hafner Publishing Co., New York, 363 pp.

TETLIE, O. E. 2007. Distribution and dispersal history of Eurypterida (Chelicerata). Palaeogeography Palaeoclimatology Palaeoecology, 252(3–4): 557–574.

_____. 2008. *Hallipterus excelsior*, a Stylonurid (Chelicerata: Eurypterida) from the Late Devonian Catskill Delta Complex, and Its phylogenetic position in the Hardieopteridae. Bulletin of the Peabody Museum of Natural History, 49(1): 19–29.

_____., and M. POSCHMANN. 2008. Phylogeny and palaeoecology of the Adelophthalmoidea (Arthropoda; Chelicerata; Eurypterida). Journal of Systematic Palaeontology, 6(2): 237–249.

TOLLERTON, V. P. 1989. Morphology, taxonomy, and classification of the Order Eurypterida Burmeister, 1843. Journal of Paleontology, 63(5): 642–657.

WATERSTON, C. D. 1957. The Scottish Carboniferous Eurypterida. Transactions – Royal Society of Edinburgh, 63, Part 2: 265–288.

_____. 1968. Further observations on the Scottish Carboniferous eurypterids. Transactions of the Royal Society of Edinburgh, 68(1): 1–20.

WATERSTON, C. D., B. W. OELOFSEN, AND R. D. F. OOSTHUIZEN. 1985. *Cyrtoctenus wittebergensis* sp. nov. (Chelicerata; Eurypterida); a large sweep-feeder from the Carboniferous of South Africa, p. 339–358. In D. R. Bowes and C. D. Waterston (eds.), Transactions of the Royal Society of Edinburgh: Earth Sciences.Volume 76.WILLARD, B. 1933. A new Chemung eurypterid from Pennsylvania. American Midland Naturalist, 14(1): 52–57.

WOODWARD, H. 1866–1878. A monograph of the British Fossil Crustacea belonging to the Order Merostomata. Palaeontographical Society (Monographs).

Museum of Paleontology, The University of Michigan
1105 North University Avenue, Ann Arbor, Michigan 48109-1085
Matt Friedman, Director

Contributions from the Museum of Paleontology, University of Michigan is a medium for publication of reports based chiefly on museum collections and field research sponsored by the museum. Jennifer Bauer and William Ausich, Guest Editors;
Jeffrey Wilson Mantilla, Editor.

Publications of the Museum of Paleontology are accessible online at: http://deepblue.lib.umich.edu/handle/2027.42/41251

Print (ISSN 0097-3556), Online (ISSN 2771-2192)

Contributions

from the Museum of Paleontology, University of Michigan
VOL. 34, NO. 3, PP. 17–33 JANUARY 18, 2022

MORPHOLOGIC EXPRESSIONS AND PALEOGEOGRAPHIC IMPLICATIONS OF EARLIEST KNOWN (FLOIAN, EARLY ORDOVICIAN) HYBOCRINIDS

BY

THOMAS E. GUENSBURG[1] AND JAMES SPRINKLE[2]

Abstract — The early hybocrinid *Syndiasmocrinus apokalypto* n. gen., n. sp. (late Floian, Early Ordovician, Laurentia), furnishes well preserved nearly complete crown morphology. The new taxon's tegmen interambulacral, or perforate extraxial, regions consist of many small platelets and epispires with the hydropore plate separate from the peristome region. This interambulacral plating extends out the arms as lateral plate fields. *Syndiasmocrinus* tegmen morphology concords with *Hoplocrinus* from the Middle to Late Ordovician, of Baltica, but not the similar aged *Hybocrinus*, of Laurentia, where interambulacra are each formed of single circumorals. In contrast, *Syndiasmocrinus'* posterior plating includes an anal X in agreement with *Hybocrinus*, but *Hoplocrinus* lacks this plate. Lateral plate fields of *Syndiasmocrinus* are unlike any other known hybocrinid but resemble those occurring in earliest crinoids such as *Apektocrinus* and *Titanocrinus*. An even earlier hybocrinid, *Parahybocrinus siewersi* n. gen., n. sp. (early Floian, Early Ordovician), posterior cup plating includes two small posterior plates distal to anal X, an expression unknown among hybocrinids until now, but widespread among other early cladids.

urn:lsid:zoobank.org:pub:1C3F1E27-939E-45A8-BA01-7DE58ECE6F75

[1]IRC, Field Museum, 1400 S. Lake Shore Drive, Chicago, IL 60605 (tguensburg@fieldmuseum.org)
[2]Department of Geological Sciences, Jackson School of Geosciences, University of Texas, 1 University Station, C1100, Austin, Texas 78712-0254 (echino@jsg.utexas.edu)

INTRODUCTION

Hybocrinids have long evoked fascination among crinoid students (e.g. Wachsmuch and Springer, 1883; Ausich et al., 2018). Aspects of their anatomy are unusual (Fig. 1). For instance, the cup base circlet is aligned with stalk meres below, in violation of the "Law of Wachsmuch and Springer" (Ubaghs, 1978). This condition has been referred to as "pseudomonocyclic" plating (Öpik, 1935; Warn, 1975; Sprinkle, 1982). Hybocrinids have non-branching food gathering structures expressed either as short atomous arms or armless ambulacra upon the cup surface, and a non-elevated posterior tegmen (Figs. 2, 3) (Sprinkle and Moore, 1978; Sprinkle, 1982; Wright et al., 2017). Some taxa are known to express a small, short, curved stalk, including *Hoplocrinus* Grewingk, 1867, *Hybocrinus* Billings, 1857, and *Hybocystites* Weatherby, 1880. *Trecrinus* Semenov, Terentyev, Mirantsev, and Rozhnov, 2021, lacks a stalk entirely.

Here, we describe earliest known hybocrinids *Syndiasmocrinus apoktalypto* n. gen., n. sp. and *Parahybocrinus siewersi* n. gen., n. sp. and compare these to later taxa to which they are most similar, the Middle to Late Ordovician Laurentian *Hybocrinus* and Baltican *Hoplocrinus* (Figs. 2, 3). Analysis of this new data includes identification of body wall regions from the perspective of the Extraxial/ Axial Theory (EAT) (Mooi and David, 1998).

Taphonomic data provides useful information for functional interpretations; methodology applied earlier by Tom Baumiller (e.g. Baumiller and Ausich, 1992; others). Specimens are relatively small, requiring hand preparation with fine needles under high magnification. Images were acquired by immersing specimens in water or coating with sublimate of ammonium chloride. Images are multi-focus montages prepared at the Field Museum using a Leica DMS digital microscope and linked software.

INSTITUTIONAL ABBREVIATIONS

NPL (----TX--) — Non-vertebrate Paleontology Laboratory, University of Texas, Austin.
PE — Field Museum, Chicago, Illinois.
PIN — Paleontological Institute, Russian Academy of Sciences, Moscow
UI X — Prairie Research Institute, University of Illinois, Champaign.

SYSTEMATIC PALEONTOLOGY

CRINOIDEA Miller, 1821
CLADIDA Moore and Laudon, 1943

Discussion.— Moore and Laudon (1943) originally conceived the Cladida as an ordinal rank taxon diagnosed, in part, by a dicyclic cup with infrabasal and basal circlets. Wright, et al. (2017), revised the Cladida to include not only the crinoid crown group, but also hybocrinids, long placed within the monocyclic disparids (see Sprinkle and Moore, 1978). Realignment within the cladids acknowledges the pseudomonocyclic hybocrinid cup in which infrabasals are secondarily lost (Warn, 1975; Sprinkle, 1982, p. 126).

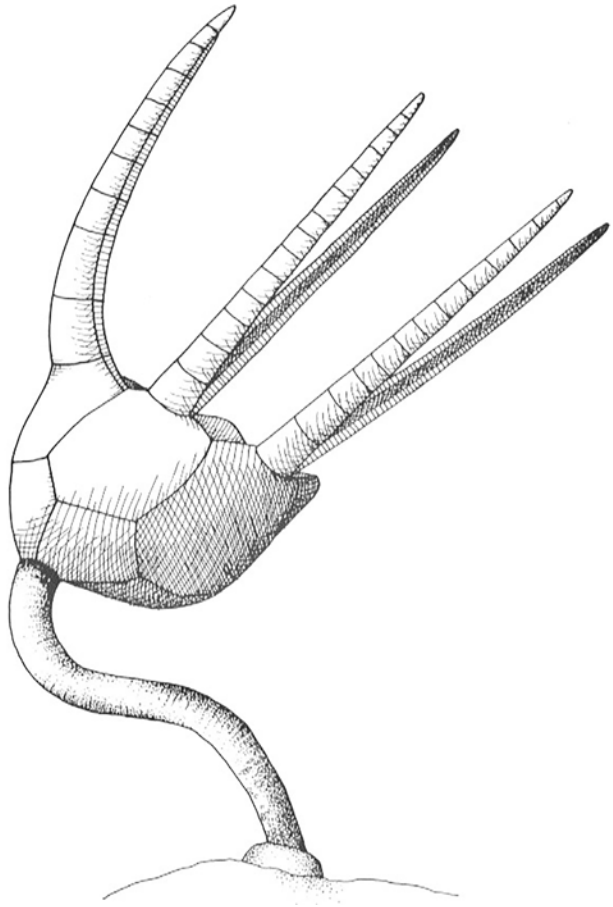

FIGURE 1— Restoration of *Hybocrinus bilateralis* Guensburg, 1984 (copyright, from Guensburg, 1992: fig. 10, reprinted with permission), Late Ordovician (Sandbian).

Order Hybocrinida Jaekel, 1918

Discussion.— The diagnosis provided by Sprinkle and Moore (1978: p. T570) is adopted here with the addition that the "monocyclic" cup is pseudomonocyclic, with the assumption that the plesiomorphic condition among cladids is a dicyclic cup with infrabasals forming the cup base.

Family Hybocrinidae Zittel, 1879

Remark.— The familial diagnosis follows Sprinkle and Moore (1978: p. T570)

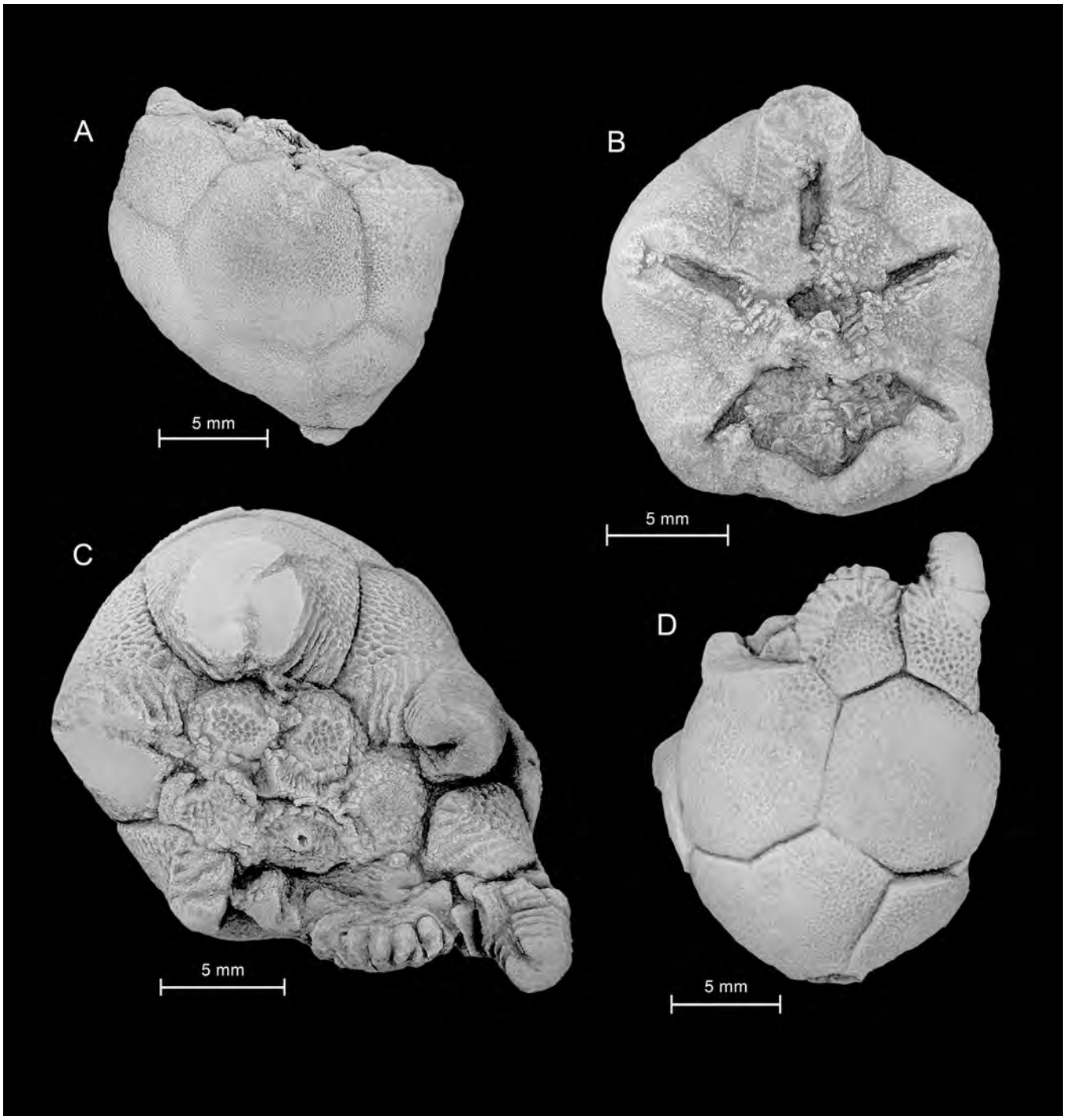

FIGURE 2 — Calyx morphology of the Late Ordovician (Sandbian) *Hybocrinus bilateralis* Guensburg, 1984. Photographs of two specimens from the same shaly interbed, morphology exemplifying the Laurentian genus *Hybocrinus:* UI X 5867 **A, B,** undistorted specimen showing fine reticulate ornament in B view of calyx (A); oral view (B), A ray at top, large circum-orals rigidly sutured to radials, pitted extraxial ornament in continuity across radials and circum-orals, radials with strong "oralward" (inward) curvature so that the tegmen is restricted to the circum-orals and peristome, hydropore plate in CD interray, incorporated into circum-oral ring; UI X 5868 **C**, **D**, slightly crushed specimen in oral view (C), with intact ambulacra, cover plates form a 2-1-2 ambulacral pattern, coarse reticulate ornament crossing from radials to circum-orals, parallel grooves extending laterally from ambulacral grooves in radials, first C brachial; Cup in CD orientation (D), crenulated, thickened, anal X distal margin.

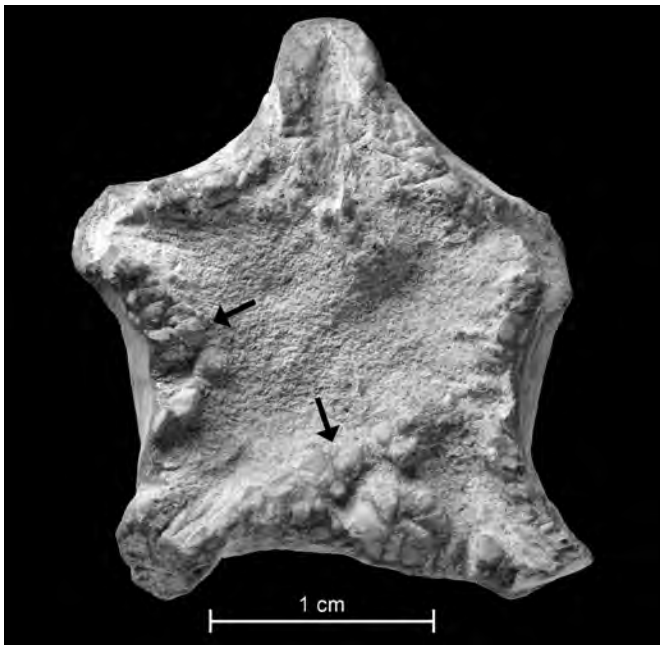

FIGURE 3 — *Hoplocrinus estonus* Öpik, 1935. PIN 4125/9, photograph of oral view of calyx showing areas with small platelets, two marked with arrows, coated. Image courtesy of S.V. Rozhnov, Paleontological Institute, Russian Academy of Sciences.

Genus *Syndiasmocrinus* gen. nov.

Type species.— *Syndiasmocrinus apokalypto* new species

Diagnosis.— As for the type species, by monotypy

Etymology.— Compounding of syndiasmos, Greek, meaning combination, in reference to morphology combining both *Hybocrinus* and *Hoplocrinus* traits, and crinus, latinized from the Greek krinos, lily.

Syndiasmocrinus apokalypto sp. nov.
Figs. 4 – 8, 9B, 9C, 9E, 9F, 10

Type specimens.— Four specimens comprise the hypodigm, the holotype 1780TX13, and paratypes: 1781TX12, 1780TX14, and 1778TX17.

Taphonomic considerations. — *Syndiasmocrinus apokalytpyo* n. gen. n. sp. (herafter *Syndiasmocrinus*, as the genus is monotypic) specimens preserve relatively complete tegmen and arm lateral plating. The four known specimens were collected in float, partly weathered free from shaly matrix. Weathering obscures plate boundaries locally, but this is a relative minor issue in terms of data loss, because most plate shapes can be confidently inferred. More significant are effects of calcitic overgrowths on small skeletal elements. In general, diminutive tegmen interray plating is darker calcite in comparison with thicker, lighter colored, cup and hydropore plates. The holotype tegmen is virtually complete and intact with minor overgrowths but shifted slightly toward the A-B side of the calyx, resulting in most complete exposure of C-E regions (Fig. 7C). Paratype 1778TX14 tegmen is more seriously affected by calcitic overgrowths but these are translucent allowing discernment of original plate outlines under strong light. As preserved, interambulacral regions sag inward in both specimens, indicating a pliable tegmen in life. The conical anal pyramid is preserved in the holotype but folded outward. Lateral plates are well-preserved in the holotype but flattened. One partially preserved arm of paratype 1778TX17 shows laterals covering an inflated region, extending well beyond, above the brachials.

Diagnosis.— A species of hybocrinid with tegmen slightly narrower than maximum cup width, tegmen interradii, interambulacra, with plate fields of tiny plates with apparent epispires, presumably embedded in a flexible integument, hydropore plate separated from the peristome, and tegmen interambulacral fields transitioning to non-pore-bearing lateral plate fields extending out atomous arms in all rays.

Occurrence.— All specimens of this new taxon were collected from the middle Ninemile Shale, *Pseuocybele nasuta* Zone, trilobite zone J (Hintze,1973; Adrain et al. 2009) in Whiterock Canyon, Eureka County, Nevada. Specimens are from an unknown distance above the slope at WR-2 or 2A (Narrows Section), approximately 1.2 km up Whiterock Canyon from the end of the north side access track. This locality is approximately 56 km southwest of Eureka, Eureka County, Central Nevada. This age falls in the upper Blackhillsian Stage, Ibexian Series, late Floian Global Stage, late Early Ordovician.

Description.— A small hybocrinid with relatively short arms; largest specimen, paratype 1780TX14, maximum cup height as measured along the C ray approximately 12.5 mm, the smallest specimen, the holotype, approximately 8.8 mm. Cup approximately as tall as wide in largest specimen paratype 1780TX14, slightly taller than wide in holotype; cup sides diverging from stalk facet at approximately 60 degrees in holotype, 70 to 80 degrees in paratype 1781TX12; C ray higher than other rays, resulting in canted oral surface and asymmetrical calyx. Cup bulbous, umbonate, slightly incurving at top, cup plates ornamented with fine pustules in holotype and paratype 1778TX17, fine reticulation in paratype 1780TX13. Cup base distinctly curved toward the posterior in holotype, slightly curved toward the anterior in paratype 1781TX12; these result in off-axis stalk attachments. Low broad ray ridges in paratype 1780TX14 (Fig. 9E), vague in other specimens.

Basals five, forming approximately lower 30% of cup; wedge-shaped with small undulating stalk facet; BC basal largest, upper facets for radial insertions slightly curved. Radials largest; anterior (A, B, D, E) radials largest cup plates with distal margins slightly curved inward toward the tegmen on average, curvature variable, A and E radials subpentagonal, B and D radials irregular hexagonal with each contacting the radianal and C radial. C radial relatively small, forming the high point of the cup, upper margin slopes distinctly away

from the C radial facet. Radial facets angustary, projecting slightly to distinctly above main body of radial, oriented nearly straight upward to angling diagonally outward. Radianal large, much larger than C radial or anal X (Figs. 4H, 9E), irregular hexagonal, bounding two basals below, B and D radials laterally, the C radial on the upper right, and anal X on the left. Anal X on the upper left, rectangular, the upper surface forming the cup top across CD and separating C and D radials, much smaller than C radial.

Tegmen (oral surface) morphology primarily taken from holotype, augmented by paratype 1778TX12 (*Taphonomic considerations* above); ambulacra (axials) in holotype narrow, converging in 2-1-2 arrangement over the peristome. Cover plate pattern obscure, larger, composed of squared-off lateral cover plates, apparent much smaller medial cover plates visible along the ambulacral mid-line (perradial suture) (Figs. 7A, B) . Interambulacra composed of a network of platelets, estimated 50 per interray, these form fields in holotype and paratype 1778TX12; individual platelets approximately 100 µm across, with estimated two to four marginal epispires along their scalloped margins, particularly well exposed in the DE interray of holotype and AB interray of paratype 1778TX12. CD interray wider than other interrays in holotype, with large ovoid hydropore plate in the holotype, distal to the peristome in CD, irregular surface with deep grooves (Figs. 6-8); at least one other large plate beyond the hydropore plate nearing the periproct. Periproct a steep-sided cone in holotype, formed of several elongate wedge-shaped plates.

Five short atomous arms; tips incomplete, maximum length estimated at slightly longer than cup height judging by arm taper in large paratype 1778TX17, slightly shorter than cup in holotype. Brachials approximately 1.5 times longer than wide in paratype 1778TX17, up to two times longer than wide in smaller holotype. Lateral plate fields separate brachials from axial plating (ambulacrals and cover plates), tapering outward, consisting of thin imbricate elongate ovoid platelets in holotype D ray; inflated ?A ray lateral field of paratype 1778TX17 nearly as wide as adjacent brachials, expanding toward the tegmen. Cover plate pattern uncertain, only exposed in holotype over the peristome; primary cover plates large, elongate, approximately twice as long as wide, squared off at the distinctly sinuous median suture in holotype sutures (Fig. 7A).

Proximal stalk segment preserving 12 very thin columnals in paratype 1780TX14; narrow, approximately 1.3 mm wide at cup juncture, tapering (Fig. 9E). Columnals with traces of pentameres, short rounded, but rough epifacets. Lumen large, pentalobate, each lobe aligned with mere, CD interray lobe larger than others.

Etymology.— *Apokalypto*, Greek, to uncover, reveal, make known, in reference to the remarkable new data furnished by this taxon's discovery.

Remarks.— Each of the four type specimens provides overlapping data representing nearly all portions of the skeleton, excepting the distal stalk and holdfast. Overlapping data also furnish some evidence for phenotypic variation, plate shape, and ornamentation, much as has been observed in *Hybocrinus* (Guensburg, 1984) and *Hoplocrinus* (Rozhnov, 1985; 2007). See COMPARATIVE ANALYISIS OF THE *SYNDIASMOCRINUS* TEGMEN below.

Paleoenvironmental context.— The Ninemile Shale is interpreted have been deposited in relatively deep shelf environment, where soft, unconsolidated substrates prevailed (Guensburg and Sprinkle, 1992; Sprinkle and Guensburg, 1995). This setting was unfavorable for early crinoids in general, judging by their relative rarity. Crinoids required suitable exposed firm or hard sites upon which to attach cementing type holdfasts.

Syndiasmocrinus sp. A
Figs. 9A, 9D

Occurrence.— A single specimen, PE 52754, from the Wah Wah Formation, approximately 2 meters above the contact with the Fillmore Formation, ridge east of Square Top, Square Top East Section, southeast quarter of the southwest quarter of the northwest quarter, Section 32, Township 21 south-Range 13 west, Millard County, Utah. This stratigraphic horizon is in the *Pseudocybele nasuta* trilobite zone J of Hintze, 1973, and Adrain et al., 2009, Blackhillsian Stage, late Floian global stage.

This taxon is represented by a single collapsed cup with parts of arms still embedded in dense matrix. Cup plates are slightly disheveled.

Remarks.— A single specimen is here referred to *Syndiasmocrinus* based on general resemblance of cup shape and plating and but without details of the tegmen and arms, assignment is tentative. Posterior plating resembles *Syndiasmocrinus apokalypto*, except that anal X is a proportionately larger plate, suggesting the possibility of a distinct species.

Paleoenvironmental context.— The single specimen was draped over a small *Calathium*-sponge mound along with other crinoids, including a small iocrinid and another taxon of unknown affinities.

?*Syndiasmocrinus* sp.
Fig. 9G

Occurrence.—Ninemile Shale, 27-29 meters above the base of the Ninemile Shale. Locality is *MJ-1* of Sprinkle, 1973 (p. 195), just out of the west gulley below southwest side of Meiklejohn Peak, northeast quarter of Section 24, Township 12 north, Range 47 east, approximately 7 miles east of Beatty, Nye County, Nevada (Bare Mountain 15-minute quadrangle).

Remarks.—A single specimen, 1968TX2, is a deeply weathered crown and stalk. Partial mouldic preservation of the cup; small, thin, tapering stalk, and atomous arms all suggest a hybocrinid with arms at least twice cup height and stalk length at least 1.3 as long as crown height. Columnals grow thicker away from the crown. Preservation is insufficient for definitive assignment.

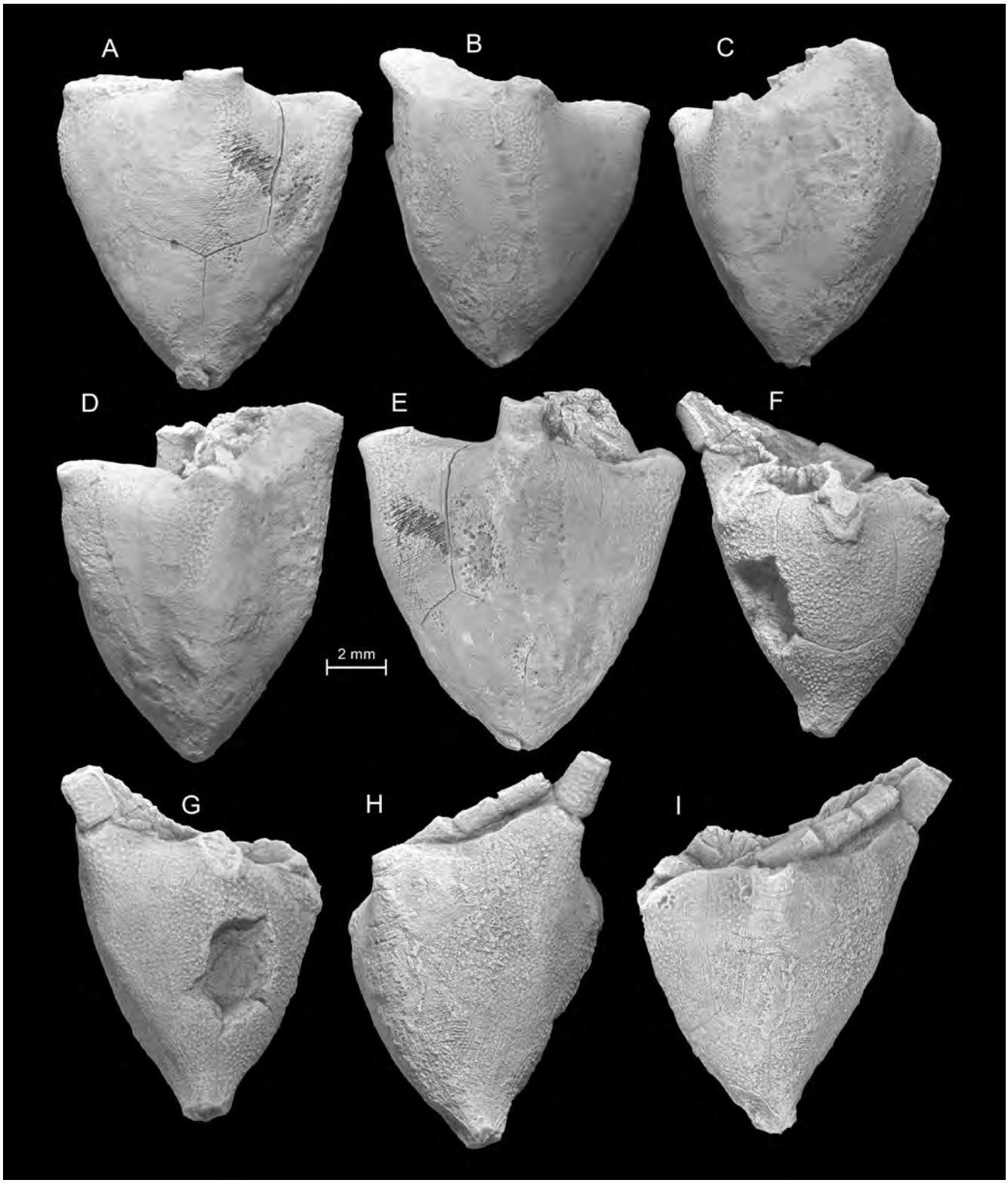

FIGURE 4 — *Syndiasmocrinus apokalypto* n. gen., n. sp. Photographs of cups in lateral views: paratype 1981TX12 **A–E**, which has fine reticulate ornament; **A**, A, **B**, B, **C**, CD, **D**, D, and **E**, E ray views. Holotype 1980TX13 **F–I**, which has fine pustulose ornament, in **F**, A, **G**, B, **H**, CD, and **I**, D ray views.

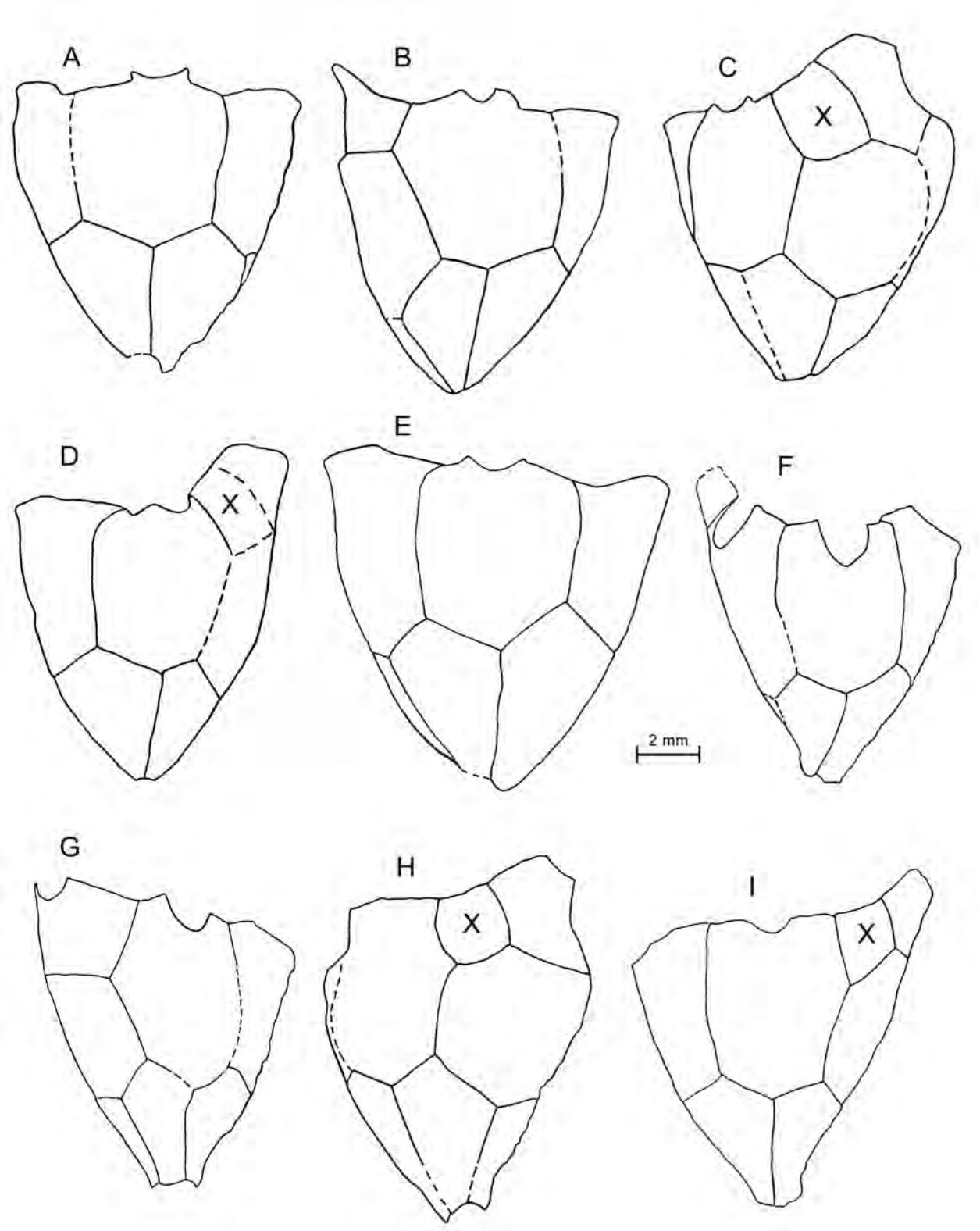

FIGURE 5 — *Syndiasmocrinus apokalypto* n. gen., n. sp. cup morphology: Tracings showing cup plate boundaries from FIGURE 4; anal X plates indicated, and other plates forming cup top are radials; plate subjacent to C radial is the radianal.

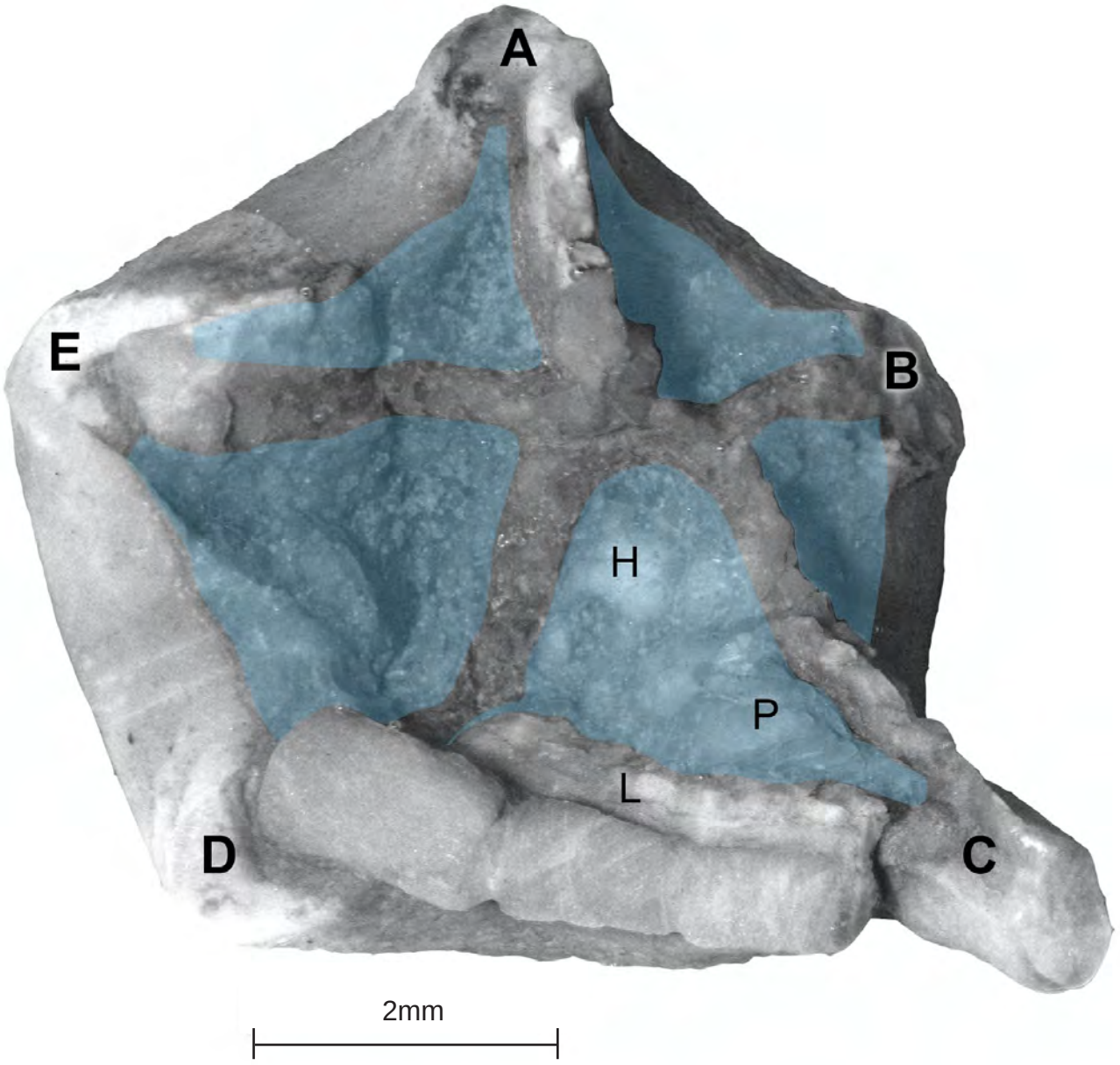

FIGURE 6 — *Syndiasmocrinus apokalypto* n. gen., n. sp., holotype 1980TX13, immersed in water, oral surface with features coded for reference to FIGURE 7. Blue shaded areas indicate interradial, perforate extraxial, portions of tegmen, separated by unshaded ambulacra, axial, area; bold letters indicate rays; H, hydropore plate; L, lateral plates of arm; P, periproct/anal cone.

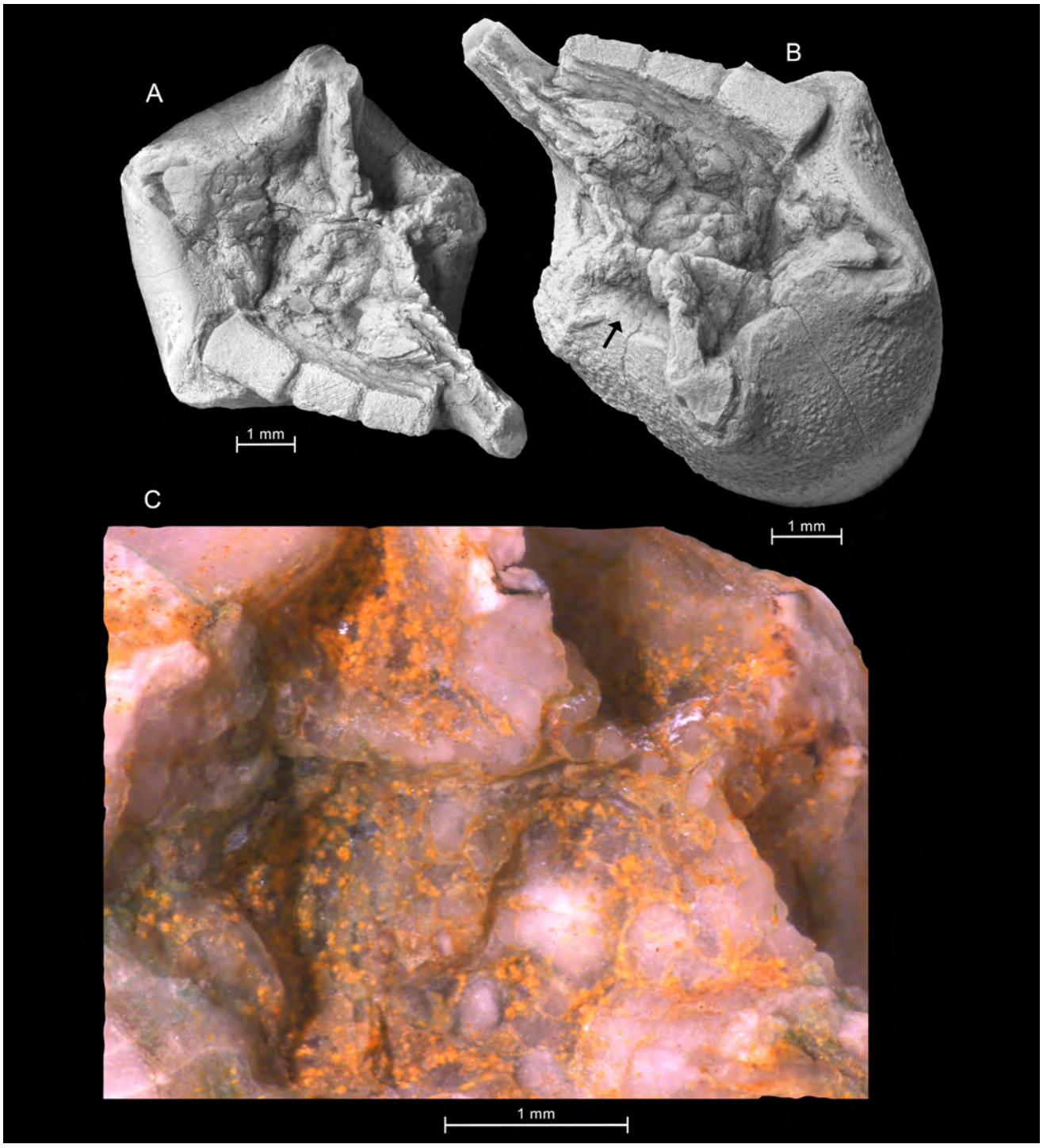

FIGURE 7 — *Syndiasmocrinus apokalypto* n. gen., n. sp. holotype 1980TX13, oral surface; **A,** photograph of entire surface viewed directly downward on coated specimen, standard orientation with A ray at top. The ambulacra are arranged in a 2-1-2 pattern, with cover plates forming sharp ridges elevated above surrounding interambulacral, sinuous perradial suture, rapidly tapering atomous arms, anal cone between C and D arms; **B,** photograph of inclined surface of coated specimen, rotated approximately 180 degrees from the orientation in FIGURE 7A, with the A-ray pointed downward. The arrow indicates BC interray showing small platelets. **C,** enlarged image of oral region, standard orientation. The interambulacra are sunken, sagged, composed of numerous platelets with epispires, large hydropore plate in CD, immersed.

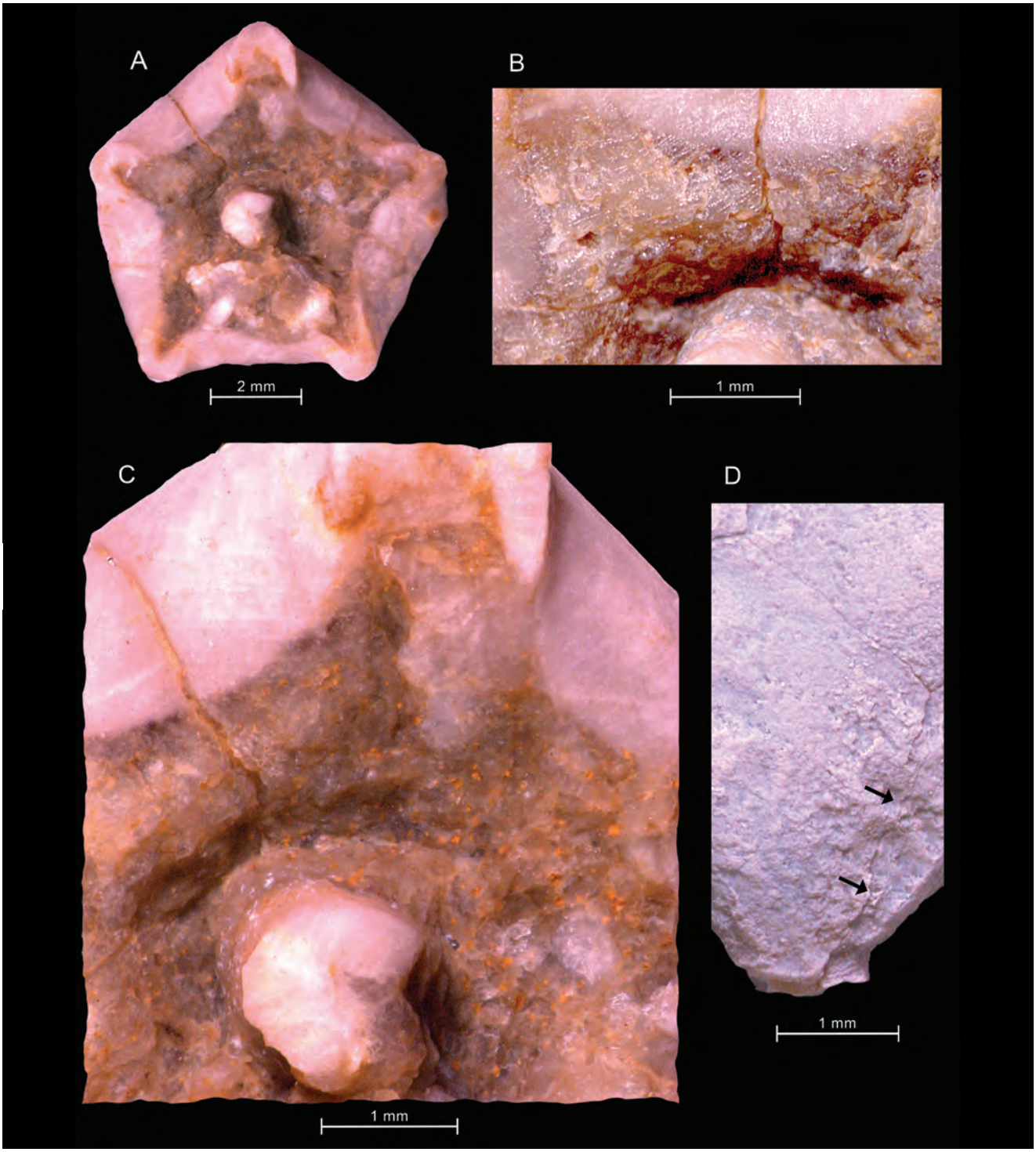

FIGURE 8 — *Syndiasmocrinus apokalypto* n. gen., n. sp.; **A–D** Photographs of paratype 1781TX12 **A–D**. Oral region **A–C**; **A,** entire surface, isolated brachial over the peristome region, standard orientation with A ray upward, radials with slight inward curvature (compared with *Hybocrinus* species), interambulacrals darker than thicker plates, immersed. **B,** EA interray, small platelets with syntaxial overgrowths, interambulacral field curved toward peristome which is pushed downward by displaced brachial, uncoated dry image. **C,** Detail of anterior cup showing lighter radials and blotchy EA and AB interambulacral regions, platelets preserved as darker spots, immersed **D,** lower cup, same CD orientation as FIGURE 3C, enlargement showing basals and thin proximal columnals, mere orientation uncertain, arrows indicate suture of BC and CD basals, coated.

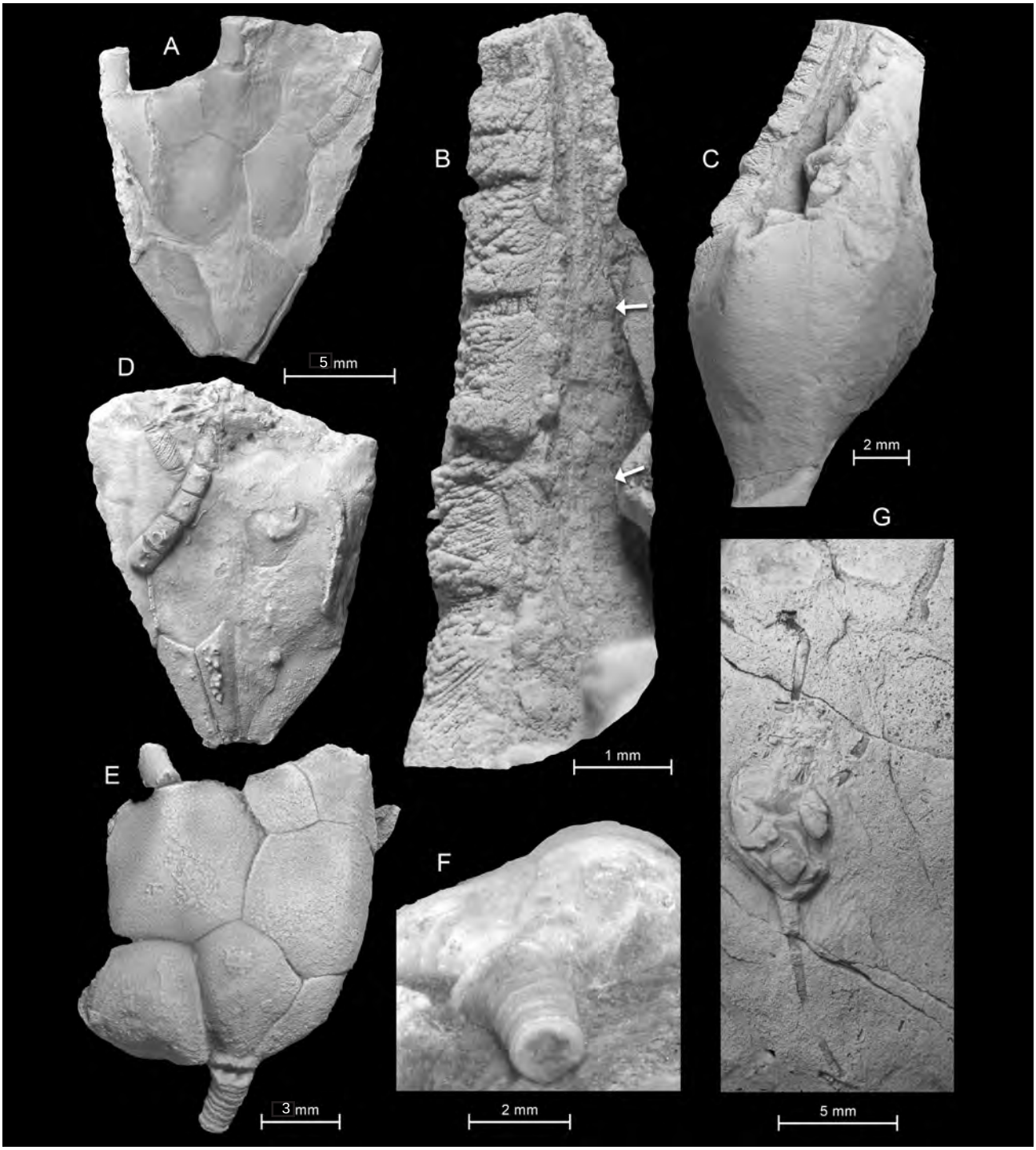

FIGURE 9 — Floian hybocrinids. Photographs of *Syndiasmocrinus* sp. A (PE 52754) **A**, **D**, coated. **A,** C ray orientation of collapsed calyx, relatively tall C radial; anal X above, left of center; **D,** A ray orientation, specimen largely buried in matrix. Photographs of *Syndiasmocrinus apokalypto* n. gen., n. sp. **B**, **C**, **E**, **F**. Paratypes 1776TX17 **B**, **C** and 1780TX14 **E**, **F**; **B**, **C**, **E**, coated, **F** immersed in water. **B,** detail of A ray with partial arm at left, brachials deeply weathered, inflated lateral plate field on right indicated by arrows, lateral plate field expanding toward the cup. **C,** anterior view of entire specimen, lower cup buried in concretion, radials with little inward upper curvature. **E**, entire specimen, partly flattened, posterior view, low broad ray ridges, pustulose ornament, proximal curved stalk, thin columnals with vague pentamere boundaries. **F**, basals and stalk showing pentalobate lumen. Photograph of ?*Syndiasmocrinus* sp. 1968TX2 **G**, Weathered partial crown and stalk.

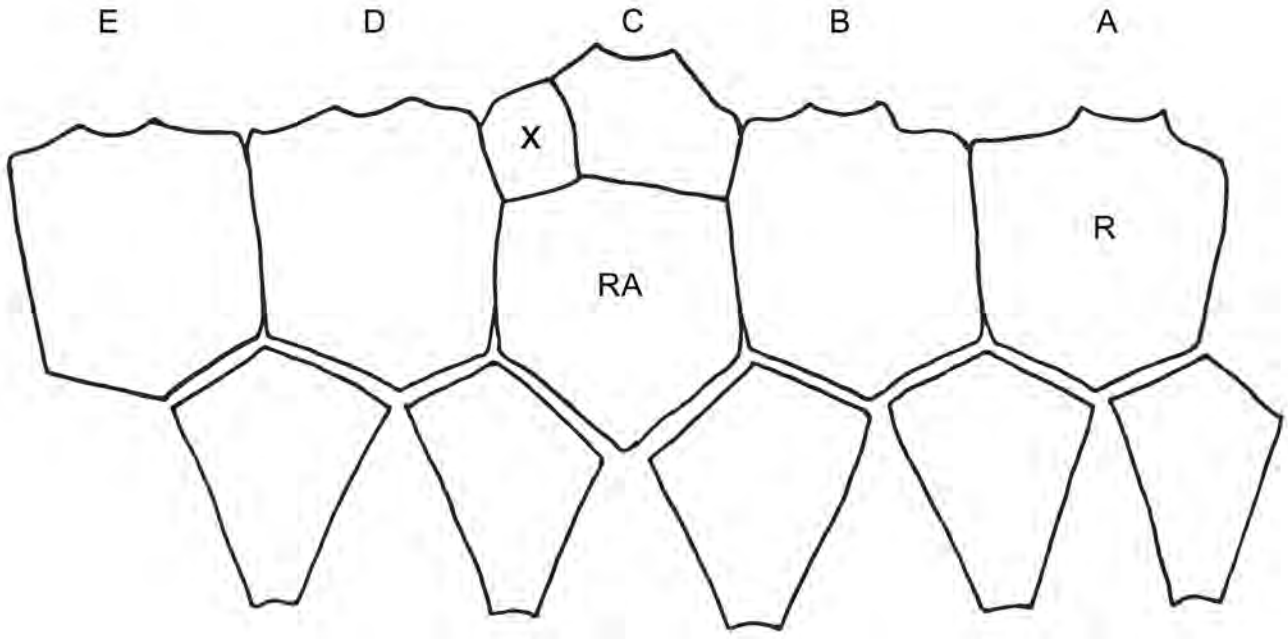

FIGURE 10 — *Syndiasmocrinus apokalypto* n. gen., n. sp., side layout plate diagram, drawn primarily from paratype 1981TX12, posterior supplemented from 1780TX14; Rays indicated above, R= radial (one indicated), RA= radianal, X= anal X.

Parahybocrinus gen. nov.

Remarks.— See *Remarks* following *Parahybocrinus siewersi* description below.

Type species.— *Prohybocrinus siewersi* new species

Diagnosis.— As for the type species, by monotypy

Etymology.— Compounding of para, Greek meaning near, hybos, Greek meaning hump (in reference to a rounded asymmetrical calyx), and crinus, lily, latinized from the Greek krinos.

Parahybocrinus siewersi sp. nov.
Figures 11, 12

Type specimen.— PE 52755

Diagnosis.— A hybocrinid with C radial and radianal approximately equal in size, two small anal series plates above anal X; the larger of the two wedged between upper shoulders of the C radial and anal X, the other smaller plate contacting the C radial.

Occurrence.— The single specimen is from the "Giza Peak megaripple bed", lower light grey ledge-forming member, approximately 253 meters above the base of the Fillmore Formation; northwest quarter of the northeast quarter of the northwest quarter of Section 25 (unsurveyed), Township 20 south, Range 14 west, House Range, Millard County, Utah. This stratigraphic horizon falls in the *Protopliomerella contracta* zone, or G(2) trilobite biozone, in the Late Tulean North American and Early Floian global stages (near the Floian-Tremadocian boundary). Associated echinoderms include the "Giza Peak" Megaripple Group of edrioasterid edrioasteroids (Guensburg and Sprinkle, 1994: p. 18), and the type specimens of *Cnemecrinus fillmorensis* Guensburg and Sprinkle, 2003, and as yet undescribed juvenile crinoid.

The single *Parahybocrinus siewersi* specimen consists of a nearly complete but etched small crown. The left margin of the anal X plate is broken away. The specimen is exposed with the posterior side facing up. Matrix was excavated from both sides of the specimen exposing the majority of the cup except for most of the E and A radials; edges of both plates are visible.

Description.— The holotype and single specimen, PE 52754, crown height estimated at 6 mm tall, D arm slightly longer than cup height as measured along the D ray below. Cup strongly asymmetrical, bulbous, cup height 2 mm as measured along D ray, 5.3 mm along C ray, 2.7 mm along B ray, and 2 mm along A ray; base of cup slightly convex, diverging from very narrow stalk at approximately 80 degrees as viewed from the CD orientation. Low thin ray ridges pass from basals to radials, ridges dissipate one third to one half the way up radials.

Basals pentagonal with very small stalk facet, approximately two times taller than wide. Radials, and radianal largest cup plates. A-ray radial short, extending only half the distance upward as adjacent B radial. B radial the tallest cup plate, heptagonal, maximum width at its mid-point, corresponding with the A radial top. C radial highest plate in cup, heptagonal, as large as radianal, slightly wider than tall, contacting radianal

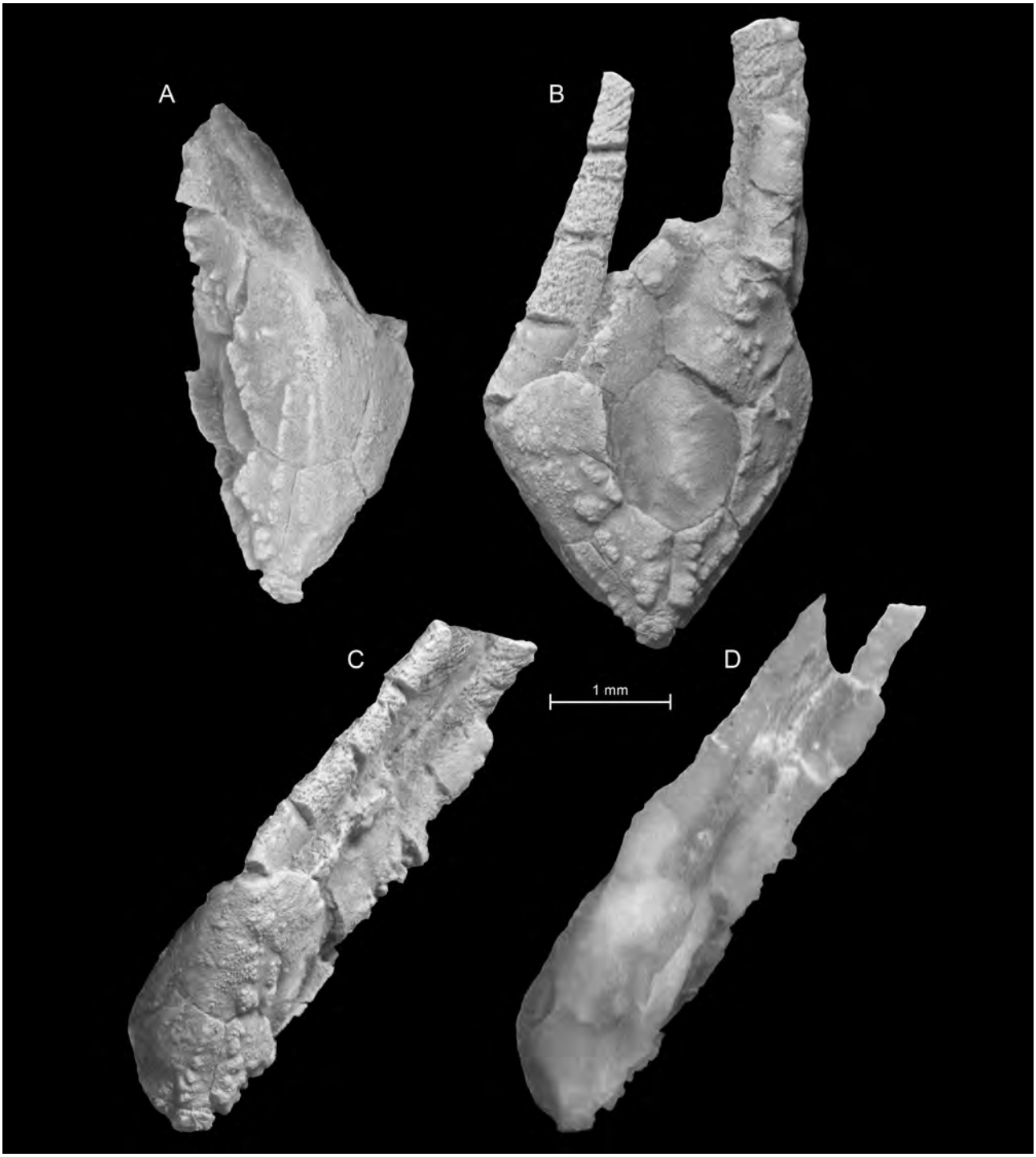

FIGURE 11 — *Parahybocrinus siewersi* n. gen., n. sp. Photographs of holotype PE 52755 **A**–**D**; **A,** B ray orientation of cup, tall B radial, one side of the A radial visible on right, and C radial at upper left, ray ridges extending from basals to the lower radials, short, thin stalk stub, with three columnals, coated; **B,** CD orientation, partly collapsed, radianal at center, large C radial at above right, B radial at right, anal X at upper left, contacting upper right shoulder of D radial, with damaged left margin, small diamond-shaped anal plate filling wedge between anal X and C radial, smaller anal plate above contacting the C radial, D arm nearly complete, C ray much taller than D ray; **C**, **D,** D ray orientation, D radial short, wide, D ray arm with four brachials, corner of E radial visible at left, coated and immersed images, respectively.

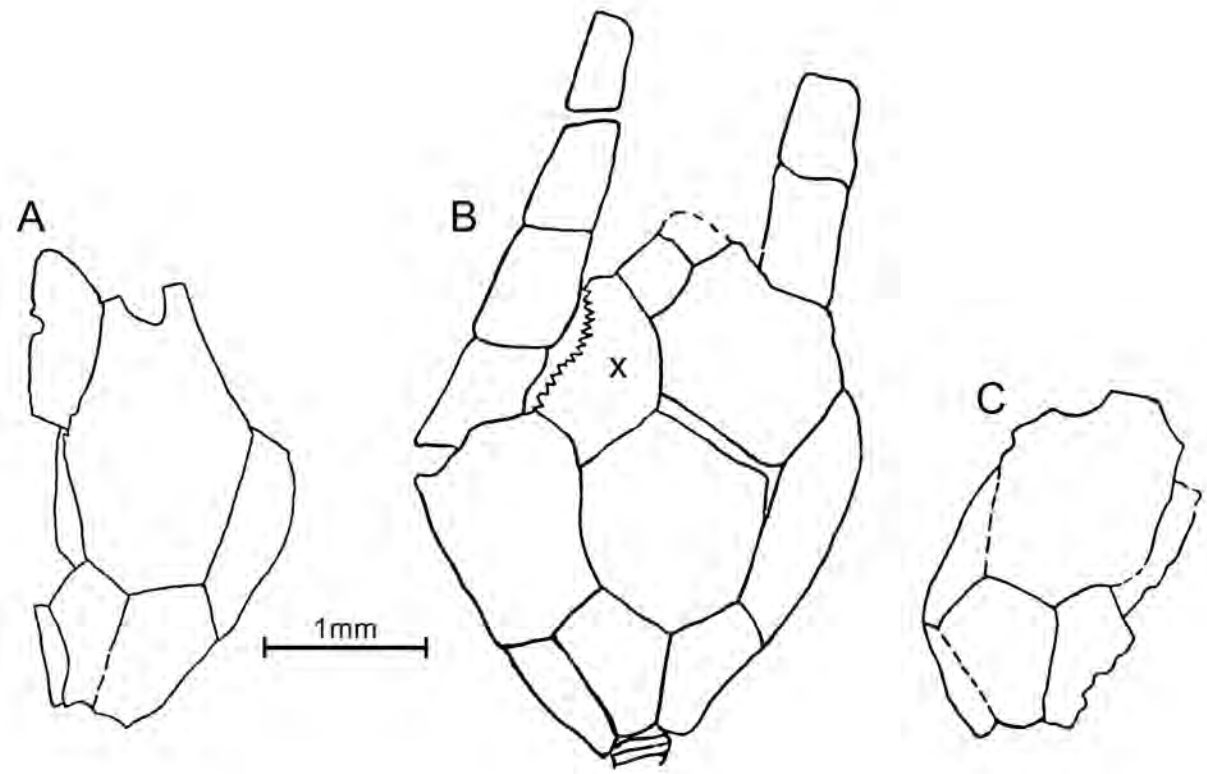

FIGURE 12 — *Parahybocrinus siewersi* n. gen., n. sp.; Holotype PE 52755 (A–C). Tracings of holotype PE 52755 based on images from Figure 11 showing plate boundaries. Abbreviations: R, radial; RA, radianal; X, anal.

on lower left, left upper shoulder of B radial on lower right, anal X on left, two small anal plates on upper left, and brachial one above. D radial hexagonal, strongly convex, contacting two basals below, the radianal on right, anal X on upper right, E basal on left. Only right margin of E radial exposed, similar in height to D radial. Radianal positioned toward in CD interray; large, hexagonal, contacting a basal on lower left and right, D radial on left, C radial on upper right shoulder. Anal X large, contacting D radial on lower right, C radial on the right, a small anal plate on upper right, broken on the left; small quadrangular anal plate contacting C radial on lower right, anal X on lower left, and another small anal plate of uncertain shape on upper right.

Partial atomous arms preserved on C, D, and ?A rays. A ray arm appears larger than C and D rays. C ray arm stub with two primibrachials, C ray arm nearly complete, with regular rapid taper, four brachials, ?A arm incomplete with unknown number of brachials, brachials average approximately twice as tall as wide. Stalk stub much weathered, with two, possibly three columnals having low rounded epifacets, lumen apparently pentalobate.

Etymology.— Specific appellation honors Fred Siewers, Geology Department, Western Kentucky University, who assisted the authors with western Utah fieldwork in 1989 and 1990, and made important echinoderm discoveries.

Remarks.— Small size and certain details such as relatively elongate few brachials suggest the type specimen represents a juvenile. However, the relatively wide cup implies an advanced growth stage (for example, contrast Fig. 11B with juvenile of *Hybocrinus bilateralis* Guensburg, 1984, pl. 9, fig. 16).

Information for this new taxon is limited, based primarily upon cup and partial arm morphology. The tegmen, distal posterior cup, arm details, and stalk are lacking. Hybocrinid apomorphies include an asymmetrical tumid cup, short tapering atomous arms, thin stalk, pseudomonocyclic cup, and cup posterior dominated by radianal and, sometimes, anal X plates. Aside from its smaller size, the general configuration of the *Parahyobcrinus* crown is comparable with that of *Syndiasmocrinus* and *Hybocrinus*. The posterior region of *Parahybocrinus* is unque among hybocrinids in expressing a proportionately larger C radial and two small plates distal to anal X. This plating pattern is intermediate between the basal condition seen in earliest (Tremadocian) cladids such as *Aethocrinus* (Ubaghs, 1969) and later hybocrinids such as *Hybocrinus* (e.g. Sprinkle, 1982, Guensburg, 1984) and *Hoplocrinus* (e.g. Öpik, 1935; Regnéll, 1948). Origin of the relatively flat hybocrinid posterior from an elevated multi-plated condition was proposed by Wachsmuth and Springer (1883: p. 377): “we further hold that the special anal plate

(anal X) in *Hybocrinus* is the first step toward a plated tube which in that genus is reduced to its minimum size, consisting of only a single plate (radianal, in *Hoplocrinus*)" (wording in parentheses added to conform with modern terminology and for clarity).

Paleoenvironmental context.—This specimen was draped over the surface of a large storm-generated megaripple bed (see Datillo, 1993) in association with a few other crinoids and edrioasteroid specimens. Modes of life of these echinoderms suggests original association and on a lithified carbonate substrate or hardground in shallow water (Guensburg and Sprinkle, 1992; Sprinkle and Guensburg, 1995).

COMPARATIVE ANALYSIS OF THE *SYNDIASMOCRINUS* TEGMEN

Tegmen body wall regions using the EAT (Mooi and David, 1998) can be divided into axial—articulated (operable) cover plate, and perforate extraxial—epispire-bearing interambulacral, hydropore, and periproct regions. The latter extend in continuity out arms as laterals (although it is uncertain whether laterals incorporated epispires. Interambulacrals and epispires end abruptly at the cup juncture; suggesting cup plates are part of the imperforate extraxial region.

There is little basis for comparing *Syndiasmocrinus*' tegmen regions with other early (Early Ordovician) crinoids for lack of data. *Titanocrinus* Guensburg and Sprinkle, 2003 (Guensburg et al., 2021), among the earliest known crinoids expresses similar tegmen interradials and lateral arm plating. Earliest known cladids *Apektocrinus* Guensburg and Sprinkle, 2009, and *Aethocrinus* Ubaghs, 1969, both express arms bearing lateral plate fields extending from the tegmen. Beyond crinoids, epispires and hydropore apart from the peristome occur in Cambrian pre-crinoid early pentardiate echinoderms such as *Stromatocystites* Pompeckj, 1896 (for instance, see Zamora et al., 2015). This limited information suggests the *Syndiasmocrinus* tegmen represents plesiomorphic, deep seated, conserved morphology.

The Laurentian *Hybocrinus* cup plating is very similar to *Syndiasmocrinus*, but the tegmen construction is remarkably different (compare Figs. 2B, C, with Fig. 7C, and Figs. 8A–C). *Hybocrinus* tegmen interradii are occupied by single large circumoral plates. These circumorals articulate firmly to radials, forming a rigid construct (e.g. Kammer et al., 2013) In contrast, no known Baltic hybocrinid expresses rigid circumoral plating (Fig. 3; Rozhnov, 1985, 2007; Semenov et al., 2021, p. 68, Sergey Rozhnov, personal contact, 2021). The many-plated integument of hybocrinids occurs throughout hybocrinid history in Baltica but, excepting *Syndiasmocrinus*, not in Laurentia. No formal phylogenetic analysis is provided here, pending inclusion of all available taxa, particularly those from Baltic material. As such, the data suggest separate histories for Laurentian and Baltican hybocrinids following their divergence from a common ancestor during the Early Ordovician.

ACKNOWLEDGMENTS

Jen Bauer, University of Michigan Museum of Paleontology, skillfully shepherded the manuscript through the various stages of preparation. D. Quednau, Field Museum, applied his considerable skill to figure preparation. The authors gratefully acknowledge two anonymous reviews. Special thanks are due to Sergey Rozhnov, Russian Academy of Sciences, Moscow, for providing the image in FIGURE 2, and important discussions on Baltic hoplocrinids. We also thank Paul Mayer, Scott Lidgard, and others at the Field Museum for helpful discussions.

LITERATURE CITED

ADRAIN, J.M., N.E.B. McADAMS, and S.R. WESTROP. 2009. Trilobite biostratigraphy and revised bases of the Tulean and Blackhillsian Stages of the Ibexian Series, Lower Ordovician, western United States. Memoirs of the Association of Australasian Paleontologists, 37: 541–610.

AUSICH, W.I., D.F. WRIGHT, S.R. COLE, and J.M. KONEICKI. 2018. Disparid and hybocrinid crinoids from the upper Ordovician (Katian) Brechin Lagerstätte of Ontario. Journal of Paleontology, 92: 850–871.

BAUMILLER, T.K. and W.I. AUSICH, 1992. The broken stick model as a null hypothesis for crinoid stalk taphonomy and as a guide to the distribution of connective tissue in fossils: Paleobiology, 7: 155-176.

BILLINGS, E. 1857. New species of fossils from the Silurian rocks of Canada: Canada Geological Survey, Report of Progress for the year 1856, p. 247–345.

DATTILO, B.F. 1993. The Lower Ordovician Fillmore Formation of Western Utah; storm- dominated sedimentation on a passive margin: Brigham Young University Geology Studies, 39, p. 71–100.

GREYWINGK, C.C.A. 1867. Über *Hoplocrinus dipentus* and *Baerocrinus ungerni*: Archive für die Naturkunde Liv-, Ehst und Kurlands, series 1, 4: 100–114.

GUENSBURG, T.E., 1984, Echinodermata of the Middle Ordovician Lebanon Limestone, Central Tennessee: Bulletins of American Paleontology, 86, 100 p.

_____. 1992. Paleoecology of hardground encrusting and commensal crinoids, Middle Ordovician, Tennessee: Journal of Paleontology, 66: 129–147.

_____, and J. SPRINKLE. 1992. Rise of echinoderms in the Paleozoic evolutionary fauna: Significance of paleoenvinronmental controls: Geology, 20: 407-420.

_____, and J. SPRINKLE. 1994. Revised phylogeny and functional interpretation of the Edrioasteroidea based on new taxa from the early and middle Ordovician of western Utah. Fieldiana, Geology, New Series, No. 29, 43 p.

_____, and J. SPRINKLE. 2003. The oldest known crinoids (Early Ordovician, Utah), and a new crinoid plate

homology system: Bulletins of American Paleontology, 364: p. 1–43.

_____, and J. SPRINKLE. 2009. Solving the mystery of crinoid ancestry: New fossil evidence of arm origin and development: Journal of Paleontology, 83: 350–364.

_____, and J. SPRINKLE, R. MOOI, B. LEFEBVRE, B. DAVID, M. ROUX, and K. DERSTLER. 2021. *Athenacrinus* n. gen. and other early echinoderm taxa inform crinoid origin and arm evolution: Journal of Paleontology, 94: 311–333.

L.F. HINTZE. 1973. Lower and Middle Ordovician stratigraphic sections in the Ibex area, Millard County, Utah: Brigham Young University Geology Studies, 20: 3–36.

JAEKEL, O. 1918. Phylogenie und system der Pelmatozoen: Paläontologische zeitschrift, 3: 1–128.

KAMMER, T.W., C.D. SUMRALL, S. ZAMORA, W.I. AUSICH, and B. DELINE, 2013. Oral region homologies in Paleozoic crinoids and other plesiomorphic pentaradial echinoderms: PLoS ONE, vol. 8, p. 1–16. (doi: 10.1371/journal.pone.0077989)

MILLER, J.S. 1821. A natural history of the Crinoidea or lily-shaped animals, with observationson the genera *Asteria, Euryale, Comatula,* and *Marsupites*: Bryan and Company, Bristol, 150 p.

MOOI, R., and B. DAVID, 1998. Evolution within a bizarre phylum: homologies of the first echinoderms: American Zoologist, v. 38: p. 965–974.

MOORE, R.C., and L.R. LAUDON. 1943. Evolution and classification of Paleozoic crinoids: Geological Society of America, Special Paper 46, 153 p.

ÖPIK, A. 1935. *Hoplocrinus*: eine stiellose Seelilie aus dem ordovizium Estlands: Tartu Ülikooli Geoloogia Instituudi Toimetused 43: 1–15.

POMPECKJ, J.A., 1896. Die Fauna des Cambrium von Tejrovic und Skrej in Böhmen: Jahrbuch der kaiserlich-königlichen geologischen Reichsanstalt, v. 45, p. 495–614.

REGNÉLL, G. 1948. Swedish hybocrinida (Crinoidea Inadunata Disparata : Ordovician—Lower Silurian: Arkiv för Zoologie, K. Svenska Vetenskapsakademien, v. 40 A, 30 p.

ROZHNOV, S.V. 1985. Morphology, symmetry, and systematic position of hybocrinid crinoids: Paleontological Journal, 280: 4–16.

_____, 2007. New data on perittocrinids and hybocrinids (Crinoidea, Echinodermata) from the Middle Ordovician of the Baltic Region. Annales de Paléontologie, 93: 261–276.

SEMENOV, N.K., S.S. TERENTYEV, G.V. MIRANSTSEV, and S.V. ROZHNOV. 2021. A new hybocrinid genus (Echinodermata, Crinoidea) from the Middle Ordovician of Ladoga Glint on the Volkhov River: Paleontological Journal, 55: 54–63.

SRINKLE, J., 1973. Morphology and evolution of blastozoan echinoderms: Special Publication, Museum of Comparative Zoology, Harvard University, Cambridge, p. 1–283.

_____, 1982. *Hybocrinus*: *in* Sprinkle, J. (ed.) Echinoderm Faunas from the Bromide Formation (Middle Ordovician) of Oklahoma: University of Kansas Paleontological Contributions, Monograph 1: 119–128.

_____, and T.E. GUENSBURG. 1995. Origin of echinoderms in the Paleozoic Evolutionary
Fauna; the role of substrates: Palaios, 10: 437–453.

_____, and R.C. MOORE. 1978. Hybocrinida: *in* Moore, R.C. and Teichert, C. (eds.) Treatise on Invertebrate Paleontology, Part T, Echinodermata 2(1). Geological Society of America, Boulder, and University of Kansas, Lawrence, pp. T564–T574.

UBAGHS, G. 1969. *Aethocrinus moorei* Ubaghs, n. gen. n. sp, le plus ancien crinoïde dicyclique connu: University of Kansas Paleontological Contributions, Paper 38, p. 1–25.

_____. 1978. Skeletal morphology of fossils crinoids: *in* Moore, R.C. and Teichert, C. (eds.) Treatise on Invertebrate Paleontology, Part T, Echinodermata 2(1). Geological Society of America, Boulder, and University of Kansas, Lawrence, p. T58–T216.

WACHSMUTH, C., and F. SPRINGER, F. 1883. On *Hybocrinus, Hoplocrinus,* and *Baerocrinus*: American Journal of Science, November 1 issue, p. 365–376.

WARN, J.M. 1975. Monocyclism vs. dicyclism, a primary schism in crinoid phylogeny?: *in* Pojeta, J. Jr., and Pope, J.K. (eds.), Studies in Paleontology and Stratigraphy: Bulletins of American Paleontology, 67: 57–69.

WETHERBY, A.G. 1880. Descriptions of new crinoids from the from the Cincinnati Group of the Lower Silurian and Subcarboniferous of Kentucky: Cincinnati Society of Natural History Journal, 2: 245–258.

WRIGHT, D.F., W.I. AUSICH, S.R. COLE, M.E. PETER, and E.C. RHENBERG. 2017. Phylogenetic taxonomy and classification of the Crinoidea (Echinodermata): Journal of Paleontology, 91: 829–846.

ZAMORA, S., B. LeFEBVRE, I. HÜSGOR, C. FRANZEN, E. NARDIN, O. FATKA, and J. ÁLVARO. 2015. The Cambrian edrioasteroid *Stromatocystites* (Echinodermata): systematics, paleogeography, and paleoecology: Geobios 48: 417–426.

ZITTEL, K.A. von. 1879. Handbuch der Paläontologie, Volume 1, Paläozoologie, No. 1, Munich, Germany, R. Oldenbourg, 765 pp.

Museum of Paleontology, The University of Michigan
1105 North University Avenue, Ann Arbor, Michigan 48109-1085
Matt Friedman, Director

Contributions from the Museum of Paleontology, University of Michigan is a medium for publication of reports based chiefly on museum collections and field research sponsored by the museum. Jennifer Bauer and William Ausich, Guest Editors;
Jeffrey Wilson Mantilla, Editor.

Publications of the Museum of Paleontology are accessible online at: http://deepblue.lib.umich.edu/handle/2027.42/41251

Print (ISSN 0097-3556), Online (ISSN 2771-2192)

Contributions

from the Museum of Paleontology, University of Michigan

VOL. 34, NO. 4, PP. 34–53 JANUARY 18, 2022

FOOD AVAILABILITY AS A TRIGGER FOR THE AGE OF CRINOIDS: EVIDENCE FROM THE PRESENT AND THE PAST

BY

DAVID L. MEYER[1] and JOHNNY A. WATERS[2]

Abstract — Crinoid and blastoid diversity and abundance peaked during the Late Devonian – early Mississippian (Famennian – Viséan), an interval known as the Age of Crinoids. In North America, localities with maximum crinoid and blastoid diversity and abundance occurred in carbonate ramp and delta platform and slope deposits offshore from the Appalachian tectonic highlands. Living shallow-water crinoids reached maximum species diversity and abundance in more heterotrophic waters of the Indo-West Pacific Coral Triangle, Great Barrier Reef, and Caribbean crinoids are less diverse around coral-rich offshore islands and atolls in more oligotrophic waters. Ancient crinoids and blastoids were suspension feeders, limited by very narrow food grooves to capturing very small food particles. Blastoids in particular had food grooves <300 μm width, but crinoid food grooves were </= 100 μm to >1.25 mm, with most species <400 μm. Living crinoids, both unstalked and stalked, also have narrow food grooves in a similar range and ingest a large proportion of detrital particles << food groove diameter. Shallow-water crinoid diversity has been associated with proximity to runoff and increased abundance of plankton and detritus over the entire evolutionary range since the early Paleozoic. Limitation of ingested food particles by narrow food grooves first appeared in Ordovician crinoids, followed by blastoids, and also characterizes present-day crinoids. New data we present here on biogeographic patterns of diversity and food groove width support the proposal of Riding, who included the Age of Crinoids peak with other globally pervasive features of this Late Devonian – early Mississippian interval that he suggested were consequences of a "bloom" of calcareous bacterioplankton in the wake of mass extinction of acritarchs during Late Devonian time coincident with a major drop of atmospheric CO_2. We suggest that the Age of Crinoids was the result of multiple driving factors, including food and nutrient supply, in addition to unique clade dynamics, open circulation free of reef development, and turnover of durophagous vertebrate predators previously proposed.

[1.] Department of Geology, University of Cincinnati, Cincinnati, OH 45221, USA;
[2.] Department of Geological and Environmental Sciences, Appalachian State University, Boone, NC 28608, USA

INTRODUCTION

For those of us who are fascinated with crinoids, we are living at the wrong time! While there are about 600 living species of crinoids, crinoid biodiversity peaked during the Mississippian Subperiod during an interval known as the "Age of Crinoids" (Kammer and Ausich, 2006; Ausich et al., 2021). Crinoids dominated the global carbonate factory to an extent not seen prior to the Mississippian and not seen after. Although the Mississippian was a time of extreme crinoid biodiversity and abundance, it was also a time in which other marine groups suffered biodiversity nadirs. A comprehensive summary of Paleozoic biodiversity by Fan et al. (2020) showed that ten invertebrate groups had lower biodiversity during the Mississippian than at any time in the Paleozoic between the beginning of the Great Ordovician Biodiversification Event (GOBE) and the onset of the End Permian Extinction Events. Their high-resolution summary shows a protracted biodiversity decline that began in the Eifelian (Devonian) and continued to the end of the Viséan. Biodiversity increases rather sharply during the Serpukhovian as part of a previously unrecognized Carboniferous – Permian Biodiversification Event that Fan et al. (2020) equated to the GOBE. No echinoderm clades were components of the Fan et al. (2020) study.

The obvious question that arises out of the discussion is why did crinoids enjoy a burst of biodiversification during the Mississippian while many other invertebrate groups suffered significant biodiversity declines? Thanks to extensive systematic reviews and revisions by Ausich and Kammer

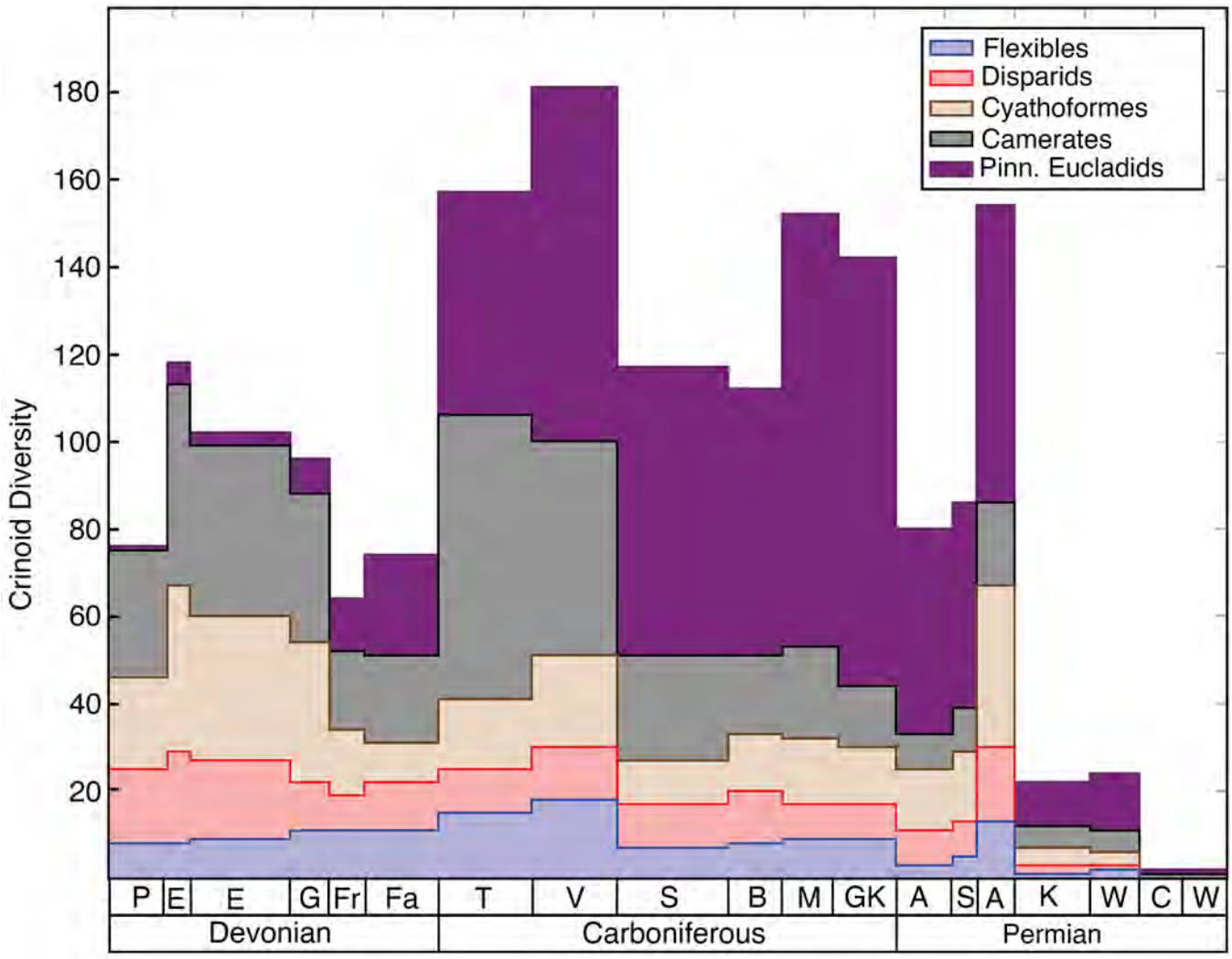

FIGURE 1 — Crinoid generic diversity from the Devonian through Permian. Stage abbreviations: P – Pragian, E – Emsian, E – Eifelian, G – Givetian, Fr – Frasnian, Fa – Famennian, T – Tournaisian, V – Viséan, S – Serpukhovian, B – Bashkirian, M – Moscovian, GK – Gzhelian and Kasimovian, A – Asselian, S – Sakmarian, A – Artinskian, K – Kungurian, W – Wordian and Roadian, C – Capitanian, W – Wuchiapingian. Data from Ausich et al. 2021.

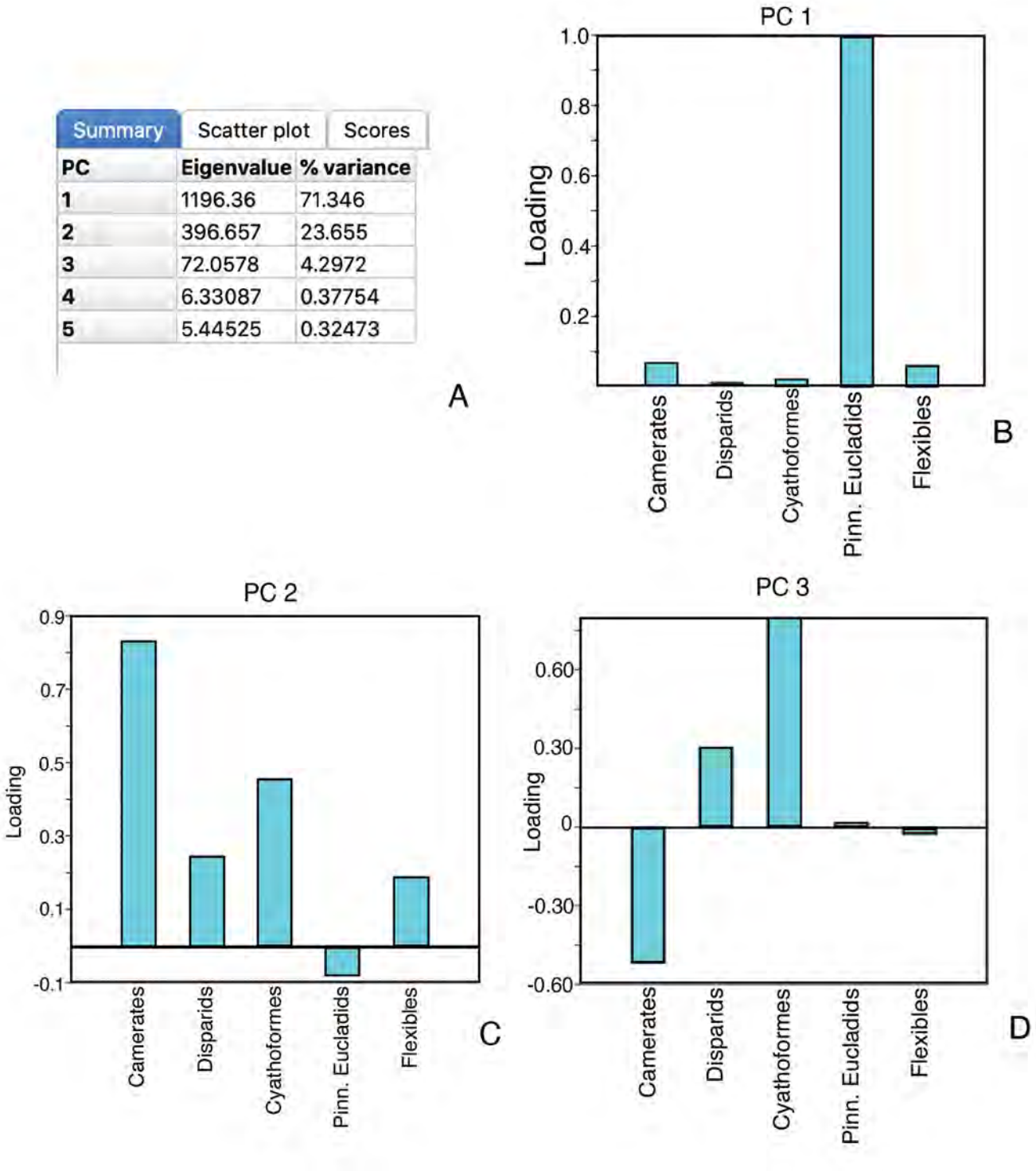

PC	Eigenvalue	% variance
1	1196.36	71.346
2	396.657	23.655
3	72.0578	4.2972
4	6.33087	0.37754
5	5.44525	0.32473

FIGURE 2 — PCA analysis of crinoid diversity data from the Devonian through the Permian. **A**, Summary of eigenvalues and % variance. **B**, pinnulate eucladids primarily responsible for PC 1 loading. **C**, Camerates, disparids and cyathoformes responsible for PC2 loading. **D**, PC 3 loading positively impacted by disparids and cyathoformes, negatively impacted by camerates.

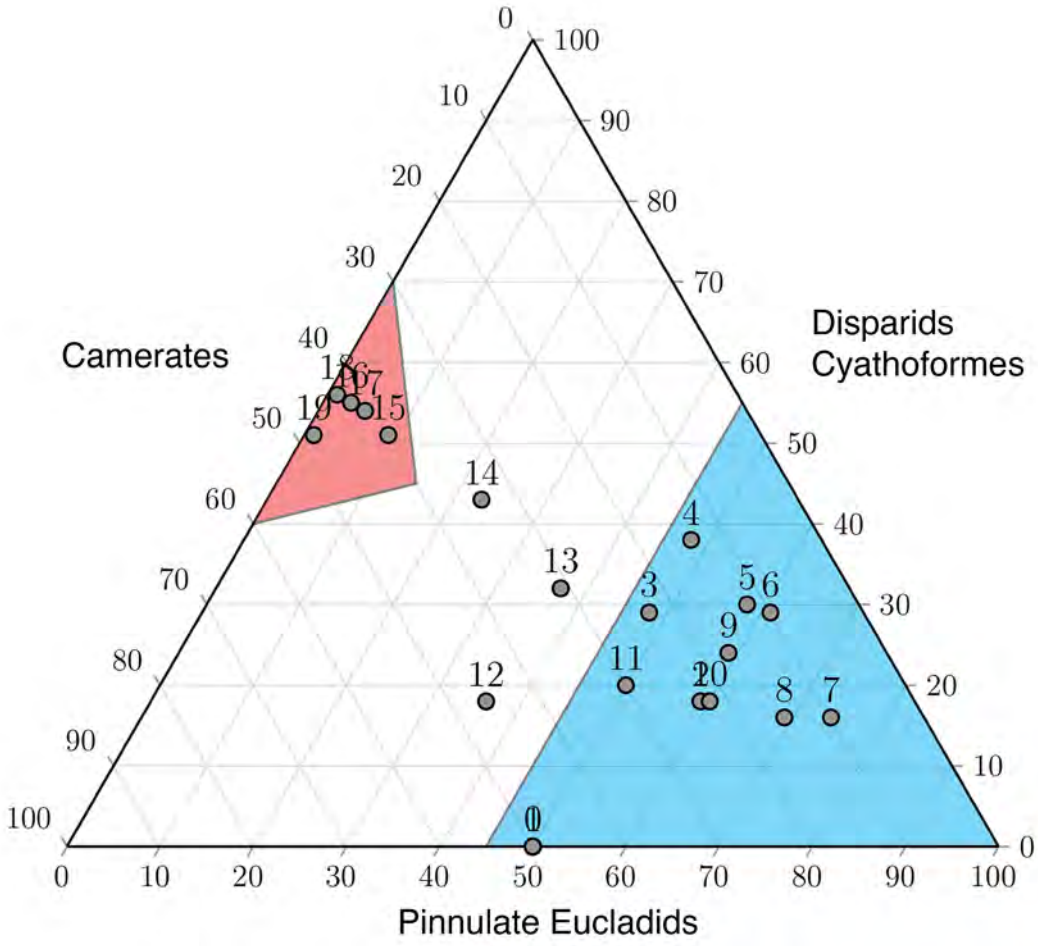

FIGURE 3 — Ternary diagram of stage-level crinoid communities. Communities segregate into MPCEF (red) with communities from the Lochkovian – Givetian, and LPCEF in Cyan (Viséan – end Permian). Frasnian, Famennian, and Tournaisian faunas plot between two groupings. Viséan is #11. The plot suggests the transition between the MPCEF and the LPCEF encompassed the Famennian through Tournaisian.

(2013), Segessenman and Kammer (2018) and Ausich et al. (2021), the Phanerozoic peak of crinoid biodiversity occurred in the Mississippian Subperiod with 157 genera in the Tournaisian and 181 genera in the Viséan. In addition, another pelmatozoan clade, the extinct blastoids, also peaked at more than 40 genera (Waters, 1988) during this time. Not only was the Mississippian the peak of pelmatozoan biodiversity, it was also a unique time of great abundance, yielding carbonate sediments dominated by echinoderm skeletal fragments as thick limestones covering vast areas of shallow seas as carbonate ramps or regional encrinites (Ausich, 1997). Crinoid-dominated sediments are nowhere to be found in modern seas and encrinites are a "vanished lithofacies" since the Jurassic (Ausich, 1997).

Paleozoic crinoid communities were organized into evolutionary faunas by Baumiller (1993). The transition from the Middle Paleozoic Crinoid Evolutionary Fauna (MPCEF) to the Late Paleozoic Crinoid Evolutionary Fauna (LPCEF) began in the early Viséan (Kammer and Ausich 1987; Baumiller 1993; Ausich et al. 1994; Kammer et al. 1998; Ausich et al. 2021). Ausich et al. (2021) concluded that the elevated crinoid biodiversity in the Tournaisian and Viséan was the result of transition between these two CEFs. Monobathrid camerates, pinnulate eucladid crinoids, and flexibles dominated the Middle Paleozoic CEF while the Late Paleozoic CEF was dominated by advanced, pinnulate cladid crinoids by the end of the Viséan. Biodiversity was high in the Mississippian because the Tournaisian primarily contains elements of the Middle Paleozoic CEF, and the early Viséan contained significant elements of both the Middle and Late Paleozoic Paleozoic CEFs (Kammer and Ausich 2006; Ausich et al. 2021).

Using data on crinoid diversity from the Devonian through the Permian from Segessenman and Kammer (2018) and

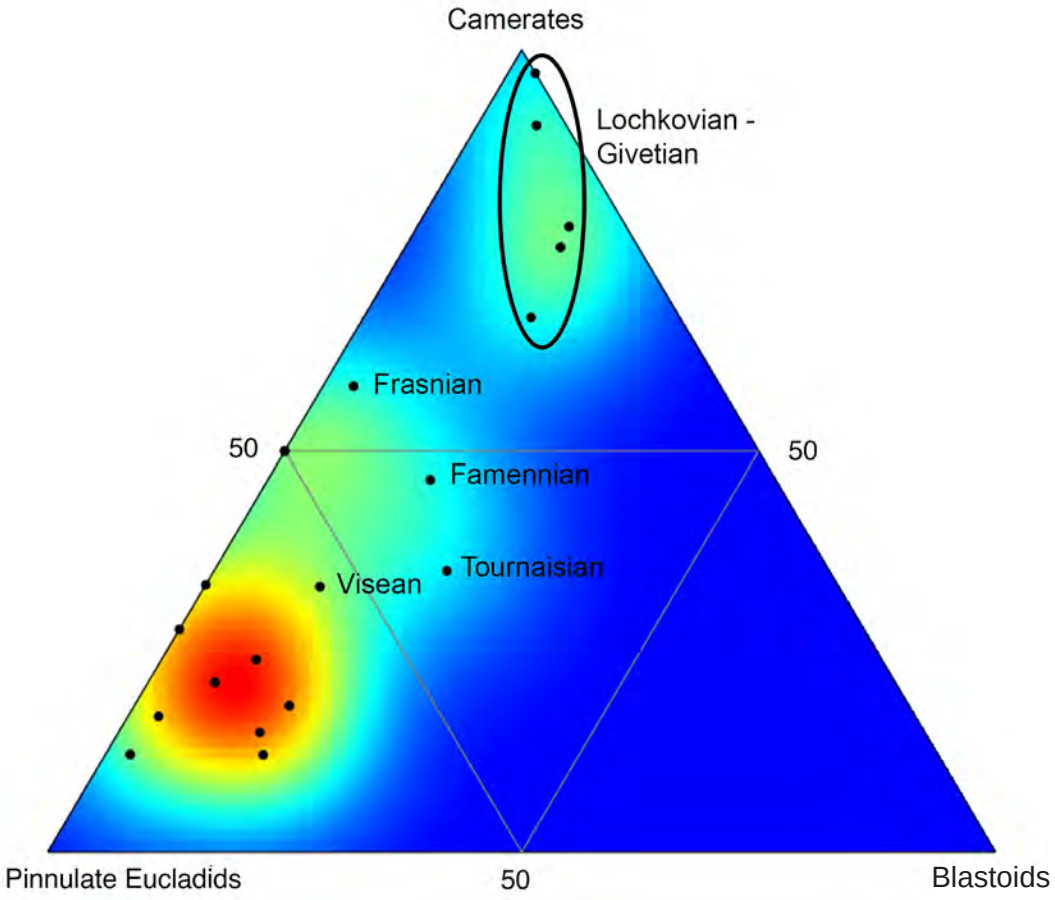

FIGURE 4 — Ternary diagram of stage level biodiversity of camerates, pinnulate eucladids, and blastoids. The Lochkovian – Givetian communities dominated by camerates and blastoids segregate as do the Viséan – Permian communities dominated by pinnulate eucladids. Frasnian, Famennian, and Tournaisian communities are intermediate in nature. Compare to Figure 3. Blastoid data from Waters (unpublished).

Ausich et al. (2021), we have investigated the transition between these two crinoid evolutionary faunas. Figure 1 shows crinoid diversity through time divided into the primary clades. Figure 1 compares favorably to figure 3 from Ausich et al., (2021), showing patterns of crinoid richness throughout the Paleozoic. Our Figure 1 shows peaks of crinoid diversity in the Emsian (MPCEF), the Tournaisian and Viséan (transition between the MPCEF and the LPCEF), Serpukhovian and Artinskian (LPCEF). Table 1 is the Correlation Matrix for biodiversity among the major crinoid groups and blastoids. Biodiversity of pinnulate eucladids is not correlated with other crinoid groups or blastoids. Biodiversity of blastoids is correlated with that of camerates and flexibles but not the other crinoid clades.

Figure 2 shows the results of a PCA analysis of the crinoid diversity data. PC1 accounts for 71% of the variance and primarily reflects the variation in the diversity of pinnulate eucladids. PC 2 accounts for 23% of the variance and reflects the diversity of camerates, cyathoformes and disparids. PC 3 accounts for 4% of the variation and has positive contributions from the cyathoformes and disparids and negative contribution from the camerates.

Figure 3 is a ternary plot of stage level crinoid diversity. The grouping outlined in red reflects the MPCEF with communities from the Lochkovian through the Givetian. The grouping outlined in blue reflects the LPCEF and ranges in age from the Viséan (11) through the end of the Permian. Data between these two groupings are Frasnian (14), Famennian (13) and Tournaisian (12). This analysis suggests that the transition from the Middle Paleozoic CEF to the Late Paleozoic CEF began in the Frasnian and continued through the Tournaisian, a time interval of some 37 million years. Figure 4 shows the crinoid biodiversity with the addition of blastoid biodiversity.

The demise of the MPCEF coincides with the collapse of reef ecosystems which began during the Eifelian extending through the Frasnian / Famennian boundary. The impact of

TABLE 1 — Correlation Matrix for biodiversity among the major crinoid groups and blastoids. Asterisk (*) indicates p>0.05. Biodiversity of Advanced Cladids is not correlated with other crinoid groups or blastoids. Biodiversity of blastoids is correlated with that of camerates and flexibles, but not the other crinoid clades. Blastoid data from Waters (unpublished).

	Camerates	Disparids	Primitive Cladids	Advanced Cladids	Flexibles	Blastoids
Camerates	—	—	—	—	—	—
Disparids	0.68*	—	—	—	—	—
Primitive Cladids	0.62*	0.88*	—	—	—	—
Advanced Cladids	0.09	0.04	0.03	—	—	—
Flexibles	0.79*	0.64*	0.60*	0.39	—	—
Blastoids	0.65*	0.43	0.44	0.41	0.66*	—

the crinoid extinction event can clearly be seen in the changes in the composition of crinoid communities. The Givetian – Tournaisian interval was a time of climatic instability, a significant drop in CO_2 and global oceanic instability recorded in anoxia events and massive carbon isotopic excursions.

Several causative factors have been proposed for the Age of Crinoids, including prevalence of widespread areas of carbonate shelves and ramps during the Tournaisian and Viséan, along with changes in circulation across shelf seas following the extinction of reefs during the Late Devonian (Kammer and Ausich, 2006), plus turnover in the composition of durophagous fish predators (Sallan et al., 2011).

For a long time, we have been intrigued by the question raised initially by N.G. Lane (1973) in his work on the world-renowned Mississippian crinoid fauna from Crawfordsville, Indiana: *What were all these suspension feeders eating?* After noting that the phytoplankton food web of the Mississippian may have been depleted in diversity and abundance, Lane stated: "Regardless of its taxonomic composition, there must have been a sufficient quantity of small organic material in the water to sustain all suspension-feeding types found at this site." We and others (Ausich and Kammer, 2013) have considered that the food supply during that part of the Mississippian could have somehow played a role in the diversification that produced the peak in crinoid and blastoid diversification, in addition to factors previously proposed. In 2009, Robert Riding brilliantly connected several key geological, biogeochemical, and paleontological events that occurred during the Late Devonian – early Mississippian interval, coinciding with the Age of Crinoids, that could be causally related to a global drawdown in atmospheric carbon dioxide. These events included: increased burial of organic carbon as black shales, worldwide extinction of coral-stromatoporoid reefs, extinction of microfossil acritarchs leading to a "phytoplankton gap", worldwide occurrence of carbonate mud mounds, and *the peak in diversity of pelmatozoan echinoderms - the Age of Crinoids itself* (Riding, 2009). Riding suggested that the drop in dissolved CO_2 in the oceans induced a carbon-concentrating mechanism in nano- or pico-bacterioplankton that "bloomed" in the seas to become the dominant marine phytoplankton following the acritarch extinction. He linked this bloom of calcareous bacterioplankton to the production of carbonate muds by cyanobacterial calcification and the abundance and diversification of marine suspension feeders including echinoderms that were well adapted for this new abundant food source. Although Riding's suggestions about relationships between the key events he listed could be debated and tested, we were especially intrigued by his recognition that the worldwide, all-time maximum of species diversity and abundance of suspension-feeding crinoids and blastoids with narrow food grooves could have been nourished by the expansion of a new component of the marine phytoplankton. Could this potentially new food source have fueled the Age of Crinoids, and acted in concert with other factors noted above as multiple drivers for this largely overlooked episode of Paleozoic marine diversity?

In this paper we present evidence from both living and fossil crinoids and blastoids of the relationship between biodiversity, abundance, and productivity of potential food sources. We will offer more information in support of Riding's suggestion that the crinoid peak was fueled by a worldwide turnover in the nature and abundance of marine phytoplankton during the early Mississippian that was particularly advantageous to benthic suspension feeders that

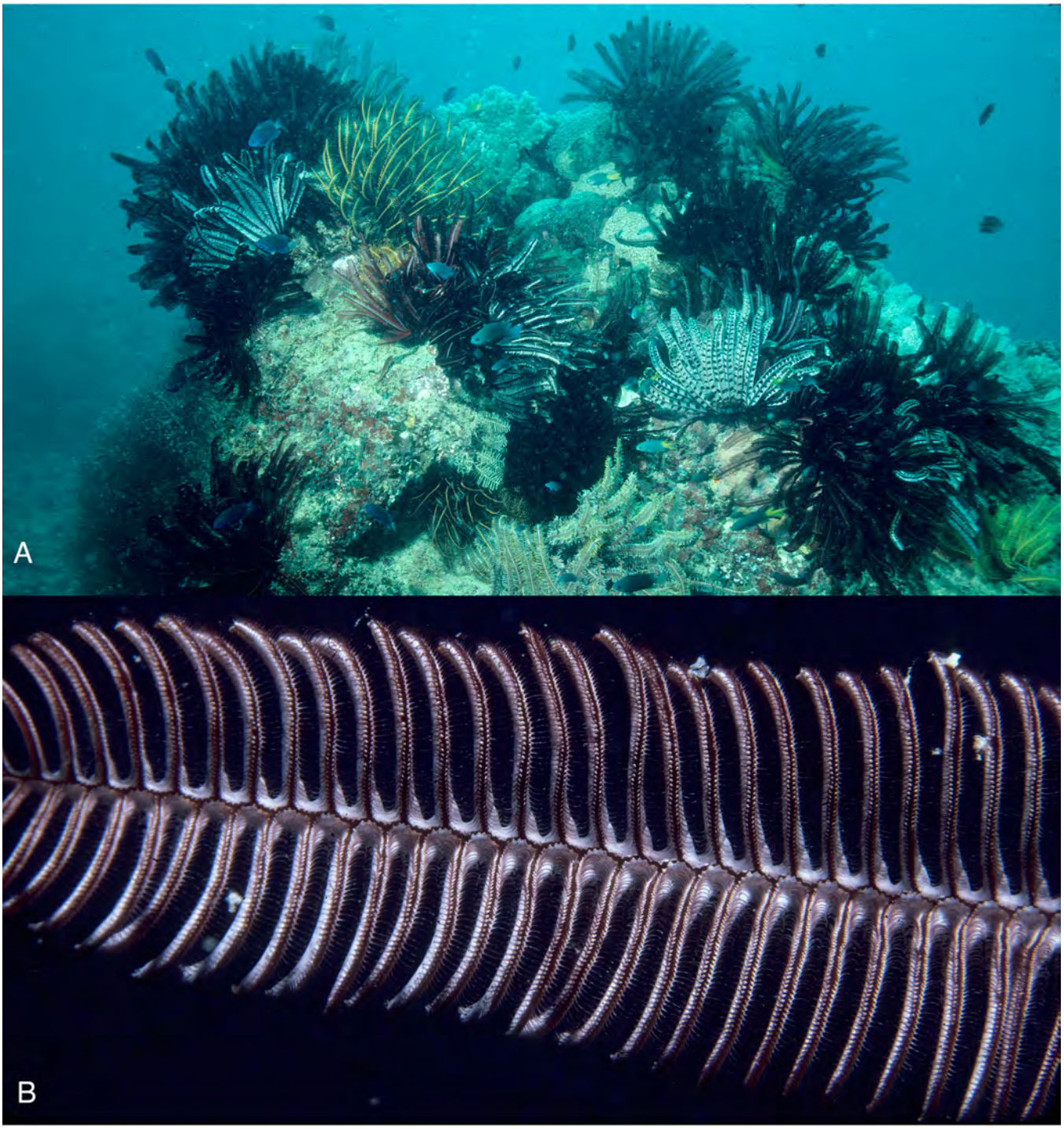

FIGURE 5 — **A**, North Reef, Lizard Island, Great Barrier Reef, depth 8 m, with ~14 crinoid spp visible by day. **B**, Arm and pinnules of Recent comatulid crinoid in life showing open food grooves and tube feet. Pinnule length ~ 1 cm. Photos by D. Meyer.

TABLE 2 — Mean density and species richness of crinoids (feather stars) of the Central Great Barrier Reef (data from Fabricius, 1994). For Davies Reef, mean crinoid density ranged from 0.7/m2 (lagoon) to 7.8/m2 (windward) and mean species number from 3.4 (lagoon) to 11.4 (windward).

Location (sites)	Mean density, m^{-2}	Mean species richness
Outer shelf (12)	2.6	7.2
Mid-shelf (10) *	8.1	9.1
Nearshore (2)	0.7	2.5

*Excluding Davies Reef

could capture very minute suspended food particles. As a kind of test of Riding's proposal, we can evaluate its underpinnings by addressing weaknesses as well as additional supporting evidence. It is very important for this analysis that we will look at the diversity and biogeographic distribution of both Recent crinoids and their feeding habits and preferences, as well as the extensive fossil record of crinoids and blastoids to determine the connections between their paleobiodiversity and their ancient environments. We find that there is considerable information in the large published literature on these groups both living and extinct that has never been collated and brought to bear on many major questions about their evolutionary history. Therefore, this paper is a review and compilation of available information, presentation of new data, and application to understanding major aspects of the half-billion-year-old evolutionary record of these echinoderms.

DIVERSITY AND ZOOGEOGRAPHY OF RECENT SHALLOW-WATER CRINOIDS

Until SCUBA diving became widely available in the years following World War II, very little was known about crinoids living in shallow marine waters (<100 m). Crinoids were described from trawling and dredging in deep waters since the 19th Century, and stalked crinoids in particular were regarded as deep-sea animals. H. L. Clark (1915) studied diverse shallow-water unstalked crinoids (feather stars) collected by a surface-supported diver on the Great Barrier Reef. The first SCUBA diving studies of reef-dwelling feather stars in the Red Sea were made by Magnus (1963, 1964) and later by Rutman and Fishelson (1969). The first reports of crinoids from similar reef environments in the tropical Western Atlantic were feather stars on shallow reefs at Dominica in the Windward Islands (Kier, 1966; pers. comm. to DM; Breimer, 1978a, fig. 210). Subsequently, Meyer (1973a, b) studied reef-dwelling crinoids found abundantly at several sites across the Caribbean such as Jamaica, Curaçao, Bonaire, Antillean islands, Colombia, and Panama. Extensive collections from deep water over the entire tropical Western Atlantic region by R/V *Pillsbury* and R/V *Gerda* were identified by Messing, Macurda, and Meyer (Meyer et al., 1978). Crinoid occurrences at many shallower reef sites across the region were recorded by Meyer and Macurda using SCUBA diving. Data from these shallow and deeper water studies were combined by Meyer et al., (1978).

Shallow Water Crinoid Diversity in the Tropical Western Atlantic

The maximum crinoid diversity at a single shallow-water site in the tropical Western Atlantic is 7 species (San Blas, Panama), and at typical well-developed coral reef sites it is 4-5 species (Meyer, 1973a; Macurda and Meyer, 1977). Despite the low diversity for the entire region compared to much higher regional diversity in the Indo-West Pacific for shallow-water invertebrates and vertebrates, including crinoids (see below), diversity in the Western Atlantic suggested an interesting pattern. The localities where shallow-water crinoids are most diverse and abundant, Panama and Colombia, are both nearshore, close to high coastal topography with nearby river outflows. In both areas, there are diverse fringing coral reefs but water clarity is often lower than that at more offshore sites such as Curaçao or Jamaica, sites known for the best-developed and most diverse reefs (also including Bonaire, Barbados, the Antillean Arc). Crinoids reach their peak diversity closer to the S. American coastline or Isthmus of Panama with sediment influx and freshwater runoff, both factors known to limit maximum reef development. A recent survey of well-developed reefs in the Jardines de la Reina, offshore of the south-central coast of Cuba by about 30 miles, yielded 3 reef-dwelling crinoid species, although more extensive study of the Cuba coast is still lacking (Meyer, pers. obs., 2016). Meyer (1973a) cited studies available at the time indicating that plankton productivity increases from the more offshore waters of the Caribbean and equatorial Atlantic toward the South American coast and that runoff from discharge of major rivers such as the Magdalena and coastal upwelling also introduced higher nutrient input and productivity for nearshore zones and islands (such as the San Blas Islands of Panama and Santa

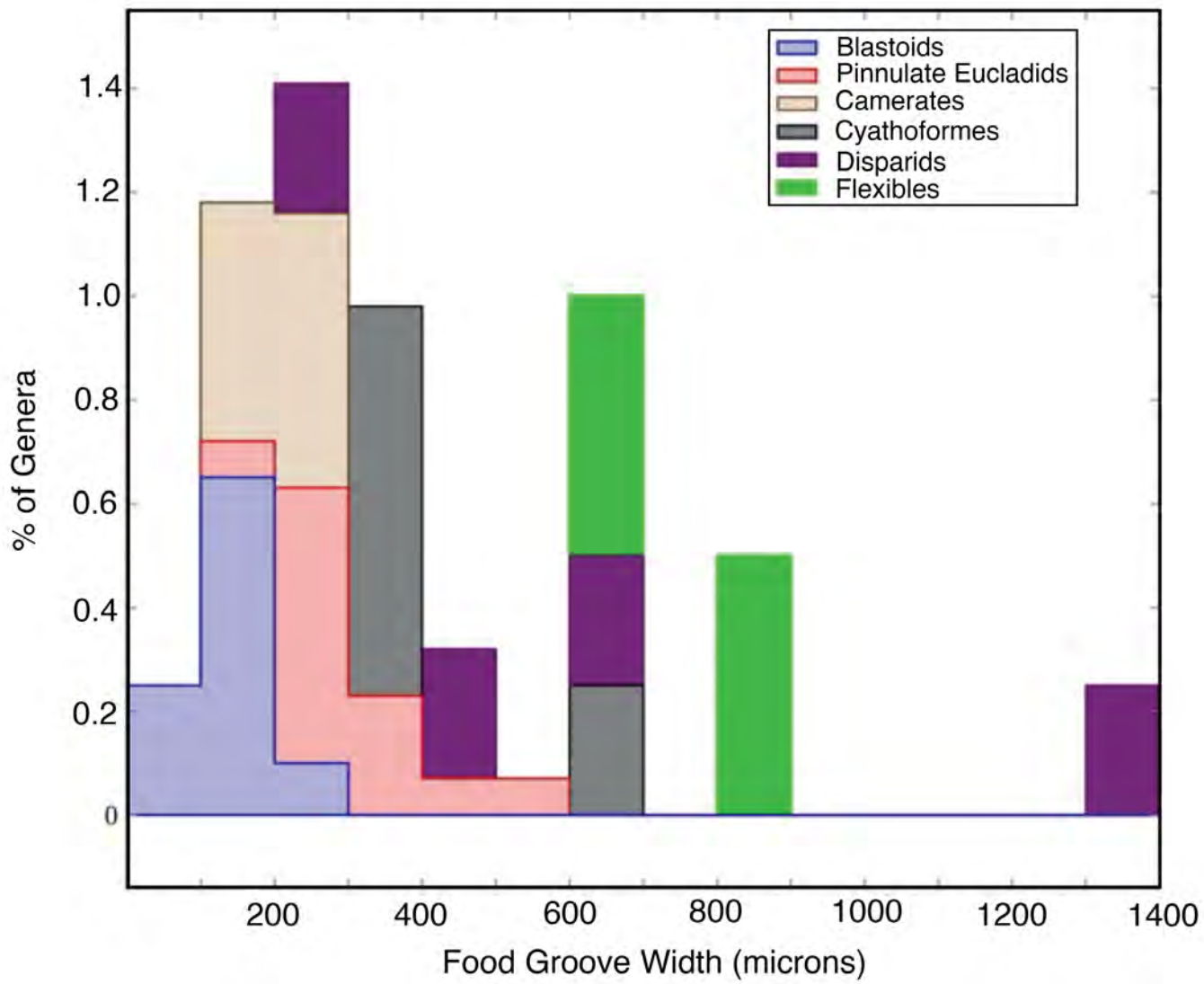

FIGURE 6 — Stacked plot of the food groove widths (microns) for blastoids and crinoid clades. Crinoid data from Ausich (1980). Blastoid data from Table 3 herein. Data for each clade normalized and reported as percent in each bin. Blastoids have very narrow food grooves in the brachioles. Camerate crinoids also have narrow food grooves even though branching arms with pinnules are the primary feeding structures. Advanced eucladids have a wider range of food groove widths but overlap blastoids and camerates. Cyathoformes have wider food grooves than camerates and most blastoids. Flexibles have significantly wider food grooves than the other clades. Disparids exhibit a very wide range of food groove widths.

Marta coast of Colombia). Meyer suggested that suspended food supply, along with favorable current flow, supported the higher diversity and abundance of suspension feeders like crinoids in shallow waters less favorable to more extensive coral reef development.

Shallow Water Crinoid Diversity in the Indo-West Pacific

In 1975 Meyer had a unique opportunity to take part in the *Rumphius* II research cruise in the Molucca Islands of Indonesia, in the heart of the famed "Coral Triangle" known for high diversity of shallow marine invertebrates and vertebrates. Although it turned out that SCUBA diving could not be supported onboard the research vessel, collection of crinoids was made using snorkel diving, aided by specimens brought to the vessel by local people at every place we stopped during a two-week cruise. Identification based on available taxonomic references resulted in a total of about 27 species (Meyer, 1976), and specimens were deposited at a university at Ambon and at the National Museum of Natural History of the Smithsonian Institution.

Since that time, many studies on Indo-West Pacific shallow-water crinoids and their symbionts have been published, extending from the Red Sea, across the Indian Ocean, Coral

Triangle, and into the Central Pacific. Messing (1998) presented a critical summary of available records of shallow-water crinoid distribution in the region. Messing pointed out several factors that should be taken into consideration when consulting records from particular localities, such as methods of collection, collecting effort, and use of updated taxonomic resources. A recent paper on the crinoids and their symbionts at Sulawesi (Virgili et al., 2020) provided an excellent summary of current knowledge of crinoid biodiversity across this vast region. These authors pointed out that many studies on the symbionts associated with shallow water crinoids have not provided comprehensive data on crinoid host species diversity or were based on now-outdated taxonomic determinations. Therefore, we will mention only those studies that are based on the latest revisions of crinoid taxonomy for the most complete sampling of crinoids at a given locality, as well as those based on personal field experience.

In the 1970s Meyer and Macurda (1980) studied reef-dwelling crinoids from the Palau Islands in Micronesia, reporting 21 species from depths <50 m. Messing (2007), using updated taxonomy, identified 22 species from the same area. Subsequently, several comprehensive studies were reported from localities closer to the Coral Triangle. From Papua New Guinea, 25 species were reported at Hansa Bay (Deheyn et al., 2006) and 40 species at Madang (Messing, 1994). Kogo et al. (2019) reported 31 species from the Indonesian islands of Ambon and Lombok. Virgili et al. (2020) reported 39 species from Bangka Island, North Sulawesi. Messing and Tay (2016) reported 39 species from waters around Singapore, based on a new survey conducted in 2013, plus previously recorded taxa.

Although outside the limits of the Coral Triangle, the Australian Great Barrier Reef has a highly diverse and abundant crinoid fauna and has received a considerable amount of attention from researchers. Beginning in 1975, Meyer and Macurda visited the Lizard Island reefs and other GBR reefs several times through 2000. Lyle Vail and Anne Hoggett, both crinoid specialists, have worked at Lizard Island Research Station as resident co-directors since 1990. Based on their longtime observations, they organized the Lizard Island Field Guide, an online illustrated guide to the reef fauna at Lizard Island (http://lifg.australian.museum/Hierarchy.html?hierarchyId=PVWrQCLG, accessed Oct. 20, 2020). This guide lists 51 shallow water crinoid species, a total comparable to that obtained during the work of Meyer and Macurda and also to the total of 57 species reported by Messing (1998) (Fig. 5A). These figures probably reflect to some degree the intensive study of the Lizard Island crinoids by specialists for nearly 50 years but suggest that similar totals might be obtained by more extensive study at other high-diversity sites mentioned above.

Another major research program was established by the Australian Institute of Marine Sciences (AIMS), to document marine diversity along a transect from the Outer Barrier Reef bordering the Coral Sea, across mid-shelf reefs to nearshore reefs close to the mainland in the Central Great Barrier Reef region. Crinoids were an invertebrate group selected for sampling using a standard protocol at designated reefs. In 1983 Meyer participated in the effort to identify the many crinoids that were sampled and also was able to visit Outer Barrier reefs such as Myrmidon and mid-shelf reefs such as Brewer and Davies. At Davies Reef a total of 27 species-level taxa were identified (Bradbury et al., 1987).

A later sampling of crinoids at <12 m depth in the Central GBR was conducted in 1988 (Fabricius and Dale, 1993; Fabricius, 1994) at 46 sites on 12 reefs, including Davies Reef. This survey is significant for the purposes of this review in being the only quantitative assessment of crinoid diversity comparing reefs across the Central GBR from the continental mainland to reefs of the mid-shelf and outer barrier. With the benefit of revised and updated taxonomy (Rowe et al., 1986), the total of approximately 44 species from Davies increased the known taxa from 27 reported by Bradbury et al. (1987). The entire dataset was analyzed using a variety of multivariate techniques. Data in Table 2 indicate that mid-shelf reefs and Davies Reef in particular have higher crinoid densities and higher number of species compared to outer shelf reefs and nearshore reefs.

A similar pattern was suggested by crinoid richness at Lizard Island, a high island on the mid-shelf, that contrasted with apparent lower crinoid diversity and abundance on outer barrier reefs (Carter-Yonge) at the same latitude (Meyer, pers. observations). On these outer barrier reefs, qualitative observations suggested maximum coral cover and richness, with exceptional water clarity (highly oligotrophic). The waters around Lizard Island, while highly diverse in all reef life, including crinoids (Fig. 5A), often seemed to have lower water clarity despite being quite far offshore (~20 miles) from mainland runoff. Was it possible that increased turbidity resulted from greater primary productivity of plankton and particulate organic matter (more heterotrophic conditions) over the mid-shelf region? Higher productivity could, in turn, provide enhanced food supply for suspension feeding reef dwellers like crinoids.

A 1982 paper published by AIMS biological oceanographers Andrews and Gentien documented nutrient enrichment and enhanced phytoplankton productivity of mid-shelf reefs from upwelling that originates along the outer shelf break that might account for the greater richness of suspension feeding crinoids around mid-shelf reefs where there is also localized upwelling. According to Fabricius (pers. comm., 2017), upwelling along the GBR is still not well understood and additional factors such as current patterns, structural complexity, and patterns of sedimentation play a role.

FOOD COMPOSITION OF LIVING CRINOIDS

The foregoing summary of the diversity and biogeography of living shallow water crinoids suggests that the highest diversity and abundance of crinoids in both the tropical Western Atlantic and Indo-West Pacific realms occurs where plankton productivity is increased in proximity to large landmasses such as islands and continents. However, this

leaves open the question: *exactly what suspended particles ingested by crinoids supply their main nutritional source?*

Suspension Feeding by Modern Crinoids

Crinoids are regarded as non-selective passive suspension feeders, capturing any particles striking the mucus-coated tube feet that flick to transfer them to the food grooves where they are entrained as a mucus string by ciliary currents leading to the mouth (Meyer, 1982b). Because the tube feet act as a "sticky filter", particles smaller than the minute gap between extended tube feet can be captured, as well as larger particles (LaBarbera, 1978). Large aggregates of suspended material can be carried along the food grooves but are usually discarded before reaching the mouth (Holland et al., 1991; video by A. Stevenson, in Meyer et al., 2021). Overall, relative nutritive value of identifiable items as well as the detrital component and DOM remain to be determined. The main limiting factor for capture of suspended particles is maximum width of the pinnular food groove (75 – ~300 microns, according to several studies cited below).

Studies of the gut and fecal contents of both stalked and unstalked crinoids from shallow as well as deep water have been reported for a number of species. A wide variety of particles have been identified from these samples, including phytoplankton, Protozoa (Foraminifera), Crustacea, fecal pellets, and sediment grains, and in most cases detritus that makes up a large proportion of the material (shallow water feather stars (LaTouche and West, 1980; Liddell, 1982; Meyer, 1982a; deep water stalked crinoid, Featherstone et al., 1998). The maximum width of most identifiable items is usually less than about 200 microns, within the width of the pinnular food grooves. However, some items can range to about 300-400 microns in width. [It should be noted that some living suspension feeders are known to ingest particles larger than microplankton normally assumed, for example, several bivalves (Lehane and Davenport, 2002)]. Detrital material appears as a mass in the samples, and single particles are unresolvable in light microscopy. Therefore, size data for the detritus are not available in size-frequency plots for identifiable items. LaTouche and West (1980) suggested that the detrital particles may have microbial material adhering that could have nutritive value for the crinoid. Actual caloric content of all food items has not been determined. Uptake by absorption of dissolved organic matter (DOM) across the body wall has been demonstrated for crinoids and may provide nutrition for a crinoid during regeneration after loss of the visceral mass from autotomy or predation (Smith et al., 1981).

Suspension Feeding by Extinct Crinoids

It is generally assumed that ancient crinoids had suspension feeding habits similar to living crinoids - passive suspension feeders utilizing tube feet for particle capture and ambulacral grooves by which particles were carried to the mouth. Detailed research on the morphology of ancient crinoid feeding structures (arms, pinnules, food grooves, column length) has revealed a wide range of variation within and among major groups of crinoids and blastoids that probably had consequences for the size-range of food particles captured.

Most significant are studies on variation within ancient communities with excellent preservation of in situ assemblages that permit comparisons between taxa with differing morphologic features of the feeding apparatus. Lane (1963) first documented the existence of co-occurring crinoid species preserved with many specimens with articulated calyxes, arms, pinnules, and columns complete to a holdfast that were "stratified" (later termed "tiered") at different heights above the sea floor. These assemblages are among the best preserved fossil crinoids ever known on large slabs of specimens from classic localities near Crawfordsville, Indiana in the Lower Mississippian Edwardsville Formation (Lane, 1963, 1973). Study of crinoid communities from distinct facies of the Edwardsville Formation. around Monroe Reservoir, Indiana, by Ausich (1980) introduced the concept of niche differentiation based on several morphologic parameters including height above substratum (column length), filtration fan density (branches/fan area), and ambulacral groove width. Ausich demonstrated that co-occurring crinoids in different facies of the Edwardsville were distributed along a niche differentiation spectrum that dictated differential capture of particles based on particle size. Furthermore, his analysis showed that the probable size range of captured particles is similar to that for living crinoids, ranging from about </= 0.1 mm to >1.25 mm (his fig. 4 and our Fig. 6 that includes blastoids). The most common crinoids in the assemblage studied by Ausich had pinnular food grooves in the range </= 0.1 - 0.4 mm in width (implying a similar size range of particles). Fewer taxa having wider food grooves occupied the tail of a right-skewed distribution of width.

Ausich stated that his data and conclusions were dictated by principles of aerosol filtration theory as applied to suspension feeding by Rubenstein and Kohl (1977) and LaBarbera (1978). Despite the fact that soft-part structures such as exact food groove width and tube feet are not preserved, the preservable morphology of the arms and pinnules permits application of these principles to a close approximation. In living crinoids the food groove width is measured from soft tissue located slightly above the pinnular ossicles (Fig. 5B; also see Breimer, 1978b: fig. 2). We would add that in many of these Mississippian crinoids, the food groove was deeply embedded in the preservable skeleton of the pinnules, sometimes with covering plates in place. [Examples are illustrated in the *Treatise on Invertebrate Paleontology*, Part T: Ubaghs, 1978, figs. 131-1d,1 136-7, 160 (fossil crinoids); Breimer, 1978b fig. 29-3 (for Recent *Neocrinus decorus*).] Thus, the width as measured by Ausich should be very close to that in the living animal. Aerosol filtration predicts that the parameters of a biological filter determine the size range of particles captured and that filters having different mesh sizes will have differing optimal size ranges. Further research by Ausich and Kammer

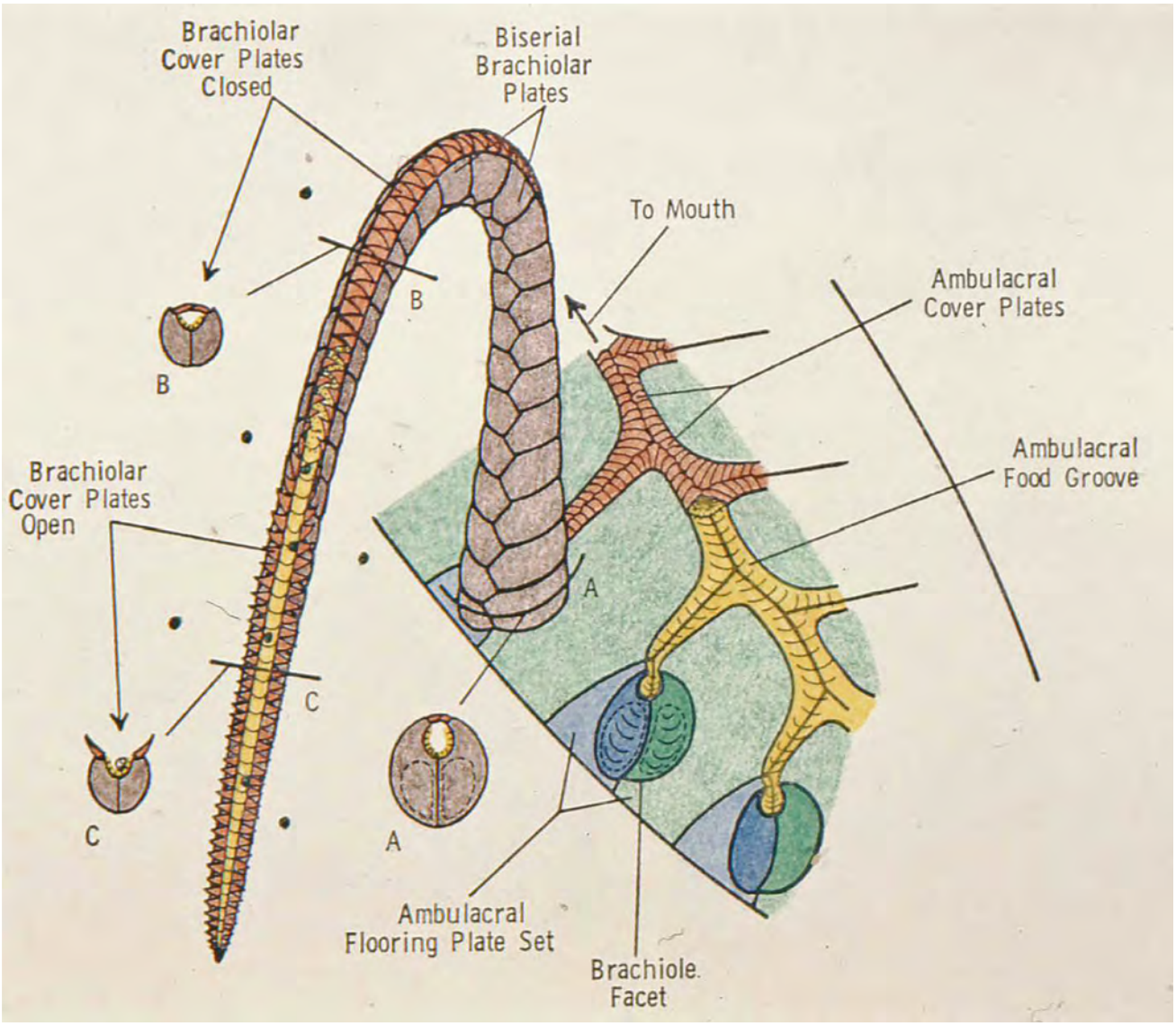

FIGURE 7 — Schematic detail of blastoid brachiole and ambulacral tract. Modified from Sprinkle, 1973, used courtesy of J. Sprinkle.

(Kammer, 1985; Kammer and Ausich, 1987) explained faunal differences among Lower Mississippian crinoid communities on the basis of aerosol filtration and current velocities.

There are no known cases of fossil preservation of stomach or fecal contents of crinoids by which direct comparisons to studies of living crinoids as described above can be made. Therefore, it is necessary to infer the size range of particles that could be entrained in the food grooves by both crinoids and blastoids (see below).

FUNCTIONAL MORPHOLOGY AND FEEDING BEHAVIOR OF BLASTOIDS

Blastoids are members of an extinct echinoderm class ranging from the Upper Ordovician to the Upper Permian. Like crinoids, blastoids were attached to the seafloor by a slender column comprised of disc-like columnals. Unlike crinoids, the blastoid column held up a regularly plated theca that encased internal structures and included five ambulacral tracts that converged on the "summit" of the theca. In crinoids, the ambulacra are termed exothecal as they elevated the arms away from the plated calyx, enabling the formation of the filtration fan discussed earlier. Blastoids lacked the arms and pinnules present in crinoids; instead, very slender, elongate, unbranched structures called brachioles lined the ambulacral tracts and extended radially, perhaps like bristles. A blastoid with a full array of brachioles might have resembled a "bottle brush". Breimer and Macurda (1972: figs. 101, 102) illustrated reconstructions of fissiculate blastoids with extended brachioles forming filtration fans oriented to filter a horizontal

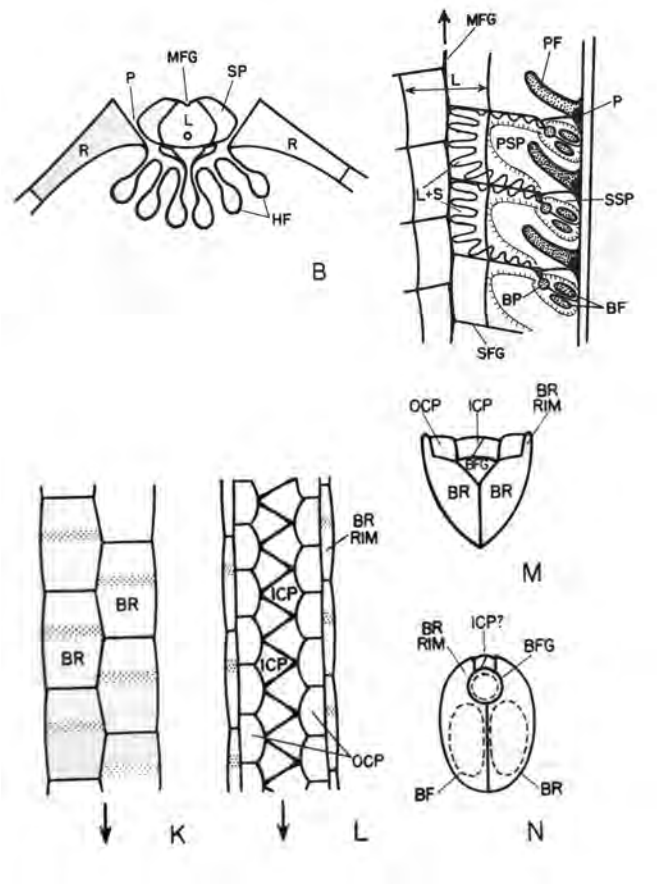

FIGURE 8 — Thecal ambulacra (upper 2 diagrams) and brachioles (lower diagrams, K-N) of *Costatoblastus*, Dev. – Miss., Montana (from Sprinkle and Gutschick, 1990, used with permission).

current or to capture particles settling from above,

James Sprinkle's (1973) reconstruction of the morphology of the brachiole attached to the theca in feeding position shows how brachioles are fundamentally distinct from arms arising from a crinoid calyx (Fig. 7). The biserial brachioles are comprised of solid, wedge-shaped ossicles (brachiolars) that bear a brachiolar groove that was covered by biserial covering plates that could be opened to expose the ambulacral groove. Sprinkle's reconstruction shows minute food particles suspended in the surrounding water and in the groove on their way to the mouth, located at the thecal summit. Sprinkle hypothesized that the food groove was lined with tissue bearing cilia that beat synchronously to create a feeding current, drawing flow around the brachioles and through the array of extended cilia. This feeding current presumably conveyed suspended particles to the exposed food groove where they were entrained by ciliary flow towards the theca.

Although Sprinkle (1973) postulated that, unlike crinoids, blastoids did not have tube feet, Breimer and Macurda (1973) suggested that tube feet could have been housed within

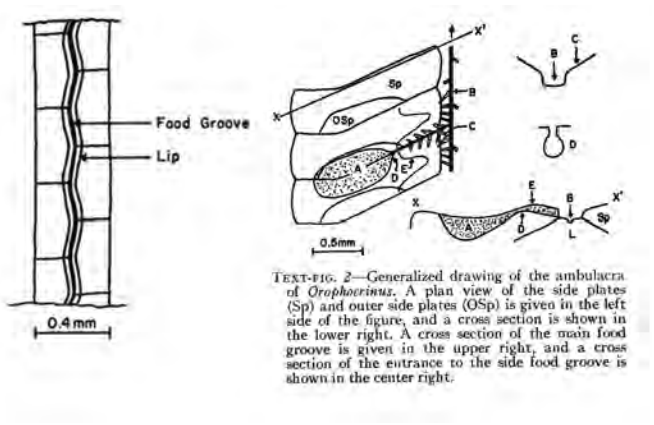

FIGURE 9 — Brachiole (left) and details of ambulacra of *Orophocrinus conicus* (right), from Macurda, 1965, used with permission.

minor grooves radiating toward the side and main ambulacral grooves, as part of the side plates. It follows from Sprinkle's reconstruction that the width of exposed food groove would be a primary limiting factor for the size of particles that could be entrained (Fig. 7). At the point where the brachiolar food groove joined the theca, particles must have entered the ambulacral food groove through the brachiolar pit (Fig. 8, BP in detail at upper right). If the diameter of the brachiolar pit was =/< the width of brachiolar food groove, entrained particles would have encountered a secondary size limiting factor. Note that in Sprinkle's reconstruction, the ambulacral groove of the thecal plates was equipped with cover plates, whereby the feeding current would have become subthecal from that point onward toward the mouth. In 1973, Sprinkle concluded that blastoids were limited to feeding on very small particles. In 2006, Sprinkle stated that "blastozoan (including blastoids) brachioles almost always had narrow food grooves, implying that they fed on small food particles."

Given that Sprinkle's 1973 reconstruction is schematic and without a scale, it is necessary to examine preserved morphology of blastoids to see if this morphology is present throughout the class and how the actual size limitations would have constrained food particle size. Blastoids preserved with attached stem and brachioles are exceedingly rare. However, several well-documented cases of exceptionally well-preserved blastoids provide data on feeding morphology. Table 3 lists sixteen taxa, both fissulates and spiraculates, for which detailed descriptions of brachiolar and ambulacral morphology are available.

Macurda (1965) provided detailed drawings with scale from which we could determine the width of the brachiolar and thecal ambulacral food groove and the brachiolar pit in the Mississippian fissiculate *Orophocrinus conicus*. In Macurda's Text-figure 1 (our Fig. 9), the width of the entire brachiole is 0.4 mm, therefore the width of the brachiolar food groove is 0.0246 mm or 24.6 microns, the narrowest width reported. In our Fig. 9 (his Text-fig. 2, plan view at left) point D marks the

TABLE 3 — Brachiolar food groove width or brachiolar pit width (bp) in some blastoids. F = fissiculate, S = spiraculate. Data obtained from published figures with scale except as indicated.

Orophocrinus conicus, F, Miss.: 24.6 μm (Macurda, 1965)

Orophocrinus cf. *O. gracilis*, F, Miss.: 195 μm (bp) (Sprinkle and Gutschick, 1990)

Pyramiblastus fusiformis, S, L. Miss.: 127 μm (Fay and Reimann, 1962)

Koryschisma elegans, F, Miss.: 167 μm (Sprinkle and Gutschick, 1990)

Montanablastus baldyensis, S, Miss.: 163 μm (Sprinkle and Gutschick, 1990)

Costatoblastus sappingtonensis , S, Devonian: 89-94 μm (Sprinkle and Gutschick, 1967)

Hyperoblastus nuciformis, S, M. Dev.: 171 μm (Fay and Reimann, 1962)

Monoschizoblastus rofei, S, Miss. 85 μm (bp) (New, SEM photo)

Monoschizoblastus rofei, S, Miss. 75 μm (bp) (New, SEM photo)

Strongyloblastus laudoni, S, Miss.: 271 μm. (Sprinkle and Gutschick, 1990)

Pentremites godoni, S, (juvenile) Miss. 55 μm (bp) (New, SEM photo)

Pentremites robustus, S, Miss. 130 μm (bp) (New, SEM photo)

Pentremites robustus, S, Miss. 136 μm (bp) (New, SEM photo)

Deltoblastus sp,, S, Permian. 145 μm (bp) (New, SEM photo)

Heteroschisma alatum, F, Devonian, 94 μm (bp) (New, SEM photo)

Cryptoschisma schultzi, F, Devonian, 169 μm (bp) (New, SEM photo)

location of the brachiolar pit (BP) that must be the same width as that of the BFG, 24.6 μm. The enlarged cross sections at the right in our Fig. 9 (his Text-fig. 2) lack a scale, but it is apparent that the BP at point D must be exceedingly small. Cross section D shows the BP to have a keyhole shape, with a pore that restricts the entrance to 24.6 μm, widening below. The main food groove at B is wider, as it is a collector for all BFG feeding into the ambulacrum.

In the description of a Mississippian spiraculate blastoid, *Costatoblastus*, Sprinkle and Gutschick (1967: fig. 9, left) illustrated a cross section of the entire ambulacrum (our Fig. 8, left) with a plan view of the half-ambulacrum at the right. In the full cross section, point P marks the pore leading into the blastoid's hydrospire folds. The brachiolar pit (BP) in the plan view is circular in section and feeds into the main food groove (MFG). From the scale provided for their figure, the width of the BFG is 89-94 μm (insets M, N). M is a cross section of the brachiole showing covering plates and BFG, and N is a cross section of the brachiolar facet, where it attached to the side plates (SP) of the ambulacrum.

Fay and Reimann (1962) illustrated a fragment of a brachiole of a Devonian blastoid *Hyperoblastus nuciformis* with a cross section with cover plates in place over the BFG. Using the scale, we determined the width of the BFG to be 171 μm. Table 3 shows other determinations of BFG widths from published illustrations in Fay and Reimann 1962) and in Sprinkle and Gutschick (1990), plus brachiolar pit width from SEM images of specimens in the collection of J. Waters.

As noted by Waters (1988), blastoids were components of echinoderm communities along with crinoids and peaked during the early Mississippian. In particular, blastoid generic diversity is highly correlated with that of monobathrid

camerate crinoids (r=0.65, P<0.02, Waters, 1988). Later during the Mississippian, blastoid diversity was not significantly correlated with that of eucladid crinoids, a group that attained a peak in diversity in the Pennsylvanian before declining toward the end of the Paleozoic. Blastoids became extinct with the end-Permian mass extinction, after regaining diversity during the Late Permian before the extinction.

Waters (1988) also pointed out that blastoids had not been successfully placed within the niche partitioning model introduced by Ausich (1980) for crinoids, because of limited information then available on the stem lengths and brachiole morphology of blastoids. This was also hindered by the contrast between crinoid filtration fans of arms and pinnules with tube feet and the blastoid brachioles that apparently lacked tube feet and could not form filtration fans like those of crinoids. Waters conjectured that blastoids might have been utilizing a specific food particle size range or even a wider particle size range than crinoids. In the present study we have presented limited data on the morphology of the brachiolar and ambulacral grooves that indicate a limitation of particle size range toward the lower end of the size spectrum (Table 3, Fig. 6). Although more data are needed for these parameters in blastoids, we can begin to assess the position of blastoids in the benthic food web of the Mississippian Age of Crinoids.

DISCUSSION

We have presented information derived from the published literature and new information that bear on the role of food availability as an additional causative factor for the all-time peak in diversity and abundance of crinoids and blastoids during the "Age of Crinoids" in Early Mississippian time. One set of information (secondary heading below) pertains to the connection between diversity of crinoids and food supply and productivity of suspended particulate food materials for both living crinoids and also extinct crinoids during the critical interval. The other set of information (next secondary heading) reviews existing knowledge of the makeup of material found in the gut and feces of living crinoids and its contribution to crinoid nutrition. We also consider the possible composition of the food of extinct crinoids in light of what is known about marine plankton at that time, particularly in terms of the available suspended particles in the size range crinoids and blastoids could ingest. We will summarize the information in both areas below and integrate it with previously published research on the relationship between species diversity and food supply, productivity, and nutrition of crinoids and shallow marine benthos over time.

Crinoid Diversity has been Closely Associated with Food Availability and Productivity Since the Paleozoic and at Present

For living shallow-water crinoids we argue that available knowledge of biogeographic distribution indicates that crinoids, chiefly feather stars, reach maximum richness and abundance in both tropical Western Atlantic and Indo-West Pacific realms where there is enhanced plankton productivity caused by influx of nutrients from terrestrial sources via river outfalls and possibly regional upwelling. These conditions occur mainly close to continental margins (South America, Central America, Australia) or high islands (Coral Triangle of the IWP).

Species diversity in the broad sense of both species richness and population size (γ diversity), for living and extinct crinoids especially during the early Mississippian, peaked 347 – 331 mya during the Viséan, ranging from the Tournaisian through the Serpukhovian and attained a secondary peak during the Pennsylvanian (Moscovian). Blastoids also reached an all-time diversity peak during the Viséan but not during the Pennsylvanian. Significant events during the Mississippian and Pennsylvanian included the plate tectonic closure of the Iapetus Sea, resulting in the orogenic uplift of the Appalachian belt and especially major clastic runoff into the epicontinental sea from the Catskill and Borden Deltaic complexes. In addition, the Age of Crinoids coincided with the drawdown of global atmospheric CO_2 that Riding (2009) inferred to have triggered a major turnover or "bloom" of marine phytoplankton following the drastic decline of planktonic acritarchs in the Late Devonian, initiating the so-called "phytoplankton blackout" (Riegel, 2008).

In his comprehensive study of species richness in marine benthic habitats through the Phanerozoic, Bambach (1977) suggested that the evolution of land plants in the Silurian initiated an increase in supply of organic nutrients that might have affected species richness in the Paleozoic. He also noted that the crinoid community at Crawfordsville, Indiana studied by Lane (1973) had the highest diversity for level-bottom communities of the entire Paleozoic. However, Ausich et al. (1979) pointed out that the total diversity for the Crawfordsville community of 73 species reported by Bambach greatly understated the actual diversity there of more than 150 invertebrate species. Later, Algeo et al. (1995) emphasized the role of land plant evolution in the middle to late Paleozoic as it affected soil weathering and introduction of nutrients into the seas.

The high species diversity of level bottom communities dominated by suspension feeders (including sponges, bryozoans, and brachiopods in addition to crinoids and blastoids) associated with the Mississippian Borden Delta (Ausich et al., 1979) suggests a parallel to the relationship discussed earlier between increased diversity of living crinoids and higher productivity closer to continental margins. Indeed, in this case, the past may well provide the key to the present.

Even though the Age of Crinoids during the Mississippian does not stand out within studies of Phanerozoic marine diversity fluctuations at taxonomic levels of family and genus, crinoids and blastoids are a significant contribution to Sepkoski's (1981) Paleozoic Evolutionary Fauna (PEF) as indicated above. The assertions we are making of the connections between pelmatozoan diversity and food supply, nutrients and productivity are fully in concert with

several large-scale analyses of the role of these factors as primary controls over diversity in Phanerozoic time by Bambach (1993), Vermeij (1995), Martin (2003), Bush and Bambach (2011), Allmon and Martin (2014) and the recent comprehensive review by Martin and Servais (2020). Closer examination of how these and other factors contributed to the diversity trends of particular component taxa of the PEF is overdue.

Suspension-Feeding by Crinoids and Blastoids was Limited to Capture of Very Small Food Items by the Narrow Width of Food Grooves

The narrow width of pinnular food grooves in crinoids and brachiolar food grooves in blastoids has been recognized for quite some time. The width of particles in gut and fecal samples from living crinoids, both unstalked and stalked, plot as right-skewed frequency distributions,with the bulk of the material in the range of about 100 – 200 μm. The presence in samples of a considerable volume of "detritus" with unresolvable particles indicates that the size distributions may be more heavily right-skewed than those drawn from resolvable, identifiable items such as plankton, fecal pellets, and even sediment grains. Detrital particles in the size range less than the minimum spacing of crinoid tube feet can be captured and retained because the tube feet are "sticky filters" coated with mucus (LaBarbera, 1978). Although blastoids lacked tube feet, the ciliated brachioles likely were also mucus coated. Fossil crinoids and blastoids had narrow food grooves in a range similar to that in living crinoids but were probably incapable of capturing larger particles because of skeletal restrictions not present in living forms in which the food grooves are in stretchable soft tissues.

We have no direct evidence of any fossilized gut contents, so that the taxonomic identification of their gut contents is not known. However, we can state with confidence that ancient crinoids and blastoids were collecting very small particles from the water mass. The immense volume of pelmatozoan-rich limestones (encrinites) of early Mississippian age from all over the world *requires* that these marine suspension feeders and others like bryozoans and sponges were supported by an abundant supply of nutritious particles from the near-bottom waters of the Paleozoic shallow seas, including phytoplankton, zooplankton, and also organic detritus and microbial pico- or nanoplankton.

Paradoxically, when we consider the fossil record of the marine plankton, we find that the Age of Crinoids coincides with a long interval from the Late Devonian through the early Mesozoic for which the fossil record is exceptionally poor (Tappan, 1968: fig. 1; Martin, 2003: fig. 2B; Riding, 2009: fig. 8; Martin and Servais, 2020: fig.1C; others). In all these records, the only component of the marine plankton present in the microfossil record during the Age of Crinoids is acritarchs with a possible trace of early dinoflagellates in some (Tappan, 1968: fig. 1) plus a trace of coccolithophorids (Martin and Servais, 2020: fig.1C). Major components of Recent phytoplankton, such as the dinoflagellates, coccolithophorids, and diatoms, do not have major increases in their abundances until the Mesozoic and Cenozoic (Knoll and Fellows, 2016). Among the zooplankton, foraminiferans and radiolarians are certainly present in Paleozoic, and diverse larvae must have been present but usually unpreservable (with possible exception of microfossils, such as from the Ediacaran Doushantuo Formation of China, 635–551 Ma). Ironically, the Age of Crinoids interval is extraordinarily rich in benthic suspension feeders with a good fossil record (crinoids, blastoids, sponges, conulariids, corals, mollusks, and especially bryozoans). The question "What were all these suspension feeders eating?" becomes all the more significant in view of the richness and abundance of the entire marine benthic suspension feeder guild.

It must be considered that the marked lack of preserved marine phytoplankton during the Age of Crinoids reflects a taphonomic artifact as a consequence of an abundance of either nonskeletonized or poorly preservable components of the microplankton at that time, a potential problem that has been discussed at length by Martin and Servais (2020). Riding (2009) discussed the possibility that the phytoplankton blackout could be "more apparent than real". As Riding suggested, it may have been the result of a major shift in plankton composition from acritarch dominance to abundance of "relatively invisible picophytoplankton" including cyanobacteria and other groups such as prasinophyte green algae (Riding, 2009). As further pointed out by Riding, as well as Martin and Servais (2020), the modern marine plankton contains bacterioplankton (< 1 μm) and picoplankton (~1–2 μm), and we also suggest that non-skeletonized protozoans such as flagellates and ciliates would have been part of the non-fossilizable Paleozoic plankton. There may be limitations on our ability to fully characterize the makeup of the Paleozoic marine plankton biota, but it is the main assertion of this paper that the richness and abundance of the Mississippian suspension feeding guild of crinoids and blastoids and other groups, like bryozoans, demonstrates that the primary producers of that time were dominated by very small organisms as suspended particles.

CONCLUSIONS

In a single paragraph Riding (2009) succinctly summarized the evidence from the Mississippian fossil record that crinoids and blastoids at their all-time peak in richness and abundance in the Age of Crinoids possessed narrow food grooves well-suited for gathering very small food particles, suggesting “both a shift and increase in food supply toward smaller particles, such as picoplankton or the microplankton that feed on them".

In the present paper we have argued that food supply, nutrients, and productivity are *among* the chief factors controlling diversity of Recent and Mississippian crinoids. We have presented an analysis of the feeding mechanism of Recent and fossil crinoids and blastoids that explains why

Mississippian crinoids and blastoids were preferentially capturing very small suspended particles. For both groups, the range of food groove width dictates that most particles were smaller than about 400 µm. For the crinoids studied by Ausich (1980) some taxa had food grooves capable of capturing larger particles, but most blastoids were more closely constrained toward the smaller end of the size spectrum. We postulate that blastoids were actually specialists at gathering very small suspended food particles. Of sixteen taxa with well-preserved brachiolar food grooves or pores, the maximum width is 271µm. Thanks to the mechanisms of aerosol filtration, blastoid cilia and larger crinoid tube feet probably acted as sticky filters (LaBarbera, 1978) that could trap particles finer than the mesh size of the filter. Both groups evolved their feeding morphologies millions of years before the Early Mississippian acme **(**Brower, 2007, 2011; Cole et al., 2019**).** When circumstances of the global atmosphere changed so as to shift primary production in the seas to the most minute bacterio- and picoplankton proposed by Riding (2009), crinoids, blastoids, and perhaps other suspension feeders could take advantage of the new food source. They were, in a sense "preadapted", to hazard an old, perhaps disfavored view. In the sense of Gould and Vrba (1982) the suspension feeding abilities of crinoids and blastoids became "exaptations" that enabled these groups to diversify opportunistically and become enormously productive. The abundance of thick regional encrinites (Ausich, 1997) became some of the most extensive limestones known, an enduring testimony to this unique phase of the Paleozoic oceans known as the Age of Crinoids.

ACKNOWLEDGMENTS

We thank James Sprinkle and D. Bradford Macurda, Jr., for kindly permitting us to reuse their published illustrations of the detailed morphology of blastoid ambulacral structures. Along with Jim Sprinkle and Brad Macurda, we learned much about the problems addressed in this article from many "companions in zealous research" including Tom Algeo, Bill Ausich, Tom Baumiller, Nick Holland, Tom Kammer, Mike LaBarbera, Ron Martin, Charles Messing, Peter Petraitis, and Colin Sumrall. We also thank Kathleen Huber for obtaining permission to reuse the illustrations of Sprinkle and Macurda published in the Journal of Paleontology. Through pure serendipity Meyer met Robert Riding on the shores of Lake Cumberland, Kentucky, where we examined the crinoid and blastoid-rich fossils associated with enigmatic carbonate mounds (Waulsortian?) from the Mississippian "Age of Crinoids". Subsequently we were inspired by Riding's 2009 Palaios paper, and we thank Robert for reading an earlier draft of the present paper and for his brilliant insight in finding the synergies of many global features of paleontology and geology of this critical interval of Earth history of the Late Devonian - Early Mississippian. We dedicate this paper to N. Gary Lane, James C. Brower, and Gary D. Webster, who contributed greatly to the knowledge of Paleozoic echinoderms and set the stage for us to seek answers to questions they had posed.

LITERATURE CITED

ALGEO, T. J., R. A. BERNER, J. B. MAYNARD, and S. E. SCHECKLER. 1995. Late Devonian oceanic anoxic events and biotic crises: "Rooted" in the evolution of vascular land plants? GSA Today, 5: 45, 64-66.

ALLMON, W. D., and R. E. MARTIN. 2014. Seafood through time revisited: the Phanerozoic increase in marine trophic resources and its macroevolutionary consequences. Paleobiology, 40: 256–287.

ANDREWS, J. C., and P. GENTIEN, 1982. Upwelling as a source of nutrients for the Great Barrier Reef ecosystem: a solution to Darwin's question? Marine Ecology Progress Series, 8: 257-69.

AUSICH, W. I. 1980. A model for niche differentiation in Lower Mississippian crinoid communities. Journal of Paleontology, 54: 273–288.

_____1997. Regional encrinites: a vanished lithofacies in C. E. BRETT AND G. C. BAIRD (eds.), Paleontological Events: Stratigraphic, Ecologic and Evolutionary Implications, Columbia University Press, New York, p. 509–519.

_____, and T.W. KAMMER 2013. Mississippian crinoid biodiversity, biogeography and macroevolution. Palaeontology, 56: 727–740.

_____, _____. and BAUMILLER, T.K. 1994. Demise of the middle Paleozoic crinoid fauna: a single extinction event or rapid faunal turnover? Paleobiology, 20: 345–361.

_____, _____, and N.G. LANE. 1979. Fossil communities of the Borden (Mississippian) Delta in Indiana and northern Kentucky, Journal of Paleontology, 53: 1182–1196.

____, _____, and G.V. MIRANTSEV. 2021. Carboniferous crinoids. In S. G. LUCAS, J. W. SCHNEIDER, X. WANG, and S. NIKOLAEVA (eds.), The Carboniferous Timescale, The Geological Society of London, Special Publications, 512, https://doi.org/10.1144/SP512-2020-71.

BAMBACH, R. K. 1977. Species richness in marine benthic habitats through the Phanerozoic. Paleobiology, 3: 152-167.

_____1993. Seafood through time: changes in biomass, energetics, and productivity in the marine ecosystem. Paleobiology, 19: 372-397.

BAUMILLER, T. K. 1993. Survivorship analysis of Paleozoic Crinoidea: effect of filter morphology on evolutionary rates. Paleobiology, 19: 304–321.

BRADBURY, R. H., R. E. REICHELT, D. L. MEYER, and R. A. BIRTLES. 1987. Patterns in the distribution of the crinoid community at Davies Reef on the central Great Barrier Reef. Coral Reefs, 5: 189-196.

BREIMER, A. 1978a. Ecology of Recent crinoids. In R. C. MOORE and C. TEICHERT, (eds.), Treatise on Invertebrate Paleontology, Part T, Echinodermata 2, vol. 1, Geological Society of America and University of Kansas, Boulder and Lawrence, p. T323.

_____ 1978b. General morphology - Recent crinoids. In

MOORE, R.C. and C. TEICHERT (eds.), Treatise on Invertebrate Paleontology, Part T, Echinodermata 2, vol. 1, Geological Society of America and University of Kansas, Boulder and Lawrence, p.T12, T29.

BREIMER, A., and D. B. MACURDA, JR., 1972. The Phylogeny of the Fissiculate Blastoids. Koninklijke Nederlandse Akademie van Wetenschappen, Eerste Reeks, Deel 26, no. 3, North Holland Publishing Company, Amsterdam, 390 pp.

BROWER, J. C. 2007. The application of filtration theory to food gathering in Ordovician crinoids. Journal of Paleontology, 81: 1284-1300.

_____ 2011. Paleoecology of suspension-feeding echinoderm assemblages from the Upper Ordovician (Katian, Shermanian) Walcott-Rust quarry of New York. Journal of Paleontology, 85: 369-391.

BUSH, A. M., and R. K. BAMBACH. 2011. Paleoecologic megatrends in marine metazoa. Annual Review of Earth and Planetary Sciences, 39: 241–269, (doi:10.1146/annurevearth-040809-152556).

CLARK, H. L. 1915. The comatulids of Torres Strait: with special reference to their habits and reactions. Papers from the Department of Marine Biology, Carnegie Institution of Washington, 8: 97-125.

COLE, S. R., D. F. WRIGHT, and W.I. AUSICH. 2019. Phylogenetic Community Paleoecology of one of the earliest complex crinoid faunas (Brechin Lagerstätte, Ordovician). Palaeogeography, Palaeoclimatology, Palaeoecology, 521: 82-98. Published online 2-20-19.

DEHEYN, D., S. LYSKIN, and I. EECKHAUT. 2006. Assemblages of symbionts in tropical shallow-water crinoids and assessment of symbionts' host-specificity. Symbiosis, 42:161–168.

FABRICIUS, K. E. 1994. Spatial patterns in shallow-water crinoid communities on the Central Great Barrier Reef. Australian Journal of Marine and Freshwater Research, 45: 1226-1236.

——, and M. B. DALE. 1993. Multispecies associations of symbionts on shallow water crinoids of the central Great Barrier Reef. Coenoses, 8: 41–52.

FAN, J. S., S. SHEN, D. H. ERWIN, P. M. SADLER, N. MACLEOD, Q. CHENG, X. HOU, J. YANG, X. WANG, Y. WANG, H. ZHANG, X. CHEN, G. LI, Y. ZHANG, Y. SHI, D. YUAN, Q. CHEN, L. ZHANG, C. LI, and Y. ZHAO. 2020. A high-resolution summary of Cambrian to Early Triassic marine invertebrate biodiversity. Science, 367: 272–277.

FAY, R. O., and I. G. REIMANN. 1962. Some brachiolar and ambulacral structures of blastoids. Oklahoma Geology Notes, 22: 30-49.

FEATHERSTONE, C. M., C. G. MESSING, and J. B. MCCLINTOCK. 1998. Dietary composition of two bathyal stalked crinoids: *Neocrinus decorus* and *Endoxocrinus parrae* (Echinodermata: Crinoidea: Isocrinidae). In: R. MOOI, and M. TELFORD, (eds.), Echinoderms: San Francisco. A. A. Balkema, Rotterdam, pp. 155–160.

GOULD, S. J., and E. S. VRBA. 1982. Exaptation - a missing term in the science of form. Paleobiology, 8: 4-15.

HOLLAND, N. D., A. B. LEONARD, and D. L. MEYER, 1991. Digestive mechanics and gluttonous feeding in the feather star *Oligometra serripinna* (Echinodermata: Crinoidea). Marine Biology, 111: 113–119.

KAMMER, T.W. 1985. Aerosol filtration theory applied to Mississippian deltaic crinoids. Journal of Paleontology, 59: 551–560.

_____, and W. I. AUSICH. 1987. Aerosol suspension feeding and current velocities: distributional controls for late Osagean crinoids. Paleobiology, 13: 379–395.

_____, and _____. 2006. The ‘‘Age of Crinoids’’: a Mississippian biodiversity spike coincident with widespread carbonate ramps. Palaios, 21: 236–248.

KIER, P. M. 1966. Bredin-Archbold-Smithsonian biological survey of Dominica. 1. The Echinoids of Dominica. Proceedings of the United States National Museum, 121: 1-10.

KNOLL, A. H., and M. J. FOLLOWS. 2016. A bottom-up perspective on ecosystem change in Mesozoic oceans. Proceedings of the Royal Society B, 283: 20161755. http://dx.doi.org/10.1098/rspb.2016.1755.

KOGO, I., T. FUJITA, and T. KUBODERA. 2019. Shallow-water Comatulids (Echinodermata: Crinoidea) from Ambon and Lombok Islands, Indonesia. Species Diversity, 24: 229–246. DOI: 10.12782/specdiv.24.229

LABARBERA, M. 1978. Particle capture by a Pacific brittle star: Experimental test of the aerosol suspension feeding model. Science, 201: 1147-1149.

LANE, N. G. 1963. The Berkeley crinoid collection from Crawfordsville, Indiana. Journal of Paleontology, 37: 1001-1008.

_____ 1973. Paleontology and paleoecology of the Crawfordsville fossil site (Upper Osagian: Indiana). University of California Publications in Geological Sciences, 99, 141 p.

LATOUCHE, R. W., and A. B. WEST. 1980. Observations on the food of *Antedon bifida* (Echinodermata: Crinoidea). Marine Biology, 60: 39–46.

LEHANE, C., and J. DAVENPORT. 2002. Ingestion of mesozooplankton by three species of bivalve; *Mytilus edulis, Cerastoderma edule* and *Aequipecten opercularis*. Journal of the Marine Biological Association of the United Kingdom, 82: 615-619.

LIDDELL, W. D. 1982. Suspension feeding by Caribbean comatulid crinoids. In J. M. LAWRENCE, (ed.), Echinoderms, Proceedings of the International Conference, Tampa Bay. A. A. Balkema, Rotterdam, pp. 33–39.

MACURDA, D. B., JR. 1965. The functional morphology and stratigraphic distribution of the Mississippian blastoid genus *Orophocrinus*. Journal of Paleontology, 39: 1045-1096.

_____. 1973. The stereomic microstructure of the blastoid endoskeleton. Contributions from the Museum of Paleontology, The University of Michigan, 24: 69-83.

_____, and D. L. MEYER. 1977. Crinoids of West Indian coral reefs. American Association of Petroleum Geologists. Studies in Geology, No. 4: 231-237.

MAGNUS, D. B. E. 1963. Der Federstern *Heterometra savignyi* im Roten Meer. Natur und Museum, Frankfurt, 98: 355-394.

_____. 1964. Gezeitenströmung und Nahrungsfiltration bei Ophiuren und Crinoiden. Helgoländer wisssenchaftliches Meeresuntersuchungen, 10: 105-117.

MARTIN, R. E. 2003. The fossil record of biodiversity: nutrients, productivity, habitat area and differential preservation. Lethaia, 36: 179-194.

_____, and T. SERVAIS. 2020. Did the evolution of the phytoplankton fuel the diversification of the marine biosphere? Lethaia, 24: 5-31.

MESSING, C. G. 1994. Comatulid crinoids (Echinodermata) of Madang, Papua New Guinea, and environs: Diversity and ecology. In B. DAVID, A. GUILLE, J.-P. FERAL, and M. ROUX, (eds.), Echinoderms through time, Balkema, Rotterdam, pp. 237–243.

_____ 1998. An initial re-assessment of the distribution and diversity of the East Indian
shallow-water crinoid fauna. In R. MOOI and M. TELFORD, (eds.). Echinoderms: San Francisco, Balkema, Rotterdam, pp. 187–192.

_____, and T. S. Tay. 2016. Extant Crinoidea (Echinodermata) of Singapore. Raffles Bulletin of Zoology, Supplement 34: 627–658.

_____ 2007. The crinoid fauna (Echinodermata: Crinoidea) of Palau. Pacific Science, 61: 91–111.

MEYER, D. L. 1973a. Feeding behavior and ecology of shallow-water unstalked crinoids (Echinodermata) in the Caribbean Sea. Marine Biology, 22: 105-130.

_____ 1973b. Distribution and living habits of comatulid crinoids near Discovery Bay, Jamaica. Coral Reef Project, Papers in Memory of Dr. Thomas F. Goreau, 10. Bulletin of Marine Science, 23: 244-259.

_____ 1976. The Crinoidea of the Rumphius Expedition II. Oseanologi di Indonesia 1976, No. 6: 39-43.

_____ 1982a. Food composition and feeding behavior of sympatric species of comatulid crinoids from the Palau Islands (Western Pacific). In J.M. LAWRENCE, (ed.), Echinoderms, Proceedings of the International Conference, Tampa Bay, A. A. Balkema, Rotterdam, pp. 43–49.

. _____ 1982b, Food and feeding mechanisms: Crinozoa. In M. JANGOUX, and J. M. LAWRENCE, (eds.), Echinoderm Nutrition, A. A. Balkema, Rotterdam, p. 25-42.

_____, and D. B. MACURDA JR. 1980. Ecology and distribution of the shallow water crinoids (Echinodermata) of the Palau Islands and Guam (western Pacific). Micronesica, 16: 59–99.

_____ C.G. MESSING, and D.B. MACURDA, JR. 1978. Zoogeography of tropical Western Atlantic Crinoidea (Echinodermata). Bulletin of Marine Science, 28: 412-441.

_____, _____, M. VEITCH, and A. STEVENSON. 2021. Crinoid Feeding Strategies: New Insights from Subsea Video and Time-Lapse. Elements of Paleontology, Paleontological Society and Cambridge University Press, doi: 10.1017/9781108893534.

RIDING, R. 2009. An atmospheric stimulus for cyanobacterial-bioinduced calcification ca. 350 million years ago? Palaios, 24: 685–69.

RIEGEL, W. 2008. The late Palaeozoic phytoplankton blackout—Artefact or evidence
of global change? Review of Palaeobotany and Palynology, 148: 73–90.

ROWE, F. W. E., A. K., HOGGETT, R.A. BIRTLES, and L. L. VAIL. 1986. Revision of some comasterid genera from Australia (Echinodermata: Crinoidea), with descriptions of two new genera and nine new species. Zoological Journal of the Linnaean Society, 86:1 97–277.

RUBENSTEIN, D. I. and M. A. R. KOEHL. 1977. The mechanisms of filter feeding: some theoretical considerations. American Naturalist, 111: 981-994

RUTMAN, J., and L. FISHELSON. 1969. Food composition and feeding behavior of shallow-water crinoids at Eilat (Red Sea). Marine Biology, 3: 46-57.

SALLAN, L. C., T. W. KAMMER, W. I. AUSICH, and L. A. COOK. 2011. Persistent predator–prey dynamics revealed by mass extinction. Proceedings of the National Academy of Science, 108: 8335–8338, https://doi.org/10.1073/ pnas.1100631108.

SEGESSENMAN, D. C., and T. W. KAMMER. 2018. Testing reduced evolutionary rates during the Late Palaeozoic Ice Age using the crinoid fossil record. Lethaia, 51: 330–343, https://doi.org/10.1111/let.12239.

SEPKOSKI, J. J., Jr. 1981. A factor analytic description of the Phanerozoic marine fossil record. Paleobiology, 7: 36-53.

SMITH, D. F., D. L. MEYER, and S. M. J. HORNER. 1981. Amino acid uptake by the comatulid crinoid *Cenometra bella* (Echinodermata) following evisceration. Marine Biology, 61: 207-213.

SPRINKLE, J. 1973. Morphology and Evolution of Blastozoan Echinoderms. Harvard University, Museum of Comparative Zoology Special Publication, 283 p.

_____. 2006. Crinoids vs. blastozoans: Some similarities but many differences. In B. LEFEBVRE, B. DAVID, E. NARDIN, and E. POTY, (eds.), Programme and Abstracts, Journees G. Ubaghs, Biogeosciences, Université de Bourgogne, p. 41-42.

_____, and R. C. GUTSCHICK, 1967. *Costatoblastus*, a channel fill blastoid from the Sappington Formation of Montana. Journal of Paleontology, 41: 385-402.

_____, and _____. 1990. Early Mississippian blastoids from Western Montana. Bulletin of the Museum of Comparative Zoology, Harvard University, 152: 89-166.

TAPPAN, H. 1968. Primary production, isotopes, extinctions and the atmosphere. Palaeogeography, Palaeoclimatology,

Palaeoecology, 4:187-210.
UBAGHS, G. 1978. Skeletal morphology of fossil crinoids. In R. C. MOORE and C. TEICHERT (eds.), Treatise on Invertebrate Paleontology, Part T, Echinodermata 2, vol. 1, Geological Society of America and University of Kansas, Boulder and Lawrence , p. T160, T136, T188.
VERMEIJ, G. J. 1995. Economics, volcanoes, and Phanerozoic revolutions. Paleobiology, 21: 125–152.
VIRGILI, R., C. CERRANO, M. PONTI, M. T. LASUT & J. D. REIMER. 2020. Crinoid diversity and their symbiotic communities at Bangka Island (North Sulawesi, Indonesia). Marine Biodiversity, 50:90 https://doi.org/10.1007/s12526-020-01097-1
WATERS, J. A. 1988. The evolutionary palaeoecology of the Blastoidea. In C. R. C. PAUL and A. B. SMITH, (eds.), Echinoderm Phylogeny and Evolutionary Biology, Clarendon Press, Oxford. p. 215-233.

Museum of Paleontology, The University of Michigan
1105 North University Avenue, Ann Arbor, Michigan 48109-1085
Matt Friedman, Director

Contributions from the Museum of Paleontology, University of Michigan is a medium for publication of reports based chiefly on museum collections and field research sponsored by the museum. Jennifer Bauer and William Ausich, Guest Editors;
Jeffrey Wilson Mantilla, Editor.

Publications of the Museum of Paleontology are accessible online at: http://deepblue.lib.umich.edu/handle/2027.42/41251

Print (ISSN 0097-3556), Online (ISSN 2771-2192)

Contributions

from the Museum of Paleontology, University of Michigan

VOL. 34, NO. 5, PP. 54–62 JANUARY 18, 2022

RECENT ADVANCES IN ICHNOLOGY OF CRAWLING STALKED CRINOIDS

BY

PRZEMYSŁAW GORZELAK,[1] DOROTA KOŁBUK,[1] MAREK DEC,[2] TATSUO OJI,[3] KAZUMASA OGURI,[4] KRZYSZTOF BROM,[5] TOMASZ BRACHANIEC,[5] KAROLINA PASZCZA,[5] MARIUSZ A. SALAMON[5]

Abstract — Stalked crinoids have generally been overlooked when considering trace fossil makers — largely because they were long considered fully sessile. However, observations both in the field and in laboratory experiments revealed that some members of the order Isocrinida use their arms to actively move along the bottom, dragging the stalk behind. This activity leaves distinct traces on the sediment surface. Here, we re-examined time-lapse movies made in 2017 and crawling traces produced by stalked crinoids (the isocrinine *Metacrinus rotundus*) in previously published neoichnological experiments using new 3D digitization techniques (laser scanning and photogrammetry) in order to provide a more detailed 3D morphology of these traces. These data reveal some previously unnoticed crawling behavior and features of the traces of *M. rotundus*. We also demonstrate that crinoid-bearing beds are sometimes associated with ichnofossils that can be potentially interpreted as crinoid crawling traces. These data sources may provide more direct evidence of active locomotion in fossil crinoids.

"If I have seen further it is by standing on the shoulders of giants." — Isaac Newton. We dedicate this paper to celebrate the scientific career of our mentor and friend Prof. Tomasz K. Baumiller who has recently retired. Our correspondence and meetings (usually accompanied with beer) guided us to the big-picture level.

[1]Institute of Paleobiology, Polish Academy of Sciences, Twarda 51/55, 00-818 Warsaw, Poland (pgorzelak@twarda.pan.pl, dkolbuk@twarda.pan.pl).

[2]Polish Geological Institute-National Research Institute, Rakowiecka 4, 00-975 Warsaw, Poland (mdec@wp.pl).

[3]University Museum, Nagoya University, Furo-cho, Nagoya, 464-8601, Japan (oji@num.nagoya-u.ac.jp).

[4]Research Institute for Global Change, Japan Agency for Marine-Earth Science and Technology (JAMSTEC), 2-15 Natsushima-cho, Yokosuka, 237-0061, Japan, current affiliation: Danish Center for Hadal Research, University of Southern Denmark, Campusvej 55, 5230 Odense M, Denmark (ogurik@biology.sdu.dk).

[5]Faculty of Natural Sciences, University of Silesia in Katowice, Będzińska 60, 41-200 Sosnowiec, Poland (krzysztofbrom@gmail.com, tomasz.brachaniec@o2.pl, karolinapaszcza@gmail.com, paleo.crinoids@poczta.fm).

INTRODUCTION

Motility in Recent crinoids has long been known. In particular, the crawling, and in some taxa swimming abilities of feather stars – those members of order Comatulida that shed the postlarval stalk – are well documented (e.g., Clark, 1915; Meyer et al., 1984; Shaw and Fontaine, 1990). Since at least the middle 1980s, however, evidence began accumulating that some stalked sea lilies (isocrinids = order Isocrinida) can also relocate by crawling with their arms along the substrate, dragging the stalk behind them (Messing, 1985). During crinoid locomotion, the crawling arms and passively pulled stalk interact with the sediment surface. *Surprisingly, however, little attention* has been paid to the traces produced during this activity. Notably, deep sea distribution of post-Paleozoic stalked crinoids and specific substrate preference of some species (carbonate hardgrounds), make ichnological study rather difficult.

Messing (1985: p. 189) was probably the first who noticed isocrinid locomotion traces: "…a single isocrinid (*E. parrae*?) was observed detached and crawling along the substrate. Although it did not move during the 5 min of observation, there was an obvious drag mark behind…". This observation was subsequently reported by Messing et al. (1988: p. 481) in the following way: "During dive JSL-I-1362 (17 June 1983, off Grand Bahama I., 403 m), a single isocrinid [probably *Endoxocrinus parrae* (Gervais)] was found detached and lying on its side on open sediment with an obvious drag mark over 1 m long behind its stalk". In the same paper the latter authors also mentioned (p. 482) that: "In September 1986, one of us (CGM) observed a *C. asterius* in the crawling posture in 260 m, the sediment slope around its crown bearing short radiating scratch marks. An area of confused but similar marks scored the sediment surface behind the crinoid, between it and a boulder about 2 m away". Unfortunately, no photos or drawings of the traces were provided in these papers. More recently, Baumiller and Messing (2007: fig. 4) took a major step forward and provided the first video footage, which shows a displacement of the sediment surface left by the stalk of crawling *Neocrinus decorus*. However, these video footages were shot at too low an angle to recognize fine details of the traces. Instead, the latter authors provided a photo of distinct traces produced by a crawling stalkless crinoid (comatulid species *Davidaster rubiginosa*), which nicely illustrated the ichnological potential of crinoids (Baumiller and Messing, 2007: fig. 5).

Recently, Brom et al. (2018) illustrated and described the morphology of the locomotory traces produced by an isocrinine crinoid in detail via neoichnological experiments on the shallowest living stalked isocrinine, *Metacrinus rotundus*. They reported that the locomotory traces are generally comprised of wide, sometimes weakly sinuous median trails consisting of few semicircular and parallel or intersecting furrows left by the stalk and cirri dragged on the bottom, and lateral short tracks of various shapes made by the crawling arms. Previously, Neto de Carvalho et al. (2016) illustrated an unidentified isocrinid fossil from the Middle Jurassic of Portugal that was found at the end of its trail, which they described as a new ichnospecies, *Krinodromos bentou*, interpreted as a mortichnial crawling trail. They diagnosed this new ichnotaxon as follows: "a narrow and flat central area with an irregular winding furrow, or almost no sedimentary disruption, bordered by shallow and large grooves externally limited by irregular piles of sediment" (p. 47).

Gorzelak et al. (2020) further explored the ichnological potential of stalked crinoids by demonstrating that autotomized arms of *Metacrinus rotundus* display vigorous movements that may produce traces on the sediment surface. These traces are comprised of straight or arched grooves, usually arranged in radiating groups, and shallow furrows. They (Gorzelak et al., 2020) also reported similar traces associated with detached arms of the oldest (Early Triassic) stem-group isocrinine (*Holocrinus*).

In this paper we re-examine our data collected during neoichnological experiments with *Metacrinus rotundus* conducted in 2017 (Brom et al., 2018). In particular, we provide unpublished time-lapse movies that reveal some previously unnoticed crawling behavior of isocrinine crinoids. We also illustrate for the first time some locomotion traces not illustrated in Brom et al. (2018) and apply a new 3D digitization techniques (laser scanning) to selected gypsum counterparts of the traces in order to provide a more detailed 3D morphology. We then show that similar traces are likely to be found at least as early as in the Triassic.

INSTITUTIONAL ABBREVIATIONS

ZPAL	—	Institute of Paleobiology of the Polish Academy of Sciences in Warsaw, Poland (ZPAL V.42ICH_N1-4) – 4 fragments of counterparts: gypsum casts of Recent traces.
GIUS	—	University of Silesia in Katowice, Faculty of Natural Sciences, Institute of Earth Sciences, Poland (GIUS 8-3696) – 1 counterpart: modeling clay cast of Triassic traces.

MATERIALS AND METHODS

Analyzed time-lapse movies (movies 1–6 in Supplementary Online Material; see also Fig. 1) and crawling traces were captured during neoichnological experiments performed in 2017 by one of us (KB). These data were published in part by Brom et al. (2018). For a detailed description of sampling and handling of crinoid specimens and movie acquisition see Brom et al. (2018). In these experiments light-gray, fine-grained sand from the Pacific coast (Nishiakazawa beach; 34.652660N, 137.363772E) was used. 3D models (.ply files

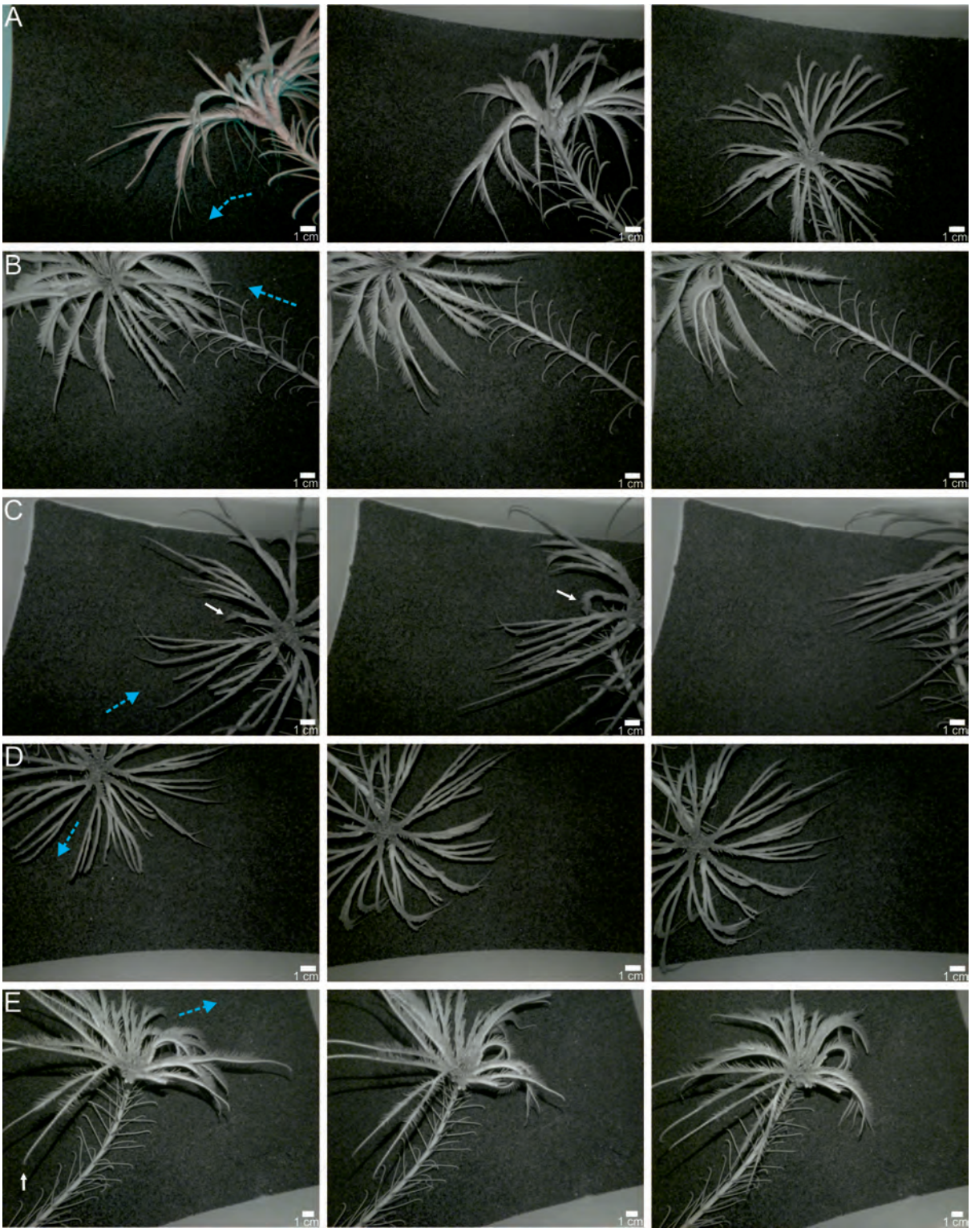

FIGURE 1— Still frames showing different crawling movements of *Metacrinus rotundus*. Rows A–E each represent a separate trial. The direction of movement is indicated by dotted blue arrows. Note that nearly all the arms can be involved in locomotion; the animal can be pulled with the leading arms and pushed with the trailing arms (e.g., white arrows).

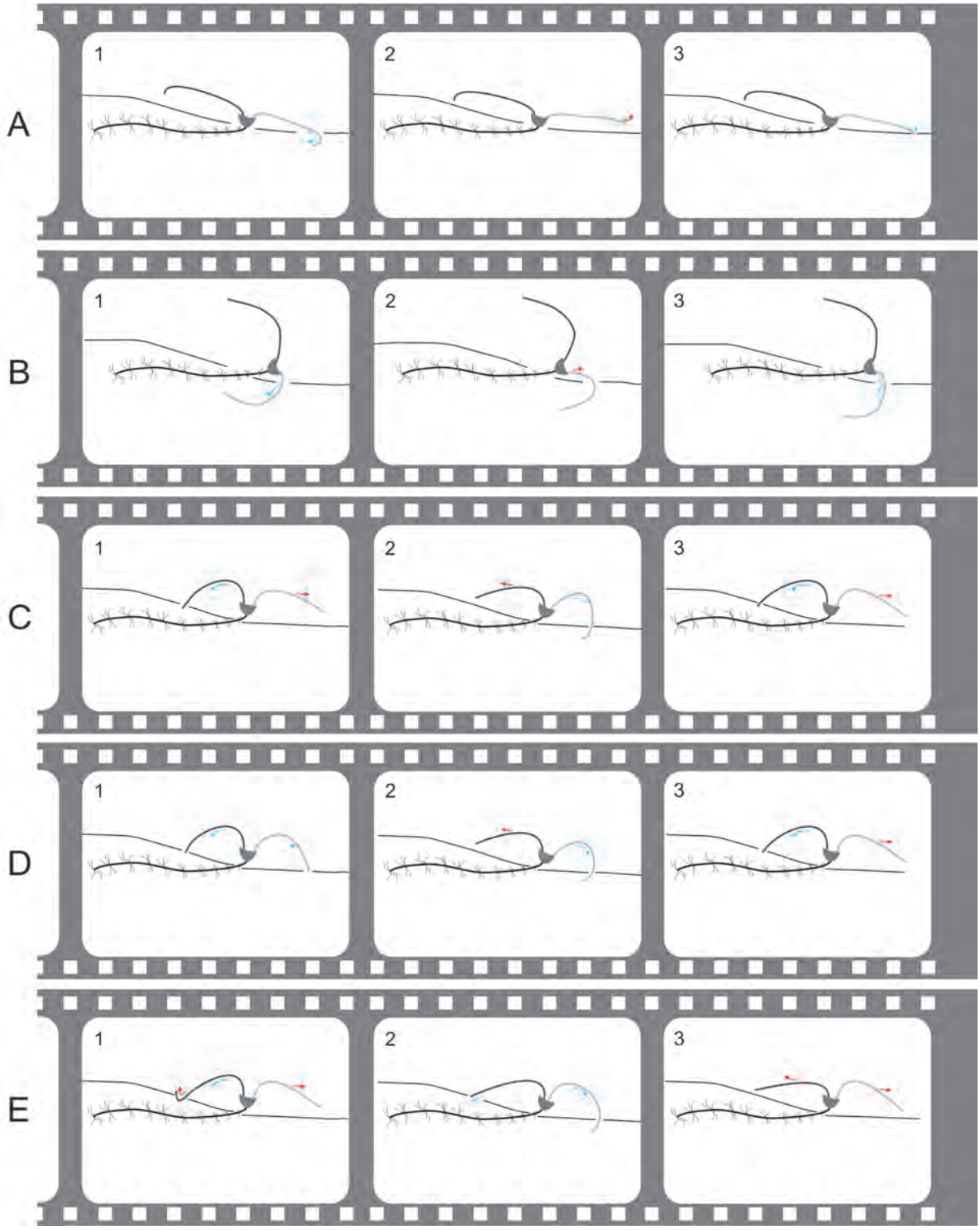

FIGURE 2— Schematic diagrams of the three major types of isocrinine locomotion (A and B modified after Baumiller and Messing, 2007: fig. 2; C and D modified after Birenheide and Motokawa, 1994: fig. 1). **A**, the finger-tip pull. **B**, the elbow-crawl. **C**–**E**, the pole push & pull. Blue arrows indicate aboral arm flexure; red arrows indicate oral arm flexure.

1–4 in Supplementary Online Material) of selected traces were acquired with a Shining 3D EinScan Pro 2X 3D scanner fixed on a tripod, EXScan Pro 3.2.0.2 software, and then processed with Meshlab 1.3.3, Blender 2.82 and ParaView 5.80 to get the false-color depth maps (see Gorzelak et al., 2020).

A set of photographs of trace fossils associated with the holocrinid stem fragments was taken at different angles. A 3D model (.ply file 5 in Supplementary Online Material) and false-color depth map were acquired by means of photogrammetric technique using Visual SFM 0.5.26 and the MeshLab 1.3.3 or Agisoft Photoscan 1.2.0. These traces were found on the surface of a large (ca. 1 m) limestone block belonging to the so-called Karchowice Fm. (Middle Triassic, middle Anisian) of Tarnów Opolski (Poland) (Szulc et al., 2015).

Quantitative data of the traces (widths, lengths, intersection angle — in map view — between the primary median trail and the grooves flanking the axial trail on both sides) were obtained using ImageJ (Rasband, 1997-2018).

CRAWLING BEHAVIOUR

Baumiller and Messing (2007) distinguished two major types of crinoid crawling: the so-called finger-tip pull (Fig. 2A) and elbow crawl (Fig. 2B). In the first type, the arms are arranged more or less radially and oriented sub-parallel to the substrate (with ambulacra facing up) (Fig. 2A1–3). The movement is generated via aboral flexure of the distal tips of the leading arms only, which press against the bottom and displace the crinoid forward (power phase) (Fig. 2A1). In the subsequent recovery phase the distalmost parts of the leading arms lift off the bottom and extend orally (Fig. 2A2). On the other hand, in the elbow crawl, movement is generated by aboral flexure of proximal articulations of the leading arms, which undergo a sequence of power and recovery strokes (Fig. 2B1–3). During this locomotion, all the arms are strongly flexed aborally and point their distal tips toward the stalk but only the pinnule-bearing oral side of the middle third to distal half of the arm adjacent to the substrate creates traction with the bottom (Fig. 2B1, 3).

Birenheide and Motokawa (1994) first briefly described a rather different mode of locomotion in *Metacrinus rotundus* during incubation in aquaria. They observed movement via pulling with the leading arms and, from time to time, via pushing with the back arms. More specifically, during pulling, the leading arms straighten by extending orally, anchor with the distal tips on the substrate, and then strongly bend aborally. This locomotion strategy was sometimes supplemented by trailing arms, which flex aborally, anchor with the distal tips on the bottom, and straighten by oral bending. Herein, we supplement these previous observations on *M. rotundus* and provide further direct proof (time-lapse movies) for its mode of locomotion, which reveal some previously unnoticed crawling behavior (Figs. 1, 2C–E, movies 1–6 in Supplementary Online Material).

The crawling pattern observed by us in *M. rotundus* is somewhat intermediate between the finger-tip pull and elbow crawl (herein referred to as the "pole pull and push" strategy). However, the movement of the leading arms seems to be mostly generated by aboral flexure at median articulations (although distal and proximal articulations may also be involved). The ambulacral pinnule-bearing surfaces of the arms during the power phase are not entirely oriented upward and sub-parallel to the substrate, as in the case of finger-tip pull; rather, some of them (from the more distal side) are more flexed aborally, though not as much as in the elbow-crawl (Fig. 2C vs. 2B). The distal arm tips point more toward the substrate (Figs. 2C2, D2) rather than toward the stalk. As a result, the distal arms still generate most of the traction against the bottom. However, both the non-pinnulate arm tips and the pinnule-bearing oral side of the distal arm contact the substrate (Fig. 2C2). Pulling with the leading arms via aboral flexure may alternate with pushing by the orally flexing trailing arms (Figs. 2C1–3), or both leading and trailing arms may flex simultaneously (Figs. 2D1–3). For the pushing power stroke, the trailing arms, which anchor to the substrate by their tips (Figs. 2C1, D1), straighten orally, while the recovery involves lifting the arm tips off the substrate and aboral arm flexure (Figs. 2C2, D2). The distalmost parts of the trailing arms may also curl orally while still against the substrate (Fig. 2E1); they suddenly straighten as they push off the bottom (Figs. 2E2–3; see movie 6 in Supplementary Online Material).

In our experiments, *Metacrinus* specimens commonly turned left or right during locomotion (Fig. 1, movies 3–6 in Supplementary Online Material). In such cases, nearly all the arms are arranged radially, and could be involved in "pole pull and push" locomotion.

CRAWLING TRACES

The crawling arms passively pull the cirriferous stalk, which leaves similar traces on the sediment surface in all types of locomotion. 3D digitization techniques applied to the traces produced in neoichnological experiments (Brom et al., 2018) provided more detailed morphologic data on these traces. Their revised description is given below.

Description (slightly emended after Brom et al. 2018).— The most common trail architecture, produced during locomotion on a more or less straight path, are horizontal traces comprised of median trails left by the cirriferous stalk dragged on the bottom (fig. 2a, b, d, e in Brom et al., 2018, see also Fig. 4B, C), and lateral short tracks made by the crawling arms (fig. 2a, c, d, f in Brom et al., 2018, see also Fig. 4B, C). Median trails can be long, rather smooth, and comprised of up to four semicircular and parallel furrows, ~ 3–8 mm (mean: 5 mm) wide. However, the width and depth of each furrow may vary along the course of the trace. Likewise, transitions between single-, double-, triple-, and four-lobed trails are present.

The lateral depressions or grooves radiate forward at different, generally low angles (5°–53°) relative to the median

trails and start from the edge of the median trails or a few centimeters away. They are straight, sometimes triangular, oval or slightly curved, short (0.5–4.8 cm long; mean: 1.9 cm), rather shallow (~ 0.2–2 mm) and narrow (~ 1–9 mm) (fig. 2c, f in Brom et al., 2018; see also Fig. 4B, C). The length-to-width ratio of these tracks ranges from 2.5 to 8.9 (mean: 6.8). They may intersect each other at different angles (forming check marks or cross marks) (Fig. 4B, C).

The median trails produced by turning individuals are similar. They are commonly sinuous and comprised of two to four smooth, semicircular parallel or intersecting furrows, 3–9 mm wide (mean: 6.2 mm), left by the cirriferous stalk (fig. 3a, b, d, e in Brom et al., 2018, see also Figs. 3, 4A, D). However, the lateral depressions (fig. 3c, f in Brom et al., 2018, see also Fig. 3) made by the arms may orient up to about 90° relative to the median trail and may start more than a few centimeters away. These tracks are commonly distributed asymmetrically and are sometimes present on only one side. Their morphology and size are virtually the same as the lateral tracks produced during locomotion on a more or less straight path.

DISCUSSION

Re-examination of our time-lapse movies made in 2017 revealed some previously unnoticed crawling behavior of stalked crinoids. More specifically, we show that crawling *M. rotundus* may display a complex moving behavior, herein referred to as the pole pull and push pattern, that takes a variety of forms. As this movement may form distinct traces on the sediment surface, it has some ichnological potential. Indeed, Neto de Carvalho et al. (2016) ascribed similar traces from the Middle Jurassic to crawling activity of a crinoid (referred to the ichnospecies *Krinodromos bentou*), and Brom et al. (2018) suggested that similar ichnofossils are likely to be present as early as in the Triassic. Notably, following the end-Permian mass extinction, crinoids underwent major functional changes, i.e., the predominantly sessile forms of the Paleozoic were largely replaced by highly motile taxa (Baumiller and Messing, 2007, Gorzelak et al., 2016). This change is thought to be related to increased predation pressure during the so-called Mesozoic Marine Revolution (Baumiller et al., 2010; Gorzelak et al., 2012). Thus, especially post-Paleozoic forms were certainly able to produce traces on the sediment surface, although some Paleozoic taxa such as advanced eucladids may have also possessed crawling abilities (e.g., Baumiller and Messing, 2007; Donovan, 2012).

Holocrinids (order Holocrinida sensu Jaekel, 1918), which were among the first crinoids to appear following the end-Permian extinction, developed highly flexible muscular arms and specialized autotomy planes at the distal nodal facets in their stalk, which allowed them to detach from the substrate and crawl (Baumiller and Hagdorn, 1995; Hagdorn, 2011; Gorzelak, 2018). Early Triassic holocrinids also likely displayed another anti-predatory trait—post-autotomy arm thrashing—as inferred from characteristic traces found

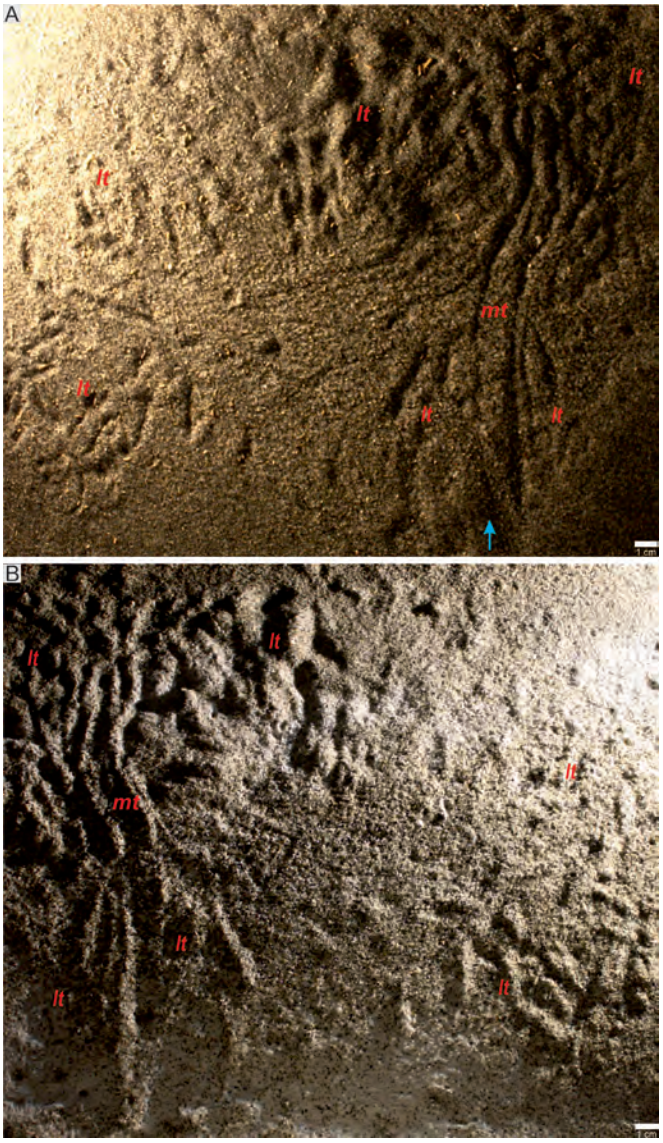

FIGURE 3— Surface features produced during locomotion of a Recent crinoid *Metacrinus rotundus*. Photographs of traces impression **A** and a positive gypsum cast taken from it **B**. Lighting is from the upper left in A and upper right in B. Blue arrow indicates direction of locomotion, lt - lateral tracks, mt - median trail.

associated with their detached arms that are similar to those produced by autotomized arms of Recent crinoids (Gorzelak et al., 2020).

Herein, we illustrate one example of a trail that can be potentially interpreted as a putative holocrinid crawling trail (Fig. 4E–G). It is comprised of median trails and some indistinct lateral short tracks. This median trail is ~25 cm long, rather smooth, and comprised of up to three semicircular and parallel furrows 2–5 mm wide (mean: 4 mm). A clear transition is visible between triple- and double-lobed trails (Fig. 4E). The lateral depressions or grooves (7–14 mm long;

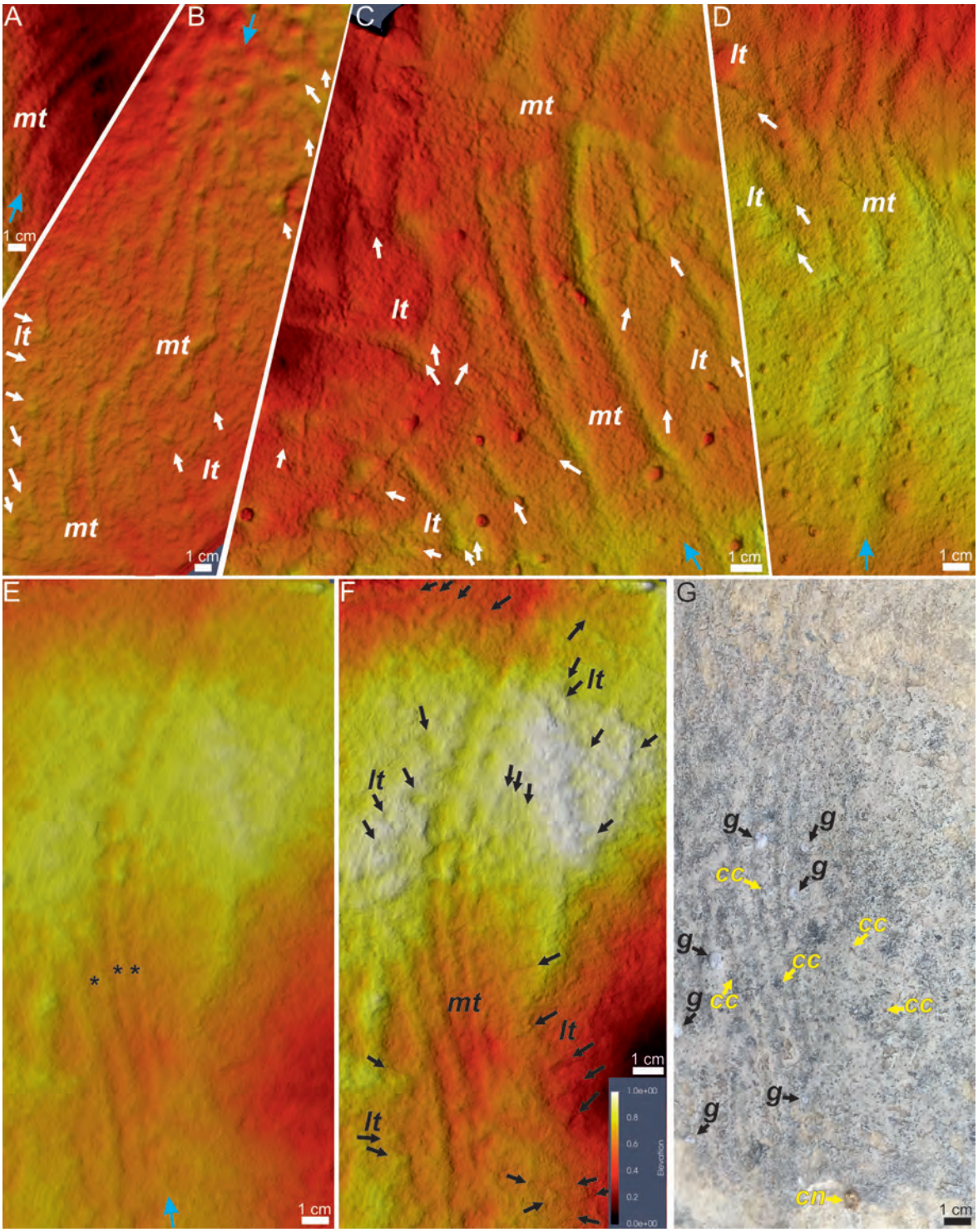

FIGURE 4 — Recent (A–D) and fossil (E–G) crinoid traces. **A**–**D**, false-color depth maps obtained from three-dimensional scans of gypsum casts of traces produced by a Recent crinoid *Metacrinus rotundus* (white arrows). **E**, **F**, false-color depth maps based on photogrammetry of the Middle Triassic traces (black arrows), GIUS 8-3696. Elevation in F has been increased (×2) to enhance depth contrast. G, photograph of the Middle Triassic slab (Karchowice Fm., Tarnów Opolski, GIUS 8-3696) containing crinoid traces and body fossils (red arrows) and *Coelostylina*-like gastropods (black arrows). Abbreviations: *cc*, crinoid cirrals; *cn*, crinoid nodal; *g*, gastropods; *lt*, lateral tracks; *mt*, middle trail.

mean: 11 mm) spread at angles ranging from 16° to 81° relative to the median trails. Notably, this trace was found on a bedding surface containing some holocrinid ossicles (one nodal and few isolated cirrals). Although the surface also includes a few small and poorly preserved *Coelostylina*-like gastropods, and although gastropods do produce roughly similar traces (ascribed to the ichnogenus *Archaeonassa* Fenton and Fenton, 1937; see Buckman, 1994: fig. 2, Baucon and Felletii, 2013: fig. 9a), their trails typically consist of a median furrow (which can be variably ornamented by oblique or transverse elements) flanked by just two regular lateral ridges. Unlike typical *Archaeonassa* traces, the putative holocrinid Triassic traces are more irregular and display transitions between double- and triple-lobed trails, as well as some lateral depressions or grooves, just like the crawling traces of Recent crinoids.

CONCLUSIONS

In this paper we describe some previously unnoticed crinoid crawling behavior and features of the traces produced during this activity. Crinoid locomotory traces have the potential to be preserved as ichnofossils. Thus, rock slabs preserving trace fossils associated with crinoid remains certainly *deserve* in-*depth investigation.* Such ichnological evidence may be particularly valuable, because it may provide more direct proof of crawling activities in fossil crinoids.

ACKNOWLEDGMENTS

This study was supported in part by PROM programme 2018/2019 – International scholarship exchange of PhD candidates and academic staff, Project No. POWR.03.03.00-IP.08-00-P13/18 (K.B.). Sampling of crinoid specimens was enabled thanks to the support from Nagoya University Grant to T.O. The underwater camera was constructed thanks to the support from Japan Society of the Promotion of Science (Kakenhi, Grant Number 15K12197). This paper was completed while M.A.S. was a recipient of a grant from the National Science Centre (Grant Number UMO-2018/31/B/ST10/00387). Dawid Dróżdż and Tomasz Szczygielski (both from Institute of Paleobiology, PAS) are acknowledged for help in gathering 3D models. Finally, we would like to thank reviewers (Charles Messing and James Thomka) for their comments, and William Ausich and Jennifer Bauer for their invitation to contribute to this special volume.

Supplemental Online Material:
https://dx.doi.org/10.7302/3815

LITERATURE CITED

BAUCON, A., and F. FELLETII. 2013. Neoichnology of a barrier-island system: The Mula di Muggia (Grado lagoon, Italy). Palaeogeography, Palaeoclimatology, Palaeoecology, 375: 112–124.

BAUMILLER, T. K., and H. HAGDORN. 1995. Taphonomy as a guide to functional morphology of *Holocrinus*, the first post-Paleozoic crinoid. Lethaia, 28: 221–228.

_____, and C. G. MESSING. 2007. Stalked crinoid locomotion, and its ecological and evolutionary implications. Palaeontologia Electronica, 10: 2A, 10 p.

_____, M. A. SALAMON, P. GORZELAK, R. MOOI, C. G. MESSING, and F. J. GAHN. 2010. Post-Paleozoic crinoid radiation in response to benthic predation preceded the Mesozoic marine revolution. Proceedings of the National Academy of Sciences of the United States of America, 107: 5893–5896.

BIRENHEIDE, R., and T. MOTOKAWA. 1994. Morphological basis and mechanics of arm movement in the stalked crinoid *Metacrinus rotundus* (Echinodermata, Crinoidea). Marine Biology, 121: 273–283.

BROM, K. R., K. OGURI, T. OJI, M. A. SALAMON, and P. GORZELAK. 2018. Experimental neoichnology of crawling stalked crinoids. Swiss Journal of Palaeontology, 137: 197–203.

BUCKMAN, J. O. 1994. *Archaeonassa* Fenton and Fenton 1937 reviewed. Ichnos: An International Journal for Plant and Animal Traces, 3:3, 185–192.

CLARK, H. L. 1915. The comatulids of Torres Strait: with special reference to their habits and reactions. Papers from the Department of Marine Biology, Carnegie Institute, Washington, 8: 97–125.

DONOVAN, S. K. 2012. Was autotomy a pervasive adaptation of the crinoid stalk during the Paleozoic? Geology, 40: 867–870.

FENTON, C. L., and M. A. FENTON. 1937. *Archaeonassa*, Cambrian snail trails and burrows. American Midland Naturalist, 18: 454–456.

GORZELAK, P. 2018. Microstructural evidence for stalk autotomy in *Holocrinus*—the oldest stem-group isocrinid. Palaeogeography, Palaeoclimatology, Palaeoecology, 506: 202–207.

_____, M. A. SALAMON, and T. K. BAUMILLER. 2012. Predator-induced macroevolutionary trends in Mesozoic crinoids. Proceedings of the National Academy of Sciences of the United States of America, 109: 7004–7007.

_____, M. A. SALAMON, D. TRZĘSIOK, R. LACH, and T. K. BAUMILLER. 2016. Diversity dynamics of post-Palaeozoic crinoids—in quest of the factors affecting crinoid macroevolution. Lethaia, 49: 231–244.

_____, M. A. SALAMON, K. BROM, T. OJI, K. OGURI, D. KOŁBUK, M. DEC, T. BRACHANIEC, and T. SAUCÈDE. 2020. Experimental neoichnology of post-autotomy arm movements of sea lilies and possible evidence of thrashing behaviour in Triassic holocrinids. Scientific Reports 10: 15147.

HAGDORN, H. 2011. Triassic: the crucial period of post-Palaeozoic crinoid diversification. Swiss Journal of Palaeontology, 130: 91–112.

JAEKEL, O. 1918. Phylogenie und System der Pelmatozoen. Palaeontologische Zeitschrift 3(1): 1–128.

MESSING, C. G. 1985. Submersible observations of deep-water crinoid assemblages in the tropical western Atlantic Ocean. Fifth International Echinoderm Conference, A. A. Balkema, Galway: 185–193.

_____, M. C. ROSESMYTH, S. R. MAILER, and J. E. MILLER. 1988. Relocation movement in a stalked crinoid (Echinodermata). Bulletin of Marine Science, 42: 480–487.

MEYER, D. L., C. A. LAHAYE, N. D. HOLLAND, A. C. ARENSON, and J. R. STRICKLER. 1984. Time-lapse cinematography of feather stars (Echinodermata: Crinoidea) on the Great Barrier Reef, Australia: demonstrations of posture changes, locomotion, spawning and possible predation by fish. Marine Biology, 78: 179–184.

NETO DE CARVALHO, C., B. PEREIRA, A. KLOMPMAKER, A. BAUCON, J. A. MOITA, P. PEREIRA, et al. 2016. Running crabs, walking crinoids, grazing gastropods: behavioral diversity and evolutionary implications of the Cabeço da Ladeira Lagerstätte (Middle Jurassic, Portugal). Comunicações Geológicas, 103 (Especial I): 39–54.

RASBAND, W.S. 1997-2018. ImageJ, U. S. National Institutes of Health, Bethesda, Maryland, USA, https://imagej.nih.gov/ij/.

SHAW, G. D., and A. R. FONTAINE. 1990. The locomotion of the comatulid *Florometra serratissima* (Echinodermata: Crinoidea) and its adaptive significance. Canadian Journal of Zoology, 68: 942–950.

SZULC, J., MATYSIK, M., and HAGDORN, H., 2015. The Mid-Triassic Muschelkalk in southern Poland: shallow-marine carbonate sedimentation in a tectonically active basin. In: HACZEWSKI, G. (ed.), Guidebook for field trips accompanying IAS 31st Meeting of Sedimentology held in Kraków on 22nd-25th of June 2015. Polish Geological Society, Kraków, pp. 195–216.

Museum of Paleontology, The University of Michigan
1105 North University Avenue, Ann Arbor, Michigan 48109-1085
Matt Friedman, Director

Contributions from the Museum of Paleontology, University of Michigan is a medium for publication of reports based chiefly on museum collections and field research sponsored by the museum. Jennifer Bauer and William Ausich, Guest Editors; Jeffrey Wilson Mantilla, Editor.

Publications of the Museum of Paleontology are accessible online at: http://deepblue.lib.umich.edu/handle/2027.42/41251

Print (ISSN 0097-3556), Online (ISSN 2771-2192)

Contributions

from the Museum of Paleontology, University of Michigan

VOL. 34, NO. 6, PP. 63–81 JANUARY 18, 2022

MICROMORPHY OFFERS EFFECTIVE DEFENSE AGAINST PREDATION: INSIGHTS FROM COST-BENEFIT ANALYSES OF THE MIOCENE MICROGASTROPOD PREDATION RECORD FROM KERALA, INDIA

BY

ANUPAMA CHANDROTH[1†] AND DEVAPRIYA CHATTOPADHYAY*[2]

Abstract — Predation, an important driver of natural selection, is studied in the fossil record using quantifiable traces like drill holes produced by gastropods and repair scars produced after durophagous attacks. Despite the abundance of such records in molluscan prey, predation records of micromolluscs (<5mm) remain largely unexplored. Using a Miocene assemblage of microgastropods from the Quilon Limestone, India, we established the predator-prey dynamics with the help of cost-benefit analyses. The overall predation intensity, measured by drilling frequency (DF) and repair scare frequency (RF) is low (DF = 0.06, RF= 0.04). The predation intensity does not depend on the relative abundance of prey families suggesting a non-random prey selection regardless of the encounter frequency. Predation is selective as revealed by higher predation observed in prey of specific family identity, ornamentation, and body size. The smallest size class has the lowest DF and RF supporting a negative size refugia. Higher frequency of incomplete drill holes (IDF) among prey in larger size classes and ornamented groups implies morphological defenses that result in higher failure. Microgastropods show a lower predation intensity than macrogastropods of the same family in a global comparison of coeval records. Results of the cost-benefit analyses explain this difference; the net energy gain from predatory drilling is found to increase monotonically with increasing prey size making the small prey less beneficial. Because the predators try to maximize net energy gain from a predatory attack, the microgastropod prey characterized by relatively low net energy yield would not be preferred in the presence of larger prey. Micromorphy, therefore, appears a viable strategy for the prey group to adopt as an evolutionary response against predation, especially in resource-limited conditions that fail to support large body size.

[1] Department of Earth sciences, Indian Institute of Science Education and Research (IISER) Kolkata, Mohanpur, WB 741246, INDIA
[2] Department of Earth and Climate Science, Indian Institute of Science Education and Research (IISER) Pune, Dr. Homi Bhaba Road, Pashan, Pune, MH 411008, INDIA
[†] Present Address: Department of Earth and Atmospheric Science, Indiana University, Bloomington, 1001 E 10th Street, IN 47408, USA

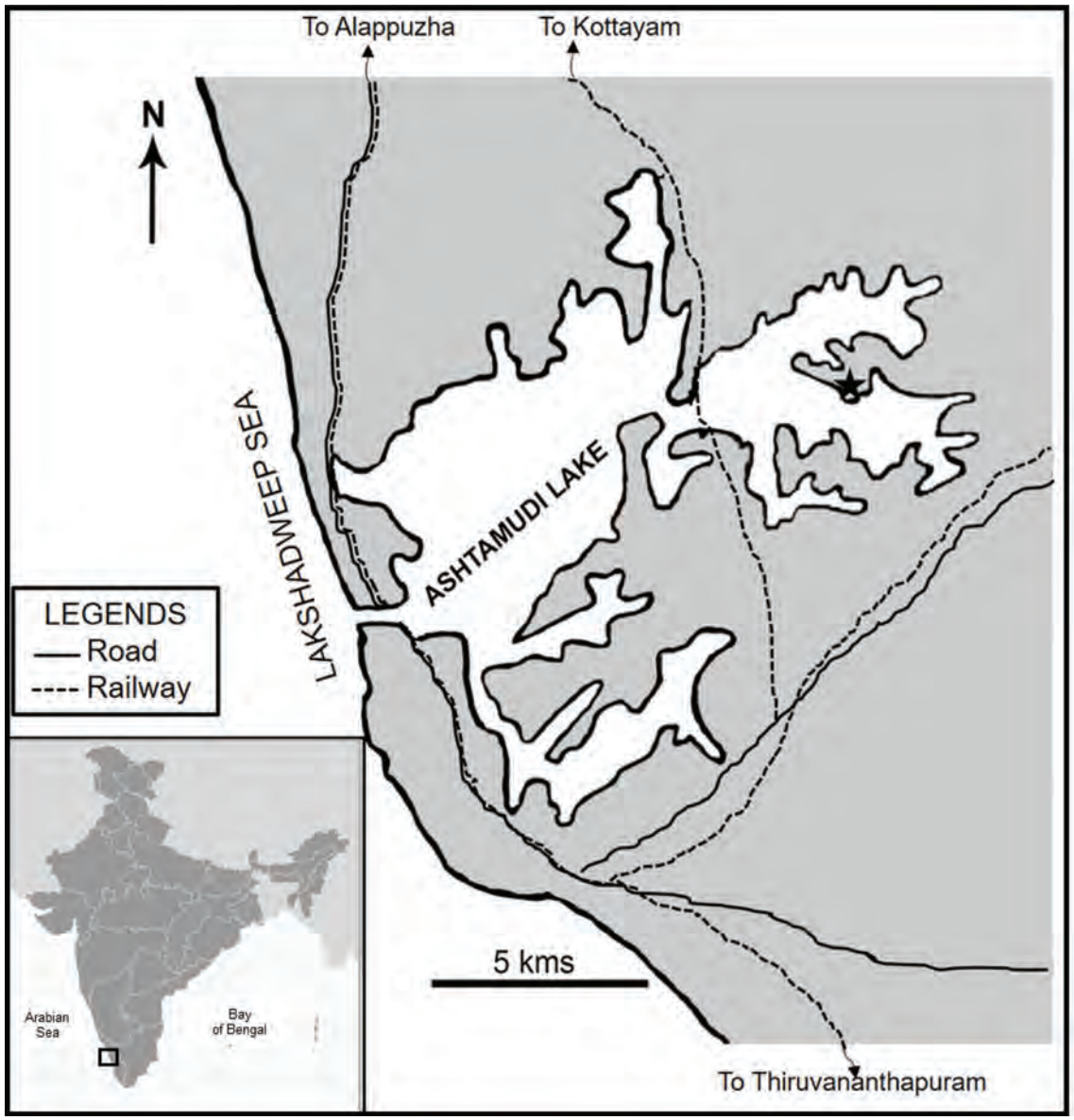

FIGURE 1 — Location of the studied locality with the map of India (inset). The star represents the location of the Quilon Limestone bed (Kerala). Modified after Chattopadhyay et al. (2020: Fig. 1.)

INTRODUCTION

Predation is an important ecological interaction and one of the major drivers of natural selection (Kitchell, 1986; Vermeij, 1987; Kelley and Hansen, 1993). It also plays a vital role in shaping community structure (Hines et al., 1990; Barnes et al., 2010). Direct evidence of predation events in the fossil record, such as the ones "caught in the act" are rare. Trace fossils like predatory drill holes and repair scars are common evidence of predation that can be studied quantitatively (Kelley et al., 2003). Complete drill holes represent a lethal attack in contrast to the traces of non-lethal attacks such as incomplete drill holes (but see Kowalewski, 2002) and repair scars. These traces reveal various aspects of predation (including the predator's identity, prey preference, and success rate) (Klompmaker et al., 2019). The fossil record of predatory traces proved crucial in understanding the evolution of marine invertebrates and restructuring of marine ecosystems as a response to biotic interactions (Vermeij et al., 1981; Huntley and Kowalewski, 2007).

The relative size of the prey and its predator often determines the outcome of a predatory interaction and plays an important role in shaping the evolutionary trajectory of the prey groups (Vermeij, 1987; Klompmaker et al., 2017).

In drilling predation, the prey size preference is primarily governed by the energy maximization of the predator for each attack (Kitchell et al., 1981; Chattopadhyay and Baumiller, 2009). Patterns like size refugia are common among the molluscs where prey greater than a specific size class are seldom attacked; the larger prey tend to be more difficult to capture and subdue (Leighton, 2002; Harper et al., 2009). Small prey is not always the most preferred size class either. Recent rhynchonelliform brachiopods from the Southern Hemisphere and tropical Northern Hemisphere demonstrated a lower intensity of shell-breaking predation among micromorph species that dominate the tropics (Harper and Peck, 2016). A fossilized assemblage of microbivalves (<5mm) also revealed a lower intensity of drilling predation in the smaller size class (<1mm) supporting the existence of a negative size refugia (Chattopadhyay et al., 2020). Such predation resistance among extremely small shelled invertebrates, such as molluscs and brachiopods, points to a complex relationship between size and predation intensity. To understand whether small size is an evolutionary response to predation, the predation record of micromolluscs needs to be explored. Except for the microbivalves, the predation record of microfossils primarily constitutes of taxa such as foraminifera (Culver and Lipps, 2003) and ostracods (Maddocks, 1988; Rayment and Elewa, 2003); microgastropods (<5mm) have not been studied extensively for their predation record.

Here we studied the microgastropod assemblage from the early Miocene Quilon Limestone bed from southwest India (Quilon, Kerala) (Harzhauser, 2014) to address the following questions:

1. What controls selectivity of microgastropod prey?
2. Is predation of microgastropods viable from the cost:benefit perspective?
3. Are predator-prey dynamics significantly different in microgastropods in comparison to macrogastropods?

MATERIALS AND METHODS

Locality and Collection

The field locality is situated on the cliffs along the shores of Ashtamudi Lake, near Padapakkara village, Kerala, India (N 08° 58’36”, E 076° 38’08”; Fig. 1). The collection protocol has been described in detail in Chattopadhyay et al. (2020)

From the collected bulk sample, 371.8g of the sample was processed. The bulk sample was soaked in normal water for 5–6 days to loosen the sediments and subsequently, wet sieved using an 18µm sieve to remove the sedimentary particles. The remaining sediments were then dried, sieved, and classified into different size classes using a set of five sieves (mesh sizes 63, 60, 35, 25, 18µm). We studied the processed samples under the microscope and identified specimens up to the family level using the detailed study by Dey (1961) and Harzhauser (2014). The identified specimens were categorized into three size classes, small (less than 1mm), medium (1–2mm), and large (greater than 2mm). The specimens were also classified into two groups based on ornamentation: the ones with smooth shells were classified as non-ornamented (Buccinidae, Eulimidae, Marginellidae, Naticidae, Phasianellidae, Scaliolidae, and Turbinidae) and rest as ornamented.

Specimens with any visible signs of predation (complete drill hole, incomplete drill hole, repair scar) were separated. Complete drillholes were further categorized into naticid drilling characterized by their parabolic shape, bevelled edges and muricid drill holes are cylindrical (Kabat, 1990; Kelley and Hansen, 2003). We used two protocols for characterizing the location of drill holes. In the first protocol, the gastropod shell was divided into two equal zones radially (apertural and abapertural) and each drill hole site was characterized using this scheme. In the second protocol, the gastropod shell was divided into three sectors vertically (top, central, basal) from the apex. Considering the total height of a specimen, the sectors were assigned based on the relative distance from the apex as the top (33% at the top), basal (33% at the base), and central (remaining 33% at the centre). We took detailed photographs of drilled specimens using a Nikon D700 attached to an Olympus SZX16 microscope. We processed the images using Image J to measure the size of the specimens and drill holes. The undrilled specimens were categorized into size-bins based on the mesh size of the sieve. For detailed imaging, representative specimens were imaged using an EVO LS10 Scanning Electron Microscope (SEM) (Carl Zeiss, Germany) where specimens were mounted on an aluminium stub using conductive carbon adhesive tape and imaged directly with low EHT (2–3 kV).

Drilling predation on Miocene macrogastropods from the same biogeographic region (Goswami et al, 2020) and other localities (Hoffmeister and Kowalewski, 2001; Kelley and Hansen, 2006; Sawyer and Zuschin, 2011) were compiled for comparative analysis. The family-specific predation matric is computed using the raw data if it is not reported in the published record.

Analysis

Drilling frequency (DF), a measure of successful predation attempts, is calculated by dividing the number of specimens with complete drill holes by the total number of specimens.

$$DF = \frac{N_D}{N} \qquad (1)$$

Where, N_D = number of specimens with complete drill hole

N= Total number of specimens.

The incomplete drilling frequency (IDF), also referred to as “prey effectiveness” is calculated by dividing the total number of incomplete drill holes by the total number of drilling attempts (Chattopadhyay & Dutta, 2013).

$$IDF = \frac{N_I}{(N_I + N_D)} \qquad (2)$$

Where, N_D = number of specimens with complete drill hole

N_I = number of incomplete drill holes

To estimate the intensity of repair scar (RF), the total number of specimens with repair scar was divided by the total number of individuals.

$$RF = \frac{N_R}{N} \quad (3)$$

Where, N_R = number of specimens with repair scar

N= Total number of specimens

To estimate the occurrence of multiple predation traces, we calculated MULT as the total number of holes in the specimens with multiple drill holes, divided by the total number of drilling attempts (Kelley and Hansen, 1993).

$$MULT = \frac{N_m}{(N_I + N_D + N_{msp})} \quad (2)$$

Where, N_m = total number of drillholes on the specimens with multiple drill holes

N_D = number of specimens with complete drill hole

N_I = number of incomplete drill holes

$N_{msp} = N_m$ – number of specimens with multiple drillholes

We used the Spearman correlation test to evaluate the correlation of predation intensity with abundance and size. We used two-tailed chi-square test to evaluate the variation in predation attempts (DF, IDF, and RF) between different size classes. For the site preference of drilling a chi-square test of goodness of fit was done. All the statistical tests were conducted using the R programming environment (R development core team, 2007).

Cost-Benefit Analyses

We reconstructed the size of the predator (*Lpd*) from the drill hole size (*OBD*) using the following equation proposed by Klompmaker et al. (2017).

$$\log(OBD) = -1.09 + 0.94 * \log(Lpd) \quad (4)$$

Where, *OBD = Outer borehole diameter (mm)*

Lpd = Length of gastopod predator (mm)

The cost-benefit analysis was done for the microgastropods by adapting the equation suggested by Kitchell et al., (1981), along with a few modifications. The total benefit is calculated using the ash-free dry weight (*Wpr*) of gastropod prey with a specific size (*Lpr*). We used the formula for the genus *Polinices* for all the species. The relation is given as (Edwards and Huebner, 1977)

$$\log Wpr = -3.6201 + 2.5969 * \log Lpr \quad (5)$$

Where, *Wpr = Ash free dry weight of the prey (g)*

Lpr = Length of the gastopod prey (mm)

The calculated ash-free dry weight (Equation.5) is then multiplied by the energetic conversion factor, 21.46kJ/g (Kitchell et al., 1981) to obtain the benefit.

$$benefit = 21.46 * Wpr \quad (6)$$

The cost is calculated as a product of metabolic rate and time taken to drill the prey species. The drilling time (t) is found to be directly related to the thickness of the shell (T). The shell thickness (T) is calculated as (Avery and Etter, 2006)

$$Log\ T = 1.49 + 1.30 * \log(Lpr) \quad (7)$$

Where, *T = Thickness of the shell (μm)*

Lpr = Length of the gastropod (mm)

Using the thickness (T), we calculated the time (t) required to produce the drill hole (Kitchell et al., 1981)

$$t = (T + 0.068)/0.026 \quad (8)$$

Where, *T = Thickness (mm)*

t = drilling time (hours)

The metabolic rate of the predator is estimated through a series of steps. Using the OBD, the length of the predator (*Lpd*) is calculated (Equation 4).

Later the ash-free dry weight is calculated using the following relationship:

$$Log\ Wpd = -3.6201 + 2.5969 * logLpd \quad (9)$$

Where, *Wpd = Ash free dry weight of the predator (g)*

Lpd = Length of the gastopod predator (mm)

The ash-free dry weight (Equation 9) is then used to find the metabolic rate in terms of the amount of oxygen consumed per hour (Harper and Peck, 2003)

$$M0_2 = 2.23 + 29.8 * Wpd \quad (10)$$

Where, *$M0_2$ = Amount of oxygen consumed (μg)*

Wpd = Ash free dry weight of the predator (g)

According to Harper and Peck (2003), 18.6μg of oxygen/ hour is equivalent to 13μl of oxygen/ hour. This relation is used to calculate the amount of oxygen consumed in litres. Using standard conversion factors, we obtain the metabolic rate in kJ/hour.

$$Mpd = M0_2 * 13.9 \quad (11)$$

Where, *Mpd = Metabolic rate of predator (kJ/hours)*

The cost is estimated as

$$cost = Mpd * t$$

Using Equation 6, the net enegy gain is estimated from the following expression:

$$benefit/cost = (21.46 * Wpr) / (Mpd * t) \quad (13)$$

TABLE 1 — Overall abundance and summary of drilling predation of microgastropods from Quilon Limestone bed.

Family	Total specimens	Completely drilled specimens	Drilling frequency (DF)	Specimens with incomplete drilling	Incomplete drilling frequency (IDF)	Specimens with repair scars	Repair scar frequency (RF)	Frequency of multiple drillholes (MULT)
Cerithiidae	717	34	0.047	4	0.105	13	0.018	0.095
Pyramidellidae	195	12	0.061	2	0.143	21	0.108	0.125
Scaliolidae	117	1	0.008	0	0.000	2	0.017	0.000
Rissoinidae	103	23	0.223	3	0.115	3	0.029	0.133
Eulimidae	28	1	0.036	1	0.500	2	0.071	0.000
Naticidae	27	3	0.111	0	0.000	2	0.074	0.000
Obtortionidae	26	1	0.038	3	0.750	2	0.077	0.000
Phasianellidae	23	3	0.13	1	0.250	2	0.087	0.000
Turbinidae	18	1	0.056	0	0.000	3	0.167	0.000
Buccinidae	13	1	0.077	0	0.000	0	0	0.000
Marginellidae	11	0	0	0	0.000	0	0	0.000
Olividae	9	2	0.222	0	0.000	0	0	0.000
Raphitomidae	9	1	0.111	0	0.000	0	0	0.000
Horaiclavidae	8	1	0.125	0	0.000	1	0.125	0.000
Triphoroidae	8	0	0	0	0.000	0	0	0.000
Turritellidae	5	0	0	0	0.000	0	0	0.000
Mangellidae	2	0	0	0	0.000	0	0	0.000
Columbellidae	2	0	0	0	0.000	1	0.5	0.000
Borsoniidae	1	0	0	0	0.000	0	0	0.000
Cerithiopsidae	1	0	0	0	0.000	0	0	0.000
Epitoniidae	1	0	0	0	0.000	0	0	0.000
Torchidae	1	0	0	0	0.000	0	0	0.000
Tornidae	1	0	0	0	0.000	0	0	0.000
Pseudomelatomidae	1	0	0	0	0.000	0	0	0.000
Ringiculidae	1	0	0	0	0.000	0	0	0.000
Total	1328	84	0.063	14	0.143	52	0.039	0.097

RESULTS

A total of 1328 microgastropod specimens in our study represent 39 species, 35 genera, and 25 families. Cerithiidae is the most abundant family, represented by 718 individuals, followed by Pyramidellidae and Scaliolidae. A total of 150 individuals from 14 families show the signature of predation yielding an overall DF of 0.063 and RF of 0.039 (Table 1, Fig. 2, 3).

Eleven families, represented by more than ten individuals each, are considered for subsequent predation analyses (Fig. 2, 3, Table 1).

Among the eleven abundant families, we find ten with complete drillings (Fig. 2, 3B, 4A), six with incomplete drill holes (Fig. 2, 3C), and nine with repair scars. Rissoinidae and Obtortionidae have the maximum DF (0.22) and IDF (0.75) respectively. The majority of the drill holes correspond to naticid drilling (76.5%) and the rest corresponds to muricid drilling (Fig. 3B). The overall incidence of multiple drillhole is low (MULT=0.097) and only three families (Rissoinidae, Cerithiidae, and Pyramidellidae) showed them (Fig. 4B).

The overall RF is 0.039 and Turbinidae has the highest RF (0.18). There is no significant correlation between the overall abundance of a family and the observed predation matric (DF, IDF, and RF) (Table 2, Fig. 5A–C). There is no significant difference in median DF or median RF between families with and without ornamentation (Fig. 5D–F); however, the ornamented shells show a significantly higher median IDF ($p= 0.03$; Fig. 5E).

RF and IDF are significantly higher in the larger size (Table 3, Fig. 6); DF shows a similar but non-statistically significant pattern (Table 4). The median size of the incompletely drilled

TABLE 2 — Results of Spearman correlation test between relative abundance and predation matrices for abundant families. *DF*, drilling frequency; *IDF*, incomplete drilling frequency; *RF*, repair frequency.

	Spearman rho	p-value
DF	0.045	0.90
IDF	0.286	0.39
RF	0.114	0.74

TABLE 3 — Predation intensity in terms of drilling frequency, incomplete drilling frequency and repair frequency with respect to size.

Size class	DF	IDF	RF
Small (< 1mm)	0.05	0.07	0.02
Medium (1–2 mm)	0.06	0.15	0.04
Large (>2 mm)	0.09	0.32	0.11

specimens is larger than the complete and undrilled specimens; however, the difference is not statistically significant (Fig. 7A).

The apertural placement of complete drill holes is significantly more common compared to the abapertural placement (Chi-square test, p=0.01); apertural placement is least favored for incomplete drilling (Fig. 7B). The central region of the shell records the highest incidences of drill holes (79%; Fig. 7C). There is a strong positive correlation between the OBD and the prey size (Spearman rho = 0.79, $p=2.2e^{-16}$), especially for naticid predation (Spearman rho= 0.81, $p= 1.23e^{-13}$; Fig. 8A). The overall prey-predator size ratio for microgastropods falls between 0.4 and 1.2 (Figure 8B). However, 'small' microgastropods have a higher prey-predator ratio compared to 'medium' and 'large' ones (Fig. 8). The cost-benefit analysis demonstrates a benefit: cost > 1 for all the successful predation (Fig. 8C–E) and this ratio increases with an increase in the size of the prey. The naticid drillings yielded a higher benefit: cost ratio than muricid drilling (Wilcox test, p=0.04; Fig. 8D, E)

When compared to other drilling predation observed in macrogastropods of Miocene age (Table 5), DF of the Quilon Limestone assemblage is lower compared to the other locations, except for Kutch (Goswami et al., 2020; Table 5, Fig. 9).

The benefit-cost ratio is significantly higher for the macro gastropods of Kutch than the micro gastropods from Kerala (Wilcox test, p<<0.01; Fig. 8D–E). The family-level global comparison also shows a low DF for microgastropods in contrast to macrogastropods, except for the Rissoinidae family (Fig. 10A). Family-level comparison of RF demonstrates similar low-frequency in microgastropods (Fig. 10B).

DISCUSSION

Drilling predation on molluscan prey is the most common fossil record of predation followed by repair scars (Klompmaker et al., 2019). Temporal and spatial patterns of predation have been established for molluscs (Kelley and Hansen, 1993; Kelley and Hansen, 2006; Klompmaker et al., 2017) using a variety of approaches including controlled experiments (Chattopadhyay and Baumiller, 2007; Chattopadhyay et al., 2014a, Das et al., 2015), ecological surveys (Mondal et al., 2014; Chattopadhyay et al., 2014b, 2015; Pahari et al., 2016) along with documentation of fossil ecosystems. Despite such a large breadth of research on molluscan predation, micromolluscs are largely ignored. Individuals of ostracods and foraminifera that are comparable to micromolluscs in size are known to be preyed upon by drilling gastropods (Reyment et al., 1987; Culver and Lipps, 2003; Reyment and Elewa, 2003). It is, therefore, expected that micromolluscs will also be targeted by predators. Chattopadhyay et al. (2020) documented the drilling predation on microbivalve prey from the Quilon Limestone and demonstrated the selective nature of drilling predation in micromolluscs for the first time. Although there have been studies on the evolution (Weigand et al., 2013) and habitat preferences (Olabarria et al., 2002) of microgastropods, there has only been a few studies on the predation patterns in microgastropods (Ortiz-Jeronimo et al., 2021) and none focussing on the cost-benefit analyses. The present study attempts to fill this gap.

Predator Identity

Naticid predators are responsible for the majority (76.5%) of the drill holes in the Quilon microgastropods as affirmed by their parabolic shape (Kabat, 1990). The presence of individuals of the naticid family in our sample and the reported presence of multiple naticid genera (*Tanea, Natica*) in the assemblage (Harzhauzer, 2014) confirms the identity of the naticid predators. Some of the naticid drill holes from the assemblage were as small as 0.035 mm, implying a shell size of approximately 0.4 mm; these could be juvenile naticids because the shells were extremely thin and lack any strong mineralization. The non-naticid drill holes had a straight cylindrical boundary indicating muricid predation (Hoffman et al., 1974; Carriker, 1981 Kabat, 1990). Although we did not find any muricid specimens in our sample, the presence of muricid family (*Triplex* and *Dermomurex*) in the same locality (Harzhauzer, 2014) reveals the identity of the muricid drilling predator.

Repair scars are primarily produced after non-lethal breakage often due to a failed predation attempt by fishes and crabs. The presence of Xanthid crabs in our sample and presence from the same locality (Verma, 1977) points towards

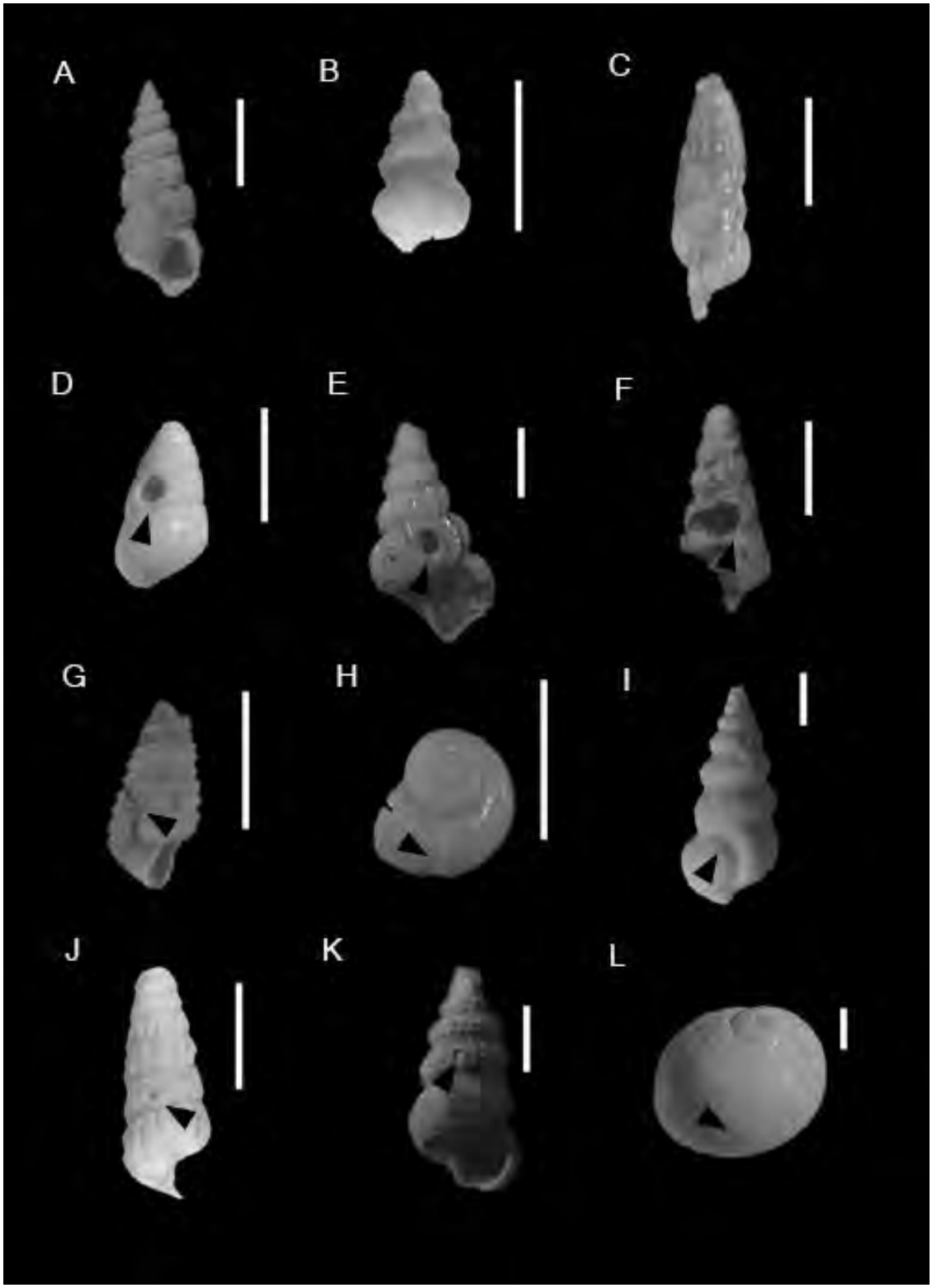

FIGURE 2 — Common gastropod families **A**, Cerithiidae, **B**, Scaliolidae and **C**, Pyramidellidae. Specimens with complete drill hole representing, **D**, Phasianellidae, **E**, Rissoinidae, **F**, Pyramidellidae. Specimens with repair marks representing **G**, Pyramidellidae, **H**, Turbinidae, **I**, Cerithiidae. Specimens with incomplete drill hole representing **J**, Pyramidellidae, **K**, Cerithiidae, and predator **L**, Naticidae. The scale corresponds to 1 mm.

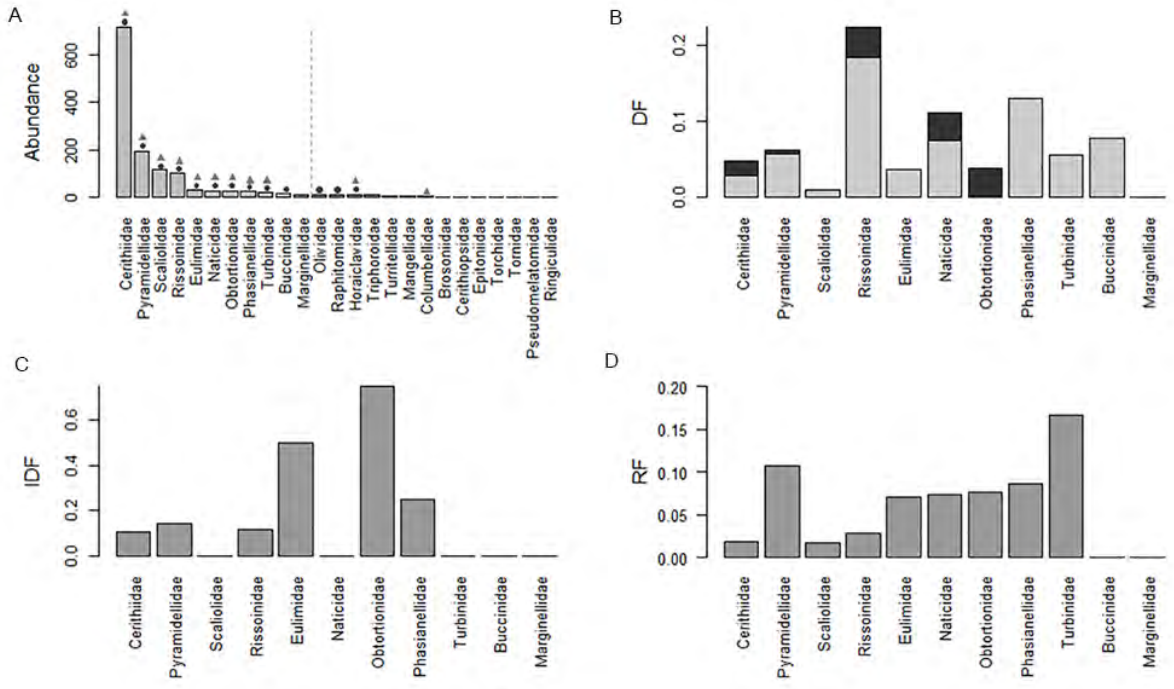

FIGURE 3 — Bar chart representing the **A**, abundance of all families. The dotted line separates the abundant (represented by more than ten individuals) and non-abundant families. The circles and triangles mark those families with drill holes and repair marks, respectively. Histograms representing the **B**, drilling frequency (DF) (the darker represents muricids and the lighter naticids), **C**, incomplete drilling frequency (IDF) and **D**, repair frequency (RF) of the eleven abundant gastropod families

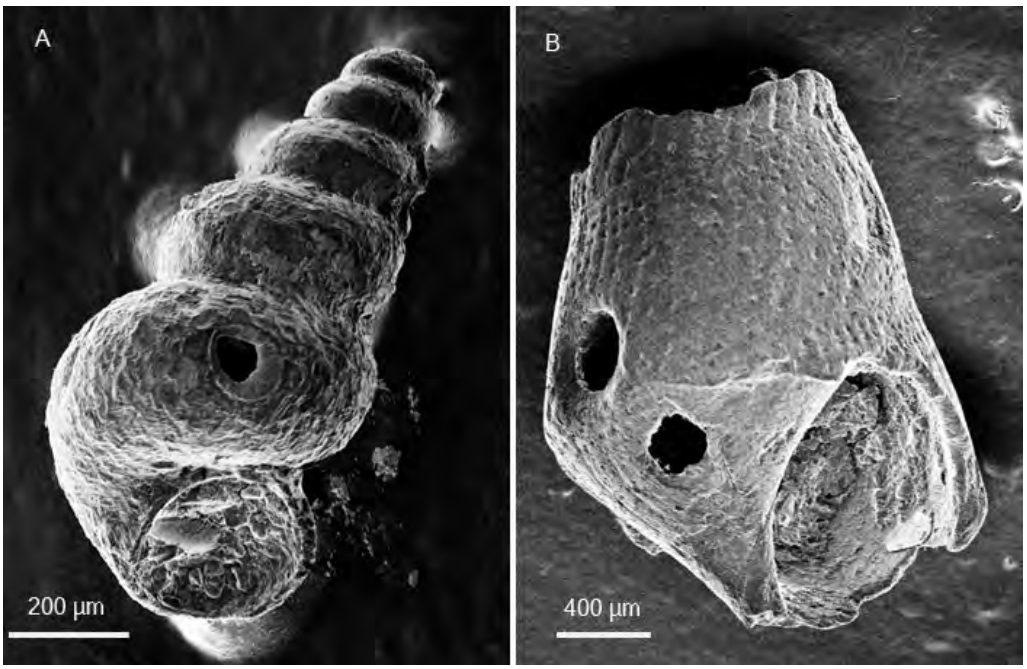

FIGURE 4 — SEM images of **A**, Complete drill hole in Scaliolidae, **B**, multiple drill hole in Pyramidellidae

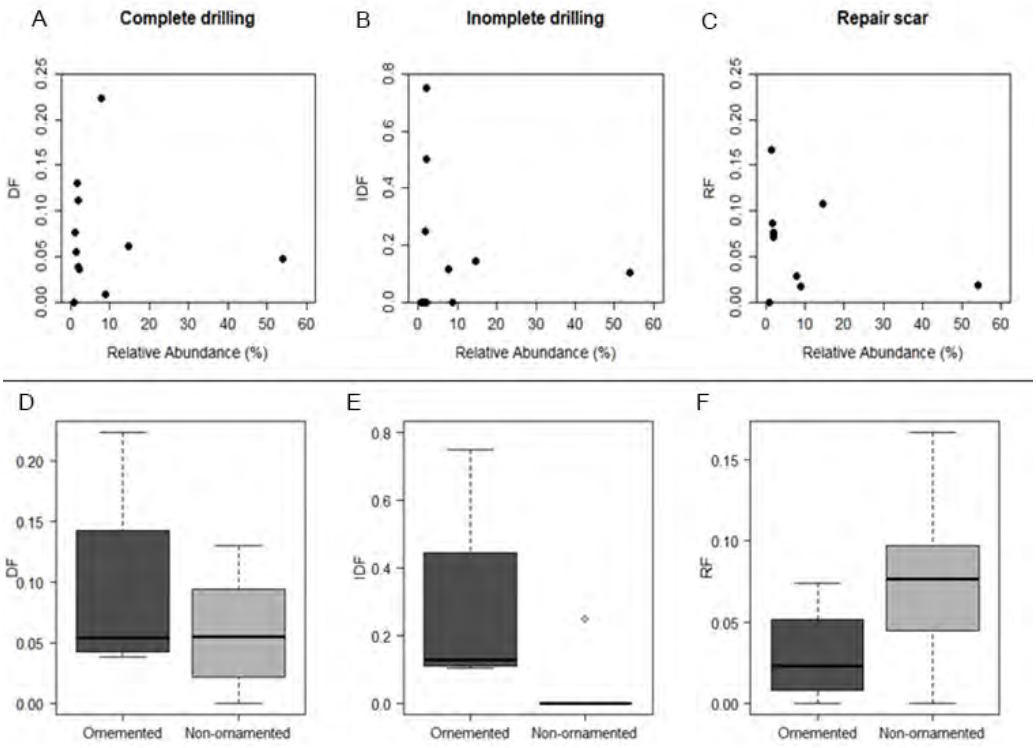

FIGURE 5 — The variation of predation marks with the relative abundance of family (**A**–**C**) and nature of ornamentation (**D**–**F**). The frequency of complete drillhole, incomplete drillhole and repair scars are represented by panels from the left to right. The boxes in the bottom panel are defined by 25th and 75th quantiles; thick line represents the median value.

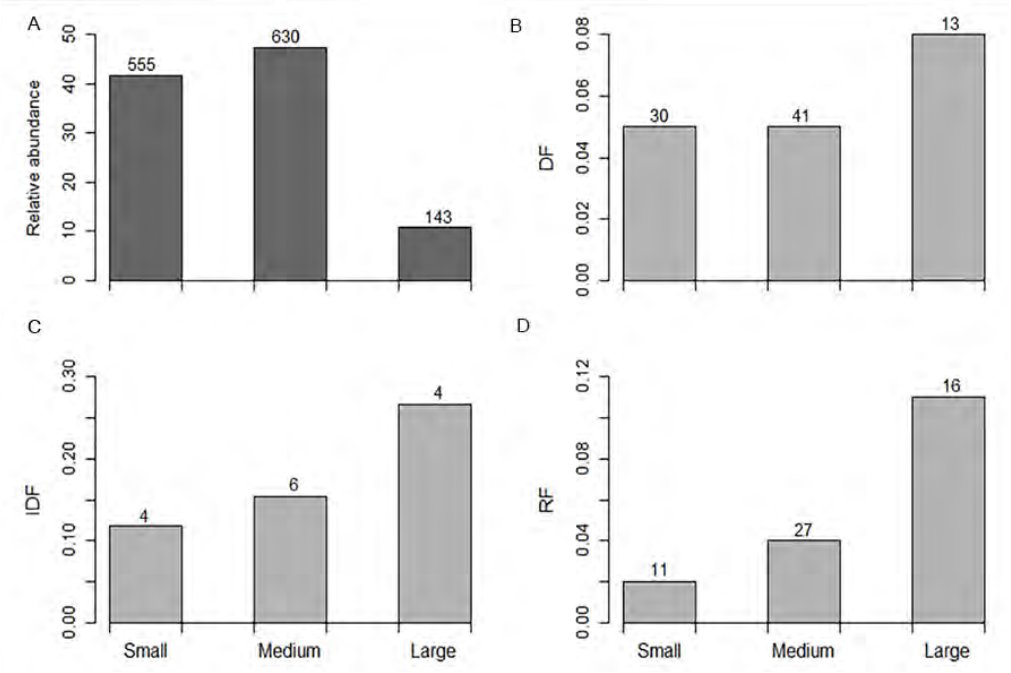

FIGURE 6 — Histogram showing the size class distribution of **A**, drilled and undrilled specimens, **B**, drilling frequency (DF), **C**, incomplete drilling frequency (IDF), and **D**, repair frequency (RF).

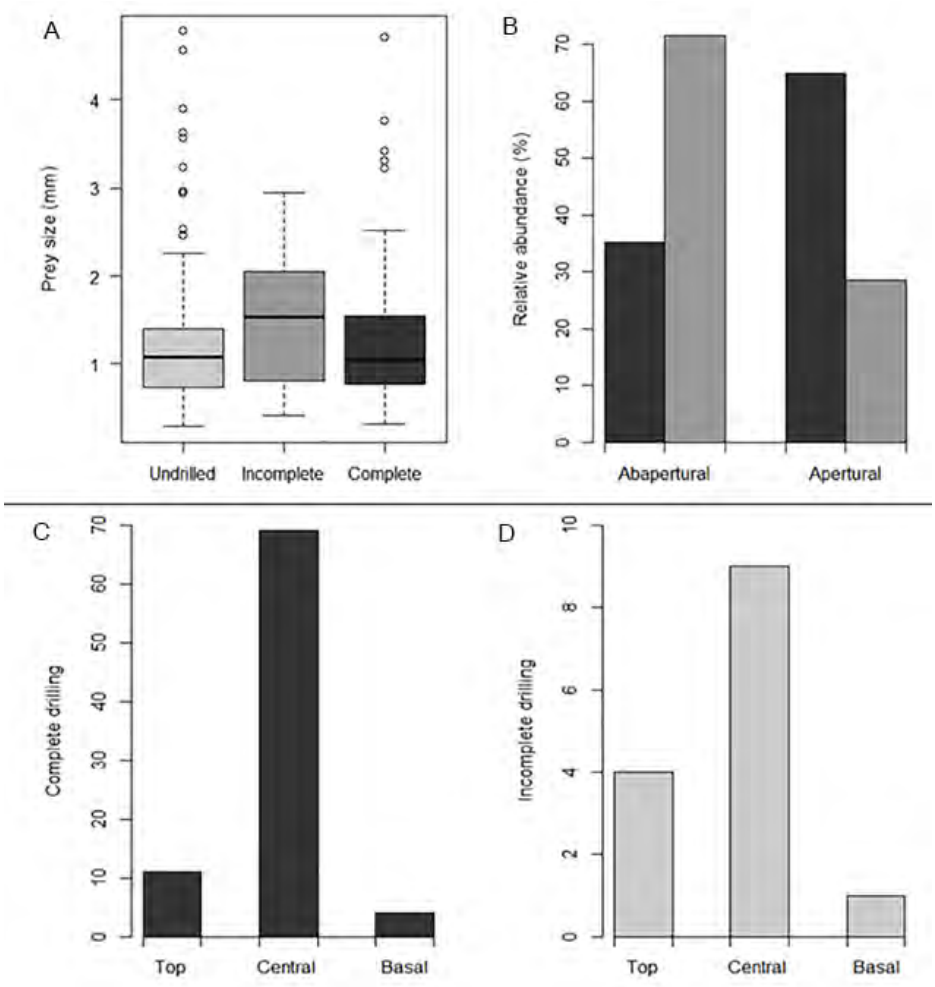

FIGURE 7 — Plot representing the variation in **A**, prey size and **B**, site selection between successful and unsuccessful predation attempts. The boxes in **A**, are defined by 25th and 75th quantiles; thick line represents the median value. The bar plots in **B**, represent relative abundance of specimens with complete drillhole (dark grey) and incomplete drill holes (light grey).

TABLE 4 — The results of the chi square tests done to evaluate the significance of variation in predation intensity interns of complete drilling, incomplete drilling, and repair scars (significant results are marked in bold).

Size class	Chi square value for DF	p-value for DF	Chi square value for IDF	p-value for IDF	Chi square value for RF	p-value for RF
Small-Medium	0.009	0.926	0.196	0.658	5.041	**0.025**
Medium-Large	3.075	0.079	4.688	**0.030**	10.572	**0.001**
Small-Large	2.771	0.096	6.188	**0.013**	25.919	**0.000**

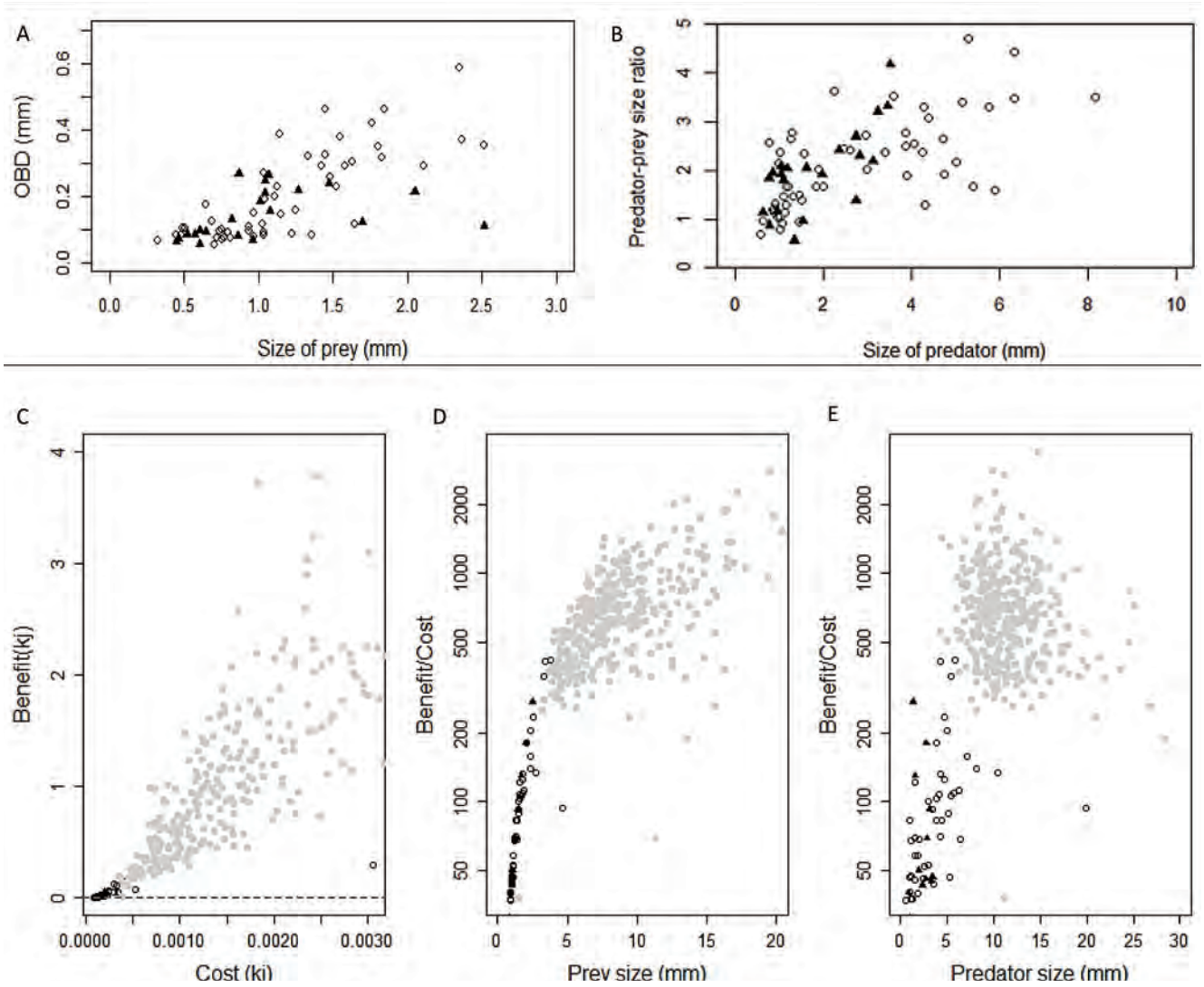

FIGURE 8 — Plot showing the relationship between **A**, size of the prey and the outer borehole diameter, **B**, the size of the predator and the prey-predator size ratio. Open circles represent naticid drilling and the closed triangles represent the muricid drilling. Cost – benefit relation for the micro gastropods, **C**, indicates the benefit gained by the predator species for a particular cost, **D**, scatter plot representing the relation between prey size and the benefit / cost ratio, **E**, relation between the inferred predator size and the benefit / cost ratio. The grey circles in the bottom panel represent data from Kutch and the dotted line in C indicate the minimum requirement for a successful predation (benefit = cost).

a potential durophagous predator. The higher number of repair scars among the 'large' microgastropods indicates a non-random predatory attack.

Factors Guiding the Prey Choice

The relative abundance of prey species is a good representation of the encounter frequency assuming the same lifespan of all the species, and studies have suggested that the predation intensity may be linked to prey availability (Leighton, 2002, 2003). However, taxon-specific DF, IDF, and RF in our study are not correlated to relative abundance (Fig. 6A–C) — a pattern consistent with findings for macro molluscs, both in the past and present ecosystems (Beu and Maxwell, 1990; Kelley et al., 2003; Mallick et al., 2014; Pahari et al., 2016). A lack of correlation between predation intensity and relative abundance indicates a predator's preference towards a particular prey species, even if it is not the most abundant; such prey is often preferred by the predator due to certain morphological traits and highlights a selective behavior demonstrated by the predator. Our specimens show a highly selective nature of prey choice for both drilling and durophagous predation primarily guided by the morphological characters of the prey, including size and ornamentation.

Size.— The size of an individual often dictates if it is targeted by a particular predator and determines the outcome of a predatory interaction. The reliable reconstruction

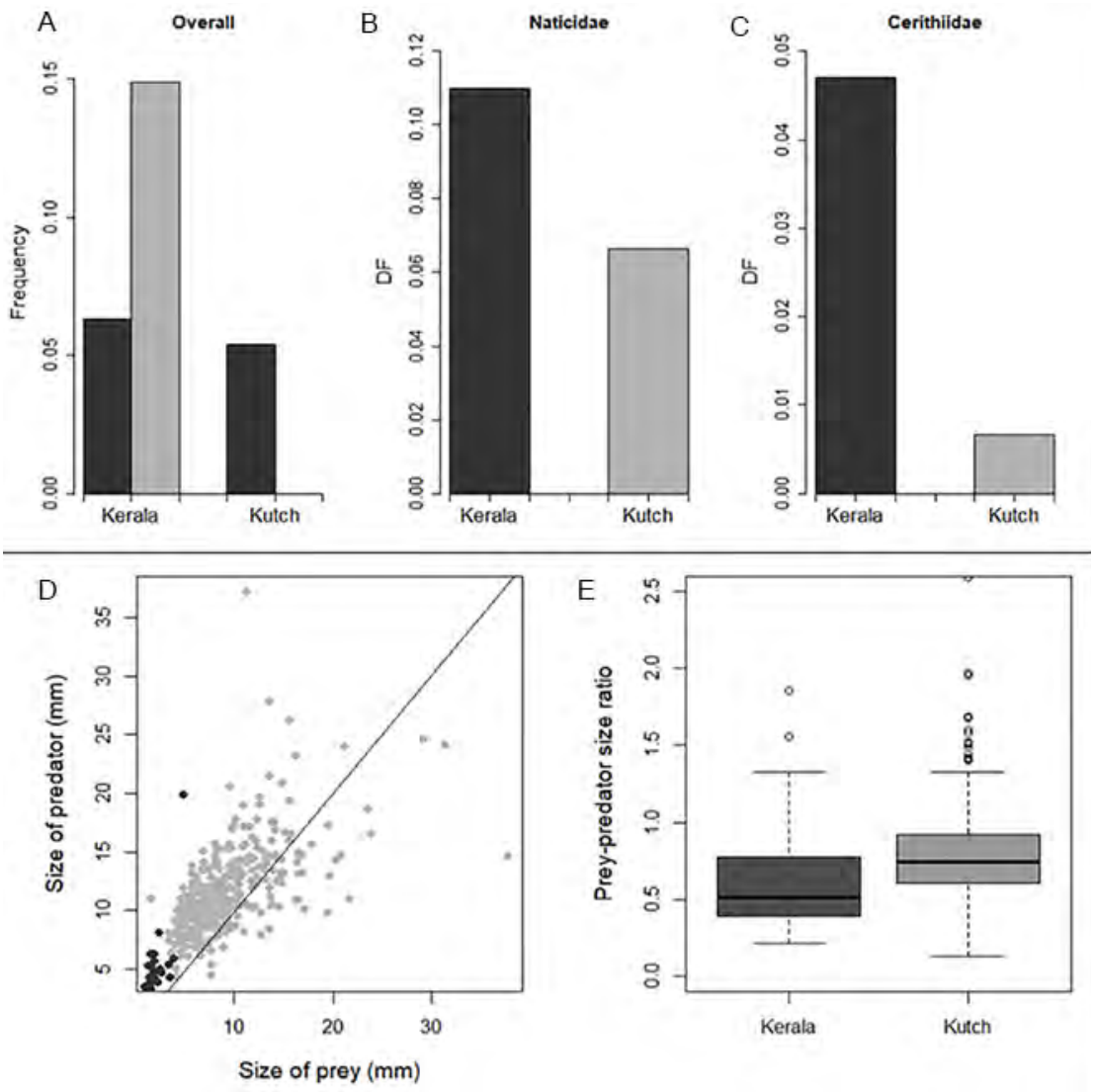

FIGURE 9 — Predatory patterns in Kerala and Kutch, India **A**, comparison of drilling frequency (DF) and incomplete drilling frequency (IDF), variation in DF for the common families **B**, Naticidae and **C**, Cerithiidae **D**, Relation between inferred size of the predator and size of the prey, grey represents Kerala specimens and black represents Kutch, **E**, boxplot representing the variation of prey predator size ratios.

of predator size is possible for drilling predation where experimental studies confirmed a strong positive correlation between the OBD and the size of the predator for specific families (Kitchell et al., 1981; Carriker and Gruber, 1999; Kowalewski, 2004; Klompmaker et al., 2017). The validity of the relationship has never been demonstrated for microgastropods. The inferred sizes of naticid and muricid predators from drill holes in the microgastropod assemblage are comparable to the size of corresponding specimens found from the locality, pointing to the validity of the approach.

Prey larger than a specific size are often avoided by predators due to difficulty in handling (Vermeij, 1987). Smaller prey are thought to offer low energetic gain and hence, not selected. Consequently, the predator targets medium-sized prey to maximize energy gain (Kitchell et al., 1981; Boggs et al., 1984; Kelley, 1988; Pahari et al., 2014; Chattopadhyay et al., 2020). The low DF in the smallest size class (although not statistically significant; Table 3) in our sample is consistent with this conclusion and suggests that the smaller size class is less likely to be attacked, providing refuge from predation. However, the higher IDF and RF in the larger size class suggest that the larger prey is efficient in escaping the predator once

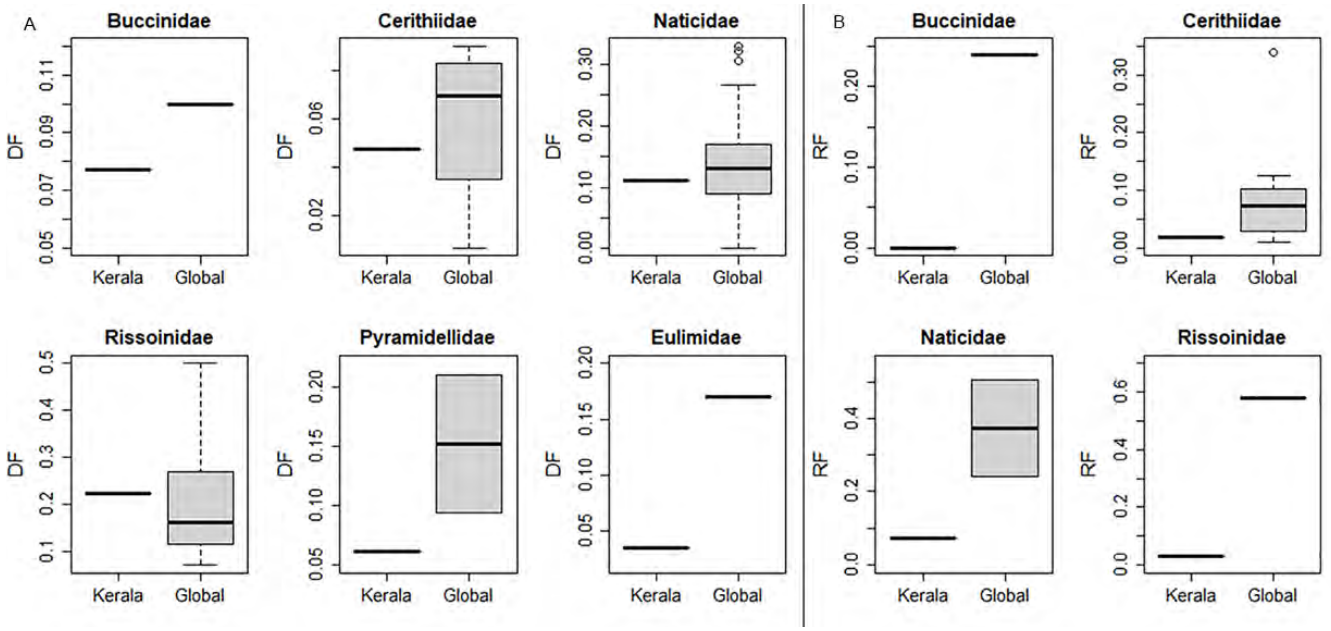

FIGURE 10 — Family-specific comparison in predatory patterns between Kerala and the other 628 coeval formations worldwide for **A**, drilling frequency (DF) and **B**, repair frequency (RF).

it is attacked. This result suggests complex prey-predator dynamics where the smaller size class is not preferred and larger prey are more successful in escaping from predators. Among two families of drilling predators, the naticids show a significant positive correlation between individual predator size and prey size demonstrating a strongly size-selective behavior (Fig. 9A–B). Because muricids do not envelope the prey within the foot unlike the naticids, muricid predators often do not show strong size-selectivity in their prey choice. The absence of size-selectivity of muricid predation not unique to micro gastropods and has been reported from macro gastropods (Tull and Böhning-Gaese, 1993).

Ornamentation.— Surface ornamentation plays an important role in determining the outcome of a predatory encounter. The ornamentation increases the effective thickness of the shell, making it more difficult to drill through. The presence of surface ornamentation such as coarse concentric ribs was found to reduce the incidence of successful drilling in bivalves (Klompmaker and Kelley 2015). Although the difference was not significant for DF and RF, the IDF was significantly higher in microgastropods with ornamentation, suggesting that ornamentation increases the probability of drilling failure. The two non-ornamented families (Eulimidae and Phasainallidae) with higher IDF have a smooth shiny surface that is hard to grab (Vermeij, 1987). Moreover, Eulimidae are parasitic and often associated with echinoderms, the defence strategies of echinids, for example the presence of spines makes them less vulnerable to predators that protect them from predators (Waren, 1983). A slightly higher, although not statistically significant, RF was found among the non-ornamented specimens, supporting the effect of ornamentation producing failures in durophagous attacks. The highest RF, however, is found in a non-ornamented microgastropod family — the Turbinidae. The small size and the smooth shell may have helped them to escape from the durophagous attacks.

Taxon.— Both drilling and durophagous predators are known to demonstrate taxon selectivity (Alexander and Dietl, 2003; Chattopadhyay and Dutta, 2013; Chattopadhyay et al., 2015). Our study suggests that some prey taxa are preferred and the preference cannot be completely explained by the lack of morphological defense, such as the Rissoinidae family. They also have ornamentation such as ribs increasing their effective thickness, which should have acted against the predatory attacks. The abundance does not explain such higher rates always; families such as Scaliolidae and Cerithiidae have a larger relative abundance yet have a lower DF. In the absence of obvious high encounter frequency or morphological weakness, their behavioral traits may have contributed to such increased predation pressure.

Individual predatory families also show distinct selective patterns. Muricids are found to prey heavily upon Obtorionidae. Kitchell et al. (1981) have found that muricids are capable of drilling deeper holes, enabling them to prey on molluscs with a thicker shell or stronger ornamentation, such as the Obtortionidae. Because the deeper drill holes require longer drilling time, the probability of interruption by other predators and prey escape increases leading to higher frequency of incomplete drillings. This interpretation is also supported by the high IDF observed among Obtortionidae (Fig. 3C, Fig. 5B). In contrast to the overall dominance of naticid drilling, the assemblage demonstrates a low incidence

TABLE 5 —. Spatiotemporal comparison of drilling predation data on gastropods from other major Miocene assemblages.

Formation/place	Age	Number of specimens	Number of drilled specimens	Drilling frequency	Source
Calvert, Maryland, USA	Middle Miocene	594	---	0.202	Kelley & Hansen, 2006
Choptank, Maryland, USA	Middle Miocene	2323	---	0.272	Kelley & Hansen, 2006
St. Marys, Maryland, USA	Middle to Late Miocene	8637	---	0.38	Kelley & Hansen, 2006
Eastover, Maryland, USA	Late Miocene	67	---	0.209	Kelley & Hansen, 2006
Boreal, central Europe	Early to Middle Miocene	1159	284	0.245	Hoffmeister & Kowalewski, 2001
Paratethys, central Europe	Early to Middle Miocene	599	84	0.14	Hoffmeister & Kowalewski, 2001
Southeastern North Atlantic, France	Middle Miocene	67	22	0.328	Hoffmeister & Kowalewski, 2001
Karpatian and Serravalian, Central Parathethys, Europe	Early to Middle Miocene	22294	1596	0.072	Sawyer & Zuschin, 2011
Chassra, Kutch, India	Early to Middle Miocene	15891	---	0.0541	Goswami et al 2020

of naticid cannibalistic behavior. Out of 64 naticid drillings, only two are cannibalistic and both of them are found in the small size class of prey supporting the experimental findings of a higher frequency of cannibalism among smaller prey (Chattopadhyay et al., 2014a).

Predator Preference for Drill Hole Site

Naticid predators often show stereotypic behavior in selecting the drilling site (Dietl and Alexander, 2005). The majority of the complete naticid drill holes are located in the central region of the microgastropods (48.6%; Fig. 7C). Similar stereotypic behavior is known from macro molluscs (Allmon et al., 1990; Hagadorn and Boyajian, 1997; Goswami et al., 2020). When a prey individual is alarmed, it withdraws the soft parts inside the shell, up to nearly its central region (Kitchell, 1986; Hansen and Kelley, 1995). The drill holes in the central region ensure access to the soft tissue. A similar pattern is present among muricid drill holes suggesting a stereotypical behavior even of the muricid predators.

Our results show that drill holes are concentrated on the apertural side, mostly between the first (top) and the fourth sectors. The position of the drill hole is also dependent on the size and the morphology of the prey and the predator (Ansell, 1960; Sohl, 1969; Negus, 1975; Kabat, 1990). During naticid predation, the predator completely covers the prey with its foot to restrict its movement and it is often seen that they release a chemical that numbs the prey (Carriker and Gruber, 1999). Dietl and Alexander (2000) have explained that in confamilial predation in naticids they observe a significant number of drilling near the umbilicus, which would help the predator to immobilize a relatively "dangerous" prey, by covering the aperture using the foot. This pattern was observed even when the prey is significantly larger and mobile. The higher intensity of naticid drill holes on the ventral side of the shell in our data thus suggests a stereotypical behavior by the predator to effectively immobilize the prey.

Prey Effectiveness and Repair Frequency

The presence of incomplete drill holes, multiple drill holes, and repair scars demonstrate the prey's ability to escape and/or the inability of the predators to complete an attack due to an interruption (Kelley et al., 2003). Incomplete drill holes do not always indicate prey's escape, because there are cases that reported the suffocation of the prey prior to the completion of drilling, thus resulting in death (Hutchings and Herbert, 2013) although rare in natural conditions (Visaggi et al., 2013). The results indicate a significant increase in IDF and RF with size. This may suggest that the shell thickness of the larger prey might be slightly higher, making it less desirable. These higher rates represent prey's physical defense mechanism acquired over its lifetime to escape predation. Chattopadhyay and Baumiller (2007) showed that the presence of secondary predators may result in the abandonment of the prey by the predatory gastropods, leading to the development of incomplete drilling. In such cases, RF is proportional to IDF and inversely proportional to DF (Chattopadhyay and Baumiller, 2010). The microgastropod assemblage, however, does not show any significant correlation ($p = 0.43$ for DF-RF, and $p = 0.92$ for IDF-RF) between the family-specific valued of these three indices suggesting limited involvement of predatory abandonment in producing an incomplete drill holes.

A high RF of an assemblage may indicate more predators, higher failure due to inefficiency of the predators or prey with stronger defenses (Vermeij et al., 1981). We have standardized the RF for both prey size and taxon. For the size standardized calculation, two reasons could account for the higher RF in the large size class: a) larger prey are usually older and, hence, accumulate scars over multiple attacks during ontogeny, b) larger prey are more likely to survive an attack in comparison to smaller prey and hence carry the signature of non-lethal attack. Multiple drill holes and incomplete drilling are not uncommon in the assemblage. Lower IDF and MULT values from macrogastropod assemblages of Miocene have been interpreted as the signature of highly efficient predation (Fortunato, 2007). The relatively higher values of IDF (14.3%) and MULT (9.7%), compared to the Kutch assemblage (0% and 0.70%) (Goswami et al., 2020) along with lower DF indicate that micro gastropods have an effective way of escaping predation.

The Energetics of Predation

The non-random prey selection is explained by the cost-benefit principle (DeAngelis and Kitchell, 1985). The cost is the invested energy by the predator in finding, capturing, and consuming the prey; the benefit is the energetic value of the prey tissue to the predator. The principle suggests that a predator selects prey to maximize the net energy gain, i.e., the difference between the benefit and cost. This principle has been shown to operate in prey selection by both naticids (Kitchell et al., 1981) and muricids (Chattopadhyay and Baumiller, 2009) on macromolluscan prey. Cost-benefit analyses confirm that selection of micromolluscan prey is non-random and each of the successful attacks yielded a positive net energy gain (Fig. 9C). The microgastropod prey yield higher energetic gain with increasing size primarily because of the increase in soft tissue volume and a negligible increase in thickness of the prey (Fig. 7A, D). This results in the exponential increase in benefit: cost ratio with prey size. This explains why smaller sizes among microgastropods are not the preferred prey confirmed by the lower DF in comparison to larger size classes (Fig. 9C–E). It is also important to note that none of the individuals below 0.35mm are drilled. This result also confirmed that a "negative size refuge" exists in microgastropods similar to microbivalve prey (Chattopadhyay et al., 2020). The cost-benefit analysis also confirms that micromorphy may act as an effective defense strategy by making the smaller sizes less preferred.

The cost-benefit analysis also brings out interesting behavioral attributes of the predator. Although the prey-predator size ratio decreases with predator size (Fig. 9B), the net energy gain increases. This implies that smaller predators, despite their selection of relatively larger prey, do not benefit energetically due to a disproportionately higher metabolic cost. When compared between two families of drillers, naticid drillings are more beneficial than muricids; the naticids are found to have a significantly higher net energy gain compared to muricids.

A Comparison to Macrogastropods

Low values of drilling frequency in microbivalves in comparison to coeval global averages have been used to establish the effectiveness of micromorphy against drilling predation (Chattopadhyay et al., 2020). Our study confirms this finding for both drilling and durophagous predation of microgastropods. The low predation intensity in family-level comparison with macrogastropods indicates the predation resistance of microgastropods (Fig. 10). Such lower intensity among the microgastropods is probably driven by their low energetic yield which makes them less preferred as demonstrated by the cost-benefit analyses. This conclusion is also supported by the higher benefit-cost ratio, observed among the macro gastropods from Kutch (Fig. 10C–E). However, there might be other factors that could affect the intensity of predation.

The studied section is interpreted to represent a seagrass environment (Reuter et al., 2011). Seagrass environments are often found to provide a natural refuge from predators (Irlandi, 1997; Wall et al., 2008) where leaf blades diminish the mobility of the predators and also makes it hard to detect the prey visually (Heck and Thoman, 1981; Irlandi, 1997). The roots also prevent digging, limiting the activity of infaunal predators (Wall et al., 2008). Since many of the predators (muricids, xanthid crabs) are epifaunal, the effect of the seagrass cannot completely explain the low predation intensity of the Quilon microgastropod assemblage.

Differential preservation of the macro-and microgastropods may also contribute to the observed low predation intensity of microgastropods. Generally, the smaller gastropods, especially juveniles, are rarely preserved in the fossil record (Kidwell, 2001; Cooper et al., 2006;) often leading to a difference in observed predation intensity across size classes (Chattopadhyay et al., 2016). One of the taphonomic biases thought to influence the inferred DF is the differential shell strength of drilled and undrilled shells (Roy et al., 1994; but see Zuschin and Stanton, 2001, Kelley, 2008, and Dyer et al., 2018). Drill holes reduce the shell strength and make the drilled shells more susceptible to point-load compression-induced breakage potentially leading to a reduced DF (Roy et al., 1994). However, the difference in breaking load between drilled and undrilled shells is more pronounced in larger shells (Fig. 3; Roy et al., 1994) — a pattern that is more likely to lower DF in macromolluscs. Moreover, the lighter shells of microgastropods are likely to be carried as suspension load in contrast to the macrogastropods that travel as bed load and get reworked in the process (Reuter et al., 2011). Most microgastropods in our collection retained their original structure without any breakage pointing to the limited role of compaction-induced breakage in developing the assemblage. Apart from this, the difference in hydrodynamic properties of drilled and undrilled shells are also known to create assemblages with reduced DF (Chattopadhyay et al., 2013a, b). However, the difference is more pronounced for larger size classes (Fig. 5; Chattopadhyay et al., 2013b). Both the taphonomic attributes

(compaction, hydrodynamics) that are known to reduce DF are more likely to affect macrogastropods and do not explain the observed low predation intensity in microgastropods implying a relatively negligible role of taphonomy in creating the pattern.

The relative abundance of predatory species is known to explain the predation intensity of a region (Allmon et al., 1990; Kardon 1998; Sawyer and Zuschin, 2011). In the recent study by Goswami et al. (2020), the low drilling intensity of macrogastropods from Kutch is explained by the low abundance of predators. Because of the low abundance of muricid gastropod in their assemblage, most muricid-like drill holes have been attributed to naticid. The microgastropod assemblage of the Quilon Limestone is characterized by a lower relative abundance of potential drillers (2.04%) in comparison to the reported values from other Miocene assemblages, such as Kutch (2.27 – 4.55%; Goswami et al., 2020). Muricid drilling is present in our collection and muricid specimens have been reported from the same locality (Harzhauser, 2014). However, the absence of muricid gastropod specimens in our documented collection is a probable indicator of their lower abundance.

Apart from the relative abundance of predators, the absence of preferred prey may also result in low predation intensity. The Quilon assemblage reports few turritellids – a family known to be a preferred prey with high DF (Kojumdjieva, 1974; Fortunato, 2007; Goswami et al., 2020). The absence of this group may have contributed to the overall lower DF of the Quilon assemblage. The availability of other preferred prey may also contribute to the lower predation intensity among microgastropods. Chattopadhyay et al. (2020) have reported a similar drilling frequency (DF = 0.06) among the microbivalves from the same locality, suggesting that microbivalves were unlikely to be a preferred prey over microgastropods. Other potential prey of this size class include ostracods and foraminifers. The thin shells of ostracods might lower the energy for drilling making them desirable prey (Reyment et al., 1987; Culver and Lipps, 2003; Reyment and Elewa, 2003). Although we do not have any direct evidence of predation from these groups, abundant ostracods (Yasuhara et al., 2020) and foraminifera (Rögl and Briguglio, 2018; Briguglio and Rögl, 2018) have been reported from the Quilon assemblage, supporting the availability of alternate prey types. This also opens the possibility for future studies to explore the predatory interactions in these groups to understand predator-prey dynamics at extremely small size classes.

CONCLUSIONS

Predation on molluscan communities from recent and past ecosystems, has been studied in-depth, with the exception of micromolluscs. The present study attempted to fill this gap by studying the predation signature in microgastropods from the Quilon Limestone of Kerala. The predation intensity of this assemblage is quite low for drilling (DF= 0.06) and durophagous (RF=0.04) predation. Also, the repair frequency (RF) and the incomplete drilling frequency (IDF) are found to be lower for the Quilon microgastropods in comparison to family-specific values of global reports of macrogastropods. These results support the previous findings of micromorphy acting against drilling predators with low drilling predation intensity as shown among microbivalves (Chattopadhyay et al., 2020). The small size of the prey species is a good defense against predation, and inverse size refugia are observed among microgastropods. However, the larger prey is found to escape predation more efficiently as demonstrated by a higher IDF among large size class. The physical features of the gastropod prey affect the intensity of predation rather than their abundance. The lower intensity of predation in this size range might be a result of multiple factors that includes a lower abundance of predators, the seagrass environment, and the presence of other prey species. Finally, the cost-benefit analysis suggests an increasing benefit to cost ratio with increasing prey size explaining the potential reason for preferring macrogastropods over microgastropods leading to the low predation intensity observed among micromolluscs.

ACKNOWLEDGMENTS

This work was supported by the Academic Research Grant of IISER Kolkata (ARF 2018–19), Start-up Research Grant of IISER Pune (2019–2021) and DST Inspire fellowship. We thank Debarati Chattopdhyay and Venugopal S Kella for collecting the samples and initial processing. We acknowledge the Microscopy Facility, IISER Pune for their support with the SEM imaging presented herein. We thank Vibhas Shevde and Santosh Poddar for their help in SEM imaging.

LITERATURE CITED

ALEXANDER, R. R., G. P. DIETL. 2003. The fossil record of shell-breaking predation on marine bivalves and gastropods. In Predator—Prey Interactions in the Fossil Record. Springer, Boston, MA. pp. 141–176.

ALLMON, W. D., J. C. NIEH, and R. D. NORRIS. 1990. Drilling and Peeling of Turritelline Gastropods since the Late Cretaceous. Palaeontology, 33: 595–611.

ANSELL, A. D. 1960. Observations on predation of *Venus striatula* (Da Costa) by *Natica alderi* (Forbes). J. Molluscan Studies, 34: 157–164.

AVERY, R., and R. J. ETTER. 2006. Microstructural differences in the reinforcement of a gastropod shell against predation. Marine Ecology Progress Series, 323: 159–170.

BARNES, C., D. MAXWELL, D. C. REUMAN, S. JENNINGS. 2010. Global patterns in predator-prey size relationships reveal size dependency of trophic transfer efficiency. Ecology, 91: 222–232.

BEU, A.G., P. A. MAXWELL. 1990. Cenozoic Mollusca of New Zealand: New Zealand Geological Survey Palaeontological Bulletin, 58: 75–454.

BOGGS, C. H., J. A. RICE, J. A. KITCHELL and J. F. KITCHELL. 1984. Predation at a snail's pace: what's

time to a gastropod? Oecologia, 62: 13–17.
BRIGUGLIO, A., and F. RÖGL, 2018. The Miocene (Burdigalian) Operculinids of Channa Kodi, Padappakkara, Kerala, Southern India. Palaeontographica Abteilung A, 17–39.
CARRIKER, M. R. 1981. Shell penetration and feeding by naticacean predatory gastropods: a synthesis. Malacologia, 20: 403–422.
_____, and G. L. GRUBER. 1999. Uniqueness of the gastropod accessory boring organ (ABO): Comparative biology, an update. Journal of Shellfish Research, 9: 257–312.
CHATTOPADHYAY, D., and S. DUTTA. 2013. Prey selection by drilling predators: A case study from Miocene of Kutch, India. Palaeogeography, Palaeoclimatology, Palaeoecology, 374: 187–196.
_____, and T. K. BAUMILLER. 2009. An experimental assessment of feeding rates of the muricid gastropod *Nucella lamellosa* and its effect on a cost-benefit analysis. Journal of Shellfish Research, 28: 883–889
_____, and _____. 2007. Drilling under threat: An experimental assessment of the drilling behavior of *Nucella lamellosa* in the presence of a predator. Journal of Experimental Marine Biology and Ecology, 352: 257–266.
_____, D. SARKAR, S. DUTTA, and S. R. PRASANJIT. 2014a. What controls cannibalism in drilling gastropods: A case study on *Natica tigrina*. Palaeogeography, Palaeoclimatology, Palaeoecology. 410: 126 –133.
_____, M. ZUSCHIN, and A. TOMASOVYCH. 2014b. Effects of a high-risk environment on edge-drilling behavior: Inference from Recent bivalves from the Red Sea. Paleobiology, 40: 34–49.
_____., M. ZUSCHIN, and A. TOMASOVYCH. 2015. How effective are ecological traits against drilling predation? Insights from Recent bivalve assemblages of the northern Red Sea. Palaeogeography, Palaeoclimatology, Palaeoecology, 440: 659–670.
_____, _____, S. DOMINICI, and, J. A. SAWYER. 2016. Patterns of drilling predation in relation to stratigraphy, locality and sieve size: Insights from the Eocene molluscan fauna of the Paris Basin. Palaeogeography, Palaeoclimatology, Palaeoecology, 459: 86–98.
CHATTOPADHYAY, D., V. G. S. KELLA, and D. CHATTOPADHYAY. 2020. Effectiveness of small size against drilling predation: Insights from lower Miocene faunal assemblage of Quilon Limestone, India. Palaeogeography, Palaeoclimatology, Palaeoecology, 551: 109742.
COOPER, R. A., P. A. MAXWELL, J. S. CRAMPTON, A. G. BEU, C. M. JONES, and B. A. MARSHALL. 2006. Completeness of the fossil record: Estimating losses due to small body size: Geology, 34: 241–244.
CULVER, S. J., and J. H. LIPPS. 2003. Predation on and by Foraminifera. In Predator-Prey Interactions in the Fossil Record. Springer US, pp. 7–32.
DAS, S., D. CHATTOPADHYAY, and D. CHATTOPADHYAY. 2015. The effect of hunger on drilling behaviour of *Natica tigrina*: An experimental assessment. Palaeogeography, Palaeoclimatology, Palaeoecology, 429: 57–61.
DEANGELIS, D. L., J. A. KITCHELL, W. M. POST. 1985. The influence of nacticid predation on evolutionary strategies of bivalve prey: conclusions from a model. American Naturalist, 126: 817–842.
DEY, A. K. 1961. The Miocene Mollusca from Quilon, Kerala (India). Memoirs of the Geological Survey of India, Palaeontologia Indica, New Series 36: 1–117.
DIETL, G. P., and R. R. ALEXANDER. 2000. Post-Miocene shift in stereotypic naticid predation on confamilial prey from the mid-Atlantic shelf: Coevolution with dangerous prey. PALAIOS, 15: 414–429.
DYER, A. D., E. R. ELLIS, D. J. MOLINARO, and L. R. LEIGHTON, 2018. Experimental fragmentation of gastropod shells by sediment compaction: implications for interpreting drilling predation intensities in the fossil record. Palaeogeography, Palaeoclimatology, Palaeoecology, 511: 332–340.
EDWARDS, D.C. and, J. D. HUEBNER. 1977. Feeding and growth rates of *Polinices duplicatus* preying on *Mya arenaria* at Barnstable Harbor, Massachusetts. Ecology, 58: 1218–1236.
FORTUNATO, H. 2007. Naticid gastropod predation in the Gatun Formation (late Middle Miocene), Panama: Preliminary assessment. Palaontologische Zeitschrift, 81: 356–364.
GOSWAMI, P., S. S. DAS, S. BARDHAN, and S. PAUL. 2020. Drilling gastropod predation on the lower Miocene gastropod assemblages from Kutch, western India: spatiotemporal implications. Historical Biology, 00: 1–18.
HAGADORN, J. W., and G. E. BOYAJIAN. 1997. Subtle Changes in Mature Predator-Prey Systems: An Example from Neogene Turritella (Gastropoda). PALAIOS, 12: 372.
HANSEN, T. A., and P. H. KELLEY. 1995. Spatial variation of naticid gastropod predation in the Eocene of North America. PALAIOS, 10: 268–278.
HARPER, E. M., and L. PECK, L. 2003. Predatory behaviour and metabolic costs in the Antarctic muricid gastropod *Trophon longstaffi*. Polar Biology, 26: 208–217.
_____, _____, and K. R. HENDRY. 2009. Patterns of shell repair in articulate brachiopods indicate size constitutes a refuge from predation. Marine Biology, 156: 1993–2000.
HARZHAUSER, M. 2014. A seagrass-associated Early Miocene Indo-Pacific gastropod fauna from South West India (Kerala). Palaeontographica, Abteilung A: Palaozoologie - Stratigraphie, 302: 73–178.
HECK, J. K., and T. A. THOMAN. 1981. Experiments on predator-prey interactions in vegetated aquatic habitats. Journal of Experimental Marine Biology and Ecology, 53: 125–134.
HINES, A. H., A. M. HADDON, and L. A. WIECHERT 1990. Guild structure and foraging impact of blue crabs and epibenthic fish in a sub-estuary of Chesapeake Bay. Marine Ecology Progress Series, 67: 105–126.
HOFFMAN, A., A. PISERA, and M. RYSZKIEWICZ. 1974.

Predation by muricid and naticid gastropods onthe lower Tortonian mollusks from the Korytnica clays. Acta Geologica Polonica, 24: 249–260.

HOFFMEISTER, A. P., and M. KOWALEWSKI. 2001. Spatial and Environmental Variation in the Fossil Record of Drilling Predation: A Case Study from the Miocene of Central Europe. PALAIOS, 16: 566– 579.

HUNTLEY, J. W., and M. KOWALEWSKI. 2007. Strong coupling of predation intensity and diversity in the Phanerozoic fossil record. Proceedings of the National Academy of Sciences of the United States of America 104, 15006–15010.

IRLANDI, E., 1997. Seagrass patch size and survivorship of an infaunal bivalve. Oikos 78: 511–518.

KABAT, A. R. 1990. Predatory ecology of naticid gastropods with a review of shell boring predation. Malacologia, 32: 155–193.

KARDON, G. 1998. Evidence from the fossil record of an antipredatory exaptation: conchiolin layers in corbulid bivalves. Evolution, 52: 68–79.

KELLEY, P. H. 1988. Evolutionary trends within bivalve prey of Chesapeake Group naticid gastropods. Historical Biology, 3: 436– 448.

_____, and T. A. HANSEN. 1993. Evolution of the naticid gastropod predator-prey system: An evaluation of the hypothesis of escalation: Palaios, 8: 358–375.

_____, _____. 2006. Comparisons of class- and lower taxon-level patterns in naticid gastropod predation, Cretaceous to Pleistocene of the US Coastal Plain. Palaeogeography, Palaeoclimatology, Palaeoecology, 236: 302–320.

_____. 2008. Role of bioerosion in taphonomy: effect of predatory drillholes on preservation of mollusc shells. In Current developments in bioerosion. Springer, Berlin, pp. 451–470.

_____, M. KOWALEWSKI, and T. A. HANSEN. 2003. Predator-Prey Interactions in the Fossil Record, Springer.

KIDWELL, S.M., 2001. Preservation of species abundance in marine death assemblages. Science, 294: 1091–1094.

KITCHELL, J. A. 1986. The evolution of predator-prey behaviour: Naticid gastropods and their molluscan preys, In Nitecki, M. H., and Kitchell, J. A. (ed), Evolution of animal behaviour: Paleontological and field approaches: New York, Oxford Press, pp. 88–110.

_____., C. H. BOGGS, J. F. KITCHELL, and J. A. RICE, J. A. 1981. Prey Selection by naticid gastropods: experimental tests and application to the fossil record. Paleobiology, 7: 533–552.

KLOMPMAKER, A. A., and P. H. KELLEY. 2015. Shell ornamentation as a likely exaptation: Evidence from predatory drilling on Cenozoic bivalves. Paleobiology, 41: 187–201.

_____, _____, D. CHATTOPADHYAY, J. C. CLEMENTS, J. W. HUNTLEY, and M. KOWALEWSKI. 2019. Predation in the marine fossil record: Studies, data, recognition, environmental factors, and behaviour. Earth-Science Reviews, 194: 472–520.

_____, M. KOWALEWSKI, J. W. HUNTLEY, and S. FINNEGAN. 2017. Increase in predator-prey size ratios throughout the Phanerozoic history of marine ecosystems. Science, 356: 1178–1180.

KOJUMDJIEVA, E. 1974. Les gastéropodes perceurs et leurs victimes du Miocène de Bulgarie du Nord-ouest. Bulgarian Academy of Science Bulletin, Geological Institute (Ser. Paleontol.), 25: 5–24.

KOWALEWSKI, M. 2004. Drill Holes Produced By the Predatory Gastropod *Nucella Lamellosa* (Muricidae): Palaeobiological and Ecological Implications. Journal Molluscan Studies, 70: 359–370.

LEIGHTON, L. R., 2002. Inferring predation intensity in the marine fossil record. Paleobiology 28: 328–342.

MADDOCKS, R. F. 1988. One Hundred Million Years of Predation on Ostracods: The Fossil Record in Texas. Developments in Palaeontology and Stratigraphy, 11: 637–657.

MALLICK, S., S. BARDHAN, S. S. DAS, S. PAUL, and P. GOSWAMI. 2014. Naticid drilling predation on gastropod assemblages across the K-T boundary in Rajahmundry, India: New evidence for escalation hypothesis. Palaeogeography, Palaeoclimatology, Palaeoecology, 411: 216–228.

MONDAL, S., S. BARDHAN, S. MALLICK, and A. ROY. 2014. Repair scars on *Mactra violacea* from the eastern coast of India: A new classification and a model for describing shell breakage on bivalves. Palaeontologia Electronica, 17: 1-13.

NEGUS, M. 1975. An analysis of boreholes drilled by *Natica catena* (Da Costa) in the valves of *Donax vittatus* (Da Costa). Proceedings of the Malacological Society of London, 41: 353-356.

OLABARRIA, C., A. J. UNDERWOOD, and M. G. CHAPMAN. 2002. Appropriate experimental design to evaluate preferences for microhabitat: An example of preferences by species of microgastropods. Oecologia, 132: 159–166.

ORTIZ-JERÓNIMO, C. G., M. C. GÓMEZ-ESPINOSA, F. R. GÍO-ARGÁEZ, O. TALAVERA-MENDOZA, L. A. F. DE DIOS, and B. B. MARTÍNEZ-VILLA., 2021. Drilling predation on juvenile and adult gastropod shells during the Pliocene in the eastern Pacific, southern Mexico. Journal of South American Earth Sciences, 110: 103352.

PAHARI, A., S. MONDAL, S. BARDHAN, D. SARKAR, S. SAHA, and D. BURAGOHAIN. 2016. Subaerial naticid gastropod drilling predation by *Natica tigrina* on the intertidal molluscan community of Chandipur, Eastern Coast of India. Palaeogeography, Palaeoclimatology, Palaeoecology, 451: 110–123.

R Core Team. 2020. R: A language and environment for statistical computing. R Foundation for Statistical Computing, Vienna, Austria.

REUTER, M., W. E. PILLER, M. HARZHAUSER, A. KROH, F. RÖGL, and S. ĆORIĆ. 2011. The Quilon Limestone, Kerala Basin, India: An archive for Miocene Indo-Pacific seagrass beds. Lethaia, 44: 76–86.

REYMENT, R. A., and A. M. T. ELEWA. 2003. Predation by drills on Ostra- coda. In P. H. Kelley, M. Kowalewski and T. A. Hansen (ed.), Predator-Prey Interactions in the Fossil Record, Springer, pp. 93–112.

_____, E. R. REYMENT, and A. HONIGSTEIN. 1987. Predation by boring gastropods on Late Cretaceous and Early Palaeocene ostracods. Cretaceous Research 8: 189–209.

RÖGL, F., and A. BRIGUGLIO, 2018. The foraminiferal fauna of the Channa Kodi section at Padappakkara, Kerala, India. Palaeontographica Abteilung A, 47–101.

ROY, K., D. J. MILLER, and M. LABARBERA. 1994. Taphonomic bias in analyses of drilling predation: effects of gastropod drill holes on bivalve shell strength. PALAIOS 9: 413–421.

SAWYER, J. A., and M. ZUSCHIN. 2011. Drilling Predation in Mollusks from the Lower and Middle Miocene of the Central Paratethys. PALAIOS, 26: 284–297.

SOHL, N. F. 1969. The fossil record of shell boring by snails. Integrative and Comparative Biology, 9: 725–734.

TULL, D. S, and K. BÖHNING-GAESE. 1993. Patterns of Drilling Predation on Gastropods of the Family Turritellidae in the Gulf of California. Paleobiology, 19: 476–486.

VERMEIJ, G. J. 1987. Evolution and Escalation, an Ecological History of Life. Princeton University Press, 527 pp.

_____, D. E. SCHINDEL, and E.ZIPSER, 1981. Predation Through Geological Time: Evidence from Gastropod Shell Repair. Science, 214: 1024–1026.

VERMA, K. K. 1977. Cranoid crabs from the Quilon Beds (Lower Miocene) of Kerala, India, Journal of the Palaeontological Society of India, 20: 305–313.

VISAGGI, C. C., G. P. DIETL, and P. H. KELLEY. 2013. Testing the influence of sediment depth on drilling behaviour of *Neverita duplicata* (Gastropoda: Naticidae), with a review of alternative modes of predation by naticids. Journal of Molluscan Studies, 79: 310–322.

WALL, C. C., B. J. PETERSON, and C. J. GOBLER, C.J., 2008. Facilitation of seagrass Zostera marina productivity by suspension-feeding bivalves. Marine Ecology Progress Series, 357, 165–174.

WARÉN, A., 1983. A generic revision of the family eulimidae (Gastropoda, Prosobranchia). Journal of Molluscan Studies, 49: 1–96.

YASUHARA, M., Y. HONG, S. Y. TIAN, W. K. CHONG, R. W. C. CHU, H. OKAHASHI, M. REUTER, W. E. PILLER and M. HARZHAUSER, 2020. Early Miocene marine ostracodes from southwestern India: implications for their biogeography and the closure of the Tethyan Seaway. Journal of Paleontology, 94: 1–36.

ZUSCHIN, M., and R. J. STANTON JR, 2001. Experimental measurement of shell strength and its taphonomic interpretation. PALAIOS, 16: 161–170.

Museum of Paleontology, The University of Michigan
1105 North University Avenue, Ann Arbor, Michigan 48109-1085
Matt Friedman, Director

Contributions from the Museum of Paleontology, University of Michigan is a medium for publication of reports based chiefly on museum collections and field research sponsored by the museum. Jennifer Bauer and William Ausich, Guest Editors;
Jeffrey Wilson Mantilla, Editor.

Publications of the Museum of Paleontology are accessible online at: http://deepblue.lib.umich.edu/handle/2027.42/41251

Print (ISSN 0097-3556), Online (ISSN 2771-2192)

Contributions

from the Museum of Paleontology, University of Michigan

VOL. 34, NO. 7, PP. 82–102 MARCH 31, 2022

SYSTEMATICS, TAPHONOMY, AND PALEOECOLOGY OF MILLERICRINIDS (MILLERICRINIDA, ARTICULATA, CRINOIDEA) FROM THE LATE JURASSIC OF SPAIN

BY

SAMUEL ZAMORA[1,2]

Abstract — Millericrinids constitute an order of extinct articulate crinoids that range from the Middle Triassic to the Late Cretaceous. Based on partially articulated material comprising calyces, columns, and holdfasts, six species (one of them new) belonging to five different genera are described from the Late Jurassic of Spain for the first time. They include *Angulocrinus tomaszi* n. sp. from the Yatova Formation (middle-upper Oxfordian); and *Millericrinus milleri*, *Liliocrinus polydactylus*, *Pomatocrinus hoferi*, *Pomatocrinus* cf. *mespiliformis*, and *Apiocrinites* cf. *parkinsoni* from the Sot de Chera Formation (Kimmeridgian). *A. tomaszi* n. sp. lived in association with sponges and other invertebrates in relatively shallow, open platform areas, with variable depths near storm wave base. The assemblage from the Sot de Chera Formation is more diverse and preliminary taphonomic and sedimentological information suggest that these millericrinids lived in high-energy conditions from shore-face environments and were transported and buried to the off-shore basin due to successive storm events. These faunas have a high number of specimens colonized by diverse sclerobionts, that combined with the presence of eroded material belonging to columnals suggest a prolonged biostratinomic phase for some specimens. Additionally, some specimens have swollen stems likely recording parasitism. The reported taxa also provide important data on the palaeobiogeographic distribution of millericrinids during the Jurassic showing that the Iberian material has affinities with other European localities.

urn:lsid:zoobank.org:pub:195B60EF-3B8F-4059-8132-33D12F34AD92

[1]Instituto Geológico y Minero de España (IGME-CSIC), C/Manuel Lasala 44, 9B, E-50006, Zaragoza, Spain. (s.zamora@igme.es)
[2]Grupo Aragosaurus-IUCA, Área de Paleontología, Facultad de Ciencias, Universidad de Zaragoza, Zaragoza, Spain.

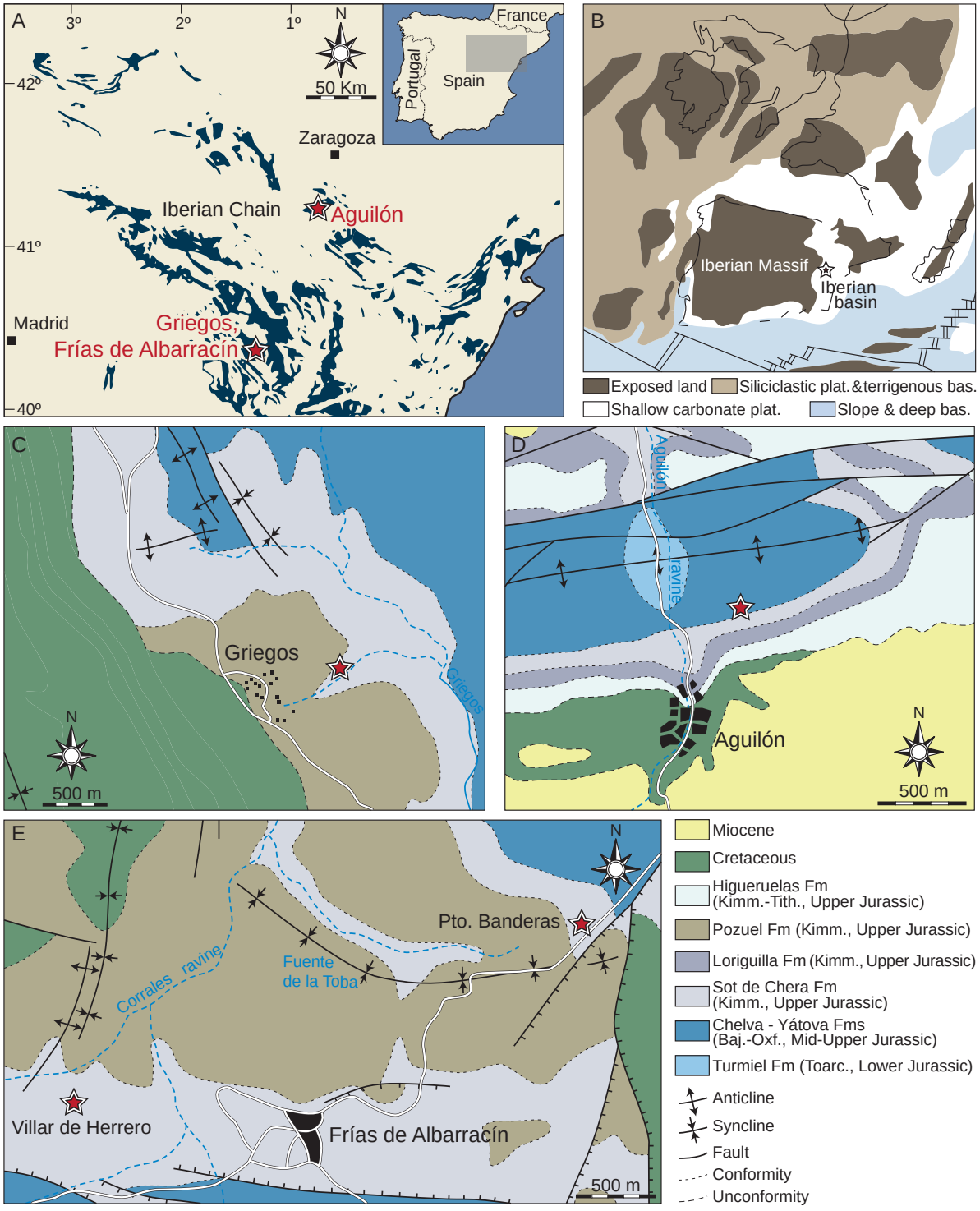

FIGURE 1 — **A**, distribution of Jurassic outcrops (blue) in NE Spain with indication of studied localities (red stars) (modified from Aurell et al., 2010, fig. 2). **B**, paleogeography of Western Europe during the Late Jurassic (modified from Dercourt et al., 1993, map 6 Early Kimmeridgian). **C**–**E**, geological maps of the studied outcrops with detailed indication of main localities. Abbreviations: Baj., Bajocian; bas., basins; Kimm., Kimmeridgian, Oxf., Oxfordian; plat., platforms; Tith., Tithonian; Toarc., Toarcian.

FIGURE 2 — Field photographs of the studied outcrops. **A**, section in the road-cut of Puerto de las Banderas. Fossiliferous levels containing crinoids appear in the marly intervals of the top of the Sot de Chera Formation. **B**, **C**, Villar de Herrero outcrop (B), with indication of some stem fragments by arrows (C). **D**, locality of Griegos with indication of the two fossiliferous levels containing crinoids. **E**, locality of Aguilón 5 with fossiliferous levels of the Yatova Formation that contain crinoid material (outcrop indicated by an arrow). **F**, partially buried specimen of *Millericrinus milleri* from the Griegos 1 locality. **G**, complete calyx of *Liliocrinus polydactylus* from the Puerto de las Banderas locality. Note that resedimented oolites are common in the surrounding sediment. **H**, partially articulated calyx of *Apiocrinites* cf. *parkinsoni* and stem fragments from the Villar de Herrero locality.

INTRODUCTION

Post-Palaeozoic crinoids includes most post-Paleozoic taxa traditionally considered articulates, including approximately 600 extant species (Wright, et al., 2017). This group comprises eight orders (sensu Hess and Messing, 2011), some of which are present in modern marine ecosystems (Comatulida, Isocrinida, Hyocrinida, Cyrtocrinida) and some including only extinct forms (Holocrinida, Encrinida, Millericrinida, Roveacrinida). Molecular clocks estimate that Articulata resulted from the diversification of a lineage that passed through the Permian-Triassic extinction event (Rouse et al., 2013). Whereas recent phylogenetic studies start to clarify the position of modern groups (Rouse et al., 2013), extinct taxa are more problematic; however, fossils provide an important source of morphological and palaeobiogeographical information helping us understand the whole evolutionary history of crinoids.

Millericrinids are characterized among other features by five basals, five radials, a column cylindrical with radiating crenulae, and absence of cirri (sensu Hess and Messing, 2011). Species identification based on incomplete material lacking dorsal cups is problematic (Salamon and Zatoń, 2005; Krajewski et al., 2019). The problem increases with the presence of a cylindrical column with radiating crenulae is also a feature convergent with other crinoid lineages such as isocrinids (Oji and Kitazawa, 2008), posing more problems in the systematics of crinoids based on isolated columns. Thus, calyx material and proximal columns are the most diagnostic parts in millericrinid systematics (Hess and Messing, 2011).

Millericrinids range from the Anisian (Triassic) to the Cenomanian (Cretaceous; Stiller, 2000; Gorzelak and Salamon, 2006; Hagdorn, 2011; Hess and Messing, 2011) and are a typical component in the Jurassic assemblages from Europe. In the Cretaceous, the group experienced a significant decline in diversity and they have been reported in only a few assemblages from France, Switzerland, Spain, Poland, and UK (Rasmussen, 1961; Gorzelak and Salamon, 2006; Hess and Gale, 2010). During the late Jurassic, shallow epicontinental seas covered wide areas of Western Europe (Fig. 1B) with carbonate sedimentation dominating the Iberian Basin, facing the Tethys Ocean to the west on the western margin of the Iberian Plate (e.g., Dercourt et al., 1993). This was an ideal area for the development of shallow carbonate platforms hosting a wide diversity of benthic organisms, including crinoids (Pomar et al., 2015). Although crinoids are an important component in Jurassic marine assemblages, the Iberian fauna has received little attention. Millericrinids are common during the Late Jurassic, but few general papers have cited their presence in Spain. These include Olagüe (1936) and Fezer (1988), who cited *Millericrinus* and *Apiocrinus* respectively in the Upper Jurassic. Several geological map memoirs from the Spanish Geological Survey also commented on the presence of millericrinids in several areas (see Abril and Rubio, 1977, among others). Hess and Messing (2011) also cited the presence of *Pomatocrinus* and *Apiocrinites* in Spain, but never figured any material. Finally, Zamora et al., (2018) first reported and figured a rich Late Jurassic fauna comprising cyrtocrinids, comatulids, isocrinids and millericrinids, but none of them received detailed systematic treatment.

The aim of this work is to formally describe the millericrinid fauna of the Late Jurassic of Northeastern Spain, which include calyx material and proximal columns. A large number of columnals and holdfast are also present in the described localities, and they provide important paleoecological and taphonomical information that increase our understanding of the occurrence of these crinoids. Because millericrinids constitute an extinct order of crinoids, their description will provide morphological information that can improve the knowledge of their systematic position, palaeoecology, and palaeobiogeographical distribution.

MATERIAL AND METHODS

Specimens described in this study were surface collected directly from the outcrops as macrofossils during the last decade (Fig. 2F–H). Crinoid remains are very common in the sampled outcrops, but thecal material, especially complete calyces, are rare. For perspective, if one person collects intensely for eight hours they will recover one specimen on average. Most specimens were covered by marly material and were prepared using potassium hydroxide (KOH), and later neutralized with hydrochloric acid (10%). Specimen were photographed using a Nikon D7100 equipped with AF-S Micro NIKKOR 60 mm objective after coating with ammonium chloride to increase contrast. Specimens are deposited in the Museo de Ciencias Naturales de la Universidad de Zaragoza (MPZ; Canudo, 2018).

Most specimens from the Sierra de Albarracín localities have sclerobionts on skeletal elements that indicate postmortem colonization. Clear examples include sclerobionts on articulating surfaces of the brachials, columnal articulations, and attachment parts of the roots. Some others appear intensively eroded and have rounded edges. The encrustation and erosion observations point to a complex taphonomic history (see discussion below) and not in situ burial of specimens.

GEOLOGICAL SETTING AND LOCALITIES

All specimens come from two formations and areas in the Iberian Ranges (Fig. 1A). Specimens of *Angulocrinus tomaszi* n. sp. were collected from the Yatova Formation (Upper Jurassic) in the surroundings of Aguilón (Zaragoza, Iberian Range). This corresponds with locality Aguilón 5 of Meléndez (1989) or its lateral equivalent (Fig. 1D, 2E). Although millericrinid columnals are common in the Yatova Formation, only this locality has provided important diagnostic material comprising the proximalmost columnal. This formation is a sponge-limestone dominated unit, which has been dated as middle-upper Oxfordian and contains abundant echinoderm remains, including a diverse crinoid fauna (Zamora et al., 2018). Here, the Yátova Formation

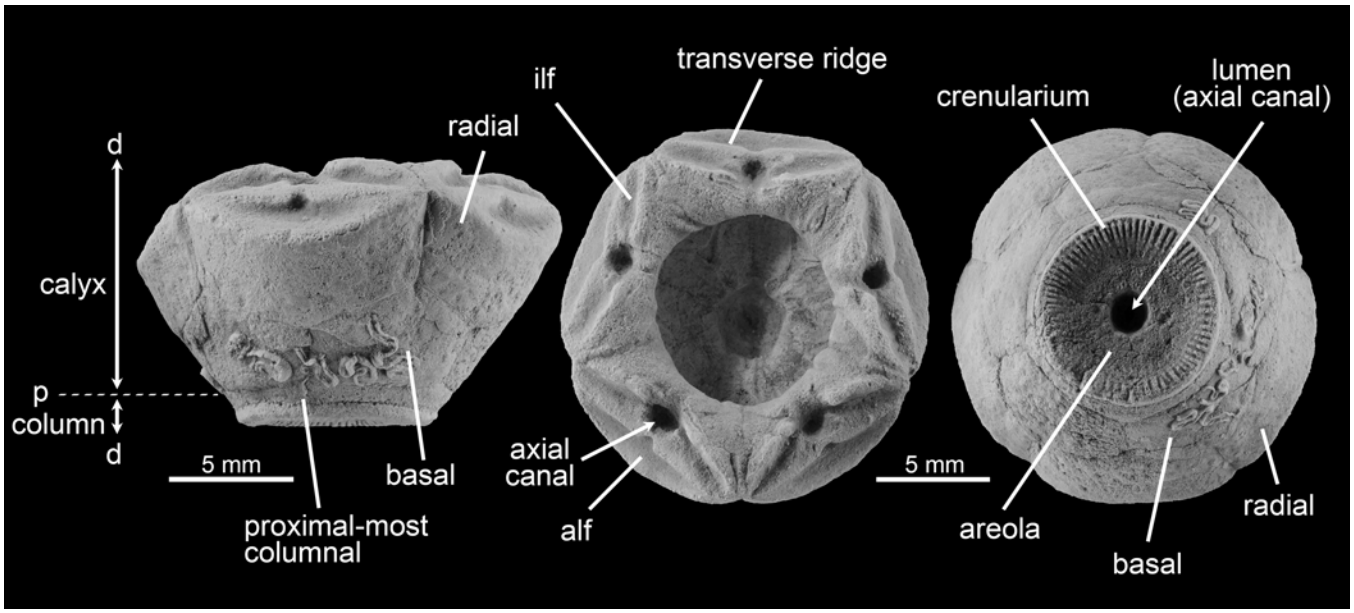

FIGURE 3 — Terminology for millericrinids used in the text. Terms follow Hess and Messing (2011). This is a photograph of *Liliocrinus polydactylus* (specimen MPZ2021/180). Abbreviations: *alf*, aboral ligament fossae; *d*, distal; *ilf*, interarticular ligament fossae; *p*, proximal.

consists of tabular to nodular limestone with marly interbeds, locally forming decimeter to meter-thick, upward-thickening sequences (Ramajo and Aurell, 2008). The main components are siliceous sponges (*Dictyida*, *Lychniskida*, and *Lithistida*, in descending order of abundance: e.g., Deusch et al., 1990) of variable morphologies (dish, cup, and tubular), typically broken and preserved in graded beds. They are associated with a microbial crust and encrusting organisms such as annelids (serpulids, *Terebella*), bryozoans, benthic foraminifera (nubeculariids, *Bullopora*), and *Tubiphytes*. Also common are tuberoids and encrusted fragments of sponges. Locally, ammonites, belemnites, bivalves, brachiopods, echinoids, asterozoans, foraminifera, ostracodes, ahermatypic corals, and crinoids can be common. The maximum age range of the Yátova Formation is middle Oxfordian (i.e., lower Transversarium Biozone) to upper Oxfordian (i.e., lower Planula Biozone, Planula Subzone). The locality of Aguilón 5 represents a small outcrop that includes the transition between the Bifurcatus and Bimammtum Biozones, which corresponds with the middle-upper Oxfordian transition (sensu Meléndez, 1989).

Other described material comes from the Sot de Chera Formation (Upper Jurassic) in Griegos and Frías de Albarracín (Teruel, Iberian Range; Fig. 1A). Two localities in Frías de Albarracin (namely Puerto de las Banderas and Villar de Herrero) and two stratigraphic levels in Griegos (Griegos 1 and 2) have provided most of the described material (Fig. 1C, E; 2A–D). The localities of Villar de Herrero (Fig. 2B, C) and Griegos (Fig. 2D) are stratigraphically lower in the Sot de Chera Formation, and Puerto de las Banderas consists of the higher levels of the Sot de Chera Formation (Fig. 2A). This formation consists of thick marly dominated successions, including decimeter-thick siliciclastic and skeletal-rich limestone intercalations. In the three localities, crinoids are abundant in skeletal-rich horizon, which includes ammonites of Galar subzone (Planula Zone) (see Zamora et al., 2018). This horizon also contains resedimented ooids from more proximal and shallow carbonate shoal environments (Pomar et al., 2015), which have implications to explain the occurrence of the crinoid material (see below). The studied bioclastic and marly intervals contain abundant echinoderm remains, including a diverse crinoid fauna. Here, the Sot de Chera Formation consists of a marly progradational wedge-shaped deposits with siliciclastics derived from the emergent areas located to the west, including abundant graded skeletal accumulations interpreted as tempestites (Aurell et al., 2003, 2010). The main skeletal components found in these mid-ramp deposits are bivalves, echinoderms, gastropods, brachiopods, siliceous sponges, serpulids, benthic foraminifera, ahermatypic colonial and solitary corals, belemnites, and ammonites. Species of crinoids per locality are summarized in Table 1.

SYSTEMATIC PALEONTOLOGY

Descriptive terminology follows Rasmussen (1978) and Hess and Messing (2011). Classification follows Hess and Messing (2011). Main morphological terms are synthetized in Figure 3.

Class CRINOIDEA Miller, 1821
Subclass ARTICULATA Miller, 1821
Order MILLERICRINIDA Sieverts-Doreck, 1952
Family MILLERICRINIDAE Jaekel, 1918

TABLE 1 — Occurrence of millericrinid crinoid genera in the different localities. The locality of Pozuel correspond to the data presented in Zamora et al. (2018). *: present as articulated specimens. +: present as disarticulated material from the calyx. -: absent.

Locality	Taxa				
	Apiocrinites	*Liliocrinus*	*Millericrinus*	*Pomatocrinus*	*Angulocrinus*
Pto. Banderas	*	*	-	+	-
Villar Herrero	*	-	-	*	-
Griegos 1	-	-	*	+	-
Griegos 2	-	-	-	+	-
Pozuel	-	-	-	*	-
Aguilón	-	-	-	-	*

Diagnosis.— Cup low cone, bowl, or globe shaped. Sharp distinction between cup and column in most forms. Few or generally no interadial plates (*sensu* Hess and Messing, 2011).

Remarks.— This family of only Jurassic forms include genera such as *Millericrinus*, *Angulocrinus*, and *Liliocrinus* among others. *Millericrinus*, *Pomatocrinus*, and *Orbignycrinus* have a very expanded calyces which clearly differ from the conical shape expressed in *Angulocrinus*, *Ailsacrinus*, and *Liliocrinus*. All forms with the exception of *Ailsacrinus* have large, modified attachment structures (Taylor, 1983; Hunter et al., 2016).

Genus *Angulocrinus* Rollier, 1911

Type species.— *Millericrinus nodotianus* d'Orbigny, 1841 by original designation.

Diagnosis.— Cup truncated conical, not tumid, increasing in diameter upward from edge of enlarged uppermost columnal, which is more or less included as a rounded to 5-sided proximale in cup with a 5-sided pyramidal proximal facet toward the basals. Synarthries between primibrachials 1 and 2 and secundibrachials 1 and 2. Proximal part of column 5-sided with columnals that may alternate in height and diameter. Mesistele mostly cylindrical, commonly ornamented with tubercles, spines, or strands of stereom attached to each other; attachment by radicular cirri as creeping roots or runners along the substrate but also by terminal root. Columnal articular facets with radiating crenulae commonly arranged in five groups, especially in proximal part of the column. Crenulae may in some species, be restricted to a marginal zone of facet (*sensu* Hess and Messing, 2011).

Remarks.— The present material is assigned to *Angulocrinus* based on the presence of enlarged uppermost columnal and crenulae arranged in five groups present in the proximal column. Hess and Messing (2011) indicated that proximal part of the column is pentagonal, but in the studied material only the proximalmost columnal facet is slightly pentagonal. Its distal facet is circular in outline.

Angulocrinus tomaszi n. sp.
Fig. 4

2018 Millericrinida indet. Zamora et al., p. 787, fig. 8C

Etymology.— Species honoring Professor Tomasz Baumiller (University of Michigan) for a lifetime dedicated to the study of modern and fossil crinoids; and for his generosity advising and encouraging me to work on post-Palaeozoic crinoids from Spain.

Type material.— Holotype includes a proximalmost columnal with second columnal (MPZ2018/472) (Fig. 4A-C). Paratype MPZ2021/178 is a fragment of a column preserving two and a half columnals (Fig. 4D-E).

Type locality.— Locality Aguilón 5 from Meléndez (1989).

Type horizon.— Yatova Formation, in the transition between the Bifurcatus and Bimammtum Biozones, middle to upper Oxfordian.

Material.— Single proximal columnal with second columnal attached and fragment of a column comprising two and a half columnals.

Diagnosis.— Proximalmost columnal flanged with five deep aureola separated by large ridges. Deep crenulae restricted to the margins of the areola and separated in five groups.

Description.— Proximal facet of the proximalmost columnal flat with a diameter of 8 mm, and 4.5 mm in height, and pentalobate in shape with a wide pentagonal lumen (ca. 2 mm). Five deep articular facets (areolas) with crenularium deep and restricted to the margins. Scattered granules in the areolas. Margins smooth without ornamentation. Distal

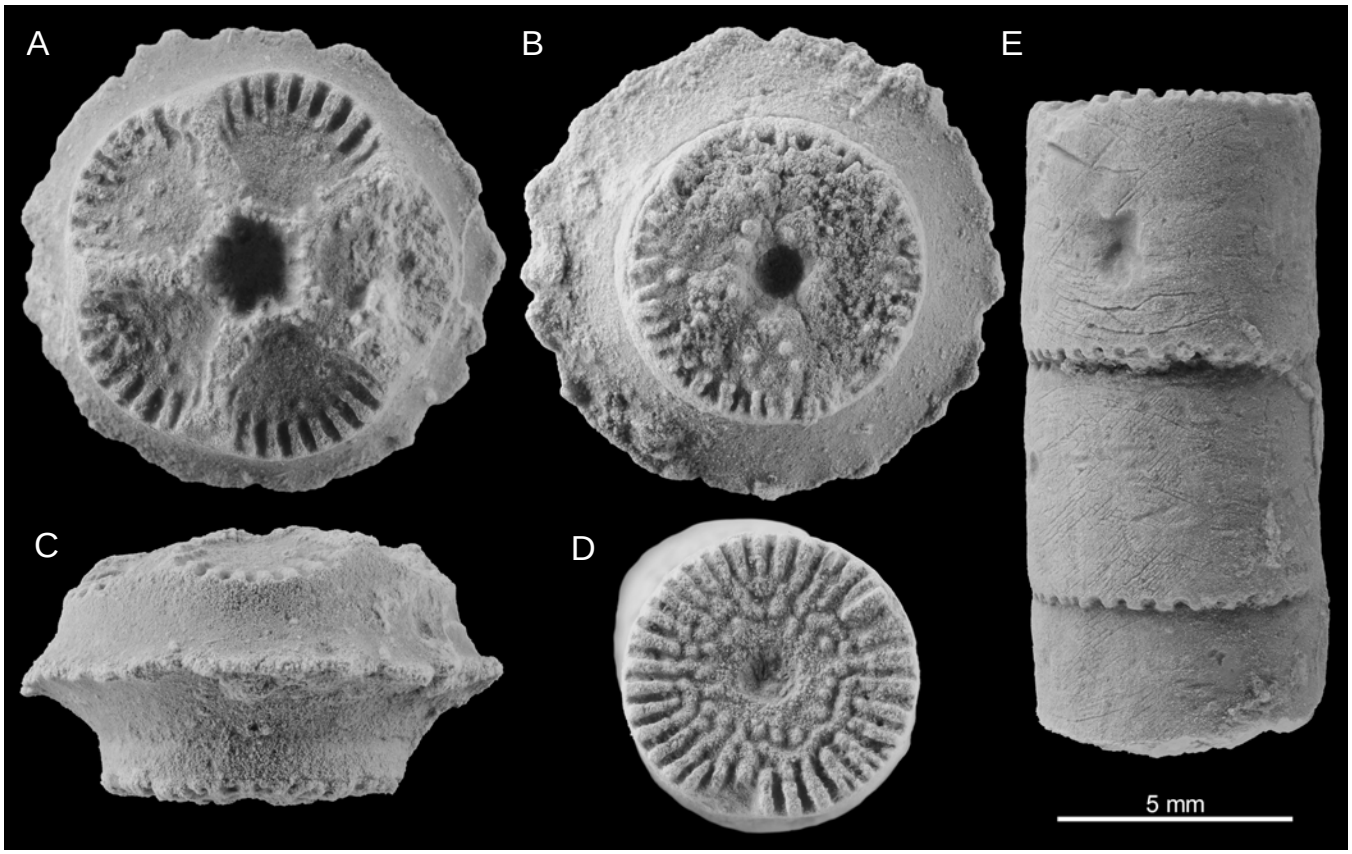

FIGURE 4 —*Angulocrinus tomaszi* n. sp., photographs of specimens from the Aguilón 5 locality in the Yatova Formation (Oxfordian, Late Jurassic). **A**–**C**, photographs of specimen MPZ2018/472 that corresponds to a proximal-most stem columnal with second columnal attached in proximal (A), distal (B), and lateral (C) views. **D**, **E**, photographs of specimen MPZ2021/178 that corresponds to columnals in axial (D) and lateral views (E).

facet of the proximalmost columnal unknown, but probably circular in outline and with marginal crenulae. Distal facet of first columnal circular in outline, with crenularium restricted to the margins and circular, wide lumen. Granules scattered in the articular facet.

Column externally smooth, with columnals that are slightly higher than wide; marginal crenularium that transform into granules to the lumen.

Remarks.— Only the proximal column with first columnal and one additional columnal is preserved. In the same level providing the proximalmost columnal there are also columns with typical crenulae and morphology of millericrinids; but only the figured specimens agree with the granules and crenulae observed in the described first columnal attached to the proximal columnal, thus this is a strong argument suggesting that this column belong to the same taxa. *Angulocrinus nodotianus*, the type species, lack a flanged proximal columnal, but has a column that has in some specimens flanged nodals (see de Loriol, 1884). Proximal part of uppermost columnal is pentagonal and with crenulae arranged in five groups, similar to *A. tomaszi* n. sp. *A. orbignyi* (figured in de Loriol, 1884, pl. 116, 1c) also preserves proximal most columnal and basals; *A. tomaszi* n. sp. differs from the later in having a flanged proximal columnal. Proper comparison with most species assigned to *Angulocrinus* based on columns only is problematic, especially because Hess and Messing (2011) pointed out that columns are highly variable.

Genus *Millericrinus* d'Orbigny, 1840

Type species. *Encrinites milleri* Schlotheim, 1823, under original designation.

Diagnosis.— Cup large and pentagonal, very low and wide. Basals form horizontal underside of cup; radials steep (*sensu* Schweigert et al., 2008).

Remarks.— *Millericrinus* is a name that has been traditionally used to many millericrinids either based on calyx or stem fragments only. Currently it includes two accepted species based on calyx material. *M. milleri* is the most represented and well-known species, having been recorded in many European localities (see Hess and Messing, 2011). *M. charpyi* is poorly known based on a few specimens described by de Loriol (1884) and considered in Rasmussen (1978).

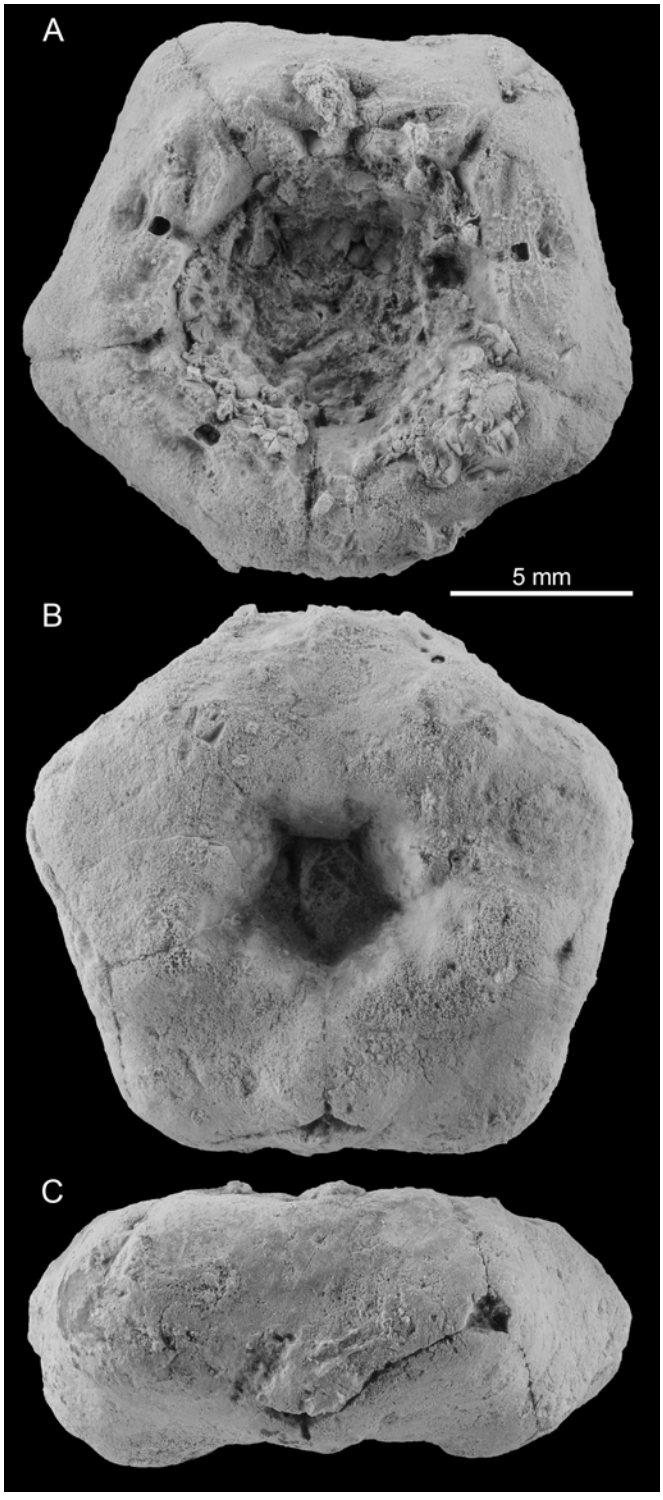

FIGURE 5 —*Millericrinus milleri*, photograph of specimen (MPZ2021/179) from the Griegos 1 locality in the Sot de Chera Formation (Kimmeridgian, Late Jurassic). A–C, complete calyx in oral (A), aboral (B), and lateral (C) views.

Millericrinus milleri Schlotheim (1823)
Fig. 5

2008 *Millericrinus milleri* Scheweigert et al., fig. 2 (with previous synonymies)

Material.— Only one specimen representing a complete calyx (MPZ2021/179).

Diagnosis.— Large pentagonal and low cup, with basals forming the floor of the calyx and radials occupying most of the sides of the calyx. Lumen clearly pentagonal. External part of proximal-most columnal lacking bosses.

Remarks.— *Millericrinus milleri* is characterized by a large and pentagonal cup which is very low (compared with other millericrinids) and wide. The basal plates form the horizontal underside of the cup. The Spanish specimen follows the aforementioned features and is thus included in this species. De Loriol (1889) figured specimens in different ontogenetic stages in plates 95-96. Large specimens have proportionately smaller facets compared with the total length of the radial plates and large proximal projections (in lateral view) in the articulation of two adjacent radials. Smaller specimens have lower radials and larger arm facets. The described specimen here is very similar to the small specimens described by de Loriol (1889) in its plates 95-96. This was also emphasized by Roux (1978) who did a comparative ontogenetic study of different millericrinids and showed that the shape of the calyx in *M. milleri* is highly dependent on its size. According to Schweigert et al., (2008), *M. charpyi* de Loriol, is the most similar form to *M. milleri*; however, the occurrence of ten oval bosses covering the lateral surface of the cup of *M. charpyi* is the most important diagnostic feature distinguishing this taxon from *M. milleri*.

Genus *Liliocrinus* Rollier, 1911

Type species.— *Millericrinus polydactylus* d'Orgigny, 1841

Diagnosis.— Cup low conical to bowl shaped, not tumid, increasing in diameter upward from edge of rather wide, uppermost columnal. Basals and radials large. Radial articular facet low and wide. Synostosis with marginal crenulae between primibrachials 1 and 2, synarthry between secundibrachials 1 and 2. Column cylindrical, proximal columnals slightly increasing in diameter toward cup, not 5-sided. Columnal articular facets covered by radiating crenulae not separated in groups. Proximal articular facet of uppermost columnal more or less pyramidal or conical to almost flat. Attachment by root (sensu Hess and Messing, 2011).

Remarks.— Desor (1845) demonstrated that the species first recorded was ambiguous. Later Rasmussen (1978) designated *M. polydactylus* as the type species; a view followed by Hess and Messing (2011) and here. Hess and Messing (2011) distinguished two species in this genus: *L. polydactylus* and *L. munsterianus*. Based on the holotype of *L. polydactylus* (Fig. 7D-F) and comparison with the well-

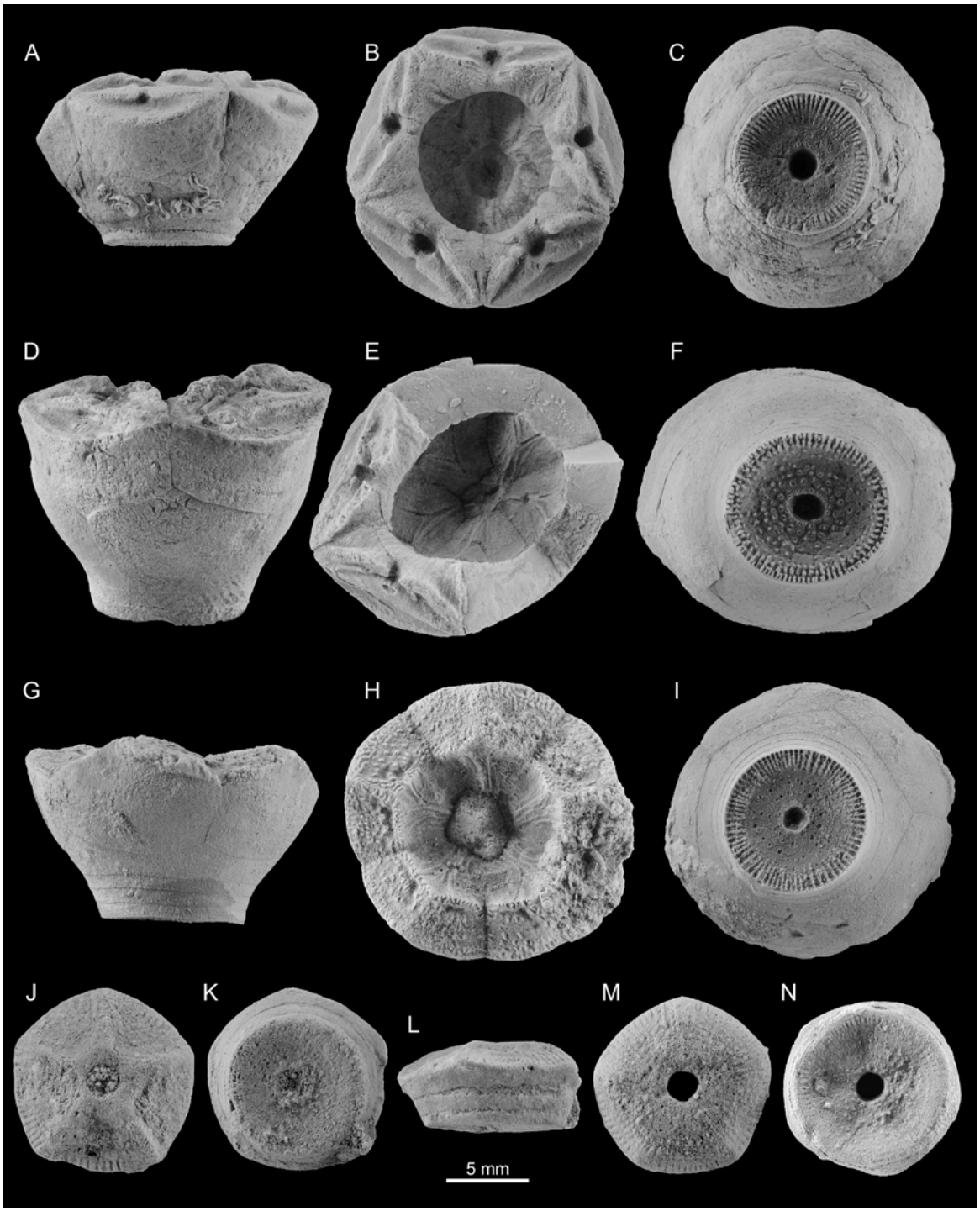

FIGURE 6 — *Liliocrinus polydactylus*, photographs of specimens from the Puerto de las Banderas locality of the Sot de Chera Formation (Kimmeridgian, Late Jurassic). **A**–**C**, MPZ2021/180 a complete calyx with first columnal in lateral (A), oral (B), and aboral views (C). **D**–**F**, MPZ2021/181, a partially complete calyx with five basals and two radials preserved, and two proximalmost columnals preserved in lateral (D), oral (E), and distal (F) views. Note granules in the articulation facet. **G**–**I**, MPZ2021/182, a partial calyx preserving the five basal plates in lateral (G), oral (H), and aboral (I) views. **J**–**L**, MPZ2021/183, a proximalmost columnal and second and third columnal in oral (J), aboral (K), and lateral (L) views. **M–N**, MPZ2021/184, a proximalmost columnal in oral (M) and aboral (N) views.

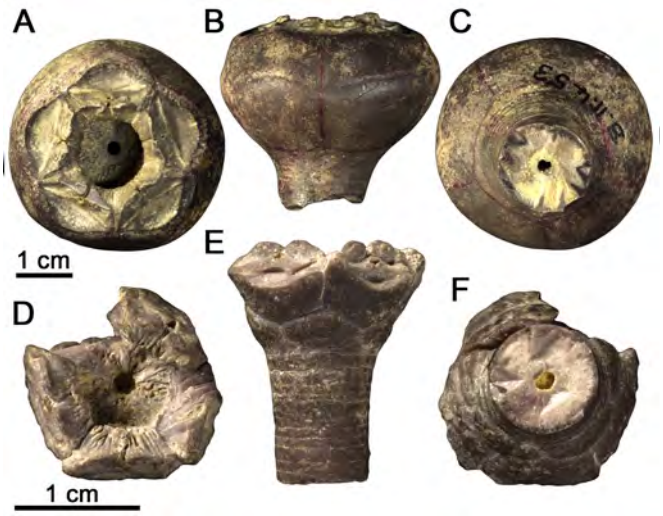

FIGURE 7 — Crinoid specimens from the Late Jurassic of Pointe-du-Chay (France) in the d'Orbigny collection of the MNHN. **A–C,** holotype of *Pomatocrinus fleuriausianus* (MNHN.F.B11453) in oral (D), lateral (E), and aboral (F) views. **D–F**, syntype of *Liliocrinus polydactylus* (MNHN.F.R62602) in oral (D), lateral (E), and aboral (F) views. Images courtesy of the Muséum National d´Histoire Naturelle (París)

figured material of *L. munsterianus* by de Loriol (1877), it became evident that shapes of the theca in the later is quiet variable in terms of basal and radial morphologies. For these reasons, *L. munsterianus* is treated here as a junior synonym of *L. polydactylus*. *L. polydactylus* is then considered the sole species of *Liliocrinus*.

Liliocrinus polydactylus (d'Orgigny, 1841)
Fig. 6

1877 *Millericrinus munsterianus* de Loriol, pl.VII, figs. 1–15 (with previous synonymies).

1884 *Millericrinus polydactylus* de Loriol, pl. 109, figs. 1–2 (with previous synonymies).

1978 *Liliocrinus polydactylus* Rasmussen, fig. 551, 2h, m.

1978 *Liliocrinus munsterianus* Rasmussen, fig. 551, 2j, k.

2011 *Liliocrinus polydactylus* Hess and Messing, fig. 80, 1a–b.

2011 *Liliocrinus munsterianus* Hess and Messing, fig. 80,1c–g.

Material.— Several complete calyces (MPZ2021/180, 181, 182) (Fig. 6A–I) with proximal most columnals, and some proximal columnals (MPZ2021/183, 184, 185, 186) (Fig. 6J–N) and a single radial plate (MPZ2021/187). Measurements of calyx material are given in Table 2.

Remarks.— Spanish material consists of well-preserved calyces, proximal columns and probably roots. The calyx material is variable in shape. There are specimens from same locality and stratigraphic level that have basals higher than radials; and others that have basals lower than radials. This is also observed in the material figured by de Loriol (1877, plate 7). Proximalmost columnal facets have five ridges that separate articulations for the five basals and marginal crenulae. In distal facets of proximal columnals the crenulae turn into fine granules toward the lumen. Granules are also present in the articulation between basals and radials.

Genus *Pomatocrinus* Desor, 1845

Type species.— *Encrinites mespiliformis* von Schlotheim, 1820 by original designation.

Diagnosis.— Cup large, globe shaped, thick walled, comprised of very large basals, smaller radials, and a rather large proximale surrounding an almost spherical central cavity. Sutures distinct. All cup plates with flat, slightly rough facets. No trace of infrabasals. Radial articular facet large, plenary; articulation with distinct fulcral ridge, aboral and interarticular ligament fossae, and small adoral muscle fossae. Primibrachials meet laterally. Arms divided at primibrachials 2 and more distally; first pinnule on secundibrachial 2. Synarthries between primibrachials 1 and 2 and secundibrachials 1 and 2. Proximal most columnal 5-sided, forming aboral pole of spherical cup, and continued as high, 5-sided, truncated pyramid inside basal circlet to bottom of central cavity; underside has a concave, circular, articular facet to receive finely granulated proximal facet of next columnal, which together with a few succeeding, very low columnals form very short, slightly conical transition to cylindrical column. Columnal articular facets with fine, radiating crenulae, closely placed, not in separate groups; crenulae might be modified to granules in central area (sensu Hess and Messing, 2011).

Remarks.— The genus *Pomatocrinus* include several species mostly described by d'Orbigny (1840) and de Loriol (1884, 1887) that have different development of basals and radials (Roux, 1978). Based on the currently known species and apparent changes in ontogeny, it is necessary to perform a morphometric analysis in order to understand changes in shape within and between different species. This is beyond the scope of the current work. Specimens described here include complete calyx, fragments of columns, and holdfasts. Disarticulated specimens including proximalmost columnal that usually appear with fused proximal columnals and isolated calyx plates are also present. Shape of the calyx in described material meets the diagnosis presented by Salamon and Zatoń (2005) and Hess and Messing (2011, see above) and should be assigned to the genus *Pomatocrinus*. The proximal part of the proximalmost columnal has the shape of a truncated pyramid which is higher than in *Liliocrinus* and also lacks crenulae in its proximal facet. These two features are important differences between two genera when only the proximal column is present. There are two clear morphotypes of *Pomatocrinus* in the described material; one includes a complete calyx plus isolated basal plates here considered as

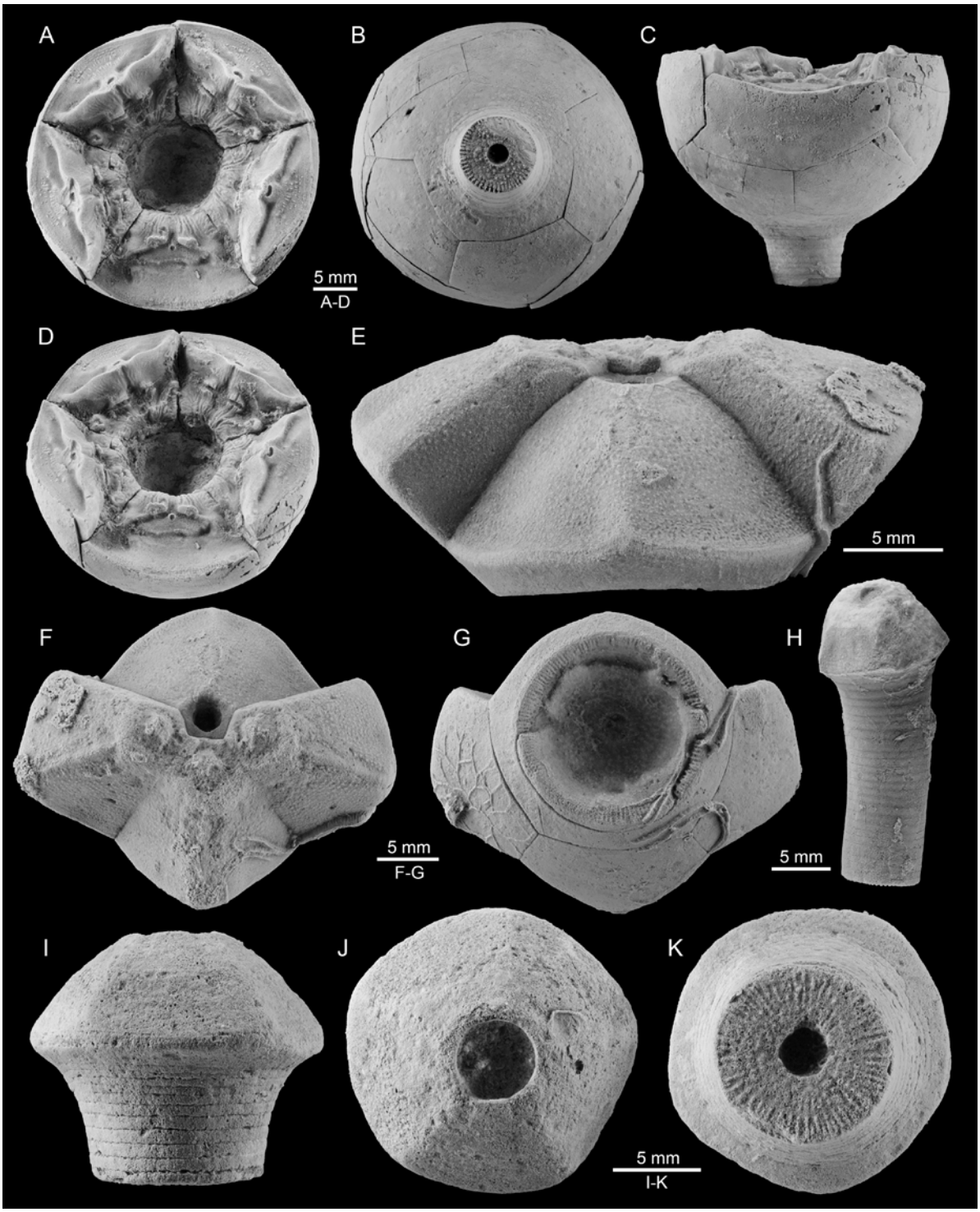

FIGURE 8 —*Pomatocrinus hoferi*, photographs of specimens from the Villar de Herrero locality of the Sot de Chera Formation (Kimmeridgian, Late Jurassic). **A**–**D**, MPZ2021/188, a complete calyx with proximal part of the stem, five basals, five radials and four brachial plates in oral (A), aboral (B), lateral (C), and oblique (D) views. **E**–**G**, MPZ2021/189, a proximal-most columnal with three basal plates, in lateral (E), proximal (F) and distal views (G). Note the morphology of the proximalmost columnal as a truncated pyramid. **H**, MPZ2021/190 a proximal-most columnal with proximal column. Compare with proximal most columnal in *Liliocrinus* from figure 6. **I**–**K**, MPZ2018/473, a proximal stem with proximal-most columnal in lateral (I), proximal (J) and distal views (K).

TABLE 2 — Measurements of *Liliocrinus polydactylus* based on the three complete or partially completed calyx materials. All measures are in millimeters.

Measure	Specimen number		
	MPZ2021/188	MPZ2021/189	MPZ2021/190
Max. cup diameter	17	ca. 20	-
Min. cup diameter	11	12	13,5
Cup height	9	13	-
Basal height	4,8/5/4,7/5/5	6,2/-/6,5/5/6,5	7/7/7/6,8/6,5
Basal width	8/8/8/8/7,5	9/10,1/10/10/10	10,1/11,5/10,8/10,5/10,5
Radial height	4/4/4/4/4	5/4,5/-/-/-	-/-/-/-/-
Radial width	11/10/11	13/12,2/-/-/-	-/-/-/-/-

Pomatocrinus hoferi (Mérian, 1849). The second morphotype is *Pomatocrinus* cf. *mespiliformis* (von Schlotheim, 1820) including only basal plates.

Pomatocrinus hoferi (Mérian, 1849)
Fig. 8, 9E-H

1760 *Trochita pentagonus* Hofer, p. 202, pl. 8, fig. 19–21.
1849 *Millericrinus* (*Pomatocrinus*) *hoferi* Mérian p. 28.
1862 *Millericrinus hoferi* Thurmann and Étallon p. 345, pl. XLIX, fig. 7.
1878 *Millericrinus hoferi* de Loriol p. 62, pl. X, figs. 1–12.
1882-84 *Millericrinus hoferi* de Loriol pl. 105, figs. 1, 2.

Material.— Complete calyx preserving proximal columnals and four brachial plates (MPZ2021/188) (Fig. 8A-D), one partial calyx (MPZ2021/189) (Fig. 8E-G), several proximalmost columnals (MPZ2018/473, MPZ2021/190) (Fig. 8H-K) and several isolated basal plates (MPZ2021/196-202) (Fig. 9E-H).

Diagnosis.— Species of *Pomatocrinus* with a bowl-shaped calyx, basals slightly higher than radials. Pentagonal basal plates, with poorly developed external curvature, proximal facets straight and internal apex acute.

Remarks.— *Pomatocrinus hoferi* was first described by Hofer (1760) as *Trochita pentagonus*. Mérian (1849) first observed important differences in the basal plates compared to *P. mespiliformis* and erected the new species *Millericrinus* (*Pomatocrinus*) *hoferi*, but never figured the specimens (sensu Thurman and Etallon, 1862). All later authors have recognized Mérian as the author of *P. hoferi*, a view followed here, pending further research on this topic. Specimens are properly figured in de Loriol (1878, plate X fig. 1-12) (reproduced here in Fig. 9J-L) and de Loriol (1882-84, plate 105 figs. 1, 2); who maintained assignment to *Millericrinus*. Neither Mérian nor de Loriol provided a proper diagnosis, which is reported here for the first time (see above). The descriptions and illustrations of de Loriol are enough to assign the Spanish material to *P. hoferi*. The species are considered valid here and transferred to *Pomatocrinus* according to characters described by Rasmussen (1978).

Pomatocrinus hoferi differs from *Pomatocrinus mespiliformis* in the shape of the basal plates (Fig. 9). These are pentagonal in *P. hoferi* and with flat sutures. For contrast, in *P. mespiliformis* they are more bulbous, with a more convex external surface, crenularium present in the articulation with proximal columnal, and double distal facet with a clear ridge in the middle.

Pomatocrinus cf. *mespiliformis* (von Schlotheim, 1820)
Fig. 9A-D

Material.— About five specimens (MPZ2021/191-195) of basal plates (Fig. 9A-D). No complete calyces have been yet reported.

Remarks.— Basal plates described here are externally very curved and have double proximal concave facets identical to those of *P. mespiliformis* figured by Rassmussen (1978, fig. 552.1a; refigured here in Fig. 9I). This typical shape of the basals suggest inclusion in *Pomatocrinus* cf. *mespiliformis* pending further and more complete material. According to Salamon and Zatoń (2005), *P. mespiliformis* and *P. fleuriausianus* (Fig. 7A–C) are distinguished by the shape of the radials and basals respectively which agree with the figures of Rasmussen (1978). In *P. fleuriausianus* radials are very low and only relegated to the uppermost part of the calyx, whereas in *P. mespiliformis* they contribute to the spherical shape of the calyx. For contrast, most of the shape of the calyx

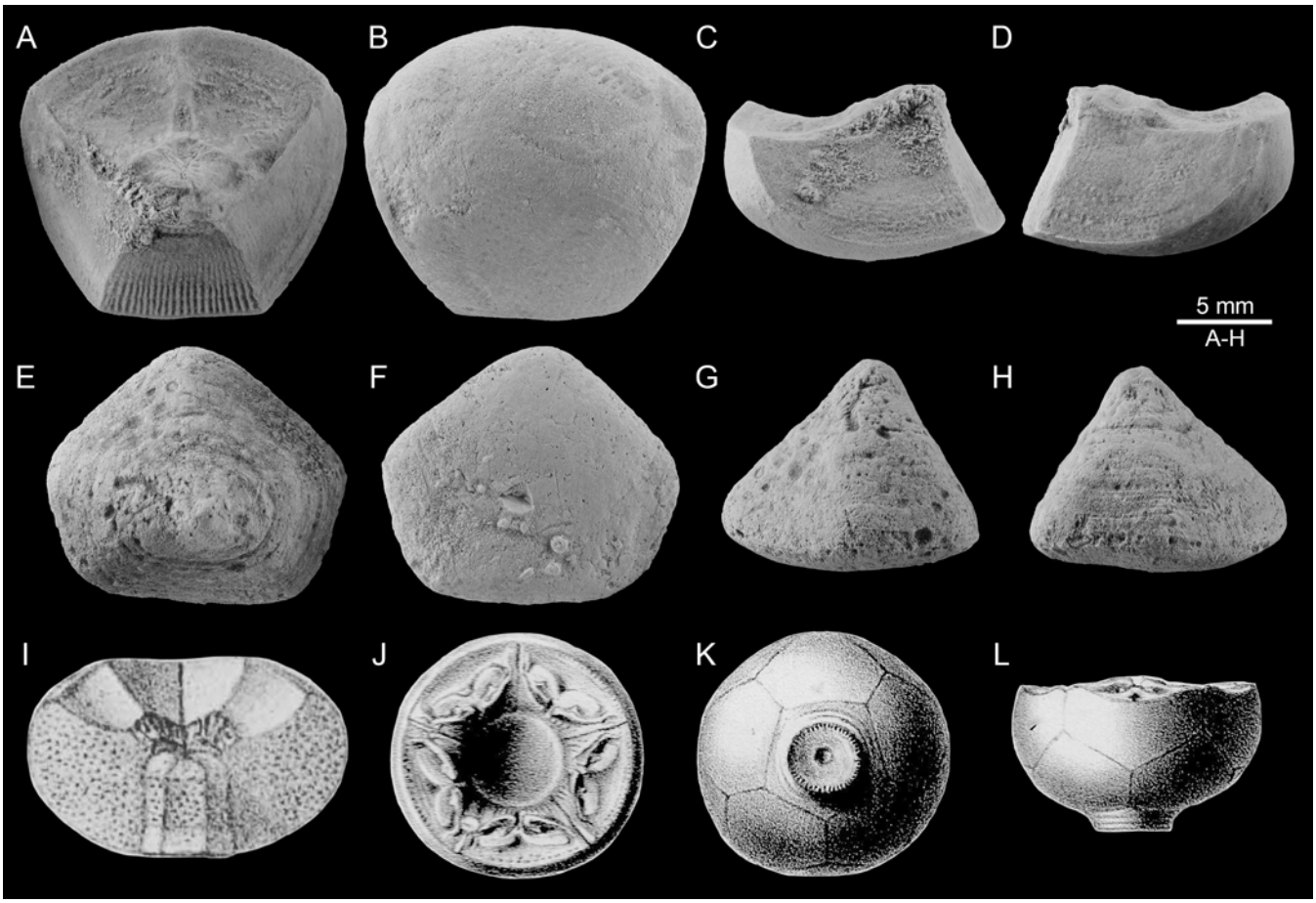

FIGURE 9 — **A**–**D**, *Pomatocrinus* cf. *mespiliformis*, photographs of the basal plate from the Puerto de las Banderas locality of the Sot de Chera Formation (Kimmeridgian, Late Jurassic). MPZ2018/473, in internal (A) (note the double facets for radials), external (B), lateral right (C), and lateral left views (D). **E**–**H**, *Pomatocrinus hoferi*, photographs of the basal plate from the Griegos 1 locality of the Sot de Chera Formation (Kimmeridgian, Late Jurassic). MPZ2021/196, in internal (E), external (F), lateral right (G), and lateral left views (H). **I**, specimen of *Pomatocrinus mespiliformis* figured in Rasmussen (1978, fig. 552. 1a). Note the shape of the basal plates and compare with A. **J**–**L**, specimen of *Pomatocrinus hoferi* figured in de Loriol (1878, pl. X, fig. 1) in oral (J), aboral (K) and lateral (L) views.

in *P. fleuriausianus* is related with the huge development of the basal plates. In the later the basals also have an external ridge that is very characteristic. This ridge is absent in *Pomatocrinus* cf. *mespiliformis*. The main differences in the latter with *P. hoferi* are related with the shape of the basal plates (see above).

Family APIOCRINITIDAE d´Orbigny, 1840

Diagnosis.— Cup very large, bowl to globe shaped, medium to high, very thick walled. Interradial plates variable in number, smaller plates may be concealed, wedge between other plates and reaching surface. Variable number of proximal columnals with increasing diameter form conical transition between cup and column (sensu Hess and Messing, 2011).

Remarks.— From all the features diagnosed by Hess and Messing (2011), the presence of proximal columnals that increase in diameter proximally is probably the most diagnostic feature of the family. This is very obvious for *Apiocrinites*. *Guettardicrinus*, the second genus included in the family also has this feature in the proximal columnals, but it has a calyx shape similar to the family Millericrinidae.

Genus *Apiocrinites* Miller, 1821

Type species.— *Encrinites parkinsoni* von Schlotheim, 1820 by original designation.

Diagnosis.— Cup typically globe- or pear-shaped to ovoid; greatest diameter at basal or radial circlet. Variable height of radials and basals. Primibrachials meet laterally, with or without a few small, polygonal, interradial plates. Synarthry

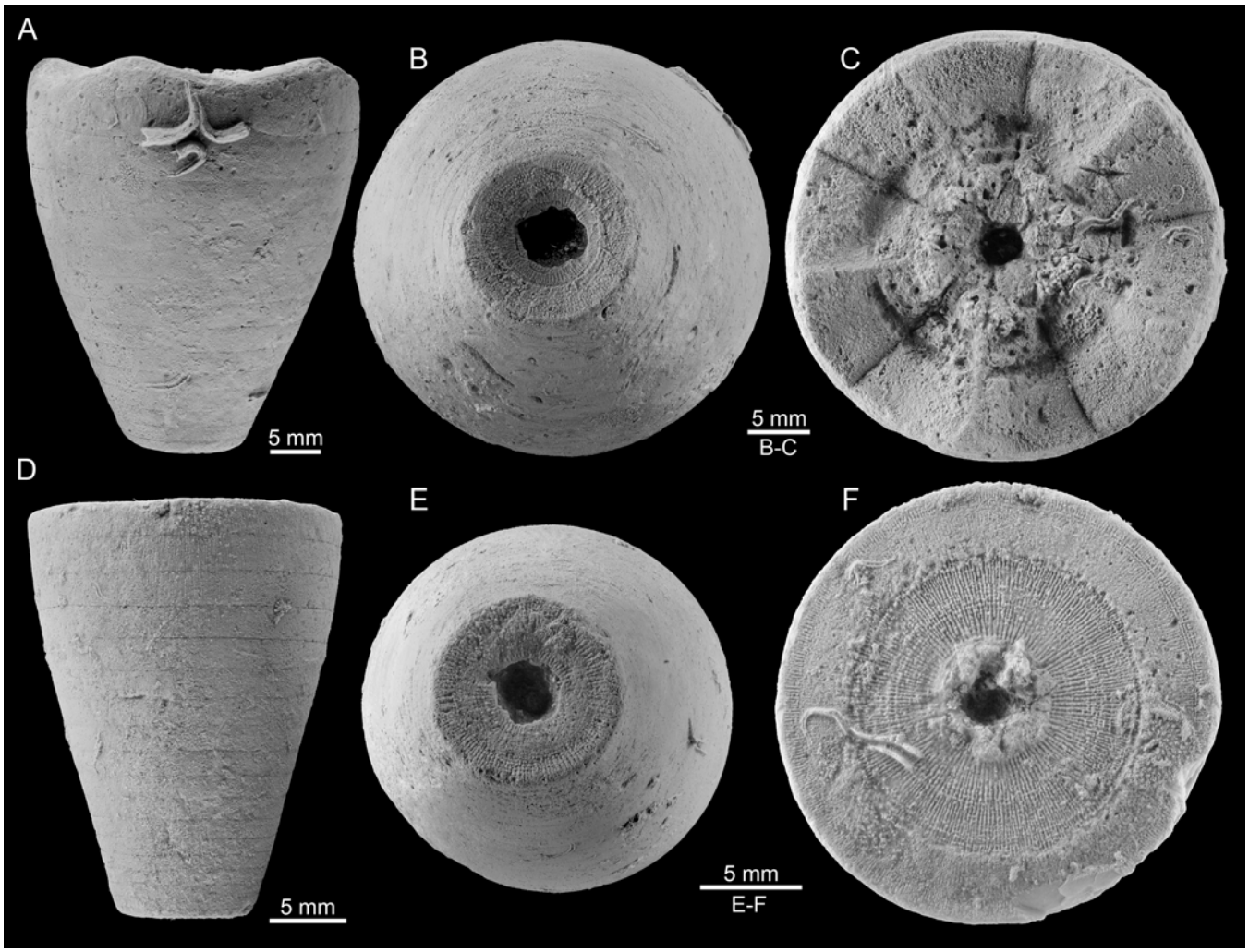

FIGURE 10 — *Apiocrinites* cf. *parkinsoni*, photographs of specimens from the Villar de Herrero locality of the Sot de Chera Formation (Kimmeridgian, Late Jurassic). **A**–**C**, MPZ2018/472, a proximal stem with the five basals but lacking radials in lateral (A), distal (B) and proximal (C) views. **D**–**F**, MPZ2021/203, a proximal stem showing increase in columnal diameters to the proximal part in lateral (D), distal (E) and proximal views.

or synostosis with marginal crenulae between primibrachials 1 and 2, synarthry between secundibrachials 1 and 2. All or most secundibrachials free. Arm divided at primibrachial 2, and in some species, further divided once or twice with variable interval. First pinnule on secundibrachial 2. Proximal column of thin, discoidal columnals increasing gradually in diameter to form long, smoothly conical transition from column to cup. Proximal columnals typically with flat proximal articular facet and concave distal facet, leaving empty central space between columnals. Proximal facet of uppermost columnal with 5 radiating ridges separating facets facing basals (sensu Hess and Messing, 2011 with modifications from Ausich and Wilson, 2012).

Remarks.— *Apiocrinites* is easily differentiated from *Guettardicrinus* by the general shape of the calyx and by the presence in the latter of radials and proximal brachials separated by several, small interradial plates.

Apiocrinites cf. *parkinsoni* von Schlotheim, 1820
Fig. 10

Material.— One calyx preserving proximal columnals and basals (MPZ2018/470; Fig. 10A–C). Other specimens include proximal columnals that are expanded and fused (MPZ2021/203) (Fig. 10D–F). Other specimens are partial proximal part of stems (MPZ2021/204-206).

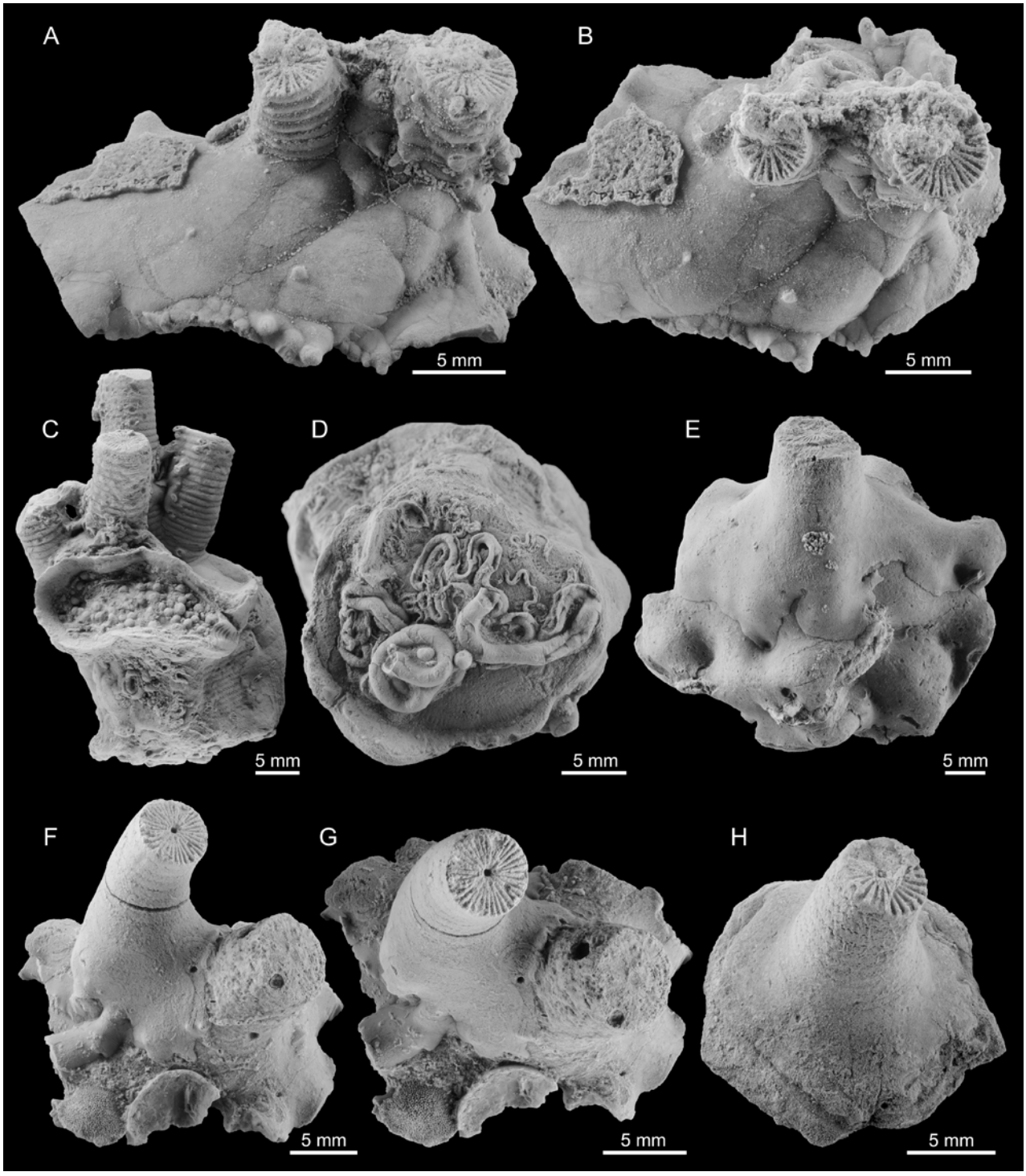

FIGURE 11 — **A**–**H**, attachment structures of millericrinids from the Sot de Chera Formation (Kimmeridgian, Late Jurassic). **A**–**B**, MPZ2021/207, is a double holdfast in lateral and proximal views from Griegos 2 locality. **C**–**D**, MPZ2021/208, are four holdfasts in the same cluster in lateral and distal views, from Griegos 2 locality. Note that the attachment surface is covered with serpulids (D). **E**, MPZ2021/209, is a specimen of holdfast overlapping a previous attachment structure from Villar de Herrero. **F**–**G**, MPZ2021/210, is a double holdfast from the Puerto de las Banderas locality. Note the different state of preservation of both individuals that suggest the left specimen was alive while the other died in the colony. **H**, MPZ2021/211, is a single holdfast from the Villar de Herrero locality.

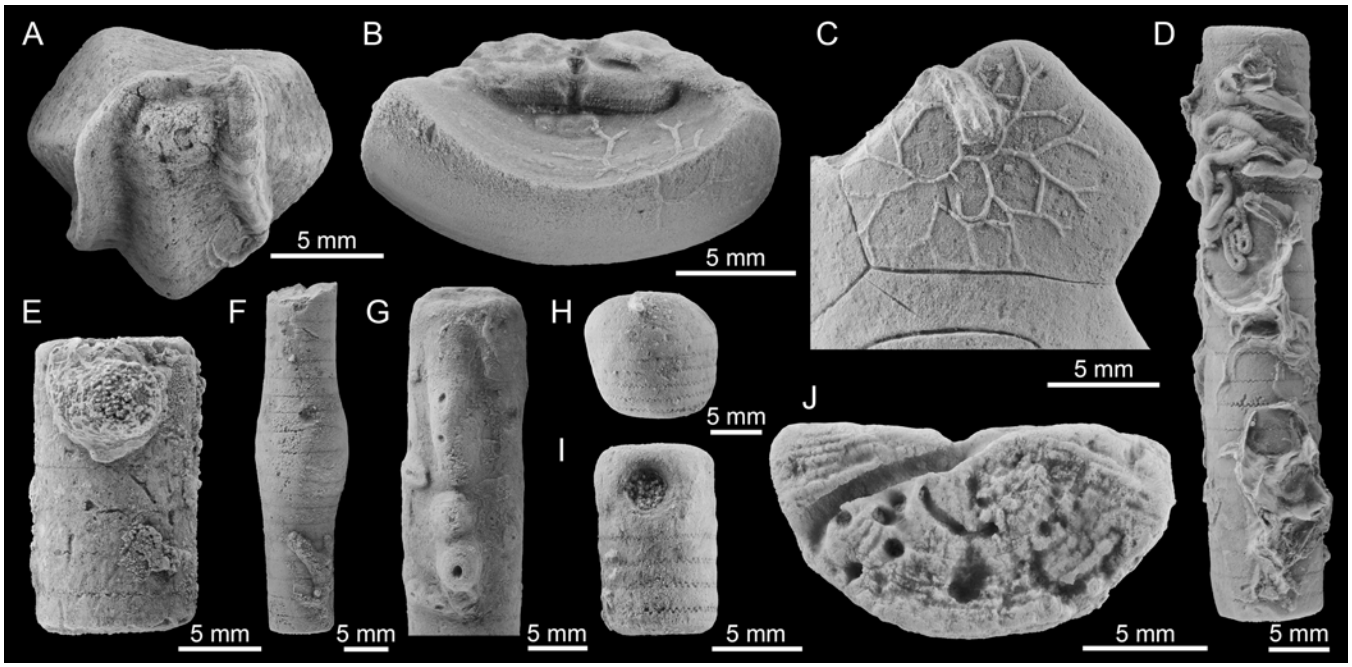

FIGURE 12 — Taphonomy of millericrinid material from the Villar de Herrero (A, C, H) and Puerto de las Banderas (B, D-G, I, J) localities of the Sot de Chera Formation (Kimmeridgian, Late Jurassic). **A**, MPZ2021/214, is a basal plate of *Pomatocrinus hoferi* with a large serpulid in the facets. **B**, MPZ2021/215, is a radial plate of a millericrinid indet. with a colonial organism growing in the attachment to brachial plate. **C**, MPZ2021/189, is a lateral view of a basal plate of *Pomatocrinus hoferi* with the bryozoan *Stomatopora* attached on its surface. Note a serpulid overlapping both, crinoid plate and *Stomatopora*. **D**, MPZ2021/216, is a stem fragment colonized by oysters and serpulids. **E**, MPZ2021/217, is a stem fragment with a small sponge attached on its surface. **F**, MPZ2021/218, is a stem fragment showing *Oichnus* isp. and a gall. **G**, MPZ2021/219, is a stem fragment infested with parasites showing crinoid reaction in life. **H**, MPZ2021/220, is a stem fragment highly eroded. **I**, MPZ2021/221, is a stem fragment showing *Oichnus* isp. **J**, MPZ2021/222 ,is a fragment of a columnal fully covered with bioerosion trace fossils.

Remarks.— Material is assigned to *A.* cf. *parkinsoni* because the general shape of the calyx and the very low basal plates. If the presence of this species is confirmed with furthermore complete material this would represent the youngest occurrence of the species because type material is from the Middle Jurassic of France. Specimens from Bradford Clay (UK) also belong to the same species and age and also have very low basal plates. *A. roissyanus* d'Orbigny from the Oxfordian of France has by comparison very high basal plates that are more comparable to those appearing in *Pomatocrinus mespiliformis*. More recently Ausich and Wilson (2012) described *A. negevensis* from the Middle Jurassic of Israel that also has high basals comparable in height to radials. Basals in *A. negevensis* are very similar to those in *A. roissyanus* but higher than in *A.* cf. *parkinsoni*. Further material from Spain preserving both basals and radials would confirm if *A.* cf. *parkinsoni* belongs to *A. parkinsoni* or to a different and new species. Wilson et al. (2014) described a second species from Israel as *A. feldmani* but figured specimens that have radial and basal plates of similar heights which seem very similar to those observed in *A. parkinsoni*. The basals in *A. feldmani* are also similar to those of *A.* cf. *parkinsoni*.

ATTACHMENT

Most stalked crinoids require permanent attachment as adults. When complete material is available from the calyx to the attachment system (see examples in Hess et al., 1999) it is easy to assign a calyx to columns and attachment structure, but when only disarticulated material is available this is a risky inference. In special cases when dealing with low diversity faunas it is sometimes possible to correlate the calyx with the rest of the animal (see Salamon and Zatoń, 2005 as a possible example), based on its morphology. Millericrinids were permanently attached by means of complex root systems or holdfast that cemented on substrates (de Loriol, 1877; Palmer and Fürsich, 1974). The column is constructed of cylindrical columnals that lack cirri, and the holdfast is the only way these crinoids attached on the substrate. In the studied material there are several types of holdfast preserved that inform about substrate preferences and attachment.

Assignation of each type of holdfast to the species of crinoids described is difficult, because they all come from the same stratigraphic horizons and coexisted. Only a few examples have been described of millericrinids in the

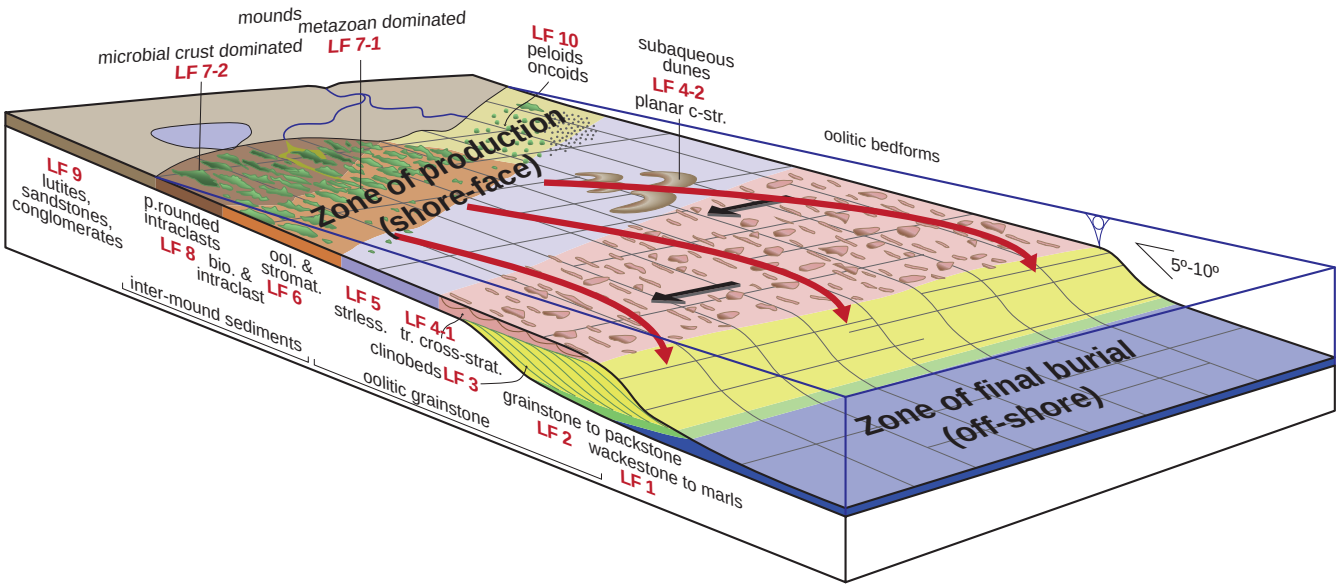

FIGURE 13 — Depositional model for the Pozuel Formation (Kimmeridgian, Late Jurassic). Studied crinoids were probably living in shore-face facies (Zone of production). Most disarticulation processes and erosion probably occurred in the high energetic oolitic grainstones. Final burial and preservation of specimens occurred in the off-shore basin, lithofacies 1 (Zone of final burial). Specimens were transported to the basin by storm-induced events. Modified from Pomar et al. (2015; fig. 11). Abbreviations: *bio*., bioclasts; *c-str.*, cross-stratification; *ool*., oolites; *p*., poorly; *stromat*., stromatolites; *strless*., structureless; *tr. cross-strat*., trought cross-stratification.

literature with the calyx, stem, and holdfast articulated. *Liliocrinus munsterianus* (*L. polydactylus* here) from the Swiss Jura developed a column up to 2 meters high that ended in a massive, cemented root; but alternatively, also developed roots on soft sediment that first attached on a hard object (Hess et al., 1999; p. 6). Specimens of *Apiocrinites parkinsoni* from the British Jurassic also developed massive holdfast that attached on hard grounds but had a considerable shorter column (Palmer and Fürsich, 1974; Hess et al. 1999 p. 198). Salamon and Zatoń (2005) figured a holdfast and column that they assigned to *Pomatocrinus mespiliformis*, and these holdfasts are notably very massive structures. Scheweigert et al., (2008) figured a specimen of *Millericrinus milleri* with a long portion of the stem preserved but lacked distal attachment structure. Based on this evidence it is impossible to correlate the described calyces with stems and holdfasts with certainty. This is especially true in the material presented here, where more than one species cooccur in the same assemblage. All columns are rather similar having millericrinid-like features such as circular outline, lack of cirri and presence of radial crenulae. Moreover, some millericrinids change the general shape of the column through ontogeny and from proximal to distal parts posing extra problems to assign column to a specific calyx. Further articulated material might clarify this issue.

Some of the reported holdfasts (Fig. 11) had more than one individual living in the same cluster (Fig. 11A, C, F). One of the specimens has up to four specimens clustered together (Fig. 11C). This suggests a gregarious lifestyle for millericrinids but also points out the possibility that space for attachment was limited. Alternatively , some restricted places were more optimal than others for attachment.

All specimens with the exception of one example (MPZ2021/212) appear unattached from the original substrate, thus determining the original substrate preferences is difficult. The sole specimen that seems attached to a fragment of rock corresponds to a large holdfast that has distal radices attached to a certain type of lithified carbonate grainstone, which is different from the marly sediment that covers the rest of the specimen. Another specimen overgrew a bivalve shell (MPZ2021/213) but have some broken radices suggesting they attached on some sort of soft substrate. These two specimens will be treated in a different paper but they suggest that millericrinids attached to either a lithified grainstone or shell fragments, supporting previous observations (Palmer and Fürsich, 1974; Hess et al., 1999).

Attachment structures are diverse in the studied material (see below) and range from very gracile structures to relatively massive ones. This probably reflects the diversity of millericrinids in the studied material. Some clusters of holdfast provide evidence that some specimens were still alive in the colony while others were dead (Fig. 11F, G). This is supported by the presence of excellently preserved specimens coexisting with other poorly preserved material in the same cluster. Attachment structures also support long post-mortem exposures with specimens preserving sclerobionts and bioerosion trace fossils that were formed after the death of the crinoids (Fig. 11D).

TAPHONOMIC OBSERVATIONS

Most of the crinoid material presented in this work comes from the Sot de Chera Formation. For this reason, the taphonomic observations and palaeoecological implications will focus only on this specific assemblage. Material from the Yatova Formation was considered in Zamora et al., (2018) and does not need to be repeated here. Crinoid material includes mostly columnals and column fragments, attachment structures, isolated brachials, and rarely partial or complete calyces. Specimens range from excellently preserved material to extremely abraded specimens (Fig. 12H), and sclerobionts, including bryozoans, serpulids, bivalves, and sponges, are common on many specimens (Fig. 12A-E). Bioerosion trace fossils are also present (Fig. 12F, G, I, J). There are also specimens of stem fragments that are swollen (Fig. 12F, G, I). Some of the sclerobionts are compatible with interactions in life, but many are located on parts that were covered with other plates in life such as brachial facets or columnal articulations (Fig. 12A, B). There are also examples of attachment structures covered with sclerobionts on the attachment surface (Fig. 11D). Similar sclerobionts on crinoids from the Jurassic have been described for the Callovian Matmor Formation (Feldman and Brett, 1998; Wilson et al., 2010). Swollen columnals in millericrinids have been previously interpreted as signs of parasitism (Wilson et al., 2014); and they show external pits with increase in stereom thickness that are interpreted as a crinoid reaction to parasitism (Fig. 12F, G). The massive roots of millericrinids offered benthic "islands" for obligate encrusters as has been demonstrated in previous observations (Seilacher and Macclintock, 2005; Lach et al., 2014), and in the many examples figured here (Fig. 11). Quantification of sclerobionts and bioerosion trace fossils has not been performed yet and will require further detailed study, but based on preliminary observations some important information can be provided. The presence of post-mortem epibiont material and abrasion suggest a long and complex taphonomic history (Zamora et al., 2018). Many specimens have evidence of abrasion that changed their original shape suggesting resedimentation in coarse grained sediment like that provided by ooids preserved with the crinoid material (see above). Size and variety of sclerobionts also support the idea that most crinoid material was on the sea floor for long periods of time (Feldman and Brett, 1998). Exceptions of rapid burial probably resulted in the preservation of complete cups having brachials in place. The theca of millericrinids was probably rigidly sutured and some of the plates were probably fused because there are examples of *Apiocrinites* and *Pomatocrinus* with the basals still present but with the articulations to radials fully covered by sclerobionts (Figs. 8E, 10A–C).

ENVIRONMENTAL INTERPRETATION

Pomar et al., (2015) provided the reconstruction of shallow carbonate platforms in the studied area. They recognized ten different lithofacies. Constructional organisms like corals, stromatoporoids, and crinoids appear associated to mounds and oolitic-skeletal grainstones of lithofacies 6 and 7. Lithofacies 3–5 are dominated by oolitic grainstones in which high energetic condition and coarse sediment favored erosion of bioclastic material. These lithofacies were developed in proximal shoreface environments. For contrast the material here described is abundant in lithofacies 1 which corresponds to basinal offshore marls (see Fig. 13).

Based on the reconstruction provided by Pomar et al., (2015); two possibilities are most suitable for the crinoids. One possibility points that most organisms including crinoids were living on shoreface meadows and were transported with the ooidal material to the lithofacies 1. A second possibility suggests that crinoids were living at the base of the talus and beginning of the basin, between lithofacies 1 and 2; and were finally buried in lithofacies 1. Based on the grade of abrasion of most material and the degree of colonization by sclerobionts the first option is most probable. Crinoids probably lived in highly energetic environments were attached in colonies to hardgrounds or small mounds (zone of production). Shortly after death, individuals rapidly disarticulated and some specimens were resedimented with the ooids in the proximal environments for long periods of time, resulting in highly abraded specimens and increase of encrusting possibilities. Finally, all the material including time-averaging assemblages was transported to the basin and buried in marly sediments (zone of final burial). This model explains the co-existence between well preserved specimens and others that are highly abraded or colonized by sclerobionts. This also explains why millericrinids are not present elsewhere in the Sot de Chera Formation and only concentrate in certain localities. Storm-driven down-welling and geostrophic currents that evolved into gravity flows at the slope (Pomar et al., 2015) were probably responsible for transporting specimens and bioclastic material from the zone of production to the zone of final burial (see direction of arrows in Fig. 13).

CONCLUSIONS

Millericrinid crinoids have been largely ignored in the Late Jurassic rocks from Spain. A rich assemblage from the Yátova and Sot de Chera Formations provides important information on the systematics, taphonomy, and palaeoecology of this important extinct clade of crinoids. Only material comprising relatively articulated specimens is described, but the diversity of millericrinids can be increased if disarticulated material is further described in the future. One taxon from the Yátova Formation is described as *Angulocrinus tomaszi* n. sp. The remaining taxa include *Millericrinus milleri*, *Liliocrinus polydactylus*, *Pomatocrinus hoferi*, *Pomatocrinus* cf. *mespiliformis* and *Apiocrinites* cf. *parkinsoni*, and are all described from the Sot de Chera Formation. The later assemblage also provides important taphonomic data on syn-vivo and postmortem interactions with other organisms. These crinoids experienced a long biostratinomic phase with long periods of exposure to erosion and colonization.

Taken together this information provides clear evidence demonstrating that millericrinids lived in relatively high energetic shore-face conditions and were transported and finally buried in deeper off-shore meadows. This provides important information to reconstruct ancient habitats from shoreface energetic meadows that rarely preserve in the fossil record.

ACKNOWLEDGMENTS

I would like to dedicate this work to Prof. Tomasz Baumiller (University of Michigan) because after a visit in 2016 he first encouraged me to describe some of the material of Post-Palaeozoic crinoids from Spain that the author collected over the last decade. Specimens studied have been collected with the help of students from the University of Zaragoza including Victoria Barrios and Fernando Ari Ferratges. The latter also helped preparing some critical specimens. Juan Carlos García Pimienta (Gobierno de Aragón, Spain) helped with field work. Isabel Pérez did incredible photography assistance. Important discussions have been taken on the sedimentology of the area with Marcos Aurell and Beatriz Bádenas, both from the University of Zaragoza. Luis Moliner classified some of the ammonites associated with the crinoids. Meg Veitch (University of Michigan) helped finding very old literature that was important to review the described species. Two reviewers, Mark A. Wilson (The College of Wooster) and Mariusz A. Salamon (University of Silesia), and editor William I. Ausich (The Ohio State University) have provided important comments that improved the resulting manuscript. Jen Bauer, editor, (University of Michigan) did a grammatical correction of an early draft of this manuscript. This is a contribution to project E18_20R "Aragosaurus: Recursos geológicos y paleoambientales" from the Government of Aragón.

LITERATURE CITED

ABRIL, J., and J. RUBIO. 1977. Memoria del Mapa Geológico de España. 1:50000, Ademuz (612). 47 pp.

AURELL, M., S. ROBLES, B. BÁDENAS, S. QUESADA, I. ROSALES, G. MELÉNDEZ, and J. C. GARCÍA-RAMOS., 2003. Transgressive/Regressive Cycles and Jurassic palaeogeography of NE Iberia. Sedimentary Geology, 162: 239–271.

_____, B. BÁDENAS, J. IPAS, and J. RAMAJO. 2010. Sedimentary evolution of an Upper Jurassic carbonate ramp (Iberian Basin, NE Spain). In van Buchem, F., K. Gerdes, M. Esteban (eds.), Reference models of Mesozoic and Cenozoic carbonate systems in Europe and the Middle East – stratigraphy and diagenesis, Geological Society of London, Special Publication, 329: 87–109.

AUSICH, W. I. and M. A.WILSON. 2012. New Tethyan Apiocrinitidae (Crinoidea; Articulata) from the Jurassic of Israel. Journal of Paleontology, 86: 1051–1055.

CANUDO, J. I. 2018. The collection of type fossils of the Natural Science Museum of the University of Zaragoza (Spain). Geoheritage, 10: 385–392.

DERCOURT, J., L. E. RICOU, and B. VRIELYNCK. 1993. Atlas Tethys Palaeoenvironmental Maps. BEICIP-FRANLAB, Gauthier-Vollars, Paris, p. 260, 14 maps.

DESOR, E. 1845. Résumé de ses études sur les crinoïdes fossiles de la Suisse. Bulletin de la Société des Sciences naturelles de Neuchâtel, 1, 211–222.

DEUSCH, M., A. FRIEBE, O. F. GEYER, and M. KRAUTTER. 1990. Las facies espongiolíticas del Jurásico español y unidades semejantes de Europa Central. Cuadernos de Geología Ibérica 14: 199–214.

FELDMAN, H. R., and C. E. BRETT. 1998. Epi- and endobiontic organisms on Late Jurassic crinoid columns from the Negev Desert. Israel: Implications for Co-evolution. Lethaia 31: 57–71.

FEZER, R. 1988. Die oberjurassische karbonatische Regressionsfazies im südwestlichen Keltiberikum zwischen Griegos und Aras de Alpuente (Prov. Teruel, Cuenca, Valencia, Spanien). Arbeiten aus dem Institut für Geologie und Paläontologie an der Universität Stuttgart. Neue Folge, 84, 1–119.

GORZELAK, P., and M. A. SALAMON. 2006. The youngest Mesozoic record of millericrinid crinoids (Millericrinida, Crinoidea) from Upper Cretaceous deposits of Poland. Freiberger Forschungshefte, 14: 39e42.

HAGDORN, H. 2011. Triassic: the crucial period of post-Palaeozoic crinoid diversification. Swiss Journal of Palaeontology, 130: 91–112.

HESS, H., W. I. AUSICH, C. E. BRETT, and M. J. SIMMS (eds.), 1999. Fossil crinoids. Cambridge University Press, Cambridge: 1–275.

_____and GALE, A. S. 2010. Crinoids from the Shenley Limestone (Albian) of Leighton Buzzard, Bedfordshire, UK. Journal of Systematic Palaeontology, 8 (3). 427–447.

_____and C. G. MESSING. 2011. Articulata. In P. Seldon (ed.) and W. I. Ausich (Coordinating Author). Treatise on Invertebrate Paleontology, Part T, Revised, Volume 3. University of Kansas Paleontological Institute, Lawrence, Kansas.

HOFER, J. 1760.Tentaminis lithologici de Polyporitis. Acta Helvetica, 4: 169-213.

HUNTER, A. W., N. L. LARSON, N. H. LANDMAN, and T. OJI. 2016. *Lakotacrinus brezinai* n. gen. n. sp., a new stalked crinoid from cold methane seeps in the Upper Cretaceous (Campanian) Pierre Shale, South Dakota, United States, Journal of Paleontology, 90 (3): 506–524.

JAEKEL, O. 1918. Phylogenie und System der Pelmatozoen. Palaeontologische Zeitschrift, 3: 1–128.

KRAJEWSKI, M., P. OLCHOWY, and M. A. SALAMON. 2019. Late Jurassic (Kimmeridgian) sea lilies (Crinoidea) from central Poland (Łódź Depression). Annales de Paléontologie, 105: 63–73.

LACH, R., D. TRZĘSIOK, and P. SZOPA. 2014. Life and death: an intriguing history of a Jurassic crinoid. Paleontological Research, 18 (1): 40–44.

LORIOL, P. de 1877–1879. Monographie des crinoïdes fossiles

de la Suisse. Mémoires de la Société Paléontologique Suisse, 4, 1–52; 5, 53–124; 6, 125–300.

LORIOL, P. de 1882–1889: Paléontologie française, Sér. 1, Animaux invertébrés. Terrain jurassique: 11, Crinoïdes, Pt. 1 (1882–84) 627 pp.; pt. 2 (1884–89) 580 pp. G. Masson, Paris.

MELÉNDEZ, G. 1989. El Oxfordiense en el sector central dela Cordillera Ibérica (provincias de Zaragoza y Teruel). Institución Fernando el Católico–Instituto de Estudios Turolenses, Zaragoza-Teruel: 418 pp.

MÉRIAN, H. R. P. 1849. Beiträge zur Kenntniss der Crinoiden des Jura in Bericht über die Verhandlungen der Naturforsch. Gesellsch. In Basel, t. VIII, p. 28.

MILLER, J. S. 1821. A natural history of the Crinoidea or lilyshaped animals, with observation on the genera *Asteria*, *Euryale*, *Comatula*, and *Marsupites*. C. Frost, Bristol. 274 pp.

OLAGÜE, I. 1936. Notas para el estudio del Jurásico en la Rioja. Boletín de la Sociedad Española de Historia Natural, XXXVI: 101–126.

OJI, T., and K. KITAZAWA. 2008. Discovery of two rare species of stalked crinoids from Okinawa Through, southwestern Japan, and their systematic and biogeographic implications. Zoological Science, 25 (1): 115–121.

ORBIGNY, A. d'. 1840–1841. Histoire naturelle, générale et particulière, des Crinoïdes, vivants et fossiles, comprenant la description géologique et zoologique de ces animaux. 1: 1–32, pls 1–6 (1840); 2–3: 33–98, pls 7–18 (1841) (republished 1858). Published by the author, Paris.

PALMER, T.J., and F.T. FÜRSICH. 1974. The ecology of a Middle Jurassic hardground and crevice fauna. Palaeontology, 17: 507-524.

POMAR, L., M. AURELL, B. BÁDENAS, M. MORSILLI, and S.F. AL-AWWAD. 2015. Depositional model for a prograding oolitic wedge, Upper Jurassic, Iberian basin. Marine and Petroleum Geology, 67: 556–582.

RAMAJO, J., and M. AURELL. 2008. Long-term Callovian-Oxfordian sea-level changes and sedimentation in the Iberian carbonate platform (Jurassic, Spain): possible eustatic implications. Basin Research, 20, 163–184.

RASMUSSEN, H. W. 1961. A monograph on the Cretaceous Crinoidea. Biologiske Skrifter udgivet af Det Kongelige Danske Videnskabernes Selskab, 12 (1): 1–428.

RASMUSSEN, H. W. 1978. Articulata. – In: MOORE, R. C. & TEICHERT, C. (Eds.): Treatise on Invertebrate Paleontology, Part T, Echinodermata 2, Crinoidea 3, T813- T928, T938-T1027; Boulder & Lawrence (Geological Society of America & University of Kansas Press).

ROLLIER, L. 1911. Fossiles noveaux ou peu connus. Mémoires de la Société Paléontologie Suisse, 37: 1–7

ROUSE, G. W., L. S. JERMIIN, N. G.WILSON, I. EECKHAUT, D. LANTERBECQ, T. OJI, C. M. YOUNG, T. BROWNING, P. CISTERNAS, L. E. HELGEN, M. STUCKEY, and C. G. MESSING. 2013. Fixed, free, and fixed: The fickle phylogeny of extant Crinoidea (Echinodermata) and their Permian-Triassic origin. Molecular Phylogenetics and Evolution, 66: 161–181.

ROUX, M. 1978. Ontogenèse, variabilité et evolution morphofonctionnelle du pédoncule et du calice chez les Millericrinida (Echinodermes, Crinoïdes). Géobios, 11: 213–241.

SALAMON, M.A., and M. ZATOŃ. 2005. First record of the Jurassic millericrinid *Pomatocrinus mespiliformis* (von Schlotheim) from Poland. Neues Jahrbuch für Geologie und Paläontologie-Monatshefte, 5: 301–320.

SCHLOTHEIM, E. F. VON. 1820. Die Petrefactenkunde auf ihremjetzigen Standpunkte durch die Beschreibung seiner Sammlung versteinerter und fossiler Überreste des Thier-und Pflanzenreichs der Vorwelt erläutert. Beck'sche Buchhandlung, Gotha.

_____. 1823. Nachträge zur Petrefactenkunde, 2. Abtheilung. – 104 pp.; Gotha (Beckersche Buchhandlung).

SCHWEIGERT, G., M. A. SALAMON, and G. DIETL. 2008. *Millericrinus milleri* (SCHLOTHEIM, 1823) (Crinoidea: Millericrinida) from the Nusplingen Lithographic Limestone (Upper Kimmeridgian, SW Germany). Neues Jahrbuch für Geologie und Paläontologie - Abhandlungen, 247: 1–7.

SEILACHER, A., and C. MACCLINTOCK. 2005. Crinoid anchoring strategies for soft-bottom dwelling. Palaios, 20 (3): 224–240.

SIEVERTS-DORECK, H. 1952. Millericrinida, p. 614, In R. C. Moore, C. Lalicker,and A. G. Fischer (eds.), Invertebrate Fossils, McGraw-Hill, New York.

STILLER, F. 2000. Two early millericrinids and an unusual crinoid of uncertain systematic position from the lower Upper Anisian (Middle Triassic) of Qingyan, Southwestern China. Journal of Paleontology, 74 (1): 32–51.

TAYLOR, P. D. 1983. *Ailsacrinus* gen. nov., an aberrant millericrinid from the Middle Jurassic of Britain. Bulletin of the British Museum (Natural History), Geology, 37: 37–77.

THURMANN, J., and C.A. ETALLON. 1862. Lethea Bruntrutana ou études paléontologiques et stratigraphiques sur les terrains jurassiques du Jura Bernois et en particulier des environs de Porrentruy. Allgemeine Schweizerische Gesellschaft für die Gesammten Naturwissenschaften19: 147–353.

WILSON, M. A., H. R. FELDMAN, and E. B. KRIVICICH. 2010. Bioerosion in anequatorial Middle Jurassic coral-sponge reef community (Callovian,Matmor Formation, southern Israel). Palaeogeography, Palaeoclimatology, Palaeoecology, 289: 93–101.

_____, E. A. REINTHAL, and W. I. AUSICH. 2014. Parasitism of a new apiocrinitid crinoid species from the Middle Jurassic (Callovian) of southern Israel. Journal of Paleontology, 88(6): 1212–1221.

WRIGHT, D. F., W.I. AUSICH, S. R. COLE, M. E. PETER, and E. C RHENBERG. 2017. Phylogenetic taxonomy and classification of the Crinoidea (Echinodermata). Journal of Paleontology, 91: 829–846.

ZAMORA, S., M. AURELL, M.VEITCH, J. SAULSBURY, M. LÓPEZ-HORGUE, F. FERRATGES, J. A. ARZ, and T. BAUMILLER. 2018. Environmental distribution of post-Palaeozoic crinoids from the Iberian and south-Pyrenean basins (NE Spain). Acta Palaeontologica Polonica, 63 (4): 779–794.

Museum of Paleontology, The University of Michigan
1105 North University Avenue, Ann Arbor, Michigan 48109-1085
Matt Friedman, Director

Contributions from the Museum of Paleontology, University of Michigan is a medium for publication of reports based chiefly on museum collections and field research sponsored by the museum. Jennifer Bauer and William Ausich, Guest Editors;
Jeffrey Wilson Mantilla, Editor.

Publications of the Museum of Paleontology are accessible online at: http://deepblue.lib.umich.edu/handle/2027.42/41251

ISSN 0097-3556

Contributions

from the Museum of Paleontology, University of Michigan

VOL. 34, NO. 8, PP. 103–122 MARCH 31, 2022

THE CALCEOCRINID PUZZLE

BY

WILLIAM I. AUSICH[1]

Abstract — Calceocrinids are among the most enigmatic crinoids by having a highly modified, bilaterally symmetrical crown and a column that was prostrate along the sediment-water interface during life. Despite or perhaps because of this highly unusual morphology and paleoecology, the Calceocrinidae had the longest duration (~170 million years) of any well-defined crinoid family. Many ideas have been proposed for the paleoecology of calceocrinids, with the runner model favored in recent years. Two questions remain, did calceocrinids have both muscles and ligaments that opened and closed the crown, and how were these bottom-dwelling crinoids positioned with respect to currents. Stereom is evaluated to infer the connective tissues that bound movable calceocrinid facets. Accordingly, calceocrinids had only ligaments present to mediate opening and closing the crown. Three potential crown postures are considered, including an erect arm posture with currents striking the aboral side of the arms and an erect arm posture with currents striking the oral side of the arms. The third, proposed herein, is a partially opened, subellipsoidal posture. It is not possible to reject any of these potential feeding orientations or postures, although ligament stretching may have imposed limitations on erect postures. It is possible that two or more of these alternative postures could have been employed to exploit changing ambient environmental conditions.

[1]School of Earth Sciences, 125 South Oval Mall, The Ohio State University, Columbus, Ohio (ausich.1@osu.edu).

INTRODUCTION

Stereotypically, crinoids are sessile, passive suspension feeders with an erect column that positions the crown for feeding up within the benthic boundary layer and into various epifaunal tiers (Ausich and Bottjer, 1982; Bottjer and Ausich, 1987). However, through the Phanerozoic several crinoid clades deviated from this Bauplan to exploit other ecological roles. Examples include crinoids attached to floating logs (*Traumatocrinus* Wöhrmann, 1889, see Hagdorn and Wang 2015; *Seirocrinus* Gislén, 1924, see Hess, 1999), and crinoids that lacked a column as an adult. Examples of the latter include a calyx cemented directly to the substratum (*Holopus* d'Orbigny, 1837), crinoids with a convex proximal calyx and no column (*Agassizocrinus* Owen and Shumard, 1852 and *Paragassizocrinus* Moore and Plummer, 1940; e.g., Ettensohn, 1975, 1980, 1984), post-Paleozoic feather stars with the proximal calyx comprised of a centrodorsal and articulated cirri, and post-Paleozoic uintacrinids that lack both a column and cirri.

Calceocrinids represent one of the more radical departures from the idealized crinoid Bauplan (Fig. 1). Rather than an erect column, the column of calceocrinids is interpreted to have lain prostrate along the substratum. Further, the crown shape and symmetry were modified for life on the sea floor. In the oldest calceocrinids, pentameral symmetry was replaced by a crown with four arms (A, B, D, and E rays) and poor bilateral symmetry (e.g., *Cremacrinus* Ulrich, 1886 and *Paracremacrinus* Brower, 1977; Fig. 1A–B). More crownward calceocrinids (e.g., *Calceocrinus* Hall, 1852 and *Halysiocrinus* Ulrich, 1886; Fig. 1C–F) had a crown with an E-BC plane of bilateral symmetry that was coincident with the axis of the column. The shapes of the basal plates were modified to form a crescent-shaped basal circlet with a straight articular ridge that was articulated in life to a similar ridge on the apposing radial circlet. Similar to the basal plates, radial plate shape was highly modified to form a radial circlet with a flat, subtrapezoidal or flattened subtubular shape (Fig. 1E–F).

As discussed below in detail, many authors have speculated on the paleoecology of these unusual crinoids, but questions remain. For example, how were calceocrinids positioned with respect to current flow? How did calceocrinids open and close the crown using the basal circlet-E inferradial plate synarthrial articulation? In this contribution, various outstanding aspects of calceocrinid paleoecology are considered.

GEOLOGICAL HISTORY OF THE CALCEOCRINIDAE

The Calceocrinidae are a well-defined family that was first recognized by Meek and Worthen (1869) and is still consistently recovered as a clade (Ausich, 2019). At present, only 25 calceocrinid genera have been described; but, the Calceocrinidae has the longest duration of any well-defined crinoid family (Fig. 2). They range from their first appearance during the Middle Ordovician (Sandbian) to the lower Permian (Artinskian). Total familial duration is as much as 170 million years and comprises a mixture of long- and short-duration genera (Fig. 2).

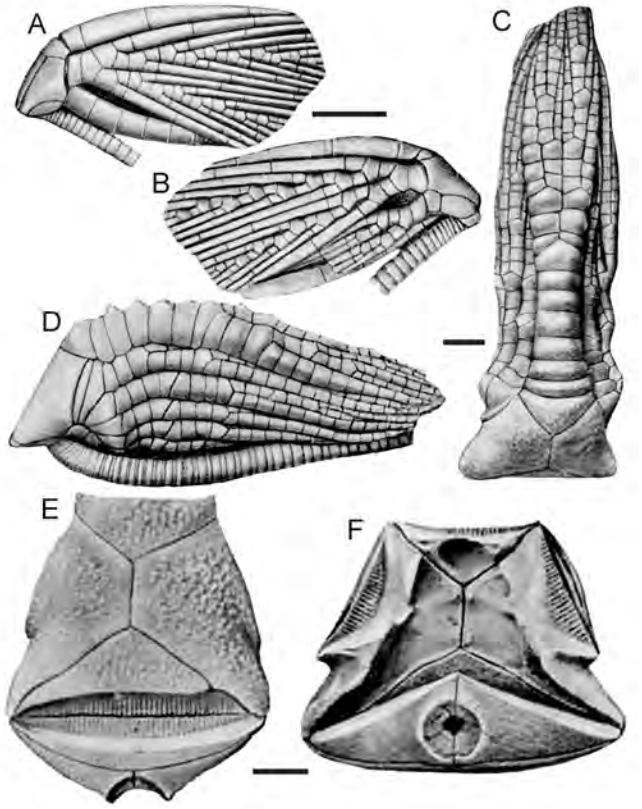

FIGURE 1 — Representative calceocrinids. **A**, **B**, Lateral views of the four-armed *Cremacrinus tubuliferus* Springer, 1926 crown (Sandbian), A, from top to bottom, E arm, A arm, and anal sac, B, from top to bottom, E arm, D arm, and B arm; **C**, **D**, Lateral views of the three-armed *Halysiocrinus tunicatus* crown (Viséan), C, view of E ray arm, D, view of D ray arm. **E**, **F**, Aboral cup of *H. tunicatus*, E, external view of open aboral cup, internal view of closed aboral cup. Images from Springer, 1926; scale bars = 5 mm.

As a whole, the Calceocrinidae were eurytopic and lived in a wide variety of epeiric sea habitats. For example, the common early Mississippian calceocrinid, *Halysiocrinus tunicatus* (Hall, 1860), studied here, lived in numerous settings (Table 1). Also, Brett (1981) discussed the range of habitats for some Silurian calceocrinids.

The biodiversity of calceocrinid genera was the highest from the Hirnantian to the Givetian (peaking during the Silurian; Fig. 2). Ausich (1986) hypothesized that the significant decline in biodiversity and occurrences of calceocrinids after the Givetian was due, in part, to competition for space on the sea floor during the radiation of fenestrate bryozoans during this time. After the middle Viséan, only two calceocrinid occurrences are known: Bashkirian (Pennsylvanian) and Artinskian (Permian), with both occurrences being *Epihalysiocrinus* Arendt, 1965.

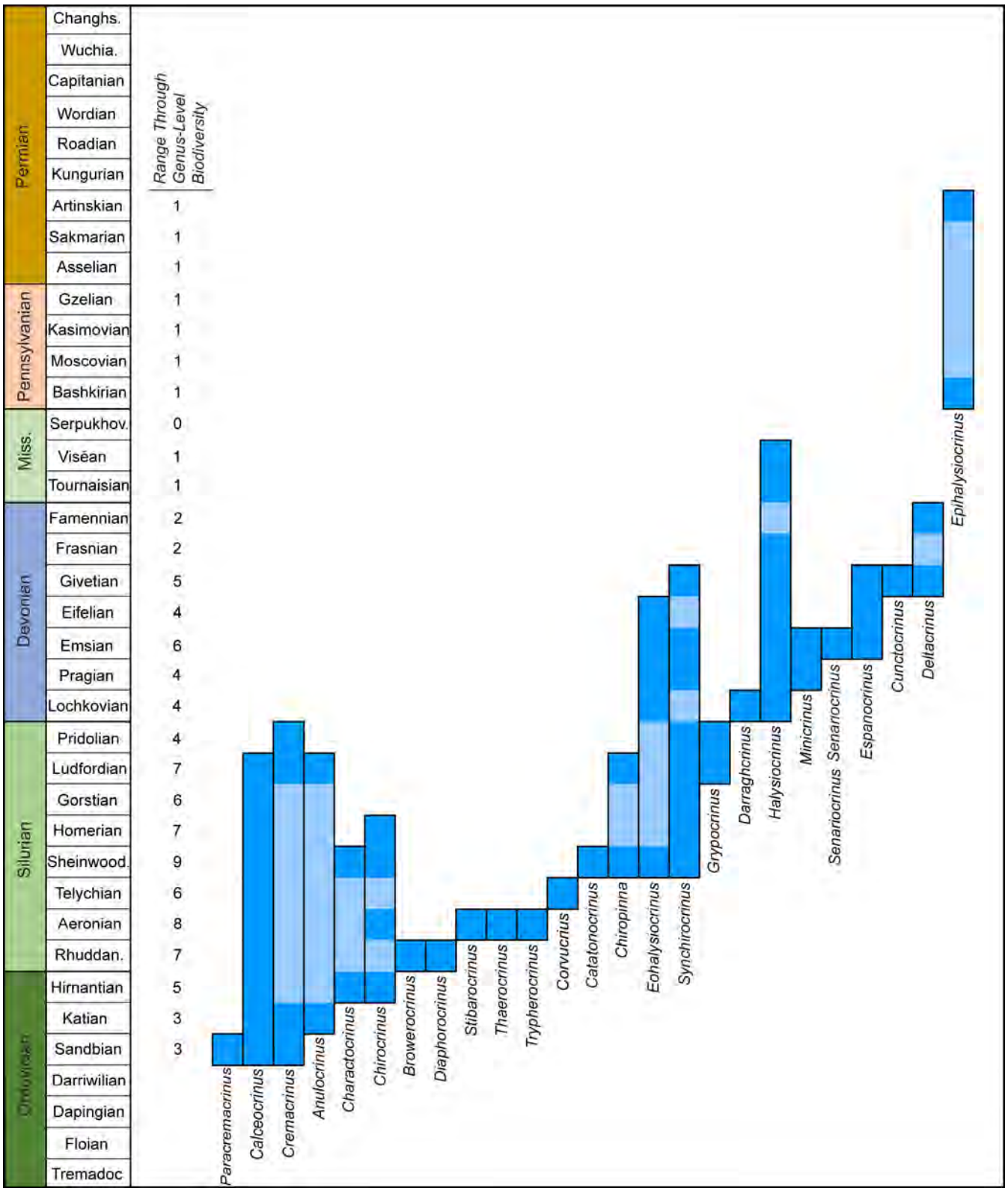

FIGURE 2 — Range chart of calceocrinid genera; dark blue presence of a genus in given time bin, light blue; range through occurrences. Range through genus diversity to the right of the time scale.

TABLE 1 — Stratigraphic and paleoenvironmental occurrences of *Halysiocrinus tunicatus* (lower Mississippian, lower to middle Viséan) of the United States.

Formation	State	Paleoenvironmental Setting	Reference
Edwardsville Formation	Indiana	Delta platform, siltstone facies	Lane (1973)
Edwardsville Formation	Indiana	Delta platform, siliciclastic mudstones facies	Ausich (1983)
Edwardsville Formation	Indiana	Delta platform, crinoidal packstone buildups	Ausich (1983)
Ramp Creek Formation	Indiana	Delta platform, mixed carbonate and siliciclastics facies	Lane (1973)
New Providence Shale Member, Borden Formation	Kentucky and Indiana	Prodelta, siliciclastic mudstone facies	Kammer (1984)
Keokuk Limestone	Illinois, Iowa, Missouri	Platform, carbonates	Kammer et al. (1997)
Warsaw Formation (lower)	Illinois, Iowa, Missouri	Platform, mixed carbonate and siliciclastics	Kammer et al. (1997)
Warsaw Formation (upper)	Illinois, Iowa, Missouri	Platform, siltstone	Kammer et al. (1997)
Fort Payne Formation	Kentucky	Basinal, siliciclastic mudstone facies	Ausich and Meyer (1980)
Fort Payne Formation	Kentucky	Basinal, crinoid packstone buildups	Ausich and Meyer (1980)
Fort Payne Formation	Kentucky	Basinal, wackestone buildup facies	Ausich and Meyer (1980)
Muldraugh Member, Borden Formation	Kentucky	Platform, mixed carbonate and siliciclastics	Ausich et al. (2000)

PALEOECOLOGY: HISTORICAL REVIEW

As summarized by Ausich (1986), three primary paleoecological models have been proposed for calceocrinids including drooper (Ringueberg, 1889), runner (Jaekel, 1918; Springer, 1926; Ramsbottom, 1952; Moore, 1962; Brower, 1966, 1977, 1990; Kesling and Sigler, 1969; Breimer and Webster, 1975; Brett, 1981; Ausich, 1986, and others; Fig. 3), and free-swimming pelagic (Schmidt, 1934). Variations of the standard runner model are the weathervane (Kesling and Sigler, 1969) and the kite (Breimer and Webster, 1975). Complete columns with holdfasts are rarely preserved on calceocrinids, so morphological adaptations demonstrating an obligate column posture along the substratum are relatively rare. However, calceocrinids are known with cemented or otherwise attached holdfasts that affixed to the substratum, which eliminates a free-swimming habit for at least these forms.

Jaekel's (1918) life reconstruction depicted *Synchirocrinus nitidus* (Bather, 1893) with the runner model and the column draped across corals and/or stromatoporoids and the crown open. The arms are erect with ramules extended and evenly spaced (Fig. 3). The arms are positioned so that the currents strike the ambulacral side of the arms. The runner model (column prostrate along the sediment-water interface) is confirmed in a few calceocrinids. In specimens of *Calceocrinus longifrons* Brower, 1977 (Sandbian, Ordovician), complete columns were shorter than the arms, negating the drooper model. An obligate, prostrate posture for the column was also demonstrated in Silurian crinoids.

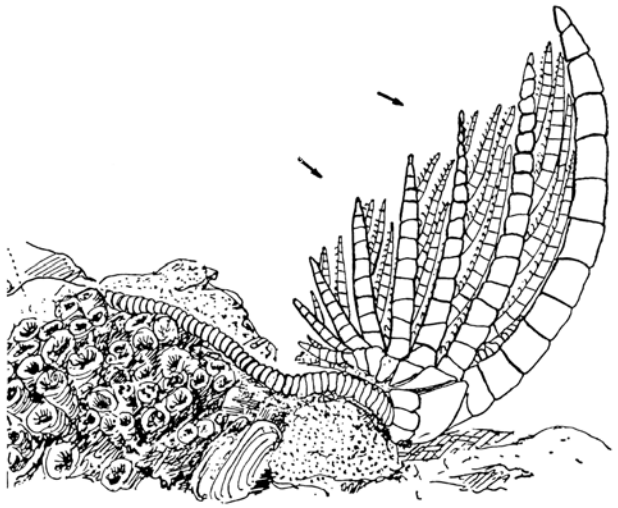

FIGURE 3 — Life reconstruction of *Synchirocrinus nitidus* in a runner mode (Jaekel, 1918: fig. 2). Arrows represent flow.

Wedge-shaped columnals in the distalmost portions of the column were reported in *Calceocrinus chrysalis* (Hall, 1860) (Brett, 1981). In *Trypherocrinus brassfieldensis* Ausich, 1984 (Aeronian, Llandovery), one specimen had a short segment of the distalmost column oriented vertically, and this section was separated from the remainder of the column by a wedge-shaped columnal making the majority of the column obligate prostrate along the substratum (Ausich, 1984). Eckert (1984) and Brett (1984, 1985) reported holdfasts with the holdfast-column articulation oriented vertically. This also produced an obligate runner orientation for the column.

Furthermore, taphonomic evidence may support the runner model. In several diverse crinoid occurrences studied by the author, specimens preserved with the arms intact appear to be more abundant for calceocrinids than for other crinoid taxa. If true, this anecdotal observation would be consistent with the runner model because a crinoid living at the sediment-water interface would have been more likely to be buried and preserved intact. Accepting the runner model as their life posture, calceocrinids fed lying on the sediment-water interface, which would have been the lowest epifaunal suspension-feeding tier.

MATERIALS AND METHODS

This study is based on experience collecting and describing Ordovician, Silurian, and Mississippian calceocrinids (e.g., Ausich, 1984; Ausich et al., 1997, 2015; Boyarko and Ausich, 2009; Ausich and Copper, 2010), as well as studies attempting to understand the evolutionary paleobiology and phylogeny of calceocrinids through the Paleozoic (Ausich, 1986; Harvey and Ausich, 1997). The specimens studied in detail herein are *Halysiocrinus tunicatus* (Hall, 1860) from the lower Viséan (upper Osagean, Mississippian) New Providence Shale Member of the Borden Formation at Button Mold Knob in north-central Kentucky (Kammer, 1984). This locality was a fossiliferous glade located in Bullitt County; but unfortunately, this classic collecting site has been destroyed by development. Material studied herein includes partial aboral cups, articulated basal plate circlets, articulated radial plate circlets, and individual radial plates. Standard petrographic thin sections were prepared from two basal plate circlets and two isolated radial plates. Two thin sections were made from each of these specimens, with the plane of thin sections perpendicular to articular facet (basal circlet facet and arm facets on radial plates).

INSTITUTIONAL ABBREVIATION

OSU — Orton Geological Museum, The Ohio State University (OSU).

CALCEOCRINID MORPHOLOGY

Crown

The synarthrial articulation between the basal circlet and the radial circlet is unique to calceocrinids. In *Halysiocrinus tunicatus*, this ridge extends across the entire E inferradial plate, and forms the proximal margin of the radial circlet. The basal circlet has three plates. The distal-most basal plate extends across the entire basal circlet margin and has one, long fossa with an articular ridge across the entire plate (Figs. 4, 5A–C). This articulates with a comparable fossa and articular ridge on the E inferradial plate (Fig. 4). Overall, the inside of the basal circlet is gently convex with the possibility of four fossa. These are arranged symmetrically on either side of the opening for the column axial canal. The distal two fossae are subtriangular and the proximal fossae subtriangular but narrower (Fig. 5).

Both the A and D radial plate arm facets are symmetrical with an articular ridge extending across most of the facet (Fig. 4A–B, 5G–I). A single, elongate aboral fossa is present along the outer margin of the articular ridge. Two adoral fossae are present on the inner side of the articular ridge (Fig. 5I). These adoral fossae are subtriangular in shape. They begin centrally on the inside of the facet and expand upward and outward toward the outer margins of the facet.

The E-ray arm articulates with the E superradial plate (Figs. 4A–B). This articulation has an articular ridge extending across the entire width of the plate; and only one, long, narrow fossa is present on the aboral side.

Kesling and Sigler (1969) depicted *Cunctocrinus* in a runner life position. They included reconstructions in both a closed, resting posture and an open, vertical fan posture (Messing et al., 2021) with the arms fully extended for feeding. In a resting posture, the radial plate circlet and arms close down over the basal circlet and onto column. When feeding, the classical interpretation is that the hinge is wide open, and the arms are erect. To attain this fully open posture, the synarthrial articulation between the basal and radial circlets would need to open by ~70°.

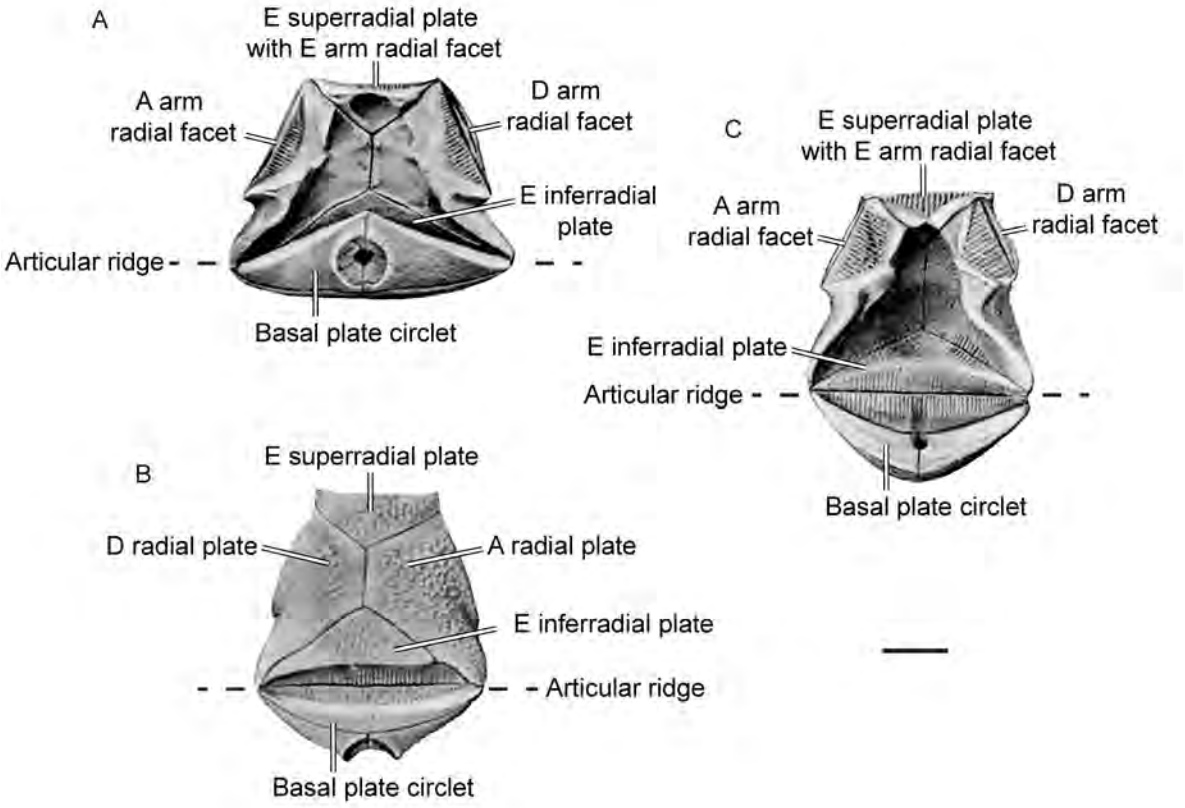

FIGURE 4 — *Halysiocrinus tunicatus* aboral cup in various orientations and with detailed explanation of the morphology. **A**, Internal view of radial plate circlet and distal view of basal plate circlets, aboral cup in a closed position; **B**, Internal view of radial and basal plate circlets, aboral cup in a an open position; **C**, External view of radial plate and basal plate circlets, aboral cup in an open position. Images from Springer, 1926; scale bar = 5 mm.

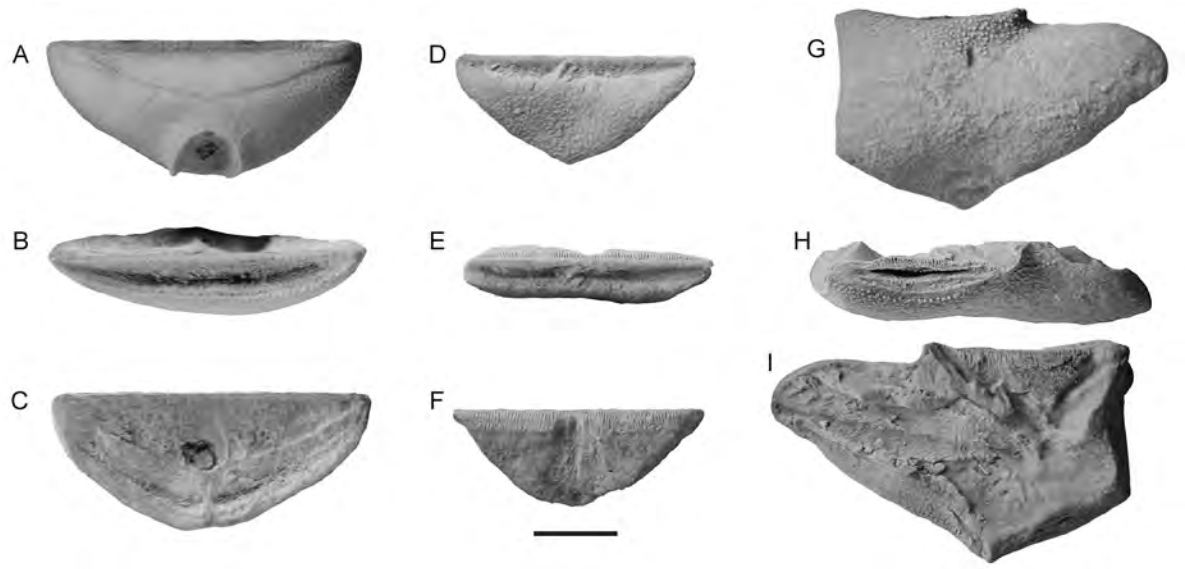

FIGURE 5 — Isolated aboral cup plates of *Halysiocrinus tunicatus.* **A**–**C**, basal circlet (OSU 54985), **A**, outside surface, **B**, basal circlet articular ridge and outer fossa, **C**, inner surface; **D**–**F, E**-superradial plate (OSU 54986), **D**, outside surface, **E**, basal circlet articular ridge and outer fossa, **F**, inner surface; **G**–**I**, E-superradial plate (OSU 54987), **G**, outside surface, **H**, basal circlet articular ridge and outer fossa, **I**, inner surface; all specimens coated with ammonium chloride, scale bar = 5 mm.

The synarthrial articulations were sites of marked movement. The basal circlet-E inferradial articulation opened and closed the crown. Tissue contraction on the outer fossae of the basal circlet-E inferradial articulation would have opened the crown, whereas contraction of tissue on the inner surface of the proximal portion of the radial circlet presumably closed the crown. Similarly, contraction of tissues on the outer fossae of the A and D radial plates and the E superradial plate would have opened the arms. On the A and D radial plates, two subtriangular fossae on the inside and beneath the articular ridge housed tissues that would have closed the arms with contracted.

Stereom Microstructure

Mesodermal calcareous plates in echinoderms have stereom microstructure, which is an echinoderm synapomorphy. Stereom is a cross-connected calcareous meshwork comprised of calcareous trabeculae that surround open pore space, which was filled with mesodermal tissue during life. Various types of stereom commonly reflect different functions (e.g., Macurda and Meyer, 1975; Roux, 1970, 1971, 1974, 1975; Macurda et al., 1978; Smith, 1980; Riddle et al., 1988; Gorzelak et al., 2014; Gorzelak, 2018). Remnants of the original stereom may be preserved in fossil echinoderms, especially in echinoderm plates preserved in siliciclastic mudstones and shales. Examples of stereom preserved in fossils include preserved stereom on the surface of plates (e.g., Strimple, 1972; Lane and Macurda, 1975; Ausich, 1977, 1983; Głuchowski, 1982; Gorzelak et al., 2014; Thomka and Smith, 2019), as well as preserved stereom on plate interiors (e.g., Ausich, 1983; Riddle et al., 1988).

Of particular interest is that different types of stereom are commonly indicative of different connective tissues, which in turn have different behavioral properties (Macurda and Meyer, 1975; Roux, 1975; Macurda et al., 1978; Smith, 1980; Gorzelak, 2018). Smith (1980: table 2) recognized ten primary types of stereom microstructure in echinoids. Relevant for the present study are imperforate, galleried, rectilinear, and labyrinthic stereom (= massive, galleried, rectilinear galleried, and labyrinthic stereom, respectively, of Macurda and Meyer, 1975). In the present study, galleried stereom is identified if linearity in the stereom is preserved as opposed the orthogonal nature of rectilinear stereom.

Specimens were examined for remnants of original stereom on both the surface of plates and within plate interiors (using thin sections). Several specimens have a fine rectilinear stereom preserved on the outside surface of the basal circlet. The key areas examined are the outer fossa and inner surface of the basal circlet, the stereom on the inner surface of radial plates, and E inferradial plates that would have housed tissue responsible for opening and closing of the crown. Also examined were the radial facets of the A radial plate, D radial plate, and E superradial plate that housed tissues for arm movement. Each is discussed separately below.

Basal circlet crescent-shaped fossa on the outside of the basal circlet.— As noted above, the distal margin of the basal circlet has an articular ridge and fossa, both extending the full width of the basal circlet (Figs. 4 and 5). The top and outer surface of the articular ridge is commonly preserved with a denser, darker colored calcite than the surrounding calcite. The denser stereom is consistent with the stereom of articular ridges and other bearing surfaces among crinoids (e.g., Macurda and Meyer, 1975; Ausich, 1977, 1983) and is comparable to the imperforate stereom of Smith (1980). Both the internal and exterior sides of this articular ridge have ridges and furrows that are perpendicular to the bearing surface of the articular ridge (Figs. 5C, 6E). Within the fossa, little stereom is preserved.

However, galleried stereom is inferred along the inside surface of the basal circlet beneath the articular ridge. This stereom is at a slight angle from perpendicular to the articular ridge. The galleried stereom is tilted toward the left on the left side of the (Fig. 6A) and toward the right on the right side (Fig. 6C).

Relatively little stereom is revealed in thin sections of basal circlet plates. In cross section, the basal circlet is an irregular crescent shape with the distal end tapering to a narrow, blunt proximal end; and the distal end is much wider with two high points separated by an indentation (Fig. 7). The high point on the concave side of the facet is the articular ridge, the indentation is the crescent-shaped aboral fossa, and high point on the convex side of the circlet is the outer edge of the crescent-shaped facet. Very faint linearly aligned stereom is present beneath the bottom of the basal circlet fossa and is interpreted to be very poorly preserved galleried stereom (Fig. 7C). Also as illustrated in Figure 8, approximately half of the interior of one specimen has poorly preserved rectilinear stereom.

In summary, little evidence of tissue-specific stereom is preserved on or in basal circlet fossae. What is preserved is all indicative of ligament tissue, and no evidence for labyrinthic stereom is present. Both the galleried stereom at the base of the basal circlet fossa (Fig. 7) and the galleried stereom along the vertical ridges and grooves in the inner surface below the articular ridge (Fig. 6) are interpreted to represent ligament tissue that connected the basal circlet to the E inferradial plate articulation.

Medial area of radial plate interiors.— Typical reconstructions of calceocrinid crowns (Brower, 1985: fig. 2; Brower, 1990: fig. 2) infer soft tissue connecting the interior of the radial plates with, perhaps the interior of basal circlet. One specimen has preserved stereom in the proximal portion of the interior a radial plate (Fig. 9). On this specimen, galleried stereom is on the plate surface. This stereom is present on the inside of a ridge adjacent to the suture between the A radial plate and the E-inferradial plate. The stereom is inclined proximally (Fig. 9A), back toward the distal portion of the basal circlet (compare to Fig. 4A and Fig. 4B).

As with the basal circlet, radial plate interiors (based on thin sections) only have preserved rectilinear and galleried stereom. In contrast to the basal circlet, the radial plates

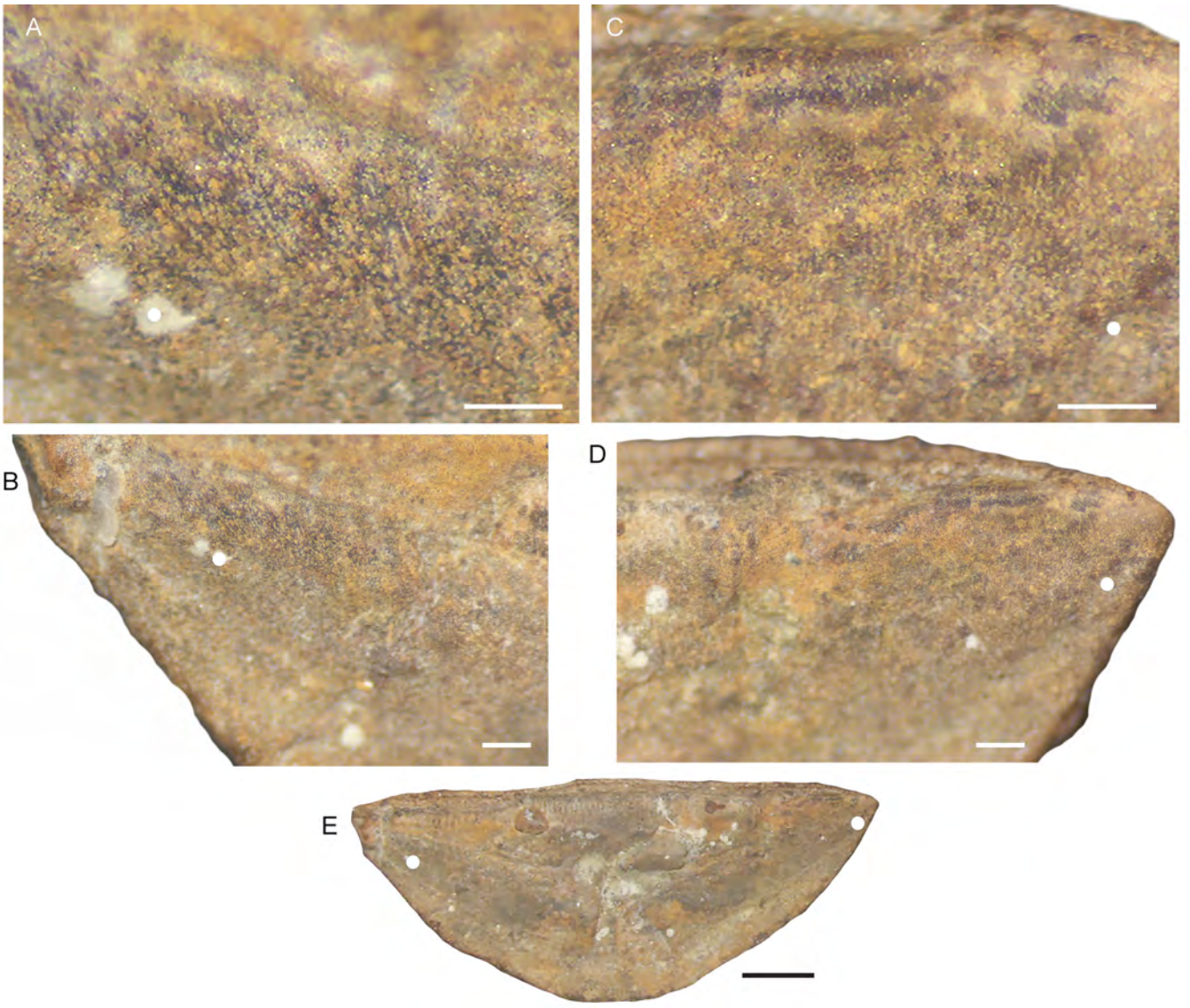

FIGURE 6 — Inner surface of a *Halysiocrinus tunicatus* basal circlet (OSU 54988). **A**, Left side of area beneath the articular ridge, enlargement of B, scale bar = 0.33 mm; **B**, enlargement of right side of area beneath the articular ridge, scale bar = 0.33 mm; **C**, Left side of articular ridge area beneath the articular ridge, enlargement of B, scale bar = 0.5 mm; **D**, Right side of area beneath articular ridge, scale bar = 0.5 mm; **E**, interior D radial plate, scale bar = 2.5; White dots are landmark points for orientation.

examined have much stereom preserved within the plates. As noted above, Figure 10 rectilinear stereom is preserved throughout the entire radial plate. However, stereom changes from rectilinear to galleried along the inner margin of the plate (Figs. 10, 11).

A and D radial arm facets.— Similar to the articular ridge of the basal circlet, the articular ridge on radial facets is commonly preserved with a denser and darker colored calcite than the remainder of the plate and is interpreted as imperforate stereom (Fig. 12). Also, similar to the basal circlet and E inferradial articular surfaces, the inside surface beneath the articular ridge has ridges and grooves perpendicular to the articular ridge (Fig. 4). Galleried stereom projects along the inner surface beneath the articular ridge parallel to the ridges and grooves and perpendicular to the articular ridge bearing surface (Fig. 13). In places where stereom is preserved within the margins of the aboral fossa of the radial plates, it is rectilinear and could be either interpreted as rectilinear or galleried stereom.

Subtriangular fossa on the inner side of the facet also has galleried stereom. It more-or-less parallels the surface of the subtriangular facet (Fig. 14). This stereom projects upward

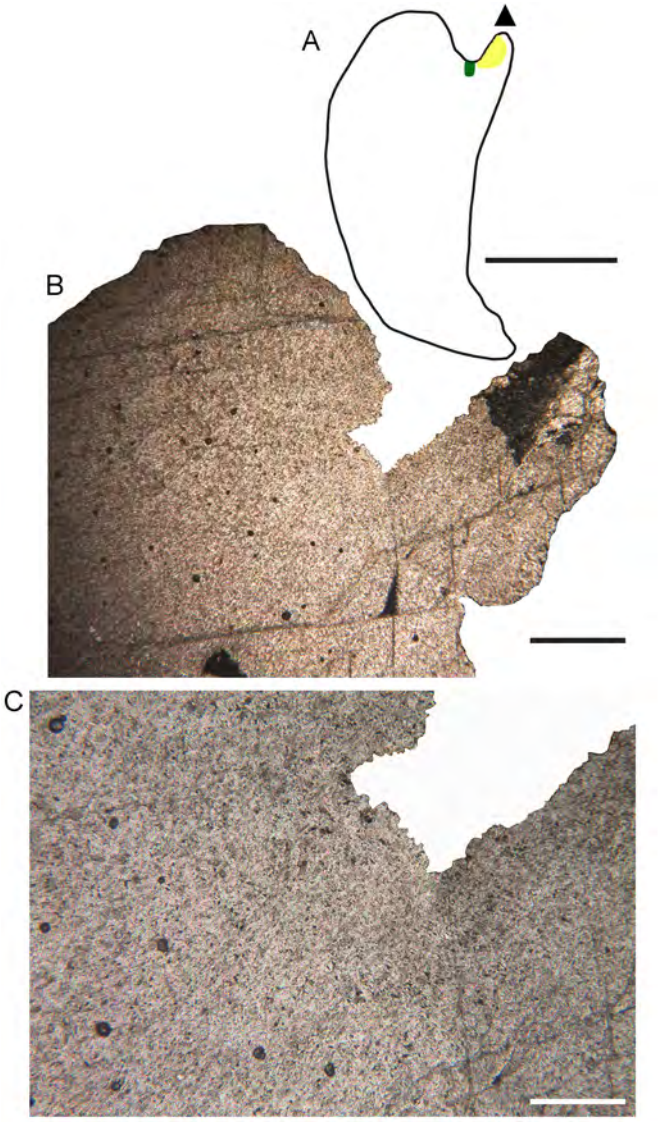

FIGURE 7 — Thin sections of *Halysiocrinus tunicatus* basal circlet (OSU 54981b), photographed in polarized light. **A**, Cross section of basal circlet (triangle, articular ridge; green, galleried stereom; yellow, rectilinear stereom); scale bar = 2.5 mm; **B**, thin section of distal end of basal, scale bar = 500 µm; **C**, enlargement of the bottom of the basal circlet fossa with faintly preserved linear stereom interpreted to be galleried stereom, scale bar = 200 µm.

along the surface of the subtriangular fossa (Fig. 14A). In thin section, galleried stereom is preserved beneath the radial facet (Figs. 11A–B).

E superradial plates.— A single, well-preserved E superradial plate is in the present collection (Figs. 5D–F). Similar to the articular ridge on the basal circlet, imperforate stereom is present along the E superradial articular ridge (Figs. 5F, 15). Ridges and grooves extend downward from

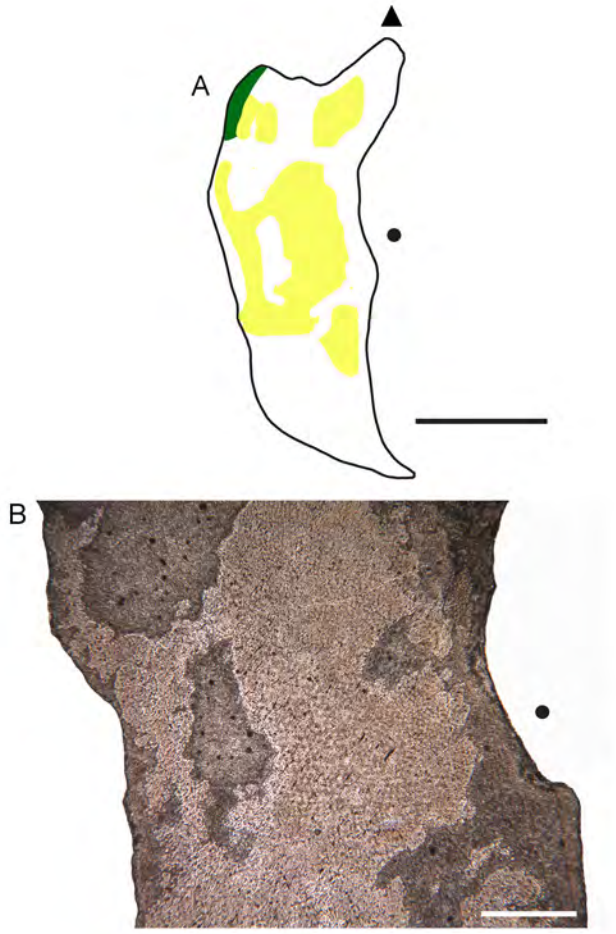

FIGURE 8 — Thin section of *Halysiocrinus tunicatus* basal circlet (OSU 54982a). **A**, Cross section of basal circlet (triangle, articular ridge; green, galleried stereom; yellow, rectilinear stereom); scale bar = 2.5 mm; **B**, thin section of the middle portion of the basal circlet with some, poorly preserved rectilinear stereom, scale bar = 500 µm. Dots are landmark points to identify position of enlargements.

the bearing surface of the articular ridge on only the inside of the articular ridge. Again, similar to the basal circlet, galleried stereom is present along the ridges and groves and is perpendicular to the articular ridge bearing surface (Fig. 15). Preserved stereom on the E superradial plate (Figs. 15D–E) would have controlled the opening and closing of the E-ray arm was presumably ligament.

FUNCTIONAL MORPHOLOGY OF THE CALCEOCRINIDAE

Despite all that has been learned since the initial description of a calceocrinid fossil, outstanding questions remain. The two fundamental questions are 1) crown position with respect

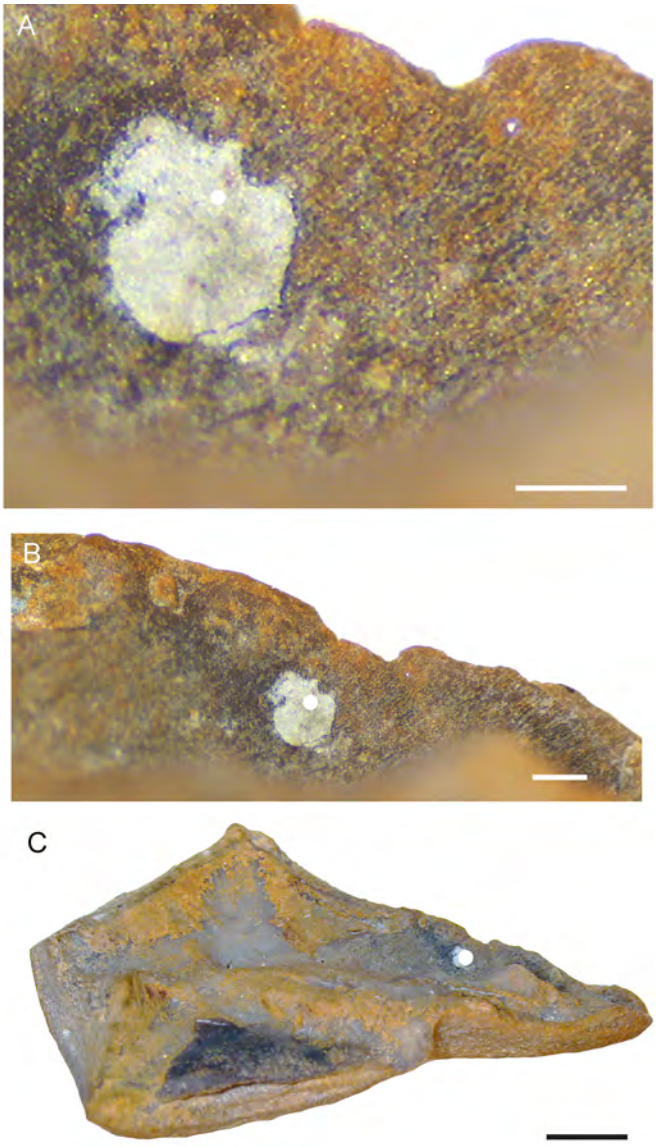

FIGURE 9 — Oblique, upside down view of an A radial facet of *Halysiocrinus tunicatus* illustrating galleried stereom in the inner side if a ridge on the lower portion of the plate (OSU 54987). **A**, scale bar = 0.33 mm; **B**, scale bar = 0.5 mm; **C**, scale bar = 2.5 mm. Dots are landmark points to identify position of enlargements.

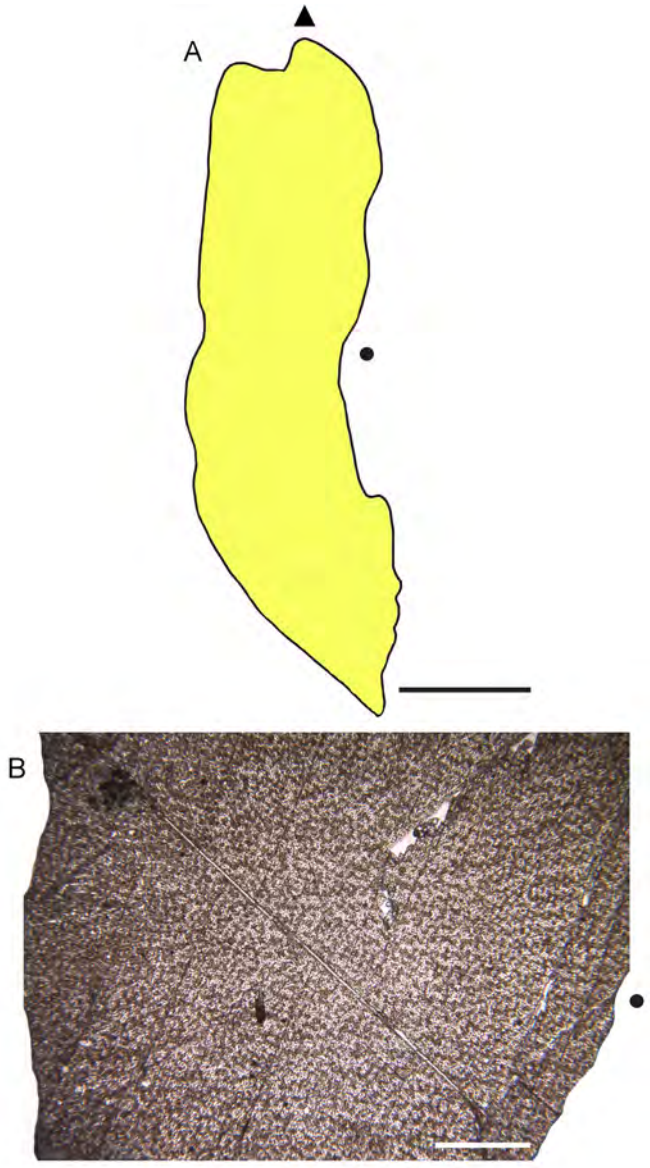

FIGURE 10 — Thin sections of *Halysiocrinus tunicatus* middle section of a radial plate (OSU 54984b). **A**, Cross section of radial plate (triangle, articular ridge; yellow, rectilinear stereom); scale bar = 2.5 mm; **B**, thin section of middle section of plate with rectilinear stereom, scale bar = 500 µm. Dots are landmark points to identify position of enlargements.

to currents during feeding and 2) what connective tissues controlled the opening and closing of the crown from a resting posture along the column to a feeding posture and back again to a resting posture?

Significant to these questions are attributes of the benthic habitat milieu. As noted by Walker and Bambach (1974), the density of organic particles in the water column is greatest at the sediment-water interface, where a flocculent layer high in organics may form. Above the sediment-water interface, the density of organic particulates decreases dramatically (Walker and Bambach, 1974). In contrast, due to frictional effects of the sea floor, current velocities asymptotically decrease toward the sediment-water interface. This height above the sediment-water interface with diminished current velocity is called the

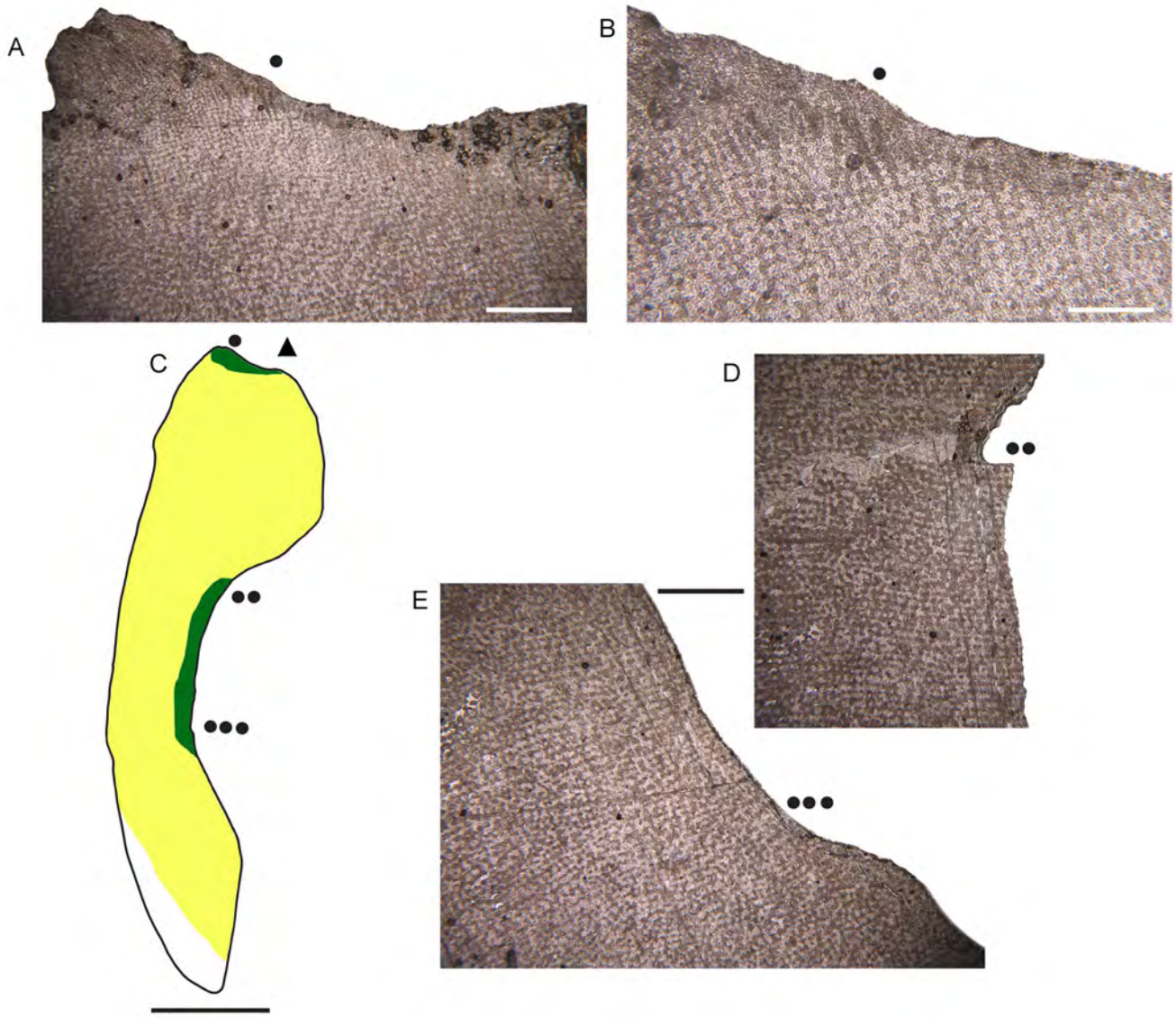

FIGURE 11 — Thin sections of a *Halysiocrinus tunicatus* radial plate; all photographs in plain light (OSU 54984a). **A**, thin section of stereom beneath the radial facet, scale bar 500 µm; **B**, enlargement of A, scale bar 200 µm; **C,** Cross section of radial plate (triangle, articular ridge; green, galleried stereom; yellow, rectilinear stereom); scale bar = 2.5 mm; **D**, thin section of inner margin of plate with rectilinear stereom transitioning outward to galleried stereom, scale bar 500 µm. **E**, thin section of inner margin of plate with galleried stereom, scale bar = 500 µm. D and E scale bar = 500 µm; dot patterns are landmark points to identify position of enlargements.

benthic boundary layer (Rhodes and Boyer, 1982). For passive suspension-feeding organisms, such as crinoids, this produces a nutrient paradox, in which the highest concentrations of potential food exist in the zone of minimal current velocity. Indeed, the entire ecological experiment of pelmatozoan echinoderms was one in which the column elevated the feeding apparatus above the sediment-water interface into a position that maximized the flux of suspended food particles through arms or brachioles. This means that during everyday conditions, calceocrinids must have fed in a setting with much reduced current velocity but a high concentration of organic particles.

Three possible feeding postures are discussed below. Key factors inferred to be significant to our understanding of calceocrinid paleoecology are the properties of echinoderm ligament tissue; the orientation of the ambulacra relative to prevailing currents, as it affects feeding; whether lift played a role in opening the arms; the ability of the column to

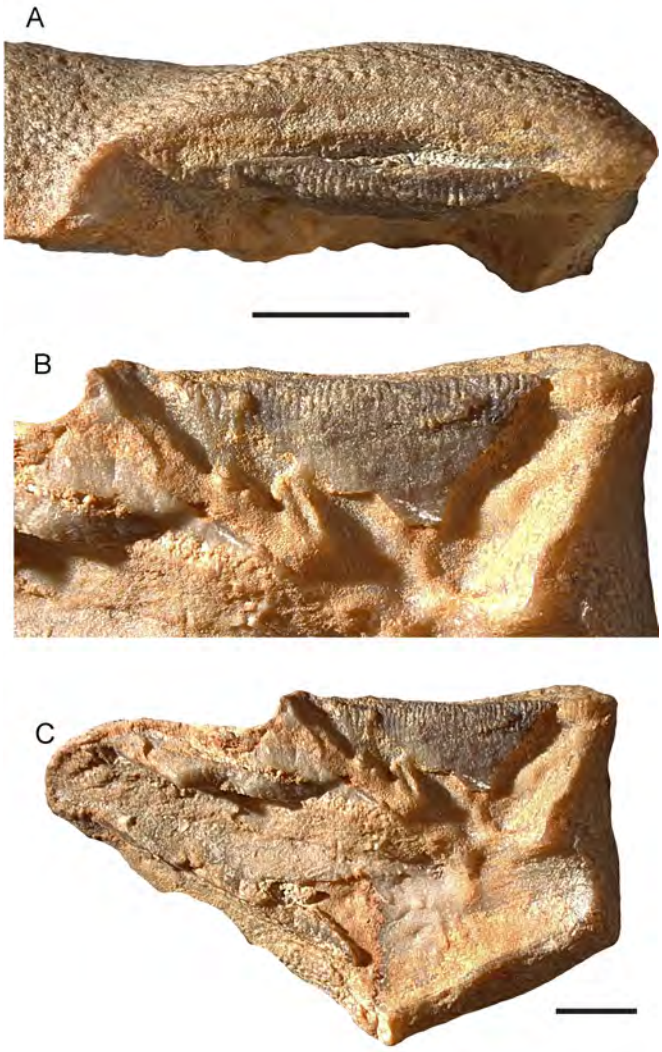

FIGURE 12 — A radial facet of *Halysiocrinus tunicatus* note darker colored and more denser stereom of the articular ridge (OSU 54987). **A, B,** scale bar = 2.5 mm;**C,** scale bar = 2.5 mm.

resist torque resulting from drag on opened arms; fouling of ambulacra with waste; closing the crown; and potential for preservation.

Echinoderm Ligaments

Mutable collagenous tissue (MCT; also catch-connective tissue) is a synapomorphy for the Echinodermata. The unique properties of this tissue have been studied extensively (e.g., Wilkie 1983, 1984, 2005; Motokawa, 1984, 1985; Wilke and Emson, 1988; Wilkie et al., 1992, 1993, 1994; Birenheide and Motokawa, 1994a, 1994b; Motokawa et al., 2004; and Wilkie et al., 2021). MCT is under nervous control. These ligaments are comprised of collagen fibrils (typically in bundles), microfibrils, and neuron-like cell processes, and they can rapidly change from being stiff to flaccid (e.g., Wilkie, 1983, 1984, 2005; Motokawa, 1984, 1985; Wilke and Emson, 1988; Birenheide and Motokawa, 1994a, 1994b; Motokawa et al., 2004; Ribeiro and others, 2011; and Wilkie et al., 2021). MCT makes autotomy of echinoderm body parts and evisceration of holothurians possible. In the stiff mode MCT allows suspension-feeding echinoderms to maintain a feeding posture with minimal expenditure of energy.

In addition to the catch-connective properties, echinoderm ligaments have also recently been demonstrated to have contractile properties (Gimmer and Holland, 1987; Birenheide and Motokawa, 1994; Motokawa et al., 2004). Ligaments have been observed to elongate by as much as 100% (Birenheide and Motokawa, 1994) as well as to contract by as much as 50% (Birenheide and Motokawa, 1996). Thus, although much slower than muscle contractions, ligament contraction can also contribute to organism movement. Unless evidence of labyrinthic stereom is identified on calceocrinid plates, it must be assumed that the degree and speed of movement in calceocrinids fell within the limits allowed by ligament tissue, as inferred by analogy with living echinoderms. As noted above, calceocrinids have a tendency to be preserved with arms intact more commonly than other coeval crinoids. Specimens with no arms but the aboral cup are exceedingly rare. These two observations also suggest that the arms and aboral cup articulations were both held together by the same connective tissues, which is inferred here to be ligaments.

Potential Feeding Postures

Three potential feeding postures are discussed here, which include a vertical fan with the current striking the oral side of the arms, a vertical fan with the currents striking the aboral side of the arms, and a partially open posture. The first is the original model proposed by Jaekel (1918: fig. 83) with the ambulacra facing the current. This posture was assumed for both the kite and weathervane hypothesis (Kesling and Sigler, 1969 and Breimer and Webster, 1975, respectively).

The second posture has a vertical filtration fan oriented with the currents striking the aboral side of the arms, which is the position assumed by most living crinoids in a unidirectional current regime. This posture was supported Brower (1985), Ausich (1986), and Messing et al. (2021).

A third alternative is proposed here, which is a partially open posture. The shape of the arms in this posture would be subellipsoidal. Messing (1994) and Messing et al. (2021) identified a relatively unusual crinoid arm posture in some extant, multiarmed Comatulidae (~40 – 80 arms). The arms are partially open and arched above the disc. This feeding posture was recognized in extant crinoids in a reef setting, where current velocities were sufficiently high to induce an erect posture in other crinoids (Stevens, 1989). A calceocrinid in this feeding posture would have fed primarily from the high concentration of organic particles immediately above the sediment-water interface.

Each of these potential feeding postures would have been affected by numerous factors, as discussed below and summarized in Table 2.

FIGURE 13 — D radial facet of *Halysiocrinus tunicatus* illustrating darker colored and more dense stereom of the articular ridge, and galleried stereom aligned vertically along the inner surface beneath the articular ridge (OSU 54989). **A**, Left side of articular ridge, enlargement of B, scale bar = 0.33 mm; **B**, enlargement of left side of articular ridge, scale bar = 0.33 mm; **C**, Right side of articular ridge, enlargement of B, scale bar = 0.5 mm; **D**, enlargement of right side of articular ridge, scale bar = 0.5 mm; **E**, interior D radial plate, scale bar = 2.5 mm.

Feeding.— In a unidirectional current regime, extant crinoids feed with the aboral side of the arms facing the current. However, food particle capture in extant crinoids is now regarded to be primarily from inertial impaction of food particles striking tube feet rather than from current eddying around the arms (Baumiller et al., 1993). Therefore, in a unidirectional current setting, whether the currents struck the oral or aboral side of the arms was probably immaterial in terms of food capture by tube feet. By the same reasoning, if tube feet were exposed, a partially opened, subellipsoidal posture would presumably have allowed particle capture, if the crown was open enough and positioning of tube feet was sufficient for currents to penetrate into this fan. Based on analogy to extant crinoids, this posture would be well-suited for a multidirectional current regime, whereas the two erect postures would not. Further, using computational fluid dynamic analyses, Dynowski et al. (2016) concluded that the partially open crown of *Encrinus liliiformis* Lamarck, 1801 would have effectively feed in an environment with variable current conditions.

Torque on the column.— Drag on the crown would produce torque on the column in any posture and in any current

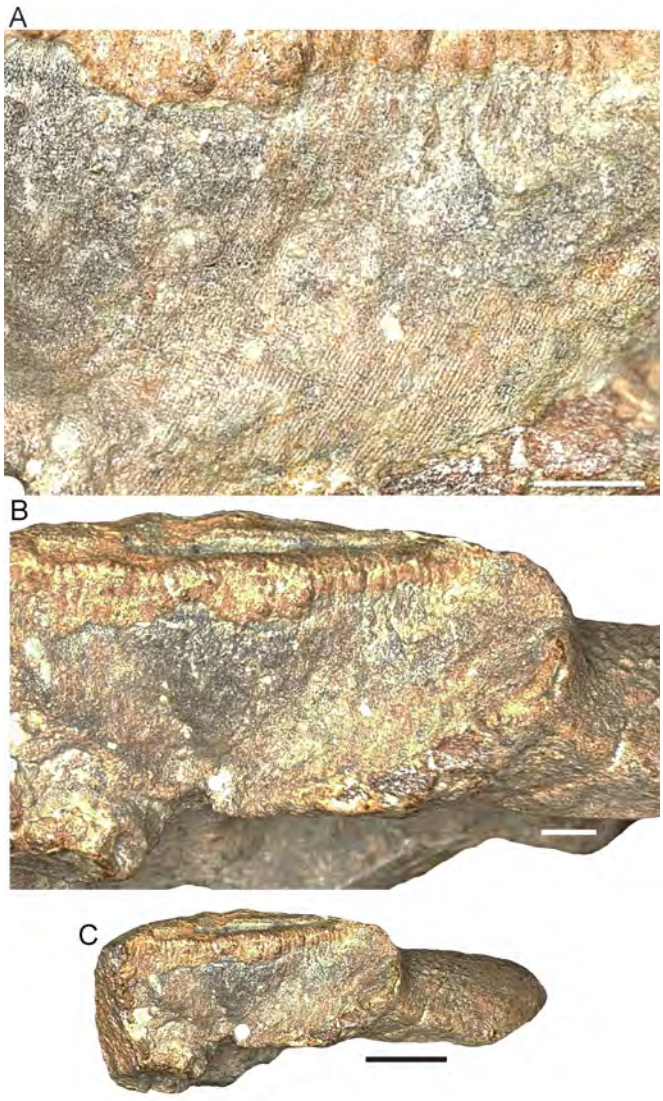

FIGURE 14 — D radial facet of *Halysiocrinus tunicatus* illustrating galleried stereom in the subtriangular inner fossa of a radial facet (OSU 54990). **A**, Enlargement of basal portion of right subtriangular inner fossa, enlargement of B, scale bar = 0.33 mm; **B**, enlargement right subtriangular inner fossa, articular ridge along top, scale bar = 0.5 mm; **C**, radial plate from a lateral perspective, scale bar = 2.5 mm.

direction except if the crown was oriented with currents striking the ambulacra and the current direction parallel to the column. The low profile of a partially open subellipsoidal posture would have experienced the least amount of column torque among the three proposed postures. One might assume that the ligaments in the column would have locked into place to prevent much movement and minimal, if any, damage to the column, but extreme turbulence events would have undoubtedly caused damage to the column, arms, or both, regardless of the arm posture.

The Kesling and Sigler (1965) weathervane mode suggested that with the currents striking the oral side of the arms the crown and column would have pivoted back and forth as dictated by currents and drag on the crown. As presently understood, there is not a single pivot point along the column that would have allowed this motion. Theoretically, it would have been possible for cumulative, coordinated contraction and relaxation of ligaments between columnals to have resulted in movement as predicted by the weathervane mode, but the motion allowed may have been slower and less extensive than imagined by Kesling and Sigler (1965).

Opening the crown.— The primary question about opening the crown is the extent to which it could open. By analogy to living echinoderm ligaments, a calceocrinid could have easily assumed a partially open, subellipsoidal posture. It is also probable that opening and closing of the outer fossae of the basal circlet-E inferradial articulation were well within the limitations imposed by ligaments. The primary question is whether ligaments on the inner surface of the radial circlet could have had contraction and stretching enough to open the crown into a fully erect posture and close it again. It is probable that the ligaments in the proximal portion of the inner radial circlet would have supported fully opening the crown into an erect posture. However, it is doubtful if this was the case for any ligaments higher up along the inner surface of the radial circlet.

Calceocrinid arms would experience lift if the crown was positioned with the currents striking the ambulacral side of the arms. This would aid opening of the crown. Indeed, this lift was the premise for the Breimer and Webster (1975) kite model of calceocrinids in which the crown gained sufficient lift to be elevated into tiering levels above the sediment-water interface. Whereas sufficient lift to slightly raise the crown was probable, the calculations of lift by Baumiller (1992) suggested that insufficient lift would have typically been generated to elevate the crown and column to the extent envisioned by Breimer and Webster (1975). Further, it is improbable that sustained current velocities would have been present low in the benthic boundary layer to maintain an elevated kite position.

In a posture with currents striking the aboral side of the arms, calceocrinids would have had to overcome drag resistance to open their arms against the currents, which is the case for living crinoids, as well as most Paleozoic crinoids that had only ligaments in the crown (Ausich and Baumiller, 1993).

The subellipsoidal posture would have experienced the least amount of resistance opening the crown simply because it opened the least. A multidirectional or unidirectional current regime would have little effect on opening the arms into a partially open subellipsoidal posture.

Closing the crown.— In a unidirectional current regime with currents striking the ambulacral side of the arms, a sudden, catastrophic current burst would severely challenge closure of the arms. Alternatively, calceocrinids feeding in either the partially open subellipsoidal posture or a posture

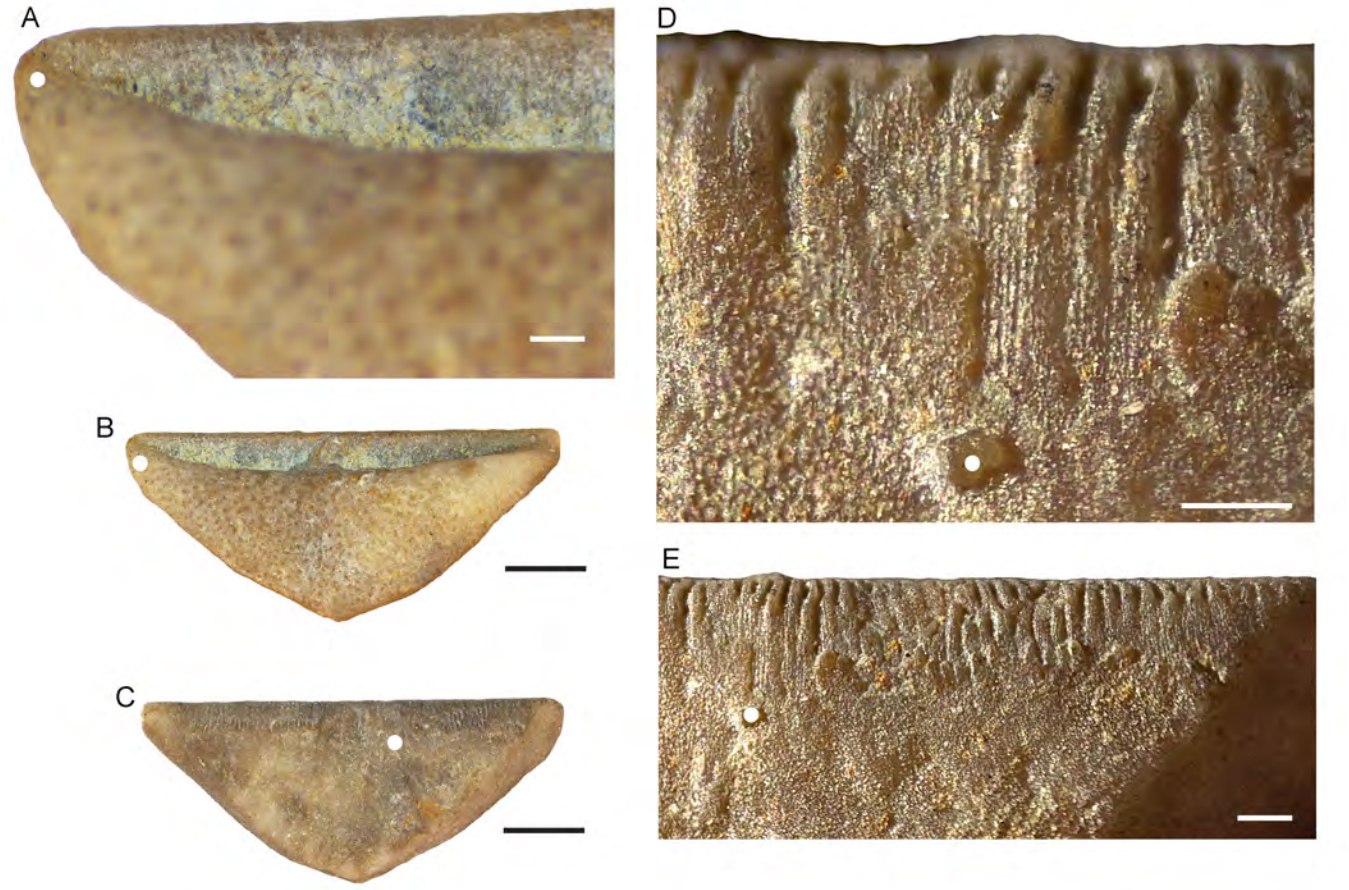

FIGURE 15 — E superradial plate of *Halysiocrinus tunicatus* illustrating ridges beneath the articular ridge and galleried stereom paralleling these ridges (OSU 54086). **A**, **B**, Exterior of E superradial plate, A an enlargement of the right side of the fossa with poorly preserved ridges beneath and perpendicular to the articular ridge. A, scale bar 0.5 mm, B, scale bar 2.5 mm. **C**, **D**, **E**, Interior of E superradial plate, C, scale bar = 2.5 mm, D, enlargement of E scale bar = 0.33 mm; **E**, enlargement of right side of C, scale bar = 0.5 mm. Dots are landmark points to identify position of enlargements.

with the currents striking the aboral side of the arms would quickly close into a resting posture with the aid of currents. As noted above, these two posture scenarios would also support the anecdotal observation of more common preservation of calceocrinid crowns in many occurrences.

Fouling from waste.— *Senariocrinus maucheri* Schmidt, 1934 is known to have had a very high anal sac that would have helped to disperse waste above and away from open arms. However, this may have presented a problem for most calceocrinids with shorter anal sacs. In calceocrinids with erect arms and currents striking the aboral side of the arms, waste products would have presumably been swept away from the ambulacra and prevented fouling. Alternatively, if arms were erect and the currents struck the oral side of the arms, waste products would have had to have been washed through the arms that were engaged in feeding, and fouling would have been inevitable. Similarly, in a partially open subellipsoidal posture with the anal sac completely enclosed within the arms, fouling would also be inevitable; however, this is presumably not a limiting factor among living crinoids.

DISCUSSION AND CONCLUSIONS

Calceocrinid crown morphology radically deviated from that of any other stalked crinoid to exploit a suspension-feeding niche immediately above the sediment-water interface. Based on the success of this lifestyle (inferred from the extreme duration of this family), it is surprising that more crinoid clades did not evolve a similar feeding position within tiered, suspension-feeding paleocommunities. Of course, feather stars also lack a column as adults. However, this morphology was inferred to primarily be a consequence of increased predation pressure before and during the Mesozoic Marine Revolution (Meyer and Macurda, 1977; Baumiller et al., 2010), and living feather stars commonly climb to the highest perch possible, presumably to maximize current flow

TABLE 2 — Various positive and negative factors that may have influenced feeding posture in the Calceocrinidae. The "+" symbol indicates a positive factor; the "0" indicates a neutral factor; the "–" symbol indicates a negative factor.

Factors	Arms Erect, Currents Strike Ambulacra	Arms Erect, Currents Strike Aboral Side of Arms	Ellipsoidal Posture
Feeding ability	+	+	+
Feeding in unidirectional currents	+	+	+
Feeding in multidirectional currents	–	–	+
Torque on column due to drag on crown	–	–	–
Lift to help to open crown	+	–	0
Currents help close crown	–	+	0
Higher probability of crown preservation	–	+	+
Fouling from waste	–	+	–

through the arms (e.g., Meyer, 1973, 1979; Messing, 1985, 1994, 1997, 2006; Stevens and Connolly, 2003; Messing et al., 2006, 2021).

Three possible suspension-feeding postures for calceocrinids are described above, including an erect arm posture with currents striking the oral side of the arms, an erect arm posture with currents striking the aboral side of the arms, and a partially open, subellipsoidal posture. Based on skeletal morphology and analogy to living crinoid feeding behavior, preserved stereom microstructure implies that opening and closing of the crown and arm movement was controlled by ligaments. It is probable that contraction and stretching limitations of echinoderm ligaments would have allowed the basal circlet-E inferradial articulation to fully open and close, but it is not clear if this is the case for the ligaments on the inner side of the radial circlet. Assuming that a vertical posture was within the limits imposed by ligaments, all three potential feeding habits are possible. Inferred pluses and minuses can be scored for each posture (Table 2), and none of the alternatives can be eliminated with certainty.

In conclusion, two primary puzzles have persisted surrounding the paleoecology of members of the Calceocrinidae. The first is solved. Based on remnants of preserved stereom, only ligament tissue is inferred to have controlled opening and closing of the crown and arms in calceocrinids. Based on the behavior of ligaments in living echinoderms, ligament tissue was sufficient to open and close the aboral cup and arms of calceocrinids. The second puzzle is calceocrinid posture during feeding. Whereas an erect fan with the current striking the aboral side of the arms has been favored by recent authors (Brower, 1985; Ausich, 1986; and Messing et al., 2021), there is no compelling criterion by which to reject this or other potential feeding orientations and posture positions, with the only caveat being the ligament stretching limits. Therefore, it is possible that two or all of three of these alternative postures could have been employed to exploit changing ambient environmental conditions. The calceocrinids remain a puzzle.

ACKNOWLEDGMENTS

Discussion with numerous people through the years have helped to crystallize the ideas presented here, and chief among them is Tomasz K. Baumiller, who has provided a unique, positive perspective to many generations who have attempted to understand living and ancient organisms, especially crinoids. I thank J. M. Lawrence, T. Oji, and I. C. Wilkie for

helping me to better understand the structure and behavior of echinoderm ligaments. I also thank W. A. Griffith, J. Leonard-Pingel, J. M. Sheets, and the Subsurface Energy Materials Characterization and Analysis Laboratory (SEMCAL) in the School of Earth Sciences, Ohio State University for their help in the preparation of figures. Przemysław Gorzelak, Jennifer Bauer, and Selina Cole greatly improved this manuscript.

LITERATURE CITED

ARENDT, Yu. A. 1965. K poznaniyu morskihh lilii kaltseokrinid [Contribution to the knowledge of crinoids from the family Calceocrinidae]. Paleontologicheskii Zhurnal, 1: 90–96.

AUSICH, W. I. 1977. The functional morphology and evolution of *Pisocrinus* (Crinoidea: Silurian). Journal of Paleontology, 51: 672–686.

_____. 1983. Functional morphology and feeding dynamics of the Early Mississippian crinoid *Barycrinus asteriscus*. Journal of Paleontology, 57: 31–41.

_____. 1984. Calceocrinids from the Early Silurian (Llandoverian) Brassfield Formation of southwestern Ohio. Journal of Paleontology, 58: 1167–1185.

_____. 1986. Palaeoecology and history of the Calceocrinidae (Palaeozoic Crinoidea). Palaeontology, 29: 85–99.

_____. 2018. Morphological paradox of disparid crinoids (Echinodermata): phylogenetic analysis of a Paleozoic clade. Swiss Journal of Paleontology, 2018: 159–176.

_____, and T. K. BAUMILLER. 1993. Taphonomic method for determining muscular articulations in fossil crinoids. Palaios, 8: 477–484.

_____, and D. J. BOTTJER. 1982. Tiering in suspension-feeding communities on soft substrata throughout the Phanerozoic. Science, 216(4542): 173–174.

_____, and P. COPPER. 2010. The Crinoidea of Anticosti Island, Québec (Late Ordovician to Early Silurian). Palaeontographica Canadiana, 29, 157 pp.

_____ A. GOLDSTEIN, and R. YATES. 2000. Crinoids from the Muldraugh Member of the Borden Formation in north-central Kentucky (Echinodermata, Lower Mississippian). Journal of Paleontology, 74: 1072–1082.

_____, T. W. KAMMER, and D. L. MEYER. 1997. Middle Mississippian disparid crinoids from the east-central United States. Journal of Paleontology, 71: 131–148.

_____, M. E. PETER, and F. R. ETTENSOHN. 2015. Echinoderms from the Lower Silurian Brassfield Formation of east-central Kentucky. Journal of Paleontology, 89: 245–256.

BATHER, F. A. 1893. The Crinoidea of Gotland. Pt. 1, The Crinoidea Inadunata. Kongliga Svenska Vetenskaps-Akademiens Handlingar, 25, 200 pP.,

BAUMILLER, T. K., 1992. Importance of hydrodynamic lift to crinoid autecology, or, could crinoids function as kites?. Journal of Paleontology, 66: 658–665.

_____, M. LABARBERA, and J. D. WOODLEY. 1991. Ecology and functional morphology of the isocrinid *Cenocrinus asterius* (Linnaeus) (Echinodermata: Crinoidea) in situ and laboratory experiments and observations. Bulletin of Marine Science, 48: 731–748.

_____, M. A SALAMON, P. GORZELAK, R. MOOI, C. G. MESSING, and F. J. GAHN. 2010. Post-Paleozoic crinoid radiation in response to benthic predation preceded the Mesozoic marine revolution. Proceedings of the National Academy of Science of the United States of America, 107: 5893–5896.

BIRENHEIDE, R., and T. MOTOKAWA. 1994. Morphological basis and mechanics of arm movement in the stalked crinoid *Metacrinus rotundus* (Echinodermata, Crinoidea). Marine Biology, 121: 273–283.

_____, and _____. 1996. Contractile connective tissue in crinoids. Biological Bulletin, 191: 1–4.

BOTTJER, D. J., and W. I. AUSICH. 1987. Phanerozoic development of tiering in soft substrata suspension-feeding communities. Paleobiology, 12: 400–420.

BOYARKO, D., and W. I. AUSICH. 2009. New calceocrinids from the Brassfield Formation of northern Kentucky and southern Ohio. Southeastern Geology, 46: 103–108.

BREIMER, A., and G. D. WEBSTER. 1975. A further contribution to the paleoecology of fossil stalked crinoids. Koninklijke Nederlandes Akademie van Wetenschappen, Proceedings, Ser. B., 76: 249–167.

BRETT, C. E. 1981. Systematics and paleoecology of Late Silurian (Wenlockian) calceocrinid crinoids from New York and Ontario. Journal of Paleontology, 55: 145–175.

_____. 1984. Autecology of Silurian pelmatozoan echinoderms. In M. G. Bassett, and J. D. Lawson, (eds.), Autecology of Silurian organisms. The Palaeontological Association Special Papers in Palaeontology, 32: 87–120.

_____. 1985. Pelmatozoan echinoderms on Silurian bioherms in western New York and Ontario. Journal of Paleontology, 59: 820–838.

BROWER, J. C. 1966. Functional morphology of Calceocrinidae with description of some new species. Journal of Paleontology, 40: 613–634.

_____. 1977. Calceocrinids from the Bromide Formation (Middle Ordovician) of southern Oklahoma. Oklahoma Geological Survey, Circular, 78: 1–28.

_____. 1985. Ontogeny and functional morphology of two Ordovician calceocrinids. In B. F. Keegan, and B. D. S. O'Connor (eds.), Echinodermata, Proceedings of the fifth international echinoderm conference Galway. A. A. Balkema, Rotterdam, p. 13–18.

_____. Ontogeny and phylogeny of the dorsal cup in calceocrinid crinoids. Journal of Paleontology, 64: 300–318.

DYNOWSKI, J. F., J. H. NEBELSICK, A. KLEIN, and A. ROTH-NEBELSICK. 2016. Computational fluid dynamics analysis of the fossil crinoid *Encrinus liliiformis* PLoS ONE, 11(5): e0156408. ?? pp. [DOI: 10.1371/journal.pone.0156408]

ECKERT, J. D. 1984. Early Llandovery crinoids and stelleroids from the Cataract Group (Lower Silurian),

southern Ontario, Canada. Royal Ontario Museum Life Sciences, Contributions, no. 137: 1–83.

ETTENSOHN, F. R. 1975. The autecology of *Agassizocrinus lobatus*. Journal of Paleontology, 49: 1044–1061.

_____. 1980. *Paragassizocrinus* systematics, phylogeny and ecology. Journal of Paleontology, 54: 978–1007.

_____. 1984. Unattached Paleozoic stemless crinoids as environmental indices. Geobios, Special Memoir 8: 63–68.

GISLÉN, T. 1924. Echinoderm studies. Zoologisk Bidrag fran Uppsala 330 pp.

GŁUCHOWSKI, E. 1982. On microstructures of columns of some Paleozoic crinoids. Acta Palaeontologica Polonica, 27: 77–83.

GORZELAK, P. 2018. Microstructural evidence for stalk autonomy in *Holocrinus* – The oldest stem-group isocrinid. Palaeogeography, Palaeoclimatology, Palaeoecology, 506: 202–207.

_____, E. GŁUCHOWSKI, and M. SALAMON. 2014. Reassessing the improbability of a muscular crinoid stem. Scientific Reports, 4(6049): 9 pp. [DOI: 10.1038/srep06049]

GRIMMER, J. C., and N. D. HOLLAND. 1987. The role of ligaments in arm extension in feather stars (Echinodermata: Crinoidea). Acta Zoologica, 68: 79–82.

HAGDORN, H. and X.-F. WANG. 2015. The pseudoplanktonic crinoid *Traumatocrinus* from the Late Triassic of Southwest China – Morphology, ontogeny, and taphonomy. Palaeoworld 24: 479–496.

HALL, J. 1852. Palaeontology of New York, v. 2, Containing descriptions of the organic remains of the lower middle division of the New-York system. Natural History of New York, New York, D. Appleton & Co. and Wiley & Putnam; Boston, Gould, Kendall, & Lincoln, v. 6, 362 p.

_____. 1860. Observations upon a new genus of Crinoidea. *Cheirocrinus*, In Appendix F. Contributions to Palaeontology, 1858 & 1859. Thirteenth Annual Report of the Regents of the University of the State of New York, on the Condition of the State Cabinet of Natural History, and the Historical and Antiquarian Collection Annexed thereto, State of New York in Senate Document 89: 121–124.

HARVEY, E. W., and W. I. AUSICH. 1997. Phylogeny of calceocrinid crinoids (Paleozoic. Echinodermata). biogeography and mosaic evolution. Journal of Paleontology, 71: 299–305.

HESS, H. 1999. Lower Jurassic Posidonia Shale of southern Germany. In H. Hess, W. I. Ausich, C. E. Brett, and M. J. Simms (eds.), Fossil Crinoids. Cambridge University Press, Cambridge, p. 183–196.

JAEKEL, O. 1918. Phylogenie und System der Pelmatozoen. Paläeontologische Zeitschrift, 3: 1–128.

KAMMER, T. W. 1984. Crinoids from the New Providence Shale Member of the Borden Formation (Mississippian) in Kentucky and Indiana. Journal of Paleontology, 58: 115–130.

_____, T. K. BAUMILLER, and W. I. AUSICH. 1997. Species longevity as a function of niche breadth: Evidence from fossil crinoids. Geology, 25: 219–222.

KESLING, R. V., and J. P. SIGLER. 1969. *Cunctocrinus*, a new Middle Devonian calceocrinid crinoid from the Silica Shale of Ohio. University of Michigan Contributions from Museum of Paleontology, 22: 339–360.

LAMARCK, J. B. P. A. DE m. DE. 1801, Système des animaux sans vertèvres. Published by the Author, Paris. 568 pp.

LANE, N. G., and D. B. MACURDA, JR. 1975. New evidence for muscular articulations in Paleozoic crinoids. Paleobiology, 1: 59–62.

MACURDA, JR., D. B., and D. L. MEYER. 1975. The microstructure of the crinoid endoskeleton. The University of Kansas Paleontological Contributions, 74, 22 pp.

_____., D. L. MEYER, and M. ROUX. 1978. The crinoid stereom. In R. C. Moore and C. Teichert (eds.), Treatise on Invertebrate Paleontology, Part T, Echinodermata 2, Volume1: The Geological Society of America and University of Kansas, Boulder, Colorado and Lawrence, Kansas, T217–T228.

MEEK, F. B., AND A. H. WORTHEN. 1869. Descriptions of new Crinoidea and Echinoidea from the Carboniferous rocks of the western states, with a note on the genus *Onychaster*. Proceedings of the Academy of Natural Sciences of Philadelphia, 21: 67–83.

MESSING, C. G. 1985. Submersible observations on deep-water crinoid assemblages in the tropical western Atlantic Ocean. In B. F. Keegan and B. D. S. O'Connor (eds.), Echinodermata: Proceedings of the Fifth Echinoderm Conference, Galway. A. A. Balkema, Rotterdam, 184–193.

_____. 1994. Comatulid crinoids (Echinodermata) of Madang, Papua New Guinea, and environs: Diversity and ecology. In B. David, A. Guille, J.-P. Feral, and M. Roux, (eds.) Echinoderms through Time: Proceedings of the Eighth International Echinoderm Conference, Dijon, France, 6–10 September 1993. A. A. Balkema, Rotterdam, 237–243.

_____. 1997. Living Comatulids. In J. Waters and C. Maples (eds.) Geobiology of Echinoderms. Paleontological Society Papers, 3. Carnegie Museum of Natural History, Pittsburgh, p. 3–30.

_____, D. L. MEYER, U. SIEBECK, L. S. JERMIIN, D. I. VANEY, and G. W. ROUSE. 2006. A modern, soft-bottom, shallow-water tropical crinoid fauna (Echinodermata) from the Great Barrier Reef. Coral Reefs, 25: 164–168. [https://doi.org/10.1007/s00338-005-0076-3].

_____, W. I. AUSICH, and D. L. MEYER. 2021. Feeding and arm postures in living and fossil crinoids Treatise on Invertebrate Paleontology Part T, Echinodermata 2, Vol. 1 Revised, Chapter 16. In Paul Seldon, and W. I. Ausich (eds.) and W. I. Ausich (Coordinating Author), *Treatise Online*, 150, 47 pp.

MEYER, D. L., 1973. Feeding behavior and ecology of shallow-water unstalked crinoids (Echinodermata) in the Caribbean Sea. Marine Biology, 22: 105–129.

_____, 1979. Length and spacing of the tube feet in crinoids (Echinodermata) and their role in suspension-feeding. Marine Biology, 51: 361–369.

_____, and D. B. MACURDA, JR. 1977. Adaptive radiation of the comatulid crinoids. Paleobiology, 3: 74–82.

MOORE, R. C. 1962. Revision of Calceocrinidae. University of Kansas Paleontological Contributions, Echinodermata Article 4: 1–40.

_____, and F. B. PLUMMER. 1940. Crinoids from the Upper Carboniferous and Permian strata in Texas. University of Texas Publication, 3945, 468 pp.

MOTOKAWA, T. 1984. Connective tissue catch in echinoderm. Biological Reviews, 59: 255–270.

_____. 1985. Catch connective tissue: the connective tissue with adjustable mechanical properties. In B. F. Keegan, and B. D. S. O'Connor (eds.), Proceedings of the 5th International Echinoderm Conference, Galway, Ireland. A. A. Balkema, Rotterdam, 69–74.

_____. 1988. Catch connective tissue: a key character for echinoderms' success. In R. D. Burke, P. V. Mladenov, P. L., and R. L. Parsley (eds.), Echinoderm Biology, A. A. Balkema, Rotterdam, 39–54.

_____., O. SHINTANI, and R. BIRENHEIDE. 2004. Contraction and stiffness changes in collagenous arm ligaments of the stalked crinoid *Metacrinus rotundus* (Echinodermata). Biological Bulletin, 206: 4–12.

ORBIGNY, A. D. d'. 1837. Mémoire sur une seconde espèce vivante de la famille des Crinoïdes ou Encrines, servant de type au nouveau genre Holope (*Holopus*). Magasin de Zoologie, (7èmé annéa), 10: 1–8.

OWEN, D. D., and B. F. SHUMARD. 1852. Descriptions of seven new species of crinoidea from the subcarboniferous of Iowa and Illinois. Journal of the Academy of Natural Sciences of Philadelphia, ser. 2, 2: 89–94.

RAMSBOTTOM, W. H. C. 1952. Calceocrinidae from the Wenlock Limestone of Dudley. Bulletin Geological Survey Great Britain, 4: 33–48.

RHODES, D. C., and L. F. BOYER. 1982. The effects of marine benthos on physical properties of sediments: a succession perspective. In P. L. McCall, and M. J. S. Tevesz (eds.) Animal-Sediment Relations. Plenum, New York, 3-52.

RIBIERO A. R., A. BARBAGLIO, C. D. BENEDETTO, C. C. RIBERIO, I. C. WILKIE, M. D. C. CARNEVALI, and M. A. BARBOSA. 2011. New insights into mutable collagenous tissue: correlations between the microstructure and mechanical state of a sea-urchin ligament. PloS One, 6(9): e24822.

RIDDLE, S. W., J. I. WULFF, and W. I. AUSICH. 1988. Biomechanics and stereomic microstructure of the *Gilbertsocrinus tuberosus* column. In R. D. Burke, and others (eds.), Echinoderm Biology, Proceedings 6th International Echinoderm Conference, Victoria. Rotterdam, A. A. Balkema, Rotterdam, p. 641–648.

RINGUEBERG, E. N. S. 1889. The Crinoidea of the lower Niagara Limestone at Lockport, N. Y., with new species. Annals of the New York Academy of Science, 5: 301–306.

ROUX, M. 1970. Introduction à l'étude des microstructures des tiges de crinoïdes. Géobios, 3: 79–98.

_____. 1971. Recherches sur las microstructure des pédonculés de crinoïdes post-paléozoïques. Travaux du Laboratoire de Paléontologie, University of Paris, Faculte Science d'Orsay, 83 pp.

_____. 1974. Observations au microscope électronique à balayage de quelques articulations entre les ossicules du squelette des crinoïdes pédonculés actuels (Bathycrinidae et Isocrinidae). Travaux du Laboratoire de Paléontologie, University of Paris, Faculte Science d'Orsay, 11 pp.

_____. 1975. Microstructural analysis of the crinoid stem. The University of Kansas Paleontological Contributions, 75, 11 pp.

SCHMIDT, W. E. 1934. Die Crinoideen des Rheinischen Devons, I. Teil; Die Crinoideen des Hunsrückschiefers. Abhandlung der Preussischen Geologischen Landesanstalt, 163: 1–149.

SMITH, A. B. 1980. Stereom microstructure of the echinoid test. Special Papers in Palaeontology, 25: 81 p.

SPRINGER, F. 1926. American Silurian Crinoids. Smithsonian Institution Publication, 2872, 1–239.

STEVENS, T. F. 1989. Species composition and distribution of the comatulid crinoids of Heron Island and Wistari Reefs. M.S. Thesis, University of Queensland, Queensland. 185 pp.

_____and R. M. CONNOLLY. 2003. Shallow water crinoids are on soft sediments too: evidence from a video survey of a subtropical estuary. Bulletin of Marine Science, 73: 593–604.

STRIMPLE, H. L. 1972. Porosity of a fossil crinoid ossicle. Journal of Paleontology, 46: 920–921.

THOMKA, J. R., and H. K. SMITH. 2019. Stereomic microstructure of crinoid spine regeneration: Examples from the Upper Pennsylvanian of eastern Ohio. Geological Society of America Abstracts with Programs, 51(5). [doi: 10.1130/abs/2019AM-341326]

ULRICH, E. O. 1886. Remarks upon the names *Cheirocrinus* and *Calceocrinus*, with descriptions of three new generic terms and one new species. Minnesota Geology and Natural History Survey, Annual Report 14: 104–113.

WALKER, K. R., and R. K. BAMBACH. 1974. Feeding by benthic invertebrates: Classification and terminology for paleoecological analysis. Lethaia, 7: 67–78.

WILKIE, I. C. 1983. Nervously mediated change in the mechanical properties of cirral ligaments of a crinoid. Marine Behavioral Physiology, 9: 229–248.

_____. 1984. Variable tensility in echinoderm collagenous tissues: a review. Marine Behavioral Physiology, 11: 1–34..

_____. 1996. Mutable collagenous tissue: extracellular matrix

as mechano-effector. In M. Jangoux and J. M. Lawrence (eds.), Echinoderm Studies, 5. A. A. Balkema, Rotterdam, 61–102.

_____. 2005. Mutable collagenous tissue: Overview and biotechnological perspective. In V. Matranga (ed.), Echinodermata. Progress in Molecular and Submolecular Biology 39 Subseries, Marine Molecular Biotechnology. Springer Verlag, Berlin, 219–248.

_____, and R. H. EMSON, 1988. Mutable collagenous tissues and their significance for echinoderm palaeontology and phylogeny. In C. R. C. Paul, and A. B. Smith (eds.), Echinoderm Phylogeny and Evolutionary Biology. Oxford University Press, Oxford, 331–330.

_____, M. D. CANDIA CARNEVALI, and F BONASORO. 1992. The compass depressors of *Paracentrotus lividus* (Echinodermata, Echinoidea): ultrastructural and mechanical aspects of their variable tensility and contractility. Zoomorphology, 112: 143–153.

_____, R. H. EMSON, and C. M. YOUNG. 1993. Smart collagen in sea lilies. Nature, 366: 519–520.

_____, R. H. EMSON, and C. M. YOUNG. 1994. Variable tensility of the ligaments in the stalk of a sea-lily. Comparative Biochemistry and Physiology A, 109: 633–641.

_____, M. SUGNI, H. S. GUPTA, M. D. CANDIA CARNEVALI, and M. R. ELPHICK. 2021. The mutable collagenous tissue of echinoderms: From biology to biomedical applications. In H. S. Azevedo, J. F. Mano, and J. Borges (eds.), Soft Matter for Biomedical Applications. Royal Academy of Chemistry, 3–33.

WÖHRMANN, S. von. 1889. Die Fauna der sogenannten Cardita- und Raibler-Schichten in den Nordtiroler und den bayerischen Alpen. Jahrbuch der Geologischen Reichsanstalt, 9: 181–258.

Museum of Paleontology, The University of Michigan
1105 North University Avenue, Ann Arbor, Michigan 48109-1085
Matt Friedman, Director

Contributions from the Museum of Paleontology, University of Michigan is a medium for publication of reports based chiefly on museum collections and field research sponsored by the museum. Jennifer Bauer and William Ausich, Guest Editors;
Jeffrey Wilson Mantilla, Editor.

Publications of the Museum of Paleontology are accessible online at: http://deepblue.lib.umich.edu/handle/2027.42/41251

Print (ISSN 0097-3556), Online (ISSN 2771-2192)

Contributions

from the Museum of Paleontology, University of Michigan

VOL. 34, NO. 9, PP. 123–140 MAY XX, 2022

MORPHOLOGICAL DYNAMICS AND RESPONSE FOLLOWING THE DISPERSAL OF ORDOVICIAN–SILURIAN DIPLOPORAN ECHINODERMS TO LAURENTIA

BY

SARAH L. SHEFFIELD[1], ADRIANE R. LAM[2], STEPHEN F. PHILLIPS[3], AND BRADLEY DELINE[3]

Abstract — The Late Ordovician Mass Extinction (LOME) left vacated niche space and brought about significant changes in echinoderm community structures across Laurentia. New echinoderm communities, having migrated into Laurentia from Baltica, did not fully establish themselves until the middle Silurian. However, the details of the evolutionary dynamics of non-crinoid echinoderms across the Ordovician–Silurian boundary is understudied. Herein, we examine the evolutionary dynamics of a clade of extinct echinoderms, the sphaeronitid diploporans. Using a combination of phylogenetic, morphologic, and biogeographic data, we analyze how sphaeronitids evolved and dispersed across the LOME and filled unoccupied niches during the Silurian in Laurentia. Analyses indicate that one dispersal event occurred from Baltica into Laurentia, during the Middle to Late Ordovician, leading to the enigmatic and well-known *Holocystites* Fauna populating central North America. As the holocystitids filled the unoccupied niches from the LOME, there was no significant expansion of morphological forms, which could be related to the narrow, previously established niches that crinoids vacated during the LOME, or possibly due to developmental constraints within the clade. Although morphological change is constrained during this event, there are some significant changes in community structure (i.e., certain species of diploporans became unusually abundant) and body size (i.e., Laurentian specimens approximately doubled in size compared to Baltic taxa). These changes indicate the importance of competitive release and dispersal events in understanding evolutionary dynamics of fossil taxa.

INTRODUCTION

The faunal composition of filter-feeding echinoderms experienced a dramatic shift across the Late Ordovician Mass Extinction. In crinoids, the fossil record shows a transition from the Ordovician early Paleozoic Crinoid Evolutionary Fauna to the Silurian–middle Mississippian middle Paleozoic Crinoid Evolutionary Fauna (Ausich et al., 1994; Baumiller, 1994; Ausich and Deline, 2012; Deline et al., 2012). This change included crinoid communities being dominated by

[1]School of Geosciences, University of South Florida, NES 107, 4202 E. Fowler Avenue, Tampa, FL, 33620, U.S.A. (ssheffield2@usf.edu).
[2]Department of Geological Sciences and Environmental Studies, Binghamton University SUNY, 165A Science 1, P.O. Box 6000, Binghamton, NY 13902, U.S.A. (alam@binghamton.edu)
[3]Department of Natural Sciences, University of West Georgia, 1601 Maples Street, Carrollton, GA, 30118, U.S.A. (Sfphillips.32@gmail.com; bdeline@westga..edu)

diplobathrid camerate, disparid, and hybocrinid crinoids to communities more dominated by monobathrid camerate, cladid, and flexible crinoids. Crinoids are dominant in Paleozoic echinoderm faunas in terms of abundance and diversity, such that their dynamics are more intensely studied. Whether a similar faunal turnover occurred within blastozoan echinoderms is largely unstudied as are the ramifications of changes in crinoid faunal structures on blastozoan communities.

Although this fundamental shift in echinoderm communities has been largely documented within crinoids, similar patterns in other filter-feeding echinoderms also occurred. These echinoderms were clearly responding to large climatic perturbations throughout the Late Ordovician–Silurian through changes in their biogeographic range, morphological disparity, and community presence. The ability to understand these evolutionary patterns in non-crinoid echinoderms has been negatively influenced by a lack of phylogenetic trees upon which to test hypotheses. In blastozoan echinoderms especially, many of the studies that have preliminarily explored global patterns (e.g., Lefebvre, 2007; Nardin and Lefebvre, 2010; Lefebvre et al., 2013; Zamora et al., 2013), such as responses to global climate changes or biogeography, treated many groups of echinoderms as monophyletic due to an absence of published phylogenetic hypotheses on these taxa. Many of these studies noted the likely non-monophyletic nature of these groups (e.g., Lefebvre et al., 2013). Such is the case with Diploporita (blastozoans with double pore respiratory structures). Many have previously hypothesized that Diploporita is polyphyletic (Paul, 1988; Sumrall, 1997; Lefebvre et al., 2013). A phylogenetic study demonstrated that this group is polyphyletic using quantitative-based methods and therefore, previous understandings of evolutionary patterns must be reassessed in light of this new information (Sheffield and Sumrall, 2019a).

Early echinoderms are excellent models for testing hypotheses of faunal responses to global climatic patterns, as these echinoderms encompass highly complex body morphologies that are disparate across different groups (Deline et al., 2020) and have been shown to be responsive to changing long-term oceanic and climatic patterns (Lefebvre and Fatka, 2003; Clausen, 2004; Dickson, 2002, 2004; Zamora and Smith, 2008; Rahman and Zamora, 2009; Sumrall et al., 2015; Lam et al., 2021). The early Paleozoic is also an excellent time in Earth's history for testing these hypotheses, specifically as the Ordovician and Silurian systems encompass great changes in climatic regimes and biotic interactions (e.g., Jeppson, 1990, 1997; Trotter et al., 2006; Finnegan et al., 2011; Albanesi et al., 2019; Stigall et al., 2019).

Major biodiversity and climatic events across the Ordovician to Silurian, combined with robust phylogenetic hypotheses, allow for the examination of interactions between evolutionary dynamics and external factors for echinoderm groups. This study focuses on an enigmatic group of Paleozoic echinoderms, the sphaeronitid diploporans, a clade of diplopore-bearing taxa. This group was biogeographically limited during the Ordovician but exploded in abundance during the Silurian in Laurentia, which was likely a response to both dispersal events and ecological opportunity following the Late Ordovician extinction and the reconfiguration of echinoderm filter feeding niches. This transition allows for the direct testing, using statistically-informed biogeographic and phylomorphospace methods, of the morphological response to competitive release, ecological opportunity, and dispersal that led to the establishment of the iconic diploporan holocystitid fauna.

BACKGROUND

The Ordovician and Silurian Earth Systems

The Ordovician system was a period of major climatic shifts, beginning with relatively high sea levels and warmer temperatures in the Early Ordovician, with shorter intervals of cooler climates and sea level falls (e.g., Trotter et al., 2008; Albanesi et al., 2019). Into the later Ordovician, a transition from greenhouse-dominated climates to an icehouse occurred, a shift that began in the Floian and grew in intensity into the Late Ordovician (Trotter et al., 2008). These events culminated in the Late Ordovician Mass Extinction (LOME), which was a two-pulsed extinction event. The first pulse, marking the Katian and Hirnantian boundary, has been closely linked to the transition to an icehouse climate and the rapid growth of continental ice sheets on Gondwana (Finnegan et al., 2011), with continental configuration likely playing a role in extinction intensity during this first extinction pulse (Saupe et al., 2020). The second event of the LOME, occurring in the later part of the Hirnantian, is linked to the sudden warming of the oceans and subsequent receding glaciers, which may have caused occurrences of ocean anoxia (Brenchley et al., 1994; Sheehan, 2001; Melchin et al., 2013). How echinoderms responded to these events is uncertain, as the glaciation and subsequent global lowstand that extended from the Late Ordovician throughout the early Silurian, was not conducive to fossil preservation (Smith, 1988; Vennin et al., 1998; Peters and Ausich, 2008).

The Silurian was also characterized by biotic events (e.g., the Ireviken, Mulde, and Lau events; Jeppson, 1990, 1997, 1998; Aldridge et al., 1993; Štorch, 1995), swings in the carbon cycle, temperature oscillations, and second- to third-order sea level changes as a result of tectonic activity (Loydell, 1998; Johnson, 2006, 2010; Haq and Schutter, 2008; Trotter et al., 2016). Such sea level changes led to large disconformities, contemporaneous within the stratigraphic records of Laurentia, Baltica, and Gondwana (Cramer and Saltzman, 2005). Namely, a large disconformity near the Llandovery-Wenlock boundary indicates that the extensive Late Ordovician glaciation continued into the Silurian (Grahn and Caputo, 1992; Finnegan et al., 2011); direct stratigraphic evidence of this glaciation in the Silurian can be found in the Soom Shale, where a record dated to the Hirnantian-Llandovery transition preserves glacial indicators (Gabbott et al., 2010; Gabbott et al., 2017; Vandenbroucke et al., 2009). Such disconformities from the glaciation and lowered

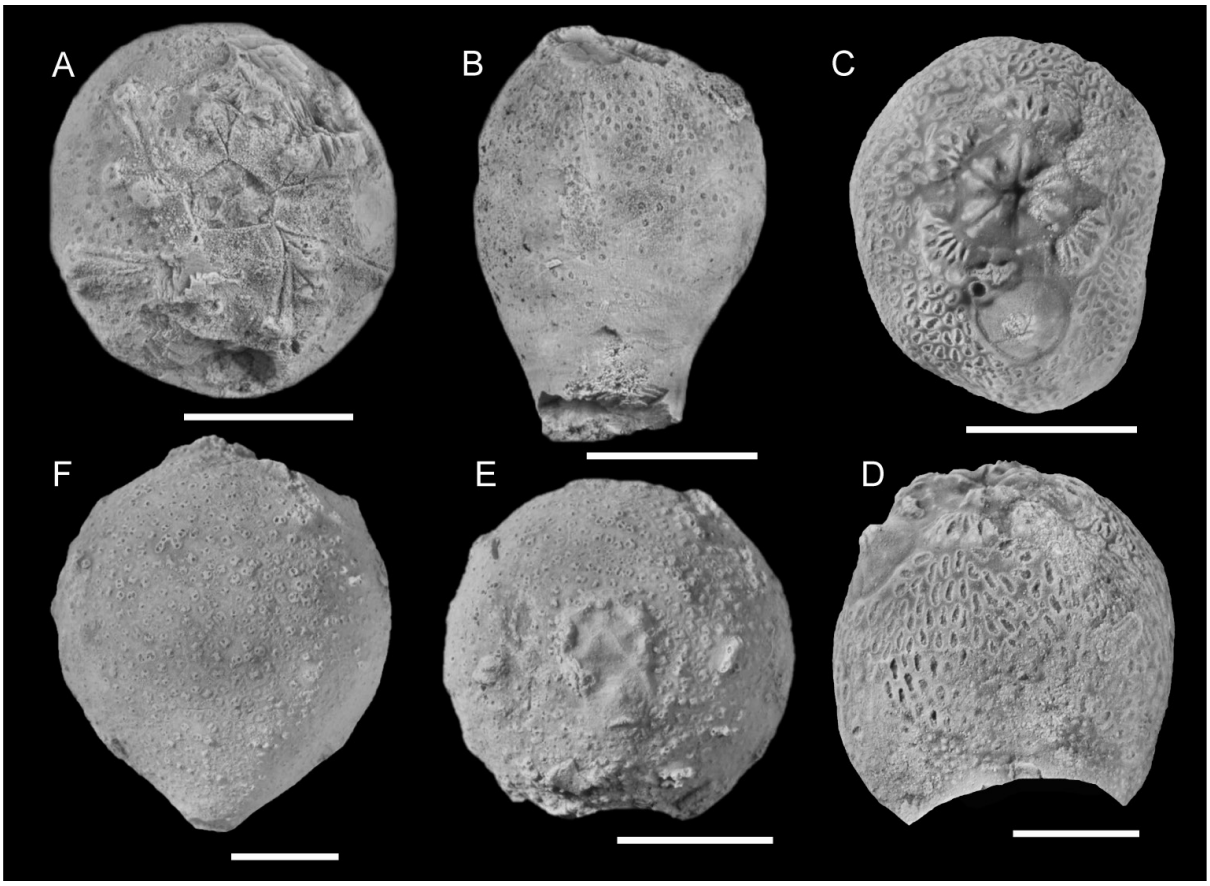

FIGURE 1 — Representative diploporan taxa from Baltica. **A**, Oral view of *Eucystis angelini* (NM-L7695). **B,** Side view of *Eucystis angelini* (NM-L7694). **C**, Oral view of *Haplosphaeronis*. (GIT 540-3). **D,** Side view of *Haplosphaeronis*. (GIT 540-3). **E**, Oral view of *Sphaeronites rossicum globosus* (GIT 540-54). **F**, Side view of *Sphaeronites rossicum globosus* (GIT 540-54). A, B, C, D modified from Sheffield and Sumrall, 2019a. Specimens whitened with ammonium chloride sublimated. Scale bars = 0.5 cm.

sea levels have made the evolutionary history of diploporan echinoderms, as well as their paleobiogeographic patterns through the early Paleozoic, extremely difficult to infer.

Sphaeronitid Diploporans and the *Holocystites* Fauna

Diploporan blastozoans encompass broad morphological diversity and disparity (Paul, 1988; Sheffield and Sumrall, 2019a; Deline et al., 2020). Phylogenetic analyses (Sheffield and Sumrall, 2019a, 2019b) showed that Diploporita is a polyphyletic group, and because of that, analyses of evolutionary patterns cannot rely on treating Diploporita as a monophyletic entity (Lam et al., 2021). Of the traditional groups named within Diploporita, only one has been recovered as a clade, the Sphaeronitida (Paul, 1988; Sheffield and Sumrall, 2019a), the clade of focus in this study (Figs. 1, 2). The sphaeronitids are united by several synapomorphic traits; namely, short ambulacral grooves that are restricted to the oral area, and a lack of floor plating associated with the ambulacral grooves (Sheffield and Sumrall, 2019a). Within the sphaeronitids, there are two smaller clades. The first clade comprises diploporans that have branching ambulacral grooves each ending in single brachiole facets (e.g., *Eucystis* (Figs. 1A–B), *Haplosphaeronis* (Figs. 1C–D), and *Sphaeronites* (Figs. 1E–F)), and the second comprises diploporans that have unbranching ambulacra ending in a single, terminal brachiole facet (e.g., *Pentacystis* (Figs. 2A–B), *Trematocystis* (Figs. 2C–D), *Holocystites* (Figs. 2E–F), and *Paulicystis* (Figs. 2G–H)).

Diploporans are first known from Lower Ordovician rocks and reached relatively high species diversity throughout the Ordovician (Lefebvre et al., 2013; Sheffield and Sumrall, 2019a). While these species reached a global distribution, there were few Ordovician occurrences of diploporans in Laurentia, with some exceptions such as *Eumorphocystis* of the Bromide Fauna (Branson and Peck, 1940; Sprinkle, 1980) and some more recent finds from the Late Ordovician, such as a diploporan from Anticosti Island (Sheffield et al., 2017). The majority of diploporan taxa did not survive across the LOME, but of those taxa that did survive, they primarily belonged to

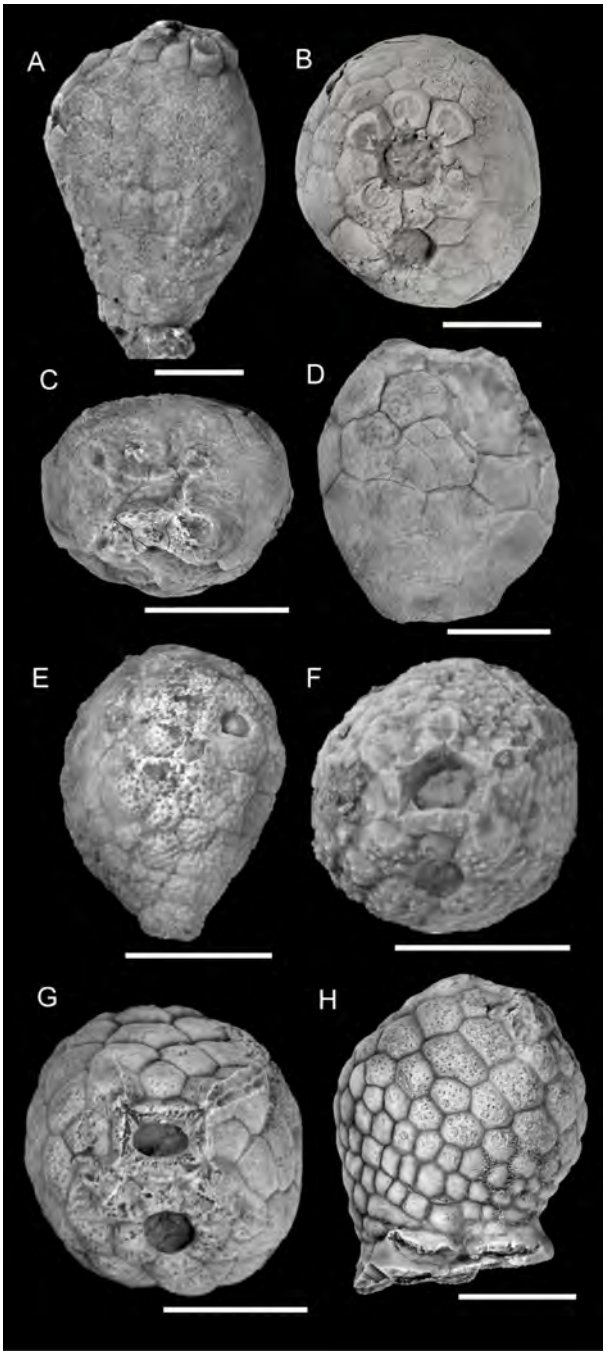

FIGURE 2 — Representative diploporan taxa from Laurentia. **A**, Side view of *Pentacystis gibsoni* (SUI 46316). **B**, Oral view of *Pentacystis gibsoni* (SUI 46316). **C**, Oral view of *Trematocystis magniporatus* (SUI 48198). **D**, Side view of *Trematocystis magniporatus* (SUI 48198). **E**, Side view of *Holocystites scutellatus* (SUI 48183). **F**, Oral view of *Holocystites scutellatus* (SUI 48183). **G**, Oral view of *Paulicystis sparsus* (SUI 48164). **H**, Side view of *Paulicystis sparsus* (SUI 48164). All modified from Sheffield and Sumrall, 2017. Specimens whitened with ammonium chloride sublimated. Scale bars = 1 cm.

the sphaeronitid clade. Similar to their taxonomic contraction, diploporans also saw a reduction in their biogeographic range and were less common globally, but they did become far more common in Laurentian strata. Sphaeronitids proliferated across central North America in the Silurian (Fig. 2), predominantly as a group informally known as the *Holocystites* Fauna (Paul, 1971; Frest et al., 2011; Sheffield and Sumrall, 2017).

The *Holocystites* Fauna is an enigmatic group that has been the focus of great scientific discussion due to their taphonomic patterns, evolutionary relationships, and their biogeographic history (Paul, 1971; Frest et al., 2011; Thomka et al., 2016; Sheffield and Sumrall, 2017, 2019a; Lam et al., 2021). Holocystitids are morphologically distinct from other diploporans and even other sphaeronitids, with a specialized type of respiratory structure (calcified, buried dipore structures called humatipores, as opposed to non-calcified, surficial diplopores), unusually large brachiole facets, a holdfast as opposed to a stem, and an enlarged mouth (Sheffield and Sumrall, 2019a). The *Holocystites* Fauna is also iconic for the sheer numbers in which they are found. Unlike the majority of other diploporan species, these holocystitids are ubiquitous in middle Silurian echinoderm deposits, with an extremely high number of fossilized specimens. Until recently, it was thought that the group existed exclusively within the middle Silurian, until a Late Ordovician representative was found (Sheffield et al., 2017).

Crinoid Faunal Dynamics Across the Ordovician–Silurian

Early Paleozoic echinoderms showed a steady morphological expansion away from the forms found in the Cambrian (Deline et al., 2020). Subsequent extinctions of transitional forms and increased stereotypy within body plans established fairly discrete and distinctive clusters by the Middle Ordovician. However, an increase in convergent evolution and continual evolutionary flexibility dampened the distinctiveness of higher order taxonomic body plans during the Late Ordovician (Deline et al., 2020). This pattern through the early Paleozoic resulted in the sustained ability within echinoderms for taxonomic, morphologic, and ecological turnover events.

These ecological turnover events have been most explored within crinoids, which experienced a dramatic shift throughout the Ordovician, including the LOME, which is known as the transition from the early to the middle Paleozoic Crinoid Evolutionary Faunas (Ausich et al., 1994; Ausich and Deline, 2012; Cole and Wright, 2021). During the LOME crinoid communities changed from being dominated by diplobathrid camerate, disparid, and hybocrinid crinoids to those dominated by monobathrid camerate, cladid, and flexible crinoids. Crinoid ecology and niche occupation are often closely tied to broad taxonomy (e.g., subclass), such that the transition between crinoid evolutionary faunas can be seen as an ecologic as well as a taxonomic event (Kammer and Ausich, 1987; Cole et al., 2019; also see Wright et al., 2017 for detailed analysis of Paleozoic crinoid systematics). These ecological differences

can also appear at lower taxonomic levels (e.g., family); in particular, lower tier crinoids with simple, unbranching, stout arms either went extinct (Porocrinidae) or suffered higher extinction rates (Hybocrinidae) during the transition between crinoid evolutionary faunas (Ausich and Deline, 2012). The ecological effect of the loss of this crinoid body plan (simple, unbranching, stout arms) was exaggerated with a significant reduction in blastozoan diversity into the Silurian (Nardin and Lefebvre, 2010). This transition likely left open niche space within the fairly structured filter-feeder community, thus enabling the establishment of broad-armed lower-tiered blastozoans such as sphaeronitid diploporitans.

INSTITUTIONAL ABBREVIATION

All taxa studied for this analysis are listed in Table 1. The specimens examined were largely limited to type specimens to ensure that the specimen data corresponded to the named species within the analyses. All specimens are housed in research collections from the following museums or institutions:

CMCIP	—	Cincinnati Museum Center, Cincinnati, Ohio, United States of America.
FMNH/UC	—	Field Museum of Natural History, Chicago, Illinois, United States of America.
GIT	—	Geological Institute of Tallinn, Tallinn, Estonia.
GSC	—	Geological Survey of Canada, Ottawa, Canada.
SUI	—	The University of Iowa, Iowa City, Iowa, United States of America.

METHODS

Time Calibrated Phylogenetic Hypothesis

We used a phylogenetic hypothesis of blastozoan echinoderms published in Sheffield and Sumrall (2019a), which tested the hypothesis that Diploporita was not a monophyletic group. Sheffield and Sumrall (2019a) chose representative species for each genus used in the analysis (with one exception where more than one species per genus was included, *Holocystites*). In Lam et al. (2021), this same phylogenetic hypothesis was used to determine biogeographic pathways of the taxa used in the study. Stratigraphic and geographic occurrence data for species in the phylogeny was collected from published literature searches and paleontological databases (i.e., The Paleobiology Database, FossilID.info), and stratigraphic occurrence information was updated to the Geologic Time Scale 2016 ages (Ogg et al., 2016) using graptolite and conodont zones to time calibrate the phylogeny. For further details on the time-calibrated phylogenetic tree, please refer to Lam et al. (2021).

For this analysis, we were most interested in the sphaeronitids' evolutionary adaptations in terms of disparity and biogeography. Therefore, we culled non-sphaeronitid taxa from the phylogenetic analysis in Sheffield and Sumrall (2019a), leaving members of the sphaeronitid clade. It should be noted that one of the taxa used in this analysis was not identical to that in Sheffield and Sumrall (2019a); we used *Haplosphaeronis* sp. instead of *Haplosphaeronis oblonga*. This substitution was necessary, as non-compacted and relatively taphonomically complete specimens were central to performing the morphological analyses discussed below. The tree in Sheffield and Sumrall (2019a) uses a singular species of *Eucystis, E. angelini*. In the current study, we also included *E. quadrangularis* in the analyses given the morphological differences between species (i.e., differing in the number of ambulacra; *E. quadrangularis* exhibits a reduction of ambulacra from five to four). However, we are confident that both of these species clearly represent *Eucystis*, as they share the same eucystitid traits (e.g., *E. quadrangularis* also bears a 36˚ rotation of the ambulacral grooves such that the grooves lie on the center of the oral plates, as opposed to along the sutures, a feature of eucystitids, as well as short, branched ambulacra that each end in single brachiole facets that do not extend past the oral summit (Sumrall, 2017; Sheffield and Sumrall, 2019a).

Geographic Framework

To infer biogeographic patterns of sphaeronitid echinoderms, we used the same basins from the BioGeoBEARS analysis of Lam et al. (2021: https://doi.org/10.5061/dryad.4tmpg4f6j). From the aforementioned study, eight areas were defined: Baltica, Gondwana, and six basins within Laurentia (Southern Appalachian Basin, Northern Appalachian Basin, Cincinnati Basin, Southern Laurentia, North of the Transcontinental Arch, and Western Midcontinent; Figs. 3, 4). The R package BioGeoBEARS (Matzke, 2013) uses a common likelihood framework to implement three programs and their key assumptions in biogeography: the dispersal-extinction-cladogenesis (DEC) of Lagrange (Ree and Smith, 2008), dispersal-vicariance-analysis (DIVA; Ronquist, 1997), and BayArea (Landis et al., 2013). Within BioGeoBEARS, DIVA and BayArea were converted into a likelihood framework, so they are referred to as DIVALIKE and BAYAREALIKE. Each of the three models allows for dispersal or range expansion, and range loss or extirpation, which are modeled within the program through the parameters *d* and *e*, respectively. Each model within the program includes a *+j* parameter, which models the relative probability of founder-event speciation, more commonly termed 'jump dispersal', during cladogenesis (Matzke, 2014).

From the Lam et al. (2021) study, BioGeoBEARS results indicated the best-fit model for the blastozoan phylogeny was DIVALIKE+*j*. In all cases within the original analysis, the addition of the *+j* parameter improved model fit. This

TABLE 1 — Diploporan taxa included in the current study.

Genus	Species	Number of Specimens	Period	Stage	Locality	Basin
Aristocystites	*bohemicus*‡	NA	Ordovician	Darriwilian to Katian	Morocco; Prague Basin, Czech Republic	Gondwana
Eucystis	*angelini*	1	Ordovician	Katian	Pskov District, Russia	Baltica
Eucystis	*quadrangularis**	1	Ordovician	Katian	Pskov District, Russia	Baltica
Haplosphaeronis	*oblonga*	1	Ordovician	Katian	Põlva County, Estonia	Baltica
Sphaeronites	*rossicum*	2	Ordovician	Sandbian	Pskov District, Russia	Baltica
Pentacystis	*gibsoni*	3	Silurian	Homerian	Indiana, USA	Cincinnati
Holocystites	*cylindricus*‡	NA	Silurian	Wenlock	Indiana, USA; Tennessee, USA; Illinois, USA	Cincinnati; Southern Appalachian
Holocystites	*salmoensis*	1	Ordovician	Hirnantian	Anticosti Island, Canada	Southern Laurentia
Holocystites	*scutellatus*	7	Silurian	Homerian	Indiana, USA; Tennessee, USA; Illinois, USA	Cincinnati; Southern Appalachian
Trematocystis	*magniporatus*	2	Silurian	Homerian	Indiana, USA	Cincinnati
Triamara	*ventricosa*‡	NA	Silurian	Wenlock	Indiana, USA; Tennessee, USA	Cincinnati; Southern Appalachian
Tristomiacystis	*globosus*‡	NA	Devonian	Givetian	Kentucky, USA	Cincinnati
Paulicystis	*densus*	4	Silurian	Homerian	Indiana, USA	Cincinnati
Pustulocystis	*pentax*‡	NA	Silurian	Wenlock	Tennessee, USA	Southern Appalachian

* Taxa included in the morphospace study only, not the biogeographic analysis
‡ Taxa included in this study but not the focus of the morphospace nor biogeographic analyses
NA= Not applicable

finding indicated that within-area speciation (sympatry) and range expansion (anagenetic dispersal) were not sufficient enough to explain the biogeographic patterns within the phylogeny, a finding that was also discovered for early Paleozoic brachiopods, trilobites, and other echinoderm groups (Lam and Stigall, 2015; Lam et al., 2018; Congreve et al., 2019; Bauer, 2021). Importantly, Lam et al. (2021) did not focus on reconstructed Silurian dispersal patterns from

TABLE 2 — Properties of the character suites used to explore sphaeronitid morphological patterns. The modified character suite was constructed by combining and binning measurements into ratio and removing characters with over 30% missing data and characters that didn't vary within the specimens being examined. The culled character suite is identical to the modified suite but removing any characters with over 10% missing data.

Character suite	Number of characters	Binary	Multistate	Measurement/Ratio	% Missing	% Non-applicable
Original	145	70	22	53	15.16%	26.68%
Modified	52	29	6	17	7.42%	17.93%
Culled	37	23	4	9	1.62%	19.85%

their BioGeoBEARS analysis. In this study, we used the DIVALIKE+*j* model of Lam et al. (2021) to infer dispersal patterns for the sphaeronitids from the Middle to Late Ordovician and into the Silurian.

Morphological Patterns and Phylomorphospace

To explore morphological trends during this biogeographic transition within diploporans, we constructed a novel character suite (Table 2). The initial character suite was constructed to exhaustively characterize any aspect of morphology based on literature sources (e.g., Kesling, 1967) and museum specimens. The characters included direct measurements of features (e.g., length of particular ambulacra or height of the theca), binary characters (e.g., presence or absence of the A ambulacrum), or multistate characters (e.g., the number of brachiole facets on a particular ambulacra). The character suite focused on characters associated with the oral system given the consistency of plating in that region compared with the rest of the organism. We utilized the Universal Elemental Homology model in the characterization of the oral system (Sumrall and Waters, 2012; Kammer et al., 2013), which has been extensively applied to understanding diploporan morphology (Sheffield and Sumrall, 2015, 2017; Sheffield and Sumrall, 2019a, 2019b; Sumrall, 2017). A total of 22 specimens from 8 genera (10 species) were then coded using this dataset following the methods outlined in Deline and Ausich (2011). Supplementary File 1 contains the characters used for this analysis; Supplementary File 2 contains the specific codings for each taxon.

The resulting dataset was then culled to eliminate any characters that did not vary across the specimens analyzed (the exclusion of invariant characters had no effect on the resulting morphospace) or included significant proportions of missing data. Missing data is unavoidable and non-random with variably preserved specimens, which can result in distorting the observed morphological patterns (Lloyd, 2016; Gerber, 2019; Deline, 2021). Even though taphonomic effects of character loss has been shown to be minimal within blastozoan echinoderms related to number of morphological features that can be coded from disarticulated material (Deline and Thomka, 2017), we still eliminated characters with significant missing unpreserved data (i.e., characters with either 30% or 10% of the states coded as missing because of incomplete preservation). We utilized thresholds for eliminating characters given the clear and non-random distribution of missing data that results from taphonomic degradation. Finally, we transformed all of the direct measurements to ratios (e.g., length/width of the peristome) to eliminate effects of specimen size, which varies extensively across the dataset. The ratios were then broadly binned to easily compare to the binary or multistate characters. This process significantly reduced the overall size of the character suites (Table 2), but also significantly reduced the amount of missing data. Morphospaces were then built using Gower similarity (Gower, 1971) and principal coordinate analysis.

To explore changes in morphology within a phylogenetic context, we then constructed a phylomorphospace using the culled tree from Sheffield and Sumrall (2019a) and the morphological character suite. There are multiple techniques that have been used to reconstruct the positions of ancestral nodes, which can broadly be broken into pre- and post-ordination methods (Lloyd, 2018). Pre-ordination ancestral character reconstruction is based on the tree, tip data, and a model of evolution using maximum likelihood or Bayesian methods such as stochastic character mapping (Huelsenbeck et al., 2003). These methods often provide more accurate placement of ancestors within the resulting morphospace as well as additional quantitative information regarding phylogenetic signals and evolutionary rates (Lloyd, 2018). In addition, Bayesian methods provide posterior probabilities of ancestral character states to assess the degree of certainty. For the current study, we first employed stochastic character mapping analyses to reconstruct ancestral character states. However, because of the tree structure or the distribution of tip data many of the ancestral character states were poorly resolved (i.e., fairly equitable posterior probabilities for all character states), thus the modeled character states and the location of ancestral taxa within morphospace were unreliable. Therefore, we used post-ordination methods

to construct the phylomorphospace. This method uses a phylogenetic tree and positions of taxa within morphospace to estimate ancestral positions using maximum likelihood (Sidlauskas, 2008). This method forces ancestral positions to be limited to the space already explored by tip data; it places ancestral data into positions that may not reflect a realistic combination of characters and imposes a strong phylogenetic signal into the position of the ancestral nodes (Lloyd, 2018; Deline, 2021). However, these methods allow a visualization of morphological evolution that has been previously utilized to understand trends in echinoderm disparity (Hopkins and Smith, 2015; Wright, 2017); thus, these methods were applied herein. All of the morphological analyses were conducted in R version 4.1.0 (R Core Team, 2021) utilizing the cluster (Maechler, 2019), ape (Paradis et al., 2004), vegan (Oksanen et al. 2020), and phytools (Revell, 2012) packages.

RESULTS

Biogeographic Patterns of Sphaeronitids

Results and discussions surrounding interpretations of biogeographic patterns are limited to the sphaeronitids (see bolded taxa names, Fig. 3). Biogeographic dispersal patterns among the sphaeronitids were inferred by taking into account the geographic areas occupied by the descendants and ancestors; dispersal events and directions from the phylogeny (Fig. 3B) were inferred using most likely areas reconstructed using the DIVALIKE+*j* analysis (Fig. 3B; Lam et al., 2021). For example, we infer a dispersal event when a descendant occupies a different or additional area than its ancestor. This inference does not take into account rare or uncertain events and does not produce an estimate of uncertainty. However, as our goal is to generally reconstruct events among a small group of species, this approach is sufficient. Below, we summarize the dispersal events (no vicariance events were inferred) that took place within our focal taxa (Table 1).

Within the Middle to Late Ordovician (470.0–443.8 Ma), it is clear from reconstructed area relationships that *Sphaeronites rossicum*, *Haplosphaeronis oblonga*, and *Eucystis angelini* were a group restricted to Baltica (Fig. 3B), the probability of which is rather high, as seen in the ancestral node reconstructions (Fig. 3A). The shared ancestor between this group and the rest of the species likely resided in Baltica, with a descendant dispersing into Laurentia, specifically into the Cincinnati Basin (Figs. 3B, 4) and establishing a population there. During the Late Ordovician, ancestors of *Holocystites salmoensis* dispersed from the Cincinnati Basin eastward into Southern Laurentia. However, it should be noted that from the BioGeoBEARS analysis, there is also a high probability that ancestors of *H. salmoensis* may have resided in Southern Laurentia (Fig. 3A), in which case *H. salmoensis* would have evolved through sympatric speciation.

Dispersal patterns within the Silurian (443.8–419.2 Ma) are mainly restricted to within Laurentian basins (Figs. 3, 4). Specifically, five dispersal events occurred into the Appalachian Basin from the Cincinnati Basin (ancestors of *Holocystites cylindricus*, *Holocystites scutellus*, *Trematocystis magniporatus*, *Triamara ventricosa*, and *Pustulocystis pentax*), with two of these events taking place among the sphaeronitids (*H. scutellus* and *T. magniporatus*), indicating a strong connection between these basins through the Silurian.

Morphological Patterns of Sphaeronitids

The resulting morphospace shows notable phylogenetic and biogeographic structure with the Baltic specimens largely clustering negatively on the first and second axes (Fig. 5A). The primary axis (PCO1) captures differences in thecal plating, shape, and ornamentation, number of brachiole facets, ambulacral width, and the overall shape of the theca. The primary axis also strongly correlates with characters associated with oral side plates (extra plates inserted within the oral frame), which only occur within *Holocystites salmoensis* resulting in its outlier position. The second axis (PCO2) captures differences in the presence and features of the A ambulacra (e.g., curvature, width, and length), which is often developmentally lost within blastozoan echinoderms (Sumrall and Wray, 2007). The first two and five axes represent 34.65% and 62.6% of the eigenvectors, respectively. Within species or genera, morphological variability is minor (Fig. 5B) with most taxa covering limited and non-overlapping areas within morphospace. The only exception to this is the large range of morphologies shown between the two included species of *Eucystis* that differ with *E. quadrangularis* reducing the number of ambulacra (loss of A). Overall, the Baltic and Laurentian taxa cover comparable regions of morphospace as shown in similar sum of ranges and sum of variation measured across the first five axes (Table 3). In addition, the Baltic and Laurentian taxa occupy distinctive and adjacent, but non-overlapping areas of morphospace (NPMANOVA, first five axes, $p=0.001$).

To test how taphonomy and the missing data alter perceived morphological patterns, we further reduced the threshold for culling characters from 30% missing data to 10% (Table 2). This reduction in the number of characters (culling 15 characters reducing the overall character number by 29%) had little effect on the resulting morphospaces (Fig. 5C, D). The taphonomically culled dataset differs in two primary ways: first, *Pentacystis* and *Paulicystis* switch positions within morphospace. Second, the distance between the two species of *Eucystis* is diminished. Both differences, shown primarily in the second axis, are the result of culling multiple characters associated with the A ambulacrum which distinguishes these taxa. In addition, there is a minor increase of within genus variation with the taphonomically culled dataset. However, the taphonomically reduced dataset retained the key aspects in terms of the hypotheses being examined in the current study such as the morphological variation within taxa from different basins as well as the strong phylogenetic structure.

Incorporating the tree structure onto the morphospace (i.e., constructing a phylomorphospace), allows us to consider the morphological structure in an evolutionary and biogeographic framework. The intercontinental dispersal from Baltica to

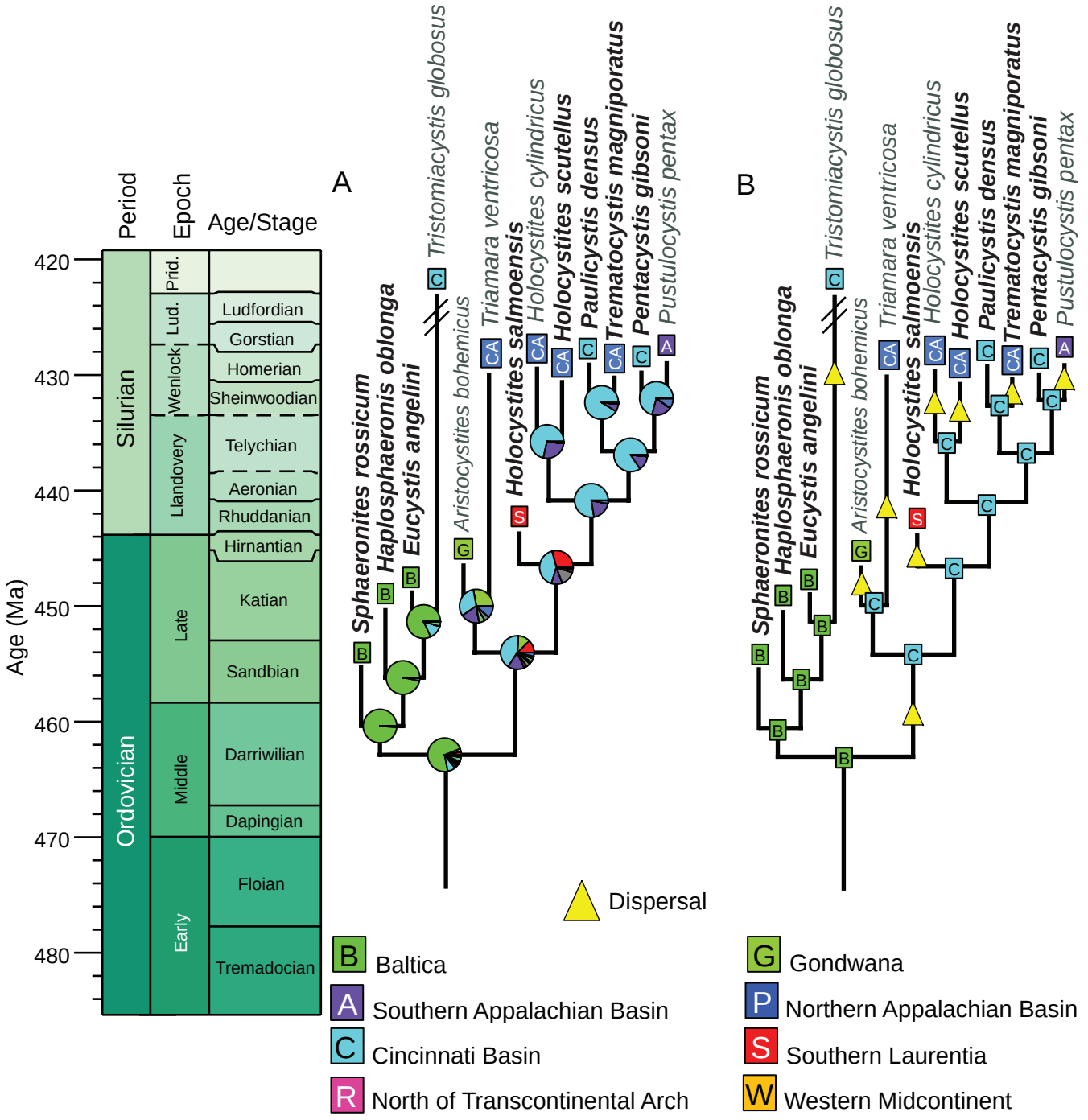

FIGURE 3 — Maximum-likelihood ancestral range estimation of the diploporan blastozoan phylogeny as modified from Lam et al. (2021) to focus on sphaeronitid taxa examined in this study (bolded genus and species names). **A**, Phylogeny with pie charts at nodes that indicate the probability of ancestral ranges from the DIVALIKE+*j* model. **B**, Most likely areas occupied by ancestors as inferred from the pie charts in A. Hatch marks on *T. globusus* range indicate this species ranges into the Devonian. Chronostratigraphy and age from the Geologic Time Scale 2016 (Ogg et al., 2016).

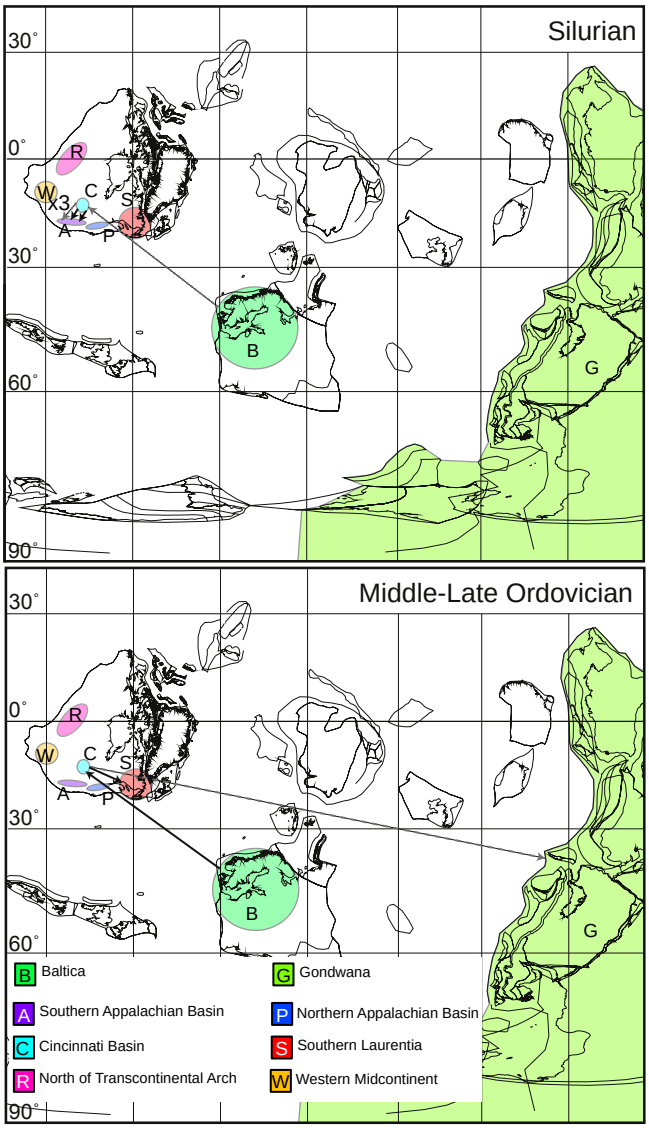

FIGURE 4 — Dispersal maps of sphaeronitid echinoderms (bolded) for two time slices: the Middle to Late Ordovician (470.0–443.8 Ma), and the Silurian (443.8–419.2 Ma). Solid black lines indicate dispersal events that took place for sphaeronitid species that are the focus of this study (Table 1), whereas dashed grey lines indicate a dispersal event that occurred for a species that is not the focus of this study. Duplicate lines (e.g., two bolded lines from the Cincinnati Basin to the Southern Appalachian Basin on the Silurian map) indicate multiple dispersal events (i.e., one line per dispersal). In the Silurian panel, the 'x3' beside the dispersal event from the Cincinnati Basin to the Southern Appalachian Basin indicates dispersal occurred three times for non-sphaeronitid species. Dispersal directions and types are inferred from the DIVALIKE+*j* analysis (FIGURE 3). Basin colors on the maps match those in Figure 3 as indicated in the key located in the bottom left corner of the Middle to Late Ordovician panel. Paleogeographic map modified from Torsvik and Cocks (2013).

Laurentia coincides with a large shift across morphospace within the Middle to Late Ordovician (Figs. 4, 5). However, the smaller intracontinental dispersals within holocystidids between Laurentian basins in the early Silurian correspond to minor shifts across morphospace. This pattern within the phylomorphospace is also retained within the taphonomically reduced dataset. Overall, the portions of the phylomorphospace representing dispersal events are not distinctive compared to the rest of the analysis. However, the relationship between morphological evolution and mode of speciation needs to be further explored in a more expansive study.

DISCUSSION

While there were some instances of dispersal between Laurentian basins during the Silurian (e.g., multiple events took place from the Cincinnati Basin to the Southern Appalachian Basin; Fig. 3), there was only one dispersal event

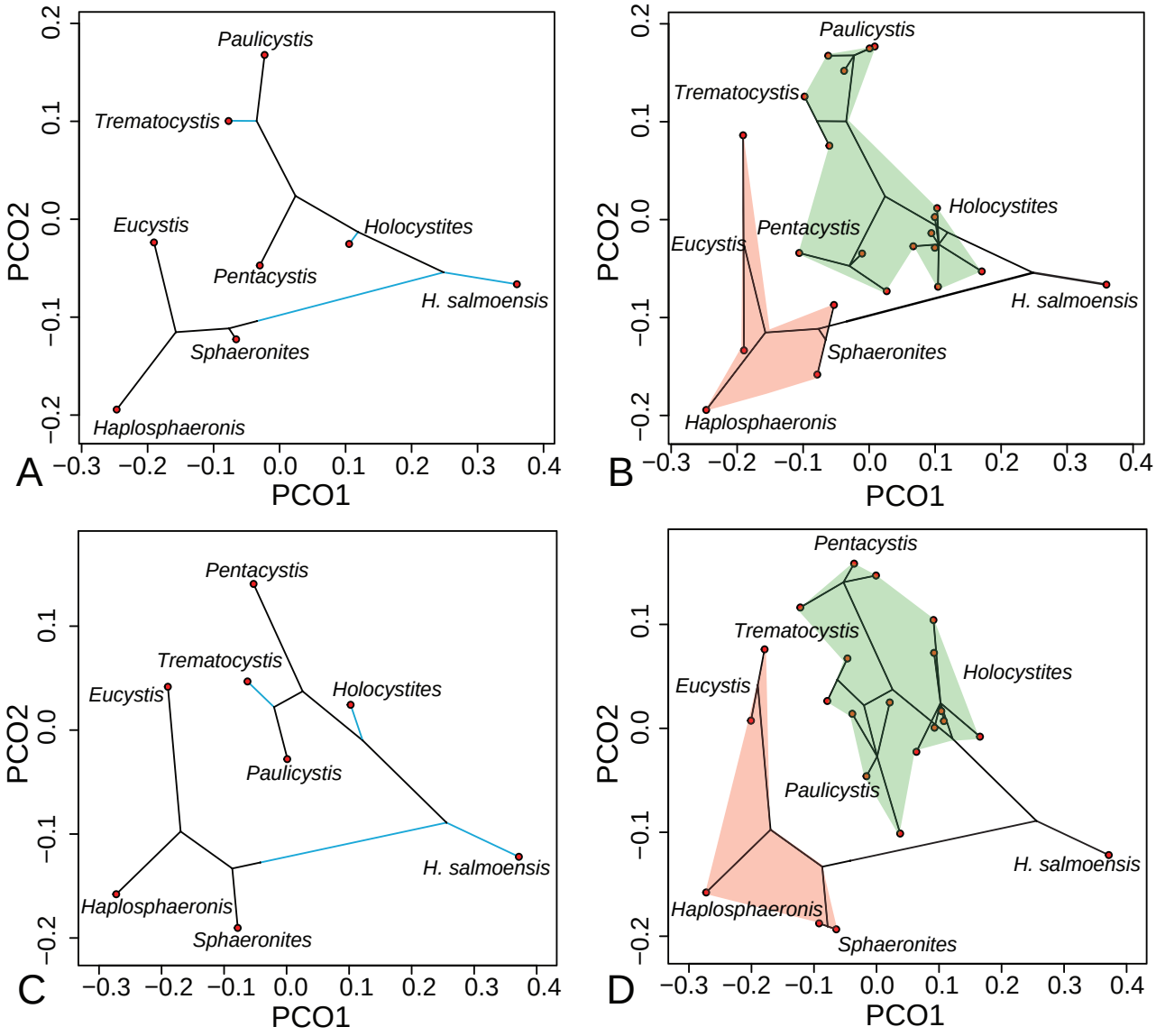

FIGURE 5 — Phylomorphospace of sphaeronitid diploporans. Ancestral positions based on post-ordination maximum likelihood. The phylomorphospaces are displayed in two ways, first, the position of the individual genera is plotted based on the ancestral node to show overall trends (A, C). Alternatively, all individual specimens are plotted in the phylomorphospace (B, D). Individual specimens within a genus are placed into a polytomy with short branch lengths. *Holocystites salmoensis* is separated from *H. scutellatus* based on its geographic position and unique morphology. **A**, **B**, phylomorphospace constructed from the modified character suite (Table 2). **C**, **D**, phylomorphospaces constructed from the culled character suite (Table 2). Specimens from Baltica are denoted in pink while those from Laurentia are in green. The portions of the phylomorphospace that represent dispersal events are shown in blue (A, C).

between Laurentia and other paleocontinents, specifically from Baltica to Laurentia (Fig. 4). This signal may indicate that as Baltica moved closer to Laurentia through the Ordovician and into the Silurian, dispersal became limited to occurring between these two paleocontinents within the sphaeronitids. Additional dispersal events between Laurentia and Gondwana may have decreased due to tectonically induced geographic barriers (e.g., the Taconic highlands from the Ordovician-early Silurian Taconic Orogeny; Van Staal et al., 2009; Torsvik and Cocks, 2013), and/or sea level fluctuations that could have limited dispersal. However, as our dataset is rather small, it is hard to infer such patterns and processes from this analysis alone.

Sphaeronitid dispersal events that occurred across ocean basins were likely controlled by wind-driven surface currents and gyre systems that operated between paleocontinents.

TABLE 3 — A comparison of European and North American sphaeronitids within morphospace (See FIGURE 5).

Region	N	Sum of Ranges	Sum of Ranges (Culled)	Sum of Variance	Sum of Variance (Culled)
Europe	5	1.170±0.20	1.215±0.19	0.050±0.011	0.054±.012
North America	17	1.223±0.15	1.108±0.14	0.029±0.008	0.026±0.007

From previous analyses of blastozoan echinoderms, it was hypothesized that dispersal between Baltica and Laurentia through the Ordovician was likely facilitated by the Iapetus Current and coastal upwelling (Pohl et al., 2016; Pohl et al., 2018; Lam et al., 2021). We invoke the same processes here to explain how species traveled, likely in their larval stages (Lam et al., 2018), between Baltica and Laurentia. Laurentian dispersal dynamics for marine invertebrates was likely facilitated by strong storm and hurricane activity, potentially sweeping species across physical and thermal barriers into new areas (Lam et al., 2018). As the Silurian is not well-preserved in Laurentian sections, it is difficult to assess the abiotic drivers of dispersal during this period. However, it is clear from our biogeographic analysis, specifically the five dispersal events from the Cincinnati Basin into the Southern Appalachian basins, that some abiotic factor(s) may have pushed species from the Cincinnati Basin to the south.

Bauer (2021) conducted a paleobiogeographic analysis for eublastoids, ranging from the Silurian through the late Permian. Through the study interval, there were limited dispersal events among paleocontinents, especially during the Silurian. However, dispersal among basins of Laurussia (i.e., the paleocontinent formed from the collision of Laurentia and Baltica) dominated during this time. Beginning in the Devonian, Bauer (2021) found that intercontinental dispersal began to increase for the eublastoids, a pattern that may be explained by reduced distances among paleocontinents (Torsvik and Cocks, 2013). Too few diploporans crossed the Devonian boundary to be able to thoroughly assess if this pattern holds true in other blastozoan groups. Bauer's (2021) finding of increased dispersal among Laurentian/Laurussian basins into and through the Silurian matches with the patterns recovered from this analysis. However, additional analyses are required to fully assess the causes of increased intracontinental dispersal more fully for blastozoans from the Late Ordovician to Silurian and increased intercontinental dispersal into the Devonian. Specifically, such additional analyses should ideally be performed in a robust phylogenetically informed and statistical framework, as patterns and processes for the Silurian are complicated for Baltica, Gondwana, and especially Laurentia due to large disconformities in the stratigraphic record that may be obscuring species' ranges (Cramer and Saltzman, 2005).

Taphonomic preservation has the potential to significantly bias morphologic interpretation and, therefore, also alter phylogenetic and morphologic conclusions, a phenomenon noted across multiple fossil groups (Sheffield and Sumrall, 2015, 2017; Murdock et al., 2016; Sansom, 2016; Deline and Thomka, 2017). However, the inclusion of taphonomic data can indicate the degree of bias and potentially increase the resolution of evolutionary studies (Murdock et al., 2016, Deline and Thomka, 2017). While diploporans are not the most susceptible echinoderms in terms of complete disarticulation (Brett et al., 1997), it is still uncommon for individuals to show complete preservation. Most often, we find that the stems or holdfasts of the specimens are disarticulated from the theca (Thomka et al., 2016) and the delicate brachiole plates are almost never found articulated (Paul, 1971; Frest et al., 2011). Furthermore, the intricate plates of the oral area, which often contain significant phylogenetic information in many blastozoans (Sumrall and Waters, 2012; Kammer et al., 2013), are often disarticulated from the theca. However, the theca itself is sutured tightly together, which presents another taphonomic difficulty in that the sutures and features of the thecal plates become significantly abraded even in articulated specimens. This taphonomic overprinting in diploporans has resulted in new taxa being erected based solely on taphonomic differences rather than morphologic differences (Sheffield and Sumrall, 2015, 2017).

Deline and Thomka (2017) explored the effects of differential taphonomic processes on blastozoan echinoderm disparity. This study found the resulting structure of the morphospace and patterns of disparity through time were stable even when taphonomic biases were significantly exaggerated. This is because many blastozoan morphological features can be observed in disarticulated specimens (e.g., respiratory structures) compared with other echinoderms, such as crinoids, that require articulated theca to discern the major features (Deline and Thomka, 2017). The current analysis of sphaeronitid diploporans is consistent with the suggestion that most blastozoans are not taphonomically sensitive regarding studies of morphologic disparity. As stricter taphonomic criteria were used to characterize morphologic patterns the overall structure of the morphospace was retained. Any difference in the resulting morphospaces with the varied taphonomic criteria are largely the result of shifting emphasis

on different body regions as characters are non-randomly removed (e.g., reducing the number of characters associated with the A ambulacrum), which is similar to patterns shown in the disparity of crinoids (Deline and Ausich, 2017). Overall, the relevant morphological patterns in the current analysis are retained even with stricter criteria for taphonomically missing data, thus these results are unlikely to be significantly biased by preservational differences between taxa.

The Late Ordovician Mass Extinction propelled ecological changes amongst filter feeding echinoderms (Ausich and Deline, 2012; Cole et al., 2019; Cole and Wright, 2021). The mass extinction paired with ecological restructuring opened potential niches and eased competitive pressures. The loss of lower-tiered Porocrinoidea (e.g., *Hybocrinus* and *Porocrinus*) and a reduction in blastozoan diversity enabled the successful establishment of holocystitids that filled the same broad ecological niche following their dispersal from Baltica to Laurentia. The morphological response to this type of biogeographic and ecological shift is understudied, but we hypothesized that the permissive ecology within niche space would result in increased disparity within the invasive taxa. This pattern of rapid morphological change often occurs following mass extinctions or the evolution of key innovations leading toward the establishment of a new niche (Hughes et al., 2013). Even though the transcontinental dispersal coincided with a large shift across regions of morphospace (i.e., the distance between centroids of the two groups ~36.4% of the range of values across PCO1), the area occupied by holocystitids was comparable to that of the Baltic diploporans (Table 3). Thus, even with the permissive ecology related to lower competition within their niche, morphology both within and between holocystitid taxa was constrained.

The reasons for this perceived lack of morphological response to the release of competitive pressure following the faunal migration could be related to the nature of a niche being filled or developmental constraints. Competition and niche partitioning has been extensively studied in late Paleozoic echinoderm communities in terms of elevation above the sea floor (Ausich and Bottjer, 1982; Bottjer and Ausich, 1986), filter density (Kammer and Ausich, 1987), and size of food particles (Meyer et al., 2002; Brower, 2006). The early Paleozoic establishment of these patterns has been recently explored in a phylogenetic context (Cole et al., 2019; Cole and Wright, 2021). Examinations of the ecomorphology of crinoid Lagerstätte in the Late Ordovician indicates a steady divergence of feeding ecologies with niches becoming more discrete and distinctive (Cole and Wright, 2021). Extensive niche partitioning would in turn lead to increasingly narrowly defined ecological niches, such that the dispersal and establishment of diploporans into one of these niches would have a stabilizing effect and prevent extensive morphological diversification. This interpretation is strengthened by the nature of many of the characters included in the current study that have ecological significance (e.g., width of ambulacra, facet shape, and number of facets per ambulacrum).

Alternatively (or in addition), the lack of morphological expansion in sphaeronitids could be related to developmental constraint. It has been hypothesized that as large-scale morphological features become more complex through time, they become increasingly evolutionarily rigid and unable to change (Riedl, 1977). This pattern has also been proposed for gene regulatory networks becoming more elaborate and static through time (Congreve et al., 2018; Erwin, 2020). Deline et al. (2020) explored early Paleozoic echinoderm morphological disparity and found that the phylogenetic signal was similar regardless of the scale of the character, which indicates a prolonged flexibility within echinoderm anatomy through time. However, observing this pattern broadly across the phylum may not necessarily translate into the evolutionary dynamics of a specific, small clade. In addition, given the focus on sphaeronitids, the characters used in the current study are smaller in scale and specific such that developmental constraints might play a larger role in the lack of morphological expansion.

The competitive release and permissive ecology following establishment in Laurentia may not have had an extensive effect in terms of characteristics and overall shape, but this ecological change might have been expressed in other manners. Foremost are changes in population ecology, wherein a decrease in competition results in high abundance of specific taxa along with uneven community structure. Baltic sphaeronitids can be locally abundant (Bockelie, 1984), but overall Ordovician diploporans, like many blastozoans, are often minor components in marine ecosystems. However, *Holocystites scutellus*, which likely filled niches vacated by crinoids, is the most common echinoderm by far within the lower Silurian Massie Formation (Frest et al., 2011; Thomka et al., 2016). In addition, there is a significant shift in body size during this transition from Baltica to Laurentia, which can be seen with the limited scale of this study with the Laurentian specimens (theca height 37.91 ± 5.53 mm, theca width 24.69 ± 2.22 mm) over double the thecal size of those from Baltica (theca height 15.04 ± 1.75 mm, theca width 13.91 ± 1.71 mm).

One particularly intriguing result of the current analyses is the shifts in phylomorphospace relative to the recognized dispersal event. The intercontinental dispersal event from Baltica to the Cincinnati Basin corresponds to a large shift across morphospace (Figs. 4, 5). The morphological shift during this transition represents roughly 48% of the range shown on the primary axis but is likely exaggerated by the aberrant morphology of *Holocystites salmoensis*. If the outlier status of *H. salmoensis* is excluded, the morphological shift corresponding to the dispersal is still robust (34.6% of the range shown on the primary axis). However, the following intracontinental dispersal events from the Cincinnati Basin to the Southern Appalachian Basin reflect minor changes in morphospace position. Dispersal events between geographically adjacent basins likely had significant gene flow and could potentially mute morphological shifts relative to migrations across wide ocean basins. However, to explore the relationship between mode of speciation (vicariance vs dispersal), dispersal distance, and morphological evolution in the future would require a more expansive study using rate-based comparative phylogenetic methods.

CONCLUSIONS

This study uses phylogenetically-informed paleobiogeography combined with a phylomorphospace analysis to infer dispersal patterns and morphological changes across the Ordovician–Silurian boundary. To date, the majority of research related to echinoderm evolutionary responses across the LOME have been focused on crinoids, leaving questions about how other groups of echinoderms may have responded to extinction dynamics. In the sphaeronitid diploporans, very little morphological change was detected across the Ordovician–Silurian boundary as these taxa dispersed in one major event from Baltica to Laurentia during the Middle–Late Ordovician; these dispersals led to the establishment of new echinoderm communities in the middle Silurian. This lack of morphological change could indicate that these diploporans filled a narrow and previously defined niche structure that was vacated by crinoids during the LOME, but it could also indicate that diploporans were under developmental constraints preventing new morphological innovation. These sphaeronitid diploporans do exhibit some changes, particularly in their body size and in their community structure. As diploporans migrated from Baltica to Laurentia, they approximately doubled their body size. In terms of community structure, some sphaeronitids became increasingly more abundant. While some sphaeronitids were locally abundant in the Ordovician, taxa such as *Holocystites scutellus* became one of the most abundant echinoderm taxa in the Silurian of Laurentia, which could be due to a decrease in competition from the vacated niches following the LOME.

We also uncover several dispersal events throughout the studied time range of the Ordovician– Silurian and increasing levels of morphospace change correlating positively with dispersal distance. Dispersal among paleocontinents virtually stopped during the Silurian and there were few intracontinental dispersal events constrained from the Cincinnati Basin to the Southern Appalachian Basin. While further studies and a larger dataset would be necessary to explore this pattern more fully, it is possible that the lack of intercontinental dispersal could have been related to a number of factors, such as tectonically-induced geographic barriers that formed during the Late Ordovician–Silurian or sea level fluctuations that would have caused further isolation of basins. Future work to better understand both the patterns of morphological shifts in relation to dispersal distance and the patterns of increased and decreased dispersal throughout this time in the early Paleozoic can be explored by weaving together datasets from multiple clades using rate-based comparative phylogenetic methods in combination with an expanded biogeographic dataset.

ACKNOWLEDGEMENTS

We are honored to submit this work to the special volume recognizing the career of Tomasz Baumiller. B. Deline volunteered at the University of Michigan Museum of Paleontology under Dr. Baumiller's supervision while he was in high school and then studied with him as an undergraduate. Dr. Baumiller provided valuable professional guidance, mentorship, encouragement, and opportunities that formed a solid foundation for his career in paleontology. S. Sheffield was supported by the Paleontological Society's Arthur James Bocout Early Career Grant. The University of South Florida's School of Geosciences provided funding to B. Deline to facilitate data collection. We thank J. Bauer, and reviewers J. Lamsdell and E. Nardin for their comments and suggestions that greatly improved this manuscript. We thank U. Toom, Geological Institute of Tallinn; G. Baranov, Geological Institute of Tallinn; B. Hunda, Cincinnati Museum Center; T. Adrain, The University of Iowa; Paul Mayer, The Field Museum; and Jean Dougherty, the Geological Survey of Canada for access to specimens. M. McCoy assisted in constructing the morphological character suite. Supplementary File 1 contains the characters used for this analysis. Supplementary File 2 contains the character codings. B. Deline and S. Sheffield designed the study, all authors collected and analyzed the data, and B. Deline, S. Sheffield, and A. Lam wrote the paper.

Supplemental Online Material:
https://dx.doi.org/10.7302/4375

LITERATURE CITED

ALBANESI, G. L., C. R. BARNES, J. A. TROTTER, I. S. WILLIAMS, and S. M. BERGSTRÖM. 2019. Comparative Lower–Middle Ordovician conodont oxygen isotope palaeothermometry of the Argentine Precordillera and Laurentian margins. Palaeogeography, Palaeoclimatology, Palaeoecology, 549: 109115. doi: 10.1016/j.palaeo.2019.03.016

ALDRIDGE, R. J., L. JEPPSSON, and K. J. DORNING. 1993. Early Silurian oceanic episodes and events. Journal of the Geological Society of London, 150, 501–513.

AUSICH, W. I., and D. J. BOTTJER. 1982. Tiering in suspension-feeding communities on soft substrata throughout the Phanerozoic. Science, 216: 173–174.

AUSICH, W. I., and B. DELINE. 2012. Macroevolutionary transition in crinoids following the Late Ordovician extinction event (Ordovician to early Silurian). Palaeogeography, Palaeoclimatology, Palaeoecology, 361: 38–48.

AUSICH, W. I., T. W. KAMMER, and T. K. BAUMILLER. 1994. Demise of the middle Paleozoic crinoid fauna: a single extinction event or rapid faunal turnover? Paleobiology, 20: 345–361.

BAUER, J. E. 2021. Paleobiogeography, paleoecology, diversity, and speciation patterns in the Eublastoidea (Blastozoa: Echinodermata), Paleobiology, 47: 221–235. doi: 10.1017/pab.2020.27.

BAUMILLER, T.K. 1994. Patterns of dominance and extinction in the record of Paleozoic crinoids. In B. David, A. Guille, J.P. Feral, and M. Roux (eds.), Echinoderms Through Time, Balkema: Rotterdam, pp. 193–198.

BOCKELIE, J. F. 1984. The Diploporita of the Oslo region, Norway. Palaeontology, 27: 1–68.

BOTTJER, D. J., and W. I. AUSICH. 1986. Phanerozoic development of tiering in soft substrata suspension-feeding communities. Paleobiology, 12: 400–420.

BRANSON, E. R., and R.E. PECK. 1940. A new cystoid from the Ordovician of Oklahoma. Journal of Paleontology, 14: 89–92.

BRENCHLEY, P. J., J. D. MARSHALL, G. A. F. CARDEN, D. B. R. ROBERTSON, D. G. F. LONG, T. MEIDLA, L. HINTS, and T. F. ANDERSON. 1994. Bathymetric and isotopic evidence for a short-lived Late Ordovician glaciation in a greenhouse period. Geology, 22: 295–298.

BRETT, C. E., H. A. MOFFAT, and W. L. TAYLOR. 1997. Echinoderm taphonomy, taphofacies, and Lagerstätten. The Paleontological Society Papers, 3, 147–190.

BROWER, J. C. 2006. Ontogeny of the food-gathering system in Ordovician crinoids. Journal of Paleontology, 80: 430–446.

CLAUSEN, S. 2004. New early Cambrian eocrinoids from the Iberian Chains (NE Spain) and their role in nonreefal benthic communities. Eclogae Geologicae Helvetiae, 97: 371–379.

COLE, S. R., and D. F. WRIGHT. 2021, September 27. Niche evolution and phylogenetic community paleoecology of Late Ordovician Crinoids. https://doi.org/10.32942/osf.io/r6jta

COLE, S. R., D.F. WRIGHT, and W.I. Ausich. 2019. Phylogenetic community paleoecology of one of the earliest complex crinoid faunas (Brechin Lagerstätte, Ordovician). Palaeogeography, Palaeoclimatology, Palaeoecology, 521: 82–98.

CONGREVE, C. R., A. Z. KRUG, and M. E. PATZKOWSKY. 2019. Evolutionary and biogeographical shifts in response to the Late Ordovician mass extinction. Palaeontology, 62: 267–285.

CONGREVE, C. R., A.R. FALK, and J.C. LAMSDELL. 2018. Biological hierarchies and the nature of extinction. Biological Reviews, 93: 811–826.

CRAMER, B. D., and M. R. SALTZMAN. 2005. Sequestration of ^{12}C in the deep ocean during the early Wenlock (Silurian) positive carbon isotope excursion. Palaeogeography, Palaeoclimatology, Palaeoecology, 219: 333–349.

DELINE, B. 2021. *Echinoderm morphological disparity: Methods, patterns, and possibilities*. Cambridge University Press.

DELINE, B., and W.I. AUSICH. 2011. Testing the plateau: a reexamination of disparity and morphologic constraints in early Paleozoic crinoids. Paleobiology, 37: 214–236.

_____. 2017. Character selection and the quantification of morphological disparity. Paleobiology, 43: 68–84

DELINE, B. and J. R. THOMKA. 2017. The role of preservation on the quantification of morphology and patterns of disparity within Paleozoic echinoderms. Journal of Paleontology, 91: 618–632.

DELINE, B., W. I. AUSICH, and C. E. Brett. 2012. Comparing taxonomic and geographic scales in the morphologic disparity of Ordovician through Early Silurian Laurentian crinoids. Paleobiology, 38: 538–553.

DELINE, B., J. R. THOMPSON, N. S. SMITH, S. ZAMORA, I. A. RAHMAN, S. L. SHEFFIELD, W. I. AUSICH, T. W. KAMMER, and C. D. SUMRALL. 2020. Evolution and development at the origin of a phylum. Current Biology, 30: 1–8. doi: 10.1016/j.cub.2020.02.054.

DICKSON, J. A. D. 2002. Fossil echinoderms as a monitor of the Mg/Ca ratio of Phanerozoic oceans. Science, 298: 1222–1224.

_____. 2004. Echinoderm skeletal preservation: calcite-aragonite seas and the Mg/Ca ratio of Phanerozoic oceans. Journal of Sedimentary Research, 74: 355–365.

ERWIN, D.H. 2020. The origin of animal body plans: a view from fossil evidence and the regulatory genome. Development, 147: dev182899.

FINNEGAN, S., K. BERGMANN, J. M. EILER, D. S. JONES, D. A. FIKE, I. EISENMAN, N. C. HUGHES, A. K. TRIPATI, and W. W. FISCHER. 2011. The magnitude and duration of Late Ordovician–Early Silurian glaciation. Science, 331: 903–906.

FREST, T. J., H. L. STRIMPLE, and C. R. C. PAUL. 2011. The North American *Holocystites* fauna (Echinodermata: Blastozoa: Diploporita): paleobiology and systematics. Bulletins of American Paleontology, 380: 1–141.

GABBOTT, S. E., J. ZALASIEWICZ, R.J. ALDRIDGE, and J.N. THERON. (2010). Eolian input into the Late Ordovician postglacial Soom Shale, South Africa. Geology, 38: 1103–1106.

GABBOTT, S. E., C. BROWNING, J.N. THERON, and R.J. WHITTLE. 2017. The late Ordovician Soom Shale Lagerstätte: an extraordinary post-glacial fossil and sedimentary record. Journal of the Geological Society, 174: 1–9.

GERBER, S. 2019. Use and misuse of discrete character data for morphospace and disparity analysis. Palaeontology, 62: 305–319.

GOWER, J. C. 1971. A general coefficient of similarity and some of its properties. Biometrics, 27, 857–871.

GRAHN, Y. G., and M.V. CAPUTO. 1992. Early Silurian glaciation in Brazil. Palaeogeography, Palaeoclimatology, Palaeoecology, 99: 9–15.

HAQ, B. U., and S.R. SCHUTTER. 2008. A chronology of Paleozoic sea-level changes. Science, 322: 64–68.

HOPKINS, M. J., and A. B. SMITH. 2015. Dynamics evolutionary change in post-Paleozoic echinoids and the importance of scale when interpreting changes in rates of evolution. Proceedings of the National Academy of Sciences, 112: 3758–3763.

HUELSENBECK, J. P., R. NIELSEN, and J.P. BOLLBACK. 2003. Stochastic mapping of morphological characters. Systematic biology, 52: 131–158.

HUGHES, M., S. GERBER, and M.A. WILLS. 2013. Clades reach highest morphological disparity early in their

evolution. Proceedings of the National Academy of Sciences, 110: 13875–13879.

JEPPSON, L. 1990. An oceanic model for lithological and faunal changes tested on the Silurian record. Journal of the Geological Society of London, 147: 663–674.

_____.1997. Recognition of a probable secondo-primo event in the Early Silurian. Lethaia, 29: 311–315.

_____.1998. Silurian oceanic events: summary of general characteristics. In E. Landing and M.E. Johnson (eds.), New York State Museum Bulletin, 491, 239–257.

JOHNSON, M. E. 2006. Relationship of Silurian sea-level fluctuations to oceanic episodes and events. GFF, 128: 115–121.

_____. 2010. Tracking Silurian eustasy: alignment of empirical evidence or pursuit of deductive reasoning? Palaeogeography, Palaeoclimatology, Palaeoecology, 296: 276–284.

KAMMER, T. W., and W. I. AUSICH. 1987. Aerosol suspension feeding and current velocities: distributional controls for late Osagean crinoids. Paleobiology, 13: 379–395.

_____, C. D. SUMRALL, S. ZAMORA, W. I. AUSICH, and B. DELINE. 2013. Oral region homologies in Paleozoic crinoids and other plesiomorphic pentaradial echinoderms. PLoS One, 8. doi: 10.1371/journal.pone.0077989

KESLING, R.V. 1967. Cystoidea. In R. C. Moore (ed.), *Tre*atise on Invertebrate Paleontology, Part S, Echinodermata 1, University of Kansas Press and Geological Society of America: Lawrence, Kansas, and Boulder, Colorado, pp. S85–S262.

LAM, A. R., and A. L. STIGALL. 2015. Pathways and mechanisms of Late Ordovician (Katian) faunal migrations of Laurentia and Baltica. Estonian Journal of Earth Sciences, 64: 62–67.

_____ _____, and N. J. MATZKE. 2018. Dispersal in the Ordovician: speciation patterns and paleobiogeographic analyses of brachiopods and trilobites. Palaeogeography, Palaeoclimatology, Palaeoecology, 489: 147–165.

_____, S. L. SHEFFIELD, and N. J. MATZKE. 2021. Estimating dispersal and evolutionary dynamics in diploporan blastozoans (Echinodermata) across the Great Ordovician biodiversification event. Paleobiology, 47: 198–220.

LANDIS, M., N. J. MATZKE, B. R. MOORE, and J. P. HUELSENBECK. 2013. Bayesian analysis of biogeography when the number of areas is large. Systematic Biology, 62: 789–804.

LEFEBVRE, B. 2007. Early Palaeozoic palaeobiogeography and palaeoecology of stylophoran echinoderms. Palaeogeography, Palaeoclimatology, Palaeoecology, 245: 156–199.

_____, and O. FATKA. 2003. Palaeogeographical and palaeoecological aspects of the Cambro–Ordovician radiation of echinoderms in Gondwanan Africa and peri-Gondwanan Europe. Palaeogeography, Palaeoclimatology, Palaeoecology, 195: 73–97.

_____, C. D. SUMRALL, R. A. SHROAT-LEWIS, M. REICH, G. D. WEBSTER, A. W. HUNTER, E. NARDIN, S. V. ROZHNOV, T. E. GUENSBERG, A. TOUZEAU. 2013. Palaeobiogeography of Ordovician echinoderms. Geological Society, London, Memoirs, 38: 173–198.

LLOYD, G. T. 2016. Estimating morphological diversity and tempo with discrete character-taxon matrices: implementation, challenges, progress, and future directions. Biological Journal of the Linnean Society, 118: 131–151.

_____. 2018. Journeys through discrete-character morphospace: synthesizing phylogeny, tempo, and disparity. Palaeontology, 61: 637–646.

LOYDELL, D. K. 1998. Early Silurian sea level changes. Geology, 135: 447–471.

MAECHLER, M. 2019. Finding groups in data: cluster analysis extended Rousseau et. *R package version*, *2*(0).

MATZKE, N. J. 2013. Probabilistic historical biogeography: new models for founder-event speciation, imperfect detection, and fossils allow improved accuracy and model-testing. Frontiers in Biogeography, 5: 242–248.

_____. 2014. Model selection in historical biogeography reveals that founder-event speciation is a crucial process in island clades. Systematic Biology, 63: 951–970.

MELCHIN, M. J., C. E. MITCHELL, C. HOLMDEN, and P. ŠTORCH. 2013. Environmental changes in the Late Ordovician–early Silurian: review and new insights from black shales and nitrogen isotopes. GSA Bulletin, 125:1635–1670.

MEYER, D. L., A. I., MILLER, S. M. HOLLAND, and B. F. DATTILO. 2002. Crinoid distribution and feeding morphology through a depositional sequence: Kope and Fairview Formations, Upper Ordovician, Cincinnati Arch region. Journal of Paleontology, 76: 725–732.

MURDOCK, D. J., S. E. GABBOTT, and M. A. PURNELL. 2016. The impact of taphonomic data on phylogenetic resolution: *Helenodora inopinata* (Carboniferous, Mazon Creek Lagerstätte) and the onychophoran stem lineage. BMC Evolutionary Biology, 16: 1–14.

NARDIN, E., and B. LEFEBVRE. 2010. Unravelling extrinsic and intrinsic factors of the early Palaeozoic diversification of blastozoan echinoderms. Palaeogeography, Palaeoclimatology, Palaeoecology, 294: 142–160.

OGG, J. G., G. OGG, and F. M. GRADSTEIN. 2016. A concise geologic time scale: 2016, Elsevier: Amsterdam.

OKSANEN, J., F. G. BLANCHET, M. FRIENDLY, R. KINDT, P. LEGENDRE, D. MCGLINN, P. R. MINCHIN, R. B. O'HARA, G. L. SIMPSON, P. SOLYMOS, M. HENRY H. STEVENS, E. SZOECS and H. WAGNER. 2020. vegan: Community Ecology Package. R package version 2.5-7. https://CRAN.R-project.org/package=vegan.

PARADIS, E., J. CLAUDE, and K. STRIMMER. 2004. APE: analyses of phylogenetics and evolution in R language. Bioinformatics, 20: 289–290.

PAUL, C. R. C. 1971. Revision of the *Holocystites* Fauna (Diploporita) of North America. Fieldiana Geology, 24: 1–166.

_____. 1988. The phylogeny of the cystoids. In C. R. C. Paul, and A. B. Smith, (eds). Echinoderm Phylogeny and Evolutionary Biology, Clarendon Press: Oxford, pp. 199–213.

PETERS, S.E., and W. I. AUSICH. 2008. A sampling-adjusted macroevolutionary history for Ordovician–Early Silurian crinoids. Paleobiology, 34: 104–116. doi:10.1666/07035.1.

POHL, A., E. NARDIN, T. R. A. VANDENBROUCKE, and Y. DONNADIEU. 2016. High dependence of Ordovician ocean surface circulation on atmospheric CO_2 levels. Palaeogeography, Palaeoclimatology, Palaeoecology, 458: 39–51.

POHL, A., D. A. T. HARPER, Y. DONNADIEU, G. LE HIR, E. NARDIN, and T. SERVAIS. 2018. Possible patterns of marine primary productivity during the Great Ordovician Biodiversification Event. Lethaia, 51: 187–197.

RAHMAN, I. A., and S. ZAMORA. 2009. The oldest cinctan carpoid (stem-group Echinodermata), and the evolution of the water vascular system. Zoological Journal of the Linnean Society, 157: 420–432.

REE, R. H., and S. A. SMITH. 2008. Maximum likelihood inference of geographic range evolution by dispersal, local extinction, and cladogenesis. Systematic Biology, 57: 4–14.

REVELL, L. J. 2012. phytools: an R package for phylogenetic comparative biology (and other things). Methods in Ecology and Evolution, 3: 217–223.

RIEDL, R. 1977. A systems-analytical approach to macro-evolutionary phenomena. The Quarterly Review of Biology, 52: 351–370.

RONQUIST, F. 1997. Dispersal-vicariance analysis: a new approach to the quantification of historical biogeography. Systematic Biology, 46: 195–203.

SANSOM, R. 2016. Preservation and phylogeny of Cambrian ecdysozoans tested by experimental decay of *Priapulus*. Scientific Reports, 6: 32817. doi: 10.1038/srep32817

SAUPE, E. E., H. QIAO, Y. DONNADIEU, A. FARNSWORTH, A. T. KENNEDY-ASSER, J.-B. LADANT, D. J. LUNT, A. POHL, P. VALDES, and S. FINNEGAN. 2020. Extinction intensity during Ordovician and Cenozoic glaciations explained by cooling and palaeogeography. Nature Geoscience, 13: 65–70.

SHEEHAN, P. M. 2001. The late Ordovician mass extinction. Annual Review of Earth and Planetary Sciences, 29: 331–364.

SHEFFIELD, S. L. 2017. Generic revision of the Holocystitidae of North America (Diploporita, Echinodermata) based on universal elemental homology. Journal of Paleontology, 91: 755–766.

_____. 2019a. The phylogeny of the Diploporita: a polyphyletic assemblage of blastozoan echinoderms. Journal of Paleontology, 93: 740–752.

____. 2019b. A re-interpretation of the ambulacral system of *Eumorphocystis* (Blastozoa: Echinodermata) and its bearing on the evolution of early crinoids. Palaeontology, 62: 163–173. doi: 10.1111/ pala.12396.

____, and C. D. SUMRALL. 2015. A new interpretation of the oral plating patterns of the *Holocystites* Fauna. In S. Zamora, and I. Rábano (eds.), Progress in Echinoderm Palaeobiology: Cuademos del Museo Geominero, Instituto Geológico y Minero de España, Madrid, 19, pp. 159–162.

_____, W.I. AUSICH, and C.D. SUMRALL. 2017. Late Ordovician (Hirnantian) diploporitan fauna of Anticosti Island, Quebec, Canada: implications for evolutionary and biogeographic patterns. Canadian Journal of Earth Sciences, 55: 1–7. DOI: 10.1139/cjes-2017-0160

SIDLAUSKAS, B. 2008. Continuous and arrested morphological diversification in sister clades of characiform fishes: a phylomorphospace approach. Evolution, 62: 3135–3156.

SMITH, A.B. 1988. Fossil evidence for the relationships of extant echinoderm classes and their times of divergence. In C.R.C. Paul and A.B. Smith (eds.), Echinoderm phylogeny and evolutionary biology: Clarendon Press, Oxford, pp. 85–106.

SPRINKLE, J. 1980. An overview of the fossil record. Studies in Geology, Notes for a short course, 3: 15–26.

STIGALL, A. L., C. T. EDWARDS, R. L. FREEMAN, and C. M. Ø. RASMUSSEN. 2019. Coordinated biotic and abiotic change during the Great Ordovician Biodiversification Event: Darriwilian assembly of early Paleozoic building blocks. Palaeoceanography, Palaeoclimatology, Palaeoecology, 530: 249–270.

ŠTORCH, P. 1995. Biotic crises and post-crisis recoveries recorded by Silurian planktonic graptolite faunas of the Barrandian area (Czech Republic). Geolines, 3: 59–70.

SUMRALL, C. D. 1997. The role of fossils in the phylogenetic reconstruction of Echinodermata. The Paleontological Society Papers, 3: 267–288.

____. 2017. New insights concerning homology of the oral region and ambulacral system plating of pentaradial echinoderms. Journal of Paleontology, 91: 604–617.

____, and J. A. WATERS. 2012. Universal elemental homology in glyptocystitoids, hemicosmitoids, coronoids and blastoids: steps toward echinoderm phylogenetic reconstruction in derived Blastozoa. Journal of Paleontology, 86: 956–972.

____, and G.A. WRAY. 2007. Ontogeny in the fossil record: diversification of body plans and the evolution of "aberrant" symmetry in Paleozoic echinoderms. Paleobiology, 33: 149–163.

____, B. DELINE, J. COLMENAR, S.L. SHEFFIELD, and S. ZAMORA. 2015. New data on late Ordovician (Katian) echinoderms from Sardinia, Italy. In S. Zamora, and I. Rábano (eds). Progress in Echinoderm Palaeobiology: Cuademos del Museo Geominero, Instituto Geológico y Minero de España, 19: Madrid, pp. 159–162.

THOMKA, J. R., C. E. BRETT, T. E. BANTEL, A. L. YOUNG, and D. L. BISSETT. 2016. Taphonomy of 'cystoids'

(Echinodermata: Diploporita) from the Napoleon quarry of southeastern Indiana, USA: The lower Silurian Massie Formation as an atypical Lagerstätte. Palaeogeography, Palaeoclimatology, Palaeoecology, 443: 263–277.

TORSVIK, T. H., and L. R. M. COCKS. 2013. New global palaeogeographical reconstructions for the Early Palaeozoic and their generation. Geological Society of London Memoir, 38: 5–24.

TROTTER, J. A., I. S. WILLIAMS, C. R. BARNES, C. LEÉCUYER, and R. S. NICOLL. 2008. Did cooling oceans trigger Ordovician biodiversification? Evidence from conodont thermometry. Science, 25: 550–554.

____, ____, ____, P. MAENNIK, and A. SIMPSON. 2016. New conodont δ18O records of Silurian climate change: Implications for environmental and biological events. Palaeogeography, Palaeoclimatology, Palaeoecology, 443: 34–48.

VAN STAAL, C. R., WHALEN, J. B., VALVERDE-VAQUERO, P., ZAGOREVSKI, A., and N. ROGERS. 2009. Pre-Carboniferous, episodic accretion-related, orogenesis along the Laurentian margin of the northern Appalachians. In J. B. Murphy, J. D. Keppie, and A. J. Hynes (eds.) Ancient Orogens and Modern Analogues, Geological Society Special Publications 327, London, pp. 271–316.

VANDENBROUCKE, T. R., S.E.GABBOTT, F. PARIS, R.J. ALDRIDGE, and J.N. THERON. 2009. Chitinozoans and the age of the Soom Shale, an Ordovician black shale Lagerstätte, South Africa. Journal of Micropalaeontology, 28: 53–66.

VENNIN, E., J.J. ÁLVARO, and E. VILLAS. 1998. High-latitude pelmatozoan-bryozoan mud- mounds from the late Ordovician northern Gondwana platform. Geological Journal, 33: 121–140. doi:10.1002/(SICI)1099-1034(1998040)33:2<121:: AID-GJ780>3.0.CO;2-D.

WRIGHT, D. F. 2017. Phenotypic innovation and adaptive constraints in the evolutionary radiation of Palaeozoic crinoids. Scientific Reports, 7: 1–10.

____, W. I. AUSICH, S. R. COLE, M. E. PETER, and E. C. RHENBERG. 2017. Phylogenetic taxonomy and classification of the Crinoidea (Echinodermata). Journal of Paleontology, 91: 829–846.

ZAMORA, S., and A.B. SMITH. 2008. A new Middle Cambrian stem-group echinoderm from Spain: paleobiological implications of a highly asymmetric cinctan. Acta Palaeontologica Polonica, 53: 207–221.

____, B. LEFEBVRE, J.J. ÁLVARO, S. CLAUSEN, O. ELICKI, O. FATKA, P. JELL, A. KOUCHINSKY, J.P. LIN, E. NARDIN, and R. PARSLEY. 2013. Cambrian echinoderm diversity and palaeobiogeography. Geological Society, London, Memoirs, 38: 157–171.

Museum of Paleontology, The University of Michigan
1105 North University Avenue, Ann Arbor, Michigan 48109-1085
Matt Friedman, Director

Contributions from the Museum of Paleontology, University of Michigan is a medium for publication of reports based chiefly on museum collections and field research sponsored by the museum. Jennifer Bauer and William Ausich, Guest Editors;
Jeffrey Wilson Mantilla, Editor.

Publications of the Museum of Paleontology are accessible online at: http://deepblue.lib.umich.edu/handle/2027.42/41251

Print (ISSN 0097-3556), Online (ISSN 2771-2192)

Contributions

from the Museum of Paleontology, University of Michigan

VOL. 34, NO. 10, PP. 141-147 APRIL 27, 2022

CRINOID ANAL SAC SPINES WITH MULTIPLE PLANES OF REGENERATION: PREDATION-GENERATED FEATURES IN THE UPPER PENNSYLVANIAN OF EASTERN OHIO, USA

BY

JAMES R. THOMKA[1], HANNAH K. SMITH[2], CARLTON E. BRETT[3] AND DONALD B. EDDY[2]

Abstract — Primibrachial spines of pirasocrinid cladid crinoids that contain two discrete regeneration planes were recently described from the Upper Pennsylvanian Ames Member of the Glenshaw Formation in eastern Ohio, USA. This occurrence constitutes the first report of isolated crinoid ossicles showing evidence for repeated breakage and regeneration, most likely reflecting multiple predation attempts throughout the lifespan of single crinoid individuals. Herein we report specimens of pirasocrinid anal sac spines bearing multiple regeneration planes from the same stratigraphic interval as the previously described brachial spines. These specimens represent the first documentation of tegmen spines that were broken and began regeneration multiple times during the lifetime of an individual. The spines with multiple regeneration planes occur in an assemblage of spines that has the highest regeneration frequency of the entire Paleozoic, suggesting that pirasocrinid crinoids in eastern Ohio during deposition of the Ames Member were subjected to anomalously high (attempted) predation intensities. Additional examples of similar specimens are needed to generate an explanatory model for the unusual frequency of breakage and regeneration, but relationships between the morphology of pirasocrinid crowns and interactions with associated non-predatory organisms may be the most important factor in explaining the high regeneration frequency of crinoid spines belonging to this group during the Pennsylvanian.

INTRODUCTION

Isolated crinoid ossicles showing evidence for regeneration following breakage, generally interpreted as evidence of attempted predation (Baumiller and Gahn, 2003), remain relatively under-studied in spite of their near ubiquity in upper Paleozoic crinoid-rich units in the North American midcontinent (Syverson et al., 2018; Thomka and Eddy, 2018). Although there are numerous challenges to understanding and/or quantifying predator-prey relationships using exclusively disarticulated crinoid remains, exceptional specimens are nevertheless useful in identifying paleoecological phenomena that were previously unrecognized and providing guiding questions for future studies.

[1]Center for Earth and Environmental Science, State University of New York at Plattsburgh, Plattsburgh, New York 12901, U.S.A. (jthom059@plattsburgh.edu)
[2]Department of Geosciences, University of Akron, Akron, Ohio 44325, U.S.A. (hks15@zips.uakron.edu, dbe9@zips.uakron.edu)
[3]Department of Geology, University of Cincinnati, Cincinnati, Ohio 45221, U.S.A. (brettce@ucmail.uc.edu)

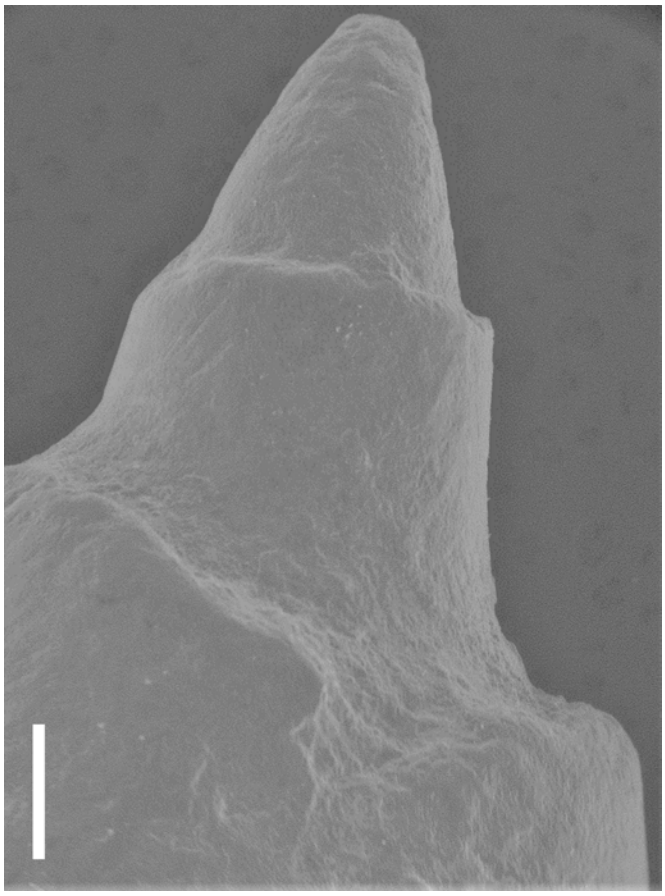

FIGURE 1 — ESEM photomicrograph of a pirasocrinid primibrachial spine with two prominent surfaces marking planes of breakage and subsequent regeneration (CMNH 9279). Thomka and Eddy (2018) reported this specimen, along with several others, from the Ames Member of the Glenshaw Formation of eastern Ohio, USA (this particular spine was depicted in Thomka and Eddy, 2018: fig. 4a). Scale bar = 1 mm.

Thomka and Eddy (2018) recently described informative primibrachial spines attributable to pirasocrinid cladid crinoids from the Upper Pennsylvanian Ames Member of the Glenshaw Formation of eastern Ohio, USA. These brachial spines were noteworthy because each specimen (five total) contained two planes of breakage and regeneration (Fig. 1), a feature not previously documented in isolated crinoid ossicles. These specimens provide unambiguous evidence that ossicles belonging to certain pirasocrinids were subjected to repeated breakage followed by partial regeneration during the lifespan of the individual. This suggests an atypically high frequency of attempted predation on pirasocrinid crinoids in the area, an interpretation that is further supported by an overall proportion of spines with evidence for regeneration that is substantially higher than that generally documented in Paleozoic spine assemblages (Syverson et al., 2018). Whereas spine regeneration frequencies typically fall within the range of 5–15% in the Paleozoic (Syverson et al., 2018), the Ames Member assemblage is characterized by an overall spine regeneration value of approximately 35% (Thomka and Eddy, 2018).

After publication of the study on Ames Member crinoid spine regeneration by Thomka and Eddy (2018), additional specimens of direct relevance have been discovered from the same stratigraphic interval. Therefore, the present report represents a supplement to Thomka and Eddy (2018), focusing on significant crinoid spines not previously described. This addendum is necessary because the initial study dealt exclusively with pirasocrinid primibrachial spines, whereas the material considered here consists of anal sac spines (Figs. 2–3). Although evidence for breakage and regeneration of pirasocrinid anal sac spines along single planes has been documented previously (e.g., Burke, 1973; Syverson et al., 2018), the presence of multiple regeneration planes on ossicles of this type has not hitherto been described. Hence, the objectives of this paper are to describe the occurrence of pirasocrinid anal sac spines with evidence of repeated regeneration and to discuss these specimens in the context of predator-prey dynamics during the late Paleozoic.

INSTITUTIONAL ABBREVIATIONS

CMNH — Cleveland Museum of Natural History, Cleveland, Ohio, USA.

MATERIALS AND METHODS

Studied material is reposited in the invertebrate paleontology collections of the Cleveland Museum of Natural History under specimen number CMNH 9211. This is a specimen lot of more than 100 isolated pirasocrinid crinoid ossicles, including anal sac spines, primibrachial spines, basal plates, and radial plates. Although some of the radials appear to belong to the genus *Plaxocrinus* Moore and Plummer 1937, the anal sac spines described here may have come from a different taxon or taxa as isolated pirasocrinid anal sac spines cannot be confidently identified to a genus (Lewis, 1974).

Specimens were collected from the Upper Pennsylvanian (Kasimovian; Missourian to Virgilian) Ames Member of the Glenshaw Formation, which is included within the Conemaugh Group. This interval comprises one of the "marine zones" within a succession of cyclothems, representing the maximum transgressive phase of the Conemaugh Group and development of shallow, open marine environments throughout eastern Ohio. The specific collection locality is a roadcut exposure along the westbound lane of OH-40 (E. Pike Rd.) in between Cambridge and Old Washington, Guernsey County, east-central Ohio, USA (N 40.03889º, W 81.39167º). The Ames Member consists of a bioturbated, fossiliferous wackestone at this locality and nearby exposures (Thomka and Eddy, 2018). An environment characterized by normal marine salinity and relatively slow sedimentation is inferred.

The collection of separated crinoid plates (CMNH 9211) was sorted by ossicle type, with anal sac spines comprising approximately one third of the specimens. All anal sac spines

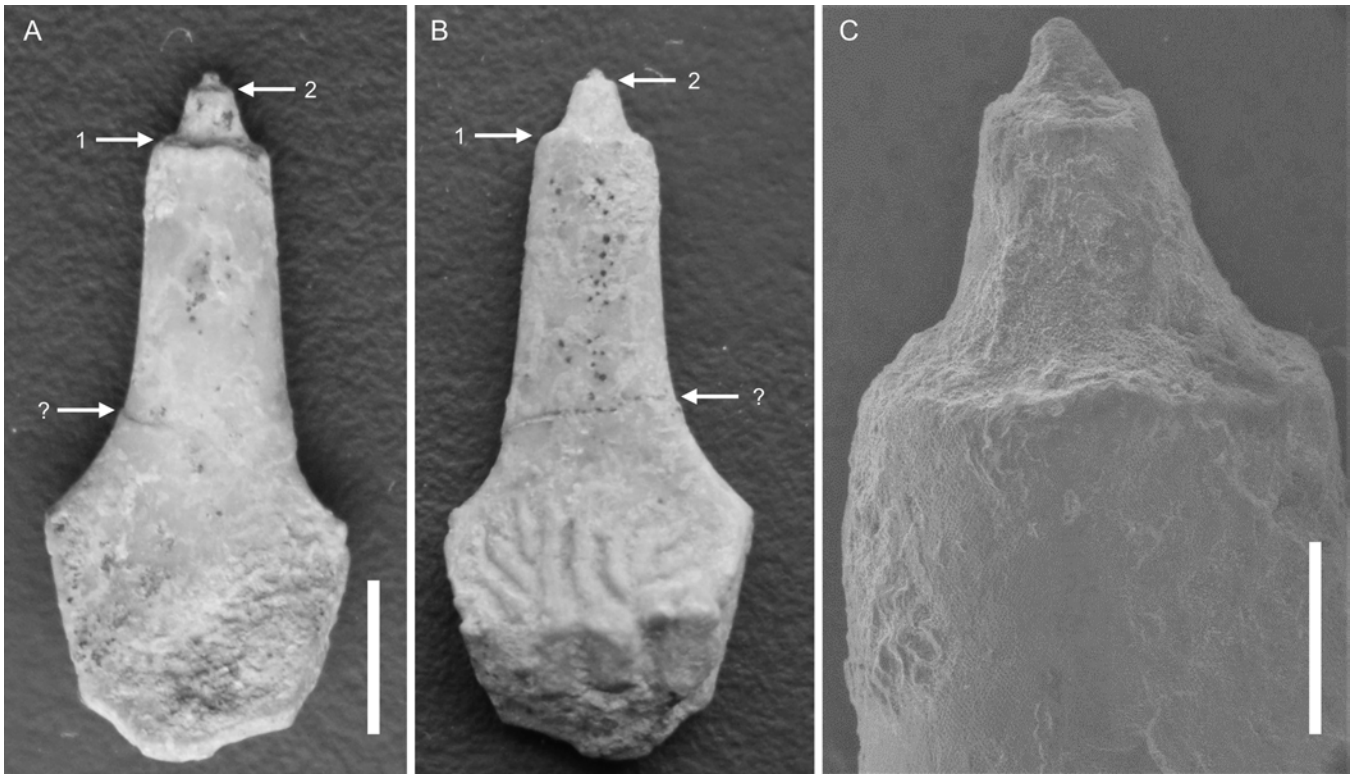

FIGURE 2 — Pirasocrinid anal sac spine (CMNH 9211-A) with multiple planes of breakage and regeneration. **A**, **B**, Upper (=ventral; A) and lower (=dorsal; B) surfaces of the entire spine with planes of regeneration marked by numbered arrows. The arrow with the question mark shows a planar feature that is most likely a fracture and not a plane of regeneration. Scale bar for both panels (shown in A) = 5 mm. **C**, ESEM photomicrograph of the distal portion of the spine showing the sharpness of the planes of breakage and regeneration. Scale bar = 1 mm.

were closely inspected for regeneration planes, and those with multiple regeneration planes were photographed using an environmental scanning electron microscope (ESEM). The ESEM permitted up to 1000x magnification, but most useful images that clearly show the regeneration planes are from 90–200x magnification; greater magnification revealed the details of surprisingly well-preserved stereomic microstructure (Thomka and Smith, 2019). Specimens required no coating for ESEM imaging to be employed.

SPECIMEN DESCRIPTIONS

Two isolated anal sac spines in CMNH 9211 display evidence of repeated regeneration in the form of two distinct planes of breakage present on each specimen (Figs. 2–3). Planes of breakage are marked by sharp discontinuities along the long axis of the spine shaft, with regenerated portions represented by sudden decreases in the diameter of spines. The regenerated portions are grown in the same direction as the unbroken parts of the spine (i.e., there has been no noticeable deflection in growth direction). Tips are relatively sharp in the distalmost portions of regenerated spines (Fig. 2C; see also Fig. 1), indicating that regeneration into a functional spine had occurred or was near completion at the time of separation from the rest of the crinoid crown (Gahn and Baumiller, 2010). There is no evidence that breakage occurred preferentially along cleavage planes in any of the specimens.

The specimen in Figure 2 (herein designated CMNH 9211-A) is slightly more than 18 mm in maximum length and is light gray in color. Two prominent planes of breakage and regeneration are present, both being relatively close to the spine tip (Figs. 2A–B). The more proximal plane is approximately 2 mm from the spine tip and is oriented perpendicular to the long axis of the spine. It is slightly irregular, with a somewhat jagged appearance, particularly on the dorsal side (Figs. 2B–C). The more distal plane is approximately 0.25 mm from the spine tip. It is oriented perpendicular to the long axis of the spine and is regular (Fig. 2C). The difference in the regularity of the regeneration planes on this spine may reflect the primary geometry of the breakage plane (i.e., the earlier event broke the spine along a more irregular plane than the later event). Alternatively, it may reflect the greater amount of regeneration associated with the earlier plane, along which spine diameter may have increased during regrowth heterogeneously rather than uniformly (see Thomka and Smith, 2019). Interestingly, there is a third planar feature at the very base of the spine shaft

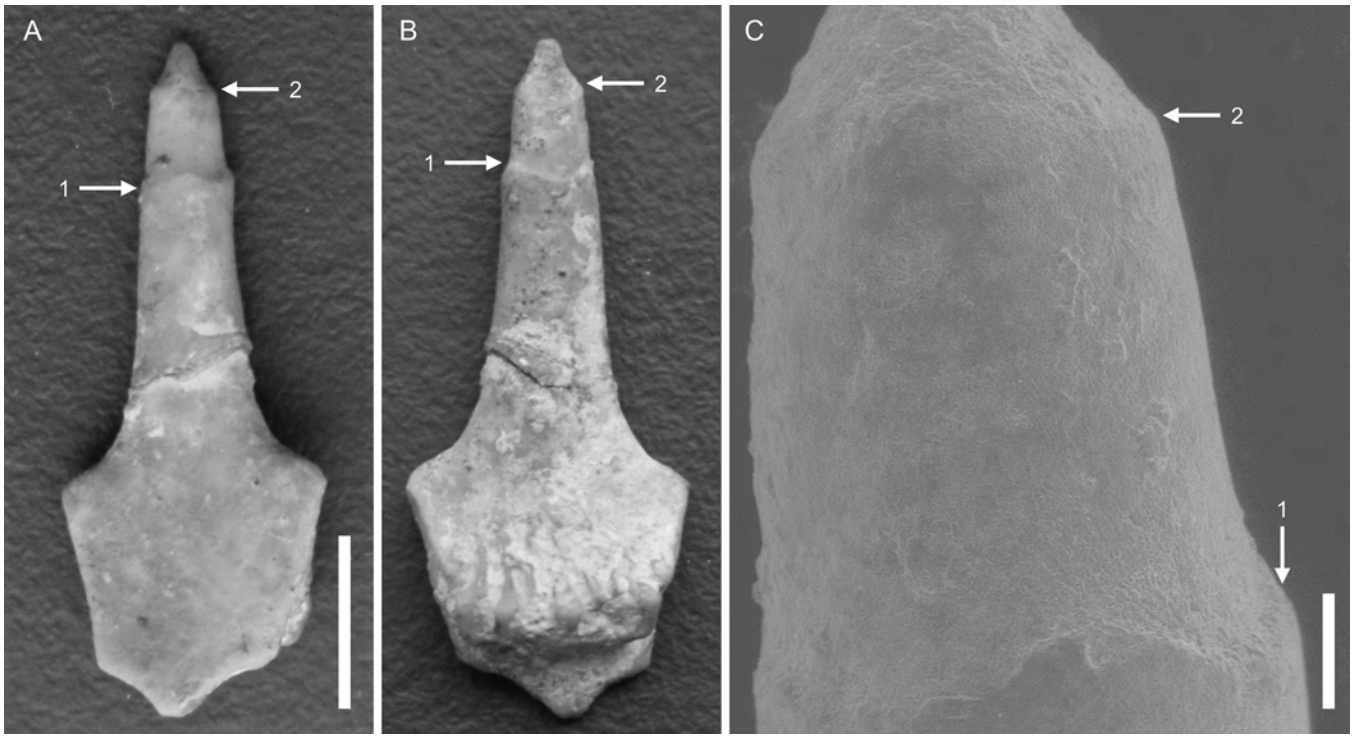

FIGURE 3 — Pirasocrinid anal sac spine (CMNH 9211-B) with multiple planes of breakage and regeneration. **A**, **B**, Upper (=ventral; A) and lower (=dorsal; B) surfaces of the entire spine with planes of regeneration marked by numbered arrows. The discontinuity running obliquely through the base of the spine is a fracture and not a third plane of regeneration. Scale bar for both panels (shown in A) = 5 mm. **C**, ESEM photomicrograph of the medial to distal portion of the spine with planes of regeneration marked by numbered arrows. Note the subtlety of the plane labeled 1, indicating that the spine had regenerated to nearly its entire pre-breakage diameter. Scale bar = 0.5 mm.

(the neck *sensu* Lewis, 1974) that is relatively subtle (marked by the question mark on Figs. 2A–B). Although there appears to be a small offset in spine diameter across this surface (Fig. 2A), this plane does not appear to be a regeneration plane and is more likely a fracture (Fig. 2B) that was produced after death of the crinoid.

The specimen in Figure 3 (herein designated CMNH 9211-B) is slightly less than 20 mm in maximum length and is purplish-brown in color. Two planes of regeneration are present, one being relatively subtle and the other being more prominent. Both planes are oriented roughly perpendicular to the long axis of the spine. The more proximal plane is located approximately 4 mm from the spine tip and is the subtler plane (Figs. 2A–B). As with the spine described above, this earlier plane of regeneration is somewhat irregular and jagged (Figs. 2A–B) and, as above, it is unclear whether this is the result of an irregular plane of breakage or heterogeneity along the re-growth margin. There is little difference in spine diameter across this plane (in contrast to both planes in the other specimen; Fig. 2), suggesting that the spine had nearly returned to its pre-breakage diameter. The more distal plane of regeneration is located 1 mm from the spine tip and is characterized by a more dramatic change in spine diameter (Fig. 3C). However, the most proximal portion of the spine regenerated from this plane appears somewhat tapered toward the spine tip rather than occurring as an immediate shift to a lower-diameter section (Fig. 3C).

In all cases, the more proximal regenerated portion is characterized by a larger diameter than the more distal regenerated portion (Figs. 2–3). This indicates that the regenerating portion of a broken spine had not yet reached its original (pre-breakage) diameter before a distal portion of the regenerating spine was, itself, broken. It is therefore indisputable that (at least) two distinct events occurred to the ossicles described here that resulted in intraplate breakage without resulting in death of the crinoid or diminished regenerative capacity of the spine.

DISCUSSION

The features described here indicate that pirasocrinid anal sac spines were broken and (at least partially) regenerated more than once during the lifespan of the crinoid from which they came. Predatory attacks, most likely by fishes, are widely accepted as the most likely cause of this style of damage to late Paleozoic crinoids, at least when occurring in association with single regeneration planes (Burke, 1973; Meyer and Ausich, 1983; Brett and Walker, 2002; Baumiller and Gahn, 2003;

Brett, 2003; Syverson et al., 2018; Thomka and Eddy, 2018), although cephalopods cannot be definitively ruled out as the cause of breakage. Several potentially durophagous fishes that could have served as the predators responsible for the broken spines are known from the Ames Member, so fish are herein considered as the most likely candidates. Post-breakage regeneration unambiguously demonstrates that the recorded predation attempts were non-lethal to the crinoids, with the individual surviving long enough to begin spine regrowth, but being damaged again before the regenerating portion of the spine could return to its full pre-breakage diameter.

Individual crinoid ossicles, in the form of pirasocrinid primibrachial spines, that contained multiple planes of regeneration were first described by Thomka and Eddy (2018). The occurrence of additional spines from a different part of the crinoid skeleton, described here, indicate that the phenomenon of repeatedly regenerated spines is not unique to the previously described specimens. However, to date, ossicles with multiple planes of breakage and regeneration have only been reported from pirasocrinids from the Ames Member of the Glenshaw Formation of eastern Ohio—representing the same stratigraphic unit, geographic area, and crinoid family that were initially described.

The restriction of spines with multiple regeneration planes to the Ames Member of the Glenshaw Formation in eastern Ohio is difficult to explain, as pirasocrinids are widespread and abundant in Upper Pennsylvanian marine strata of North America (Holterhoff, 1997; Webster, 2018), and isolated pirasocrinid ossicles, including brachial and anal sac spines, are common bioclasts in many marine sedimentary deposits of this age. This may be the result of specimens from other localities simply being overlooked in existing collections. This does not appear to be a sufficient explanation by itself, however, as the relatively comprehensive study of cladid crinoid spines by Syverson et al. (2018), which evaluated hundreds of pirasocrinid spines from throughout the North American midcontinent, including collections from similar depositional environments to the Ames Member, did not yield specimens with multiple regeneration planes. Further, the high overall frequency of regeneration planes in pirasocrinid spines from the Ames Member in eastern Ohio—35% (Thomka and Eddy, 2018), which is more than double the typical frequency for Pennsylvanian crinoids (Syverson et al., 2018)—indicates that predation intensity may have truly been unusually high in this region. The state of preservation of spines from the Ames Member is not spectacular and is identical to the spines studied by Syverson et al. (2018), so taphonomy does not appear to be a factor. More information is needed to resolve this issue.

The restriction of spines with multiple regeneration planes to this single cladid family may be related to certain morphological aspects of pirasocrinids. First, pirasocrinids are among the most spinose of crinoids to have ever evolved (Lewis, 1974; Syverson et al., 2018). With numerous spines on each arm in addition to a radial array of spines atop the hypertrophied, mushroom-shaped anal sac (Lewis, 1974; Thomka and Eddy, 2018: fig. 1), a large number of spines are present on each pirasocrinid individual. Rare or unusual features of isolated spines belonging to pirasocrinids may be more likely to be discovered simply because of the sheer number of spines that can be collected from deposits that contain a rich pirasocrinid fauna. However, as also noted above, such specimens were not identified among the Pennsylvanian cladid crinoid spine assemblages studied by Syverson et al. (2018).

Biotic interactions may play a more important role in explaining the high pirasocrinid spine breakage values. Thomka and Eddy (2018) outlined the morphological and ecological factors that relegated pirasocrinids to the category of relatively poor prey items compared to co-occurring and/or common and coeval crinoid taxa—but taxa that were nevertheless subjected to frequent predation attempts. Pirasocrinids themselves do not make sense as targets of intense predation; for example, the large size of anal sacs was attained primarily through addition of roofing plates, spines, and intercalated, spine-bearing tegmen plates rather than expansion of the interior cavity of the tegmen. The hypertrophied anal sac may have assisted with respiration but did not appear to house an unusually voluminous or nutritious gonadic payload (Lewis, 1974; Lane, 1984). Rather, the most logical explanation for this apparent paradox is that the pirasocrinids were not the actual intended target and that associated organisms that were interacting with the pirasocrinids, specifically in the region of their crowns, were the true targets of predation (see Brett and Walker, 2002; Brett, 2003; Syverson et al., 2018; Thomka and Eddy, 2018).

It has been suggested that attacks on late Paleozoic crinoids may have involved non-lethal predation on expendable anal sacs and their contained gonads (Lane, 1984) followed by regeneration. The occurrence of repeatedly regenerated anal sac spines in these pirasocrinids, however, indicates that, at least in these cases, the anal sacs were retained through repeated predation attempts. As a corollary of the model of secondary targeting (Syverson et al., 2018; see also Brett, 2003), we suggest another variant of predatory behavior, non-lethal to the crinoids. Attacks on commensals, parasites, or organisms involved in some other form of association with the crinoids may actually have been successful without causing death of the crinoids, which may have encouraged repeated foraging on host crinoids. While these attacks were somewhat deleterious to crinoid hosts (via broken spines and perhaps other collateral damage), they could have been largely innocuous, or even beneficial to some extent if antagonistic organisms were removed without significant damage to the crinoid. Thus, the high frequency of attacks on pirasocrinids may involve their propensity to attract associated symbionts and/or epifauna.

For Devonian and Mississippian crinoids, it has been postulated that the known association of platyceratid gastropods with particular host crinoids increased the frequency of attacks on the hosts and may have driven an evolutionary response in the form of increasing spinosity through time; evidence for this hypothesis lies in the non-random association of platyceratid hosts and evolution of

spinosity (Brett, 2003; Syverson et al., 2018; Thomka and Brett, 2021). Although pirasocrinids have not yet been found in association with platyceratids in the Ames Member, three factors must be considered when evaluating the secondary targeting hypothesis in this instance. First, pirasocrinid crowns disarticulate rapidly after death, making them among the most likely of Pennsylvanian crinoid morphotypes to be discovered exclusively as isolated ossicles (Thomka et al., 2012). This would obscure the evidence for association with a platyceratid unless the attached gastropod shell managed to hold identifiable cup plates together. Second, platyceratids are known to infest Pennsylvanian stellarocrinid crinoids (e.g., Strimple and Moore, 1971: pls. 18.5, 19.4), which are similar in morphology to pirasocrinids in having spinose brachials and a spinose tegmen capped by a radiating set of anal sac spines. Hence, it is not unreasonable to infer that pirasocrinids were at least capable of serving as hosts to platyceratids, although this association has not been confirmed. Third, a preliminary assessment of evidence for biotic interactions recorded on isolated cup plates from the Ames Member showed that 50.0% of pirasocrinid ossicles (33 out of 66 specimens) had encrusters, borings/embedment structures, short slashes, and/or meandering bioerosion structures. This value was higher than that for co-occurring, moderately spinose catacrinids (33.3%, 11 out of 33 specimens) and non-spinose cromyocrinids (24.6%, 49 out of 199 specimens). An abundance of specimens bearing such features is consistent for pirasocrinids described from other Pennsylvanian localities (Pabian et al., 1997; Pabian and Rushlau, 2002). Hence, despite the absence of a definitive association with platyceratids, pirasocrinids may have been subjected to secondary targeting. Modern crinoids serve as hosts to large numbers of commensals and parasites, including annelids, arthropods, ophiuroids, and cnidarians (e.g., Meyer and Ausich, 1983; Zmarzly, 1984; Fabricius and Dale, 1993), many of which are entirely soft-bodied, lightly mineralized, or not tightly associated with the crinoid and, therefore, incapable of leaving a robust record of the interaction. It is quite probable that Paleozoic crinoids similarly harbored symbionts and faunal associates, which could have provided a ready food source for swimming predators. At present, however, this must remain a hypothesis pending evidence of such interactions.

In a larger sense, the discovery of pirasocrinid anal sac spines that were broken and at least partially regenerated more than once during the lifespan of the associated crinoid individual demonstrates that the specimens described by Thomka and Eddy (2018) were more than isolated anomalies. At least within the Ames Member and at least among pirasocrinid cladids, spines present on crinoid crowns were being broken repeatedly. Further, given the fact that at least one plane of breakage that occurred earlier in the life history of the crinoid was relatively subtle due to attainment of near-pre-breakage spine diameter, it is worthwhile to consider the number of former planes of breakage that cannot be recognized in the fossil record due to full regeneration of missing portions of the spine in areas of less frequent non-fatal breakage. The number of episodes of breakage determined from analysis of partially regenerated Paleozoic crinoid spines must be an under-estimation, although the extent to which this influences estimates of predatory attacks on crinoids is not known and may not be significant. Careful attention to separated crinoid ossicles, which are commonly overlooked in favor of articulated material, is needed to provide additional information on the spatio-temporal and taxonomic distributions of this phenomenon and, perhaps more importantly, on the underlying cause(s) for this biotic interaction.

ACKNOWLEDGEMENTS

This contribution is dedicated to the illustrious career of Tomasz K. Baumiller, whose work on predation upon crinoids and regeneration of portions of the crinoid skeleton has been invaluable to our research. We thank W. Ausich (Ohio State University) and J. Bauer (University of Michigan Museum of Paleontology) for initiating, organizing, and editing this special volume. Access to studied specimens was provided by J. Hannibal and D. Dunn of the CMNH. T. Quick (University of Akron) ran the scanning electron microscope and assisted with obtaining some of the images in this study. Previous versions of this article were significantly improved by the constructive reviews provided by D. Meyer (University of Cincinnati), V. Syverson (Clovis Community College), and the editors.

LITERATURE CITED

BAUMILLER, T. K., and F. J. GAHN. 2003. Predation on crinoids. In P. H. KELLEY, M. KOWALEWSKI, and T. A. HANSEN (eds.), Predator-Prey Interactions in the Fossil Record, Kluwer Academic/Plenum Publishers, New York, pp. 263–278.

BRETT, C. E. 2003. Durophagous predation in Paleozoic marine benthic assemblages. In P. H. KELLEY, M. KOWALEWSKI, and T. A. HANSEN (eds.), Predator-Prey Interactions in the Fossil Record, Kluwer Academic/Plenum Publishers, New York, pp. 401–432.

_____, and S. E. WALKER. 2002. Predators and predation in Paleozoic marine environments. In M . KOWALEWSKI and P. H. KELLEY (eds.), The Fossil Record of Predation. Paleontological Society Papers 8, pp. 93–118.

BURKE, J. J. 1973. Four new pirasocrinid crinoids from the Ames Limestone, Pennsylvanian, of Brooke County, West Virginia. Annals of the Carnegie Museum, 44: 157–169.

FABRICIUS, K. E., and M. B. DALE. 1993. Multispecies associations of symbionts on shallow water crinoids of the central Great Barrier Reef. Coenoses, 8: 41–52.

GAHN, F. J., and T. K. BAUMILLER. 2010. Evolutionary history of regeneration in crinoids (Echinodermata). Integrative and Comparative Biology, 50: 514a–514m.

HOLTERHOFF, P. F. 1997. Paleocommunity and evolutionary

ecology of Paleozoic crinoids. In J. A. WATERS and C. G. MAPLES (eds.), Geobiology of Echinoderms. Paleontological Society Papers 3, pp. 69–106.

LANE, N. G. 1984. Predation and survival among inadunate crinoids. Paleobiology, 10: 453–458.

LEWIS, R. D. 1974. Studies in the inadunate crinoid family Pirasocrinidae. Unpublished M. S. thesis, University of Iowa, Iowa City, 181 pp.

MEYER, D. L., and W. I. AUSICH. 1983. Biotic interactions among Recent and among fossil crinoids. In M. J. S. TEVESZ and P. S. MCCALL (eds.), Biotic Interactions in Recent and Fossil Benthic Communities, Plenum Press, New York, pp. 377–427.

MOORE, R. C., and F. B. PLUMMER. 1937. Upper Carboniferous crinoids from the Morrow Subseries of Arkansas, Oklahoma and Texas. Denison University Bulletin, Journal of the Scientific Laboratories, 32: 209–303.

PABIAN, R. K., and W. J. RUSHLAU. 2002. Taphonomic analysis and systematic descriptions of some Late Pennsylvanian and Early Permian crinoids from southeastern Nebraska, eastern Kansas, and southwestern Iowa. Nebraska Geological Survey Papers, 20: 1–45.

_____, D. MOSHER, R. D. LEWIS, and P. F. HOLTERHOFF. 1997. Prey-predator, parasitic, and commensal relationships with Late Pennsylvanian crinoids and associated fauna from the Barnsdall Formation (Late Pennsylvanian, Missourian/Virgilian) of northeastern Oklahoma. Proceedings of the Nebraska Academy of Sciences, 107: 49.

STRIMPLE, H. L., and R. C. MOORE. 1971. Crinoids of the LaSalle Limestone (Pennsylvanian) of Illinois. University of Kansas Paleontological Contributions, 55: 1– 48.

SYVERSON, V. J., C. E. BRETT, F. J. GAHN, and T. K. BAUMILLER. 2018. Spinosity, regeneration, and targeting among Paleozoic crinoids and their predators. Paleobiology, 44: 290–305.

THOMKA, J. R., and C. E. BRETT. In press. Parasitism of Paleozoic crinoids and related stalked echinoderms: Paleopathology, ichnology, coevolution, and evolutionary paleoecology. In K. DE BAETS and J. W. HUNTLEY (eds), The Evolution and Fossil Record of Parasitism: Coevolution and Paleoparasitological Techniques, Springer, Berlin, pp. 289-316.

_____, and D. B. EDDY. 2018. Repeated regeneration of crinoid spines in the Upper Pennsylvanian of eastern Ohio: Evidence of elevated predation intensity and significance for predator-driven evolution of crinoid morphology. Palaios, 33: 508–513.

_____, and H. K. SMITH. 2019. Stereomic microstructure of crinoid spine regeneration: Examples from the Upper Pennsylvanian of eastern Ohio. Geological Society of America Abstracts with Programs, 51.

_____, D. MOSHER, R. D. LEWIS, and R. K. PABIAN. 2012. The utility of isolated crinoid ossicles and fragmentary crinoid remains in taphonomic and paleoenvironmental analysis: An example from the Upper Pennsylvanian of Oklahoma, USA. Palaios, 27: 465-480.

WEBSTER, G. D. 2018. Mississippian-Permian evolution and paleogeographic distribution of the Cromyocrinidae and Pirasocrinidae (Crinoidea, Dendrocrinida). Swiss Journal of Palaeontology, 137: 265–278.

ZMARZLY, D. L. 1984. Distribution and ecology of shallow-water crinoids at Enewetak Atoll, Marshall Islands, with an annotated checklist of their symbionts. Pacific Science, 38: 105–122.

Museum of Paleontology, The University of Michigan
1105 North University Avenue, Ann Arbor, Michigan 48109-1085
Matt Friedman, Director

Contributions from the Museum of Paleontology, University of Michigan is a medium for publication of reports based chiefly on museum collections and field research sponsored by the museum. Jennifer Bauer and William Ausich, Guest Editors;
Jeffrey Wilson Mantilla, Editor.

Publications of the Museum of Paleontology are accessible online at: http://deepblue.lib.umich.edu/handle/2027.42/41251

Print (ISSN 0097-3556), Online (ISSN 2771-2192)

Contributions

from the Museum of Paleontology, University of Michigan

VOL. 34, NO. 11, PP. 148–157 APRIL 27, 2022

FISH PREDATION ON *CLYPEASTER HUMILIS* FROM THE RED SEA: POTENTIAL FOR RECOGNITION IN THE FOSSIL RECORD

BY

JAMES H. NEBELSICK[1] AND ANDREA MANCOSU[2]

Abstract — Fish predation on *Clypeaster humilis* produces characteristic traces on the test. The predatory attacks are lethal, removing much of the oral surface and exposing the internal organs of the animal. There are various stages of test removal, generally expanding from the peristome to the ambitus. In some cases, the wound can be highly irregular and even extend to the aboral surface. In a few instances, accompanying scratch marks are found on the oral surface. In others, discrete indentations can be correlated to bite marks at the rim of the wound. Intraplate fragmentation is mostly prevalent, though interplate breakage along plate boundaries also occurs. Intraplate fragmentation often results in oblique breakage planes reaching toward the oral surface. The potential for recognizing such events in the fossil record depends on the preservation of these specific features. The described predation events can compromise the fossilization potential of such traces unless rapidly buried or encrusted by bioinfestation.

INTRODUCTION

Recognizing predation events in the fossil record is an important tool for studying synecological interactions through time (e.g., Walker and Brett, 2002; Huntley and Kowalewski, 2007; Klompmaker et al., 2019). Detecting these interactions, however, can be problematic as the act of predation itself is inherently destructive. Predation events on skeletonized organisms lead not only to the death of the prey, but also to the demolition of protective or associated hard parts (e.g., Nebelsick, 1999a). This circumstance thus compromises the potential recognition of these events in folssil ecosystems, as well as affecting the completeness of the fossil record as a whole, because predation is pervasive in most ecosystems.

Gastropod predation on invertebrates leave neat round holes that may or may not affect the preservation potentials of the shelly remains (e.g., Nebelsick and Kowalewski, 1999; Grun et al., 2014; Harper, 2016; Farrar et al., 2020),

[1]Department of Earth Sciences, University of Tübingen, Schnarrenbergstraße 94-96, 72076 Tübingen, Germany (nebelsick@uni-tuebingen.de).

[2] Dipartimento di Scienze Chimiche e Geologiche, Università degli studi di Cagliari, “Citadella Universitaria di Monserrato, 09127, Cagliari, Italy (andrea.mancosu@gmail.com).

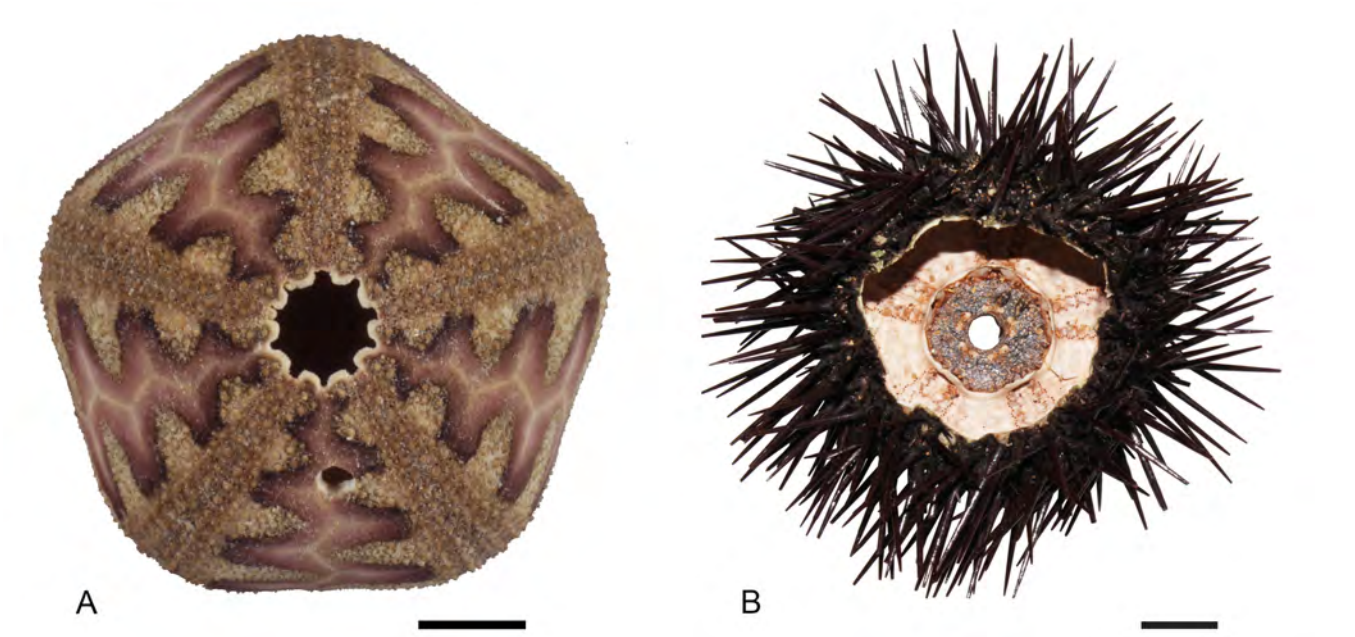

FIGURE 1 — Comparison of predation scars from gastropod and fish predation. **A**, Predatory gastropod bore hole on the regular echinoid *Microcyphus rousseaui* from the Northern Bay of Safaga, Red Sea. The round bore hole is clearly placed within an interambulacral plate row, which in this species is largely devoid of tubercles (Sample JS87-162) **B**, Predation by sparid fish removing the aboral surface of *Paracentrotus lividus*. Spines and peristomal membrane are still preserved indicating a recent predation event. Mediterranean Sea, Torre del Porticciolo, Sardinia (TP-PL-001). Scale bars = 1 cm.

predation by durophagous organisms is usually destructive. The resulting damage to the skeleton may be difficult to differentiate with respect to specific predators as well as from other destructive taphonomic processes such as fragmentation resulting from transport and sediment agitation. Furthermore, such massive wounds potentially weaken the skeletons such that the predated-upon skeletons have poorer preservation potentials. Gastropod predation on echinoids has been studied with respect to changes through deep time (e.g., Kowalewski and Nebelsick, 2003; Farrar et al., 2020; Petsios et al., 2021; and literature therein). Predation by other predators including fish, crustaceans, birds, and mammals can also be common (e.g., Estes et al., 1978; Andrew and MacDiarmid, 1991), although they have received comparatively little attention with respect to their preservation in the fossil record (see Belaústegui et al., 2017). There have been a few specific actualistic studies on predator-prey interactions on echinoids with respect to their preservation potentials besides those concerning gastropods including investigations involving shorebirds, stingrays, and bony fish (Sievers et al., 2014; Grun, 2016; Sievers and Nebelsick, 2018). Variations in the wounds found on sea urchins are consistent with the different types of predators that attack echinoids (see Fig. 1). The degree to which predatory attacks can be recognized and attributed to specific predators depends on the careful analysis of not only wound morphologies but also of the architecture of the prey skeletons.

In the echinoid fossil record, reports of predation on echinoids is again dominated by gastropod drilling in the form of drill holes (see literature in Złotnik and Ceranka, 2005; Meadows et al., 2015; Grun et al., 2017; Farrer et al., 2020; Petsios et al., 2021). Publications concerning other types of predation on echinoids are less common and have been restricted to fish predation on regular echinoid spines and tests (Borszcz and Zatoń, 2013; Wilson et al., 2015) and predation on echinoids from marine reptiles (Neumann and Hampe, 2018). The preservation potential of echinoids is influenced by a wide range of factors (e.g., Allison, 1990; Donovan, 1991; Kidwell and Baumiller, 1990; Greenstein, 1991; Kowalewski et al., 2018; Nebelsick and Mancosu, 2021). Although durophagous predation may be intuitively destructive, Kidwell and Baumiller (1990) showed in tumbling experiments on regular echinoids that collagenous ligaments continue to connect test plates after death until they fully decay. Breakage crossing plate boundaries thus does not necessarily imply predation events. In addition, some predation events have shown to enhance preservation potentials (Tyler et al., 2018).

In this study, predation by fish on a recent clypeasteroid echinoid, *Clypeaster humilis* (Leske, 1998) from the Red Sea, is described with respect to the wounds and potential recognition in the fossil record. *Clypeaster humilis* is a common Indo-Pacific echinoid in shallow water carbonate sediments typically reaching lengths of 5 to 8 cm (Clark and Rowe, 1971; Nebelsick 1992a, b, 1995b, c, 2008; Nebelsick and Kampfer, 1994). As a clypeasteroid, it has a flattened test with a prominent petalodium on the aboral side containing modified respiratory ambulacral tube feet (Fig. 2). The oral

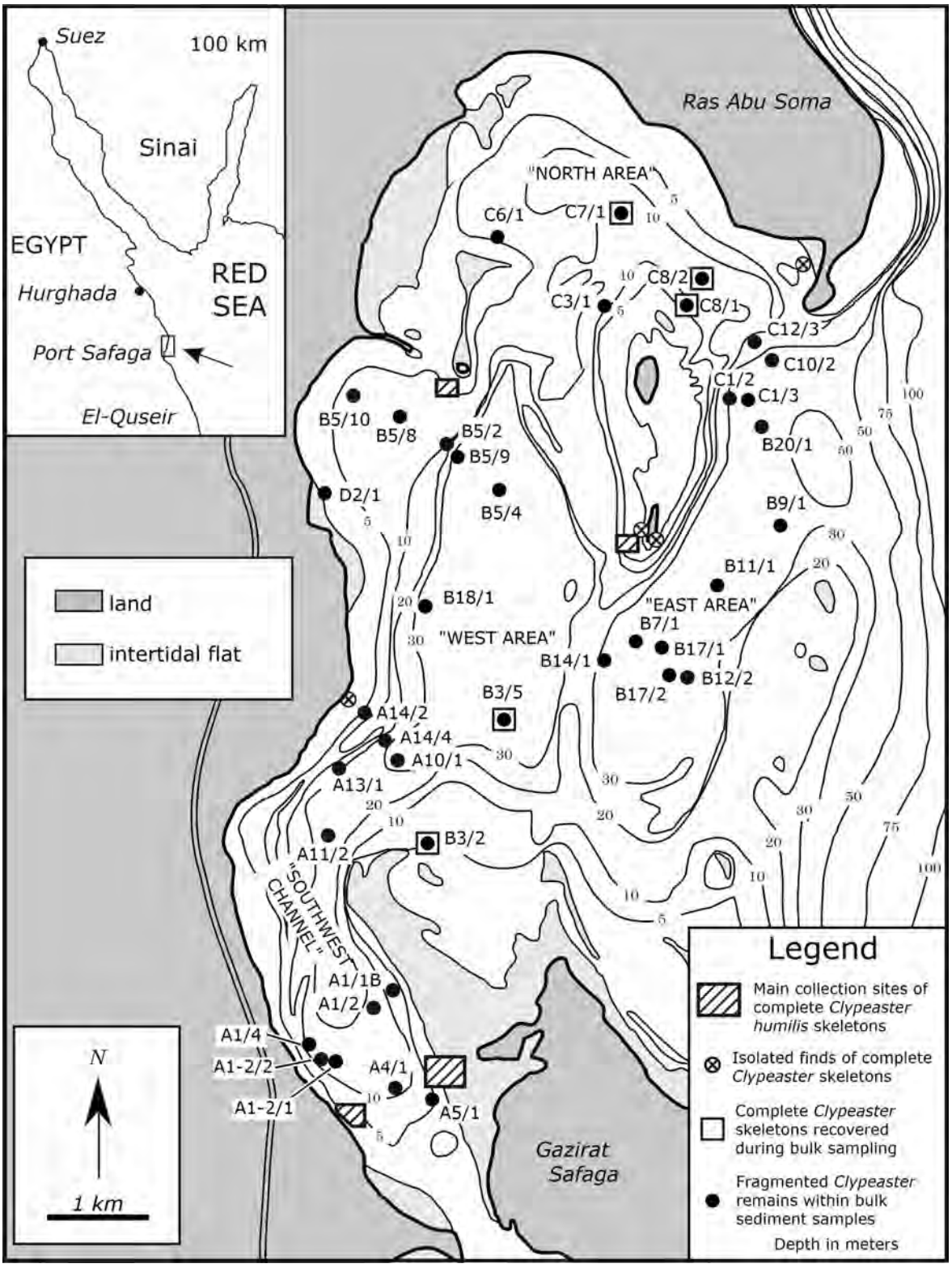

FIGURE 2 — Northern Bay of Safaga, Egypt showing 4 main areas of collection of *Clypeaster humilis* specimens. Specimens found separately as well as those recovered during bulk sampling are also indicated. In addition, bulk samples containing *Clypeaster* fragments are shown.

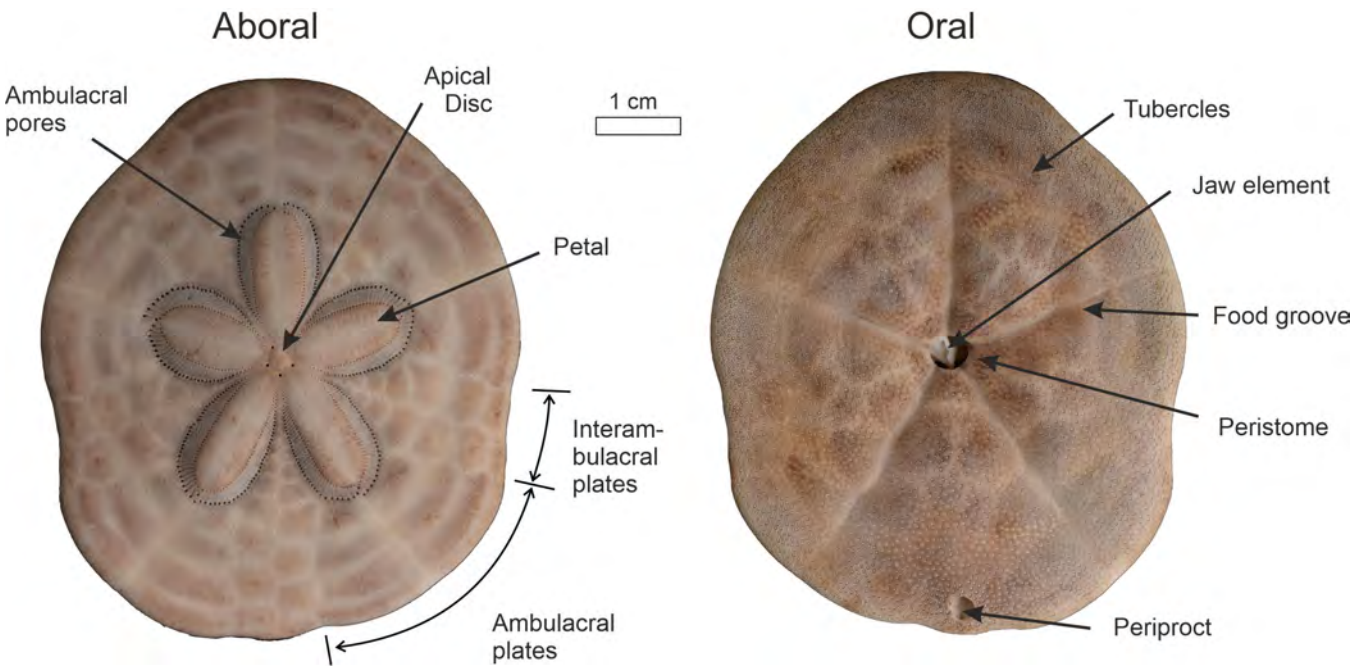

FIGURE 3 — *Clypeaster humilis* from the Northern Bay of Safaga, Red Sea, Egypt. Scale bar = 1 cm. **A** and **B**, Complete, well preserved tests showing plate boundaries and tuberculation. Note that slightly differential length of the left- and right-hand side of the test. The aboral side **A**, shows the central apical system and five petals of the petalodium containing the ambulacral pores in which the modified respiratory tube feet are found during life. The oral side. **B**, shows the centrally positioned mouth (peristome), the posterior anus (periproct) and straight food grooves leading to the mouth. Elements of the jaw apparatus are just visible within the peristome. Sample RS-CL2/13.

side of the test is characterized by a central peristome, posteriorly placed periproct, and straight food grooves leading to the mouth. The external test surface is covered by small tubercles that support the spines. The test is stabilized by internal supports that conjoin the oral and aboral sides consisting of more central pillars and peripheral supports near the ambitus. For a detailed morphological description of test features in *Clypeaster* see Durham (1966) and Mihaljević et al. (2011).

MATERIAL AND METHODS

Clypeaster humilis is a shallow burrower living just underneath the sediment surface. This species belongs to the most widely distributed irregular echinoids in shallow environments of the Red Sea (Clark and Rowe, 1971). Distribution and taphonomy of echinoid remains in general and their correlation to sediment parameters within the Northern Bay of Safaga, Egypt (26°48'9.46"N, 33°58'11.64"E) was analyzed in detail by Nebelsick (1992a, b, 1995a, c). *Clypeaster* is the most widely distributed echinoid genus in the study area (Fig. 3). Three species of *Clypeaster* were recognized in the Northern Bay of Safaga, Egypt, which were totally dominated in shallow water by *Clypeaster humilis*. Rare examples of *Clypeaster fervens* Koehler, 1922 were restricted to deeper water, while only few dead tests of *Clypeaster reticulatus* (Linnaeus, 1758) were recovered. The taphonomy of complete tests as well as fragments of *Clypeaster* has also been studied (see Nebelsick and Kampfer, 1994; Nebelsick, 1999a, c, 2008). Nebelsick (1999c) showed the distribution of taphofacies based on *Clypeaster* fragments and correlated the preservation styles (abrasion, interplate fragmentation, and encrustation) to environmental factors such as exposure and surface residence times. Finally, Nebelsick (2008) recognized a taphonomic gradient from: 1) tests still retaining spines; to 2) well preserved, denuded tests; 3) tests showing initial abrasion of tubercles and loss of the apical discs; 4) highly abraded, encrusted and bioeroded tests; and finally 5) highly corroded tests that could just be recognized as belonging to the genus *Clypeaster*.

Clypeaster humilis was common throughout the study area in shallow coarse sands, as well as in small sand patches within seagrass meadows and within sand veneers on reef flats (Fig. 3). Living specimens were found either completely or slightly covered by sediment. Numerous tests and fragments were recovered during scuba diving trips conducted in order to collect sediment cores as well as samples of micro- and macrofauna. Living specimens were collected following visual identification of their outlines if shallowly buried, or recovered by raking the sediment by using a modified rake revealing densities of ca 1.5 to 2 specimens/m^{-2}. The main areas where complete specimens of *Clypeaster humilis* were

FIGURE 4 — Oral views of predated specimens of *Clypeaster humilis*. **A**, Massive wound restricted to the central area of the oral surface. Internal supports surrounding the petals are broken. The wound is dominated by intraplate fragmentation. The remaining oral surface is well preserved as well as the internal surface of the aboral surface with a slight encrustation by coiled serpulid worm tubes (JS87-321). **B**, Wound dominated by intraplate fragmentation with slanting surfaces. The remaining well-preserved oral surface has some marks (upper right) that could be interpreted as tooth marks. The wound reaches the ambitus on the left-hand side revealing the marginal buttresses that are present near the edge of the test (JS87-318). **C**, Poorly preserved test surface showing abrasion of tubercles and high irregular wound showing indentation (JS87-312). **D**, Specimen showing almost complete removal of the oral surface with breakage predominantly along plate edges (JS87-230). **E**, Highly irregular wound reaching the ambitus. The test surface and interior show encrustation by serpulids (JAE-45). **F**, Larger fragments showing broken oral surfaces which resemble wound found on more complete tests (West Safaga Island).

collected (Fig. 3) were screened for predation scars and compared with respect to the position and the extent of the wound, as well as details of the wound borders.

WOUND MORPHOLOGY

All specimens were collected on and in the sediment surface in the Northern Bay of Safaga. The predation events were never observed, despite numerous (daytime) scuba dives in the environments in which dead tests were collected. All predation events represent lethal attacks as the prey was eviscerated removing the internal organs and jaw apparatus. Predation events were recorded on tests showing a wide range of taphonomic grades (see Nebelsick, 2008) from echinoids still retaining spines, to denuded, well preserved tests, to tests with slight abrasion and encrustation. Heavily abraded tests show few such predation events.

The wounds are mostly restricted to the oral surface, the

peristome is not preserved. Successive stages of destruction are shown by the wounds (see Fig. 4) including: 1) A large central oral wound, removing a number of both ambulacral and interambulacral plates (Fig. 4A). Internal interambulacral pillars that abut the ambulacral petals are destroyed such that only the top halves of these pillars attached to the aboral side of the test are still present. 2) More extensive wounds extend toward the test rim exposing the marginal buttresses that run parallel to the ambitus (Figs. 4B, D, E, F, 5). The periproct, which is adjacent to the posterior rim of these sea urchins, can also be included or fully removed in this stage. 3) Damage extending beyond the oral surface to the aboral side of the test (Figs. 4C, 5). These are intervening stages between those listed above; and, in some cases, the wounds are quite irregular in shape. The wound borders are dominated by intraplate fractures, though interplate fracturing can also occur.

These wounds can be accompanied by the following features: 1) Shallow scratch marks up to 1 mm wide up and 5 mm long can faintly be discerned in a few examples (Fig. 5). These marks radiate away from the wound rim toward the ambitus and are only present on those surfaces in which areas are still intact. 2) The wound borders not only have intraplate fragmentation, but also reveal common highly oblique fracture surfaces that are visible on the outside of the test (Fig. 5). 3) Some highly irregular wound outlines have constrained indentations of skeletal removal extending from the wound toward the ambitus (Figs. 4B, C, E, F, 5). In some cases, these indentations occur along interambulacral plate rows.

Following the above-mentioned characteristics, wound damage can also be recognized in larger fragments representing broken *Clypeaster* tests (Fig. 4F). These fragments also have interplate fragmentation of the oral surface and more completely preserved aboral surfaces. Scratch marks on *Clypeaster* fragments from the study area have already been reported by Nebelsick (1999c).

INTERPRETATION AS FISH PREDATION

Based on the size and morphology of the wound, the cause of this type of test damage is very likely due to fish predation. A large number of fish species are known to prey on echinoids, and they play an important role in controlling sea urchin populations and further ramification for herbivory and bioerosion (see review in Sievers and Nebelsick, 2018; Nebelsick, 2020).

Similar wound morphologies are described and figured by Kier and Grant (1965: pl. 15, fig. 8) on the Caribbean *Clypeaster subdepressus* (Gray, 1825), which is larger than the *Clypeaster humilis* specimens studied herein, but similar in having a flattened test and an endobenthic lifestyle. The authors report (Kier and Grant, 1965: p. 55) that "Several dead tests of *Clypeaster subdepressus* were collected, in which the ventral surface was almost completely excavated, and the remaining rim marked by numerous short radiating scratches…The organism that preyed upon the urchin was not observed, but presumably it was a fish."

In Indo-Pacific reefal environments, Fricke (1971, 1974, 1975) analyzed the ethology of predator-prey relationship involving labrids and triggerfish prey on regular echinoids. Detailed accounts of hunting and handling techniques are given along with the observation that these fish hunt infaunal prey by blowing away the sediment. Fricke (1971) described how labrids carry regular echinoids in their mouths to rocky substrates where the prey is smashed open, whereas trigger fish snip off the spines of diademed echinoids, before the fish plunge into the test exposing the inner organs. The echinoid tests are completely consumed, leaving a pile of broken spines behind. Opened sea urchins then attract numerous fish other than the few species that are able to open the specimen.

By studying gray triggerfish feeding on *Mellita, Leodia,* and *Encope* in the Gulf of Mexico, Frazer et al. (1991) described in detail the hunting procedures and resulting damage on sand dollars. Foraging behavior with the fish directing a jet of water at the sand with enough force to reveal the sand dollars. The edge of the prey item is exposed by repeated jetting action. The triggerfish then dart in and grasps the sand dollar between the teeth releasing it 2m off the sediment surface. If the sand dollar does not land on its oral surface, the process is repeated. With jaws closed, the triggerfish crushes the center of the overturned sand dollar consuming the soft tissues in the damaged area. The feeding action is then modified in order to access remaining tissue along irregular edges of the broken test leaving distinct teeth marks.

Kurz (1995) documented triggerfish attacking four different species of sand dollars (*Clypeaster*, *Encope*, *Mellita* and *Leodia*) in the Gulf of Mexico in a study analyzing predator-prey interactions and foraging strategies. The possibility for recognizing these interactions using the distinct marks left on the test was emphasized. Stingray predation on the spatangoid *Meoma ventricosa* and the sand dollar *Leodia sexiesperforata* was described by Grun (2016). The sand dollar is crushed with most of the oral side missing with bite marks across thin test and half of the test missing.

McClanahan (1995) found a wide variety of species off the coast of Kenya preying on the common regular echinoid *Echinometra mathaei*, including eight outright predators including triggerfish, wrasses, and an emperor fish. An additional seven species were placed into an attempted predator guild that failed to prey on the echinoid (although potentially could prey on juveniles) and finally a larger number of fish (18 in all) in a scavenger guild. When studying fish predation on regular sea urchins on the Great Barrier Reef Australia, Young and Bellwood (2012) found four fish predators of adult sea urchins including triggerfish, an emperor fish, and a wrasse with clear differences with respect to attack frequencies and handling duration.

Following the above described observations, the central wound on the oral surface of echinoids studied here, together with the accompanying scratch marks, strongly suggests that trigger fish are responsible for the wounds. Massive test destruction as to be expected from predation by stingrays (Grun, 2016) is not present. The scratch marks, as also

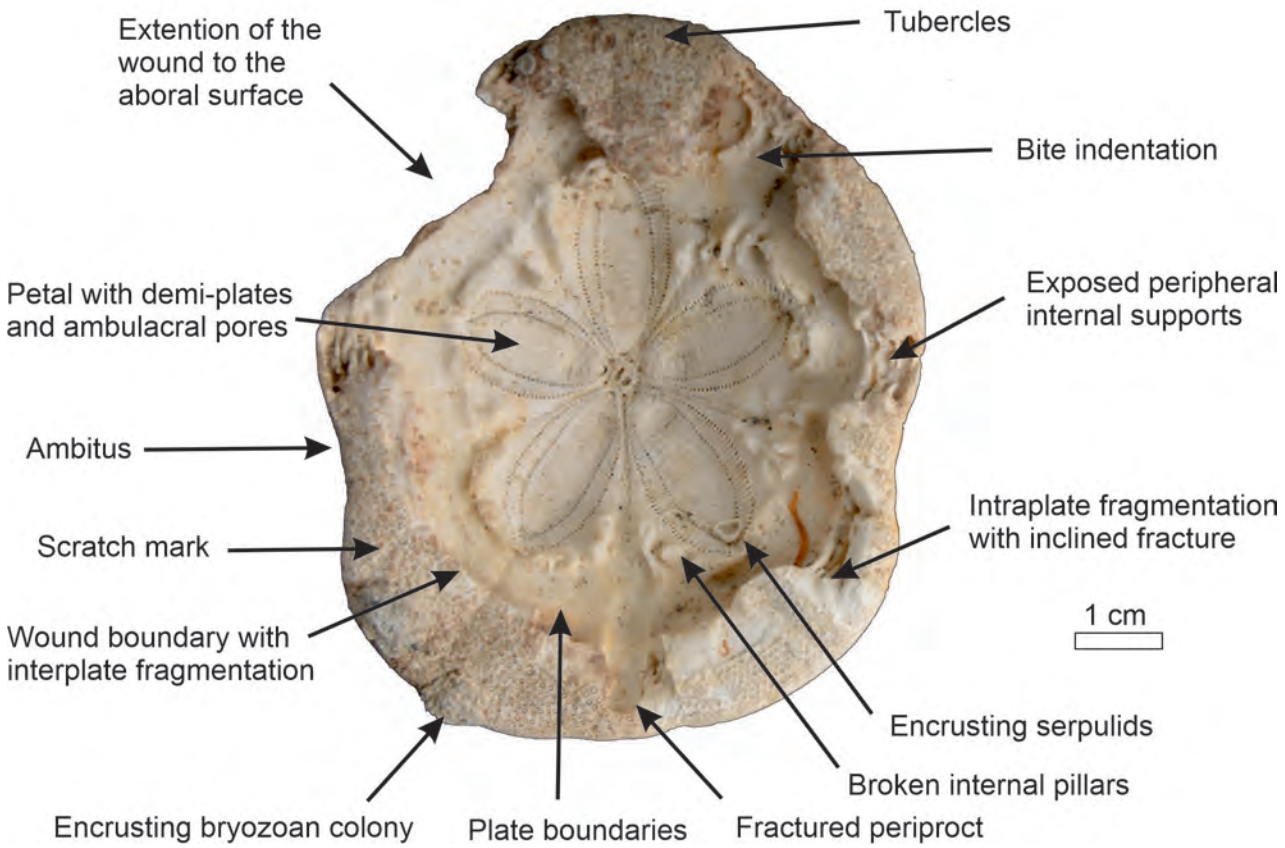

FIGURE 5 — Detailed oral view of predated *Clypeaster humilis* from the Northern Bay of Safaga, Red Sea, Egypt showing test morphology and characteristic wound features. The extensive wound removed much of the oral surface and extends to the aboral surface leading to an irregular outline with a damaged ambitus. The inner surface of the aboral skeleton shows plate boundaries (poorly visible from the outer view) and ambulacral pores. The preserved outer surface of the test shows numerous well-preserved tubercles. Wound features include irregular outline, intra- and interplate fragmentation, bite indentations, fractured periproct and scratch marks on the oral surface. Internal pillars and peripheral internal supports are exposed. Post-mortem encrustation by bryozoans and serpulids are present (JS87-2).

described by Kier and Grant (1965) and Fraser et al. (1991) are not as prominent in *Clypeaster humilis* as in *Sculpsitechinus auritus* (Leske, 1778), which has a broader more flattened test, from the study area (see Nebelsick and Kampfer, 1994; Nebelsick, 1999b). These differences may be due to prey handling techniques and the morphology of the prey skeletons. The oblique breakage on intraplate fractures may also represent a handling effect. These fractures are clearly visible from the outside and may be a result of manipulation by fish teeth breaking the test open from the center of the test toward the rim.

The sole presence of the wound on the oral surface and the extension of the wound toward the ambitus suggests a stereotypic behavior of the predators. The oral test surface is evidently weaker than that of the aboral surface. The area around the peristome lack internal supports, and it is here that the fish first destroy the test surface before expanding the wound. Highly irregular outlines as well as the fact that the wound can unnecessarily extend toward the aboral surface suggests that variation in this behavior can occur. These may be due to the fact that predation events commonly attract the attention of other predators and/or scavengers, thus disturbing the predation event and leading to an irregular outline.

RECOGNITION OF FISH PREDATION IN THE FOSSIL RECORD

Predation events described here were successful despite a number of morphological features that support the structural integrity of the test of *Clypeaster humilis*. These consist of both soft and hard parts: 1) The epidermis covering both internal and external surfaces of the plates (echinoderm skeletons are mesodermal in origin). 2) Collagenous fibers crossing plate boundaries. 3) Skeletal connections consisting of stereomic projections between the plates, and 4) Internal supports in the form of both central pillars and marginal buttresses (Seilacher, 1979; Mihaljević et al., 2011; Grun and Nebelsick, 2018a, b; Grun et al., 2018). High energy stress events are thus needed to break open the test. These are provided by the ballasted fish plunging with their snouts into the weaker oral side of

test. This instantly produces fragments and produces the characteristic wound.

The collected examples have been taken out of their taphonomic context in this warm water, well oxygenated environment. Attached spines will invariably be lost, and it is to be expected that these attacks will weaken the test. After the structural integrity of the *Clypeaster humilis* test is compromised, it can readily break apart into separate plates (e.g., Nebelsick and Kampfer, 1994). Preservation of specimens damaged by predation could be enhanced if included in sedimentation events rapidly burying the specimens, a process that can occur in near shore environments (e.g., Mancosu and Nebelsick, 2017). In addition, surface encrustation can cross plate boundaries and help preserved specimens (see discussion in Nebelsick and Kampfer, 1994; Nebelsick and Mancosu, 2021).

Differentiating these wounds from other possible non-predatory mediated fragmentation in *Clypeaster* and other clypeasteroids in the fossil record should be based on the presence of: 1) accompanying scratch marks, 2) oblique surfaces of intra-plate fragmentation, and/or 3) specific bite marks leading to highly irregular wounds. Larger fragments can also show such wounds that can be associated with predation events. The predation produces fragmented plates by wound production and probably weaken the test as well.

AKNOWLEGEMENTS

We thank Jeffrey Thompson, Adiël Klompmaker and William Ausich for significantly improving upon an earlier version of this manuscript.

LITERATURE CITED

ANDREW, N. L. and A. B. MACDIARMID. 1991. Interrelations between sea urchins and spiny lobsters in northeastern New Zealand. Marine Ecology Progress Series, 70: 211– 222.

ALLISON, P. A. 1990. Variations in rates of decay and disarticulation of Echinodermata, implications for the applications of actualistic data. Palaios, 5: 432–440.

BELAÚSTEGUI, Z., F. MUÑIZ, J. H. NEBELSICK, R. DOMÈNECH, and J. MARTINELL, J. 2017. Echinoderm ichnology: bioturbation, bioerosion and related processes. Journal of Paleontology, 91: 643–661.

BORSZCZ, T. and M. ZATOŃ. 2013. The oldest record of predation on echinoids: Evidence from the Middle Jurassic of Poland. Lethaia, 46: 141–145.

CLARK, A. M. and F. W. E. ROWE. 1971. Monograph of Shallow-Water Indo-West Pacific Echinoderms. London, Trustees of the British Museum (Natural History). 238 pp.

DONOVAN, S. K. 1991. The taphonomy of echinoderms: Calcareous multielement skeletons in the marine environment. In S. K. Donovan (ed.), The Processes of Fossilization. London: Belhaven Press, pp. 241–269.

DURHAM, J. W. 1966. Clypeasteroids. In R. G. Moore (ed.), Treatise on Invertebrate Paleontology. Part U, Echinodermata 3., Geological Society of America, University of Kansas Press, Lawrence Kansas, pp. U450–U491.

ESTES, J. A., N. S. SMITH, and J. F. PALMISANO. 1978. Sea otter predation and community organization in the wester Aleutian Islands, Alaska. Ecology, 59: 822–833.

FARRAR, L., E. GRAVES, E. PETSIOS, R. W. PORTELL, T. B. GRUN, M. KOWALEWSKI, and C. L. TYLER. 2020. Characterization of traces of predation and parasitism on fossil echinoids. Palaios, 35: 215–227.

FRAZER, T. K., W. J. LINDBERG, and G. R. STANTON. 1991. Predation on sand dollars by gray triggerfish *Balistes capriscus*, in the northeastern Gulf of Mexico. Bulletin of Marine Science, 48: 159–164.

FRICKE, H. W. 1971. Fische als Feinde tropischer Seeigel. Marine Biology, 9: 328–338.

_____. 1974. Möglicher Einfluß von Feinden auf das Verhalten von *Diadema*-Seeigeln. Marine Biology, 27: 59–64.

_____. 1975. Lösung einfacher Probleme bei einem Fisch (Freiwasserversuche an *Balistes fuscus).* Zeitschrift für Tierpsychologie, 38: 18–33.

GREENSTEIN, B. J. 1991. An integrated study of echinoid taphonomy: Predictions for the fossil record of four echinoid Families. Palaios, 6: 519–540.

GRUN, T. B. 2016. Echinoid test damage by a stingray predator. Lethaia, 49: 285–286.

_____. and J. H. NEBELSICK. 2018a. Biomechanics of an echinoid's trabecular system. PLoS ONE, 13(9): e0204432.

_____. 2018b. Structural design analysis of the minute clypeasteroid echinoid *Echinocyamus pusillus*. Royal Society Open Science, 5: 171323.

_____, D. SIEVERS, and J. H. NEBELSICK. 2014. Drilling Predation on the Clypeasteroid Echinoid *Echinocyamus pusillus* from the Mediterranean Sea (Giglio, Italy). Historical Biology, 26: 745–757.

_____, A. KROH, and J. H. NEBELSICK. 2017. Comparative drilling predation on time–averaged phosphatized and non–phosphatized specimens of the minute clypeasteroid echinoid *Echinocyamus stellatus* from Miocene offshore sediments (Globigerina Limestone Fm., Malta. Journal of Paleontology, 91: 633–642.

_____, A. MANCOSU, Z. BELAÙSTEGUI, Z., and J. H. NEBELSICK. 2018. Clypeaster Taphonomy: a paleontological tool to identify stable structures in natural shell systems. Neues Jahrbuch für Geologie und Paläontologie, Abhandlungen, 288: 189–202.

HARPER, E. 2016. Uncovering the holes and cracks: from anecdote to testable hypotheses in predation studies. Palaeontology, 59: 597–609.

HUNTLEY, J. W. and M. KOWALEWSKI. 2007. Strong coupling of predation intensity and diversity in the Phanerozoic fossil record. Proceedings of the National Academy of Sciences of the United States of America,

104(38): 15006–15010.

KIDWELL, S. M. and T. BAUMILLER. 1990. Experimental disintegration of regular echinoids: Roles of temperature, oxygen, and decay thresholds. Paleobiology, 16: 247–271.

KIER, P. M. and R. E. GRANT. 1965. Echinoid distribution and habits, Key Largo Coral Reef Preserve. Florida Smithsonian Miscellaneous Collections, 149(6): 1–68.

KLOMPMAKER, A. A., P. H. KELLEY, D. CHATTOPADHYAY, J. C. CLEMENTS, J. W. HUNTLEY, and M. KOWALEWSKI. 2019. Predation in the marine fossil record: Studies, data, recognition, environmental factors, and behavior. Earth–Science Reviews, 194: 472–520.

KOWALEWSKI, M. and J. H. NEBELSICK. 2003. Predation on recent and fossil echinoids. In P. H. Kelley, M. Kowalewski, and T. A. Hansen (eds.), Predator–Prey Interactions in the Fossil Record. Topics in Geobiology Series, Plenum Press, Kluwer, pp. 279–302.

_____, S. CASEBOLT, Q. HUA, K. E. WHITACRE, D. S. KAUFMAN, and M. A. KOSNIK. 2018. One fossil record, multiple time resolutions: Disparate time–averaging of echinoids and mollusks on a Holocene carbonate platform. Geology, 46: 51–54.

KURZ, R. C. 1995. Predator–prey interactions between gray triggerfish (*Balistes capriscus* Gmelin) and a guild of sand dollars around artificial reefs in the northeastern Gulf of Mexico. Bulletin of marine science, 56: 150–160.

McCLANAHAN, T. R. 1995. Fish predators and scavengers of the sea urchin *Echinometra mathaei* in Kenyan coral–reef marine parks. Environmental Biology of Fishes, 43: 187–193.

MANCOSU, A. and J. H. NEBELSICK. 2017. Ecomorphological gradient of clypeasteroid–dominated echinoid assemblages along a mixed siliciclastic–carbonate shelf from the Early Miocene of northern Sardinia, Italy. Acta Palaeontologica Polonica, 62: 627–646.

MEADOWS, C. A., R. E. W. FORDYCE, and T. K. BAUMILLER. 2015. Drill holes in the irregular echinoid, *Fibularia*, from the Oligocene of New Zealand. Palaios, 30: 810–817.

MIHALJEVIĆ, M. I. JERJEN, and A. B. SMITH. 2011. The test architecture of *Clypeaster* (Echinoidea, Clypeasteroida) and its phylogenetic significance. Zootaxa, 2983: 21–38.

NEBELSICK, J. H., 1992a. Echinoid distribution by fragment identification in the Northern Bay of Safaga; Red Sea, Egypt. Palaios, 7(2): 316–328.

_____. 1992b. The Northern Bay of Safaga (Red Sea, Egypt): An actuopalaeontological approach. III Distribution of echinoids. Beiträge zur Paläontologie von Österreich, 17: 5–79.

_____. 1995a. The uses and limitations of actuopalaeontological investigations on Echinoids. Geobios, M.S., 18: 329–336.

_____. 1995b. Comparative taphonomy of Clypeasteroids. Eclogae geologicae Helvetiae, 88: 685–693.

_____.1995c. Actuopalaeontological investigations on echinoids: The potential for taphonomic interpretation. In R. H. Emson, A. B. Smith, and A. C. Campbell (eds.), Echinoderm Research, Balkema, Rotterdam, pp. 209–214.

_____. 1999a. Taphonomic legacy of predation on echinoids. In M. D. Candia Carnevali and F. Bonasoro (eds.), Echinoderm Research, Proceedings of the Fifth European Conference on Echinoderms: Balkema, Rotterdam, pp. 347–352.

_____.1999b. Taphonomic comparison between recent and fossil sand dollars. Palaeogeography, Palaeoclimatology, Palaeoecology, 149: 349–358.

_____. 1999c. Taphonomy of *Clypeaster* fragments: preservation and taphofacies. Lethaia, 32: 241–252.

_____. 2008. Taphonomy of the irregular echinoid *Clypeaster humilis* from the Red Sea: Implications for taxonomic resolutions along taphonomic grades. In W. I. Ausich and G. D. Webster (eds.), Echinoderm Paleobiology. Indiana University Press, pp. 114–128.

_____. 2020. Clypeasteroids. In J. M. Lawrence (ed.), Biology and Ecology of Sea Urchins (4th Edition). Elsevier, Amsterdam, pp. 315–332.

_____, and S. KAMPFER. 1994. Taphonomy of *Clypeaster humilis* and *Echinodiscus auritus* from the Red Sea. In B. David, A, Guille, A., J.–P. Féral, and M. Roux, (eds.), Echinoderms through time, Balkema, Rotterdam, pp. 803–808.

_____, and M. KOWALEWSKI. 1999. Drilling predation on recent clypeasteroid echinoids from the Red Sea. Palaios, 14: 127–144.

_____, and A. MANCOSU. 2021. The taphonomy of echinoids: Skeletal morphologies, environmental factors and preservation pathways. (Elements of Paleontology). Cambridge: Cambridge University Press. doi:10.1017/9781108893411.

NEUMANN, C. and O. HAMPE. 2018. Eggs for breakfast? Analysis of a probable mosasaur biting trace on the Cretaceous echinoid *Echinocorys ovata* Leske, 1778. Fossil Record, 21: 55–66.

PETSIOS, E. R., W. PORTELL, L. FARRAR, S. TENNAKOON, T. B. GRUN, M. KOWALEWSKI, and C. L. TYLER. 2021. An asynchronous Mesozoic marine revolution: The Cenozoic intensification of predation on echinoids. Proceedings of the Royal Society B, 288: 20210400.

SEILACHER, A. 1979. Constructional morphology of sand dollars. Paleobiology, 5: 191–221.

SIEVERS, D. and J. H. NEBELSICK. 2018. Fish predation on a Mediterranean echinoid: Identification and preservation potential. Palaios, 33: 1–8.

_____, and J.–P. FRIEDRICH, and J. H. NEBELSICK. 2014. A feast for crows: bird predation on irregular echinoids from Brittany, France. Palaios, 29: 87–94.

TYLER, C. I., T. A., DEXTER, R. W. PORTELL, and M. KOWALEWSKI. 2018. Predation–facilitated

preservation of echinoids in a tropical marine environment. Palaios, 33: 478–486.
WALKER, S. and C. E. BRETT. 2002. Post–Paleozoic patterns in marine predation: Was there a Mesozoic and Cenozoic Marine Predatory Revolution? Paleontological Society Papers, 8: 119–193.
WILSON, M.A., T., BORSZCZ, and M. ZATOŃ. 2015. Bitten spines reveal unique evidence for fish predation on Middle Jurassic echinoids. Lethaia, 48: 4–9.
YOUNG, M. A. L. and D. R. BELLWOOD. 2012. Fish predation on sea urchins on the Great Barrier Reef. Coral Reefs, 31: 731–738.
ZŁOTNIK, M. and T. CERANKA. 2005. Patterns of drilling predation of cassid gastropods preying on echinoids from the middle Miocene of Poland. Acta Palaeontologica Polonica, 50: 409–428.

Museum of Paleontology, The University of Michigan
1105 North University Avenue, Ann Arbor, Michigan 48109-1085
Matt Friedman, Director

Contributions from the Museum of Paleontology, University of Michigan is a medium for publication of reports based chiefly on museum collections and field research sponsored by the museum. Jennifer Bauer and William Ausich, Guest Editors;
Jeffrey Wilson Mantilla, Editor.

Publications of the Museum of Paleontology are accessible online at: http://deepblue.lib.umich.edu/handle/2027.42/41251

Print (ISSN 0097-3556), Online (ISSN 2771-2192)

Contributions

from the Museum of Paleontology, University of Michigan
VOL. 34, NO. 12, PP. 158-192 JUNE 9, 2022

A REVISION OF THE FEATHER STAR GENERA *POECILOMETRA* AND *STROTOMETRA* (ECHINODERMATA: CRINOIDEA: CHARITOMETRIDAE)

BY

ALOIS ROMANOWSKI AND CHARLES G. MESSING

Abstract — The chiefly tropical, deep-water (>100 m) feather star family Charitometridae (Echinodermata: Crinoidea: Comatulida) currently consists of 34 species in eight genera and has not been revised since 1950. Recent molecular analyses and the discovery of both new specimens of known species and a new species prompted a morphological re-examination of those genera with abruptly expanded genital pinnules. As a result, *Poecilometra* is redescribed, and now includes four species, including two formerly placed in *Strotometra*, plus *Poecilometra baumilleri* n. sp. *Poecilometra scalaris* is placed in synonymy under *P. acoela*. *Strotometra* is redescribed and *S. hepburniana* placed in synonymy under *S. parvipinna*. The diagnoses of both genera and their component species are revised.

INTRODUCTION

Charitometridae A. H. Clark, 1909a, is a family of feather stars (Order Comatulida) that currently includes 34 species in eight genera, with the majority of specimens collected at depths between 200 and 600 m. The family is restricted to the Indo-western Pacific region except for monotypic, western Atlantic *Crinometra brevipinna* (Pourtalès, 1868). Most records are tropical, with a few species extending to temperate latitudes: Sagami Bay, Japan (Gislén, 1922, 1927; A. H. Clark, 1950; Kogo, 1998; Kogo and Fujita, 2005), East London, South Africa (Gislén, 1938), Ulladulla, NSW, Australia (Rowe and Gates, 1995), northern Gulf of Mexico (Meyer et al. 1978), Rio Grande do Sul, Brazil (Tommasi, 1969), and St. Helena (Gislén, 1933). Charitometrids can be important and sometimes dominant megafauna on hard substrates (Messing et al. 2019, and unpublished observations). The taxonomy of the family was most recently revised more than one half a century ago (A. H. Clark, 1950) and remains based exclusively on morphology. Its history is particularly convoluted and is, therefore, summarized here.

Carpenter (1888) first arranged the species eventually placed in the family in a hierarchy of groups within series in genus *Antedon* and distinguished them based on arm number (i.e., ten vs. more than ten) and number of ossicles in brachitaxes (i.e., IIBr2 versus IIBr4(3+4) (see terminology and abbreviations below). A. H. Clark (1907a) established two genera for species formerly placed in Carpenter's groups: *Charitometra* A. H. Clark, 1907a, with 19 species (type species: *Antedon incisa* Carpenter, 1888) and *Poecilometra* A. H. Clark, 1907a (type species: *Antedon acoela* Carpenter, 1884, plus *A. scalaris* A. H. Clark, 1907b). His genus-level

[1] Department of Marine and Environmental Sciences, Nova Southeastern University, 8000 North Ocean Drive, Dania Beach FL 33004, U.S.A. (messingc@nova.edu)

diagnostic features included up to 50 arms in the former, and only ten arms with sharply expanded genital pinnules in the latter. He (A. H. Clark 1908a) first placed *Charitometra* in the family Thalassometridae A. H. Clark, 1908a. Next, A. H. Clark (1909a) grouped it with *Poecilometra* in the thalassometrid subfamily Charitometrinae A. H. Clark, 1909a, with five new genera: *Glyptometra, Strotometra, Crinometra, Pachylometra,* and *Chlorometra*; and finally (A. H. Clark (1911) elevated the subfamily to family-level status as Charitometridae. Hartlaub (1912), who had inherited the large U.S. Coast and Geodetic Survey Steamer *Blake* collection from the late Carpenter, felt bound to use the earlier classification and restored all the included species to *Antedon*, an arrangement not followed since.

A. H. Clark (1916) added five more genera: *Crossometra* (3 species), *Perissometra* (11), and *Monachometra* (1) for species formerly in *Pachylometra* and *Glyptometra*; *Chondrometra* (3) for species formerly in *Chlorometra*; and *Calyptometra* for *Charitometra lateralis* A. H. Clark, 1908b. A. H. Clark's (1918) detailed key to the family included 42 species (including nine nominal species and 11 varieties of *Crinometra*) in twelve genera. Genus-level characters included relative lengths of proximal versus middle and distal pinnules; brachitaxes all of two ossicles versus IIBr4(3+4), narrow and laterally well-separated versus apposed with laterally flattened ossicles, and aborally keeled or not; genital pinnules with the third and fourth pinnulars ($P_{(3–4)}$) abruptly expanded versus a slight, gradually tapered expansion; 10 versus >10 arms; distal arms laterally compressed or not; centrodorsal shape, and overall size ("large" versus "small").

In a series of papers, Gislén (1922) first added *Diodontometra* (for *D. bocki* n. sp.), which raised the number of genera to 13. Although Gislén (1927, 1933) identified ambiguities among generic diagnoses, recommended transferring several species to different genera, and proposed characters of the centrodorsal and cirri as more reliable than arm ornamentation and relative pinnule lengths in distinguishing genera, e.g., cirri stout versus slender and with versus without aboral spines (Gislén, 1928), he maintained the 13 genera (Gislén, 1934).

In the last complete revision of the family, A. H. Clark (1950) concluded that many standard characters used in differentiating the genera were unimportant. He reduced the number of genera to eight, placing *Diodontometra* under *Chlorometra*; and *Calyptometra, Crossometra, Perissometra,* and *Pachylometra* under *Glyptometra*; and divided the genera among two informal groups based on differences in genital pinnule structure: 1) tapering from more or less broadened proximal segments to a longer delicate distal portion (*Chondrometra, Crinometra, Monachometra,* and *Glyptometra*) versus 2) two to four abruptly broader pinnulars with a shorter slender tip (*Chlorometra, Strotometra, Poecilometra,* and *Charitometra*). Within these two groups, distinguishing features at the generic level included compressed versus rounded arms, development of synarthrial tubercles, IIBr series of two versus four ossicles, and relative lengths of oral and genital pinnules (A. H. Clark, 1950). Inconsistencies remain, however. In his remarks on the family, he considered the type of genital pinnules and length of oral pinnules as "unreliable and undiagnostic" (p. 198), but a few lines later noted that the "characters presented by the genital pinnules seem to be reliable." Although he placed *Monachometra* in the first group and *Chlorometra* in the second, he noted (p. 199) that the "genital pinnules of *Chlorometra* are very little different from those of *Monachometra*, of which *Chlorometra* should perhaps be regarded as a synonym." Similarly, he used similar variations in ornamentation to distinguish species of *Glyptometra* but only varieties (accepted as subspecies; ICZN 45.6.4) of *Crinometra brevipinna*. The taxonomy of the family has not been altered since, except for the addition of *Monachometra kermadecensis* McKnight, 1977a; and *Chondrometra crosnieri* Marshall and Rowe, 1981; and slight modifications of the familial and generic diagnoses in Hess and Messing (2011). Hemery's (2011) molecular phylogeny included 13 charitometrid terminals representing five genera. Of those with multiple species-level taxa, *Chondrometra* (2 terminals) returned as monophyletic, but both *Strotometra* (5) and *Glyptometra* (2) returned as polyphyletic. However, no species were re-assigned, and no taxonomy was revised. Other additions have been new faunal records, e.g., off Japan and adjacent waters (Kogo, 1998; Kogo and Fujita, 2005), New Zealand (McKnight, 1975, 1977a,b,c, 1989a,b,c), and in the tropical western Atlantic (Meyer et al., 1978) and ecological relationships, e.g., in the tropical western Atlantic (Messing et al., 1990) and northeastern Atlantic (Bullimore et al., 2013).

Within the order Comatulida, Charitometridae was long placed with several other families in a grouping variously treated as a suborder, tribe, subtribe, or superfamily (e.g., A. H. Clark, 1908b, 1932; Gislén, 1924) based primarily on the possession of pinnules that are triangular in cross section (prismatic) with a sharp or sharply rounded aboral (dorsal in earlier literature) keel. Other characters have included well-developed ambulacral plates (except in Tropiometridae), and distalmost pinnules extending beyond the minute terminal brachials (Gislén, 1924; A. H. Clark, 1931, 1947, 1950; Rasmussen, 1978). The other families in the most recent arrangement, as superfamily Tropiometroidea (Hess and Messing, 2011), are Thalassometridae A. H. Clark, 1908a, Calometridae A. H. Clark, 1911, Tropiometridae A. H. Clark, 1908a, Ptilometridae A. H. Clark, 1914, Asterometridae Gislén, 1924, and the fossil families Conometridae Gislén, 1924, Pseudoconometridae Eagle, 2001, and Pterocomidae Rasmussen, 1978. However, recent molecular analyses returned the superfamily as polyphyletic, with monophyletic Charitometridae sister to a deep-sea clade composed of the stalked Guillecrinidae Mironov and Sorokina, 1998, and the feather star family Pentametrocrinidae A. H. Clark, 1908a, (Cohen and Pisera 2016; Rouse et al. 2013; Hemery et al. 2013; Hess and Messing, 2011).

Hemery's (2011) Maximum Likelihood and Bayesian Inference analyses of 13 charitometrid terminals (combined CO1, 16S, 28S and 18S) represent the most inclusive sequence data yet available for the family. Both analyses returned two

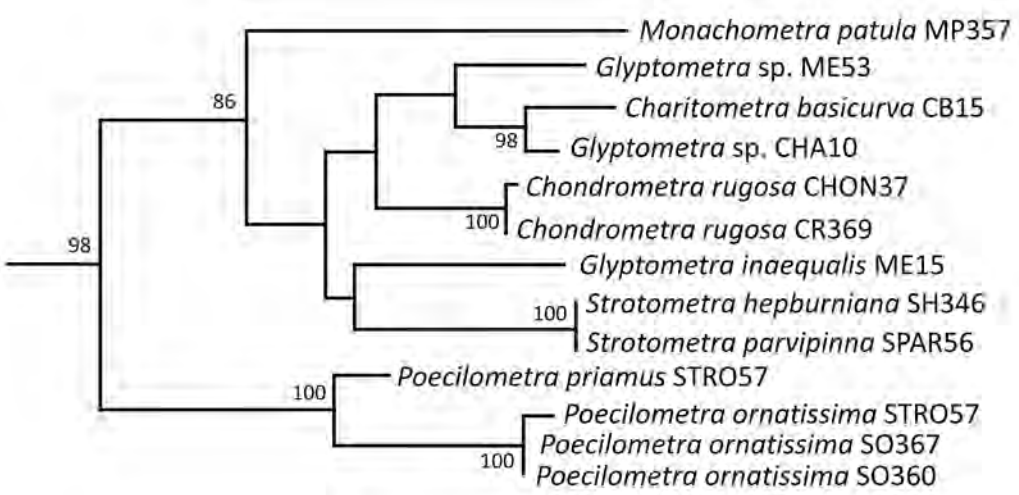

FIGURE 1 — Phylogeny of Charitometridae assembled from a Maximum Likelihood analysis of four combined genes (COI, 16S, 28S and 18S). Adapted from Hemery (2011, figure 4.B.9; bootstrap values shown on nodes are those >80%).

sister clades with the same composition. One clade returned with the same topology in both analyses: a *Poecilometra priamus* (originally identified as *Strotometra* n. sp.) sister to a clade of three *P. ornatissima* (originally a *Strotometra* sp. and two *S. ornatissimus*) terminals. The topology of the other clade differed between the two analyses. Figure 1 shows the ML results. In BI, a clade of *Strotometra hepburniana* and *S. parvipinna* returned basal to the seven remaining terminals representing five other charitometrid genera. Both analyses support the monophyly of *Poecilometra* and *Strotometra* as treated herein but returned *Glyptometra* as polyphyletic.

As noted above, A. H. Clark (1950) used the characters of the genital pinnules to divide the genera into two groups. The current work was prompted by an initial examination of several specimens, which suggested that the supposedly diagnostic expansion of the genital pinnules was not structurally similar among these genera and included specimens of an apparently new species. This paper focuses on two of the four genera and six of the nine species in A. H. Clark's (1950) second group: those supposedly with abruptly expanded genital pinnules followed by a short slender tip: *Poecilometra* (2 species) and *Strotometra* (4). Of the other two genera in that group, we point out here that *Charitometra* has genital pinnules more similar to those of A. H. Clark's other group of genera and provide evidence that monotypic *Chlorometra garrettiana* A. H. Clark, 1907b, also belongs with the first group of genera.

Terminology chiefly follows Messing and Dearborn (1990), Messing *et al.* (2000), and Hess (2011). Abbreviations are as follows: number of cirri in Roman numerals followed by the number of component segments (cirrals) in Arabic numerals (e.g., X–XV, 11–17), with individual cirrals indicated by 'C' (e.g., C5 = fifth cirral from the base). Arm branching series (brachitaxes, or division series) are numbered from the arm base (following the radial ossicle) with a Roman numeral followed by 'Br' and the number of component ossicles by an Arabic numeral (e.g., IIIBr2 = third brachitaxis composed of two ossicles). 'br' indicates individual arm ossicles (brachials; brr = plural) (e.g., IVbr2 = second ossicle of the fourth brachitaxis; br5 = fifth brachial of an undivided arm following the distalmost axil). Axils (the ossicles at which a ray branches) are indicated by 'ax' (e.g., IIIax4 = the fourth ossicle of the third brachitaxis is an axil). A plus sign (+) indicates a syzygy between two brachials (e.g., IIBr4(3+4) = second brachitaxis composed of four ossicles, with the third and fourth joined by syzygy; br9+10 = ninth and tenth brachials of an undivided arm joined by syzygy).

For ossicle proportions, LW = ratio of length to median width of a cirral or pinnular (in side view); WL = ratio of median width to midaboral length of a brachial (in aboral view) (the different ratios used in order to maintain values generally >1.0); DH = ratio of centrodorsal basal diameter to height. Pinnules are abbreviated P, with interior pinnules (those closest to the extrapolated axis of the preceding brachitaxis) indicated by lower case letters and exterior pinnules by Arabic numerals, e.g., Pe and P5 = fifth interior and exterior pinnules, respectively, counting from the most proximal. Following Messing (2020a, 2020b), individual pinnulars are indicated as Arabic subscript numerals in parentheses (e.g., $P8_{(3–6)}$ = third through sixth pinnulars of the eighth pinnule). Pinnulars of pinnules with unknown placement along the arm (e.g., detached) are noted with just the parenthetical (e.g., P(3–6), or perhaps $Pgen_{(3–6)}$ or $Pmid_{(3–6)}$, if the pinnule is recognizable as genital or arising from the middle portion of the arm, respectively). Pinnulars expanded over the gonad on genital pinnules are referred to as gonadal.

MATERIALS AND METHODS

We examined 12 specimens originally identified as *Poecilometra* (including the new species); 31 of *Strotometra*; three of *Glyptometra lateralis* (A. H. Clark, 1908c); one

of *Monachometra patula* (Carpenter, 1888); several of *Crinometra brevipinna* (Pourtalès, 1868); and photographs of type specimens belonging to *Charitometra basicurva* (Carpenter, 1888), *Charitometra incisa* (Carpenter, 1888), *Chondrometra rugosa* A. H. Clark, 1918, *Chondrometra crosnieri* Marshall and Rowe, 1981, *Chlorometra garrettiana*, *Glyptometra* spp., and *Monachometra* spp.

Specimens were examined with Wild M-5 or Leica M275 dissecting microscopes, both with camera lucida attachment. Most photographs were taken with a Canon EOS Rebel T3 camera directed through the Leica M275. Some specimens photographed in museums (e.g., Smithsonian, London, Amsterdam, Copenhagen, Leiden) were taken with equipment available at the institution. Images taken at multiple focal points were combined and rendered with Helicon Focus 7 Lite focus-stacking software and edited in a photo-editing program.

Pinnulars of some specimens were dissociated with full-strength commercial bleach (5% sodium hypochlorite solution) to examine ossicles using scanning electron microscopy (SEM). Ossicles were rinsed in distilled water, dried, and mounted on scanning electron microscopy stubs, sputter-coated with palladium, and examined with either an ISI-DS130 SEM (NSU Ocean Campus) or FEI ESEM Quanta 200 Environmental SEM (NSU School of Dentistry).

INSTITUTIONAL ABBREVIATIONS

FLMNH	—	Florida Museum of Natural History, Gainesville, Florida, U.S.A.
MNHN	—	Muséum national d'Histoire naturelle, Paris, France.
NHM	—	Natural History Museum, Cromwell Road, London, U.K.
NSU-CRI	—	Nova Southeastern University, Ocean Campus, Dania Beach, Florida, U.S.A. (Crinoid collection, Schure bldg. rm 205).
NIWA	—	National Institute of Water and Atmospheric Research, Auckland, New Zealand.
RMNH	—	Rijksmuseum van Natuurlijke Historie (formerly Amsterdam, now housed at Naturalis Biodiversity Centre, Leiden, Netherlands).
USNM	—	National Museum of Natural History, Smithsonian Institution, Washington, D.C., U.S.A. (United States National Museum)
UUZM	—	Uppsala University Museum of Evolution, Zoology section, Uppsala, Sweden.
NHMD	—	Natural History Museum Denmark.

TAXONOMIC SECTION

CHARITOMETRIDAE A. H. Clark, 1909a

Diagnosis.— Aboral apex of centrodorsal commonly rugose or tuberculate; no adoral radial pits. Cirrus sockets commonly with distinct articular tubercles and, in some genera, with marginal crenulae; sockets large, irregularly crowded or in 5, 10, or 15 distinct columns. Cirri typically of 20-30 cirrals (range 10-50); generally less than 20% of arm length, cylindrical or laterally compressed, and lacking transition segment. Cirrals usually <25 (rarely up to ~30), without aboral spines, but sometimes carinate or with low distal tubercle. Distal cirrals usually as long as wide or longer, often not much shorter than proximal cirrals. Rod-shaped basals exposed interradially or concealed. Subradial cleft commonly present. Radials concealed or narrowly exposed. Radial articular facet moderately sloping inward adorally; profile of facet straight with no angle or bend. Muscle fossae tall and narrow. Radial cavity narrow. Arms 10 to 33. IBr2 joined by synarthry; IIBr either 2 or 4(3+4); following brachitaxes 2, 2(1+2), or 4(3+4) (rarely 3(2+3) or 4 [no syzygy]); initial syzygies of undivided arms at br1+2, br3+4, or br1+2, 3+4; distal intervals between syzygies 2 to 26 (commonly 6 to 11) articulations. Arms aborally rounded or laterally compressed and carinate, often with rugose or tuberculate surface. P1, P2, and sometimes P3 (oral pinnules) more flexible and composed of more, mostly short, pinnulars than succeeding pinnules; lengths similar, or increasing or decreasing from the most proximal; number of pinnulars of oral pinnules usually decreasing from P1 onward. Pinnules triangular or rounded triangular in cross section (=prismatic), with distinct ambulacral covering plates; oral pinnules sometimes more rounded in cross section. Genital pinnules with proximal segments at least somewhat broadened, or with a few segments abruptly broadened, and covering gonad (modified from A. H. Clark, 1950; Hess and Messing, 2011).

Remarks.— Characters included in the diagnosis in Hess and Messing (2011) but omitted here, as they are widely variable and present in other feather star families as well or restricted to one genus within Charitometridae, are: centrodorsal hemispherical, conical, or truncated conical to discoidal with rounded or flattened, cirrus-free aboral apex; some species of *Monachometra* with a dorsal star.

Key to the Genera and Species of *Poecilometra* and *Strotometra*

1a. Genital pinnules with 3–5 narrow basal pinnulars following a usually wider $P_{(1)}$ and preceding expanded pinnulars bearing the gonad (pedunculate); expanded gonadal pinnulars symmetrical in cross-sectional view, with small articular area, especially the abambulacral ligament fossa, and long, thin lateral "wing-like" flanges; pinnulars distal to expanded gonadal pinnulars abruptly narrower; abambulacral side of $P_{(1)}$ of proximal pinnules with weak to well-developed

flange, or flattened, curved tongue directed aboral side of arm; arms 10–20.....*Poecilometra* (2)

1b. Genital pinnules with 1–2 narrow basal pinnulars or broadening gradually from the base and tapering gradually distal to gonad; no abambulacral projection on $P_{(1)}$; expanded gonadal pinnulars asymmetrical in cross-sectional view, with a longer, curved flange and usually shorter, thicker triangular flange, and articulation proportionally larger than in *Poecilometra*; arms 10.....*Strotometra parvipinna*

2a. Brachitaxes and brr1-2 well separated with distinct gaps between adjacent ray bases, but with projecting lateral and/or proximal flanges; distal portion of genital pinnules shorter than gonad; 10 arms only.....3

2b. Brachitaxes and brr1-2 laterally flattened and apposed against adjacent ossicles, often with everted lateral margins; 10 or up to 20 arms.....4

3a. Proximal and lateral aboral margins of Ibr1 with continuous curved flange overhanging radial proximally and almost bridging gap between adjacent rays laterally; cirri XX–~XXV, up to 18, and ~22 mm long; longest cirrals with LW up to 2.2; distal portion of genital pinnules typically consisting of only 3–4 small, abruptly narrower pinnulars ....*Poecilometra acoela*

3b. Ibr1 with proximal margin almost straight to slightly convex, and lateral margins converging and bearing low thick lateral flange or ridge; cirri X–~XVI, up to 19 cirrals, and 42 mm long; longest cirrals with LW chiefly 2.4–2.7; distal portion of genital pinnules consisting of up to 7 small, narrow pinnulars.....*Poecilometra baumilleri* n. sp.

4a. Distal edges of br2, br4, and br5 strongly everted as a high crest perpendicular to midaboral axis; 10 arms; $P_{(1)}$ of proximal pinnules with at most weak abambulacral projection.....*Poecilometra ornatissima*

4b. No strongly everted crest on distal edges of any proximal brachials; up to 20 arms; $P_{(1)}$ of proximal pinnules (sometimes excluding P1) bearing elongated, flat, abambulacral projection, sometimes weak, but often curved, tongue-like and, in larger specimens, extending around to aboral surface of arm.....*Poecilometra priamus*

Poecilometra A. H. Clark, 1907a

Antedon (Part) Carpenter 1880: pl. 6, fig. 10

Poecilometra A. H. Clark 1907a: 361; 1908a: 136; 1908c: 211–212; 1908d: 245; 1909a: 18; 1912a: 9, 11, 25, 60, 225; 1918: 172, 19.—Gislén 1928: 9; 1934: 18.—Hess and Messing 2011: 115

Revised diagnosis.— Centrodorsal hemispherical or discoidal; cirrus sockets in 1–3 irregular marginal tiers, or in 2–3 irregular columns of 1–3 sockets in each radial area; arms 10 to 20; brachitaxes and proximal brachials well separated with gaps bridged by lateral flanges, or closely laterally apposed; abambulacral side of $P_{(1)}$ of proximal pinnules with weak to well-developed flange, or flattened, curved tongue directed toward aboral side of arm; genital pinnules usually with 3–5 narrow basal pinnulars (infrequently 2–7) following a usually wider $P_{(1)}$ and preceding abruptly expanded pinnulars bearing the gonad (pedunculate); pinnulars expanded over gonad, symmetrical in cross-sectional view, with small articular area, especially the abambulacral ligament fossa, and long, thin lateral "wing-like" flanges; pinnulars distal to gonad abruptly narrower.

Type species.— *Antedon acoela* (Carpenter, 1888).

Other included species.— *Antedon scalaris* (A. H. Clark, 1907b); *Strotometra ornatissimus* A. H. Clark, 1912b; *Strotometra priamus* A. H. Clark, 1912b*; Poecilometra baumilleri* n. sp.

Distribution.— Northwestern, western, southwestern, and central Pacific Ocean; 345 to 1800 m.

Remarks.— The genital pinnules consist of 2–7 narrow basal pinnulars followed by 3–8 abruptly expanded pinnulars, and terminate in 4–10 abruptly thinner, much smaller pinnulars, an appearance referred to here as pedunculate (see Figs. 4, 7, 12, 14, 18, 22I–L). Such genital pinnules are unique among charitometrids and appear to represent a synapomorphy. On this basis, *Strotometra priamus* and *Strotometra ornatissimus* are herein moved to *Poecilometra. Poecilometra baumilleri* n. sp., described below, also has similar pedunculate genital pinnules.

In addition to the pedunculate genital pinnules, all four species placed in *Poecilometra* herein have brachitaxes and proximal arm brachials with lateral extensions referred to here as flanges, either prominent, smooth, and associated with well-separated ray bases (*P. acoela* (including *P. scalaris*, see below) and *P. baumilleri* n. sp.) or comparatively narrow, with ossicle margins often everted and irregular, and associated with laterally flattened and apposed ray bases (*P. priamus* and *P. ornatissima*) (A. H. Clark 1950, and herein). However, because Hemery's (2011) analysis did not include either *Poecilometra* species with prominent lateral flanges and well-separated ray bases (*P. acoela, P. baumilleri*), additional data is needed to determine if these different ray base features warrant generic-level distinctions or not. If so, *P. priamus* and *P. ornatissima* might require a new generic name, as *acoela* is the type species of *Poecilometra*.

Poecilometra acoela (Carpenter, 1888)
Figures 2–4, 8–9, 22J, 23F

Antedon sp. Carpenter 1880: pl. 6, fig. 10, pl. 15, fig. 9

Antedon acoela Carpenter 1884: 57, 83–84, 93, 109–110, 113, 128, pl.54, figs. 1–4, pl 55, fig. 5; 1887: 391, pl. 30, fig. 3; 1888: 132, pl. 2, fig. 3 a-d, pl. 16., figs 1–5.—Hartlaub 1891: 113.—Shipley and MacBride 1901: 269.—Minckert 1905: 190.—Hamann 1907: 1578, pl. 12, fig. 1.—A. H. Clark 1912a: 33, 225; 1915a: 43.

Poecilometra acoela: A. H. Clark 1907a: 362; 1909a: 18; 1912a: 33, 225; 1913a: 50; 1915a: 43, 63 (fig. 8), 367 (fig. 493); 1918: 190, 273; 1921: 49, 75, 152, 228, 230, 359, 754, 763, pl. 26, fig. 1161.—Gislén 1924: 280.—A. H. Clark 1950: 355–359.

Antedon scalaris A. H. Clark 1907b: 141; 1908a: 437, 493.

Poecilometra scalaris: A. H. Clark 1907a: 362; 1909a: 18; 1912a: 225; 1913a: 50; 1915b: 215; 1918: 190; 1921: 79

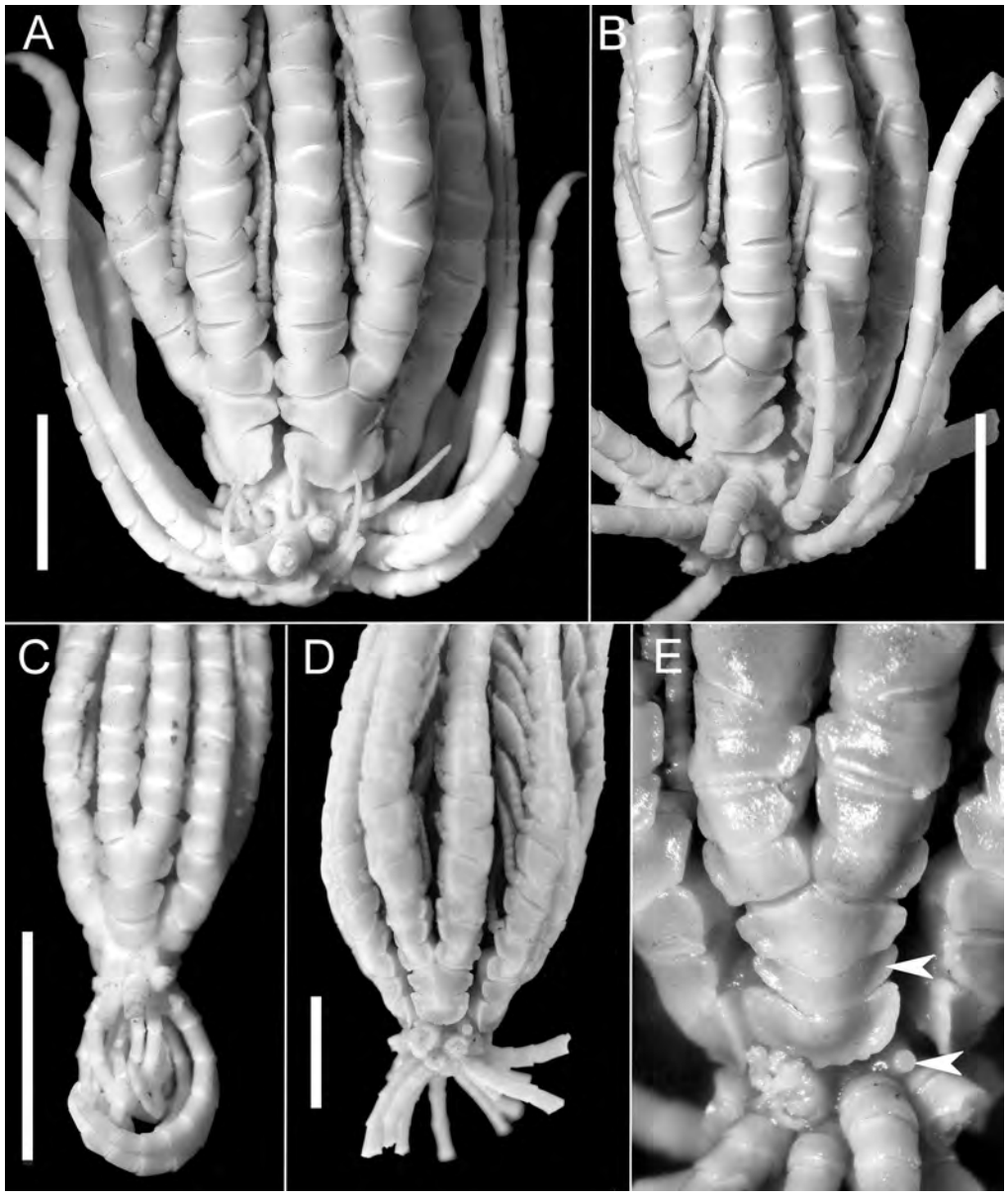

FIGURE 2 — **A–C**, *Poecilometra acoela* (Carpenter, 1884), syntypes, NHM 88.11.9.31. **A**, specimen 1, proximal portion in lateral view (composite image). **B**, specimen 2, proximal portion in lateral view. **C**, specimen 3, proximal portion. **D–E**, *Antedon scalaris* A. H. Clark, 1907b, holotype, USNM 22629. **D**, proximal portion in lateral view. **E**, close-up of a different ray showing small extra ossicle in IBr series (upper arrow) and round projection at interradial angle of centrodorsal (lower arrow); scale bars = 5 mm (E, no scale recorded).

(figs. 118, 132), 186 (fig. 229), 221 (fig. 288), 263, 279, 286, 289 (figs. 539–542), 293, 412 (figs. 849–855), 722, 729; 1950: 359–360

Poecilometra acoela: A. H. Clark 1908a: 265, fig. 1, 318

Material examined.— INDONESIA: *Challenger* sta. 214, SW of Pulau Kakalotan, Kepulauan Talaud (=Meangis Is.), 4°33'N, 127°06'E, 914 m, bottom temp. 5.44°C, blue mud, 10 Feb 1875 (NHM 88.11.9.31 (3 of 6 specimens), NHMD-873490 (1), *Antedon acoela* syntypes); *Siboga* sta. 122, N of the NE tip of Sulawesi, 01º58'30"N, 125º00'30"E, 1,165–1,264 m, stone, 17 Jul 1899 (USNM E439, 1). JAPAN: *Albatross* sta. 4918, East China Sea SW of Kagoshima, Japan, 30°22'N, 129°08'E, 660 m, bottom temp. 5.95 C, gray sand, foraminifera, and broken shells, 13 Aug 1906 (USNM 22629, holotype of *Antedon scalaris*).

Diagnosis.— A species of *Poecilometra* with 10 arms; IBr and proximal brachials well separated; proximal and

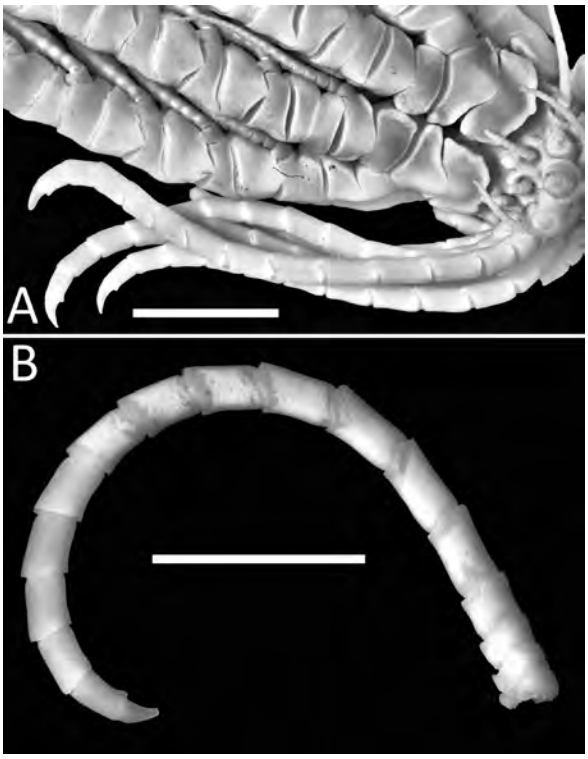

FIGURE 3 — *Poecilometra acoela* (Carpenter, 1884). **A**, syntype, NHM 88.11.9.31, specimen 1, base of one ray and cirri. **B**, *Antedon scalaris* A. H. Clark, 1907b, holotype, USNM 22629, detached cirrus; scale bar = 5 mm.

lateral aboral margins of Ibr1 with continuous curved flange overhanging radial proximally and almost bridging gap between adjacent rays laterally; flange continued but weaker on lateral ends of Iax2 and brr1–2 (flanges reduced in small specimens); cirri in large specimens (centrodorsal diameter 3.5–5.0 mm) XX–~XXXV, up to 18, and ~22 mm long; longest cirrals with LW up to 2.2. Distal portion of genital pinnules shorter than gonad, typically consisting of only 3–4 small, abruptly narrower pinnulars.

Description.— Centrodorsal rounded conical or hemispherical, 1.7–5.2 mm across adoral (basal) diameter; DH 1.2–1.5, with interradial ridge or knob adjacent to base, ranging from short and rounded to narrow, irregular and almost half centrodorsal height (the latter visible in Figure 2B). Aboral pole convex or dome-like, 0.3–0.4x centrodorsal diameter. Cirrus sockets in 2 columns (3 in largest specimens) per radial area of chiefly 2 or 3 (rarely 1) sockets each (Figs. 2, 3).

Cirri XX to ~XXXV, 14–18, up to at least 22 mm long (XV, 11, 6.2 mm long in small NHM 88.11.9.31 syntype with centrodorsal diameter 1.7 mm). Cirrals increasing in length from very short or squarish C1; C2 and at least following few cirrals with proximal and distal margins sinuous in lateral view; C4–6 longest, up to C6–8 in larger specimens; these long middle cirrals with LW 1.8–2.2 (small NHM 88.11.9.31 syntype with longest cirral C3–4, LW 1.7); following cirrals becoming shorter but remaining longer than wide; cirri slightly tapering near tip; penultimate cirral distinctly narrower than those preceding; opposing spine tiny, distally-directed, rounded-conical and located at distal end of cirral; terminal claw curved, shorter or longer than preceding cirral (Figs. 2A–C, 3).

Radials hidden, or very short and almost completely hidden in larger specimens, by overhanging proximal flange of Ibr1; radial WL rarely measurable (3.6 in one specimen); some larger specimens with a small beadlike tubercle on at least some radials; another with a small low bump on either side of midaboral line (or just one) on two radials; and with WL 3.6. Radials in small NHM 88.11.9.31 syntype crescent-shaped with distal margin shallowly concave and no ornamentation; WL 1.4 (Fig. 2C).

Brachitaxes and arm bases separated laterally, but IBr2 and br1 with lateral flanges at least partly bridging gaps between adjacent rays (Figs. 2A–B, D–E, 3A). IBr2 with low, midaboral, convex synarthrial swelling; Ibr1 crescent-shaped, WL 2.4–3.4, with broad, thick, continuous flange extending outward from proximal and lateral margins, sometimes slightly sinuous or irregular laterally, and with distal margin shallow or deeply concave. Iax2 wider than Ibr1, hexagonal with short, diverging lateral flanged margins, or rhombic with flanges either restricted to lateral portions or running along entire shallow V-shaped proximal margin; WL 1.4–2.1. One IBr series of *A. scalaris* holotype with an additional, shallow V-shaped ossicle between Ibr1 and Iax2, with lateral flanges but not as wide as either other ossicle; WL 4.5 (Fig. 2E). Small NHM syntype with IBr2 smoothly rounded aborally and no synarthrial swelling; Ibr1 with weak straight flange on diverging lateral margins; distal margin very slightly concave; WL 2.0; Iax2 hexagonal with proximal margin slightly convex; lateral margins with ear-like flanges; WL 1.4 (Fig. 2C).

Arms 10, up to 110 mm (incomplete in most specimens). Br1 roughly rectangular or slightly longer exteriorly, with convex or straight lateral flanges; weaker, shorter or absent interiorly, and distal margin slightly concave; WL 2.2–2.7. Br2 roughly pentagonal, shallow V-shaped proximally, with lateral margins diverging or straight, with or without flanges; WL 1.8–1.9. Br3+4 oblong or with exterior lateral margin longer than interior; 0.8–2.0 mm across; WL 1.2–1.5; br3 with lateral flanges weak, present only interiorly in some specimens. Brr5–8 or 9 wedge-shaped; WL 1.6–2.2; one or two following brachials almost rectangular. Middle brr almost triangular; WL 1.8. Distal brachials strongly wedge-shaped; distal margins slightly raised but not overlapping; WL 1.1–1.2. Small NHM syntype with br1 oblong, with convex exterior lateral flange; WL 1.7 (Fig. 2C). Br2 almost oblong but with diverging interior lateral margin and no flange; WL 1.5. Br3+4 oblong, slightly longer than wide, 0.9 mm across; WL 0.9; following few brr only slightly wedge-shaped; WL 1.1–1.3.

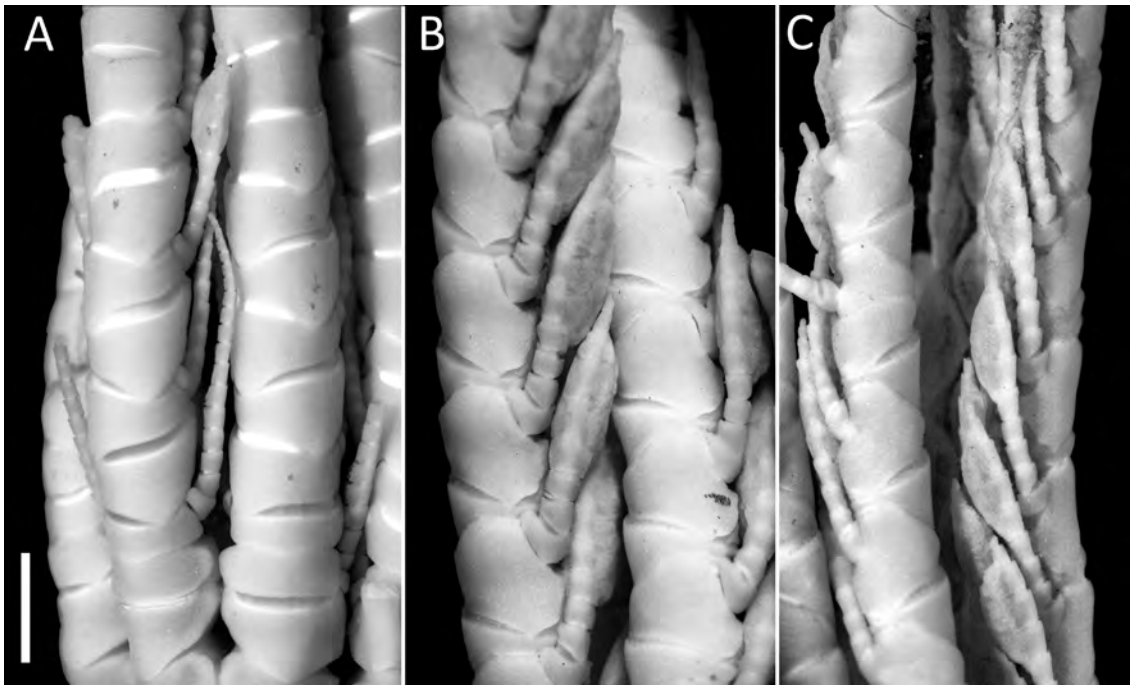

FIGURE 4 — *Poecilometra acoela* (Carpenter, 1884), syntype, NHM 88.11.9.31, specimen 2. **A**, proximal interior pinnules (center) Pa, Pb, Pc (genital). **B**, Middle genital pinnules. **C**, More distal genital pinnules; A scale bar = 2 mm; B, C = no scale recorded.

Second syzygy at br9+10 to br13+14. Distal intersyzygial interval usually 4–5 (sometimes 3–6). In small specimen (NHM 88.11.9.31), second syzygy at br13+14 to br15+16; following intersyzygial interval 7 to at least 12 (longest remaining arms broken beyond br12 to br26).

P1 of 18–24 pinnulars, up to 7.1 mm long (2.5 mm in small NHM syntype); $P1_{(1)}$ wider than those following, with convex or truncated abambulacral flange; following proximal pinnulars squarish; middle pinnulars slightly longer than wide; LW at most 1.3; distal pinnulars almost squarish. Pa similar but with a weak convex abambulacral keel spanning $Pa_{(5–6)}$ or $_{(5–8)}$. P2 shorter than P1, with fewer pinnulars; in small NHM syntype segments longer than in P1 with very slight expansion at $P2_{(5–6)}$ or $_{(6–7)}$. P3 first genital pinnule; genital pinnules with 9–14 pinnulars; $Pgen_{(1)}$ wider than those following, usually with weak to well-developed convex abambulacral flange (Fig. 4); following 2–4 pinnulars squarish or slightly longer than wide—$P_{(2–3 \text{ or } 4)}$ on proximal genital pinnules, $P_{(2–4 \text{ or } 5)}$ on middle genital pinnules; following 3–5 pinnulars, e.g., $Pgen_{(4–7), (5–7), (4–8)}$, or $_{(6–8)}$, abruptly expanded over gonad; following few distal pinnulars abruptly narrower, tapering to pinnule tip. Distal pinnules of up to 19 pinnulars, 11 mm long; $Pdist_{(1)}$ much wider than long and wider than following pinnulars; $Pdist_{(2)}$ roughly trapezoidal and narrower distally; $Pdist_{(3)}$ squarish; following pinnulars increasingly longer than wide except near tip; LW at most 1.7. One NHM syntype with gonads weaker on P8, absent by P10 of 10 pinnulars; longest pinnular with LW 2.0. Another smaller NHM syntype with no genital expansion; middle pinnules of 8 pinnulars, and middle pinnulars with LW to 2.6.

Disk completely covered with irregular plates bearing short and blunt rodlike spines.

Distribution.— Northern Indonesia to just south of Japan; 660–1,327 m (A. H. Clark, 1950).

Remarks.— The preceding description is based on A. H. Clark's (1950) text plus photographs of three syntypes of *Antedon acoela* (*Challenger* sta. 214) and the holotype of *Antedon scalaris* (taken by CGM), and direct examination of one syntype (NHMD-873490). A. H. Clark (1950) distinguished *P. acoela* from *P. scalaris* on the basis of differences in the profiles of the brachitaxes and arm bases in side view of the specimens: in *P. acoela* "the lateral profiles of the IBr series are almost parallel, those of the arm bases slightly diverging; the IBr series are constricted so that there is a sudden broadening at the first brachial" (p. 355); in *P. scalaris* "the profiles of the IBr series and arm are smooth and continuous, those of the two sides making with each other an angle of about 60º" (p. 359). However, the profiles are smooth and continuous in at least one *P. acoela* syntype (Fig. 2B), whereas the holotype of *P. scalaris* and at least one syntype of *P. acoela* both exhibit a similar gentle "broadening at the first brachial" (Fig. 2A, D). The remaining diagnostic characters listed by Clark either overlap or are minor and size-related, i.e., centrodorsal diameter 4 versus 5 mm; cirri XXV–XXX, 15–18 versus XX, 20, and arm length 100 versus 110 mm, for *P. acoela* versus *P. scalaris*, respectively. [Note: for the single known specimen of *P. scalaris*, Clark indicated 20 cirrals in the diagnosis but 15 cirrals in the description; the specimen no longer has any attached complete cirri, but a complete detached cirrus has 17 cirrals (Fig. 3B), so 20 is its

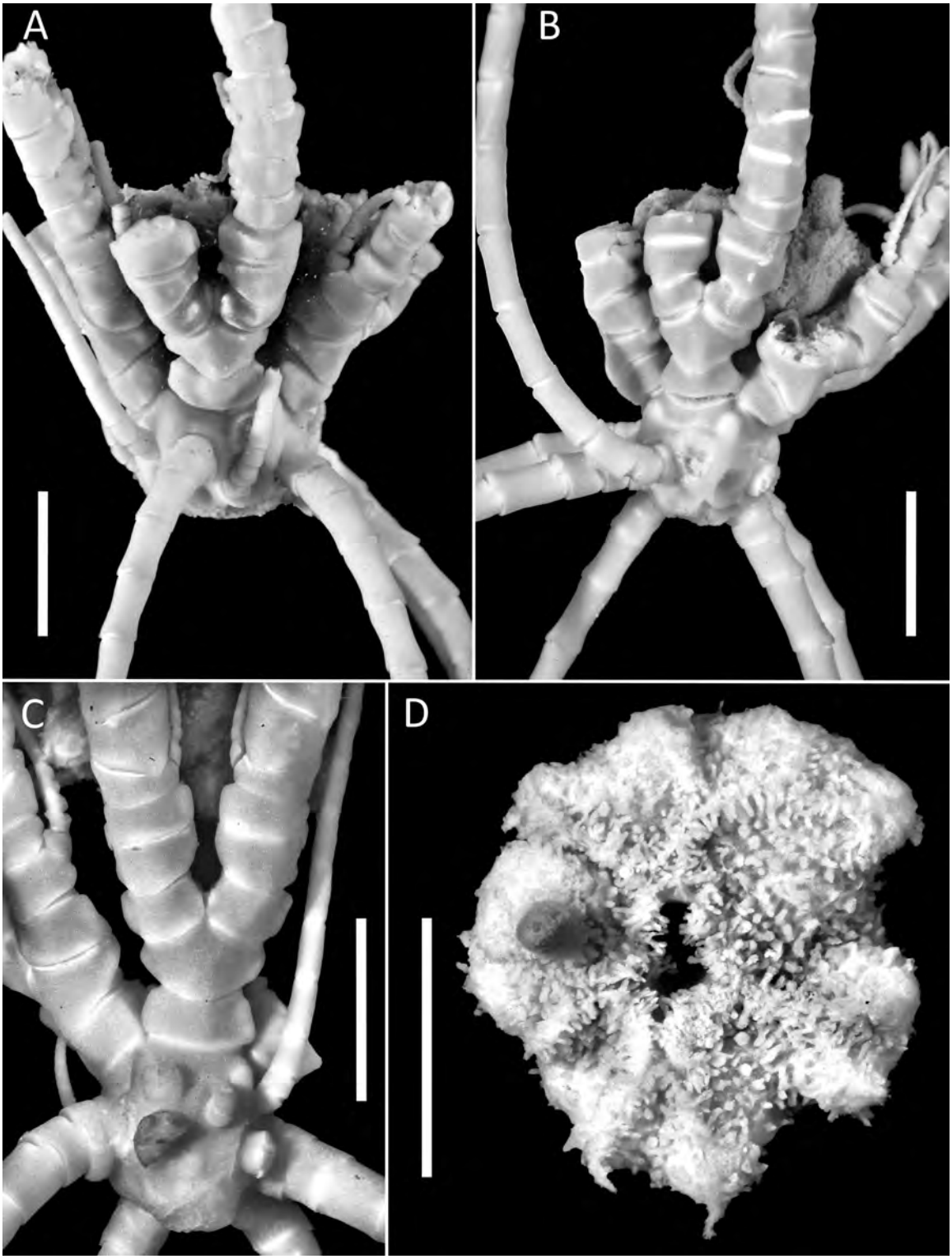

FIGURE 5 — *Poecilometra baumilleri* new species. **A-C**, centrodorsals, and bases of rays and cirri; **A**, FLMNH 21594, **B**, USNM 1660641, **C**, FLMNH 21597. **D**, detached disk, oral surface, FLMNH 21597; scale bars = 5 mm.

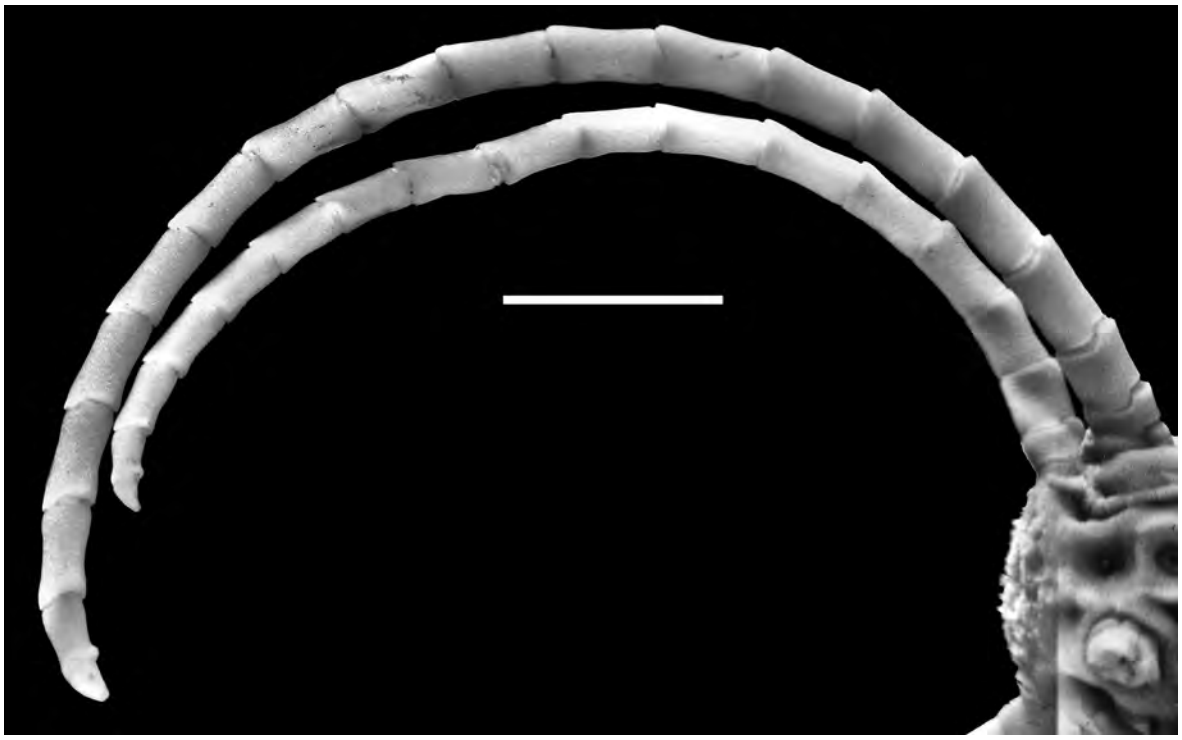

FIGURE 6 — *Poecilometra baumilleri* new species, cirri, FLMNH 21594; scale bar = 5 mm. (Composite image.)

likelier maximum number of cirrals.] We, therefore, treat *P. scalaris* as a junior synonym of *P. acoela*. The addition of *P. scalaris* extends the distribution of *P. acoela* to just south of Japan. The shallower depth record is not surprising given its considerably more northern latitude. More recent mentions of *P. scalaris* refer to no additional material (Kogo, 1998; Kogo and Fujita, 2005).

Small specimens differ from larger ones in having more widely exposed radials and proportionally more elongated proximal brachials with less developed or absent flanges (Fig. 2C).

Poecilometra baumilleri sp. nov.
Figures 5–9, 22I

Holotype.— NOAA *Okeanos Explorer* sta. P4-256, Necker Ridge, SW of Necker I., 21°38'N, 167°49'W, 14 Oct 2011, 1,746 m (FLMNH 21594, 1 specimen).

Paratypes.— NOAA *Okeanos Explorer* sta. P4-257, Necker Ridge, SW of Necker I., 21°31'N, 167°56'W, 15 Oct 2011, 1,802 m (FLMNH 21597, 1; USNM 1660641, 1).

Other material examined.— HAWAIIAN ISLANDS: NOAA *Okeanos Explorer* sta. P4-256, Necker Ridge, SW of Necker I., 21°38'N, 167°49'W, 14 Oct 2011, 1,748 m (FLMNH 21590 (1), 21592 (1)), 1,746 m (FLMNH 21593 (1)).

Diagnosis.— A species of *Poecilometra* with 10 arms; IBr and proximal brachials well separated; Ibr1 with proximal margin almost straight to slightly convex, distal margin shallowly concave, and lateral margins converging and bearing low thick lateral flange or ridge that may be more strongly developed along one side; flange continued but weaker on lateral edges of Iax2 and br1 (sometimes to br2; flanges reduced in small specimens); cirri in large specimens (centrodorsal diameter 3.9–6.5 mm) X–~XVI, up to 19 cirrals, and 42 mm long; longest cirrals with LW typically 2.4–2.7. Distal portion of genital pinnules shorter than gonad, consisting of up to 7 small, narrow pinnulars.

Description.— Centrodorsal dome-shaped, or rounded or truncated conical, and with short thick interradial ridges adjacent to base continuous with slightly swollen proximal corners of radials; centrodorsal proportionally taller in smaller specimens (DH 1.3–1.4 with adoral diameter 3.9–4.6 mm; 1.9 with diameter 6.5 mm); adoral margin in radial area variable, from shallowly concave to deeply V-shaped. Aboral pole flat or gently convex, bearing fine papillae, irregular fine spinules, or radiating ridges; convex without ornament in smallest specimen. Cirrus sockets in two columns per radial area of 1–2 sockets each, often with one socket rudimentary and peripheral, or one obsolete and apical, so that most radial areas have at most 3 sockets; rims of at least some mature peripheral sockets slightly projecting.

Cirri X–XVI (including up to 4 rudimentary), 16–19, to 42 mm long; proximal cirrals increasing in length from base; C1–2 short; C5–6 to C7–8 longest (C7–10 in one specimen), LW chiefly 2.4–2.7 (extremes 2.0–2.9); following cirrals gradually shorter and slightly compressed but remaining longer than wide; penultimate cirral slightly tapering distally,

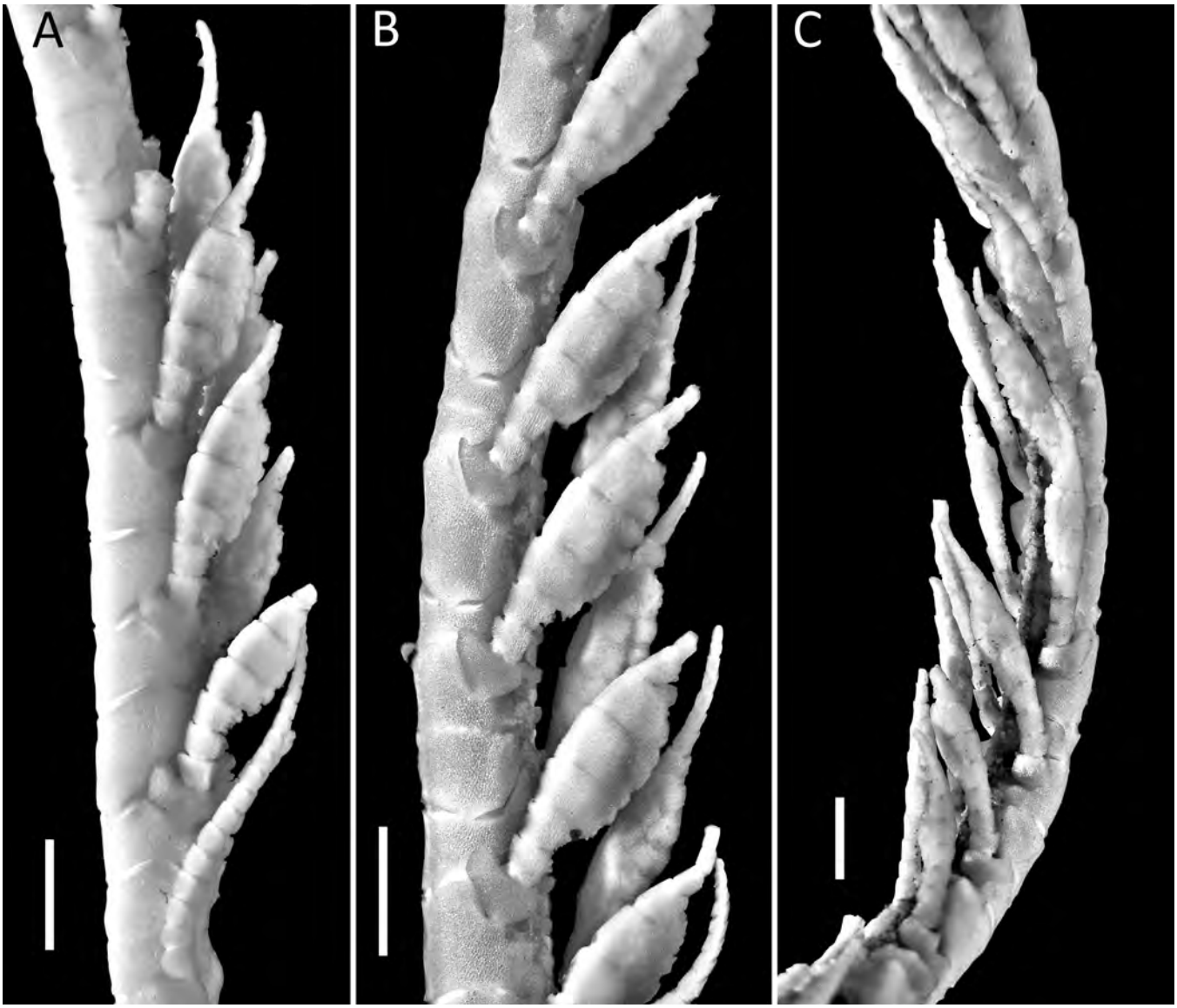

FIGURE 7 — *Poecilometra baumilleri* new species, genital pinnules. **A**, FLMNH 21597. **B**, USNM 1660641. **C**, FLMNH 21594, genital expansion weaker; scale bars = 2 mm.

with weak distal rounded opposing knob, LW 1.8–2.2; terminal claw shorter than preceding cirral, usually gently curved; proximal and distal margins (in lateral view) of C1–2 or 3 sinuous.

Radials hidden or visible as narrow band or small area recessed within V-shaped incision in centrodorsal margin, WL 3.3–4.9. When exposed, with proximolateral corners slightly swollen against interradial ridges of centrodorsal.

IBr2 and brr1–2 with weak to moderately developed, broad rounded synarthrial swelling. Ibr1 narrower distally; proximal margin almost straight, slightly projecting proximally in one specimen; distal margin weakly concave or shallowly V-shaped; lateral margins converging, with low, straight or rounded, thick flange projecting beyond ossicle margin, WL 2.2–3.4. Iax2 rhombic to hexagonal with short lateral margins, wider than Ibr1; lateral corners with small knob, weak rounded flange or irregular projection, WL 1.6–1.9; narrow distolateral margin of Ibr1 and projecting lateral margins of Iax2 create roughly rhombic gap between adjacent rays.

Arms 10, up to ~110 mm long (reconstructed from detached arm). Br1 oblong or with converging interior lateral margin; exterior lateral margin flattened with distolateral knob, or with low ridge or flange, WL 1.4–2.3. Br2 with proximal margin rounded V-shaped; interior lateral margin diverging, sometimes with distolateral knob (3 small knobs on one arm) or weak flange; exterior lateral margin flattened

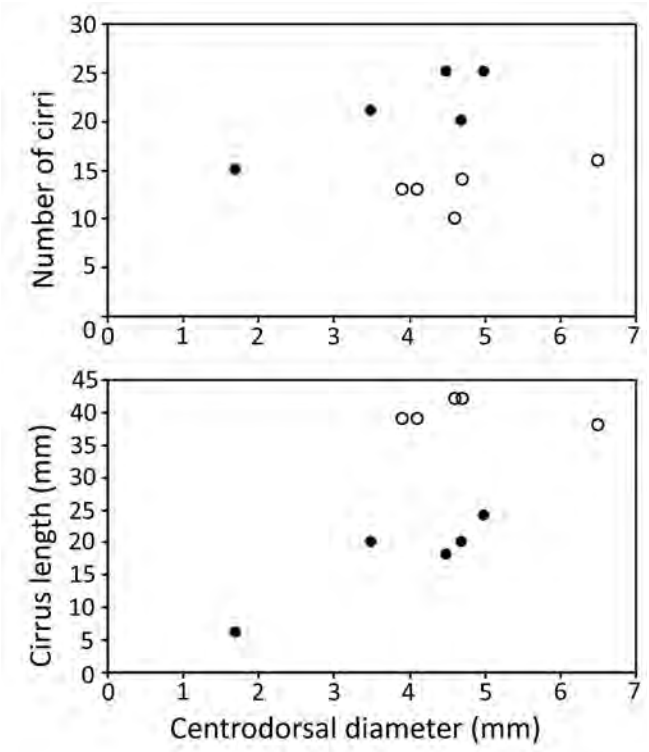

FIGURE 8 — Graph illustrating differences in cirrus number and length relative to centrodorsal diameter in *Poecilometra acoela* (solid circles) versus *Poecilometra baumilleri* new species (open circles).

or with short flange or small knob similar to that on Iax2; WL 1.1–2.0. Truncated interior distolateral corner of br1 and projecting interior lateral margin of br2 create gap between bases of arms arising from the same axil. Most arms detached following br3; most remaining attached arm fragments regenerating at br3+4. br3+4 on attached arm with WL ~1.0; br3 interior lateral margin with distolateral projection, knob, or flange—a continuation of distolateral projection of br2—also on br4 to br6 on a few arms. Following brr increasingly wedge-shaped, but 1 or 2 ossicles from br8 to br10 oblong or almost square; subsequent brr becoming more strongly wedge-shaped, almost triangular by br15. Middle brr strongly wedge-shaped or almost triangular, WL 1.0–1.4, with long lateral margin up to 3.5x length of short lateral margin. Distal brr becoming less strongly wedge-shaped, longer than wide, WL 0.6–1.0 (0.5 nearer arm tip); longer lateral margin ~2x longer than shorter lateral margin; distal margins slightly raised but smooth. Second syzygy at br8+9 to 14+15 (br22+23 on a regenerating arm); distal intersyzygial interval variable, chiefly 2–4, chiefly 4, or 5–9.

P1 of up to 28 pinnulars, 7.8 mm long; all pinnulars short, mostly shorter than wide; some middle segments squarish; $P1_{(1)}$ wider than those following, with abambulacral projection tongue-like and as tall as pinnular width, or weak and rounded or triangular; $P1_{(2)}$ wider distally; $P1_{(3–4)}$ with thick adambulacral keel. P2–P4 first genital pinnule. P2 with up to 16 pinnulars, 5.7 mm long, with weak genital expansion on 2–3 middle pinnulars (e.g., $P2_{(5–7)}$ or $_{(6–8)}$), and middle and distal pinnulars longer than wide, or without genital expansion and resembling P1. Following genital pinnules of up to 14 pinnulars, to 6.9 mm long, shorter with fewer pinnulars (9–13) in most specimens; $Pgen_{(1)}$ with tongue-like abambulacral flange as tall as pinnular width, diminishing on more distal genital pinnules; initial pinnules with well-developed gonad (e.g., Pb, P2–3) with 4 narrow basal pinnulars and genital expansion widest on $Pgen_{(5–7)}$; following genital pinnules with only 2–3 narrow basal pinnulars and genital expansion often widest on $Pgen_{(4–6)}$; segments distal to gonad much narrower. Genital expansion variable (e.g., wide in fig. 7A, B; narrow in figs. 7C, 22I); expansion over gonad reduced on more distal genital pinnules and developing more gradually from proximal pinnulars. Distal pinnules of up to 17 pinnulars, to 12 mm long, tapered near tip, more strongly prismatic than proximal pinnules; $Pdist_{(1)}$ wider than those following, with concave distal margin and weak abambulacral projection (if any); following pinnulars longer than wide, LW 1.8–2.7, except for short, smaller distalmost 1–3 pinnulars.

Disk poorly preserved; sides apparently paved with irregular polygonal plates; plates covering oral surface bearing rounded knob or short blunt spine; disk ambulacra apparently lined with short fingerlike spines.

Distribution.— Currently only known from Necker Ridge, south of the Hawaiian Islands; 1,746–1,802 m.

Etymology.— The species is named *baumilleri* in celebration of Tomasz K. Baumiller, Ph.D., long-term Professor of Earth and Environmental Sciences and Curator of Invertebrates at the Museum of Paleontology, University of Michigan, for his many important contributions to research on both living and fossils crinoids, including evolution, ecology, functional morphology, biomechanics, and taphonomy.

Remarks.— *Poecilometra baumilleri* n. sp. differs from *P. acoela* in having 1) substantially fewer, much longer cirri at similar centrodorsal diameters (Figs. 8, 9); 2) differently shaped Ibr1, in particular with distinctly converging lateral margins and lacking a projecting proximal flange; 3) fine papillae or irregular fine spinules on the centrodorsal apex, at least in larger specimens, and 4) radials remaining more visible in similarly sized specimens. The converging lateral margins of Ibr1 and the narrowing lateral portions of Iax2 create distinct, large, more-or-less rhombic gaps, referred to by A. H. Clark (1915a, 1950) as water pores, between adjacent ray bases.

Poecilometra ornatissima A. H. Clark, 1912a
Figures 10–11

Strotometra ornatissimus A. H. Clark 1912a: 82; 1918: 192–193, figs.10–11; 1950: 362–363, pl. 20 fig. 65.—McKnight, 1989a: 34.—Hess and Messing 2011: 115.—Hemery 2011: 179–188, figs. IV.B.1–IV.B.10.

Strotometra ornatissimns: A. H. Clark 1918: 191 (sic.).

Strotometra ornatissima: A. H. Clark, 1915a: 163, figs. 101–102; 1918: 273, pl. 24, fig. 70.

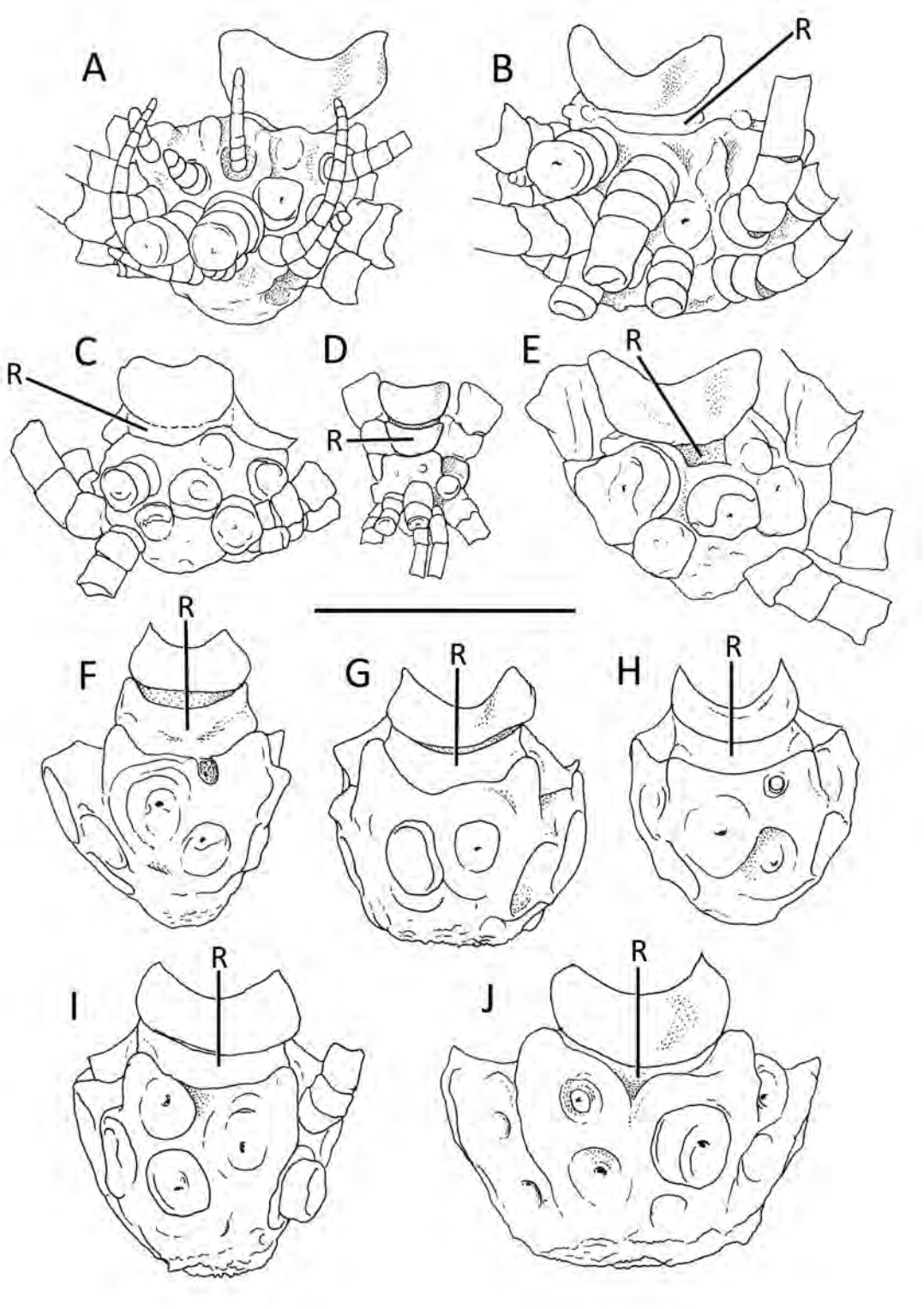

FIGURE 9 — Centrodorsal schematics illustrating numerous versus relatively few cirri in *P. acoela* versus *P. baumilleri*, respectively. **A**–**E**, *Poecilometra acoela* (Carpenter, 1884). **A**, NHM 88.11.9.31 spec. 1. **B**, NHM 88.11.9.31 spec. 2. **C**, NHMD-873490. **D**, NHM 88.11.9.31 spec. 3. **E**, USNM 22629 (holotype of *Antedon scalaris*). **F**–**J**, *Poecilometra baumilleri* new species. **F**, FLMNH 21590. **G**, USNM 1660641. **H**, FLMNH 21592. **I**, FLMNH 21597. **J**, FLMNH 21594. R = exposed surface of radial; scale bar = 5 mm.

Material examined.— INDONESIA: *Albatross* sta. 1899, Celebes Sea, 1°58'30"N, 125°00'30"E, 1035–1264 m, 1906 (NHMD E2088, holotype, photographs only); KERMADEC IS.: M/V *Tangaroa* sta. T243, 30°05'S, 178°15'E, 1035 m, 24 Mar 1982 (NIWA 115369, drawing of 1 of 2); FIJI: MUSORSTOM 10 sta. CP1361, 18°00'S, 178°53'42.6192"E, 1058–1091 m, 13 Aug 1998, sample STRO81 (MHNH-IE-2012-876, 1).

Diagnosis.— A species of *Poecilometra* with 10 arms and distal edges of br2, br4, and br5 strongly everted as a high crest perpendicular to midaboral axis; axils chevron-shaped instead of triangular; C4 or 5 to C6 with LW 2.8–3.4, with expanded distal margins.

Description.— Centrodorsal low hemispherical or discoidal, 2.4–3.0 mm across, DH 2.5. Aboral pole convex. Cirri XXII–XXXVI, 10–15, arranged in one and a partial second, or two to three, irregular marginal tiers (Fig. 10A, 11A). C1 very short; C2 LW 1.1-2.2; C3 LW 2.4-3.3; proximal cirrals strongly constricted centrally; cirrals becoming laterally compressed distally; C4 or 5 to C6 longest, LW 2.8–3.4 (Fig. 10D) (longest cirral unidentified, LW to 2.0 in McKnight (1989a)); distal ends of most cirrals except distalmost 2–3 expanded; distal cirrals with LW 2.0–2.7; distalmost 3-4 cirrals gradually slightly narrower; penultimate cirral slightly smaller than preceding, with small opposing spine and LW 1.4; terminal claw about as long as preceding cirral.

Radials narrowly visible over rim of centrodorsal or hidden by Ibr1, or visible only at interradial angles. IBr2 flat-sided, closely apposed laterally, and with lateral margins of each ossicle diverging and extended as short, often slightly everted and sometimes irregular or weakly scalloped flange; synarthry with weak midaboral swelling. Ibr1 with slightly convex or shallowly Λ-shaped distal margin and with diverging lateral margins, WL 3.3–3.8. Note that the illustration of this feature in the type specimen in A. H. Clark, 1915a (p. 163, Figs. 101–102), is more strongly Λ-shaped than in the photographs (Figs. 10A, C) of the same specimen herein. Iax2 pentagonal or weakly chevron-shaped, WL 2.5–2.8. Lateral thirds of Ibr1 distal margin and Iax2 proximal margin irregularly scalloped or bearing small tubercles that interlock across the articulation.

Arms 10, longest known 40 mm. Brr1–2 also closely apposed laterally, with parallel proximal and distal margins; exterior lateral margins straight; interior lateral margins diverging; lateral eversions and synarthrial swelling weaker than on IBr2. Br1 with interior distal corner extended as triangular projection, WL 2.4–2.7. Br2 with distal margin everted and projecting aborally at right angle to midaboral axis of arm as enormous thin, roughly fan-shaped, crest or shelf, with projecting edge rounded, irregularly scalloped or divided midaborally (Figs. 10A, C); crest height up to three times br2 length; exterior proximolateral corner sometimes produced proximally over distal exterior corner of br1 and scalloped or with weak tubercles; WL ~2.6–2.7. Br3+4 short, oblong; distal margin of br4 bearing crest similar to that of 2. Distal margin crests present to brr10–12 but gradually weakening and projecting more distally, sometimes chiefly reduced to tongue-like projection on one side of distal margin. Middle brachials to br16 triangular, with distal margins projecting distally but not overlapping succeeding brachial; WL 1.7–1.8. Distal brachials wedge-shaped, smooth, with distal margin finely spinose, LW 1.0.

$P_{(1)}$ of proximal pinnules with abambulacral projection similar to those on smaller *P. priamus* specimens. Remaining portion of P1 in holotype of +17 pinnulars, 4.8 mm long (26 pinnulars, 5 mm long in McKnight (1989a)). Remaining P2 in holotype missing narrow terminal portion distal to gonad, of ~11 remaining pinnulars, 4.6 mm long. $P1_{(1)}$ with small, rounded ambambulacral flange as tall as width of $P1_{(2)}$ (Fig. 10B, bottom), also present on following pinnules. Gonads on P3 to P6–7, occasionally P1 or P2 (P2–P3 in McKnight (1989a)); genital pinnules distinctly pedunculate (Fig. 10E), to 4 mm long; $Pgen_{(1)}$ as in P1; following 3–4 pinnulars narrow; abrupt gonadal expansion variable, of 3–4 pinnulars ($Pgen_{(4–6)}$ to $_{(5–8)}$); gonad covered by large plates; gonad followed by up to 6 abruptly narrower, fragile pinnulars. Distal pinnules of 12–16 pinnulars, 8–10 mm long; all pinnulars elongated except for short $Pdist_{(1)}$, which bears distinct aboral keel.

A large specimen (MHNH-IE-2012-876) differs as follows (Fig. 11): centrodorsal 3.6 mm across, DH 1.7, with convex polar area 0.66x basal diameter and cirrus sockets in 2–3 crowded irregular tiers. Cirri LXVII, 15; C4-7 longest, LW diminishing from 3.1 to 2.4 as cirrals become slightly wider distally; distal 2–3 cirrals preceding penultimate sometimes with distal aboral end expanded; antepenultimate cirral of one cirrus with rounded distal projection similar to but weaker than opposing spine (Fig. 11C).

Distal corners of radials barely visible in interradial angles. IBr2 aborally smooth, not laterally flattened or apposed, and with large rhombic gap ("water pore") between adjacent ray bases (similar gap between adjacent brr1-2; Fig. 11A). Ibr1 with lateral margins converging and bearing smooth, short lateral flange, WL 2.0. Iax2 short, rhombic, much wider than Ibr1, with portion of proximal margin extending beyond Ibr1 bearing smooth or irregular flange, WL 1.9-2.2. Longest remaining attached arm 19 mm. Br1 oblong with proximal and distal exterior corners and proximal interior corner everted, and with interior distal corner cut away, WL 2.0; one br1 with interior half of distal margin strongly everted as a broad, fan-like shelf projecting at right angle to arm axis. Br2 short, with strongly diverging lateral margins, WL 2.3. Br3+4 oblong, WL 2.0, 2.4 mm across; br4 shorter than br3. Br5 oblong or wedge-shaped, WL 2.6. Brr5-7 or 8, short, wedge-shaped, with diverging lateral margins, WL 2.1-2.5. Distal margins of brr2, 4, 5, and 6 or 7 bearing projecting crests as in other specimens, strongest on br2, chiefly divided or reduced to 2-3 thick flattened knobs on following brachials. Brachials smooth and triangular by br12. Second syzygy at br9+10 or br10+11. No pinnules intact. $P_{(1)}$ of proximal pinnules with elongated, abambulacral, tongue-like projection similar to that of large *P. priamus*. Disk covered with small, rounded plates (Fig. 5D) similar to those of *P. priamus* but with those lining disk ambulacra apparently not as elongated (Fig. 11B).

Distribution.— Celebes Sea, Indonesia, Kermadec Is., Fiji; 1,035 to 1,264 m (A. H. Clark, 1950; McKnight, 1989a).

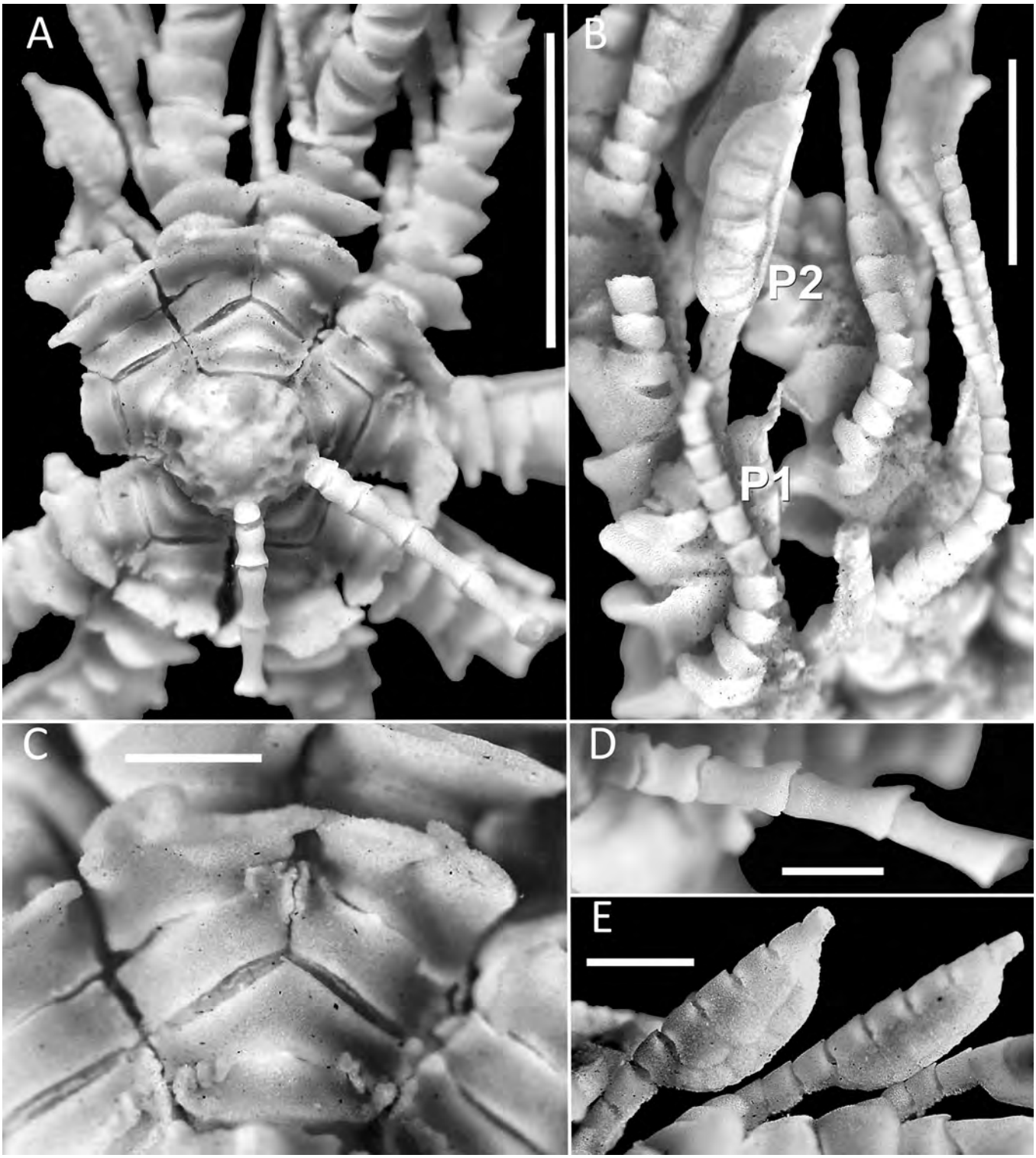

FIGURE 10 — *Poecilometra ornatissima*, holotype, RMNH ECH.2088. **A**, centrodorsal and ray bases, aboral view. **B**, proximal pinnules, lateral view. **C**, IBr2 and proximal brachials of one ray, aboral view. **D**, base of cirrus. **E**, genital pinnules, lateral view; A scale bar = 5 mm; B scale bar = 2 mm; C–E scale bars = 1 mm.

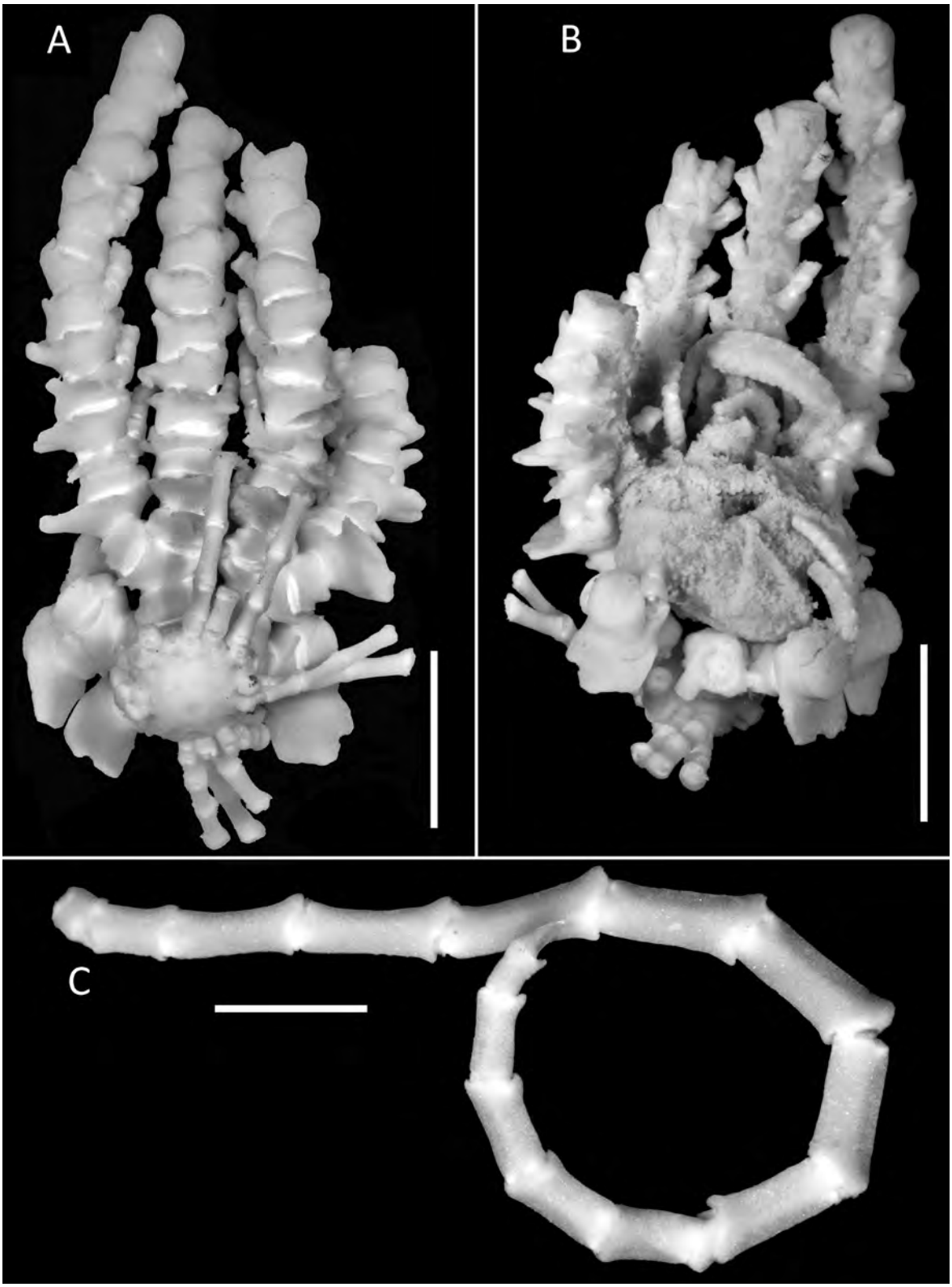

FIGURE 11 — *Poecilometra ornatissima*, MHNH-IE-2012-876. **A**–**B**, entire specimen. **A**, aboral view. **B**, oral view showing disk and one enlarged genital pinnule. **C**. Cirrus; A, B scale bars = 5 mm; C scale bar = 2 mm.

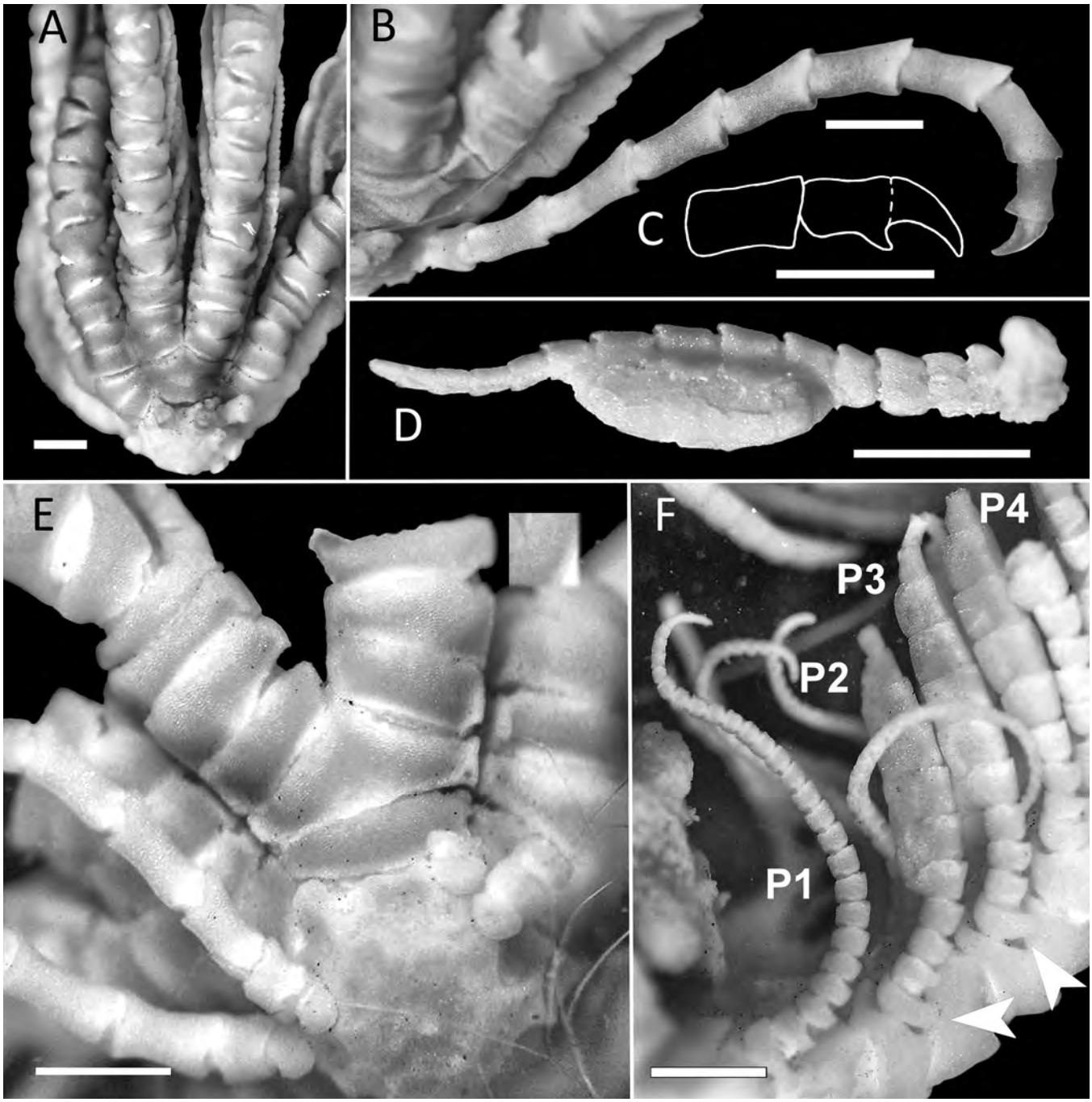

FIGURE 12 — *Poecilometra priamus*, small specimens. **A**–**B**, RMNH.ECH.1813 A, centrodorsal and proximal rays, lateral view. B, cirrus with opposing spine triangular in profile. **C**–**F**, USNM E427. **C**, cirrus tip opposing spine distally curved in profile. **D**, detached genital pinnule with tongue-like projection on $P_{(1)}$, adambulacral view. **E**, centrodorsal and ray base, aboral view. **F**, proximal pinnules with narrow genital expansions on P2-P4, lateral view; arrows indicate short, tongue-like projections on $P2_{(1)}$ and $P3_{(1)}$; scale bars = 1 mm.

Remarks.— Although A. H. Clark (1915a, 1918) repeatedly spelled the species epithet as *ornatissima*, the genus and species epithets of his (A. H. Clark 1912a) original description (and his full description (A. H. Clark 1950)) did not agree in gender (*Strotometra* feminine; *ornatissimus* masculine). As *Poecilometra* is also feminine, the species epithet is herein

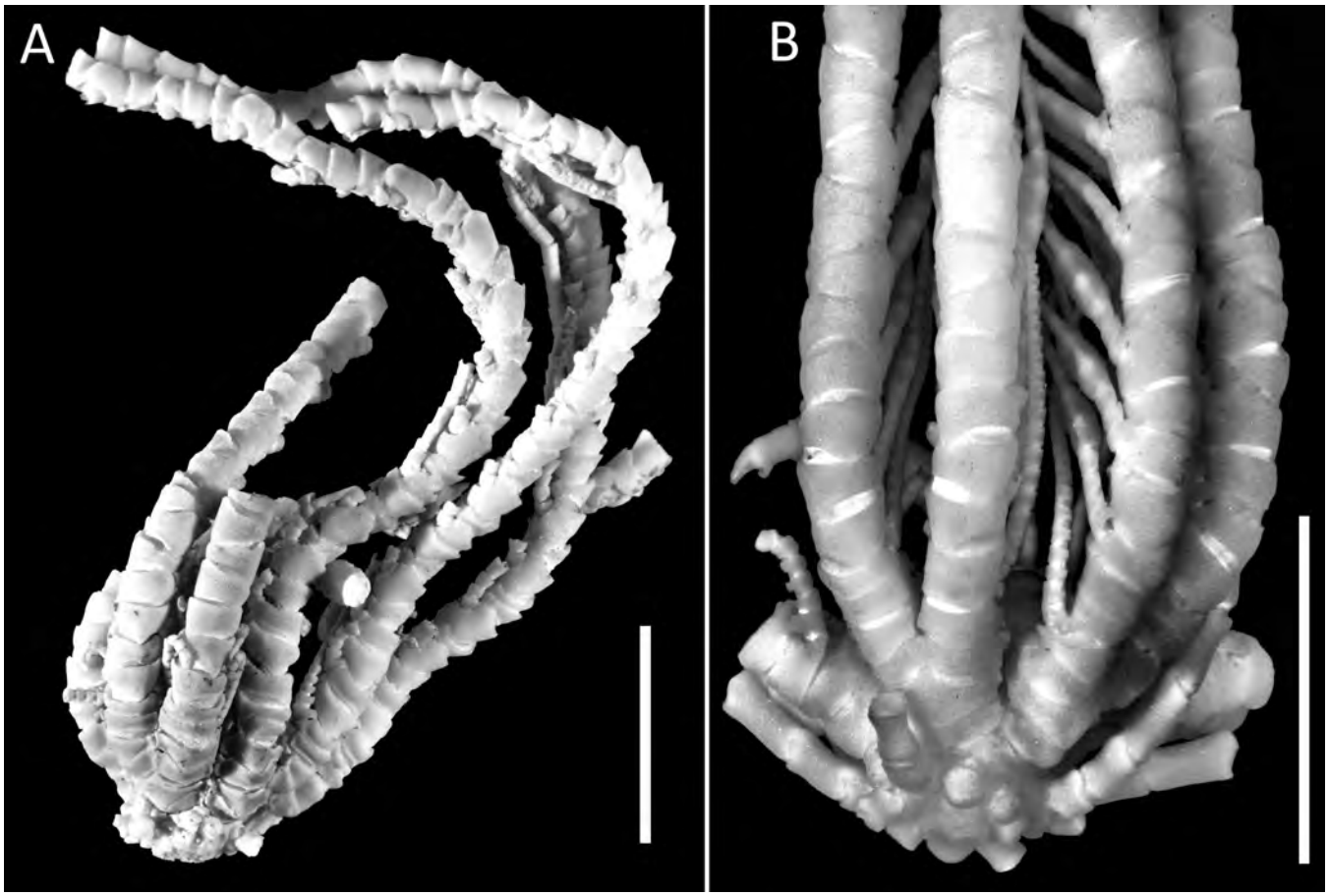

FIGURE 13 — *Poecilometra priamus*, small specimens. **A**, MNHN IE-2019-4434, entire specimen, lateral view. **B**, MNHN IE-2007-5904, centrodorsal and proximal rays, lateral view; scale bars = 5 mm.

formally modified to *ornatissima* (feminine) following Article 31.2 of the International Code of Zoological Nomenclature (ICZN, 1999).

The description above includes information from McKnight (1989a), who found two specimens off the Kermadec Islands that differed somewhat from the holotype, likely associated with their much more complete condition. Those specimens were not examined.

Poecilometra priamus (A. H. Clark, 1912a)
Figures 12–17, 22K, L, 23G

Strotometra priamus A. H. Clark 1912b: 81; 1918: 192, 194, 275, pl.4, figs. 64, 65; 1950: 363–365, pl. 31, fig. 97.— Hess and Messing 2011: 115.

Material examined.— KEPULAUAN KAI (KEI IS.), INDONESIA: *Siboga* sta. 266, 05º56'30"S, 137º47'42"E, 595 m, gray mud with coral and stones; 19 Dec 1899 (USNM E427 (syntypes, 3 of 10 specimens); RMNH.ECH.1813 (syntypes, 2)); Danish Expedition to the Kei Islands, sta. 1, 5°34'S, 132°50'E, 370 m, mud, 30 Mar 1922 (NHMD-873541, 2); Danish Expedition to the Kei Islands, sta. 56, 5°30'20"S, 132°51'E, 345 m, mud, 10 May 1922 (NHMD-873492, 1). NEW CALEDONIA: *Alis* sta. DW790, BATHUS 3, 23°49'S, 169°48'E, 685–715 m, 25 Nov 1993 (MNHN IE-2019-4434, 1, dry); *Vauban* sta. DR04, VAUBAN, 22°17'S, 167°13'E, 400 m, 22 May 1978 (MNHN-IE-2012-831, 3, dry); EXBODI sta. DW3784, 22°13'12"S, 167°09'18"E, 353–365 m, 02 Sep 2011 (MNHN IE-2007-5904, 1); *Alis* sta. CP3833, EXBODI, 22°01'36.0012"S, 167°03'42.0012"E, 325-332 m, 08 Sep 2011 (MNHN IE-2007-6012, 1); *Vauban* sta. CP216, MUSORSTOM 4, 22°59'S, 167°22'E, 490–515 m, 29 Sep 1985 (MNHN IE-2019-4432, 1; MNHN IE-2019-4433, 2); *Alis* sta. CP1721, NORFOLK 1, 23°18'14.8212"S, 168°00'52.1856"E, 416–443 m, 26 Jun 2001, sample STRO57 (MHNH-IE-2012-875, 4 (3 badly fragmented)).

Diagnosis.— A species of *Poecilometra* with as many as 20 arms; IBr and brr1–2 laterally flattened and apposed against adjacent ossicles, with lateral margins bearing projecting and often everted short flange; cirri in large specimens (3.4–4.6 mm across) XXVIII–LXIV, 12–17, to 23 mm long; longest cirrals with LW 2.2–2.5 (to 3.2 in small specimens); first pinnular (P(1)) of proximal several pairs of

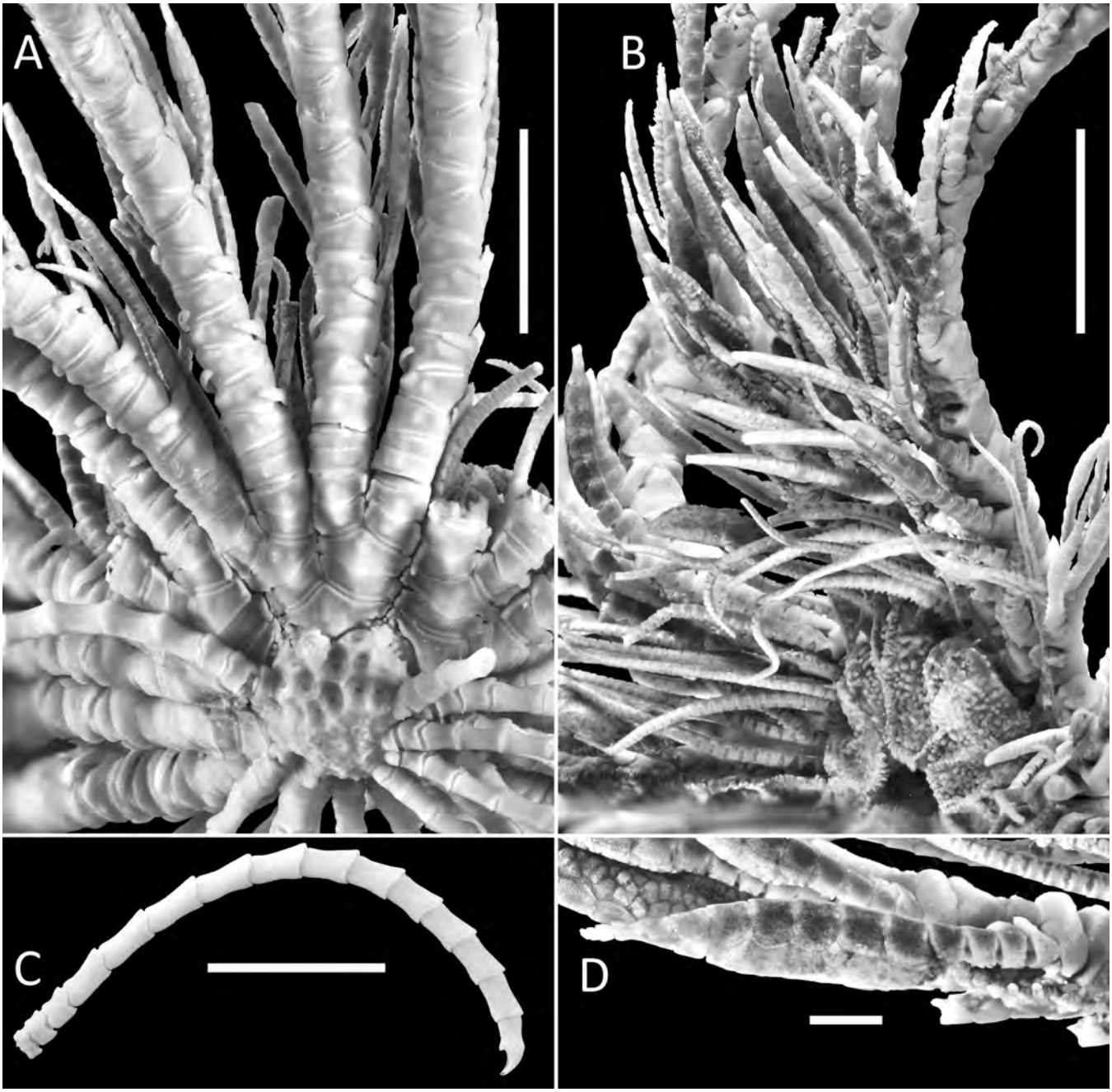

FIGURE 14 — *Poecilometra priamus*, large specimen, MNHN IE-2019-4432. **A**, centrodorsal and ray bases, aboral view. **B**, proximal pinnules and portion of disk showing pavement of nodules, lateral view. **C**, cirrus. **D**, genital pinnule, lateral view; A–C scale bars = 5 mm; D scale bar = 1 mm.

pinnules (sometimes excluding P1) bearing elongated, flat, abambulacral projection, often curved, tongue-like and, in larger specimens, extending around to aboral surface of arm. Distal portion of genital pinnules shorter than or occasionally as long as gonad, composed of up to 7 small, abruptly narrower pinnulars.

Description of smaller specimens (including syntypes).— Centrodorsal a pentagonal convex disk, shallow dome or flattened hemisphere, 1.5–2.9 mm across; DH 1.4–2.5 (Fig. 12A, 13). Interradial corners sometimes with weak irregular papillae or distinct tubercle (Fig. 12E). Aboral pole flat or convex, smooth or with irregular low papillae or traces

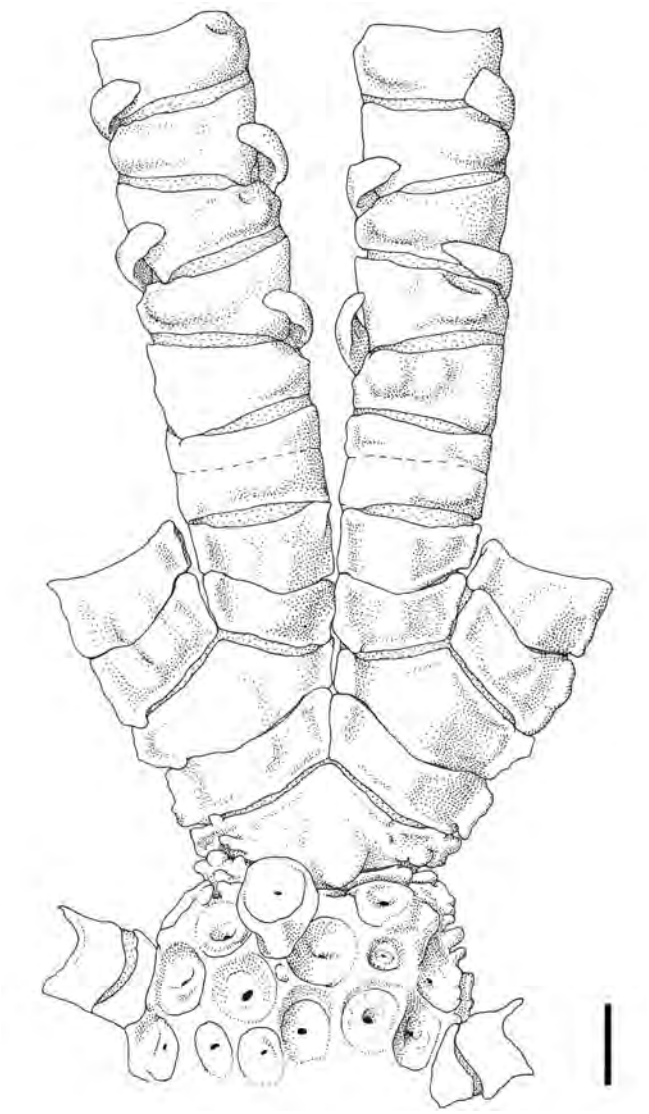

FIGURE 15 — *Poecilometra priamus*, MNHN IE-2019-4432, large specimen. Centrodorsal and base of one ray, aboral view; scale bar = 1 mm. Illustration by C. G. Messing.

of obsolete sockets, 0.5–0.75x centrodorsal diameter; one specimen with tiny apical bump; another with a small apical pit. Cirrus sockets crowded in single and partially double, irregular marginal tiers, rarely encroaching on polar area.

Cirri XI–XXII, 9–13 (possibly to ~15), 8 to ~14 mm long, slender, increasing in length from very short C1; C1 usually with weak to large aboral knob; C2 usually squarish; C4–5 (sometimes C5–6) longest, with LW 2.4–3.2; following cirrals slightly shorter, becoming compressed, wider and slightly constricted centrally with prominent distal end overlapping oral side of succeeding cirral, LW 2.5; distal cirrals with LW 2.0–2.4; antepenultimate cirral LW 1.4–2.1; penultimate cirral narrower, LW 1.5–1.8; opposing spine small, terminal, prominent, distally curved (rarely conical); terminal claw sharp, curved, slightly shorter than or as long as penultimate cirral (Figs. 12B, C).

Radials not exposed, or visible as extremely short, shallow concave band, WL ~6.0–6.5; sometimes only articulation between radial and Ibr1 visible.

IBr2 and brr1–2 flat-sided and closely apposed laterally, with lateral margins of each ossicle diverging and extended as short, often slightly irregular and slightly everted flange, sometimes with weakly scalloped edge and rounded ends (Figs. 12A, E, 13). Synarthrial swelling usually low and rounded, sometimes negligible, typically stronger on IBr2 than brr1–2. Both Ibr1 and Iax2 with lateral margins diverging so that axil is much wider than base of the ray. Ibr1 oblong or shallowly V-shaped, or with lateral portions of proximal and distal margins straight and midaboral portions of proximal margin gently convex and distal margin gently concave; WL chiefly 3.1–4.2 (extremes 2.6–5.0). Iax2 ranging from almost triangular or rhombic (with straight versus shallowly V-shaped proximal margin), both with very short diverging and projecting lateral margins, to distinctly pentagonal or hexagonal (straight versus convex proximal margin, respectively) with more distinct short diverging lateral margins; everted and projecting lateral margins similar to those of Ibr1 but shorter; WL chiefly 2.0–2.3 (extremes 1.8–2.6).

Arms 10–13, longest intact 40–45 mm. All proximal through middle brachials wider than long. Brr1–2 similar to IBr2 in having lateral margins apposed; lateral everted flanges continued from IBr2 but usually weaker. Br1 oblong or with exterior lateral margin longer; distal margin straight or shallowly concave to accommodate synarthrial swelling of br2; exterior lateral margin sometimes ending in rounded triangular projection; WL chiefly 2.1–2.6 (extremes 1.5–2.7). Br2 shorter than br1, almost oblong or slightly wedge-shaped with longer exterior lateral margin and with proximal margin usually convex; WL 2.0–3.0; one specimen with exterior lateral flange rounded and bifid. Br3+4 short, oblong, with lateral margins as in brr1–2 or with lateral eversion weak or absent; WL 1.5–2.0. Brr5–6 (sometimes also br7) weakly to strongly wedge-shaped, wider distally, with or without weak alternating synarthrial swellings; WL 1.8–2.3 (Fig. 12A). Brr7–8 usually almost oblong; WL chiefly 1.7–2.0 (2.3 in one specimen; Fig. 13). Following brachials wedge-shaped, becoming almost triangular; middle brachials ranging from almost triangular to less strongly wedge-shaped; distal margins raised and finely spinose; WL 1.3–1.7. Triangular middle brachials with longer lateral margin to 3.5x length of shorter lateral margin. More distal brachials becoming less wedge-shaped, with finely spinose distal margins; WL 1.0–1.6; weakly wedge-shaped distal brachials with longer lateral margin often only 1.3x length of shorter lateral margin.

Second syzygy from br10+11 to br14+15; following interval 3–4.

First pinnular ($P_{(1)}$) of proximal pinnules from P1 to P4–P7 with abambulacral projection ranging from weak and triangular to well-developed, flattened, and tongue-like (rounded, truncated or irregular), usually strongest on

proximal genital pinnules on which the tip of the "tongue" may curve around to the aboral side of the arm (Figs. 14A, 15), and weakening on more distal pinnules. Although least developed on smallest specimens (Figs. 12F, 13), as indicated by the width ratio of $P1_{(1)}$ to $P1_{(2)}$ no more than about 1.5 (Fig. 17C), this projection is variably developed on similarly sized larger specimens (based on centrodorsal diameter) and is often not uniformly developed on different arms, i.e., weak or absent on one arm (Figs. 16 D, G) but well developed on another (Figs. 16E, H). Second pinnular ($P_{(2)}$) on P1 to P2 or P3 sometimes with weak abambulacral triangular projection. P1 of up to 35 pinnulars, 6 mm long (usually fewer and shorter, e.g., 17–23 segments, 4.7–5.0 mm), slender, delicate; pinnulars chiefly short; mid-distal pinnulars with LW up to 1.5. P2 sometimes not genital, 14 segments, 4.2 mm, similar to P1 but shorter, with more elongated middle pinnulars with LW to 2.25. Genital pinnules usually P2–P4 (Pa on at least one arm of one specimen with $Pa_{(8–10)}$ expanded; P3–P6 on another specimen, with expansion on P6 weaker), pedunculate and composed of distinctly narrower pinnulars preceding and following those bearing gonad; genital expansion variable, of 3–5 (rarely 6) pinnulars, e.g., $P_{(4–6 \text{ or } 7,\ 5–7 \text{ or } 9,\ 6–9,\ 10 \text{ or } 11)}$ (Fig. 12D; Figs. 22K vs. 22L), with broadest pinnulars ranging from 1.1x – 1.7x wider than more proximal narrower pinnular in abambulacral view; 3–7 pinnulars distal to gonad fragile, tapering to pinnule tip; initial pinnular distal to gonad no more than half width of widest genital pinnule. Genital P2 of 12–18 pinnulars, 4–6 mm. P3 similar to P2, 11–14 pinnulars, 3.75–4.5 mm long. P5 of 10 short, prismatic segments, 2.9–3.0 mm; sometimes with slight gonadal expansion on $P5_{(4–5)}$. P6 chiefly non-genital. Following pinnules gradually increasing in length. Middle pinnules of 10–12 pinnulars, 4.0–5.0 mm; most middle pinnulars of equal length, LW 1.4–1.75, becoming proportionally longer as pinnule narrows distally. Distal pinnules longer, probably reaching ~16–17 pinnulars.

Disk covered with rounded nodules.

Description of larger specimens.— Centrodorsal a flattened pentagonal hemisphere, 3.7–5.1 mm across, DH 1.6–3.1; Aboral pole usually no more than half adoral diameter of centrodorsal, flat or slightly convex, irregularly shaped, pitted or with traces of obsolete sockets, usually with apical sockets encroaching around margin. Centrodorsal margin shallowly concave radially, sometimes with a few small, rounded projections. Cirrus sockets in 2–3 crowded, irregular tiers, sometimes with each radial area having sockets arranged in a lateral column of 2–3 sockets each with midradial sockets arranged irregularly (Fig. 14A, 15).

Cirri XXXVII–XL, 12–18, 12–20 mm long (Fig. 14C). C1 short; following cirrals increasing in length; longest cirrals varying from C4–5 to C6–8, with LW chiefly 1.7–2.2 (to 2.4 on apical cirri); following cirrals decreasing gradually in length but remaining longer than wide; penultimate cirral narrower, WL 1.3; opposing spine located distally on cirral, triangular or rounded in profile, well developed (Fig. 12B, C) or small (Fig. 14C), with spine tip directed aborally (Fig. 12B) or curved distally (Fig. 12C); opposing spine on some cirri of one specimen (MNHN IE-2019-4433) broad and scoop-shaped in distal view; terminal claw usually shorter than preceding cirral, sometimes shorter and rounded (possibly eroded); cirrals beyond basal few with expanded distal margins.

Radials either hidden by centrodorsal or just visible in interradial angles; distal margin with a few weak tubercles. IBr2, IIBr2 and brr1–2 closely apposed and laterally flat-sided; aboral surface ranging from flat through gently to strongly convex, usually with rounded midaboral synarthrial swellings; swellings weaker on IIBr2, and sometimes absent on brr1–2. Lateral margins of brachitaxes ossicles extending beyond articulations as short thick flange, slightly everted, often weakly scalloped or wrinkled, and sometimes interlocking with adjacent ossicle; proximal and distal margins of ossicles sometimes raised as weak, narrow ridge, smooth or slightly wrinkled. Interior distal corners of IIbr1 and br1 sometimes with extended triangular or rounded tip (Fig. 14A, 15). Ibr1 shallowly V-shaped, extremely short, partly to mostly hidden by centrodorsal; lateral portion of distal margin sometimes with few weak knobs. Iax2 pentagonal or hexagonal with short diverging lateral margins; WL 1.8–2.6. IIbr1 oblong or shallowly V-shaped, with diverging lateral margins, WL 2.3–3.4; IIax2 similar to Iax2, WL 1.5–2.25.

Arms 18–20; longest intact arms ~80–100 mm. Brr1–2 flat-sided and apposed, sometimes with lateral margins weakly extended beyond articulation (Fig. 14A, 15). Br1 oblong or slightly longer exteriorly, sometimes with shallowly concave distal margin, WL 1.8–2.4. Br2 longer exteriorly, WL 1.9–2.4. Br3+4 oblong, WL 1.2–1.7; 1.2–1.66 mm across; low midaboral swelling sometimes present; br4 shorter than br3. Following few brachials weakly wedge-shaped, sometimes with low, broad swelling on alternating sides of successive brachials, WL 1.9–2.4. Brr9–10 or brr10–11 (sometimes only one) oblong, WL 2.0–2.1. Following brachials becoming triangular with weakly raised, finely spinulose distal margins, WL 1.7–2.1 (rarely to 2.4). Middle brachials strongly wedge-shaped to almost triangular, with longer lateral margin gently convex, WL 1.4–1.9 (rarely to 2.2). Brachials becoming wedge-shaped again distal to mid-arm, becoming weakly wedge-shaped distally, with longer lateral margin slightly convex and with distal margins slightly raised and weakly spinulose, WL 1.0–1.1, becoming longer than wide near arm tip.

Second syzygy widely variable, including on same specimen, from br8+9 to at least br24+25 (one specimen with 5+6 and 7+8 on separate arms); distal interval 3–6 (sometime to 9).

P1 with up to 41 short pinnulars, to 8.8 mm long, tapering from base to slender flexible tip (Fig. 14B); $P1_{(1)}$ usually with abambulacral flange or irregularly triangular projection ranging from weak to taller than width of body of pinnular, often variably developed on different arms of a specimen and infrequently absent (Fig. 16F–I); following several pinnulars with abambulacral keel; remaining pinnulars cylindrical. Abambulacral flange on following several pinnules increasingly longer, tongue-like, and in larger specimens often

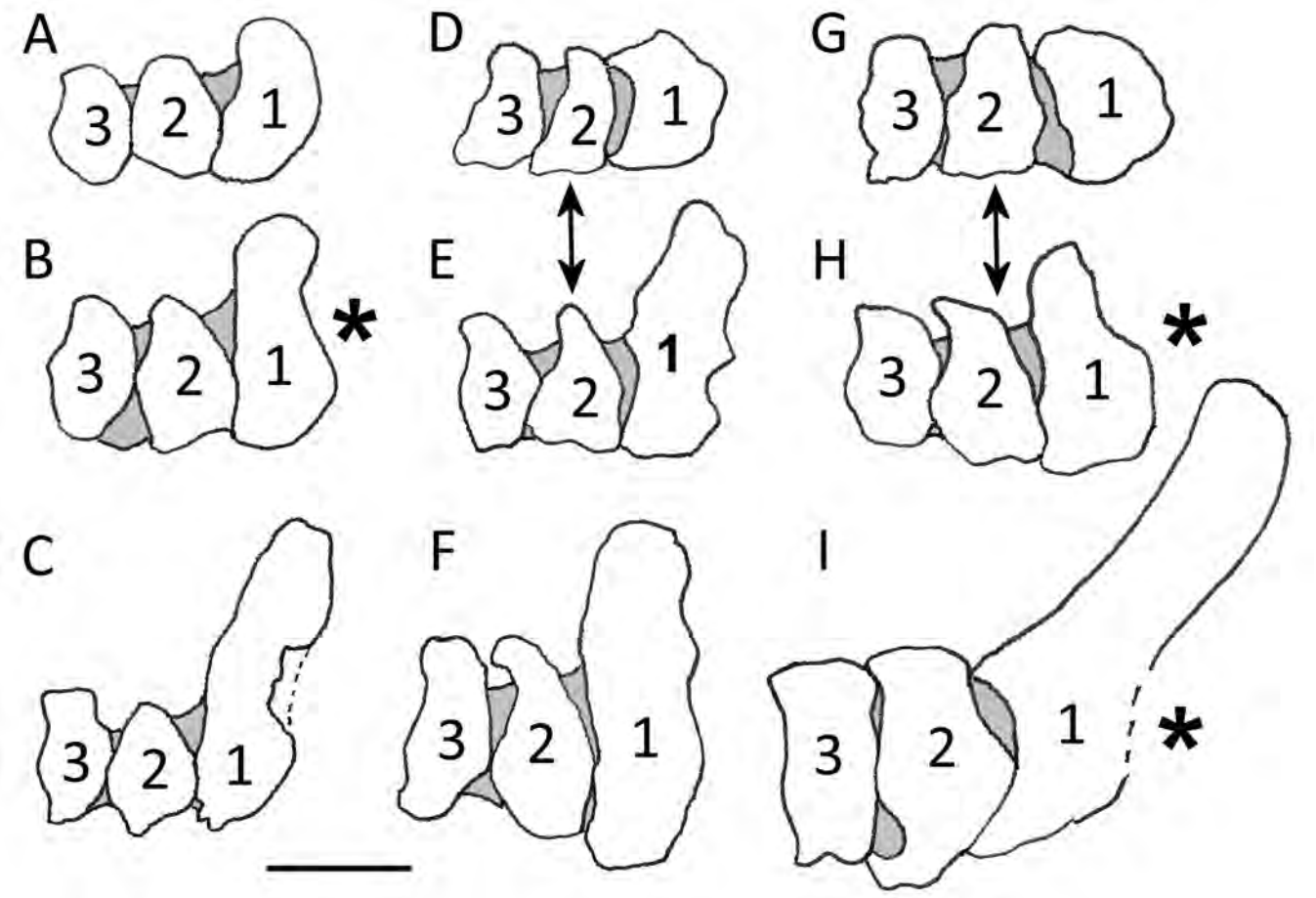

FIGURE 16 — *Poecilometra priamus*. Variations in abambulacral flange development on P1. **A**, NHMD-873492. **B**, NHMD-873541. **C**, MNHN IE-2012-831. **D**–**E**, MNHN IE-2007-5904, different arms. **F**, MHNH-IE-2012-875. **G**–**H**, MHNH-IE-2012-875 [different specimen than F], adjacent arms. **I**, MNHN IE-2019-4432, slightly oblique view. Numbers inside ossicles indicate first through third pinnulars ($P1_{(1\text{-}3)}$). Asterisks (*) indicate images that have been reversed for ease of comparison. Double-ended arrows indicate pinnules from different arms on the same specimen. Dashed line on right side of $P1_{(1)}$ in C indicates broken portion. Dashed line on right side of $P1_{(1)}$ in I indicates portion of ossicle hidden by adjacent arm; scale bar = 0.5 mm.

curving around onto aboral surface of arm (Fig. 15); becoming weaker anywhere from P5 to P12; absent on distal pinnules. Non-genital P2 similar to P1, of up to 29 pinnulars, 8.7 mm long; middle and following pinnulars longer than wide except near tip. Gonads usually on P2–P6, sometimes to P10; sometimes only 1–2 pinnules with fully developed gonads per side of arm; genital expansion ranging from narrow to broad (Figs. 14B, D). Genital P2 with narrow to well-developed gonad on $P2_{(9 \text{ or } 10 \text{ to } 15,\ 6\text{–}11,\ \text{or } 8\text{–}14)}$, on $P2_{(4\text{–}6)}$ of smaller specimen; narrow distal portion of pinnule shorter than gonad, of up to 10 pinnulars, each longer than wide except near tip. Gonad irregularly plated. P3 of up to 22 pinnulars, to 8.4 mm long; genital expansion variable, of 4–5 pinnulars beginning anywhere from $P3_{(6)}$ to $P3_{(9)}$; up to ~7 narrow pinnulars distal to gonad. Middle and distal pinnules prismatic; middle pinnules up to 18 pinnulars, to 8.7 mm long; distal pinnules up to 17 pinnulars to 7.9 mm long; $Pdistal_{(1)}$ short and wide, no flange; $Pdistal_{(2)}$ squarish; following pinnulars with LW 1.2–1.3.

Disk covered with numerous small, rounded nodules (Fig. 14B).

Distribution.— South of Timor I., eastern Indonesia, and New Caledonia; 245–685 (possibly 715) m (A. H. Clark, 1950 and herein).

Remarks.— Small and large specimens have been described separately above, because the larger specimens were initially thought to be a species distinct from *S. priamus* based on the enormously elongated, tongue-like projections on the first pinnular of proximal pinnules that often wrapped around to the aboral arm surface and looked like the fingers of a reed instrument player (Romanowski, 2015), and because specimens of intermediate size are lacking. However, examination of the type material of *S. priamus* (all small and ten-armed) revealed weakly developed versions of these projections in some specimens. In addition, new, small

specimens collected off New Caledonia with the distinctive large specimens resemble type specimens. A comparison of all specimens indicated that the pinnular projection is somewhat size related (i.e., least developed on smallest individuals) but may vary substantially among different arms of an individual (Figs. 16, 17C).

A. H. Clark (1912a) based his original description of *Strotometra priamus* on more than one specimen from *Siboga* sta. 266 (e.g., "centrodorsal…1.5 mm. to 2.0 mm in diameter", p. 81), which he designated as the type locality, but he did not indicate the number of specimens. His re-description (A. H. Clark, 1950, p. 365) indicates the number and location of specimens from this sta. as "(39, U.S.N.M., E. 427; Amsterdam Mus.)". However, USNM E427 includes 10 specimens; C.G.M. examined 2 specimens in RMNH. ECH.1813, and ZMA.ECH.CR.2089 includes 39 specimens listed as syntypes that were not examined. All are from sta. 266, indicating a total of 51 syntype specimens. Note: the original NHMD labels indicate 370 m and 345 m for the specimens from stations 1 and 56, respectively, but A. H. Clark (1950) gives the depths as 370-400 m and 245 m.

The new specimens extend this species' range to New Caledonia and increase the depth range to about 700 m.

Hemery's (2011) Maximum Likelihood tree placed a specimen identified as *Strotometra* n. sp. (MHNH-IE-2012-875, here treated as *P. priamus*) close to *Poecilometra ornatissima*. Both species have similar cirrals, brachitaxes, pedunculate genital pinnules, and an aboral P(1) flange.

Strotometra A. H. Clark, 1909a

Antedon (Part) Carpenter 1888: 127
Charitometra (Part) A. H. Clark 1907a: 361
Strotometra A. H. Clark 1909a: 19; 1912a: 9, 11, 25, 60, 226; 1918: 172, 191.—Gislén 1928: 9; 1934: 18.—A. H. Clark 1950: 361.—Hess and Messing 2011: 115.

Type species.— *Antedon hepburniana* A. H. Clark 1907b.

Other included species.— *Strotometra parvipinna* Carpenter, 1888.

Diagnosis.— A genus of Charitometridae with centrodorsal hemispherical or discoidal; cirrus sockets in irregular marginal rows; cirri short and stout, X-XV, 10–15; ten arms; rays extending outward from oral-aboral axis; genital pinnules either with 1–2 narrow basal pinnulars or broadening gradually from the base; genital expansion over gonad usually at P(3–5) and tapering gradually distally; expanded pinnulars asymmetrical in cross-sectional view, with a longer, curved flange and usually shorter, thicker triangular flange, and articulation proportionally larger than in *Poecilometra*.

Distribution.— SW of Timor, eastern Indonesia (Kepulauan Kai), East China Sea, Ogasawara Is. and southern Japan; (160?) 183 to 660 m (A. H. Clark, 1950; Utinomi and Kogo 1968; Kogo, 1998; Kogo and Fujita, 2005).

Remarks.— With the transfer of *Strotometra ornatissimus* and *S. priamus* to *Poecilometra* herein, *Strotometra* retains only *S. parvipinna* and *S. hepburniana*. However, a combination of morphological and molecular data strongly suggest that they represent a single species, and we treat the genus as monotypic (see below).

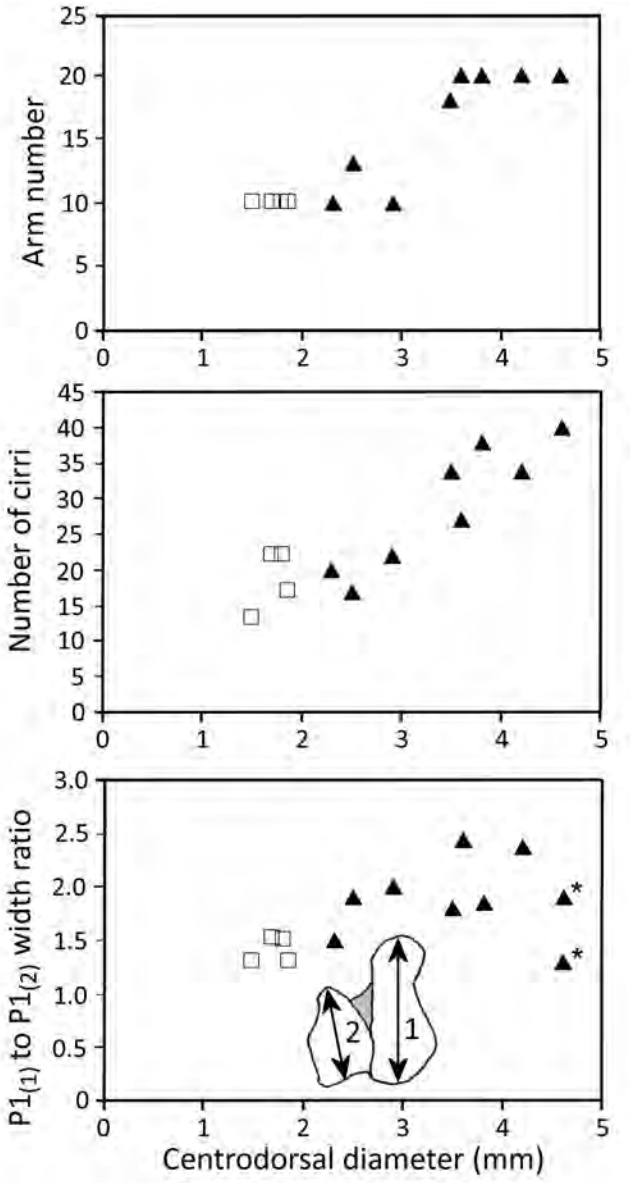

FIGURE 17 — *Poecilometra priamus*. Graphs illustrating variations in arm number, number of cirri, and width ratio of first two pinnulars ($P1_{(1)}$ to $P1_{(2)}$) relative to specimen size based on centrodorsal diameter. Double-ended arrows in bottom graph indicate width measurements of illustrated $P1_{(1)}$ and $P1_{(2)}$, giving a width ratio = 1.53. Open squares = syntypes: USNM E427, NHMD-873492, and NHMD-873541 (2). Black triangles, MNHN specimens from New Caledonia: IE-2019-4434, IE-2007-6012, IE-2007-5904, IE-2012-831 (2), IE-2012-875, IE-2019-4432, and IE-2019-4433 (2). * indicates values from two arms of one specimen.

Strotometra parvipinna (Carpenter, 1888)
Figures 18–21, 22M–O

Antedon parvipinna Carpenter 1888: 127, pl. 15, fig. 9.—Hartlaub 1895: 130.—Hamann 1907: 1578.—A. H. Clark 1912a: 33, 226.
Antedon hepburniana A. H. Clark 1907b: 139; 1912a: 33, 226.
Charitometra parvipinna: A. H. Clark 1907a: 361.
Charitometra hepburniana: A. H. Clark 1907a: 361; 1908a: 603.
Strotometra parvipinna: A. H. Clark 1909a: 20; 1912a: 33, 226; 1913a: 50; 1918: pl. 10, 192, 194, 274–275.—Gislén 1928: 9; 1934: 18.—A. H. Clark 1950: 365–368, 370.
Strotometra hepburniana: A. H. Clark, 1909a: 20; 1909b: 187; 1912a: 33, 226; 1913a: 50; 1913b: 179; 1915b: 215; 1918: 192, 194, pl. 9; 1921: pl. 2, fig. 28; 1950: 367–370, pl. 31, figs. 95–96, pl. 32 fig. 104.—Utinomi and Kogo 1968: 51; Kogo, 1998: 111, 115–116, fig. 93.—Kogo and Fujita, 2005: 350.—Hemery 2011: 179–188, figs. IV.B.1–IV.B.10.

Holotype.— *Antedon parvipinna* Carpenter, 1888, NHM 88.11.9.26, *Challenger* sta. 192, Kei Islands, 5°49’15”S, 132°14’15”E, 256 m, 26 Sep 1874.

Material Examined.— INDONESIA: *Challenger* sta. 192, Kepulauan Kai (Kei Is.), 5°49’15”S, 132°14’15”E, 256 m, 26 Sep 1874 (NHM 88.11.9.26, holotype, photographs only); Danish Expedition to the Kei Islands sta. 56, 5°33’S, 132°51’30”E, 345 m, 10 May 1922 (USNM E3142 (identified as *S. parvipinna*, 1 specimen, photographs only), NHMD-874397, 4). JAPAN: *Albatross* sta. 4890; 10 miles SW of Goto Is., 32º26'30"N, 128º36'30"E, 243 m, 9 Aug 1906, bottom temp. 11.28ºC, rocky bottom (USNM 35692 (identified as *S. hepburniana*, photographs only); Captain Schönau, Eastern Sea, S of Goto Is., 32°10’N, 128°20’E, 183 m [180 m in AHC 1950], 23 Apr 1898 (NHMD-873531, 1, as *S. hepburniana*). “EAST ASIA” [probably East or South China Sea]: [Capt.] Suensson, [Danish cable-repair ship] Eastern Asia, 19 Apr 1911 (NHMD-873536, 1, as *S. hepburniana*).

Description.— Centrodorsal discoidal or low hemispheric, with strongly projecting, rounded or irregularly triangular interradial projections visible in some specimens (identified as basal rays in A. H. Clark (1950)), ~2.0–3.3 mm diameter, DH 2.1–2.5. Interradial projections sometimes roughened or bearing tiny conical tubercles. Cirrus sockets crowded in single or partly double, irregular, marginal row(s) (apical aboral to basal socket in an irregularly columnal arrangement in one specimen). Apical pole flat or gently convex, covered with weak irregular sculpture (irregular tubercles, ridges) imparting a sponge-like appearance, rarely smooth, 0.6–0.8x centrodorsal diameter; one specimen with a gently convex center surrounded by small irregular bumps and vestiges of apical sockets.

Cirri short, stout, X–XVIII (chiefly XIII–XVI), 9–15 (chiefly 11–13), up to ~12 mm long; C1 very short; following cirrals progressively longer; C4–5 to C5–6 (rarely to C7) longest, LW 0.9 to 1.2 (maximum 1.6); following cirrals shorter, LW 0.7 to 1.0; cirrals in distal half slightly compressed and wider than proximal cirrals; distal few cirrals preceding penultimate with swollen, rounded aboral distal end; antepenultimate cirral sometimes narrower than preceding; penultimate cirral always narrower than preceding, LW 1.1–1.3; small opposing spine usually rounded triangular and distally directed, sometimes sharply conical and/or erect, sometimes eroded and blunt; terminal claw curved, shorter or longer than penultimate cirral.

Radials completely hidden by centrodorsal or cirri, visible only in interradial angles, or exposed as extremely short, gently curved bands (concave distally), with lateral margins sometimes swollen. IBr2 gently to moderately convex aborally, laterally flattened and apposed, with midaboral rounded synarthrial swelling or weak narrow keel; lateral margins sometimes projecting as thin flange or short ridge. Ibr1 oblong to slightly crescentic (concave distally), often narrowing laterally, with lateral portions of aboral surface bearing one or more rounded knobs or small irregular conical tubercles (sponge-like appearance); lateral margins sometimes weakly everted; WL 3.7–5.2. Iax2 usually pentagonal, often with proximal margin slightly V-shaped; lateral margins diverging or straight (rarely negligible so that axil appears triangular), usually slightly everted with slightly irregular flange, WL 1.8–3.0; lateral portions of either proximal or distal margins (or both) sometimes slightly everted and lined with fine tubercles or tiny irregular teeth; distal margin sometimes irregularly swollen.

Arms 10, to 75 mm long, increasing in width from base to brr6–10; weak (usually barely noticeable), narrow midaboral ridge present, sometimes a low round or slightly elongated knob on proximal brachials, sometimes limited to proximal brachials, rarely absent on some or all brachials. Brr1–2 laterally flattened and apposed; lateral margins with weak projecting flange, sometimes weakly everted with finely irregular or dentate edge. Br1 oblong or weakly wedge-shaped and slightly longer exteriorly, sometimes slightly curved (concave distally); interior distolateral corner a rounded or triangular projection; WL 1.9–2.6. Br2 longer exteriorly, WL 2.1–2.8. Br3+4 oblong; lateral margins at least slightly flattened (rounded in one specimen); br4 (rarely also br3) with thickened, flared distal margin; WL 1.4–1.9, 1.1–1.55 mm across. Br5 oblong or with interior margin slightly longer; one or both lateral margins often diverging; distal margin thickened and flared; WL 2.0–2.8. Following several brachials (to brr9–10) short, wedge-shaped, with diverging lateral margins, and distal margin thickened, flared and concave, much wider than visible span of succeeding articular ligament; WL 1.9–3.0. Following brachials becoming strongly wedge-shaped, then triangular, with distal margin not as thickened, flared and concave as more proximal brachials; middle brachials proportionally more elongated, but remaining wider than long. Brachials becoming wedge-shaped distally, with distal margin less thickened than on

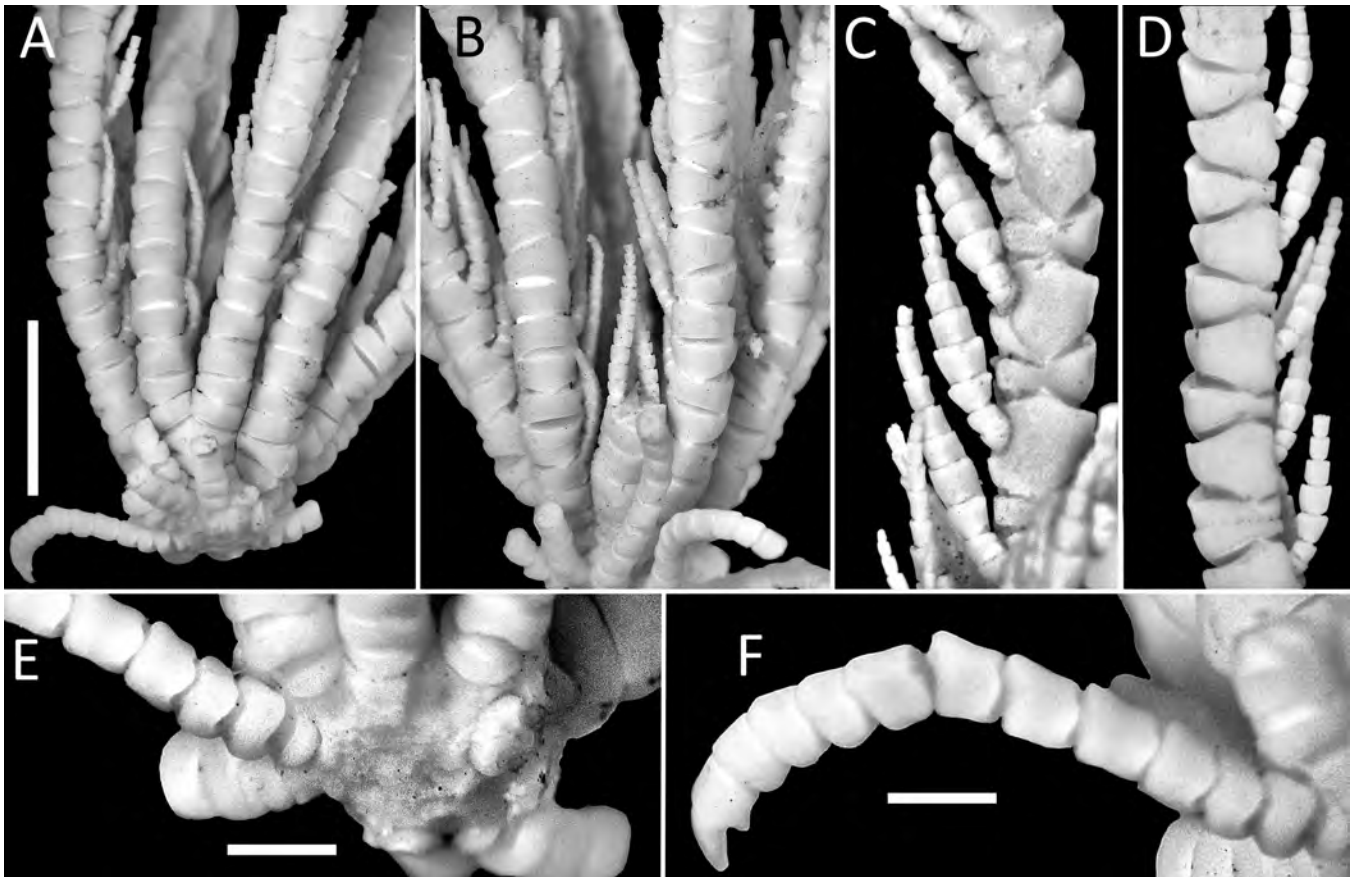

FIGURE 18 — *Strotometra parvipinna* NHM 88.11.9.26 (holotype). **A**, centrodorsal and proximal arms, lateral view. **B**, proximal arms showing proximal pinnules, lateral view. **C**, genital pinnules. **D**, middle arm. **E**, centrodorsal. **F**, cirrus. Portions of strongly out-of-focus cirri deleted in **E** and **F**; A–D scale bars = 5 mm; E–F scale bars = 1 mm

more proximal brachials; WL 1.5–1.7, and proportionally more elongated near arm tip; WL 1.0–1.3.

Syzygies at br3+4 (absent on at least 4 arms (1 on each ray) on one specimen); second widely variable, usually br13+14 to br15+16 (extremes br8+9 to br18+19); distal interval chiefly 4–9 (extremes 3–10).

P1 to 23 pinnulars, 5.0 mm long (usually shorter with fewer pinnulars, e.g., 13–17, 4.4–4.6 mm), sometimes much smaller and shorter on at least some arms; pinnulars all short, most with abambulacral margin slightly diverging and distal corner projecting; 1–3 pinnulars near tip sometimes longer than wide, LW to 1.3; ambulacral groove present; $P1_{(1)}$ wider than $P1_{(2)}$, with abambulacral projection; $P1_{(2)}$ short; $P1_{(3\text{-}4)}$ wider with diverging abambulacral margin; following pinnulars gradually narrower, with lateral margins becoming parallel. P2 usually non-genital, similar to P1 (sometimes shorter or longer) with up to 17 pinnulars, 4.2 mm long; $P2_{(3–5)}$ to $_{(4–6)}$ with diverging lateral margins, expanded but not as much as on genital pinnules; following pinnulars gradually narrower; distal few pinnulars squarish or with LW to 1.2. One specimen with P2 genital, 12 pinnulars, 4.0 mm long, with $P2_{(3–6)}$ expanded over gonad; $P2_{(4)}$ widest, LW 0.55, rapidly narrowing distally with 2–3 pinnulars near tip longer than wide, LW to 1.7. P3 genital or not.

P4 usually first genital pinnule, up to 13 pinnulars, 4.8 mm long; $Pgen_{(1)}$ wider than $Pgen_{(2)}$; $Pgen_{(2)}$ short, with diverging lateral margins; $Pgen_{(3 \text{ or } 4)}$ to $_{(5 \text{ or } 6)}$ (rarely to $Pgen_{(7)}$) expanded over plated gonad; expanded pinnulars either with both lateral margins diverging, or with abambulacral margin diverging with rounded triangular distal end, and adambulacral margin rounded, LW 0.5–0.8; pinnule distal to gonad gradually tapering; longer distal pinnulars with LW 1.2–1.7. Mid-abambulacral ridge on expanded gonadal pinnulars in NHMD-873531 (identified as *S. hepburniana*) with rounded distal projection so that distal margins of these pinnulars appear to have a pair of rounded distal knobs (Fig. 22O). Distalmost gonad variable, on P8 to P12, sometimes variably developed on different pinnules of a single arm. Middle (non-genital) pinnules to 14 pinnulars, 5.2 mm long; $Pmid_{(3–4)}$ weakly expanded; 1–3 pinnulars near tip with LW to 1.3. Distal pinnules to 17 pinnulars, 5.0 mm long; $Pdist_{(1)}$ short, $Pdist_{(2)}$ with LW ~1.0; following pinnulars longer than wide, to LW 1.8 near tip; distal end of abambulacral ridge pointed and slightly projecting distally.

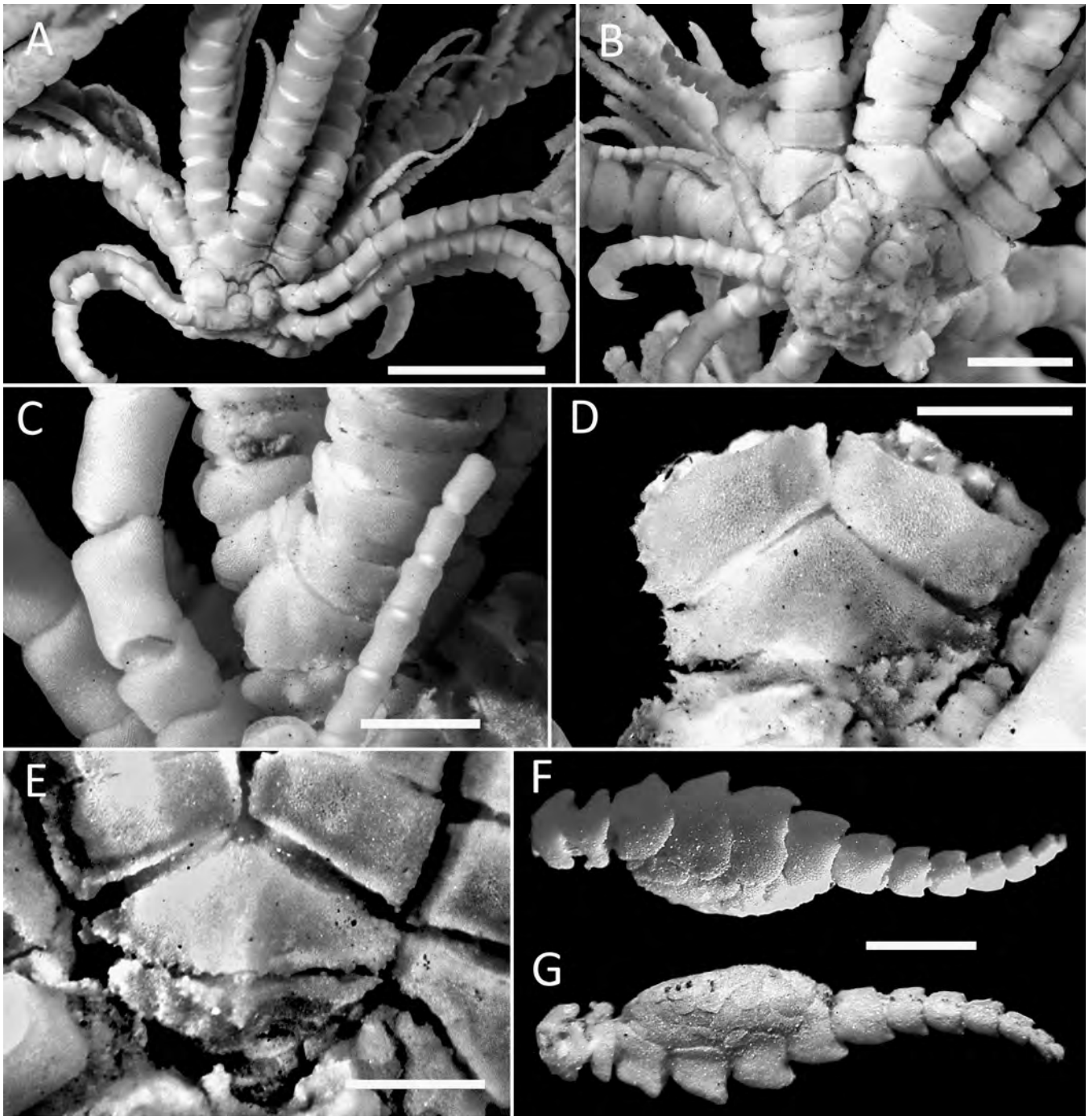

FIGURE 19 — *Strotometra parvipinna*. **A**–**D**, NHMD-874397, four specimens illustrating variations in ray base features. **A**, Ibr1 with weak irregular surface; Iax2 with finely irregular lateral and proximal margins. **B**, Ibr1 with midaboral knob and second knob to left of right-hand axil; Iax2 with weak midaboral swelling and lateral margins almost smooth. **C**, Ibr1 with multiple knobs; Iax2 with strong, midaboral "nose-like" synarthrial swelling. **D**, Ibr1 partly hidden by centrodorsal, with blunt spines on right side and short fine spines along lateral margin; Iax2 with fine spines along lateral margins (and on left-hand lateral margin of br1). **E**–**G**, USNM E3142. **E**, ray base with sponge-like aboral surface of Ibr1 and weakly dentate proximal margin of Iax2. **F**–**G**, genital pinnules, abambulacral (F) and adambulacral (G) views; A scale bar = 5 mm; B scale bar = 2 mm; C–D, F–G scale bars = 1 mm.

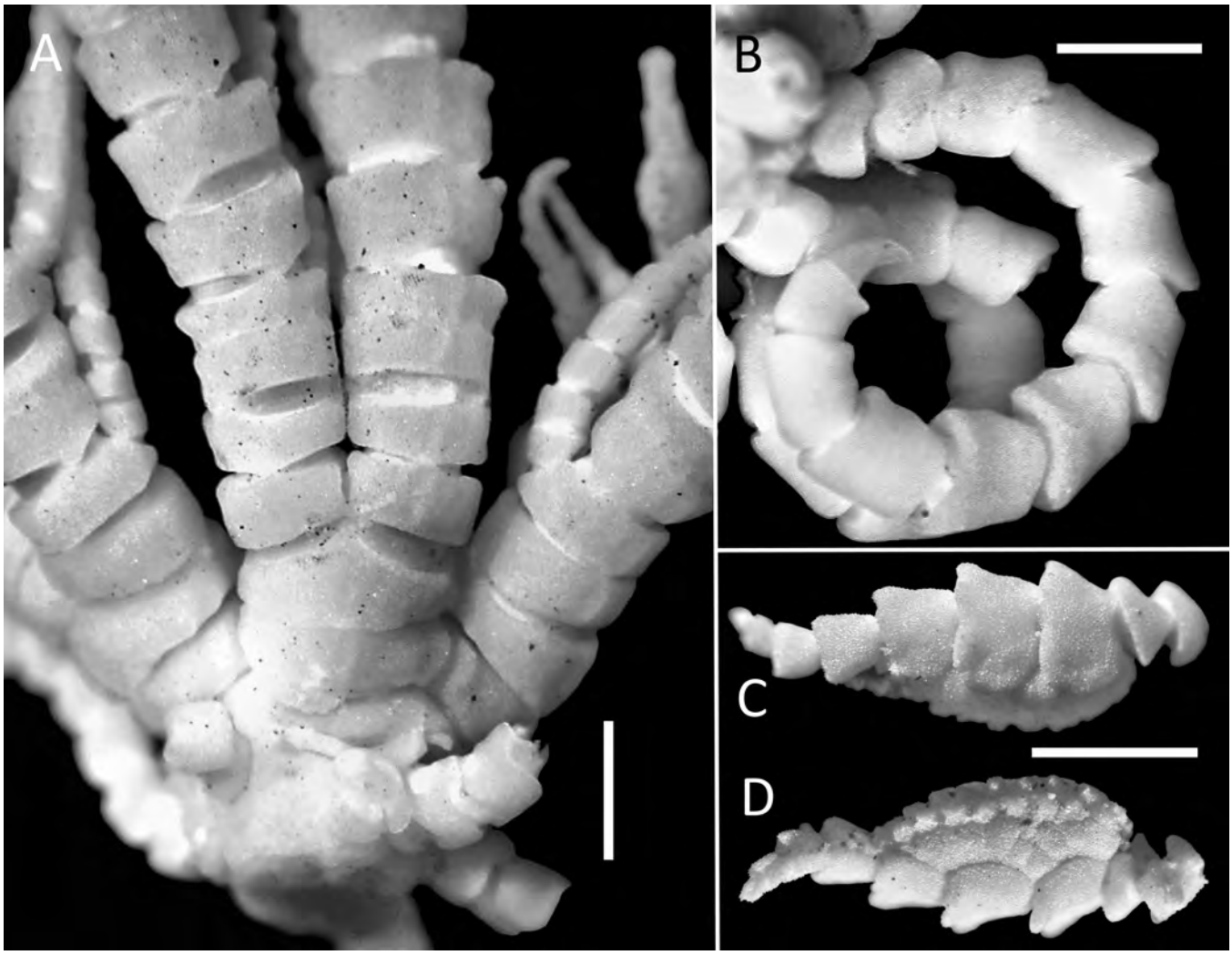

FIGURE 20 — *Strotometra hepburniana* USNM 35692. **A**, centrodorsal and ray bases. **B**, cirrus. **C**–**D**, detached genital pinnule. **C**, abambulacral view. **D**, oblique adambulacral view showing side and covering plates on gonad; scale bars = 1 mm.

Interambulacral areas of disk with separated or sparse small nodules, round or irregular; nodules crowded in thick band along ambulacra.

Color yellow or dull orange.

Distribution.— Same as for genus.

Remarks.— A. H. Clark (1950) distinguished *Strotometra parvipinna* from *S. hepburniana* chiefly on the basis of size-related characters, i.e., P1 with 20–22 versus 10–11 segments and 6 mm vs. 3.5 mm long, arms 60–75 mm vs. 45 mm long, and cirri with 10 vs. 11–15 cirrals, respectively. His other distinction was between the proximal pinnules: "smooth or nearly so" in *S. parvipinna* versus "with conspicuously flaring and overlapping distal ends, appearing very rough" in *S. hepburniana* (pp. 361–362). However, examination of type material and other specimens identified by A. H. Clark revealed no consistent difference in proximal pinnule characters between the two nominal species (Figs. 18B, 19A, 20A, 21). His reference to the "flaring and overlapping distal ends appears to apply more to the genital pinnules of *S. hepburniana* than to the proximal pinnules (Figs. 20C-D, 21B). The expansion of the genital pinnules is wider in the examined specimens of *S. hepburniana* (Figs. 20C, D, 21B) relative to *S. parvipinna* (Figs. 18C, 19F, G, 21A). However, genital pinnule expansion may vary even within an individual (see fig. 14B above center); and it is possible, though not documented in Charitometridae, that male and female genital pinnules might differ, as they do in brooding *Isometra* (Holland, 1991).

Other features also do not appear to vary consistently between the two. As examples, specimens attributed to both species have a weak midaboral ridge or keel on the brachials, although A. H. Clark (1950) did not mention it in

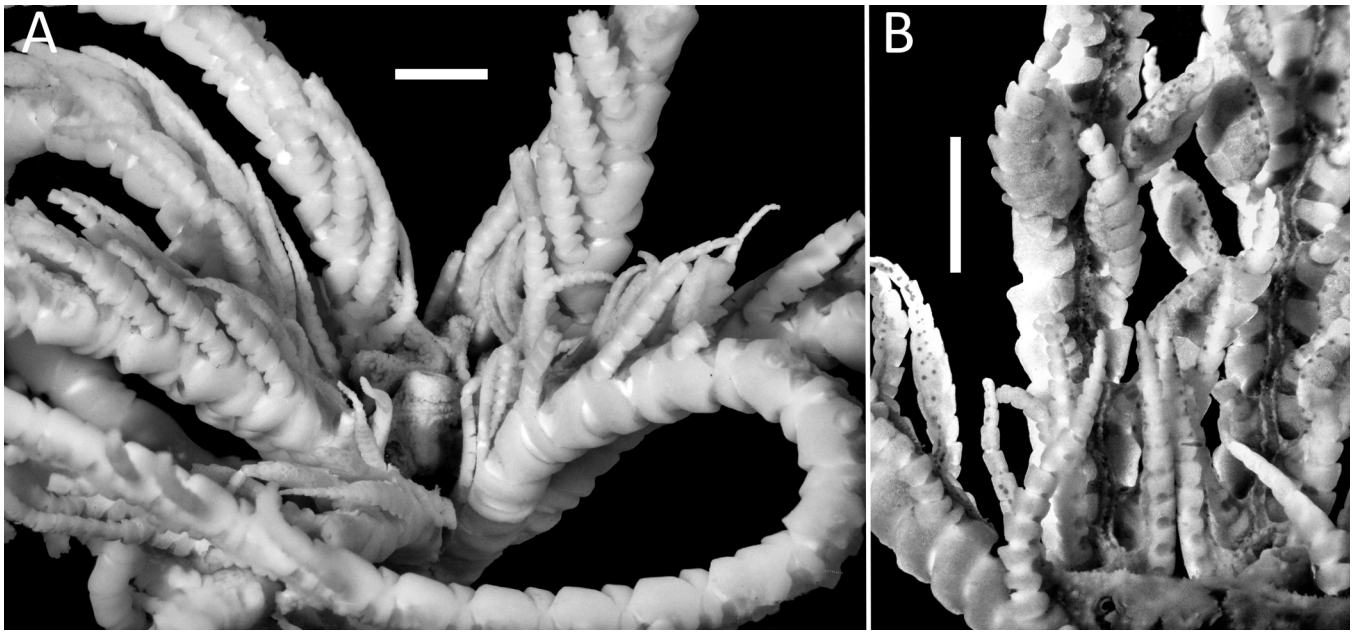

FIGURE 21 — Proximal pinnules. **A**, *Strotometra parvipinna* NHMD-874397. **B**, *Strotometra hepburniana* NHMD-873531, proximal pinnules; scale bars = 5 mm.

his description of *S. hepburniana*, and it was not recognizable in one of four *S. parvipinna* examined from NHMD-874397. The IBr2 ossicles vary from having little or no sculpture (apart from lateral flanges) along the margins in both the holotype of *S. parvipinna* (Fig. 18A) and specimens of *S. hepburniana* (e.g., Fig. 20A), to an irregularly dentate proximal margin on the Iax2 and irregularly sponge-like sculpture on the aboral surface of Ibr1 in specimens of *S. parvipinna* (Figs. 19D, E), or distinct knobs especially on Ibr1 in other *S. parvipinna* (Fig. 19B, C). Although all *S. hepburniana* specimens examined for the current paper lack any spiny or knobby ornamentation on IBr2, Kogo (1998) described new specimens identified as *S. hepburniana* from Japan as having the division series "granulated with minute tubercles" (p. 116), accompanied by an illustration showing irregular ornamentation along the lateral margins (his fig. 93a). We therefore treat *S. hepburniana* as a junior synonym of *S. parvipinna*. In addition, Hemery (2011) returned specimens identified as *S. parvipinna* and *S. hepburniana* as well-supported sister terminals (Fig. 1).

A. H. Clark identified (according to the specimen label) a small specimen (NHMD-873536) collected by Capt. Suensson in "East Asia" as *S. hepburniana* (catalogued 19 Sep 1911) but did not include it in his monograph (A. H. Clark, 1950), although he did include other NHMD-874397 specimens that he identified as *S. parvipinna* collected later (10 May 1922). The omission might have been due to the small size and immaturity of the specimen: arms 10, ~15 mm long, curled over the aboral surface, obscuring the centrodorsal, most cirri and brachitaxis. Cirri stout, of 8 short cirrals, 3.2 mm long. P1 developed on some arms, 8 short segments, ~1.5 mm long; following several pairs of pinnules not developed or rudimentary; no genital expansion. Cirri, brachials, and pinnules similar to those of *S. parvipinna*. A. H. Clark (1913b) also noted the provenance of this specimen as "probably Korean Straits."

Alcohol-preserved specimens attributed to both *S. parvipinna* and *S. hepburniana* have no obvious ambulacral groove on most pinnules with large gonads. Instead, the mid-ambulacral surface is a series of sacculi alternating with covering plates. However, this may be a function of preservation, although podia and a distinct groove are visible on many distal pinnules.

DISCUSSION

As noted in the introduction, A. H. Clark (1950) placed the genera of Charitometridae in two informal groups based on differences in genital pinnule structure: 1) tapering from more or less broadened proximal segments to a longer delicate distal portion (*Chondrometra*, *Crinometra*, *Monachometra*, and *Glyptometra*) versus 2) two to four abruptly broader pinnulars with a shorter slender tip (*Strotometra*, *Poecilometra*, *Chlorometra*, and *Charitometra*). A comparison of genital pinnules across all charitometrid genera (Fig. 22), plus the descriptions and illustrations in the taxonomic section above, and additional details discussed below, support placing *Charitometra* (Fig. 22A–B), *Chlorometra* (Fig. 22C), and *Strotometra* (Fig. 22M–O) in the first group, leaving *Poecilometra* as the only genus with genital pinnules characteristic of his second group, what we have termed "pedunculate". Hemery's (2011) sequence results (Fig. 1) also place *Strotometra* in the same charitometrid clade as

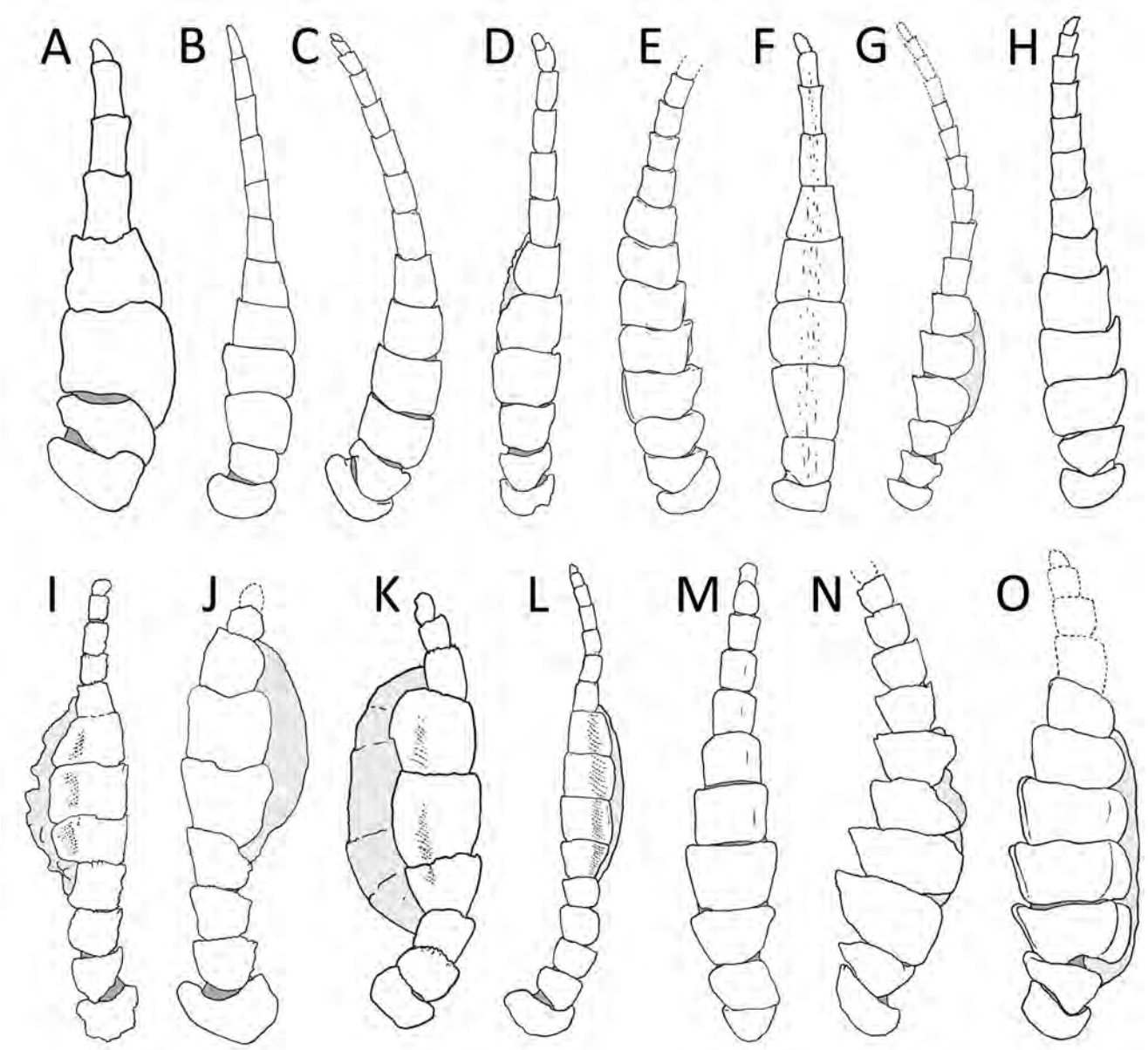

FIGURE 22 — Charitometrid genital pinnules (not to scale). **A**, *Charitometra basicurva* NHM 88.11.9.22, syntype. **B**, *Charitometra incisa*, NHM 88.11.9.23, syntype. **C**, *Chondrometra rugosa*, RMNH.ECH.2101. **D**, *Crinometra brevipinna* NSU-CRI 649. **E**, *Monachometra flexilis* NHM 88.11.9.27, cotype (distal end out of photograph). F, *Chlorometra garrettiana* (holotype of *Diodontometra bocki*, UUZM 254 (redrawn from Gislén, 1922, fig. 82, p. 88). **G**, *Glyptometra tuberosa*, NHM 88.11.9.25, syntype (distal four pinnulars missing, reconstructed from adjacent pinnule). **H**, *Glyptometra inaequalis* NHM 88.11.9.81, cotype. **I**, *Poecilometra baumilleri* USNM 1660641 (FLMNH 21597 spec. 2) paratype. J, *Poecilometra acoela* NHMD-873490 (tip reconstructed from nearby pinnule). **K**, *Poecilometra priamus* RMNH.ECH.1813, syntype. **L**, *Poecilometra priamus* USNM E427. **M**, *Strotometra parvipinna* NHM 88.11.9.26, holotype. **N**, *Strotometra parvipinna* NHMD-874397 (tip missing). **O**, *Strotometra hepburniana* NHMD-873531 (distal four pinnulars missing, reconstructed from adjacent pinnule). A–C, E–H, K, M. from photographs. D, I–J, L, N–O. from specimens.

representatives of three other group-one genera (per A. H. Clark's usage) (*Chondrometra*, Fig. 22C; *Monachometra*, Fig. 22E; *Glyptometra*, Fig. 22G), separate from a *Poecilometra* clade (although those sequences did not include either *P. acoela* or *P. baumilleri*). We have also re-assigned both *priamus* and *ornatissima* to *Poecilometra* based on genital pinnule features, leaving only *parvipinna* and its synonym *hepburniana* in *Strotometra*. Synonymizing the latter two was supported by the broadly overlapping morphology revealed by our re-examination of type and other specimens.

Of the other two genera in Clark's second grouping, *Chlorometra* and *Charitometra*, the former has genital pinnules more similar to those of genera in his first group (Fig. 22F). The holotype of *Chlorometra garrettiana* A. H. Clark, 1907b (USNM 22633) is badly fragmented, and no images of its genital pinnules are available. A. H. Clark (1950, p. 221) diagnosed this monotypic genus as having genital pinnules with $P_{(3\text{-}5 \text{ or } 6)}$ "flattened and expanded with winglike borders, the portion of the pinnules beyond being abruptly narrower and shorter than the expanded portion." However, he described them (p. 223) as having the pinnulars following $P_{(1\text{-}2)}$ wider than long, and the following pinnulars longer than wide, with the two terminal pinnulars small [no mention of the expansion, but see below]. He then distinguished shorter genital pinnules as having $P_{(3\text{-}4)}$ "markedly longer and slightly broader than those following, though they are not broader than the two basal segments". He synonymized *Diodontometra bocki* Gislén, 1922, under *C. garrettiana*, and considered the latter as an immature specimen of the former. In comparing the two, he wrote: "In the genital pinnules of *garrettiana* the third and fourth segments are often abruptly larger than those following and flattened; but they are not broader than those preceding and do not have produced lateral borders as in *bocki*; this is probably an indication of immaturity…" Gislén's (1922) drawing of a *D. bocki* genital pinnule (Fig. 22F) shows similarities to those of *Glyptometra* (Fig. 22H), *Crinometra* (Fig. 22D), and some *Strotometra* (Fig. 22M), all members of the first group of genera. Despite placing *Chlorometra* in group two, A. H. Clark (1950, p. 199) also wrote: "the genital pinnules are not so abruptly and greatly swollen as they are in the other members of this [second] group and they may not be swollen at all, though the genital segments are usually enlarged. The genital pinnules of *Chlorometra* are very little different from those of *Monachometra* [group one], of which *Chlorometra* should perhaps be regarded as a synonym." His comment that "they may not be swollen at all" reflects our observation that the expansion of genital pinnules may vary substantially among arms of an individual and from small to large specimens, even at similar distances along the arms (Fig. 14B).

For the final genus in group two, A. H. Clark (1950, p. 348) diagnosed *Charitometra* as having genital pinnules with an abruptly narrower distal portion shorter than the expanded gonadal portion (group two). However, examination of type specimens reveals that, although many genital pinnules of *Charitometra basicurva* (Carpenter, 1884) have an abruptly narrower distal portion, it is often just as long as or longer than the expanded gonadal portion (Fig. 22A) and tapers rather gradually in some. Likewise, those of the type species, *Charitometra incisa* (Carpenter, 1888), have a gradually tapering distal portion that may be longer than the expanded gonadal portion (Fig. 22B). Hemery's (2011) sequence results place *Charitometra basicurva* well within the clade of genera characterized by group one genital pinnules (Fig. 1).

An initial examination of expanded gonadal pinnulars in a selection of genera using scanning electron microscopy (SEM) supports separating *Poecilometra* (Fig. 23F–G) from representatives of all four other genera examined: *Monachometra* (Fig. 23A), *Crinometra* (Fig. 23B), *Glyptometra* (Fig. 23C), and *Strotometra* (Fig. 23D–E). Viewed in cross-section, these pinnulars in *Poecilometra* are symmetrical, with a proportionally much smaller articular area, especially the abambulacral ligament fossa, and proportionally much longer, thinner lateral "wing-like" flanges than in the other genera. They appear to be uniform across the genus; those of *P. baumilleri* (not shown) are similar in all respects to those of *P. acoela* (Fig. 23F) and *P. priamus* (Fig. 23G). Although not examined with SEM, those of *P. ornatissima* appear similar (see Figs. 10E, 11B). By contrast, those of *Monachometra*, *Glyptometra*, *Crinometra*, and *Strotometra* are asymmetrical, with one flange longer and curved, and the other shorter, thicker, and triangular and a proportionally larger articular facet with a larger ligament fossa than in *Poecilometra*. However, the "wing-like" flanges approach similar lengths in a specimen originally identified as *S. hepburniana* (here treated as a synonym of *S. parvipinna*). As a result, these flanges and articular features require additional inquiry to evaluate their potential diagnostic status, e.g., how they vary with growth along and among arms, with gonadal development, and among additional charitometrid taxa.

CONCLUSION

Family Charitometridae appears to be divisible into two groups based on both morphological and molecular sequence data: those with a series of narrow basal pinnulars followed by an abruptly expanded short series of pinnulars associated with the gonad (pedunculate) versus those with gradually tapering genital pinnules. Symmetrically versus asymmetrically expanded gonadal pinnulars may offer an additional distinction. Two species formerly placed in *Strotometra* (*priamus* and *ornatissima*) have been re-assigned to *Poecilometra* based on these genital pinnule features, although the former differs from the other members of the genus in having up to 20 rather than just 10 arms. As no consistent morphological features distinguish the remaining two *Strotometra* species (*S. hepburniana* and *S. parvipinna*), they are treated as synonyms herein, as the senior *S. parvipinna*. We re-diagnosed *Poecilometra* to include both the features of the genital pinnules as well as the aborally-directed flange on P(1). *Poecilometra baumilleri* n. sp. was described and placed in *Poecilometra* on the basis of both of these features. Future studies should combine molecular analyses and morphological re-evaluation, including ontogenetic variations, of the remaining charitometrid genera. Both generic- and specific-level distinctions remain unclear in many cases, e.g., similar characters currently diagnose species of *Glyptometra* but only varieties of *Crinometra* (A. H. Clark, 1950).

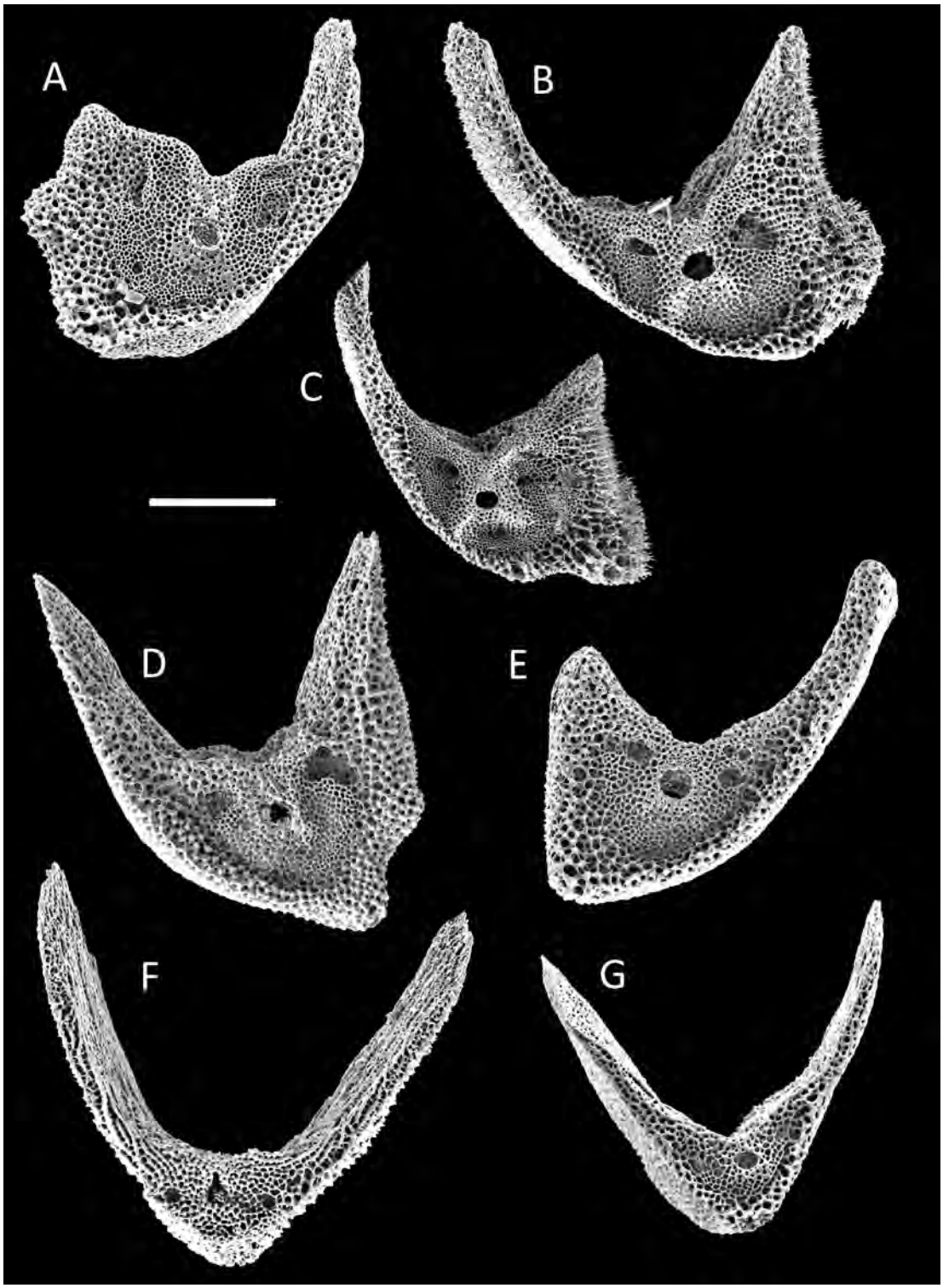

FIGURE 23 — Expanded gonadal pinnulars. **A**, *Monachometra patula* MNHN IE-2007-6012. **B**, *Crinometra brevipinna* NSU-CRI 649. **C**, *Glyptometra lateralis* FLMNH 21599. **D**–**E**, *Strotometra parvipinna*. **D**, NHMD-873531 (originally *S. hepburniana*). **E**, USNM E3142. **F**, *Poecilometra acoela* NHMD-873490. **G**, *Poecilometra priamus* NHMD-873492. Note that A, E and G versus B, C, D and F are from pinnules on opposite sides of arms; scale bar = 250 µm.

ACKNOWLEDGEMENTS

The authors wish to thank David Pawson, William Keel, and William Moser (National Museum of Natural History, Smithsonian Institution); Marc Eléaume, Nadia Améziane, and Pierre Lozouet (Muséum national d'Histoire naturelle, Paris); Amy Baco-Taylor, John Slapcinsky, and Gustav Paulay (Florida State University), and Tom Schiøette (Zoologisk Museum Købnhavn) for loans of specimens from their respective institutions and collections. We also wish to thank Dr. Patricia Blackwelder and Ria Achong-Bowe (NSU) for their invaluable expertise and assistance with the scanning electron microscopes. This research was partly funded through the Collaborative Research: Assembling the Echinoderm Tree of Life project (National Science Foundation, Award ID: 1036219), to one of us (CGM).

LITERATURE CITED

BULLIMORE, R. D., N. L. FOSTER, and K. L. HOWELL. 2013. Coral-characterized benthic assemblages of the deep Northeast Atlantic: defining "Coral Gardens" to support future habitat mapping efforts. ICES Journal of Marine Science, 70: 511–522.

CARPENTER, P. H. 1880. Feather-stars, recent and fossil. Popular Science Review, 4(15): 193–204.

_____. 1883. On a new crinoid from the Southern Sea. Annals and Magazine of Natural

History (5th series), 12, 143–144.

_____. 1884. Report upon the Crinoidea collected during the Voyage of H.M.S. Challenger during the Years 1873-76, Report of the Scientific Results of the Voyage of H.M.S. Challenger, Zoology, Part I, General morphology, with descriptions of the stalked crinoids, v. 11 (1884): 1–442 pp., text-figs. 1–21, pl. 1–62.

_____. 1887. Notes on echinoderm morphology, No. X. On the supposed presence of symbiotic algae in Antedon rosacea. Quarterly Journal of Microscopical Science (New series), 27: 379-391, pl. XXX, fig. 3

_____. 1888. Report upon the Crinoidea collected during the voyage of H.M.S. Challenger during the Years 1873-76, Report of the Scientific Results of the Voyage of H.M.S. Challenger, Zoology, Part II, The Comatulae, v. 26 (1888): 1–400 pp., text-fig. 1–6, pl. 1–70.

CLARK, A. H. 1907a. New genera of recent free crinoids. Smithsonian Miscellaneous Collection, Quarterly Issue, 50(3): 343–364.

_____. 1907b. Description of new species of recent unstalked crinoids from the coast of northeastern Asia. Proceedings of the United States National Museum, 33: 127–156.

_____. 1908a. New genera of unstalked crinoids. Proceedings of the Biological Society of Washington, 21: 125–136.

_____. 1908b. Some points in the Ecology of Recent Crinoids. American Naturalist, 42(503): 717–726.

_____. 1908c. Description of new species of crinoids, chiefly from the collections made by U.S. Fisheries steamer "Albatross" at the Hawaiian Islands in 1902; with remarks on the classification of the Comatulida. U.S. National Museum, Proceedings 34: 209–239.

_____. 1908d. Notice of some crinoids in the collection of the Museum of Comparative Zoology. Bulletin of the Museum of Comparative Zoology, Harvard, 51(8): 233–248.

_____. 1909a. A revision of the crinoid families Thalassometridae and Himerometridae. Proceedings of the Biological Society of Washington, 22: 1–22.

_____. 1909b. On a collection of crinoids from the Zoological Museum of Copenhagen. Videnskabelige Meddelelser den naturhistoriske Forening I Kjøbenhavn, 61:115–194.

_____. 1911. The recent crinoids of Australia. Memoir of the Australian Museum, 4(15) :705–804.

_____. 1912a. The crinoids of the Indian Ocean. Echinoderma of the Indian Museum, pt. 7, Crinoidea. The Indian Museum, Calcutta, 325 pp.

_____. 1912b. Six new East Indian crinoids belonging to the family Charitometridae. Proceedings of the Biological Society of Washington, 25: 77–84.

_____. 1913a. Notes on the recent crinoids in the British Museum. Smithsonian Miscellaneous Collection, 61(15): 1–89.

_____. 1913b. Description of a collection of unstalked crinoids made by Captain Suenson in Eastern Asia. Proceedings of the Biological Society of Washington, 26: 177–182.

_____. 1914. Une étude philosophique de la relation entre les crinoïdes actuels et la temperature de leur habitat. Bulletin de l'Institut océanographique, Monaco, 294: 1–11.

_____. 1915a. A monograph of the existing crinoids. 1. The comatulids. Part 1. Bulletin of the United States National Museum, 82(1): 406 pp., 17 pls.

_____. 1915b. The bathymetrical and thermal distribution of the unstalked crinoids, or comatulids, occurring on the coasts of China and Japan. Journal of the Washington Academy of Sciences, 5(6): 213–218.

_____. 1916. Six new genera of unstalked crinoids belonging to the families Thalassometridae and Charitometridae. Journal of the Washington Academy of Sciences, 6(17): 605–608.

_____. 1918. The unstalked crinoids of the Siboga Expedition. Siboga Expedition, 42b: 1–300, 28 pl.

_____. 1921. A monograph of the existing crinoids. 1. The comatulids. Part 2. Bulletin of the United States National Museum, 82(2): 1–795, fig. 1–949, pl. 1–57.

_____. 1931. A monograph of the existing crinoids. 1. The comatulids. Part 3. Superfamily Comasterida. Bulletin of the United States National Museum, 82(3): 816 pp., 82 pls.

_____. 1932. On a collection of crinoids from the Indian Ocean and the Bay of Bengal. Records of the Indian Museum, 34: 551–566.

_____. 1947. A monograph of the existing crinoids. 1. The comatulids. Part 4b. Superfamily Mariametrida (concluded- the family Colobometridae) and Superfamily Tropiometrida (except the families Thalassometridae and Charitometridae). Bulletin of the United States National Museum, 82(4b): 473 pp., 43 pls.

_____. 1950. A monograph of the existing crinoids. 1. The comatulids. Part 4C. Superfamily Tropiometrida (the families Thalassometridae and Charitometridae). Bulletin of the United States National Museum, 82(4c): 383 pp., 32 pls.

EAGLE, M. K. 2001. New fossil crinoids (Articulata: Comatulida) from the Late Oligocene of Waitete Bay, northern Coromandel Peninsula, New Zealand. Records of the Auckland Museum 37: 81–92, 22 fig.

GISLÉN, T. 1922. The crinoids from Dr. S. Bock's expedition to Japan 1914. Nova Acta Regiae Societatis Scientiarum Upsaliensis, (4)5(6): 1–183, text-fig. 1–162, pl. 1, 2.

_____. 1924. Echinoderm studies. Zoologisk Bidrag från Uppsala, 9: 1–316.

_____. 1927. Papers from Dr. Th. Mortensen's Pacific Expedition 1914–16. 37. Japanese crinoids. Videnskabelige Meddelelser frå Dansk Naturhistorisk Forening i København, 83: 1–69, fig. 1–80, pl. 1–2.

_____. 1928. Notes on some crinoids in the British Natural History Museum. Kungliga Svenska Vetenskapsakademiens, Arkiv för Zoologi, 19A (32): 1–15.

_____. 1933. Papers from Dr. Th. Mortensen's Pacific Expedition 1914-16. LXVII. A small collection of crinoids from St. Helena. Videnskabelige Meddelelser frå Dansk Naturhistorisk Forening i København, 93: 475–485.

_____. 1934. A reconstruction problem: Analysis of fossil comatulids from North America, with a survey of all known types of comatulid arm ramifications. Lunds Universitets Årsskrift (Acta Univ. Lundensis), new series, 30(2): 1–59.

_____. 1938. Crinoids of S. Africa. Kungliga Svenska Vetenskapsakademiens Sällskapets Lund, Handlingar, (series 3) 17(2): 1–22, pl. 1–2.

HAMANN, O. 1907. Dr. H. G. Bronne's Klassen und Ordnungen des Tier-Reichs. Leipzig und Heidelberg, Leipzig, Germany, Bd. 2, Abt. 3, Bu. 5, 1602 pp.

HARTLAUB, C. 1891. Beitrag zur Kenntniss der Comatuliden Fauna des Indischen Archipels. Nova Acta Leopoldina (Abhandlungen der Kaiserlich Leopoldinisch-Carolinischen Deutschen Akademie der Naturforscher) 58(1): 1–120, pl. 1–5.

_____. 1895. Reports on the dredging operations off the west coast of Central America to the Galapagos, to the west coast of Mexico, and to the Gulf of California, charge of Alexander Agassiz, carried on by the U.S. Fish Commission steamer "Albatross," during 1891, Lieut.-Commander Z. L. Tanner, U. S. N., commanding. Die Comatuliden. Bulletin of the Museum of Comparative Anatomy, Harvard, 27(4): 129–152, pls. 1-4.

_____. 1912. XLV. Die Comatuliden. Reports on the results of dredging under the supervision of Alexander Agassiz in the Gulf of Mexico (1877-78), in the Caribbean Sea (1878-79), and along the Atlantic Coast of the United States (1880) by the U.S. Coast Survey Steamer "Blake". Memoirs of the Museum of Comparative Zoology, Harvard, 27(4): 277–491, pl. 1–18.

HEMERY, L. G. 2011. Diversité moléculaire, phylogéographie et phylogénie des Crinoïdes (Echinodermes) dans un environnement extrême : l'océan Austral. PhD Dissertation. Museum national d'Histoire naturelle, Paris, 381 pp.

_____., M. ROUX, N. AMÉZIANE, and M. ELÉAUME. 2013. High-resolution crinoid phyletic inter-relationships derived from molecular data. Cahiers de Biologie Marine, 54: 511–523.

HESS, H. 2011. Articulata: Introduction. In Hess, H., and C. G. Messing. Part T: Echinodermata 2. Revised Crinoidea, Volume 3, P. A. Selden (ed.), Treatise on Invertebrate Paleontology. University of Kansas Paleontological Institute, Lawrence, Kansas, pp. 1–22.

_____., and C. G. MESSING. 2011. Part T: Echinodermata 2. Revised Crinoidea, Volume 3. In P. A. Selden (ed.), Treatise on Invertebrate Paleontology. University of Kansas Paleontological Institute, Lawrence, Kansas, pp.1–261.

HOLLAND, N. D. 1991. Echinoderms and Lophophorates. In Giese, A. C., Pearse, J. S. & Pearse, V. B. (eds.), *Reproduction of Marine Invertebrates*, Boxwood Press, Pacific Grove, CA, vol. 6, pp. 247–299.

ICZN (International Commission on Zoological Nomenclature). 1999. International Code of Zoological Nomenclature, 4th edition. International Trust for Zoological Nomenclature, London, 289 pp. https://www.iczn.org/the-code/the-international-code-of-zoological-nomenclature/the-code-online/

KOGO, I. 1998. Crinoids from Japan and its adjacent waters. Special publications from Osaka Museum of Natural History, 30: 1–148.

_____., and T. FUJITA, T. 2005. Geographic distribution of crinoids (Echinodermata) in southwestern Japan. In Hasegawa, K., G. Shinohara, and M. Takeda (eds.) Deep-Sea Fauna and Pollutants in Nansei Islands, National Science Museum Monographs, Tokyo, no. 29, pp. 297-355.

MARSHALL, J. I., and F. W. E. ROWE. 1981. The Crinoids of Madagascar. Bulletin du Muséum national d'Histoire naturelle, Paris, 4(3): 379-413.

MCKNIGHT, D. G. 1975. Some echinoderms from the northern Tasman Sea. NZOI Records / New Zealand Oceanographic Institute, 2(5): 49–76.

_____. 1977a. Some crinoids from the Kermadec Islands. NZOI Records / New Zealand Oceanographic Institute, 3(13): 121–128.

_____. 1977b. Additions to the New Zealand crinoid fauna. NZOI Records / New Zealand Oceanographic Institute, 3(11): 93–112.

_____. 1977c. Crinoids from Norfolk Island and Wanganella Bank. NZOI Records / New Zealand Oceanographic Institute, 3(14): 129–137.

_____. 1989a. Further crinoids (Echinodermata) from off the Kermadec Islands, southwest Pacific Ocean. DMFS Reports (NZOI) 3(3): 31–35.

_____. 1989b. Some echinoderm records from the tropical south-western Pacific Ocean. DMFS Reports (NZOI) 3(2): 19–30.

_____. 1989c. Further records of Tasman Sea and Coral Sea Echinoderms. DMFS Reports (NZOI) 3(1): 3–17.

MESSING, C. G. 2020a. A revision of the unusual feather star genus *Atopocrinus* with a description of a new species (Echinodermata: Crinoidea). Zootaxa, 4731(4): 471–491. https://doi.org/10.11646/zootaxa.4731.4.2

_____. 2020b. Erratum: A revision of the unusual feather star genus *Atopocrinus* with a description of a new species (Echinodermata: Crinoidea). Zootaxa, 4772 (3): 600. https://doi.org/10.11646/zootaxa.4772.3.11

_____., and J. H. DEARBORN. 1990. Marine flora and fauna of the northeastern United States. Echinodermata: Crinoidea. National Oceanic and Atmospheric Administration Technical Report, National Marine Fisheries Service 91: 1–29.

_____., N. AMÉZIANE, and M. ELÉAUME. 2000. Echinodermata Crinoidea: Comatulid crinoids of the KARUBAR Expedition to Indonesia. The families Comasteridae, Asterometridae, Calometridae and Thalassometridae. In Crosnier, A. (ed.), Résultats des Campagnes MUSORSTOM, vol. 21. Mémoires du Muséum national d'Histoire naturelle, 184: 627–702.

_____., A. C. NEUMANN, and J. C. LANG. 1990. Biozonation of deep-water lithoherms and associated hardgrounds in the northeastern Straits of Florida. Palaios, 5: 15–33.

_____., V. J. SYVERSON, M. A. VEITCH, K. STANLEY, AND T. K. BAUMILLER. 2019. Advances in Understanding the Deep Tropical Western Atlantic Crinoid Fauna (Echinodermata). ASLO Aquatic Sciences Meeting, "Planet Water: Challenges and Successes," San Juan, Puerto Rico, 23 Feb-2 Mar 2019. https://www.aslo.org/wp-content/uploads/ASLO-2019-Program-Book-with-addendum.pdf

MEYER, D. L., C. G. MESSING, and D. B. MACURDA Jr. 1978. Biological results of the University of Miami deep-sea expeditions. 129. Zoogeography of tropical western Atlantic Crinoidea (Echinodermata). Bulletin of Marine Science, 28(3): 412-441.

MINCKERT, W. 1905. Das Genus *Promachocrinus*, zugleich ein Beitrag zur Faunistik der Antarktis. Zoologische Anzeiger, 28: 490–501.

NORMAN, A. M. 1865. On the genera and species of British Echinodermata. 1, Crinoidea, Ophiuroidea, Asteroidea. Annals and Magazine of Natural History (series 3), 15, 98–129.

POURTALÈS, L. F. de. 1868. Contributions to the fauna of the Gulf Stream at great depths. Bulletin of the Museum of Comparative Zoölogy, 1(6), 103-142.

RASMUSSEN, H. W. 1978. Articulata. In Moore, R. C. and Teichert, C. (eds.) Treatise on Invertebrate Paleontology, Part T. Echinodermata 2(3). The Geological Society of America, Inc. & The University of Kansas Press. Boulder, CO & Lawrence, Kansas, pp. T813-T928, T938-T998.

ROMANOWSKI, A. 2015. A Revision of the Genera of Charitometridae with Abruptly Expanded Genital Pinnules. M. S. Thesis, Nova Southeastern University. 87 pp. https://nsuworks.nova.edu/occ_stuetd/383/

ROUSE, G. W., L. S. JERMIIN, N. G. WILSON, I., EECKHUAT, D. LANTERBECQ, T. OJI, C. M. YOUNG, T. BROWNING, P. CISTERNAS, L. E. HELGEN, M. STUCKEY, and C. G. MESSING. 2013. Fixed, free, and fixed: The fickle phylogeny of extant Crinoidea (Echinodermata) and their Permian-Triassic origin. Molecular Phylogenetics and Evolution, 66: 161–181.

ROWE, F. E. W., and J. GATES. 1995. Echinodermata. In Wells, A. (ed.) *Zoological Catalogue of Australia*, CSIRO Australia, Melbourne, vol. 33, pp. xiii + 510.

SHIPLEY, A. E., and E. W. MACBRIDE. 1901. Zoology: An elementary textbook. The MacMillan Company, New York City, New York, 632 pp.

TOMMASI, L. R. 1969. Nova contribucão a lista dos crinóides recentes do Brasil. Contribuições avulsas do Instituto Oceanográfico, Universidade de São Paulo, sér. Oceanográfia biológica. 17, 8 pp.

UTINOMI, H. and KOGO, I. 1968. A revised catalogue of crinoids collected from Japanese waters. Proceedings of the Japan Society of Systematic Zoology, 4: 46–53 (In Japanese).

Museum of Paleontology, The University of Michigan
1105 North University Avenue, Ann Arbor, Michigan 48109-1085
Matt Friedman, Director

Contributions from the Museum of Paleontology, University of Michigan is a medium for publication of reports based chiefly on museum collections and field research sponsored by the museum. Jennifer Bauer and William Ausich, Guest Editors;
Jeffrey Wilson Mantilla, Editor.

Publications of the Museum of Paleontology are accessible online at: http://deepblue.lib.umich.edu/handle/2027.42/41251

Print (ISSN 0097-3556), Online (ISSN 2771-2192)

Contributions

from the Museum of Paleontology, University of Michigan

VOL. 34, NO. 13, PP. 193–208 JUNE, 24, 2022

ATELESTOCRINUS BAUMILLERI, N. SP., A NEW EARLY MISSISSIPPIAN (VISÉAN) CRINOID, AND RELATED PSEUDOMONOCYCLIC FORMS

BY

FOREST J. GAHN[1]

Abstract — *Atelestocrinus* is a rare cladid crinoid that ranges from the Middle Devonian (Givetian) to Mississippian (Viséan) of Iran, Ireland, and North America. Unlike most crinoids, it has quadrangular symmetry, possessing only four arm-bearing rays; the anterior radial usually lacks an arm and associated facet. The type species of the genus is clarified as *Atelestocrinus robustus* Wachsmuth and Springer 1885, by monotypy. A lectotype is established for *A. robustus*. *Atractocrinus* and *Fiannacrinus* are synonyms of the genus. *Atelestocrinus indianensis* and *Atelestocrinus kentuckyensis* are likely monocyclic crinoids, but they are too poorly preserved to be reasonably diagnostic for any genus or species. They are considered *nomina dubia*. *Atelestocrinus baumilleri* is a new species from the Ramp Creek Formation of Montgomery, County, Indiana. Stratigraphically, it is the youngest known species of the genus. The only known specimen bears a regenerated ray that shows evidence of autotomy. Cooccurring with *A. robustus* and *A. baumilleri* are similar monocyclic forms, both of which violate the typical symmetry principles for crinoids. They are interpreted as pseudomonocyclic crinoids that have lost their basal circlets. *Belemnocrinus*, currently classified as a disparid, has likely been misdiagnosed for 160 years. Instead of possessing five arm-bearing radials, it has a radial circlet constructed of only four arm-bearing plates; the basals and anterior radial are entirely absent. It represents an extremely reduced developmental form of *Atelestocrinus* or its direct descendant. Patterns of symmetry suggest the cup base circlets of most monocyclic crinoids from the Paleozoic are better interpreted as infrabasals than basals.

UUID: http://zoobank.org/ea8bbb01-19e2-4c1f-80db-eba46982d507

INTRODUCTION

Wachsmuth and Springer pondered an unusual crinoid. They considered it abnormal until acquiring more specimens of the new genus, which they later named *Atelestocrinus* for the Greek ατελής, incomplete. Ironically, two of the three specimens they possessed were very complete for fossils, preserving fine details of the stem, dicyclic calyx, and arms. However, it is in this last trait *Atelestocrinus* is lacking. It has an anterior (or "A") radial that fails to develop an arm, giving the genus only four arm-bearing rays with eight arms total. Rather than having pentameral symmetry typical of most crinoids, the crown of *Atelestocrinus* is quadrangular, though without perfect bilateral symmetry because of a posterior interray that includes three anal plates.

This armless radial not only puzzled Wachsmuth and Springer in the late 19th century, but it continues to generate confusion in the 21st. In a recent paper, focused on the anal plates of Paleozoic crinoids, Ausich et al. (2020: fig. 3) mistook the anterior side of the animal for its posterior,

[1]Department of Geology, Brigham Young University, Idaho, Rexburg, Idaho 83460-0510, U.S.A. (gahnf@byui.edu).

identifying the A radial as the radianal. As discussed near the end of this contribution, I made a similar mistake while considering a new population of crinoids from the Wassonville Formation of Iowa.

The first specimen in the possession of Wachsmuth and Springer was collected from the Early Mississippian (upper Tournaisian) Burlington Limestone of Iowa. They named it *Atelestocrinus delicatus* Wachsmuth and Springer, 1896. They assigned the other two specimens to a second species, *Atelestocrinus robustus* Wachsmuth and Springer, 1895 (Figs. 1A–F, I; 2A) with one specimen each from the Burlington Limestone of Iowa and the lower Viséan Fort Payne Formation of Tennessee. The latter specimen is figured here for the first time (Fig. 1B–F). McIntosh (1983: pl. 26, fig. 7) recognized a third specimen of *A. robustus* from the Burlington Limestone, but despite the thousands of crinoids amassed from this formation since the 19th century, no additional specimens of *A. delicatus* or *A. robustus* are known.

Two additional North American species were later described from rocks of similar age, *Atelestocrinus indianensis* Ausich and Lane, 1982 (Fig. 3) from the Edwardsville Formation (Viséan) and *Atelestocrinus kentuckyensis* Lee, Ausich, and Kammer, 2005 from the Nada Member of the Borden Formation (Tournaisian). These species are likewise known from few specimens (one and two, respectively) but only as incomplete calyxes, specifically little more than radial circlets. Despite naming the genus for its incompleteness, this is not the kind of imperfection Wachsmuth and Springer had in mind. Regardless, the scant morphology available for study in these specimens is more consistent with coeval monocyclic crinoids, but it is impossible to know if *A. indianensis* and *A. kentuckyensis* were monocyclic or dicyclic since no morphology is preserved below the radial plates.

A specimen recovered from Indiana that does preserve the lowermost plate circlets, and can be confidently assigned to the genus, is *Atelestocrinus baumilleri*, n. sp., from the Ramp Creek Formation (Viséan) of Indian Creek, Montgomery County (Fig. 4A–B, E–G). This is the stratigraphically youngest known species of the group. As usual for its congeners, *A. baumilleri* is known from a single dicyclic specimen. It is associated with another individual from the same locality that is nearly identical except for possessing only one plate circlet below the radials (Fig. 4I), meaning it is monocyclic rather than dicyclic as is the holotype of *A. baumilleri*. Curiously, there is also a monocyclic specimen labelled as *A. robustus* (USNM S2410; Figs. 1G–H, J–K; 2B) that is likewise similar to its dicyclic counterpart (Figs. 1A–F, I; 2A).

Such morphological equivalence, despite differing numbers of cup base circlets, is noteworthy given that higher-level (e.g., ordinal) crinoid classification is largely grounded in the number of plate circlets below the radials. An extreme example of this is Bather's (1900) proposal to divide all crinoids into two grand subclasses, the Dicyclica and Monocyclica, based on this difference alone. Generally, dicyclic crinoids bear two plate circlets below the radials: infrabasals and basals; and monocyclic crinoids possess only one, variably interpreted as either infrabasals or basals (Guensburg and Sprinkle, 2003). However, some groups of crinoids are known to exhibit both dicyclic and monocyclic forms, even within the same species (e.g., *Uintacrinus socialis* Grinnell 1876; Springer, 1901).

Monocyclic crinoids that originated from within a dicyclic clade are termed pseudomonocyclic. As originally applied, pseudomonocycly refers to the loss of the infrabasal circlet as is characteristic of extant crinoids (Ubaghs, 1978). The Triassic crinoid *Aszulcicrinus* provides a compelling example of this transition (Hagdorn, 2020). However, pseudomonocyclic crinoids may also emerge from dicyclic clades through the loss of basals (McIntosh, 1979) or radials (Lane, 1967).

With the above in mind, the monocyclic semblances of *A. robustus* and *A. baumilleri* prompt unresolved questions. Do they represent undescribed taxa that are morphologically convergent with species of *Atelestocrinus*, or are they simply aberrant forms of this same genus? If they are pseudomonocyclic, did they achieve this condition (developmentally or phylogenetically) through loss of the infrabasal, basal, or radial circlets? The purpose of this contribution is to consider these questions, in addition to describing a new species, *Atelestocrinus baumilleri*, within the context of Mississippian forms of the genus. Finally, I discuss the relationship between *Atelestocrinus* and *Belemnocrinus* (White, 1862), a genus currently assigned to the monocyclic Disparida (Moore and Laudon, 1943; Moore and Lane, 1978a), and potential implications for the homology of the primary cup circlets of Paleozoic crinoids.

MATERIALS AND METHODS

The holotype and only known specimen of *Atelestocrinus baumilleri*, n. sp., was commercially collected from private land on Indian Creek, Montgomery County, Indiana. Scott Vergiels prepared the crinoid on behalf of Tom Witherspoon. Vergiels brought the specimen to my attention knowing I was interested in both *Atelestocrinus* and *Belemnocrinus*. I purchased the specimen from Witherspoon, and commissioned Vergiels to remove the crown from the matrix, so both the anterior and posterior sides could be studied and described. Vergiels also provided me with a cast and photograph of the monocyclic semblance of *A. baumilleri* (Fig. 4I). That specimen was likewise commercially collected from Indian Creek, but by Bob Howell in 1990. Unfortunately, the original has yet to be located despite querying numerous private collectors, universities, and museums. George McIntosh (pers. comm., 2021) saw the specimen in the possession of Gary Lane at an annual meeting of the Geological Society of America. Because of restrictions related to the SARS-CoV-2 pandemic, I was unable to visit Lane's collection at Indiana University. However, Claudia Johnson and David Polly searched for it on my behalf but were unable to locate it.

Restrictions imposed by the pandemic also made it

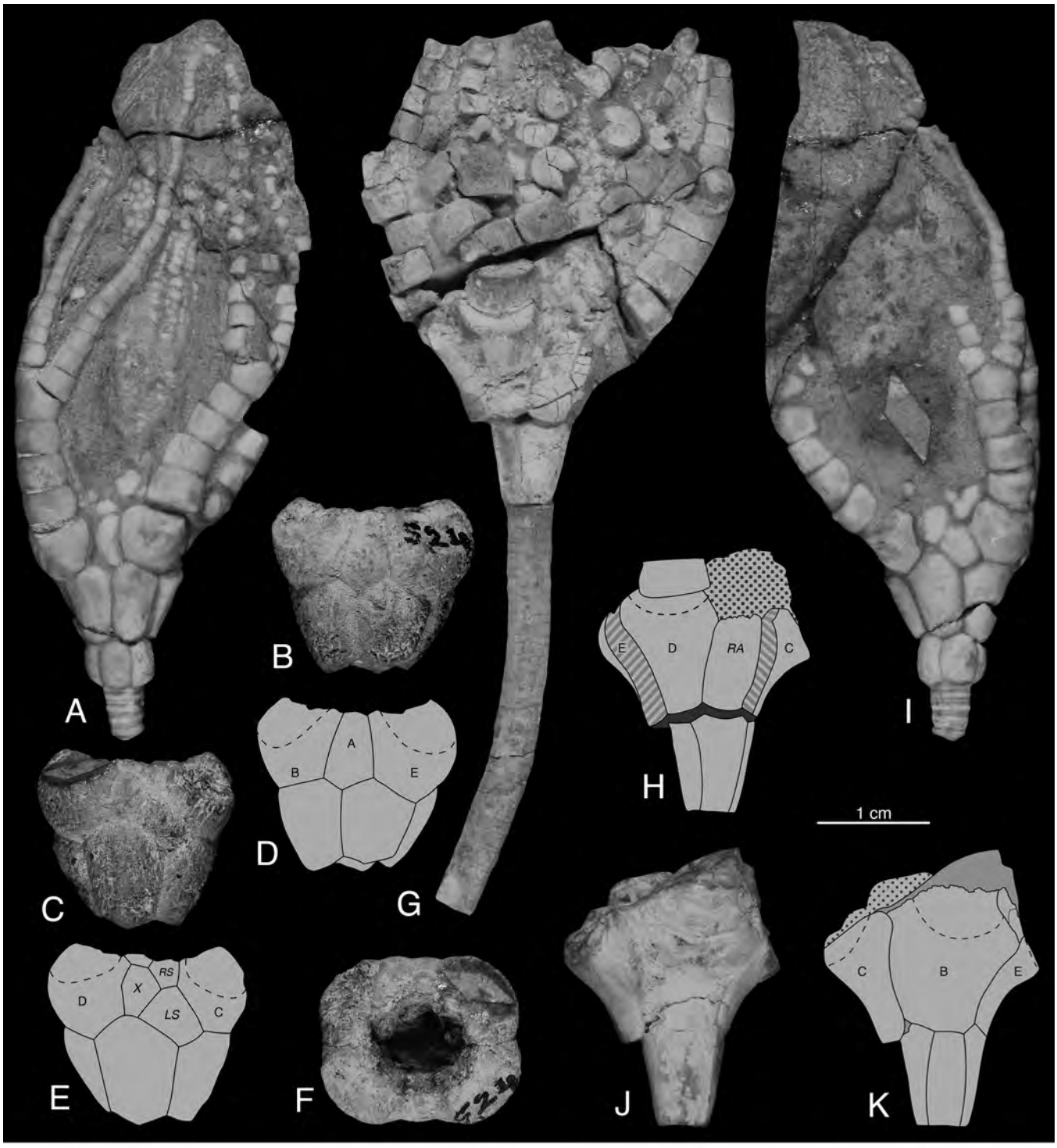

FIGURE 1 — Specimens of *Atelestocrinus robustus* and a related pseudomonocyclic form. **A, I,** anterior (A) and posterior (I) views of the lectotype of *A. robustus* (USNM S2409) from the Burlington Limestone, Iowa. **B–F,** anterior (B, D), posterior (C, E), and ventral (F) views of the paralectotype of *A. robustus* (USNM S2411) from the Fort Payne Formation, Tennessee. **G–H, J–K,** left posterior (G, H) and right anterior (J, K) views of the pseudomonocyclic specimen labeled and identified as *Atelestocrinus robustus* in the NMNH (USNM S2410); compare with Figure 2B. Scale bar is 1 cm for all specimens.

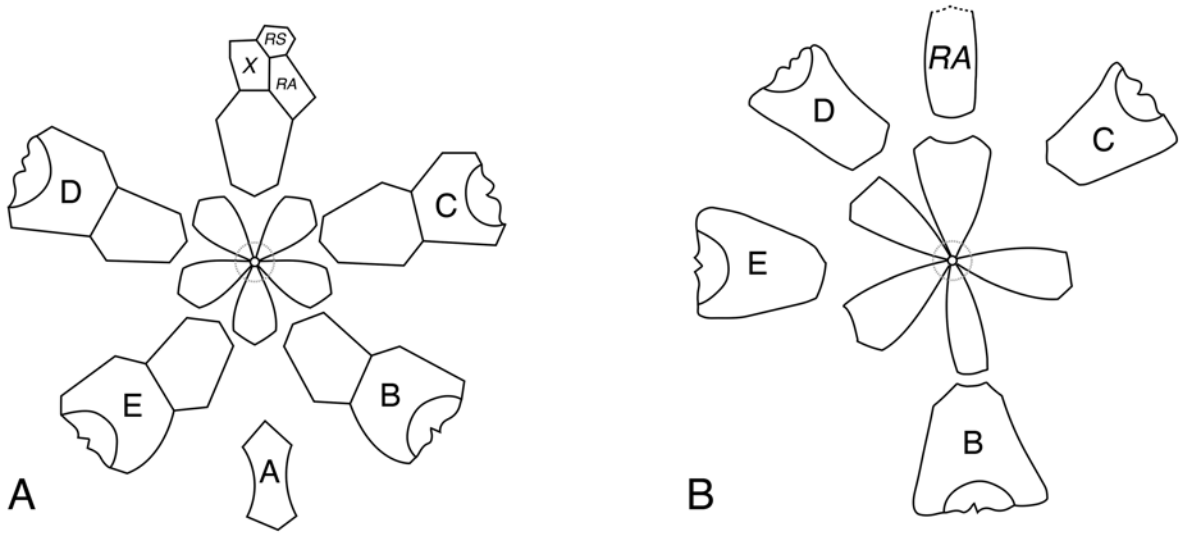

FIGURE 2 — Plate diagrams for *Atelestocrinus* and a related pseudomonocyclic form. **A,** *Atelestocrinus robustus*, modified from the original diagram of Wachsmuth and Springer, 1885: pl. 6, fig. 4. **B,** Diagram of a pseudomonocyclic specimen labeled and identified as *Atelestocrinus robustus* in the NMNH (USNM S2410). The basal circlet and anterior radial are entirely missing forcing a radical change in calyx plate morphology and symmetry.

impossible to visit the National Museum of Natural History to more carefully examine specimens of *Atelestocrinus*, including the monocyclic form similar to *A. robustus* (Figs. 1G–H, J–K; 2B). Ideally more precise descriptions for these fossils would have been provided (as for *A. baumilleri*; see "Systematic Paleontology"), but given the circumstances, the best I could do was evaluate the specimens from photographs and notes I took fifteen years prior. Specimens from the Wassonville Formation and *A. baumilleri* were accessible in the research collections of Brigham Young University, Idaho, Department of Geology, where they currently reside. These were photographed with a Nikon D7100 connected to a MacBook Pro and using the most recent version of Helicon Remote [heliconsoft.com]. Stacked images, up to 40 for some specimens, were then combined using the default settings in Helicon Focus. Unless otherwise stated in the figure captions, all photos were taken without coating or immersion. Measurements of *A. baumilleri* were taken using digital calipers under a binocular microscope and are included with the species description. Species of *Atelestocrinus* not mentioned above were examined from McIntosh's unpublished PhD dissertation (1983; University of Michigan) and the primary literature (Kirk, 1948; Ausich and Lane, 1982; Ausich and Sevastopulo, 2001; Webster et al., 2003; Lee et al., 2005). Classification, terminology, and abbreviations generally follow the *Treatise on Invertebrate Paleontology* (Ubaghs, 1978), but for the latest interpretation of crinoid classification see Wright et al. (2017). For clarity and convenience, a list of abbreviations used in the text and figures is provided below. Note that crinoid orientation is consistently given in capital letters, and specific plates that compose the crown are given in italics; thus, the position of the B radial is clearly differentiated from a basal plate, *B*.

INSTITUTIONAL ABBREVIATIONS

SUI	—	University of Iowa, Iowa City, Iowa, U.S.A.
UMMP	—	University of Michigan Museum of Paleontology, Ann Arbor, Michigan, U.S.A.
USNM	—	United States National Museum, National Museum of Natural History (NMNH), Washington D.C., U.S.A.

MORPHOLOGY AND MEASUREMENT ABBREVIATIONS

IAx	primaxil	DE	left posterior interray
IBr	primibrachial	E	E ray
IIBr	secundibrachial	EA	left anterior interray
A	A ray, anterior	*IB*	infrabasal plate
AB	right anterior interray	H	height
B	B ray, right anterior	*LS*	left sac plate
B	basal plate	*R*	radial
BC	right posterior interray	*RA*	radianal
C	C ray, right posterior	*RS*	right sac plate
CD	posterior interray	W	width
D	D ray, left posterior	*X*	anal X plate

SYSTEMATIC PALEONTOLOGY

Class CRINOIDEA Miller, 1821
Subclass CLADIDA Moore and Laudon, 1943
Order DENDROCRINIDA Bather, 1899

Genus *Atelestocrinus* Wachsmuth and Springer, 1885
Fig. 2A

Atelestocrinus Wachsmuth and Springer, 1885, pl. 6, fig. 4; pl. 9. fig. 4.
Atractocrinus Kirk, 1948, pp. 701–703.
Fiannacrinus Ausich and Sevastopulo, 2001, p. 85.

Type species.— *Atelestocrinus robustus* Wachsmuth and Springer, 1885: pl. 6, fig. 4; pl.9. fig 4, by monotypy.

Other species.— *Atelestocrinus baumilleri* n. sp.; *Atelestocrinus campanulatus* (Kirk, 1948); *Atelestocrinus concinnus* (Kirk, 1948); *Atelestocrinus curtus* (Kirk, 1948); *Atelestocrinus delicatus* Wachsmuth and Springer, 1886; *Atelestocrinus hutkensis* Webster, Maples, Mawson, and Dastanpour, 2003; *Atelestocrinus meszarosi* Kammer and Roeser, 2012; *Atelestocrinus quinquangularis* (Austin & Austin, 1843), n. comb.; and *Atelestocrinus tenuis* (Kirk, 1948).

Distribution.— Middle Devonian (Givetian) to Mississippian (Viséan) of Canada, Iran, Ireland, and the United States, specifically: Indiana, Iowa, Michigan, New York, Ohio, and Tennessee.

Discussion.— *Atelestocrinus* has been most commonly assigned to the family Mastigocrinidae (Jaekel, 1918; Moore and Laudon, 1978b; Webster et al., 2003; Lee et al., 2005; Kammer and Roeser, 2005). Many of the genera previously included within the Mastigocrinidae, as defined by the *Treatise on Invertebrate Paleontology* (Ubaghs, 1978), have been formally reassigned to other families (e.g., McIntosh and Brett, 1988; McIntosh, 2001). *Atelestocrinus* should likewise be removed from the Mastigocrinidae based on differences in the construction of the posterior interradius and arms. However, since higher-level cladid taxonomy remains in significant need of revision (McIntosh, 1983; Wright et al., 2017), but is beyond the scope of the present study, I leave *Atelestocrinus* unassigned at the family level. Regardless, I address some relationships among *Atelestocrinus* and other crinoid genera in the subsequent section.

The publication date for *Atelestocrinus* is typically given as "Wachsmuth and Springer, 1886" and the type species as *A. delicatus* by subsequent designation (Miller, 1889: 226; Jaekel, 1918; Moore and Laudon, 1943; Ausich and Lane, 1982; Kammer and Gahn, 2003; Webster et al., 2003; Lee et al., 2005; Kammer and Roeser, 2012). However, *Atelestocrinus robustus* was named and figured nearly a year earlier (Wachsmuth and Springer, 1885: pl. 6, fig. 4; pl.9, fig 4). The figures include a labeled plate diagram for the genus (Fig. 2A) and a drawing of the specimen of *A. robustus* (USNM S2409) from the Burlington Limestone. Thus, the genus name *Atelestocrinus* was established by Wachsmuth and Springer in 1885 rather than 1886 (following ICZN, 1999: Article 23.1). Likewise, *A. robustus* gained nominal priority in 1885 since it satisfies all nomenclatural requirements (ICZN, 1999: Articles 11, 12.1, 12.2.7).

Although Wachsmuth and Springer (1885, 1886) did not explicitly define a type species for the genus, it is reasonable to assume *A. robustus* best captures their concept given it was the only species they figured; they never illustrated *A. delicatus*. Moreover, *A. delicatus* is ineligible as the type because it was published after the establishment of the genus (ICZN, 1999: Article 67.2). When only a single species is named under a new genus, that species must be considered the type species (ICZN, 1999: Article 68.3). Simply put, Miller (1889: 226) was incorrect in recognizing *A. delicatus* as the type — a mistake repeated by subsequent authors. The type species for *Atelestocrinus* is corrected herein as *Atelestocrinus robustus* Wachsmuth and Springer, 1885 by monotypy (ICZN 1999: Article 70.3).

Atelestocrinus delicatus Wachsmuth and Springer 1886 was originally published under a misspelling of the genus, *"Attelesocrinus"*, likely a typesetting error, but it is the only spelling of the name in the entire *Revision of the Palaeocrinoidea*. Fortunately, they provided an erratum at the end of that work (Wachsmuth and Springer, 1986: 229–303), in which they corrected numerous "exceedingly annoying" errors, including that for *Atelestocrinus delicatus* (ICZN, 1999: Article 32.5.1.1).

Webster et al. (2003) provided a revised diagnosis for the genus that is largely followed here. The only correction is that in addition to being pentagonal, the stem of *Atelestocrinus* may also be round or nearly so. The most pertinent revisions to the genus (Webster et al., 2003) relate to the radials and brachials. Although the most diagnostic feature of the genus is an atrophied anterior radial without an arm or facet, rarely an atavistic facet may develop as in the holotype of *A. concinnus* (USNM S4608). This arm facet may or may not be functional, occasionally bearing a few extremely reduced brachials; and rarer still, it may possess a functional arm. Within a population of 25 undescribed *Atelestocrinus* from the Early Mississippian (Tournaisian) Wassonville Formation of Iowa, two individuals bear atavistic facets in a reduced anterior ray that supports at least one atrophied brachial (Fig. 4C), and one specimen has an arm of normal thickness (Fig. 4D). Another relevant revision of Webster et al. (2003) is that *Atelestocrinus* may possess two to six primibrachials. This is a highly variable character for the genus, even among individuals of the same species and within different rays of the same specimen. On one end of this spectrum is *A. delicatus*, which has only two primibrachials in each ray, and on the other end are species such as *A. campanulatus*, *A. hutkensis*, and *A. quinquangularis*, in which the sixth primibrachial may be axillary.

McIntosh (1983) proposed synonymizing *Atractocrinus* (Kirk,1948) with *Atelestocrinus*, a move formalized by Webster et al. (2003). The two genera are indistinguishable given the current genus concept for *Atelestocrinus*. Webster (2014: 1141) also considered *Fiannacrinus* Ausich and

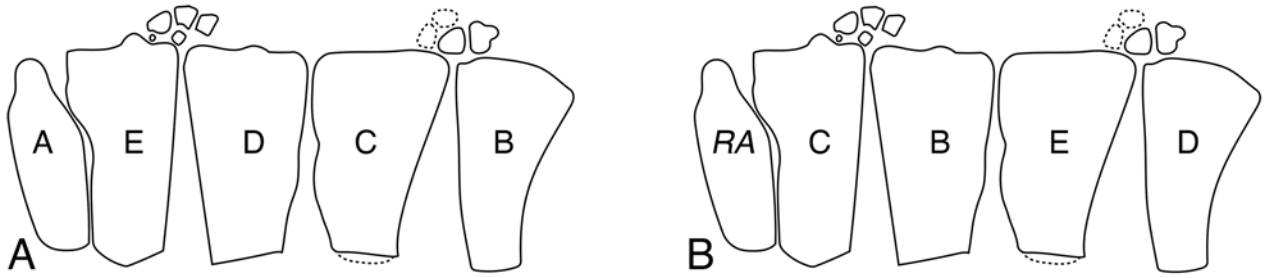

FIGURE 3 — Plate diagrams for *Atelestocrinus indianensis*, modified from Ausich and Lane, 1982: fig. 2. Note the paucity of preserved morphology above and below the radial circlet, the series of plates labeled with capital letters. **A**, Plate interpretation of the original authors. **B,** Plate interpretation of this paper.

Sevastopulo (2001) a synonym of *Atelestocrinus*, a change formalized here. The diagnostic differences separating *Atelestocrinus* from *Fiannacrinus* were presented as the latter genus having "three anal plates in the cup, a radianal of typical size and shape, small C radial, and four or more primibrachials" (Ausich and Sevastopulo, 2001: 85). *Atelestocrinus* has 3 anal plates in the cup (not 2 as indicated by Ausich and Sevastopulo, 2001; see Fig. 2A), a pentagonal radianal that is in contact with the basals (not the infrabasals as indicated by Ausich and Sevastopulo, 2001), and a C radial that may be the smallest in the cup. As such, *Fiannacrinus* is synonymized with *Atelestocrinus* (following ICZN 1999: Article 23.3). When compared to *A. robustus*, *A. quinquangularis* has a more strongly pentagonal stem, less bulbous infrabasals, and in some specimens, depressed triple-plate junctions and an additional primibrachial, but these are species-level, not genus-level, differences. In fact, many of these traits are variable within individuals of the same species.

Known primarily from radial circlets, *A. indianensis* (Ausich and Lane, 1982) and *A. kentuckyensis* (Lee et al., 2005) are here considered *nomina dubia*. They simply lack enough characters to be reasonably diagnostic for any species (see Fig. 3). Webster et al. (2003: 11), citing as evidence the uncharacteristically long radials, rejected *A. indianensis* from the genus and instead suggested it was a disparid. I disagree with this opinion and present evidence below for both species being cladids that are missing the basal circlets. However, this cannot be unquestionably demonstrated given the dearth of characters preserved in the holotypes of these two species (Ausich and Lane, 1982; Lee et al., 2005).

Atelestocrinus robustus, Wachsmuth and Springer, 1885
Figs. 1A–F, I; 2A

Atelestocrinus robustus Wachsmuth and Springer, 1885, pl. 6, fig. 4; pl. 9, fig. 4. Wachsmuth and Springer, 1886, p. 147. Miller, S. A., 1889, p. 226. Weller, S., 1898, p. 101. Moore and Lane *in* Moore and Teichert, 1978b, p. T621, fig. 404, no. 2. Ausich and Lane, 1982, p. 1350. Webster, 1986, p. 69. Webster, 1988, p. 40. Kammer and Ausich, 1996, p. 838. Kammer and Gahn, 2003, p. 122, figs. 1.1-1.2. Webster et al., 2003, p. 13. Lee et al., 2005, p. 349. Kammer and Roeser, 2012, pp. 475-476. Ausich et al., 2020, p. 528, fig. 3.

Atelestrocrinus robustus (Wachsmuth and Springer, 1886). Bassler and Moodey, 1943, p. 314.

Lectotype.— USNM S2409 *Atelestocrinus robustus* Wachsmuth and Springer, 1885: pl. 9. fig. 4. from the uppermost Burlington Limestone, Cedar Fork Member, near Burlington, Iowa.

Other material.— Paralectotype USNM S2411 from the Fort Payne Formation, Whites Spring Creek, Davidson County, Tennessee. McIntosh (1983: pl. 26, fig. 7) figured a third specimen of *A. robustus* from the NMNH, but I have not had the opportunity to examine it except from the dissertation. Additionally, USNM 2410, a specimen from the collection of Wachsmuth and Springer labeled as *A. robustus* despite being monocyclic.

Discussion.— Wachsmuth and Springer (1885, 1886) established *A. robustus* with two specimens in hand, syntypes USNM S2409 and USNM S2411. The latter specimen from the Fort Payne Formation is based on a partial calyx, figured here for the first time (Fig. 1B–F). Despite a paucity of characters, including the absence of an infrabasal circlet, it convincingly belongs to the genus given the armless anterior ray and the structure of the posterior interray. Regardless, because of the incomplete nature of this specimen, and considering it was never figured by Wachsmuth and Springer, USNM S2411 is established as a paralectotype, leaving USNM S2409 as the lectotype of *A. robustus*.

The stratigraphic provenance of the lectotype has been a point of confusion. Wachsmuth and Springer (1886: 147) described it as being from the "Burlington and Keokuk Transition bed near Burlington, Iowa." Based on accompanying specimen labels, Kammer and Gahn (2003: 122) questionably reported it as being from "either the upper part of the Burlington Limestone or Montrose Chert Member

of the Keokuk Limestone." The first author and I disagreed on this point, so both views were presented at the time. However, I am confident the lectotype is from the Cedar Fork Member of the Burlington Limestone. In southeast Iowa, the uppermost Burlington Limestone is characterized by thin bedded, orange dolomitic mudstones that alternate with medium bedded crinoidal packstones and some chert. In addition, there are several interspersed bone beds with a rich chondrichthyan fauna, often bearing abundant glauconite. Conodont research places the "transition beds" in the *Gnathodus bulbosus* Zone (Thompson, 1967; Brenckle, 2005) of the Cedar Fork Member. This zone accumulated during a lowstand period of reduced sedimentation on the Burlington Shelf immediately prior to the transgressive event associated with Keokuk deposition (Witzke and Bunker, 1996; Lane and Brenckle, 2005). The thin orange mudstones at the top of the Cedar Fork Member preserve some of the most spectacular crowns in the Burlington Limestone, consistent with the preservation and associated matrix of the lectotype (Fig. 1A, I). In contrast, fossils from the lowermost Keokuk Limestone are more heavily silicified, and the fossil preservation is different, mostly yielding crushed, solution-weathered calyxes; crowns of any quality are rare. Finally, the "Montrose Chert" has been abandoned as a formal division of the Keokuk Limestone (Witzke and Bunker, 2005) because of stratigraphic misplacement by Keyes (1895). The chert at Montrose, Iowa, is positioned near the top, not the base, of the Keokuk Limestone.

Although a precise description of *A. robustus* is not possible because of the current inaccessibility of the NMNH, much can be said of the types from available photographs (Fig. 1A–F, I). Among the most diagnostic characters of the species are the uniformly tumid plates and relatively large radial facets that support four to five heavy primibrachials. The radial facets and associated brachials of this species appear to be proportionally larger than those of any other *Atelestocrinus*. The lectotype (Fig. 1A, I) appears more gracile and with less tumid plates than the paralectotype (Fig. 1B–F), but the absence of infrabasals in the latter gives it a deceptively globose aspect. Other differences include faint granulose ornamentation on the paralectotype (especially visible on the A and E radials) and more equant basals, but this could represent intraspecific variation, if indeed the two fossils represent the same species. The specimen of *A. robustus* figured by McIntosh (1983: pl. 26, fig. 7) likewise has more equant basals than the lectotype. It also has less tumid plates and shorter infrabasals. Regrettably, the rarity of *A. robustus* limits our understanding of intraspecific variation in this species. Fortunately, large numbers of some *Atelestocrinus* species are available for study (McIntosh, 1983), including the undescribed population from the Wassonville Formation (see Fig. 4C–D). In short, some of the most variable characters seem to include plate ornamentation and tumidity, relative size of the basals, the number of primibrachials, and whether the ramules branch — which is variable even along single arms of some individuals.

The monocyclic specimen described as *A. robustus* (USNM S2410; Fig, 1G–H, J–K; 2B) exhibits many of the same traits as the lectotype of the species. Most notably, it has a nearly round stem, large radial facets, and thick arms with four to five primibrachials. However, it also exhibits some exceptional differences, the most glaring being only a single plate circlet below very elongate radials. When I first saw the specimen, I thought it might represent a new species of *Belemnocrinus*, or perhaps even a new genus. Yet another possibility is that it is an abnormal specimen of *A. robustus*. Upon further examination of the calyx, which is free from the matrix, it has a radial circlet consisting of five plates, only four of which are arm-bearing. The two most reasonable interpretations of the armless plate are that it is either a typical anterior radial for *Atelestocrinus* or it represents the posterior interray, conceivably a hypertrophied radianal or anal *X*. Given the former interpretation, it is inconsistent with *Atelestocrinus* because it would lack any posterior plates. Given the latter interpretation, it is inconsistent with *Belemnocrinus*, at least as historically defined, because that genus is described as having five arm-bearing rays with one radial-sized posterior plate in the cup, resulting in a radial circlet composed of six plates (White, 1862; Wachsmuth and Springer, 1877; Moore and Lane, 1978a). Under any interpretation, the calyx is unusual (Fig. 2B). The plates of the lowermost circlet are variable in shape, width, and some of the lateral sutures are bowed. This specimen appears to have lost entirely the basals and anterior radial. Moreover, the calyx deviates from the typical pattern of 36º offset of superadjacent plate circlets.

Atelestocrinus baumilleri, n. sp.
Fig. 4A–B, E–G

Holotype.— UMMP 75465, which consists of a strongly compressed partial crown and stem; the crown was removed from the matrix for more thorough study. The holotype and only known specimen is from the Mississippian (Viséan) Ramp Creek Formation, Indian Creek, Montgomery County, Indiana, U.S.A.

Diagnosis.— The most distinctive feature of *A. baumilleri* is the fine, granulose texture that covers all plates of the dorsal cup. Proximally, these granules are weakly organized into radiating ridges that run across the basals and infrabasals. Such radiating granulose ornamentation has not been observed in any other species of *Atelestocrinus*. It is clearly distinguished from *A. robustus*, *A. delicatus*, and *A. meszarosi* by the absence of a bulbous infrabasal circlet and the presence of a strongly pentagonal stem. In this regard it is most similar to *A. hutkensis* and *A. quinquangularis*; however, *A. baumilleri* differs from those taxa in possessing fewer primibrachials, nodose tegmen plates, and ornamented cup plates.

Etymology.— This species is named in honor of Tomasz K. Baumiller for his monumental contributions to crinoid paleontology, stellar mentorship, and invaluable friendship. Like the holotype specimen, long may he regenerate.

Description.— The crown of *A. baumilleri* is tall and gracile with eight ramulate arms that make up 75% of crown height. It has a high conical cup that is slightly higher than wide (H:W 1.1). The plates of the calyx are relatively thin.

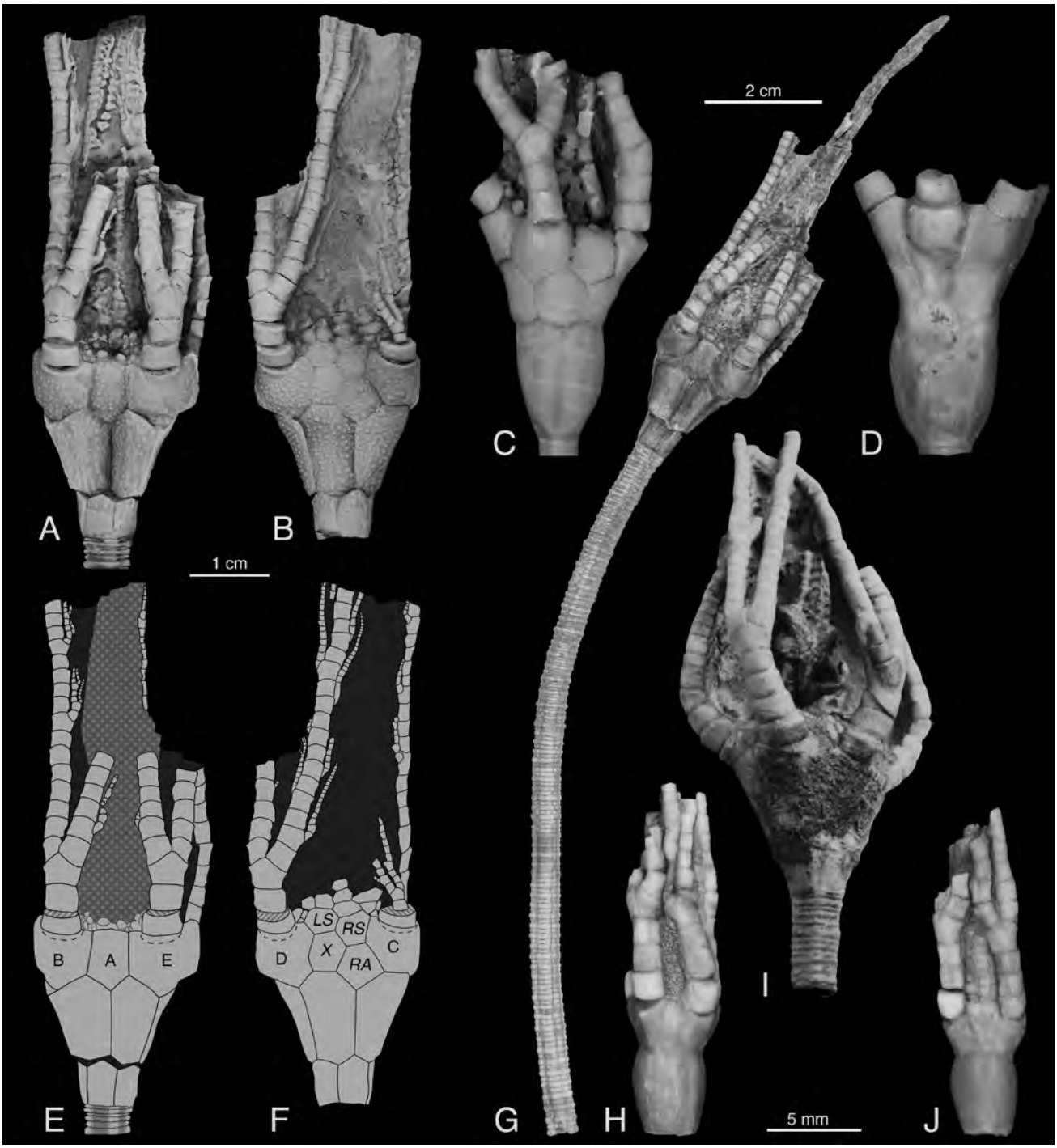

FIGURE 4 — Specimens of *Atelestocrinus*, *Belemnocrinus*, and another pseudomonocyclic individual. **A–B, E–F,** anterior (A, E) and posterior (B, F) views of the crown of *Atelestocrinus baumilleri*, n. sp. (UMMP 75465) from the Ramp Creek Formation, Indiana (left scale bar, 1 cm); specimen coated with ammonium chloride. **G,** anterior view of the same specimen (UMMP 75465) with stem (upper right scale bar, 2 cm). **C–D**, **H, J,** undescribed crinoids from the Wassonville Formation of Iowa, including: (C) An *Atelestocrinus* with an atavistic radial facet and primibrachial in the A ray (SUI 148482); (D) an abnormal specimen of the same species (SUI 98386); and anterior (H) and posterior (J) views of a *Belemnocrinus* specimen (SUI 148483) (all lower right scale bar, 5 mm). **I,** a pseudomonocyclic crinoid similar to *A. baumilleri* from the Ramp Creek Formation, Indiana, that has an ophiuroid attached to its anal sac (left scale bar, 1 cm).

The five infrabasal plates are higher than wide (H:W 1.5–1.6), uniformly pentagonal, entirely visible in side view, and make up about 24% of cup height. The five basal plates are higher than wide with the DE and EA basals being notably tall and thin (H:W 2.3 and 1.8, respectively) relative to the AB, BC, and CD basals (H:W 1.5–1.6). All the basals are hexagonal except for CD, which is septagonal. The AB, DE, and EA basals have peaked upper surfaces, whereas those of BC and CD are flat. The basal circlet makes up roughly 43% of cup height. The five radial plates are slightly higher than wide (H:W 1.1–1.3), except for the C radial, which is slightly wider than high (H:W 0.9). The A radial is the tallest and thinnest radial plate and lacks an arm or associated facet. The C radial is the smallest arm-bearing plate. All radials are roughly septagonal with the exception of the A radial, which is hexagonal. All of the radials have peaked lower surfaces except for the C radial, which articulates with the underlying CD basal along a flat surface, the two plates being perfectly aligned and lacking the 36º offset typical of superadjacent plate circlets. Because of the atrophied A radial and relatively wide posterior interray, the C radial is shifted into the BC interradial position. The radial circlet makes up about 33% of cup height. The radial facets are peneplenary, moderately declivate, and are broadly U-shaped with weakly developed marginal rims. They occupy approximately 23–33% of radial height, with the C radial being an outlier (43%), and 63–73% of radial plate width.

Three plates are fully incorporated into the posterior interray of the dorsal cup. These include a pentagonal radianal (H:W 0.9) equally supported by the BC and CD basals, a hexagonal anal *X* (H:W 0.8), and a hexagonal right sac plate (H:W 0.7). The left sac plate is also partially integrated into the dorsal cup, being supported by the upper right shoulder of the D radial. The anal sac is incomplete but extends to at least the height of longest preserved arm in the B ray. It appears to be relatively narrow and elongate, composed of eight uniserial rows of thin, hexagonal plates that are uniformly wider than high. Small circular pores are developed at the plate corners. The anal sac emerges from a tegmen composed of numerous tiny, nodose plates that are irregularly arranged. Embedded within this pebbly integument, along the outer margins of most interrays, are two to three larger elongate plates with their long axes directed radially toward the center of the calyx. Near the base of the sac is a large, elongated dome-shaped plate, possibly an oral, directed perpendicularly to the anterior-posterior axis though slightly displaced taphonomically. Ambulacra on the tegmen are not apparent, possibly due to partial disarticulation and severe compression of the holotype.

The longest preserved arm, right branch of the D ray, is approximately four times longer than the dorsal cup and consists of 42 secundibrachials. The arms branch once isotomously on the third primibrachial, resulting in eight arms total, and are of moderate thickness. Their lateral margins are sharply rounded and deep. Primibrachials are about twice as wide as high (IBr_1 H:W 0.4–0.6), and proximal secundibrachials are more equant (H:W 0.8–0.9). All the brachials possess nearly parallel articular surfaces and form a relatively linear stack of uniserial plates. Each arm gives rise to a ramule on alternating secundibrachials, beginning with $IIBr_2$. The ramules are heterotomous and complexly branched, emerging from robust, rimmed facets that occupy about half the height of their supporting brachials. Where visible, all secondary ramule branches arise first from the second ramular and subsequently from every third ramular; the smallest branches are directed away from the main arm branch. The ventral groove may be observed in two places in the holotype, $IIBr_{8\text{-}10}$ and $IIBr_{25\text{-}26}$ of the right branch of the D ray. The groove is deep and U–shaped, occupying nearly 40% of secundibrachial width proximally and 50% distally, where it also appears to become shallower. Two rows of paired cover plates adorn the ventral grooves of both the brachials and ramulars.

The stem is strongly pentagonal with the lobes oriented interradially. In the holotype, the stem appears to be pentameric (Fig. 4G), but this is not the case. What appears to be meres are irregular fractures generated by compaction. Proximally, the noditaxis pattern is N3231323, and it becomes N212 distally. Proximal nodals are nearly four times thicker than the thinnest internodals, and their points bear bulbous ornamentation. The columnals have well developed crenulae on their outer margins, which are clearly visible in side view; otherwise the articular surfaces are smooth. The lumen is tiny, its shape obscured by compaction. Evidence for cirri or cirral scars is lacking.

Measurements.— All in mm. Length of the full specimen, 225. Crown H, 90.8. Calyx H:W, 22.8:20.8. H:W for the following plates: *IB* A, 5.6:3.7; *IB* B, 5.8:3.6; *IB* C, 6.1:3.9; *IB* D, 6:3.7; *IB* E, 5.7:3.6; *B* AB, 10.9:7.2; *B* BC, 11.8:7.4; *B* CD, 11.9:7.8; *B* DE, 12.1:5.1; *B* EA, 11.4:6.4; *R* A, 7.8:5.8; *R* B, 9.5:7.9; *R* C, 6.9:7.8; *R* D, 8.7:7.8; *R* E, 9.6:8.9; *RA*, 5.8:6.1; *X*, 5.2:4.9; *RS*, 3.8:4.5; *LS*, 3.2:4.2. IBr_1 B, 2.5:4.9; IBr_1 C, 2.2:5; IBr_1 D, 2.4:4.8; IBr_1 E, 3:5.1; IAx_1 B, 3.5:4.9; IAx_1 C, 1.6:1.9; IAx_1 D, 3.8:5; IAx_1 E, 4.3:5.1. Radial facet height from the bottom of the facet to the top of the radial plate:the width of the radial facet: *R* B, 5.8:2.4; *R* C, 5.2:3; *R* D, 5.6:2.3; *R* E, 5.6:2.9. Height of the primibrachial series: B, 10.3; C, 5.1; D, 10.2; E, 10.6. Length of the longest preserved arm (including primibrachials), 90.1. Length of the longest preserved ramule, 12.1; Stem length, 134.2. Proximal stem width, 6.3. Proximal nodal thickness, 1.3. Proximal internodal thickness, 0.3.

Discussion.— For the most part, *Atelestocrinus* is exceedingly rare, even from localities world renowned for producing thousands of complete specimens in dense, multispecies associations such as Crawfordsville. Despite searching major crinoid collections, public and private, having close ties to individuals in the commercial fossil community, and even posting queries to large social media groups, I was unable to discover a second specimen of *A. baumilleri*. As far as is known, this species is also the last surviving member of a lineage that first appears in the Middle Devonian (Givetian) of North America (McIntosh, 1983).

Fitting for its namesake, Tom Baumiller, and our collaborative research on predation, the holotype bears a regenerated arm in the C ray. The entire arm is regenerated above the first primibrachial. The absence of any mechanical

damage to this plate is consistent with autotomy of the arm whether the loss was triggered by an exploitive biotic interaction or otherwise. McIntosh (1983; pl. 26, fig. 9) figured a similarly regenerated arm in the D ray of an *A. campanulatus*, also originating from an unfractured first primibrachial. This suggests at least some brachials in *Atelestocrinus* may have had an autotomy function like the cryptosyzygies of some extinct and extant crinoids (Gahn and Baumiller, 2010).

Geographically and temporally, *A. baumilleri* shows some affinities with *A. indianensis* (Ausich and Lane, 1982: pl. 1, figs. 5, 9,13). They have similar radial facet development, and although not mentioned in the original description, *A. indianensis* appears to have finely granulose ornamentation. However, the comparison must largely end there given the holotype of *A. indianensis* lacks a stem, infrabasals, basals (if it had them), tegmen, anal sac, and arms. Unlike *A. baumilleri*, *A. indianensis* has only five plates in the radial circlet. These were interpreted by Ausich and Lane (1982) as five radials with an armless A ray as in *Atelestocrinus* but without the posterior plates characteristic of the genus (Fig. 3A). The arrangement of the radial circlet in *A. indianensis* is like that of the monocyclic form of *A. robustus* (USNM S2410; Figs. 1G–H, J–K; 2B), and it is also reinterpreted as being composed of only four radials and a hypertrophied radianal (Fig. 3B).

Atelestocrinus kentuckyensis (Lee et al., 2005) is in most ways identical to *A. indianensis* in both preservation and morphology. It is known from little more than a radial circlet that is composed of only five plates, interpreted by the original authors as representing five radials without any anal plates. It also has similarly developed radial facets and granulose ornamentation. The plate they interpreted as the armless anterior radial has a peaked upper surface, forming two facets that each support large, equant "tegmen" plates (Lee et al., 2005: fig. 1.12). This is not an armless A radial with two tegmen plates but rather three posterior plates. A similar configuration is seen in some individuals of *Belemnocrinus*.

The radial circlets of *A. indianensis* and *A. kentuckyensis* bear resemblance to the unusual form of *A. robustus* (Figs. 1G–H, J–K; Fig. 2B; Fig. 3). They are also similar to the undescribed (and as of yet unlocated) monocyclic crinoid from Indian Creek (Fig. 4I). Based on the photograph and cast I have of this specimen, it has similarly elongated radials. There is no clear evidence of a fifth arm-bearing ray, but this is difficult to rule out since the specimen is embedded in matrix. However, the proportions of the visible plates are consistent with a radial circlet composed of four arm-bearing radials and a large posterior plate. Under magnification, there is some indication in the 1990-vintage photograph (Fig. 4I) of a possible fifth arm-bearing ray, mostly buried in the matrix; but it's difficult to say without the specimen in hand.

The monocyclic specimen from Indian Creek (Fig. 4I) shares numerous similarities with *A. robustus*, and especially with *A. baumilleri*. Like *A. robustus*, it has four to five primibrachials in each ray. Like *A. baumilleri*, it has a strongly pentagonal stem with bulbous ornamentation at the lobes. It also has finely granulose plate ornamentation on the dorsal cup, somewhat obscured by heavy pyritization. It has similarly developed radial facets and arms that are less "robust" than those of *A. robustus* and with complexly branched ramules. Finally, the monocyclic semblance of *A. baumilleri* has on the tegmen, radially oriented, elongate plates at the margins of the interradial areas like those of its dicyclic counterpart. See below for a discussion on possible explanations for this unusual crinoid from Indian Creek and other monocyclic crinoids that share similarities with *Atelestocrinus*.

EVOLUTIONARY AND DEVELOPMENTAL IMPLICATIONS OF *ATELESTOCRINUS*

The documentation of new species is foundational to paleontological science, but such efforts have their greatest value when framed in questions of organismal development, evolution, and ecology. The description of *Atelestocrinus baumilleri* is no exception. What may have driven the loss of an entire food gathering ray in *Atelestocrinus*? How do the morphologically similar but monocyclic crinoids relate to *Atelestocrinus*, and developmentally, how did they achieve this form? Some possible answers to these questions, among other considerations, are addressed in the following paragraphs.

McIntosh (1983) suggested *Atelestocrinus* is closely related to *Bactrocrinites*, both genera rife with abnormal individuals (McIntosh, 1979). *Bactrocrinites* is a dicyclic crinoid that includes teratological monocyclic forms, in addition to intermediates that retain basals in some interrays but not others. For example, McIntosh (1979) considered *Hypsocrinus*, *Perissocrinus*, and *Kalpidocrinus* to be aberrant forms of *Bactrocrinites fieldi* (Springer and Slocum, 1906). Abnormalities in these crinoids were associated with the midcup, generating a rarely demonstrated type of pseudomonocycly. Whereas pseudomonocycly is mostly associated with loss of the infrabasal circlet, these individuals lost some or all their basal plates. The reduction or elimination of the midcup in these taxa often disrupted typical patterns of calyx plate symmetry. *Belanskicrinus westoni* (Belanski, 1928), a species formerly aligned with *Bactrocrinites*, likewise shows midcup instability, but instead of reducing or eliminating the midcup, it added plates immediately below the radials (Strimple and Levorson, 1969). Both the addition and subtraction of plates can disrupt expected patterns of calyx plate symmetry.

Wachsmuth and Springer (1885) highlighted fundamental differences in patterns of symmetry between dicyclic and monocyclic crinoids with pentagonal stems and lumens, the so-called "Law of Wachsmuth and Springer" (LWS; Bather, 1898). Among such dicyclic crinoids, stem lobes are interradial and lumen lobes are radial. Monocyclic crinoids show the opposite: Stem lobes are radial and lumen lobes are interradial. These structural principles are valuable for determining whether monocycly was achieved through infrabasal loss. For example, among articulates with pentagonal stems, the stem lobes are interradial, providing evidence in favor of these

crinoids having originated from dicyclic ancestors via loss of the infrabasal circlet; a pattern consistent with ontogeny (Amemiya et al., 2016).

In crinoids that develop monocycly through loss of the basals, McIntosh (1979) observed they lack the expected 36º offset of superadjacent plate circlets. This generates inconsistent patterns of symmetry, with radial stem lobes in some rays and interradial stem lobes in others. This pattern is here defined as "McIntosh's rule" and may be used as evidence for identifying monocyclic crinoids that originated from dicyclic ancestors through loss of the midcup. For example, in *Hypsocrinus*, McIntosh (1979: 27) observed two interradial and three radial stem lobes. Moreover, some of the infrabasals in this specimen have sinuous lateral sutures; the plates are radially disposed proximally, and they are interradially disposed distally. This pattern of midcup instability is an indication of plate reorganization and compensatory growth due to loss of the basals, most likely before the calyx plates became fixed during the cystidean stage of development (Springer, 1920; Amemiya et al., 2016). This same pattern is observed in *Belemnocrinus*, a genus McIntosh (1979: 28) suggested might likewise be a pseudomonocyclic cladid.

Belemnocrinus (White, 1862) is an unusual monocyclic crinoid that has been formally described only from the Burlington Limestone. It is currently classified as a disparid, the namesake of an entire superfamily, the Belemnocrinacea (Miller, 1883; Moore and Lane, 1978a). *Belemnocrinus* continues to be included in phylogenetic analyses of the Disparida (Ausich, 2018) despite numerous suggestions that it is a pseudomonocyclic cladid (Ubaghs, 1953; McIntosh, 1979; Sevastopulo and Lane, 1988; Gahn, 2006). New observations herein provide further evidence for the interpretation that *Belemnocrinus* is an abnormal cladid that possibly arose from *Atelestocrinus*, either phylogenetically or developmentally.

Since 1994, I have been collecting an undescribed crinoid fauna from the Wassonville Formation of Iowa that includes a substantial population of *Belemnocrinus* (Gahn and Baumiller, 2004). Stratigraphically, the Wassonville Formation immediately underlies the Burlington Limestone. Although I have collected hundreds of articulated crinoids from the Wassonville Formation and coeval strata in a dozen quarries from central Iowa to northeastern Missouri, all the *Belemnocrinus* specimens come from a single quarry and horizon. Alongside nearly 25 specimens of *Belemnocrinus* (Fig. 4H, J) are an equal number of crinoids that are dicyclic but otherwise nearly indistinguishable (Fig. 4C–D). They occur exclusively in the same quarry and horizon as the monocyclic *Belemnocrinus*. I initially considered these crinoids to be monocyclic and dicyclic variants of the same species.

When I first began unearthing this population of crinoids, and despite their simplicity, I did not fully appreciate the morphology of either the dicyclic or the monocyclic forms. *Belemnocrinus* is consistently described as having five armed rays and a single anal plate (White, 1862; Wachsmuth and Springer, 1877; Moore and Lane, 1978a). Since the Wassonville specimens were embedded in matrix, I could typically observe only half of any crown. When I first observed a single, armless plate in the radial circlet of a "dicyclic *Belemnocrinus*", I assumed it was the single anal plate diagnostic for that genus. However, I soon wondered if these dicyclic crinoids could be *Atelestocrinus*. The only way to resolve this question was to remove a dicyclic variant from the matrix, and so I did. The first extricated specimen had only four arm-bearing rays with an armless anterior radial and three plates in the posterior interray, fitting the diagnosis for *Atelestocrinus*.

Still working under a model of these monocyclic and dicyclic forms being of the same species of cladid, I faced a quandary. How could a crinoid with three cup circlets and four armed rays develop into a variant with two cup circlets and five armed rays? First, I searched the population of Wassonville *Atelestocrinus* for specimens with fully developed arms in the anterior ray. Strikingly, I discovered one such specimen (Fig. 4D) and two additional specimens with atavistic arm facets and brachials in the anterior ray (Fig. 4C).

Next, I turned to specimens of the monocyclic *Belemnocrinus* and started removing them from the matrix. The first specimen extracted had only five plates in the radial circlet — four arm-bearing radials (not five as expected) and a single, radial-sized anal plate (Fig. 4H–J). This is the same configuration as in the monocyclic form of *A. robustus* discussed previously (Figs. 1G–H, J–K; 2B). Did I serendipitously find yet another new species of an undocumented genus, specifically the one that includes the monocyclic forms of *A. robustus* and *A. baumilleri*? No, *Belemnocrinus* has likely been misdiagnosed for 160 years. Upon removing additional monocyclic variants from the matrix, I was unable to discover a single specimen of *Belemnocrinus* with five radials. Perhaps more importantly, I was unable to confirm that a single specimen of *Belemnocrinus typus* White, 1862 has five radials, even after examining all known specimens of the type species. *Belemnocrinus*, like *Atelestocrinus*, has only four arm-bearing radials. However, it has taken the reduction of the anterior ray one step further by eliminating it entirely. The loss of the anterior arm in *Atelestocrinus* and absence of the associated radial in *Belemnocrinus* may be explained by neoteny; in some Paleozoic crinoids, the A radial is the last to develop ontogenetically (Lane, 1978; Sevastopulo and Lane, 1988). This same radial is likewise missing in *Hypsocrinus* (McIntosh, 1979).

The degree of variation observed in both the dicyclic and monocyclic individuals from the Wassonville population is unusual but will not be fully documented here. However, to contextualize the monocyclic semblances of *A. robustus* and *A. baumilleri* (Figs. 1G–H, J–K; 4I), one abnormal *Atelestocrinus* from the Wassonville Formation (Fig. 4D) is especially insightful. Despite being dicyclic, it has starkly malformed calyx plates and misaligned cup circlets. The infrabasal and basal circlets appear to have been partly resorbed at the expense of one another, and the radials, which show evidence of thickening in areas consistent with normally

developed plates of this type (Fig. 4C), have thinner tongues of stereom extending into regions of the calyx typically occupied by the basals. This abnormal growth likely occurred prior to the pentacrinoid stage of development. Once closure of the calyx was completed, the nearly isometric growth that is typical of most calyx plates would have conserved this aberrant form in the adult. Regardless, this specimen (Fig. 4D) may provide insight into the development of the monocyclic forms of *A. robustus* and *A. baumilleri*, specifically their relatively elongate radials. Complete resorption of the basals and compensatory growth of the radials in early (cystidean) stages of growth could explain this difference between the monocyclic and dicyclic forms of these taxa.

Such compensatory growth is also observed among individuals of Wassonville *Belemnocrinus*, but the larger sample size permits study of variability. Relative to the dicyclic variants (*Atelestocrinus*), some specimens exhibit normal infrabasals with greatly extended radials. Others exhibit normal radials with greatly extended infrabasals, occasionally with sinuous lateral sutures as in *Hypsocrinus*. Yet others seem to have lost the basals without any compensatory growth of either the infrabasals or the radials. However, consistent with McIntosh's rule, many individuals deviate from the expected 36º offset of superadjacent plate circlets.

Another critical observation relates to the underlying explanation for the LWS and homology of the cup base circlet among dicyclic and monocyclic crinoids. Like *A. baumilleri* and its monocyclic counterpart (Fig. 4A, I), some specimens from the Wassonville *Atelestocrinus-Belemnocrinus* population have pentalobate stems. In all of these, the stem lobes are offset with the radially disposed infrabasals. However, whereas the infrabasals are aligned with the radials in dicyclic forms (*Atelestocrinus*), they are generally misaligned with the radials in monocyclic forms (*Belemnocrinus*). In other words, the radial circlets of most monocyclic variants, as well as their corresponding arms and ambulacra, are interradially disposed. The stem-infrabasal junction is fixed in both the dicyclic and monocyclic forms, but with the loss of the basals, the radial circlet generally rotates clockwise (from a ventral perspective) into an interradial position. With emphasis, using the infrabasals as a fixed reference, the alimentary system may be oriented interradially in monocyclic crinoids.

This observation rejects a fundamental assumption of Carpenter's (1878) plate homology system, which interprets the lowermost cup circlet of most monocyclic crinoids (e.g., disparids and monobathrids) as basal plates. Miller (1821), author of the Crinoidea, universally referred to the cup base circlets of all crinoids as the "pelvis". Likewise, Müller (1843) suggested the cup plates immediately above the stem were homologous for both dicyclic and monocyclic crinoids (based on the translation and interpretation of Carpenter, 1878: 366). Using current terminology, Müller (1843) would have referred to the lowermost plate circlet of both forms as infrabasals. Carpenter (1878) objected to this interpretation because he firmly held that a plate circlet could not be radially disposed in some taxa and interradially disposed in others. This assumption was championed by Wachsmuth and Springer (1897) and perpetuated in subsequent publications (e.g., Moore and Laudon, 1943; Ubaghs, 1978). The Carpenter system of plate homology and concomitant view that radial and interradial plate positions are fixed in crinoids generally persist to this day. This is true despite evidence to the contrary, including the work of Lane (1978) who demonstrated that primary plate circlets, notably the orals, shift from a radial to an interradial position during ontogeny of the microcrinoid *Cranocrinus*. Similarly, the population of Wassonville *Atelestocrinus-Belemnocrinus* decisively rejects Carpenter's assumption by demonstrating that the radial circlet can be radially or interradially disposed. Careful examination of McIntosh's (1979) work illustrates this for individuals of the same species. The infrabasals and radials are aligned in normal specimens of *Bactrocrinites fieldi*, but they are misaligned in the pseudomonocyclic *Kalpidocrinus eriensis* Goldring, 1954, its aberrant junior synonym.

Variation in the orientation of the radial plates can even occur within a single individual. Such irregularity is normal for many cladids, including *Atelestocrinus*. The C radial is typically displaced (counterclockwise) into the BC interradial position, directly over the right posterior basal plate, to accommodate a wide posterior interray. This plate shift is also conserved in the transition to *Belemnocrinus*. However, with the loss of the basals and the anterior radial in this taxon, in addition to hypertrophy of the radianal, the remaining radials shift up to 36° in the opposite (clockwise) direction such that the D radial shifts into the DE interray, the E radial shifts into the EA interray, and the B radial shifts into the AB interray; thereby regaining the expected offset of superadjacent cup plate circlets.

Interpreting the lowest plate circlet of most monocyclic crinoids as infrabasals instead of basals (Müller, 1843) better explains the origin of symmetry patterns elucidated by the LWS than does the Carpenter system (1878). Keeping the infrabasals fixed in a radial position while rotating the radial circlet conserves the offset of the stem lobes with the lowermost plate circlet. Moreover, this rotation explains the observed alignment of the stem lobes with the radials, though now the radials are interradially, not radially, disposed. On the contrary, when the infrabasals are lost without rotation of superadjacent cup plates, leaving basals as the lowermost circlet, the LWS is violated, permitting recognition of true pseudomonocyclic (sensu stricto) crinoids such as extant articulates.

Based on the LWS, Simms (1994) likewise argued for using the stem-cup base junction, not the radials, as the foundation for evaluating the homology of primary plate circlets. He also noted the consistent patterns of symmetry between the stem and calyx base among dicyclic and monocyclic crinoids (as observed for *Atelestocrinus* and *Belemnocrinus*). However, instead of arguing for the loss of the basals and rotation of the radial circlet, he suggested that in many monocyclic crinoids, specifically disparids and glyptocrine camerates, the radials are missing, and the arms developed on basal plates.

Simms (1994) and I agree that the arms can be interradially disposed, but we differ in our explanation for the probable origin of this condition. Evidence presented here also supports the interpretation that the cup base circlets of most disparids and monobathrids are infrabasals, likewise proposed by Guensburg and Sprinkle (2003; see also Moore, 1954: 144), and in opposition to the widely favored Carpenter system (Ubaghs, 1978).

Consistent with McIntosh's rule and this contribution, Guensburg and Sprinkle (2003) argued that the midcup instability they observed among monocyclic camerates from the Early Ordovician suggests retention of infrabasals and radials in these taxa. I generally agree and suspect other examples of variable plate circlet alignment have been overlooked. Even in the absence of a stem, and perhaps especially so, the relative orientations of lumen lobes and radials may be analyzed from the cup base. Recall that according to the LWS, lumen lobes should be consistently aligned with the radials in dicyclic crinoids (e.g., cladids and diplobathrids) and offset by 36 in monocyclic crinoids (e.g., disparids and monobathrids). Variability in the orientations of lumen lobes among monocyclic crinoids is predicted for taxa that achieved this form through loss of the basal circlet. Examination of eight calyxes (USNM S1137) of *Thinocrinus scitulus* (Meek and Worthen, 1860), a monobathrid (Actinocrinitidae) from the Burlington Limestone, reveals stark inconsistency in the orientation of the lumen lobes and radial plates — only about half are interradially disposed. I observed similar inconsistency within large populations of Batocrinidae and Coelocrinidae. Such variability could be the result of reorganization of the radial circlet with loss of the midcup, but it could be also generated by the addition of a sixth plate to the radial circlet, the primanal, as is characteristic of compsocrines. A less ambiguous test could be made among glyptocrines (and disparids), which typically possess only a five-plate radial circlet. However, consistency in the alignment of superadjacent plate circlets does not necessarily rule out loss of the midcup. As demonstrated by *Belemnocrinus*, crinoids that have lost their basal circlets often regain the symmetry patterns expected from the LWS for monocyclic crinoids.

Returning to *Atelestocrinus*, there are at least three competing hypotheses for the relationship among the dicyclic and monocyclic forms of the genus. First, despite their many similarities, *Atelestocrinus* and *Belemnocrinus* may represent distinct genera. The Wassonville population could simply be capturing the origin of a genus. As these linages continued to evolve independently, they could have done so in parallel. Under this scenario, the monocyclic forms of *A. robustus* and *A. baumilleri* are new species of *Belemnocrinus*. Second, the monocyclic *A. robustus* could represent a new pseudomonocyclic genus (not *Belemnocrinus*) that originated independently from its dicyclic counterpart, which perhaps in turn gave rise to the monocyclic *A. baumilleri*, also potentially a member of this same new genus. Under this scenario, *Atelestocrinus* gave rise to more than one genus of pseudomonocyclic crinoid. Third, *Belemnocrinus* could be a phenotypic variant of *Atelestocrinus* that recurs iteratively throughout the range of the genus — a persistent abnormality. Under this scenario, the two genera are synonymous.

There is observational evidence for and against each of these hypotheses, but I withhold much further discussion until thoroughly documenting the Wassonville population, which will include extensive morphological and phylogenetic analysis of the associated clade. Presently, the weight of evidence seems to favor the Wassonville population of *Atelestocrinus-Belemnocrinus* being members of the same species that exhibit extreme phenotypic variation. Likewise, the monocyclic semblances of *A. robustus* and *A. baumilleri* may be best considered aberrant forms of their respective species, not unique taxa. Springer (1901) documented similarly dramatic polymorphism in large populations of *Uintacrinus socialis* (Grinnell, 1876), notably in the number of calyx plate circlets. In a population of specimens from the same lens, 44% of 435 individuals were dicyclic and the rest were monocyclic. It is inconceivable to regard these specimens of *Uintacrinus* as being from distinct species, and much less distinct genera or higher taxa, because of this difference alone.

Suffice it to say, *Belemnocrinus* is a pseudomonocyclic derivative of *Atelestocrinus*, whether developmentally or phylogenetically. But if the two are synonymized, *Belemnocrinus* has priority by over two decades (White, 1862; Wachsmuth and Springer, 1885). Perhaps *Atelestocrinus baumilleri* is *Belemnocrinus baumilleri*. Regardless of the verdict, both are remarkable forms that provide new evidence for a compelling developmental and evolutionary narrative.

Finally, the Belemnocrinacea (Miller, 1883; Moore and Lane, 1978a) is nonmonophyletic. McIntosh (1979) removed *Hypsocrinus* and *Perissocrinus* from the group, and ironically, the namesake genus must now be rejected as well. Through the application of McIntosh's rule, additional dicyclic crinoids that have lost their basal circlets will undoubtedly be recognized. However, loss of the midcup may represent the rule, not the exception, for the origin of monocyclic crinoids in the Paleozoic.

ACKNOWLEDGEMENTS

I am grateful to Jen Bauer and Bill Ausich for organizing this tribute to Tom Baumiller. Jen was especially gracious in answering many questions about style and formatting and provided feedback on earlier drafts. Tiffany Adrain, Jen Bauer, Claudia Johnson, Mark Florence, and David Polly assisted with collections and specimen numbers. Scott Vergiels shared information regarding the provenance of the fossil material from Crawfordville. Tom Baumiller, Tom Guensburg, Hans Hagdorn, and George McIntosh provided some needed references and replied to important queries of a scientific nature. Chris Mah and Simon Coppard provided feedback on my interpretation of the ICZN for *Atelestocrinus*. Mackenzie Mitchell, an undergraduate student in the Art Department, Brigham Young University—Idaho, generated the line illustrations and provided invaluable assistance in formatting the figures. The BYUI Department of Geology facilitated this

work by providing space, equipment, and financial support. Tom Guensburg, Sarah Sheffield, and Samuel Zamora provided helpful reviews of earlier drafts. I am indebted to all. It is an honor this manuscript could be accepted for publication in 2021 as a tribute to the 200th anniversary of Miller's (1821) establishment of the Crinoidea.

LITERATURE CITED

AUSICH, W. I. and N. G. Lane, N. G. 1982. Crinoids from the Edwardsville Formation (Lower Mississippian) of southern Indiana. Journal of Paleontology, 56: 1343–1361.

_____ and G. D. SEVASTOPULO. 2001. The Lower Carboniferous (Tournaisian) crinoids from Hook Head, County Wexford, Ireland. The Palaeontological Society Monograph, 216: 1–136.

_____, D. F. WRIGHT, S. R. COLE, and G. D. SEVASTOPULO. 2020. Homology of posterior interray plates in crinoids: A review and new perspectives from phylogenetics, the fossil record and development. Palaeontology, 63: 525–545

AUSTIN, T. and T. AUSTIN. 1843. XXXII. Description of several new genera and species of Crinoidea. Annals and Magazine of Natural History, 69: 195–207.

BASSLER, R. S. and M. W. MOODEY. 1943. Bibliographic and faunal index of Paleozoic pelmatozoan echinoderms: Geological Society of America Special Paper 45: 1–734.

BATHER, F. A. 1898. Wachsmuth and Springer's monograph on crinoids, third notice. Geological Magazine, New Series, Decade IV, 5: 419–428.

_____. 1899. A phylogenetic classification of the Pelmatozoa. British Association for the Advancement of Science (1898), pp. 916–923.

_____, assisted by J. W. GREGORY and E. S. GOODRICH. 1900. Part III. The Echinoderma. The Pelmatozoa: In E. R. Lankester (ed.), A Treatise on Zoology. Adam and Charles Black, London, pp. 1–344.

BELANSKI, C. H. 1928. Descriptions of some typical fossils of the Shellrock stage. American Midlands Naturalist, 11: 171–212.

CARPENTER, P. H. 1878. On the oral and apical systems of the echinoderms. Quarterly Journal of microscopial science, 18: 351–383.

GAHN, F. J. 2002. Crinoid and blastoid biozonation and biodiversity in the Early Mississippian (Osagean) Burlington Limestone. In B. J. Witzke, B. J. Bunker, and R. anderson (eds.), Pleistocene, Devonian, and Mississippian Stratigraphy of the Burlington, Iowa Area. Iowa Department of Natural Resources, Geological Survey Bureau, Guidebook Series, no. 23: 53–74.

_____. 2006. From dicycly to monocycly: Revision of *Belemnocrinus* and implications for crinoid phylogeny. In B. LeFebvre, B. David, E. Nardin, and E. Poty (eds.), Journées Georges Ubaghs, Programme & Abstracts: 18

_____ and T.K. BAUMILLER. 2004. A bootstrap analysis for comparative taphonomy applied to Early Mississippian (Kinderhookian) crinoids from the Wassonville cycle of Iowa. PALAIOS, 19: 17–38.

_____ and _____. 2010. Evolutionary history of regeneration in crinoids (Echinodermata). Integrative and Comparative Biology, 50: 514a–514m.

GOLDRING, W. 1954. Devonian crinoids. new and old, II. New York State Museum, Circular 37: 1–51.

GRINNELL, G. B. 1876. On a new crinoid from the Cretaceous formation of the West. American Journal of Science and Arts, 12: 81–83.

GUENSBURG, T. E., and J. SPRINKLE. 2003. The oldest known crinoids (Early Ordovician, Utah) and a new crinoid plate homology system: Bulletins of American Paleontology, 364: 1–43.

HAGDORN, H. 2020. *Aszulcicrinus*, a new genus of the Triassic crinoid family Dadocrinidae (Articulata; Encrinida) from Poland. Annales Societatis Geologorum Poloniae, 90: 381–390.

ICZN, 1999. International Code of Zoological Nomenclature. Fourth Edition. The International Trust for Zoological Nomenclature, London, UK. 306 pp [https://www.iczn.org/the-code/the-code-online/]

JAEKEL, O. 1918. Phylogenie und System der Pelmatozoen: Paläeontologische Zeitschrift, 3: 1–128.

KAMMER, T. W., and W. I. AUSICH. 1996. Primitive cladid crinoids from upper Osagean–lower Meramecian (Mississippian) rocks of east-central United States. Journal of Paleontology, 70: 835–866.

_____ and F. J. GAHN. 2003. Primitive cladid crinoids from the early Osagean Burlington Limestone and the phylogenetics of Mississippian species of *Cyathocrinites*. Journal of Paleontology, 77: 121–138.

_____ and E. W. ROESER. Cladid crinoids from the late Kinderhookian Meadville Shale, Cuyahoga Formation of Ohio. Journal of Paleontology, 86: 470–487.

KEYES, C. R. 1895. Geology of Lee County; Geology of Des Moines County. Iowa Geological Survey, Annual Report, 3: 305–492.

KIRK, E., 1948. Two new inadunate crinoid genera from the Middle Devonian. American Journal of Science, 246: 701–710.

LANE, H. R. and P. L. BRENCKLE. 2005. Type Mississippian Subdivisions and Biostratigraphic Succession. In P. H. Heckel (ed.), Stratigraphy and Biostratigraphy of the Mississippian Subsystem (Carboniferous System) in Its Type Region, the Mississippi River Valley of Illinois, Missouri, and Iowa. Illinois State Geological Survey Guidebook 34: 76–105.

LANE, N. G. 1967. Revision of suborder Cyathocrinina (Class Crinoidea). University of Kansas Paleontological Contributions, Paper 24: 1–13.

_____. 1978. Postlarval ontogeny of fossil crinoids: Inadunates. In R.C. Moore and C. Teichert (eds.), Treatise on Invertebrate Paleontology, Part T, Echinodermata 2, Crinoidea. Geological Society of America and University of Kansas, pp. T263–266.

LEE, K. G., W. I. AUSICH, and T. W. KAMMER. 2005. Crinoids from the Nada Member of the Borden Formation (Lower Mississippian) in eastern Kentucky. Journal of Paleontology, 79: 337–355.

MCINTOSH, G. C. 1979. Abnormal specimens of the Middle Devonian crinoid *Bactrocrinites* and their effect on the taxonomy of the genus. Journal of Paleontology, 53: 18–28.

_____. 1983. Review of the Devonian cladid inadunate crinoids: Suborder Dendrocrinina. Ph.D. dissertation, University of Michigan, pp. 1–521.

_____. 2001. Devonian cladid crinoids: Families Glossocrinidae Goldring,1923, and Rutkowskicrinidae new family. Journal of Paleontology, 75: 783–807.

_____ and C. E. Brett. 1988. Occurrence of the cladid inadunate crinoid Thalamocrinus in the Silurian (Wenlockian) of New York and Ontario. Royal Ontario Museum, Life Sciences Contributions, 149: 1–17.

Meek, F. B. and A. H. Worthen. 1860. Descriptions of new species of Crinoidea and Echinoidea from the Carboniferous rocks of Illinois, and other western states. Proceedings of the Academy of Natural Sciences of Philadelphia, 12: 379–397.

MILLER, J. S. 1821. A natural history of the Crinoidea, or lily-shaped animals; with observations on the genera, *Asteria*, *Euryale*, *Comatula* and *Marsupites*. Bryan & Co., Bristol, England, pp. 1–150.

MILLER, S. A. 1883. The American Palaeozoic fossils. a catalogue of the genera and species, with names of authors, dates, places of publication, groups of books in which found, and the etymology and signification of the words, and an introduction devoted to the stratigraphical geology of the Palaeozoic rocks. The author, Cincinnati, Ohio, Second Edition. Echinodermata, pp. 247–334.

_____. 1889. North American geology and paleontology. Western Methodist Book Concern, Cincinnati, pp. 1—664.

Moore, R. C., 1954. Status of invertebrate paleontology, 1953, IV Echinodermata; Pelmatozoa. Harvard University Museum of Comparative Zoology Bulletin, 112: 125–149.

_____ and L. R. LAUDON. 1943. Evolution and classification of Paleozoic crinoids: Geological Society of America, Special Paper 46: 1–151.

_____ and N. G. LANE. 1978a. Superfamily Belemnocrinacea S. A. Miller, 1883. In R.C. Moore and C. Teichert (eds.), Treatise on Invertebrate Paleontology, Part T, Echinodermata 2, Crinoidea. Geological Society of America and University of Kansas, pp. T557–562.

_____ and _____. 1978b. Superfamily Mastigocrinacea Jaekel, 1918. In R.C. Moore and C. Teichert (eds.), Treatise on Invertebrate Paleontology, Part T, Echinodermata 2, Crinoidea. Geological Society of America and University of Kansas, pp. T618–626.

MÜLLER, J., 1843. Über den Bau des *Pentacrinus caput Medusae*. Abhandlungen der Königlichen Academie der Wissenschafften zu Berlin, 1841, pp. 177–248.

SEVASTOPULO, G. D. and N. G. LANE. 1988. Ontogeny and phylogeny of disparid crinoids. In C. R. C. Paul and A. B. Smith (eds.), Echinoderm phylogeny and evolutionary biology, Clarendon Press, Oxford, pp. 245–253.

SPRINGER, F., 1901. Uintacrinus, its structure and relations. Harvard Museum of Comparative Zoology, Memoir 25: 1–89.

_____. 1920. The Crinoidea Flexibilia. Smithsonian Institution Publication 2501: 1–486.

_____ and A. W. SLOCUM. 1906. *Hypsocrinus*, a new genus of crinoids from the Devonian. Field Columbia Museum Publication, 114, Geology Series, 2: 267–271.

STRIMPLE, H. L. and C. O. Levorson, 1969. Two Upper Devonian crinoids. In Fossil Crinoid Studies. University of Kansas Paleontological Contributions, Paper 42: 17–20.

THOMPSON, T. L. 1967. Conodont zonation of lower Osagean Rocks (lower Mississippian) of southwestern Missouri. Missouri Geological Survey and Water Resources, Report of Investigations 39: 1–88.

UBAGHS, G. 1953. Classe des Crinoides. In J. Piveteau (ed.), Traité de paléontologie, Volume 3, Masson & Cie, Paris, pp. 658–773.

_____. 1978, General morphology, In R. C. Moore and C. Teichert (eds.), Treatise on Invertebrate Paleontology, Pt. T Echinodermata 2: Geological Society of America and University of Kansas Press, pp. T58–T216.

WACHSMUTH, C. and F. SPRINGER, F. 1877. Revision of the genus *Belemnocrinus*, and description of two new species. American Journal of Science, 13: 253–259.

_____ and _____. 1885. Revision of the Palaeocrinoidea. Pt. III, Sec. 1. Discussion of the classification and relations of the brachiate crinoids, and conclusion of the generic descriptions. Proceedings of the Academy of Natural Sciences of Philadelphia, pp. 225–364.

_____ and _____. 1886. Revision of the Palaeocrinoidea. Pt. III, Sec. 1. Discussion of the classification and relations

of the brachiate crinoids, and conclusion of the generic descriptions. Proceedings of the Academy of Natural Sciences of Philadelphia, pp. 64–226.

WEBSTER, G. D. 1986. Bibliography and index of Paleozoic crinoids, 1974-1980. Geological Society of America, Microform Publication 16: 1–405.

_____.1988. Bibliography and index of Paleozoic crinoids and coronate echinoderms 1981-1985. Geological Society of America, Microform Publication 18: 1–235.

WEBSTER, G. D., 2014. Bibliography and index of Paleozoic crinoids, coronates, and hemistreptocrinoids, 1758–2012. The author, Pullman, Washington, pp. 1–2,694 [http://crinoids.azurewebsites.net/].

WEBSTER, G. D., C. G. MAPLES, R. MAWSON, and M. DASTANPOUR. 2003. A cladid-dominated Early Mississippian crinoid and conodont fauna from Kerman Province, Iran and revision of the glossocrinids and rhenocrinids. Journal of Paleontology, Memoir 60: 1–35.

WELLER, S. 1898. A bibliographic index of Carboniferous invertebrates. U. S. Geological Survey, Bulletin 153: 1–653.

WHITE, C. A. 1862. Description of new species of fossils from the Devonian and Carboniferous rocks of the Mississippi Valley. Boston Society of Natural History Journal, 9: 8–33.

WITZKE, B. J. and B. J. BUNKER. 1996. Relative sea-level changes during Middle Ordovician through Mississippian deposition in the Iowa area, North American craton, In B. J. Witzke, G. A. Ludvigson, and J. Day (eds.), Paleozoic sequence stratigraphy: Views from the North American Craton. Geological Society of America, Special Paper, 306: 307–330.

_____ and _____. 2005. Comments on the Mississippian Stratigraphic Succession in Iowa. In P. H. Heckel (ed.), Stratigraphy and Biostratigraphy of the Mississippian Subsystem (Carboniferous System) in Its Type Region, the Mississippi River Valley of Illinois, Missouri, and Iowa. Illinois State Geological Survey Guidebook 34: 63–75.

WRIGHT, D., W. AUSICH, S. COLE, M. PETER, and E. RHENBERG. 2017. Phylogenetic taxonomy and classification of the Crinoidea (Echinodermata). Journal of Paleontology, 91: 829–846.

Museum of Paleontology, The University of Michigan
1105 North University Avenue, Ann Arbor, Michigan 48109-1085
Matt Friedman, Director

Contributions from the Museum of Paleontology, University of Michigan is a medium for publication of reports based chiefly on museum collections and field research sponsored by the museum. Jennifer Bauer and William Ausich, Guest Editors;
Jeffrey Wilson Mantilla, Editor.

Publications of the Museum of Paleontology are accessible online at: http://deepblue.lib.umich.edu/handle/2027.42/41251

Print (ISSN 0097-3556), Online (ISSN 2771-2192)